ASTEROSEISMOLOGY IN THE KEPLER ERA

EDITED BY: Andrzej S. Baran, Anthony Eugene Lynas-Gray and Karen Kinemuchi
PUBLISHED IN: Frontiers in Astronomy and Space Sciences

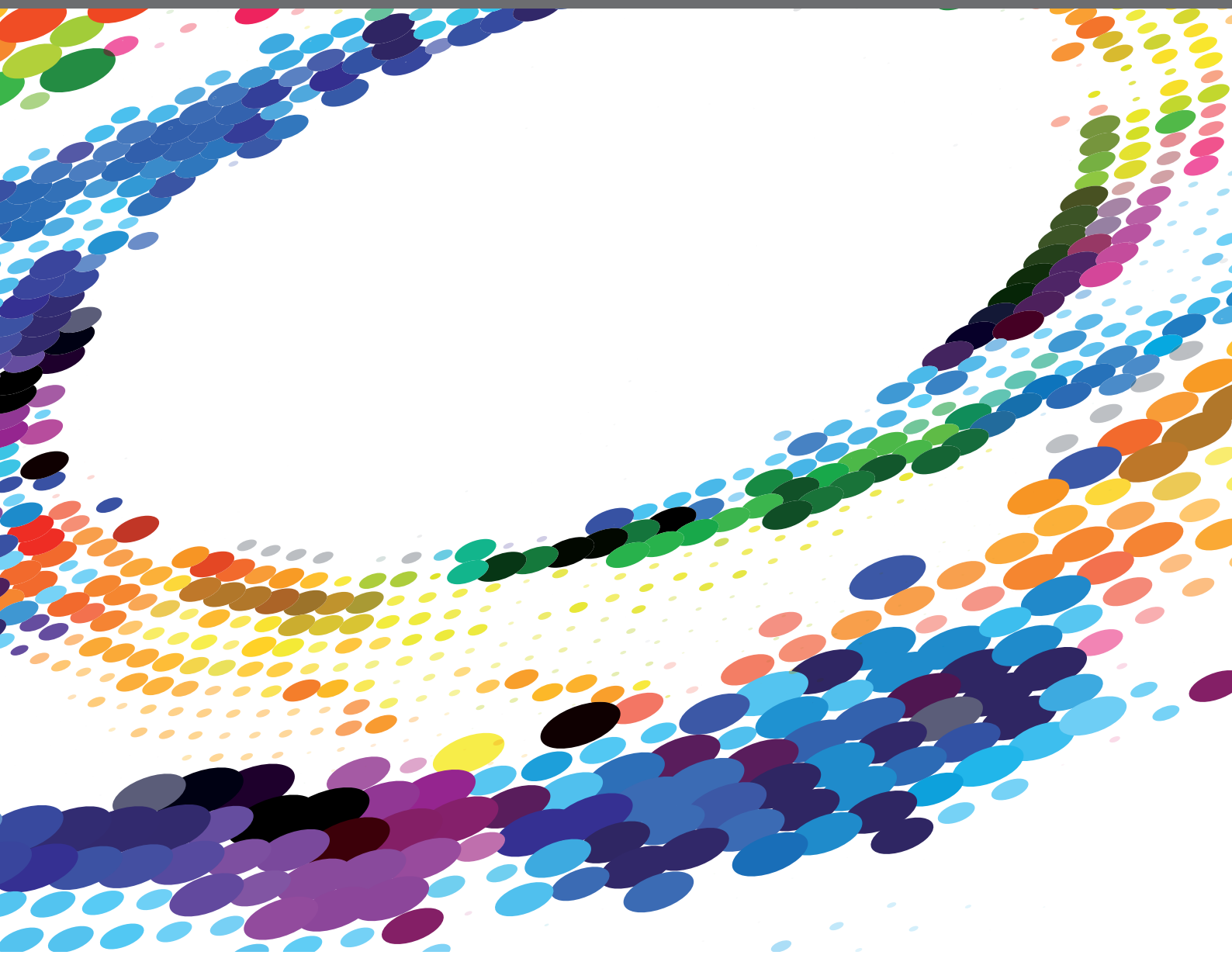

frontiers Research Topics

frontiers

ISSN 1664-8714
ISBN 978-2-88971-477-3
DOI 10.3389/978-2-88971-477-3

About Frontiers

Frontiers is more than just an open-access publisher of scholarly articles: it is a pioneering approach to the world of academia, radically improving the way scholarly research is managed. The grand vision of Frontiers is a world where all people have an equal opportunity to seek, share and generate knowledge. Frontiers provides immediate and permanent online open access to all its publications, but this alone is not enough to realize our grand goals.

Frontiers Journal Series

The Frontiers Journal Series is a multi-tier and interdisciplinary set of open-access, online journals, promising a paradigm shift from the current review, selection and dissemination processes in academic publishing. All Frontiers journals are driven by researchers for researchers; therefore, they constitute a service to the scholarly community. At the same time, the Frontiers Journal Series operates on a revolutionary invention, the tiered publishing system, initially addressing specific communities of scholars, and gradually climbing up to broader public understanding, thus serving the interests of the lay society, too.

Dedication to Quality

Each Frontiers article is a landmark of the highest quality, thanks to genuinely collaborative interactions between authors and review editors, who include some of the world's best academicians. Research must be certified by peers before entering a stream of knowledge that may eventually reach the public - and shape society; therefore, Frontiers only applies the most rigorous and unbiased reviews.
Frontiers revolutionizes research publishing by freely delivering the most outstanding research, evaluated with no bias from both the academic and social point of view. By applying the most advanced information technologies, Frontiers is catapulting scholarly publishing into a new generation.

What are Frontiers Research Topics?

Frontiers Research Topics are very popular trademarks of the Frontiers Journals Series: they are collections of at least ten articles, all centered on a particular subject. With their unique mix of varied contributions from Original Research to Review Articles, Frontiers Research Topics unify the most influential researchers, the latest key findings and historical advances in a hot research area! Find out more on how to host your own Frontiers Research Topic or contribute to one as an author by contacting the Frontiers Editorial Office: frontiersin.org/about/contact

ASTEROSEISMOLOGY IN THE KEPLER ERA

Topic Editors:
Andrzej S. Baran, Pedagogical University of Kraków, Poland
Anthony Eugene Lynas-Gray, University College London, United Kingdom
Karen Kinemuchi, New Mexico State University, United States

Citation: Baran, A. S., Lynas-Gray, A. E., Kinemuchi, K., eds. (2021). Asteroseismology in the Kepler Era. Lausanne: Frontiers Media SA.
doi: 10.3389/978-2-88971-477-3

Table of Contents

frontiers in Astronomy and Space Sciences

EDITORIAL
published: 23 August 2021
doi: 10.3389/fspas.2021.708266

Editorial: Asteroseismology in the Kepler Era

Anthony E. Lynas-Gray[1,2,3], *Andrzej S. Baran*[4,5,6]* *and Karen Kinemuchi*[7]

[1]University College London, London, United Kingdom, [2]University of Oxford, Oxford, United Kingdom, [3]University of the Western Cape, Bellville, South Africa, [4]ARDASTELLA Research Group, Institute of Physics, Pedagogical University of Kraków, Kraków, Poland, [5]Department of Physical Science, Embry-Riddle Aeronautical University, Daytona Beach, FL, United States, [6]Department of Physics, Astronomy, and Materials Science, Missouri State University, Springfield, MO, United States, [7]New Mexico State University, Las Cruces, NM, United States

Keywords: kepler spacecraft, pulsating stars, asteroseismology, space photometry, fourier technique

Editorial on the Research Topic

Asteroseismology in the Kepler Era

The Kepler spacecraft, launched by the National Aeronautics and Space Administration (NASA) on 2009 March 7th, proved to be an important pioneering astronomical survey instrumental, making crucial discoveries during its primary mission over the ensuing 4 years. Looking longitudinally along the Local Spiral Arm in the general direction of Cygnus maximised the number of nearby (and therefore bright) stars that could be monitored almost continuously over the lifetime of the mission. A 0.95-m mirror with detectors sensitive to wavelengths in range 430–890 nm offered the best prospect of detecting earth-sized planets with orbital periods of about one-year, transiting across the disks of solar-type stars. While the search for planets orbiting nearby stars, and those in habitable zones in particular, persuaded NASA to support the Kepler mission, it would be a mistake to suppose that asteroseismic studies constituted a secondary scientific objective. Stellar pulsation generates light-curve features which could be of the same order as the flux lost from a solar-type star when an earth-sized planet in its habitable zone transits across its disk; it is critical that the two are not confused. Asteroseismology therefore plays a role in the search for planets beyond the Solar System. Furthermore, the existence of a planetary system is likely to affect evolution and internal structure of the host star, thereby determining its asteroseismic properties. Searches for planets orbiting nearby stars, and asteroseismology of these objects, are therefore inextricably linked.

The Editors are extremely grateful to the authors and reviewers who have contributed papers on asteroseismology with the Kepler spacecraft. While only a tiny fraction of the scientific returns are presented, the sample is understood to be representative and serve to inspire and support future space missions which will achieve even more than the impressive results secured by the Kepler mission.

In particular, we look forward to theoretical developments which allow the full potential of asteroseismic observations to be realised.

AUTHOR CONTRIBUTIONS

All authors listed have made a substantial, direct, and intellectual contribution to the work and approved it for publication.

Conflict of Interest: The authors declare that the research was conducted in the absence of any commercial or financial relationships that could be construed as a potential conflict of interest.

Publisher's Note: All claims expressed in this article are solely those of the authors and do not necessarily represent those of their affiliated organizations, or those of the publisher, the editors and the reviewers. Any product that may be evaluated in this article, or claim that may be made by its manufacturer, is not guaranteed or endorsed by the publisher.

OPEN ACCESS

Edited and reviewed by:
Scott William McIntosh, National Center for Atmospheric Research (UCAR), United States

***Correspondence:**
Andrzej S. Baran
andrzej.baran@up.krakow.pl

Specialty section:
This article was submitted to Stellar and Solar Physics, a section of the journal Frontiers in Astronomy and Space Sciences

Received: *11 May 2021*
Accepted: *11 August 2021*
Published: *23 August 2021*

Citation:
Lynas-Gray AE, Baran AS and Kinemuchi K (2021) Editorial: Asteroseismology in the Kepler Era. Front. Astron. Space Sci. 8:708266. doi: 10.3389/fspas.2021.708266

frontiers in Astronomy and Space Sciences

REVIEW
published: 04 August 2020
doi: 10.3389/fspas.2020.00044

Unveiling the Structure and Dynamics of Red Giants With Asteroseismology

Sarbani Basu[1]* *and Saskia Hekker*[2,3]

[1] Department of Astronomy, Yale University, New Haven, CT, United States, [2] Max Planck Institute for Solar System Research, Göttingen, Germany, [3] Stellar Astrophysics Centre, Department of Physics and Astronomy, Aarhus University, Aarhus, Denmark

The *Kepler* mission observed many thousands of red giants. The long time series, some as long as the mission itself, have allowed us to study red giants with unprecedented detail. Given that red giants are intrinsically luminous, and hence can be observed from very large distances, knowing the properties of red giants, in particular ages, is of immense value for studies of the formation and evolution of the Galaxy, an endeavor known as "Galactic archaeology." In this article we review what we have learned about red giants using asteroseismic data. We start with the properties of the power spectrum and move on to internal structure and dynamics of these stars; we also touch upon unsolved issues in red-giant asteroseismology and the prospects of making further progress in understanding these stars.

Keywords: stellar oscillations, fundamental parameters of stars, stellar evolution, stellar interiors, stellar rotation

OPEN ACCESS

Edited by:
Karen Kinemuchi,
New Mexico State University,
United States

Reviewed by:
Tiago Campante,
Instituto de Astrofísica e Ciências do Espaço (IA), Portugal
Paul G. Beck,
University of Graz, Austria

***Correspondence:**
Sarbani Basu
sarbani.basu@yale.edu

Specialty section:
This article was submitted to Stellar and Solar Physics, a section of the journal Frontiers in Astronomy and Space Sciences

Received: *12 May 2020*
Accepted: *17 June 2020*
Published: *04 August 2020*

Citation:
Basu S and Hekker S (2020) Unveiling the Structure and Dynamics of Red Giants With Asteroseismology. Front. Astron. Space Sci. 7:44. doi: 10.3389/fspas.2020.00044

1. INTRODUCTION

Red-giant stars mark that stage of stellar evolution when a star has exhausted its central hydrogen, fusion occurs in a very thin shell around an inert helium core, and the envelope is cool enough that the convection zone encompasses most of the star making the stars almost fully convective (see, e.g., Salaris and Cassisi, 2005; Kippenhahn et al., 2012, etc.). Being almost fully convective, the stars are constrained to take an almost vertical path on the Hertzsprung-Russell (HR) diagram (see **Figure 1**). Along the red-giant branch (RGB) the stars exhibit a very narrow range of temperatures. The stars follow the vertical path, briefly disrupted by a short phase in which the star decreases its luminosity, i.e., the RGB bump, until the onset of helium fusion in the core. For stars with masses below about 2 $M_\odot$ at the tip of the RGB the onset of helium fusion occurs in degenerate conditions. This is a fast process referred to as the helium-flash. For higher-mass stars, the onset of helium burning occurs in non-degenerate conditions. After the onset of helium burning in the core, the star reduces in luminosity and radius, and has a slightly higher temperature. High-metallicity low-mass stars in this stage settle into the red clump and higher-mass stars form the so-called secondary clump; low-metallicity stars form the horizontal branch. While these stars are fascinating on their own accord, their high luminosities make them visible from large distances, and thus useful tools in studying the Galaxy.

Stellar oscillation frequencies can be derived from radial velocity measurements, [e.g., from the Stellar Oscillation Network Group; Grundahl et al. (2007)], as well as photometry from space with missions like *CoRot* (Baglin et al., 2006) and *Kepler* (Borucki et al., 2010) The recent *Kepler* space mission provided long ($\sim$ 4 years) of near-uninterrupted high-precision high-cadence photometric timeseries data. These data are of unprecedented quality and frequency resolution,

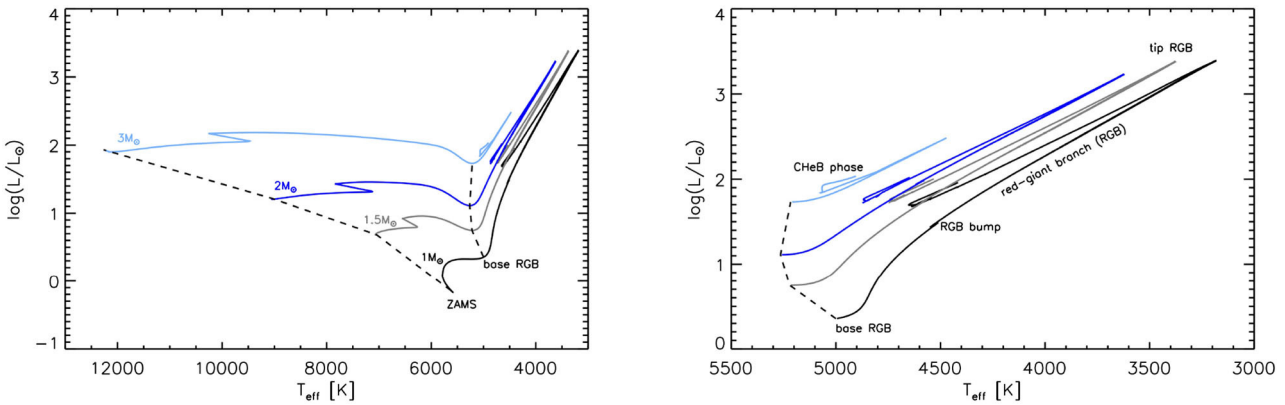

FIGURE 1 | Left: HR Diagram with four evolutionary tracks of models of masses 1.0, 1.5, 2.0 and 3.0 $M_{\odot}$ in black, gray, blue, and light blue, respectively. The tracks are shown from the zero age main sequence (ZAMS) through the red-giant branch (RGB) and the core helium burning (CHeB) phase until the helium core mass fraction drops below 10^{-3}. **Right**: The same tracks as in the left panel now starting from the base of the red-giant branch. The models were computed using MESA (Paxton et al., 2019, and references therein) version r-10398 and solar metallicity. See **Appendix A** for the inlist of the MESA computations.

and are a treasure trove for red-giant asteroseismology. This has led to many ground-breaking results published over the last decade. These include the detection of g-mode period spacings (Beck et al., 2011), the discovery that g-mode spacings can be used to distinguish inert-helium core red giants from core helium burning giants (Bedding et al., 2011; Mosser et al., 2011), the unequivocal detection of core rotation (Beck et al., 2012b), that red giant cores might actually slow down rather than spin up as they contract (Mosser et al., 2012b; Gehan et al., 2018), that precise estimates of red-giant surface gravities can be derived from the contribution that granulation makes to the photometric time series (Kallinger et al., 2016), etc. These data have also resulted in catalogs of stellar properties (Pinsonneault et al., 2014, 2018; Yu et al., 2018, etc.) that are proving invaluable to the study of Galactic archaeology. Many such results are also highlighted in recent reviews by Hekker (2013), Mosser et al. (2016), and Hekker and Christensen-Dalsgaard (2017). In this review, we focus on the properties of the power spectra of red-giant stars and how they can be interpreted in terms of their structure and dynamics.

2. PROPERTIES OF THE POWER SPECTRUM

Red-giant stars are solar-like oscillators, i.e., their oscillations are stochastically excited and damped by near-surface turbulent convection (see e.g., Goldreich and Keeley, 1977a,b; Balmforth, 1992). Unlike classical pulsators, many oscillation modes are excited, however the amplitudes of the modes are small. The frequencies of the modes are determined by the internal structure of the star, which makes asteroseismic inferences on stellar structure possible. Spherical harmonics are used to describe the angular dependence of the modes, with the degree l being the number of nodal planes intersecting the surface, and the azimuthal order m the number of nodes along the equator. In the radial direction, the models are described by the radial order n, which is the number of nodes in the radial direction. Conventionally, acoustic modes are denoted by positive values of n and while gravity modes, i.e., modes with buoyancy as restoring force, are denoted by negative values of n. The azimuthal order comes into play only if rotation or magnetic fields (or both) break spherical symmetry. In the absence of these symmetry-breaking factors, there is a single mode with a given (l, n); rotation "splits" the modes into $2l + 1$ components labeled by m. For stars other than the Sun only low-degree oscillations can be observed due to cancellation effects that are a result of observing stars as point sources. Typically one observes radial ($l = 0$), dipole ($l = 1$) and quadrupole ($l = 2$) modes, though sometimes octupole ($l = 3$) modes can be detected as well. More details about the characteristics of oscillation frequencies and how they are related to internal structure and dynamic are described in textbooks such as Unno et al. (1989) and Aerts et al. (2010). Whether, and how many, rotationally split modes are observed depends on the inclination angle of the star (Gizon and Solanki, 2003) assuming of course, that the frequency resolution is good enough. These rotationally split modes provide insight in the rotation rate from the size of the splitting and on the inclination angle from the relative amplitudes of the split components.

We show a power spectrum of a typical red giant in **Figure 2**. The power density spectrum of red-giant stars, as well as other solar-like oscillations such as low-mass main-sequence stars and subgiants, is dominated by granulation – the observable part of the near-surface turbulent convection– as a frequency-dependent signal and is commonly modeled as red noise. The power spectrum is modulated by a broad bell-shaped envelope whose maximum is at a frequency often called $\nu_{\rm max}$, the frequency of maximum oscillation power. The value of $\nu_{\rm max}$ provides a direct rough indication of the size of the star, i.e., it takes longer for the waves to travel through a larger star and hence stars with larger radii have oscillations occurring at lower values of $\nu_{\rm max}$. Brown et al. (1991) and Kjeldsen and Bedding (1995) argued that $\nu_{\rm max} \propto \nu_{\rm ac}$, where $\nu_{\rm ac}$ is the acoustic cutoff frequency i.e., the frequency beyond which acoustic modes are no longer trapped in the star

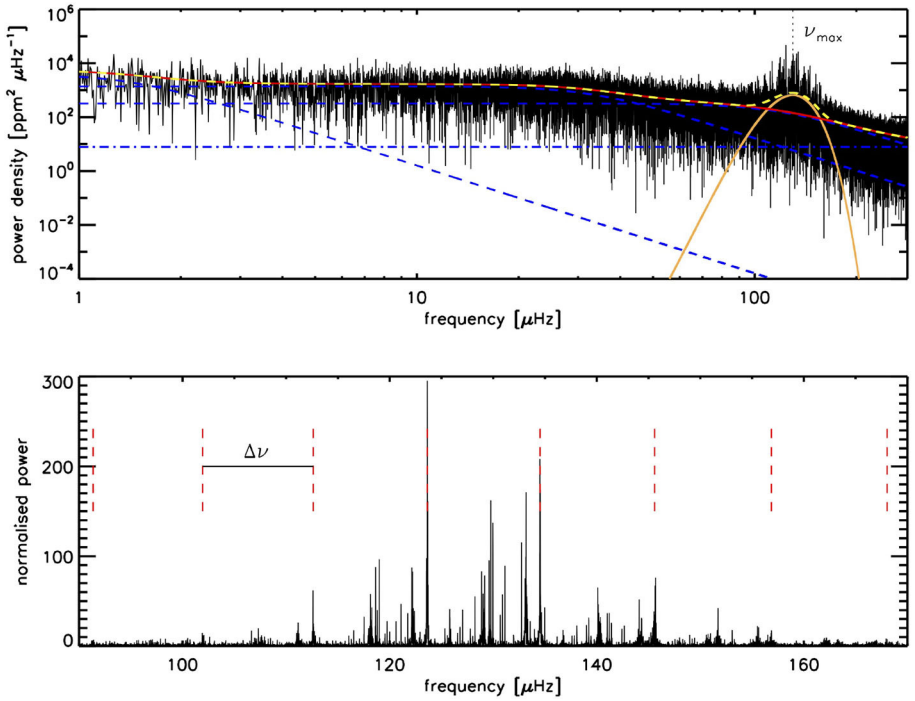

FIGURE 2 | Top: Power density spectrum of KIC 6144777 with the data shown in black. The granulation components are indicated with blue dashed lines and the white noise with the blue dashed-dotted line. The sum of the granulation components and noise comprise the background fit, which is shown with the red solid line. The Gaussian fit to the power excess is shown in orange with the frequency of maximum oscillation power (ν_{max}) indicated by the vertical dotted line. The complete fit (background + oscillation power excess) is shown with the yellow dashed line. **Bottom:** The power spectrum after the background correction. The regular pattern of radial modes is indicated with the vertical red dashed lines. The distance in frequency between these lines is the large frequency separation $\Delta\nu$.

and behave as traveling waves. Under the assumption of an isothermal atmosphere, one can show that ν_{ac} is proportional to $g/\sqrt{T_{\rm eff}} \propto M/(R^2\sqrt{T_{\rm eff}})$, where $g, M, R, T_{\rm eff}$ are surface gravity, mass, radius and effective temperature, respectively. Both the shape of the envelope and the value of ν_{max} are determined by the excitation and damping of the oscillation modes. There is as yet no theoretical understanding as to why ν_{max} is proportional to ν_{ac}.

Another property of the power spectra of solar-like oscillators is the picket-fence, or comb-like, pattern of low degree modes. The modes of a given degree l and consecutive radial orders n are approximately equidistant in frequency, and the separation is called the large frequency separation, $\Delta\nu$. Ulrich (1986) and Christensen-Dalsgaard (1988) showed that the large frequency separation scales approximately with the square root of the mean density ($\bar{\rho}$) of the star: $(\Delta\nu/\Delta_{\nu_\odot}) \sim \sqrt{(\bar{\rho}/\bar{\rho_\odot}}$. The expression is not exact and has well-known deviations that are a function of temperature (White et al., 2011), metallicity (Guggenberger et al., 2016) and at the red-giant end the deviation also depends on mass (Guggenberger et al., 2017). For an extensive overview of ways to mitigate these deviations see Hekker (2020) and references therein. However, despite these deviations, the $\Delta\nu$ scaling relation, along with the relation for ν_{max}, have been very useful in getting initial mass and radius estimates of all types of stars (Chaplin et al., 2010; Pinsonneault et al., 2014, 2018). As shown by Ong and Basu (2019a), we now understand why these deviations occur, and have derived ways of calculating $\Delta\nu$ for models that give much better approximations to $\Delta\nu$, without resorting to calculating the frequencies.

Solar-like oscillation modes can be divided into acoustic modes (i.e., sound waves with pressure as the restoring force) or gravity modes (with buoyancy as the restoring force). The acoustic modes are the ones that are equidistant in frequency and separated by $\Delta\nu$; gravity modes on the other hand are equidistant in period. Whether a mode is acoustic or gravity depends on two frequencies: the Lamb frequency S_l which depends on the sound-speed profile of the star as well as the degree of a mode; and the buoyancy or Brunt-Väisälä frequency N that is related to the convective stability criterion and is imaginary in convection zones. Acoustic modes have frequency ω such that $\omega^2 > S_l^2$ and $\omega^2 > N^2$, and gravity modes occur in the region where $\omega^2 < N^2$ and $\omega^2 < S_l^2$. For main-sequence solar-like oscillators, the acoustic modes and gravity modes are trapped in well-separated regions of a star and the observed modes are purely acoustic modes. However, in evolved solar-like oscillators the non-radial ($l > 0$) oscillation modes are not necessarily pure acoustic modes. As a star evolves, the density of the core increases leading to an increase of the buoyancy frequency values, while at the same time the outer layers of the star expand leading to a decrease of ν_{max}. This can result in a coupling of the acoustic and gravity

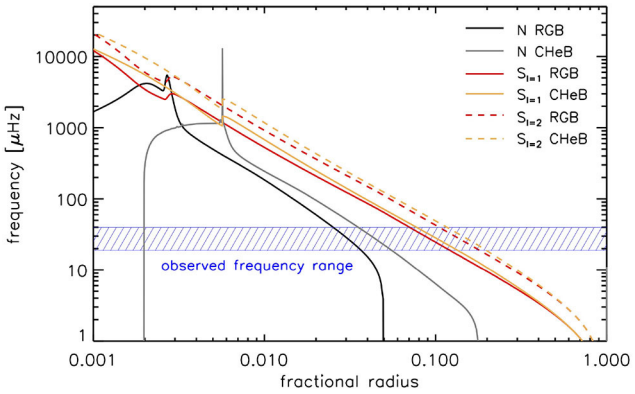

FIGURE 3 | Propagation diagram of a 1 $M_\odot$ model of an ascending the red-giant branch (RGB) star and a core helium burning (CHeB) star on the same evolutionary track. For the RGB model, the Brunt-Väisälä frequency N is shown in black and the Lamb frequency S for dipole ($l = 1$) and quadrupole ($l = 2$) modes are shown with the red solid and dashed line, respectively. The Brunt-Väisälä frequency and Lamb frequencies for the core helium burning (CHeB) model are indicated in gray and orange. The region around the ν_{max} value of both models is indicated by the horizontal blue bar.

mode cavities. In **Figure 3**, we show a so-called "propagation diagram" for red-giant models. This diagram shows the Lamb frequency for $l = 1$ and $l = 2$ modes along with the buoyancy frequency. We can see that around ν_{max} for these models, the radial distance between the cavity for acoustic $l = 1$ modes and for gravity modes is small, allowing g modes (gravity modes) to couple with p modes (acoustic modes). The "mixed" modes have gravity-mode characteristics in the deep interior, and acoustic mode characteristics in the outer layers. In red giants, multiple g modes can couple with a single p mode leading to multiple mixed modes per acoustic radial order. The presence of mixed modes causes multiple peaks for a given $l = 1$ p mode. We show this in **Figure 4**. The mixed modes of degree $l = 1$ (dipole modes) are most evident in red-giant power spectra. Coupling is weaker for the $l = 2$ (quadrupole) modes because of the larger evanescent zone between the Lamb and Brunt-Väisälä frequency (see **Figure 3**), as a result only the most p-dominated quadrupole modes are observed easily. Additionally, the $l = 2$ g-dominated modes would be harder to resolve since the frequency differences between the more p-dominated and the neighboring g-dominated modes is often unresolved given the frequency resolution and width of the modes. More about the nature of the modes can be found in Unno et al. (1989), Aerts et al. (2010), etc.

The mixed dipole modes appear at frequencies that are equidistant in period ($\Delta\Pi$) as dictated by the gravity-part of the mode, modulated by the strength of the coupling to the pressure part of the mode (e.g., Mosser et al., 2012c). In other words, close to the nominal pressure mode the coupling is strongest and the observed period spacing deviates from the underlying period spacing of the gravity part of the mode, while further away from the nominal pressure mode the period spacing approaches the underlying value. This underlying period spacing acts as a direct probe of the core of red-giant stars.

In reality, mode-frequencies do not follow a strict separation in frequency (or period for g modes), i.e., the frequency/period separation between adjacent modes differs from the average value of $\Delta\nu$ or $\Delta\Pi$, although these deviations are small. These deviations are a result of the fact that stars are not homogeneous balls of gas, but are stratified, and this leaves a "curvature" in the frequency spacings that is easily seen in an échelle diagram of the frequencies (see **Figure 5**). Abrupt changes, so-called glitches, leave an oscillatory pattern in the frequency separations, and the deeper inside the star the location of the glitch occurs, the shorter the wavelength of the pattern (Gough, 1990). The base of the convection zone, and the helium second ionization zone are places where an acoustic glitch occurs. In evolved stars, the hydrogen-burning shell can leave a glitch in the buoyancy frequency which affects period spacings. These glitches provide a direct probe of the location and nature of the change in the stellar structure. We refer reader to Basu and Chaplin (2017) for details on the behavior of acoustic, gravity and mixed modes in different types of solar oscillators, as well as the effect of glitches and how they may be used to study stellar structure.

3. DIFFERENTIATING RED-GIANT AND RED-CLUMP STARS

One of the important results obtained with *Kepler* data was the realization that asteroseismic data can be used to differentiate RGB stars from core-helium burning red-clump stars. Red-clump stars are important because they are standard candles since their luminosity depends very weakly on mass and metallicity (Girardi, 2016). These stars can be used as distance tracers out to $\sim$ 10 Kpc (e.g., Bovy et al., 2014; Mathur et al., 2016; Ting et al., 2018). Currently, the Gaia mission is providing parallaxes for billions of stars, however, beyond about 3 Kpc Gaia uncertainties can become larger than those provided by standard candles such as red-clump stars (e.g., Mints and Hekker, 2018). In fact red-clump stars have revealed zero-point errors in Gaia data and have aided in showing how these errors can be corrected (Davies et al., 2017; Khan et al., 2019). However, because red-clump stars occur in a $T_{\rm eff}$ and $\log g$ range where ascending branch red-giant stars are also found, it is almost impossible to pick them out among field red giants; in clusters on the other hand, the over-density of points in the color-magnitude diagram (CMD) at the characteristic $\log g$ facilitates detection.

Bedding et al. (2011) showed that asteroseismic data can distinguish between the two types of giants, and the key discriminant is the period spacing of the dipole model in the two types of stars (see **Figure 6**) with red-clump stars having higher period spacings than red giants. Secondary clump stars, i.e., stars massive enough to initiate helium burning before their cores become degenerate have intermediate values. It is actually quite easy to understand the result, and in fact, it should have been anticipated. Asymptotically, the period spacing ($\Delta\Pi_0$) of the g-mode oscillations can be expressed as $\Delta\Pi_0 = 2\pi^2(\int_{r_1}^{r_2} N(r)\mathrm{d}r/r)^{-1}$, where r_1 and r_2 are the boundaries of the radiative zone; for modes of a given l, the spacing ($\Delta\Pi_l$) is then $\Delta\Pi_0/\sqrt{l(l+1)}$ (Aizenman et al., 1977; Tassoul, 1980). The key

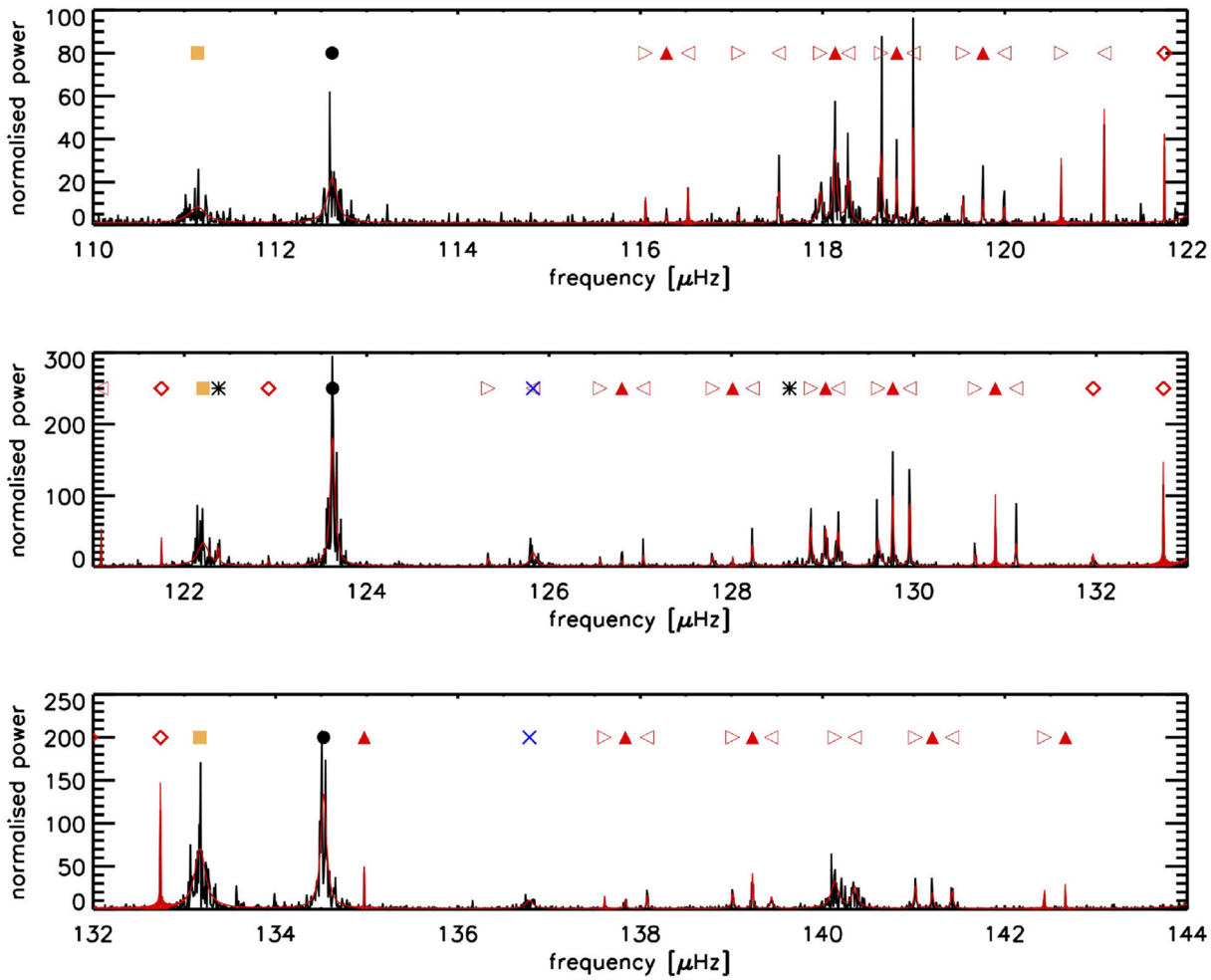

FIGURE 4 | A close look into the region of the three radial orders closest to ν_{max} in the power density spectrum of KIC 6144777. Each row focuses on one radial mode and the adjacent $l = 1$ and $l = 2$ modes. The fit to the data as computed with TACO (Hekker et al., in prep) is indicated in red. The radial, dipole, quadrupole and octupole modes are indicated with black dots, red triangles, orange squares and blue crosses, respectively. Note that there are multiple dipole modes associated with each radial mode—these are the mixed modes. Additionally, the dipole modes show rotational splitting, where the $m = -1$ and $m = +1$ modes are indicated with right and left pointing open triangles respectively. Dipole modes for which the azimuthal order could not (yet) be identified are indicated with red diamonds. Modes for which no identification could be obtained are indicated with black asterisks.

to understand the difference in $\Delta\Pi$[1] for RGB and CHeB stars is in the integral over the buoyancy frequency. As can be seen in **Figure 3**, the core convection zone in RC stars means that the integral is smaller, and hence $\Delta\Pi$ is larger. The utility of the period spacing has led to the development of automated methods of determining $\Delta\Pi$ values (e.g., Vrard et al., 2016) and from that the evolutionary phases of observed red-giant stars.

Deriving a reliable value of $\Delta\Pi$ requires a power spectrum that has a reasonably high signal-to-noise, which is not always the case. Kallinger et al. (2012) showed that the asteroseismic phase function ϵ can help. Asymptotically, frequencies follow the relation $\nu \simeq \Delta\nu(n + l/2 + \epsilon)$, where ϵ is the "phase function." The phase function can be a function of frequency (due to the curvature mentioned earlier), though the value of ϵ around ν_{max} can be defined in a straight forward manner. Kallinger et al. (2012) showed that in a plot of ϵ against $\Delta\nu$ or ν_{max}, red-clump stars stand out. There has been some attempts to explain why the phase function behaves different in red-clump stars. Christensen-Dalsgaard et al. (2014) showed that the differences between the phase functions of red-giant and red-clump stars arise from differences in the thermodynamic state of their convective envelopes. Ong and Basu (2019b) subsequently showed that this sensitivity to evolutionary stage arises from differences in the local frequency derivative of the underlying phase function which has a large contribution from the interior of the star too, and as a result this can be used to classify other types of stars as well; interestingly all the RGBs follow a much more well-defined sequence than stars in other states of evolution (**Figure 7**).

[1]We drop the degree identification here as we focus only on dipole mixed modes.

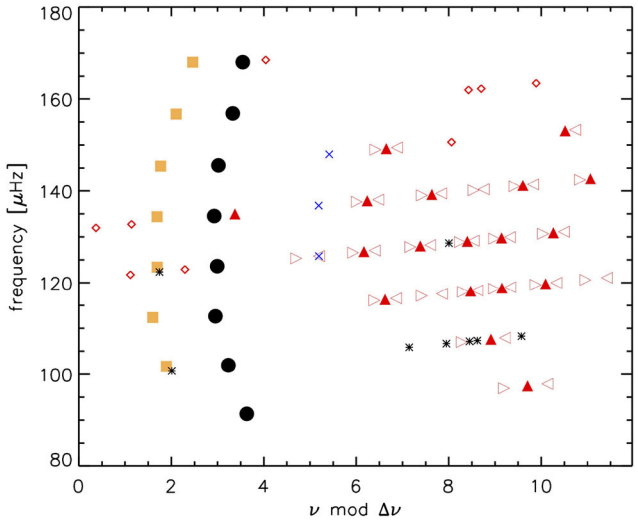

FIGURE 5 | The échelle diagram of the modes of KIC 6144777. As in **Figure 4**, the black dots are radial modes, the red symbols are dipole modes with the $m = 0$ indicated by filled triangles, while the $m = -1$ and $m = +1$ modes are indicated with right and left pointing open triangles, respectively, the dipole modes with unidentified azimuthal orders are indicated with red diamonds. The orange squares are quadrupole modes and the blue crosses the octupole ($l = 3$) modes. Modes that could not be identified are indicated by black asterisks. Note that the radial modes line up vertically, but not perfectly, and there is a curvature (see text for more details).

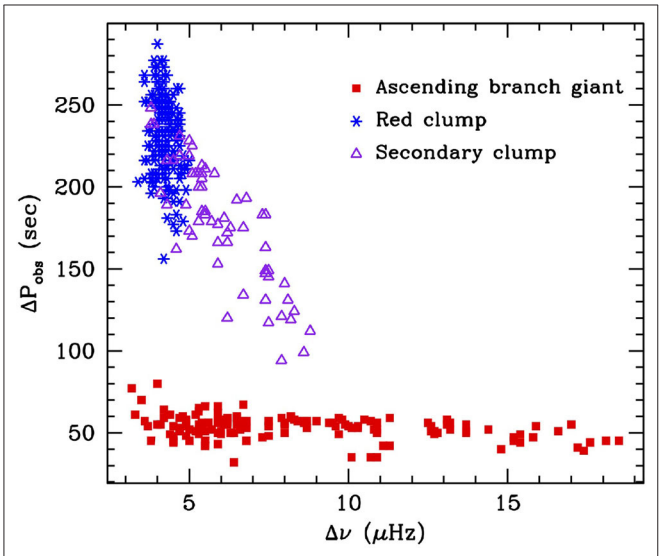

FIGURE 6 | Observed mixed-mode spacings for a sample of red giants observed by *Kepler*. Data are from Bedding et al. (2011).

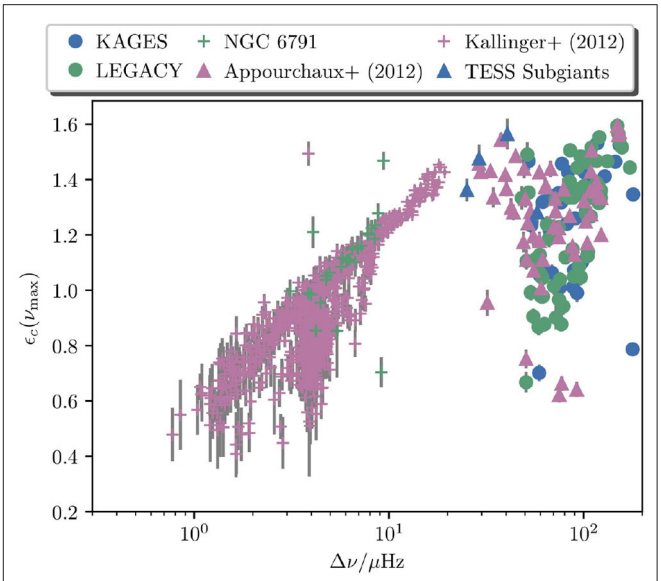

FIGURE 7 | The asteroseismic phase function ϵ at ν_{max} as a function of $\Delta\nu$ for stars observed with *Kepler*. The pink crosses are RGB and RC stars from Kallinger et al. (2012), with the red-clump stars forming a distinct group around a $\Delta\nu$ of 4 μHz. KAGES refers to the exoplanet-host sample of Davies et al. (2016) and Silva Aguirre et al. (2015), and LEGACY to the sample of main-sequence stars in Lund et al. (2017) and Silva Aguirre et al. (2017). Appourchaux et al. (2012) has a mix of main-sequence and subgiant stars. NGC 6791 refers to the sample analyzed by McKeever et al. (2019), and "TESS subgiants" are a set of sungiants in the TESS southern continuous viewing zone that show clear oscillations. Image courtesy of Joel Ong.

The importance of red-clump stars to Galactic archaeology has led to the development of a number of automated pipelines that look at different seismic properties in order to classify the stars. These include using a method that uses the measured period spacings (Mosser et al., 2014, 2015), the morphology of the power spectrum (Elsworth et al., 2017), a grid-based method using the ratio $\Delta\nu/\nu_{max}$ (Hekker et al., 2017), use of the phase factor ϵ (Kallinger et al., 2012), as well as some machine learning based methods based on the power spectrum (Hon et al., 2018), and based directly on the timeseries data (Kuszlewicz et al. in press). None of the techniques is perfect, and a comparison of some of the methods can be found in Elsworth et al. (2019), where the consensus evolutionary stage of the sample of red giants in Pinsonneault et al. (2018) has been presented.

4. STRUCTURE AND DYNAMICS

Most of the asteroseismic characterization of red giants that has been done thus far has involved determining the global properties of the stars—surface gravity, masses, radii, and ages—with the ultimate aim of using these to study the chemo-dynamical evolution of the Galaxy. Pinsonneault et al. (2014, 2018) released a catalog of red-giant properties based on asteroseismic data combined with spectroscopy. The uncertainties in the asteroseismic parameters were low enough that the red-clump stood out clearly in a Kiel diagram (see **Figure 8**). These have been used extensively in studying the evolution of the Galaxy (see, e,g, Nidever et al., 2014; Valentini et al., 2019; Lian et al., 2020; Spitoni et al., 2020, etc.), and have also been used as training sets to for machine-learning based methods of deriving red-giant properties from spectra alone (e.g., Martig et al., 2016). The stellar properties derived in Pinsonneault et al. (2014) were determined

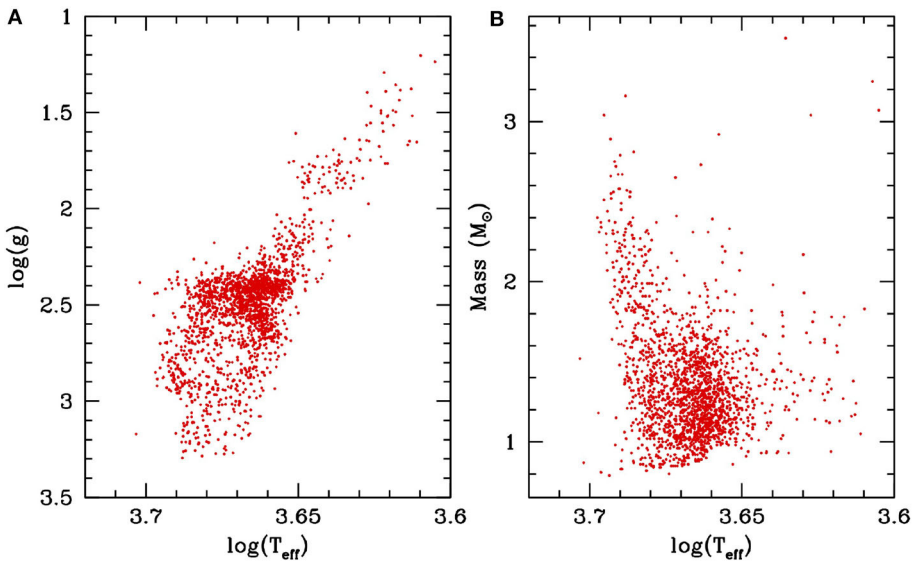

FIGURE 8 | Asteroseismically derived surface gravity **(A)** and mass **(B)** of the sample of red giants in Pinsonneault et al. (2014). The over-density of points in **(A)** around $\log g \sim 2.5$ is caused by the presence of red-clump stars. There is a corresponding over-density in masses, though here the overdensity is confined to low masses; higher-mass stars do not form red-clump stars.

from $\Delta\nu$, $\nu_{\rm max}$, $T_{\rm eff}$ and metallicity by searching among pre-computed grids of models. A different approach was taken by Pinsonneault et al. (2018); in this paper masses and radii were determined using the scaling relations for $\nu_{\rm max}$ and $\Delta\nu$, after correcting the $\Delta\nu$ scaling relation empirically using asteroseismic data of stars in clusters. This work was prompted in part by the result that the use of scaling relations yield masses for halo stars that are well above reasonable values for old stellar populations (Epstein et al., 2014). One of the interesting discoveries made with such analyses is that there are high-mass stars that have a high [α/Fe] ratio (Chiappini et al., 2015; Martig et al., 2015). This is interesting because a high [α/Fe] ratio has been believed to be a hallmark of old, and hence, low-mass stars. Hekker and Johnson (2019) and references therein proposed that the origin of these "α-rich young" stars are main sequence merger remnants.

4.1. Structure

Global asteroseismic parameters are not sufficient to determine the internal structure of red giants. Information about the structure is however, imprinted on the individual oscillations. While there have been concerted efforts in modeling the individual frequencies of main-sequence stars (e.g., Silva Aguirre et al., 2015, 2017), there have been few such efforts in the case of red giants (e.g., Li et al., 2018), even though there are thousands of red giants with high-signal-to-noise oscillation power spectra. One of the main reasons is that the extraction of this wealth of information present in the data has caused difficulties that have been slow to overcome. Some codes have now been developed to extract and identify these modes (e.g., Corsaro and De Ridder, 2014; García Saravia Ortiz de Montellano et al., 2018; Kallinger, 2019; Hekker et al., in prep.). Another main reason for the lack of results based on individual frequencies is the incredibly complicated frequency structure with all the mixed modes. The frequencies of mixed modes depend on details of the buoyancy-frequency profile, which in turn depends on uncertain internal processes such as convective overshoot and mixing; this is a challenge in modeling. Fortunately, the uncertainties of the modeling outcome will be reduced by accurate data on mixed modes.

A more practical challenge in modeling the frequencies of red giants is the issue of the so-called "surface term." The surface term is a frequency-dependent frequency offset between models and stars caused by our inability to model the near-surface layers of a star properly, the main culprit being the approximations used to model convection. The way this is taken care of in main-sequence stars is to subtract out a slowly varying function of frequency from the models. There are many ways of doing this (see e.g., Kjeldsen et al., 2008; Ball and Gizon, 2014; Sonoi et al., 2015, etc.), though currently the most popular model is that of Ball and Gizon (2014), who, based on work by Gough (1990) claimed that the surface term produces a frequency difference that can be expressed as

$$\delta\nu_{nl} = \nu_{nl}^{\rm obs} - \nu_{nl}^{\rm model} = \frac{1}{I_{nl}}\left[a\left(\frac{\nu_{nl}}{\nu_{\rm ac}}\right)^{-1} + b\left(\frac{\nu_{nl}}{\nu_{\rm ac}}\right)^{3}\right], \quad (1)$$

where $\delta\nu_{nl}$ is the difference in frequency ν_{nl} for a mode of degree l and order n between a star and its model, I_{nl} is the inertia of the mode, and $\nu_{\rm ac}$ is the acoustic cut-off frequency. The coefficients a and b can be determined through a generalized linear least-squares fit. This form appears to work quite well for main-sequence stars and subgiants, and even for radial modes of red giants (Schmitt and Basu, 2015; Ball et al., 2018). However, the $l = 1$ modes of red giants pose a challenge. Mixed modes, particularly the g-dominated ones, have large inertia and hence

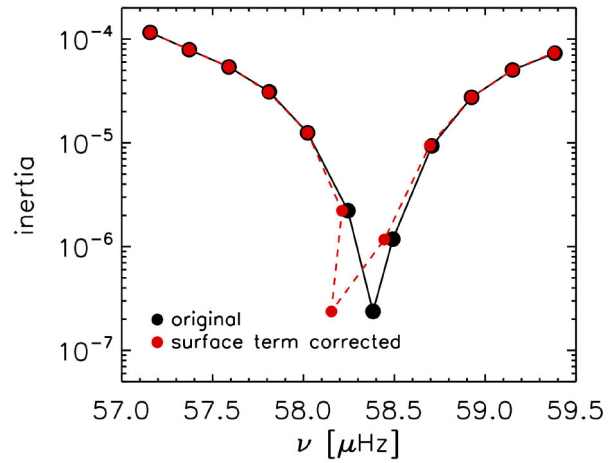

FIGURE 9 | The effects of the Ball and Gizon (2014) surface-term correction on $l = 1$ modes of red-giant models. Note that the most p-dominated mode shifts enough to confuse its frequency with the more g-dominated mode at lower frequency. Data are from Ball et al. (2018).

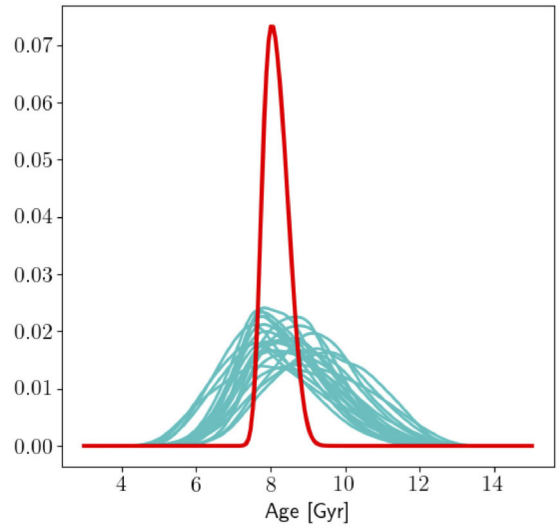

FIGURE 10 | The cyan curves mark the individual probability density functions for age for a sample of red giants in NGC 6791. The red curve is the joint probability assuming that all stars in a cluster have the same age. Note the precision to which the age of the cluster can be determined. Image courtesy of Jean McKeever.

the surface effect is small, as a result they do not change much when a surface-term correction is applied. Consequently the usual surface-effect corrections can be large enough to put the non-radial mixed modes in red giants out of order, which is unphysical (see Ball et al., 2018, and **Figure 9**). Ball et al. (2018) proposed a method to modify the structure of the models to suppress g modes in the cores of stellar models, so that they have only pure p modes on which to apply the surface-term correction. The authors showed that this did work for three double-lined eclipsing binaries, KIC 8410637, KIC 9540226, and KIC 5640750. Note that suppressing the g modes means that information from the core is neglected, but this provides a possible way to begin exploiting the data, and allows us to determine the mass and age of the star quite precisely. There are efforts under way (Ong and Basu, 2020) of calculating pure p- and g-mode frequencies of stars without resorting to modifying the structure of the models. There are also efforts underway to determine red-giant surface-term corrections from simulations of stellar convection (see e.g., Jørgensen et al., 2020).

Masses and ages of red giants can be determined quite precisely from their radial and quadrupole modes, where the surface term behaves well. This was exploited by McKeever et al. (2019) to determine the age and initial helium abundance of the cluster NGC 6791 using cluster red giants. NGC 6791 is a rather strange cluster—it is old, and yet very metal rich. Although the ages, or for that matter the helium abundance, of individual stars could not be determined to a high precision, using the fact that all cluster stars have the same age and initial metallicity allowed them to obtain a precise age of 8.2 ± 0.3 Gyr (see **Figure 10**) and an initial helium abundance of $Y_0 = 0.297 \pm 0.003$. This is to date, the most precise age and helium estimate for this cluster.

4.2. Dynamics

Unlike the case of red-giant structure, a lot more attention has been paid to the internal rotation of red giants. Beck et al. (2012b) showed unequivocally that rotational splittings of red-giant modes can be observed and measured. This opened up the possibility of determining the rotation of RGB cores since mixed modes are most sensitive to conditions in the core. Beck et al. (2012b) and Beck et al. (2012a) showed that the cores of red giants rotate ten times faster than the surface, as is expected from the principle of conservation of angular momentum—as stars evolve, the core contracts while the envelope expands, and the contracting core rotates faster to conserve angular momentum.

Clearly, interpreting the rotational splittings require the knowledge of how the splittings depend on internal rotation. Goupil et al. (2013) showed how the contrast between core and envelope rotation are encoded in the frequency splittings. They showed that the splittings have a linear dependence on the contribution of the core to the total mode inertia and that the slope of this linear relation is related to the ratio of the average envelope rotation to that of the core. The linear theory of rotational splittings predicts symmetric splittings around the $m = 0$ mode for rotation that does not depend on latitude. However, this is not the case for strongly couple mixed modes. Such asymmetries were first observed by Beck et al. (2014). Deheuvels et al. (2017) showed how the splittings might be calculated under conditions of strong coupling. Their work implied that it is important to obtain a good model of the star being studied in order to obtain the eigenfunctions needed to interpret the data.

Rotational splittings only indicate an average rotation rate, and one has to invert the rotational splittings to determine what the real rotation rate is. Deheuvels et al. (2012) inverted the splittings of KIC 7341231, a star very close to the base of the red-giant branch, and found that the core of the star is rotating at least five times faster than the envelope. This result is interesting

because while it shows that the core of stars spin up as they evolve, the spin up is not as fast as simple models of angular momentum transport in stars would suggest. Deheuvels et al. (2014) examined six more stars, all evolved subgiants and red-giants low on the red-giant branch. They obtained estimates of their core rotation rates and upper limits for the rotation in their convective envelopes. The results by Deheuvels et al. (2014) confirmed that the contrast between the rotation rates of the core and the envelope increases along the subgiant branch. They also find evidence of an abrupt change in the radial rotation profile in two of the stars, with the hydrogen-burning shell being the likely location of this change. The evidence for a an abrupt change in rotation rate causing a shear layer was also found by Di Mauro et al. (2016) and Di Mauro et al. (2018) in the star KIC 4448777. They inferred that the entire core rotates rigidly and provide evidence for an angular velocity gradient around the base of the hydrogen-burning shell. In particular their analysis revealed that the shear layer lies partially inside the hydrogen shell above $r \sim 0.05\ R_{star}$ and extends across the core-envelope boundary. KIC 4448777 is not the only giant with a measured gradient in the rotation rate. By comparing the rotation rate of the convective envelope with the measured surface rotation (Beck et al., 2018) showed that a radial gradient in rotation is also present in KIC 9163796.

While inversions have been very successful in determining the rotation rate of red-giant cores, there has been less success when it comes to inversion results of the envelope. Theoretical work in this regards (Ahlborn et al., 2020) shows how sensitive inversion results are to envelope rotation depends on where the star is on the red-giant branch (see **Figure 11**). This behavior is associated with a glitch in the buoyancy frequency which is caused by the composition discontinuity left behind by the convective envelope. The authors only looked at models below the luminosity bump as those are the stars for which mixed modes are observed and rotational splittings are resolved. This theoretical results shows that the sensitivity of the resolution kernels obtained from the inversions imply that we may have better success resolving the envelope of higher-luminosity red giants compared with the lower luminosity ones.

The most puzzling results about core-rotation have come from ensemble studies of red giants. Mosser et al. (2012b) claimed that the cores of red giants, contrary to all expectations, spin down instead of spinning up, as they ascend the red-giant branch. Gehan et al. (2018) confirmed this on examining a larger sample of stars, however, they found a smaller trend. Tayar et al. (2019) looked at core-helium burning stars rather than ascending branch stars, and they find that the core-rotation rates of these stars decrease strongly with decreasing surface gravity during the core He-burning phase.

The results above clearly indicate that our models of angular momentum transport within stars are deficient. It is clear that the different layers of a star are dynamically coupled and that angular momentum is transferred from the core to the outer layers. The results have spurred work on trying to understand how angular momentum is transferred between different layers (see e.g., Eggenberger et al., 2012, 2017; Ceillier et al., 2013; Cantiello et al., 2014; Belkacem et al., 2015a,b; Fuller et al., 2019, etc.). The processes being studied range from how models of rotation on shells (so-called "shellular rotation") can be modified to give the observed splittings, to meridional circulation, as well as internal gravity modes and magnetic instabilities. A comprehensive discussion of the investigations is beyond the scope of this article. Interested readers are directed to Aerts et al. (2019) for a review of angular momentum transport in stars.

5. UNSOLVED ISSUES AND NEGLECTED DATA

The seismic study of red giants is quite new, and their oscillation power spectra, and how best to extract information from them, still poses challenges.

It is known empirically that the power spectra of red-clump stars look noisier than those of inert-core red giants, and we can see this in **Figure 12**. Given that oscillations in these stars are excited by convection, it is to be expected that granulation would play a role in this. Indeed, Mathur et al. (2011) showed that the granulation power for red-clump stars can be higher than for a red-giant star of the same radius. However, as expected from theory of stellar convection which states that granulation depends only on $T_{\rm eff}$, $\log g$, and metallicity, there does not appear to be any difference between RGB and RC stars when granulation power is plotted against $\log g$ (see Figures 7,11 in Mathur et al., 2011).

The power spectra of some red giants show suppressed dipole modes (Mosser et al., 2012a; García et al., 2014). The suppression has been explained as being caused by remnant magnetic fields in red-giant cores (Fuller et al., 2015; Stello et al., 2016), but this interpretation has been challenged (Mosser et al., 2017), because the depressed dipole modes in these red giants are mixed modes and not the pure depressed acoustic modes that would be seen if the modes were suppressed by magnetic fields. The exact cause of the phenomenon is still under debate and remains a puzzle. See also Loi and Papaloizou (2017, 2018) for updated core magnetic field scenarios that could be consistent with the observational findings of suppressed mixed modes by Mosser et al. (2017).

As mentioned earlier, there have not been many attempts to determine the internal structure of many red giants by modeling their frequencies, partly because of issues with correcting for the surface term. However, without modeling the frequencies, a complete analysis of their rotation is not possible either. Thus clearly to understand red giants properly, the available data need to be exploited fully.

Another overlooked piece of information is the signature of glitches in the buoyancy frequency on period spacings. Cunha et al. (2015) presented a theoretical study of how the spacings will be affected. On the observational side, Mosser et al. (2015) showed how this signature may be extracted from the data. However, there has been little progress in terms of using the signature to determine the properties of red-giant cores. This is not completely surprising, since interpretation depends both on individual frequencies, which are not commonly extracted, and on models whose physics is uncertain. However, there is a wealth of data which should allow us to make progress despite the uncertainties.

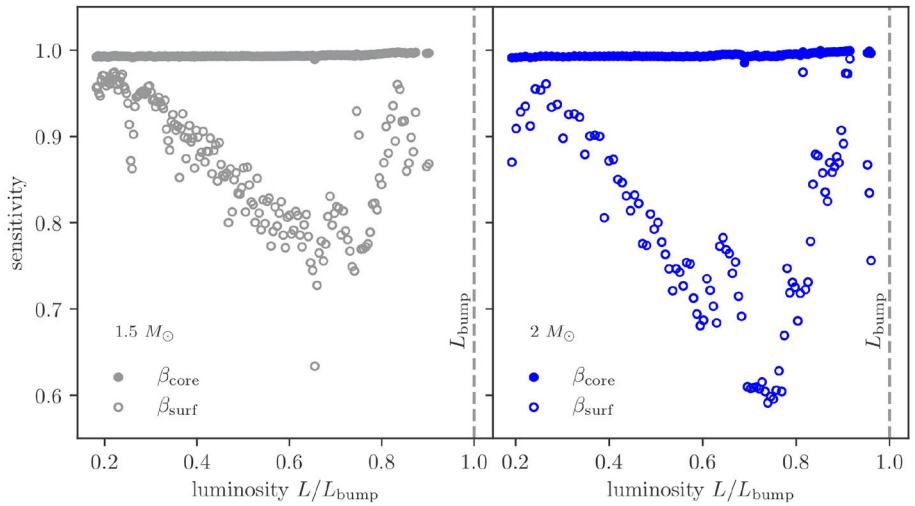

FIGURE 11 | The sensitivity of the resolution, i.e., averaging kernels for models with a mass of 1.5 $M_\odot$ **(Left)** and 2.0 $M_\odot$ **(Right)** obtained using dipole mode splittings plotted as a function of luminosity along the red-giant branch. The sensitivity for the core ($\beta_{\rm core} = \int_0^{r_{\rm core}} K(r_0, r)dr$, where $K(r_0, r)$ is the averaging kernel and $r_{\rm core} = 0.003$ $R_{\rm star}$) is shown as filled circles, and the surface sensitivity ($\beta_{\rm surf} = 1 - \int_0^{r_{\rm lim}} K(r_0, r)dr$, $r_{\rm lim} = 0.98$ $R_{\rm star}$) is shown as open circles. The vertical dashed lines mark the luminosity of the bump. Note that while there is almost complete sensitivity at the core, the sensitivity to near-surface rotation decreases and then increases again. Image with results from Ahlborn et al. (2020) is courtesy of Felix Ahlborn.

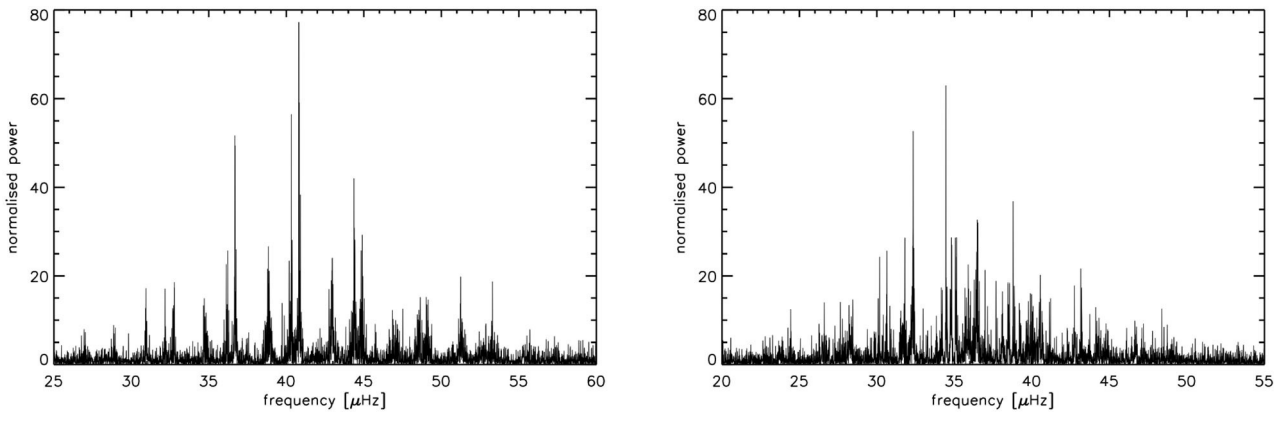

FIGURE 12 | Power spectra of an RGB star (**Left**, KIC 1433730) and an RC star (**Right**, KIC 1161618).

6. FINAL THOUGHTS

The oscillation spectra of red giants are fascinating and complicated. They reflect the large density contrast in the interior. The presence of mixed modes has allowed us to study core rotation of these stars, which in turn will allow us to study processes involved with angular-momentum transport inside stars. Methods to exploit mixed modes to study the interior structure of red giants are still under development. Although *Kepler* has ceased functioning, the red-giant data obtained by the observatory will be exploited for years to come.

AUTHOR CONTRIBUTIONS

SB planned the outline of the review. Both authors had equal share in the writing.

REFERENCES

Aerts, C., Christensen-Dalsgaard, J., and Kurtz, D. W. (2010). *Asteroseismology*. Springer Netherlands. doi: 10.1007/978-1-4020-5803-5

Aerts, C., Mathis, S., and Rogers, T. M. (2019). Angular momentum transport in stellar interiors. *Ann. Rev. Astron. Astrophys.* 57, 35–78. doi: 10.1146/annurev-astro-091918-104359

Ahlborn, F., Bellinger, E. P., Hekker, S., Basu, S., and Angelou, G. C. (2020). On the asteroseismic sensitivity to internal rotation along the red-giant branch. *arXiv preprints arXiv:2003.08905*. doi: 10.1051/0004-6361/201936947

Aizenman, M., Smeyers, P., and Weigert, A. (1977). Avoided crossing of modes of non-radial stellar oscillations. *Astron. Astrophys.* 58:41.

Appourchaux, T., Chaplin, W. J., García, R. A., Gruberbauer, M., Verner, G. A., Antia, H. M., et al. (2012). Oscillation mode

frequencies of 61 main-sequence and subgiant stars observed by Kepler. *Astron. Astrophys.*, 543:A54. doi: 10.1051/0004-6361/201218948

Baglin, A., Auvergne, M., Boisnard, L., Lam-Trong, T., Barge, P., Catala, C., et al. (2006). "CoRoT: a high precision photometer for stellar ecolution and exoplanet finding," in *36th COSPAR Scientific Assembly*, Vol. 36 (Beijing), 3749.

Ball, W. H., and Gizon, L. (2014). A new correction of stellar oscillation frequencies for near-surface effects. *Astron. Astrophys.* 568:A123. doi: 10.1051/0004-6361/201424325

Ball, W. H., Themeßl, N., and Hekker, S. (2018). Surface effects on the red giant branch. *Mon. Not. R. Astron. Soc.* 478, 4697–4709. doi: 10.1093/mnras/sty1141

Balmforth, N. J. (1992). Solar pulsational stability - III. Acoustical excitation by turbulent convection. *Mon. Not. R. Astron. Soc.* 255:639. doi: 10.1093/mnras/255.4.639

Basu, S., and Chaplin, W. J. (2017). *Asteroseismic Data Analysis: Foundations and Techniques*. Princeton, NJ: Princeton University Press. doi: 10.23943/princeton/9780691162928.001.0001

Beck, P. G., Bedding, T. R., Mosser, B., Stello, D., Garcia, R. A., Kallinger, T., et al. (2011). Kepler detected gravity-mode period spacings in a red giant star. *Science* 332:205. doi: 10.1126/science.1201939

Beck, P. G., De Ridder, J., Aerts, C., Kallinger, T., Hekker, S., García, R. A., et al. (2012a). Constraining the core-rotation rate in red-giant stars from Kepler space photometry. *Astronomische Nachrichten* 333:967. doi: 10.1002/asna.201211787

Beck, P. G., Hambleton, K., Vos, J., Kallinger, T., Bloemen, S., Tkachenko, A., et al. (2014). Pulsating red giant stars in eccentric binary systems discovered from Kepler space-based photometry. A sample study and the analysis of KIC 5006817. *Astron. Astrophys.* 564:A36. doi: 10.1051/0004-6361/201322477

Beck, P. G., Kallinger, T., Pavlovski, K., Palacios, A., Tkachenko, A., Mathis, S., et al. (2018). Seismic probing of the first dredge-up event through the eccentric red-giant and red-giant spectroscopic binary KIC 9163796. How different are red-giant stars with a mass ratio of 1.015? *Astron. Astrophys.* 612:A22. doi: 10.1051/0004-6361/201731269

Beck, P. G., Montalban, J., Kallinger, T., De Ridder, J., Aerts, C., García, R. A., et al. (2012b). Fast core rotation in red-giant stars as revealed by gravity-dominated mixed modes. *Nature* 481, 55–57. doi: 10.1038/nature10612

Bedding, T. R., Mosser, B., Huber, D., Montalbán, J., Beck, P., Christensen-Dalsgaard, J., et al. (2011). Gravity modes as a way to distinguish between hydrogen- and helium-burning red giant stars. *Nature* 471, 608–611. doi: 10.1038/nature09935

Belkacem, K., Marques, J. P., Goupil, M. J., Mosser, B., Sonoi, T., Ouazzani, R. M., et al. (2015a). Angular momentum redistribution by mixed modes in evolved low-mass stars. II. Spin-down of the core of red giants induced by mixed modes. *Astron. Astrophys.* 579:A31. doi: 10.1051/0004-6361/201526043

Belkacem, K., Marques, J. P., Goupil, M. J., Sonoi, T., Ouazzani, R. M., Dupret, M. A., et al. (2015b). Angular momentum redistribution by mixed modes in evolved low-mass stars. I. Theoretical formalism. *Astron. Astrophys.* 579:A30. doi: 10.1051/0004-6361/201526042

Borucki, W. J., Koch, D., Basri, G., Batalha, N., Brown, T., Caldwell, D., et al. (2010). Kepler planet-detection mission: introduction and first results. *Science* 327:977. doi: 10.1126/science.1185402

Bovy, J., Nidever, D. L., Rix, H.-W., Girardi, L., Zasowski, G., Chojnowski, S. D., et al. (2014). The APOGEE red-clump catalog: precise distances, velocities, and high-resolution elemental abundances over a large area of the milky way's disk. *Astrophys. J.* 790:127. doi: 10.1088/0004-637X/790/2/127

Brown, T. M., Gilliland, R. L., Noyes, R. W., and Ramsey, L. W. (1991). Detection of possible p-mode oscillations on procyon. *Astrophys. J.* 368:599. doi: 10.1086/169725

Cantiello, M., Mankovich, C., Bildsten, L., Christensen-Dalsgaard, J., and Paxton, B. (2014). Angular momentum transport within evolved low-mass stars. *Astrophys. J.* 788:93. doi: 10.1088/0004-637X/788/1/93

Ceillier, T., Eggenberger, P., García, R. A., and Mathis, S. (2013). Understanding angular momentum transport in red giants: the case of KIC 7341231. *Astron. Astrophys.* 555:A54. doi: 10.1051/0004-6361/201321473

Chaplin, W. J., Appourchaux, T., Elsworth, Y., García, R. A., Houdek, G., Karoff, C., et al. (2010). The asteroseismic potential of Kepler: first results for solar-type stars. *Astrophys. J. Letters* 713, L169–L175. doi: 10.1088/2041-8205/713/2/L169

Chiappini, C., Anders, F., Rodrigues, T. S., Miglio, A., Montalban, J., Mosser, B., et al. (2015). Young [α/Fe]-enhanced stars discovered by CoRoT and APOGEE: what is their origin? *Astron. Astrophys.* 576:L12. doi: 10.1051/0004-6361/201525865

Christensen-Dalsgaard, J. (1988). "A Hertzsprung-Russell diagram for stellar oscillations," in *Advances in Helio- and Asteroseismology, Volume 123 of IAU Symposium*, eds J. Christensen-Dalsgaard and S. Frandsen, 295 (Aarhus). doi: 10.1017/S0074180900158279

Christensen-Dalsgaard, J., Silva Aguirre, V., Elsworth, Y., and Hekker, S. (2014). On the asymptotic acoustic-mode phase in red giant stars and its dependence on evolutionary state. *Mon. Not. R. Astron. Soc.* 445, 3685–3693. doi: 10.1093/mnras/stu2007

Corsaro, E., and De Ridder, J. (2014). DIAMONDS: a new Bayesian nested sampling tool. Application to peak bagging of solar-like oscillations. *Astron. Astrophys.* 571:A71. doi: 10.1051/0004-6361/201424181

Cunha, M. S., Stello, D., Avelino, P. P., Christensen-Dalsgaard, J., and Townsend, R. H. D. (2015). Structural glitches near the cores of red giants revealed by oscillations in g-mode period spacings from stellar models. *Astrophys. J.* 805:127. doi: 10.1088/0004-637X/805/2/127

Davies, G. R., Lund, M. N., Miglio, A., Elsworth, Y., Kuszlewicz, J. S., North, T. S. H., et al. (2017). Using red clump stars to correct the Gaia DR1 parallaxes. *Astron. Astrophys.* 598:L4. doi: 10.1051/0004-6361/201630066

Davies, G. R., Silva Aguirre, V., Bedding, T. R., Hand berg, R., Lund, M. N., Chaplin, W. J., et al. (2016). Oscillation frequencies for 35 Kepler solar-type planet-hosting stars using Bayesian techniques and machine learning. *Mon. Not. R. Astron. Soc.* 456, 2183–2195. doi: 10.1093/mnras/stv2593

Deheuvels, S., Doğan, G., Goupil, M. J., Appourchaux, T., Benomar, O., Bruntt, H., et al. (2014). Seismic constraints on the radial dependence of the internal rotation profiles of six Kepler subgiants and young red giants. *Astron. Astrophys.* 564:A27. doi: 10.1051/0004-6361/201322779

Deheuvels, S., García, R. A., Chaplin, W. J., Basu, S., Antia, H. M., Appourchaux, T., et al. (2012). Seismic evidence for a rapidly rotating core in a lower-giant-branch star observed with Kepler. *Astrophys. J.* 756:19. doi: 10.1088/0004-637X/756/1/19

Deheuvels, S., Ouazzani, R. M., and Basu, S. (2017). Near-degeneracy effects on the frequencies of rotationally-split mixed modes in red giants. *Astron. Astrophys.* 605:A75. doi: 10.1051/0004-6361/201730786

Di Mauro, M. P., Ventura, R., Cardini, D., Stello, D., Christensen-Dalsgaard, J., Dziembowski, W. A., et al. (2016). Internal rotation of the red-giant star KIC 4448777 by means of asteroseismic inversion. *Astrophys. J.* 817:65. doi: 10.3847/0004-637X/817/1/65

Di Mauro, M. P., Ventura, R., Corsaro, E., and Lustosa De Moura, B. (2018). The rotational shear layer inside the early red-giant star KIC 4448777. *Astrophys. J.* 862:9. doi: 10.3847/1538-4357/aac7c4

Eggenberger, P., Lagarde, N., Miglio, A., Montalban, J., Ekström, S., Georgy, C., et al. (2017). Constraining the efficiency of angular momentum transport with asteroseismology of red giants: the effect of stellar mass. *Astron. Astrophys.*, 599:A18. doi: 10.1051/0004-6361/201629459

Eggenberger, P., Montalban, J., and Miglio, A. (2012). Angular momentum transport in stellar interiors constrained by rotational splittings of mixed modes in red giants. *Astron. Astrophys.* 544:L4. doi: 10.1051/0004-6361/201219729

Elsworth, Y., Hekker, S., Basu, S., and Davies, G. R. (2017). A new method for the asteroseismic determination of the evolutionary state of red-giant stars. *Mon. Not. R. Astron. Soc.* 466, 3344–3352. doi: 10.1093/mnras/stw3288

Elsworth, Y., Hekker, S., Johnson, J. A., Kallinger, T., Mosser, B., Pinsonneault, M., et al. (2019). Insights from the APOKASC determination of the evolutionary state of red-giant stars by consolidation of different methods. *Mon. Not. R. Astron. Soc.* 489, 4641–4657. doi: 10.1093/mnras/stz2356

Epstein, C. R., Elsworth, Y. P., Johnson, J. A., Shetrone, M., Mosser, B., Hekker, S., et al. (2014). Testing the asteroseismic mass scale using metal-poor stars characterized with APOGEE and Kepler. *Astrophys. J. Letters* 785:L28. doi: 10.1088/2041-8205/785/2/L28

Fuller, J., Cantiello, M., Stello, D., Garcia, R. A., and Bildsten, L. (2015). Asteroseismology can reveal strong internal magnetic fields in red giant stars. *Science* 350, 423–426. doi: 10.1126/science.aac6933

Fuller, J., Piro, A. L., and Jermyn, A. S. (2019). Slowing the spins of stellar cores. *Mon. Not. R. Astron. Soc.* 485, 3661–3680. doi: 10.1093/mnras/stz514

García Saravia Ortiz de Montellano, A., Hekker, S., and Themeßl, N. (2018). Automated asteroseismic peak detections. *Mon. Not. R. Astron. Soc.* 476, 1470–1496. doi: 10.1093/mnras/sty253

García, R. A., Pérez Hernández, F., Benomar, O., Silva Aguirre, V., Ballot, J., Davies, G. R., et al. (2014). Study of KIC 8561221 observed by Kepler: an early red giant showing depressed dipolar modes. *Astron. Astrophys.* 563:A84. doi: 10.1051/0004-6361/201322823

Gehan, C., Mosser, B., Michel, E., Samadi, R., and Kallinger, T. (2018). Core rotation braking on the red giant branch for various mass ranges. *Astron. Astrophys.* 616:A24. doi: 10.1051/0004-6361/201832822

Girardi, L. (2016). Red Clump Stars. *Ann. Rev. Astron. Astrophys.* 54, 95–133. doi: 10.1146/annurev-astro-081915-023354

Gizon, L., and Solanki, S. K. (2003). Determining the inclination of the rotation axis of a sun-like star. *Astrophys. J.* 589, 1009–1019. doi: 10.1086/374715

Goldreich, P., and Keeley, D. A. (1977a). Solar seismology. I. The stability of the solar p-modes. *Astrophys. J.* 211, 934–942. doi: 10.1086/155005

Goldreich, P., and Keeley, D. A. (1977b). Solar seismology. II. The stochastic excitation of the solar p-modes by turbulent convection. *Astrophys. J.* 212, 243–251. doi: 10.1086/155043

Gough, D. O. (1990). "Comments on helioseismic inference," in *Progress of Seismology of the Sun and Stars*, eds Y. Osaki and H. Shibahashi (Berlin, Heidelberg: Springer), 281–318.

Goupil, M. J., Mosser, B., Marques, J. P., Ouazzani, R. M., Belkacem, K., Lebreton, Y., et al. (2013). Seismic diagnostics for transport of angular momentum in stars. II. Interpreting observed rotational splittings of slowly rotating red giant stars. *Astron. Astrophys.* 549:A75. doi: 10.1051/0004-6361/201220266

Grundahl, F., Kjeldsen, H., Christensen-Dalsgaard, J., Arentoft, T., and Frandsen, S. (2007). Stellar oscillations network group. *Commun. Asteroseismol.* 150:300. doi: 10.1553/cia150s300

Guggenberger, E., Hekker, S., Angelou, G. C., Basu, S., and Bellinger, E. P. (2017). Mitigating the mass dependence in the $\Delta\nu$ scaling relation of red giant stars. *Mon. Not. R. Astron. Soc.* 470, 2069–2078. doi: 10.1093/mnras/stx1253

Guggenberger, E., Hekker, S., Basu, S., and Bellinger, E. (2016). Significantly improving stellar mass and radius estimates: a new reference function for the $\Delta\nu$ scaling relation. *Mon. Not. R. Astron. Soc.* 460, 4277–4281. doi: 10.1093/mnras/stw1326

Hekker, S. (2013). CoRoT and Kepler results: solar-like oscillators. *Adv. Space Res.* 52, 1581–1592. doi: 10.1016/j.asr.2013.08.005

Hekker, S. (2020). Scaling relations for solar-like oscillations: a review. *Front. Astron. Space Sci.* 7:3. doi: 10.3389/fspas.2020.00003

Hekker, S., and Christensen-Dalsgaard, J. (2017). Giant star seismology. *Astron. Astrophys. Rev.* 25:1. doi: 10.1007/s00159-017-0101-x

Hekker, S., Elsworth, Y., Basu, S., and Bellinger, E. (2017). "Evolutionary states of red-giant stars from grid-based modelling," in *European Physical Journal Web of Conferences, Volume 160 of European Physical Journal Web of Conferences* (Azores Islands), 04006. doi: 10.1051/epjconf/201716004006

Hekker, S., and Johnson, J. A. (2019). Origin of α-rich young stars: clues from C, N, and O. *Mon. Not. R. Astron. Soc.* 487, 4343–4354. doi: 10.1093/mnras/stz1554

Hon, M., Stello, D., and Yu, J. (2018). Deep learning classification in asteroseismology using an improved neural network: results on 15 000 Kepler red giants and applications to K2 and TESS data. *Mon. Not. R. Astron. Soc.* 476, 3233–3244. doi: 10.1093/mnras/sty483

Jørgensen, A. S., Montalban, J., Miglio, A., Rendle, B. M., Davies, G. R., Buldgen, G., et al. (2020). Investigating surface correction relations for RGB stars. *arXiv preprint arXiv:2004.13666*. doi: 10.1093/mnras/staa1480

Kallinger, T. (2019). Release note: massive peak bagging of red giants in the Kepler field. *arXiv preprint arXiv:1906.09428*.

Kallinger, T., Hekker, S., Garcia, R. A., Huber, D., and Matthews, J. M. (2016). Precise stellar surface gravities from the time scales of convectively driven brightness variations. *Sci. Adv.* 2:1500654. doi: 10.1126/sciadv.1500654

Kallinger, T., Hekker, S., Mosser, B., De Ridder, J., Bedding, T. R., Elsworth, Y. P., et al. (2012). Evolutionary influences on the structure of red-giant acoustic oscillation spectra from 600d of Kepler observations. *Astron. Astrophys.* 541:A51. doi: 10.1051/0004-6361/201218854

Khan, S., Miglio, A., Mosser, B., Arenou, F., Belkacem, K., Brown, A. G. A., et al. (2019). New light on the Gaia DR2 parallax zero-point: influence of the asteroseismic approach, in and beyond the Kepler field. *Astron. Astrophys.* 628:A35. doi: 10.1051/0004-6361/201935304

Kippenhahn, R., Weigert, A., and Weiss, A. (2012). *Stellar Structure and Evolution*. Berlin; Heidelberg: Springer-Verlag. doi: 10.1007/978-3-642-30304-3

Kjeldsen, H., and Bedding, T. R. (1995). Amplitudes of stellar oscillations: the implications for asteroseismology. *Astron. Astrophys.* 293, 87–106.

Kjeldsen, H., Bedding, T. R., and Christensen-Dalsgaard, J. (2008). Correcting stellar oscillation frequencies for near-surface effects. *Astrophys. J. Letters* 683:L175. doi: 10.1086/591667

Li, T., Bedding, T. R., Huber, D., Ball, W. H., Stello, D., Murphy, S. J., et al. (2018). Modelling Kepler red giants in eclipsing binaries: calibrating the mixing-length parameter with asteroseismology. *MNRAS* 475, 981–998. doi: 10.1093/mnras/stx3079

Lian, J., Thomas, D., Maraston, C., Zamora, O., Tayar, J., Pan, K., et al. (2020). The age-chemical abundance structure of the Galaxy I: evidence for a late-accretion event in the outer disc at z $\sim$ 0.6. *Mon. Not. R. Astron. Soc.* 494, 2561–2575. doi: 10.1093/mnras/staa867

Loi, S. T., and Papaloizou, J. C. B. (2017). Torsional Alfvén resonances as an efficient damping mechanism for non-radial oscillations in red giant stars. *Mon. Not. R. Astron. Soc.* 467, 3212–3225. doi: 10.1093/mnras/stx281

Loi, S. T., and Papaloizou, J. C. B. (2018). Effects of a strong magnetic field on internal gravity waves: trapping, phase mixing, reflection, and dynamical chaos. *Mon. Not. R. Astron. Soc.* 477, 5338–5357. doi: 10.1093/mnras/sty917

Lund, M. N., Silva Aguirre, V., Davies, G. R., Chaplin, W. J., Christensen-Dalsgaard, J., Houdek, G., et al. (2017). Standing on the shoulders of dwarfs: the Kepler Asteroseismic LEGACY sample. I. Oscillation mode parameters. *Astrophys. J.* 835:172. doi: 10.3847/1538-4357/aa9658

Martig, M., Fouesneau, M., Rix, H.-W., Ness, M., Mészáros, S., García-Hernández, D. A., et al. (2016). Red giant masses and ages derived from carbon and nitrogen abundances. *Mon. Not. R. Astron. Soc.* 456, 3655–3670. doi: 10.1093/mnras/stv2830

Martig, M., Rix, H.-W., Silva Aguirre, V., Hekker, S., Mosser, B., Elsworth, Y., et al. (2015). Young α-enriched giant stars in the solar neighbourhood. *Mon. Not. R. Astron. Soc.* 451, 2230–2243. doi: 10.1093/mnras/stv1071

Mathur, S., García, R. A., Huber, D., Regulo, C., Stello, D., Beck, P. G., et al. (2016). Probing the deep end of the milky way with Kepler: asteroseismic analysis of 854 faint red giants misclassified as cool dwarfs. *Astrophys. J.* 827:50. doi: 10.3847/0004-637X/827/1/50

Mathur, S., Hekker, S., Trampedach, R., Ballot, J., Kallinger, T., Buzasi, D., et al. (2011). Granulation in red giants: observations by the Kepler mission and three-dimensional convection simulations. *Astrophys. J.* 741:119. doi: 10.1088/0004-637X/741/2/119

McKeever, J. M., Basu, S., and Corsaro, E. (2019). The helium abundance of NGC 6791 from modeling of stellar oscillations. *Astrophys. J.* 874:180. doi: 10.3847/1538-4357/ab0c04

Mints, A., and Hekker, S. (2018). Isochrone fitting in the Gaia era. *Astron. Astrophys.* 618:A54. doi: 10.1051/0004-6361/201832739

Mosser, B., Barban, C., Montalban, J., Beck, P. G., Miglio, A., Belkacem, K., et al. (2011). Mixed modes in red-giant stars observed with CoRoT. *Astron. Astrophys.* 532:A86. doi: 10.1051/0004-6361/201116825

Mosser, B., Belkacem, K., Pinçon, C., Takata, M., Vrard, M., Barban, C., et al. (2017). Dipole modes with depressed amplitudes in red giants are mixed modes. *Astron. Astrophys.* 598:A62. doi: 10.1051/0004-6361/201629494

Mosser, B., Benomar, O., Belkacem, K., Goupil, M. J., Lagarde, N., Michel, E., et al. (2014). Mixed modes in red giants: a window on stellar evolution. *Astron. Astrophys.* 572:L5. doi: 10.1051/0004-6361/201425039

Mosser, B., Elsworth, Y., Hekker, S., Huber, D., Kallinger, T., Mathur, S., et al. (2012a). Characterization of the power excess of solar-like oscillations in red giants with Kepler. *Astron. Astrophys.* 537:A30. doi: 10.1051/0004-6361/201117352

Mosser, B., Goupil, M. J., Belkacem, K., Marques, J. P., Beck, P. G., Bloemen, S., et al. (2012b). Spin down of the core rotation in red giants. *Astron. Astrophys.* 548:A10. doi: 10.1051/0004-6361/201220106

Mosser, B., Goupil, M. J., Belkacem, K., Michel, E., Stello, D., Marques, J. P., et al. (2012c). Probing the core structure and evolution of red giants using gravity-dominated mixed modes observed with Kepler. *Astron. Astrophys.* 540:A143. doi: 10.1051/0004-6361/201118519

Mosser, B., Miglio, A., and CoRot Team (2016). *The CoRoT Legacy Book: The Adventure of the Ultra High Precision Photometry From Space.* EDP Sciences. doi: 10.1051/978-2-7598-1876-1.c042

Mosser, B., Vrard, M., Belkacem, K., Deheuvels, S., and Goupil, M. J. (2015). Period spacings in red giants. I. Disentangling rotation and revealing core structure discontinuities. *Astron. Astrophys.* 584:A50. doi: 10.1051/0004-6361/201527075

Nidever, D. L., Bovy, J., Bird, J. C., Andrews, B. H., Hayden, M., Holtzman, J., et al. (2014). Tracing chemical evolution over the extent of the milky way's disk with APOGEE red clump stars. *Astrophys. J.* 796:38. doi: 10.1088/0004-637X/796/1/38

Ong, J. M. J., and Basu, S. (2019a). Explaining deviations from the scaling relationship of the large frequency separation. *Astrophys. J.* 870:41. doi: 10.3847/1538-4357/aaf1b5

Ong, J. M. J., and Basu, S. (2019b). Structural and evolutionary diagnostics from asteroseismic phase functions. *Astrophys. J.* 885:26. doi: 10.3847/1538-4357/ab425f

Ong, J. M. J., and Basu, S. (2020). Semi-analytic expressions for the isolation and coupling of mixed modes. *arXiv [Preprint]. arXiv:2006.13313*. Available online at: https://ui.adsabs.harvard.edu/abs/2020arXiv200613313O.

Paxton, B., Smolec, R., Schwab, J., Gautschy, A., Bildsten, L., Cantiello, M., et al. (2019). Modules for experiments in stellar astrophysics (MESA): pulsating variable stars, rotation, convective boundaries, and energy conservation. *Astrophys. J. Suppl. Ser.* 243:10. doi: 10.3847/1538-4365/ab2241

Pinsonneault, M. H., Elsworth, Y., Epstein, C., Hekker, S., Mészáros, S., Chaplin, W. J., et al. (2014). The APOKASC catalog: an asteroseismic and spectroscopic joint survey of targets in the Kepler fields. *Astrophys. J. Suppl. Ser.* 215:19. doi: 10.1088/0067-0049/215/2/19

Pinsonneault, M. H., Elsworth, Y. P., Tayar, J., Serenelli, A., Stello, D., Zinn, J., et al. (2018). The second APOKASC catalog: the empirical approach. Astrophys. J. Suppl. Ser.239:32. doi: 10.3847/1538-4365/aaebfd

Salaris, M., and Cassisi, S. (2005). *Evolution of Stars and Stellar Populations*. Chichestor: John Wiley and Sons. doi: 10.1002/0470033452

Schmitt, J. R., and Basu, S. (2015). Modeling the asteroseismic surface term across the HR diagram. *Astrophys. J.* 808:123. doi: 10.1088/0004-637X/808/2/123

Silva Aguirre, V., Davies, G. R., Basu, S., Christensen-Dalsgaard, J., Creevey, O., Metcalfe, T. S., et al. (2015). Ages and fundamental properties of Kepler exoplanet host stars from asteroseismology. *Mon. Not. R. Astron. Soc.* 452, 2127–2148. doi: 10.1093/mnras/stv1388

Silva Aguirre, V., Lund, M. N., Antia, H. M., Ball, W. H., Basu, S., Christensen-Dalsgaard, J., et al. (2017). Standing on the shoulders of dwarfs: the kepler asteroseismic LEGACY sample. II. Radii, masses, and ages. *Astrophys. J.* 835:173. doi: 10.3847/1538-4357/835/2/173

Sonoi, T., Samadi, R., Belkacem, K., Ludwig, H. G., Caffau, E., and Mosser, B. (2015). Surface-effect corrections for solar-like oscillations using 3D hydrodynamical simulations. I. Adiabatic oscillations. *Astron. Astrophys.* 583:A112. doi: 10.1051/0004-6361/201526838

Spitoni, E., Verma, K., Silva Aguirre, V., and Calura, F. (2020). Galactic archaeology with asteroseismic ages. II. Confirmation of a delayed gas infall using Bayesian analysis based on MCMC methods. *Astron. Astrophys.*, 635:A58. doi: 10.1051/0004-6361/201937275

Stello, D., Cantiello, M., Fuller, J., Huber, D., García, R. A., Bedding, T. R., et al. (2016). A prevalence of dynamo-generated magnetic fields in the cores of intermediate-mass stars. *Nature* 529, 364–367. doi: 10.1038/nature16171

Tassoul, M. (1980). Asymptotic approximations for stellar nonradial pulsations. *Astrophys. J. Suppl. Ser.* 43, 469–490. doi: 10.1086/190678

Tayar, J., Beck, P. G., Pinsonneault, M. H., García, R. A., and Mathur, S. (2019). Core-envelope coupling in intermediate-mass core-helium burning stars. *Astrophys. J.* 887:203. doi: 10.3847/1538-4357/ab558a

Ting, Y.-S., Hawkins, K., and Rix, H.-W. (2018). A large and pristine sample of standard candles across the milky way: 100,000 red clump stars with 3% contamination. *Astrophys. J. Letters* 858:L7. doi: 10.3847/2041-8213/aabf8e

Ulrich, R. K. (1986). Determination of Stellar Ages from Asteroseismology. *Astrophys. J. Letters* 306:L37. doi: 10.1086/184700

Unno, W., Osaki, Y., Ando, H., Saio, H., and Shibahashi, H. (1989). *Nonradial Oscillation of Stars*. Tokyo: University of Tokyo Press.

Valentini, M., Chiappini, C., Bossini, D., Miglio, A., Davies, G. R., Mosser, B., et al. (2019). Masses and ages for metal-poor stars. A pilot programme combining asteroseismology and high-resolution spectroscopic follow-up of RAVE halo stars. *Astron. Astrophys.* 627:A173. doi: 10.1051/0004-6361/201834081

Vrard, M., Mosser, B., and Samadi, R. (2016). Period spacings in red giants. II. Automated measurement. *Astron. Astrophys.* 588:A87. doi: 10.1051/0004-6361/201527259

White, T. R., Bedding, T. R., Stello, D., Christensen-Dalsgaard, J., Huber, D., and Kjeldsen, H. (2011). Calculating asteroseismic diagrams for solar-like oscillations. *Astrophys. J.* 743:161. doi: 10.1088/0004-637X/743/2/161

Yu, J., Huber, D., Bedding, T. R., Stello, D., Hon, M., Murphy, S. J., et al. (2018). Asteroseismology of 16,000 Kepler red giants: global oscillation parameters, masses, and radii. *APJS* 236:42. doi: 10.3847/1538-4365/aaaf74

Conflict of Interest: The authors declare that the research was conducted in the absence of any commercial or financial relationships that could be construed as a potential conflict of interest.

APPENDIX A

Here we present the inlist of the MESA computations used to compute the tracks shown in **Figure 1**. We show here the inlist of the 1 $M_{\odot}$ track and computed the other tracks with exactly the same physics and only changed the mass.

```
 ! inlist to evolve a 1 solar mass star

! For the sake of future readers of this file (yourself included),
! ONLY include the controls you are actually using.  DO NOT include
! all of the other controls that simply have their default values.

&star_job

  ! begin with a pre-main sequence model
    create_pre_main_sequence_model = .true.


  ! begin with saved model
    load_saved_model = .false.

  ! save a model at the end of the run
    save_model_when_terminate = .true.
    save_model_filename = 'bottomAGB10.mod'

  ! display on-screen plots
    pgstar_flag = .true.

  pause_before_terminate=.true.

/ !end of star_job namelist


&controls

  ! starting specifications
    initial_mass = 1.0 ! in Msun units

  ! stop when the star nears ZAMS (Lnuc/L > 0.99)
    stop_near_zams = .false.

  ! stop when the center mass fraction of h1 drops below this limit
    xa_central_lower_limit_species(1) = 'he4'
    xa_central_lower_limit(1) = 1d-3


   !control output
   history_interval = 1
   write_profiles_flag = .true.
   profile_interval = 20
   profiles_index_name='profile1.0.index'
   profile_data_prefix = 'profile'
   max_num_profile_models = 1000
   star_history_name = 'historym1.0zsun.data'

/ ! end of controls namelist
```

frontiers in Astronomy and Space Sciences

REVIEW
published: 28 August 2020
doi: 10.3389/fspas.2020.00047

White-Dwarf Asteroseismology With the *Kepler* Space Telescope

Alejandro H. Córsico [1,2]*

[1] Facultad de Ciencias Astronómicas y Geofísicas, Universidad Nacional de La Plata, La Plata, Argentina, [2] Instituto de Astrofísica La Plata, CONICET-UNLP, La Plata, Argentina

In the course of their evolution, white-dwarf stars go through at least one phase of variability in which the global pulsations they undergo allow astronomers to peer into their interiors, making it possible to shed light on their deep inner structure and evolutionary stage by means of asteroseismology. The study of pulsating white dwarfs has undergone substantial progress in the last decade, and this is largely thanks to the arrival of continuous observations of unprecedented quality from space, like those of the CoRoT, *Kepler*, and *TESS* missions. This, along with the advent of new detailed theoretical models and the development of improved asteroseismological techniques, has helped to unravel the internal chemical structure of many pulsating white dwarfs, and, at the same time, has posed new questions that challenge theoreticians. In particular, uninterrupted monitoring of white-dwarf stars for months has allowed discovering phenomena impossible to detect with ground-based observations, despite previous admirable efforts like the Whole Earth Telescope (WET). Here, we start by reviewing the essential properties of white-dwarf and pre-white dwarf stars and their pulsations, and then, we go through the different families of pulsating objects known to date. Finally, we review the most outstanding findings about pulsating white dwarfs and pre-white dwarfs made possible with the unprecedented-quality observations of the *Kepler* space telescope, although we envisage that future analyses of space data from this mission that still await examination, may reveal new secrets of these extremely interesting variable stars.

Keywords: stellar evolution, white dwarf stars, stellar interiors, stellar oscillations, asteroseismology

OPEN ACCESS

Edited by:
Anthony Eugene Lynas-Gray, University College London, United Kingdom

Reviewed by:
J. J. Hermes, Boston University, United States
Vasili Kukhianidze, Ilia State University, Georgia

***Correspondence:**
Alejandro H. Córsico
acorsico@fcaglp.unlp.edu.ar

Specialty section:
This article was submitted to Stellar and Solar Physics, a section of the journal Frontiers in Astronomy and Space Sciences

Received: *13 April 2020*
Accepted: *18 June 2020*
Published: *28 August 2020*

Citation:
Córsico AH (2020) White-Dwarf Asteroseismology With the Kepler Space Telescope. Front. Astron. Space Sci. 7:47. doi: 10.3389/fspas.2020.00047

1. BASIC PROPERTIES OF WHITE-DWARF AND PRE-WHITE DWARF STARS

White-dwarf stars constitute the most common compact remnants of the evolution of stars with initial masses below $\sim 10-11 M_{\odot}$ (Woosley and Heger, 2015), including our Sun. Comprehensive accounts referring to the origin and evolution of white dwarfs can be found in the review articles of Fontaine et al. (2001) and Althaus et al. (2010). White dwarfs are extremely old objects, with typical ages in the range $1-10$ Gyr (1 Gyr $\equiv 10^9$ yr). These stellar fossils are found in a range of masses of $0.15 \lesssim M_{\star}/M_{\odot} \lesssim 1.25$, with an average value of $M_{\star}/M_{\odot} \sim 0.60$ (Tremblay et al., 2016), although for the majority of white dwarfs the mass lies between $M_{\star}/M_{\odot} \sim 0.50$ and $M_{\star}/M_{\odot} \sim 0.70$. Since they are characterized by planetary dimensions ($R_{\star} \sim 0.01 R_{\odot}$), the matter inside is highly concentrated, with average densities of white dwarfs being in the order of $\overline{\rho} \sim 10^6$ g/cm^3. Consequently, the prevailing equation of the state inside white dwarfs is that of a

highly-degenerate Fermi gas (Chandrasekhar, 1939). Indeed, the hydrostatic equilibrium in the interior of a white dwarf is provided by the pressure of degenerate electrons counteracting the gravity force, thus avoiding the collapse of the star. In particular, electron degeneracy is responsible for a curious relationship between the stellar mass and radius: the more massive the white dwarf, the smaller its radius. The process of discovery of white dwarfs, starting from the observation of variations of the proper motion of Procyon and Sirius by Friedrich Wilhelm Bessel in 1844 (Bessel, 1844), was fascinating. The emergence of the quantum-mechanics theory toward the first quarter of the 20th century paved the way in explaining the existence of white dwarfs. An excellent historical account of the discovery of white dwarfs and the theoretical arguments that led to explaining the existence of these compact objects in nature is provided by Van Horn (2015).

Apart from the degenerate electrons, the interior of white dwarfs is composed by non-degenerate ions that store the thermal energy generated by previous nuclear burning—generally extinct in the white-dwarf stage. White dwarfs are found at a huge interval of effective temperatures ($4,000 \lesssim T_{\rm eff} \lesssim 200,000$ K) thus spanning seven orders of magnitude in luminosity, $10^{-4} \lesssim \log(L_\star/L_\odot) \lesssim 10^3$. Regarding their inner chemical composition, average-mass white dwarfs are characterized by cores likely made of ^{12}C and ^{16}O—the products of He burning—although ultra-massive white dwarfs ($M_\star/M_\odot \gtrsim 1.0$) could contain cores composed of ^{16}O, ^{20}Ne, and ^{24}Mg as well, and the lowest-mass white dwarfs (low-mass and extremely low-mass white dwarfs, abbreviated as LM and ELM white dwarfs, respectively) could harbor cores made of ^{4}He. In particular, ELM white dwarfs ($M_\star/M_\odot \lesssim 0.2$) must be formed in interacting binary systems, otherwise they would be much older than the Universe. A description of the different formation channels of white dwarfs, either single- or binary-star evolution, can be found in the review articles of Althaus et al. (2010) and Córsico et al. (2019). Unlike other stages of stellar evolution, the white-dwarf phase is characterized by a relatively simple process of gradual cooling of the star, shining at the expense of the heat stored in its core during the prior evolutionary history. This process was first described in a simplified way by Mestel (1952). The cooling rate of white dwarfs depends on many factors: surface temperature, stellar mass, core chemical composition, surface chemical composition, etc. The surface chemical composition of white dwarfs defines the spectral type. Most white dwarfs ($\sim$ 80%) have atmospheres rich in ^{1}H, and are called DA white dwarfs. About a $\sim$ 15% of white dwarfs have atmospheres rich in ^{4}He, and are denominated by DB and DO white dwarfs. The remaining population of white dwarfs ($\sim$ 5%) show atmospheres rich in ^{4}He, ^{12}C, and ^{16}O (PG1159 stars)[1], ^{12}C and ^{4}He (DQ white dwarfs), and metals without ^{1}H or ^{4}He present (DZ white dwarfs). There are also some exotic objects, such as SDSS J0922+2928 and SDSS J1102+2054, that exhibit O in their atmospheres (Gänsicke et al., 2010), SDSS J1240+6710 that has a nearly pure ^{16}O atmosphere, diluted only by traces of ^{20}Ne, ^{26}Mg, and ^{28}Si (Kepler et al., 2016a), and finally WD J0551+4135, that shows a mixed ^{1}H and ^{12}C atmosphere (Hollands et al., 2020). The origin of these unfamiliar objects is not yet known, but might involve stellar mergers. By virtue of the high densities and small radii of the white dwarfs, they are characterized by very high surface gravities, in the range of $\log g \sim 6 - 9$ [cm/s^2]. The extremely high gravities of white dwarfs force heavy elements to sink and light nuclear species to float on the white-dwarf surface. This effect, called gravitational settling, explains the purity of the atmospheres of DA and DB/DO white dwarfs. Any "impurity" observed in white dwarf atmospheres at intermediate temperatures—for instance, photospheric trace metals found in many white dwarfs—must be attributed either to accreted material (i.e., tidally disrupted planetesimals; see Koester et al., 2014), material floating on the surface due to radiative levitation, or material dredged up from the interior due to convection. The typical chemical structure of an average-mass DA white dwarf consists of a core composed of ^{12}C and ^{16}O—in unknown proportions—containing $\sim$ 99% of the mass, surrounded by a ^{4}He layer with a mass $M_{\rm He} \lesssim 10^{-2} M_\star$, it is in turn enclosed by a thin ^{1}H envelope with a mass of $M_{\rm H} \lesssim 10^{-4} M_\star$. The thickness of the ^{1}H and ^{4}He mantles depends on the mass of the white dwarf. Despite the thinness of these layers, they play a fundamental role in the cooling rate (Wood, 1990).

The population of known white dwarfs has increased dramatically in recent years. Ground-based observations, principally with the spectral observations of the Sloan Digital Sky Survey (SDSS; York et al., 2000), have enlarged the number of known white dwarfs by a factor of 15 (Kleinman et al., 2013; Kepler et al., 2016b, 2019). Recently, Gentile Fusillo et al. (2019) presented a catalog of $\sim$ 260,000 high-confidence white-dwarf candidates selected from *Gaia* DR2.

White-dwarf research has relevant applications to various areas of modern astrophysics. A primary application of the analysis of white-dwarf properties, either individual or collective—like the mass distribution, core chemical composition, and cooling times—is to place constraints on the evolution of low-mass stars, including third dredge up and mass loss on the Asymptotic Giant Branch (AGB), the efficiency of extra-mixing during core He burning, and nuclear reaction rates (Kunz et al., 2002; Metcalfe, 2003; Straniero et al., 2003; Salaris et al., 2009; Fields et al., 2016).

By virtue of the large number of white dwarfs that are currently known, and thanks to the extreme longevity of these stars (they are among the oldest objects of the Galaxy), they are a key part in our understanding of the formation and evolution of stars, evolution of planetary systems, and the history of our Galaxy itself. For instance, since the existing population of white dwarfs holds a detailed account of the early star formation in the Galaxy, then accurate white-dwarf luminosity functions can be employed to deduce the age, structure, and evolution of the Galactic disk and the nearest open and globular clusters, through what is called *cosmochronology* (Fontaine et al., 2001; Bedin et al., 2009, 2015; García-Berro et al., 2010; Campos et al., 2013, 2016; García-Berro and Oswalt, 2016; Kilic et al., 2017).

From another perspective, since the majority of low-mass stars will evolve into white dwarfs, then most of the host stars of

[1]Strictly speaking, since these stars still have substantial nuclear burning, they should be considered pre-white dwarfs.

planetary systems will end their lives as white dwarfs. At present, many white dwarfs with planetary debris are currently being detected, and their study provides valuable information about the chemical composition of extra-solar planets (Gänsicke et al., 2012; Hollands et al., 2018). In particular, Gänsicke et al. (2019) have detected a white dwarf accreting material probably coming from a giant planet.

In a different context, white dwarfs are found in binary systems. This allows exploring the interactions among stars, and in particular, to study type Ia supernovae progenitors (Maoz et al., 2014). Indeed, since the mechanical properties of a white dwarf are described by a Fermi gas of degenerate electrons, there exist a limit mass—the Chandrasekhar mass, $\sim 1.4 M_{\odot}$—beyond which the structure of a white dwarf becomes unstable. Therefore, a ^{12}C/^{16}O-core white dwarf in a binary system that receives mass from its companion, can approach the Chandrasekhar mass and explode as a supernova.

Finally, another very important aspect of white dwarfs is that, due to the high density prevailing in their interiors, they are extremely useful as cosmic laboratories to study dense plasma physics and solid state physics (crystallization; Montgomery and Winget, 1999; Montgomery et al., 1999; Winget et al., 2009; Tremblay et al., 2019), and "exotic physics" (axions, neutrino magnetic dipole moment, variation of fundamental constants, etc; Isern et al., 1992, 2008, 2018; Córsico et al., 2001, 2012b, 2013, 2014; Miller Bertolami, 2014; Miller Bertolami et al., 2014).

2. PULSATION PROPERTIES OF WHITE DWARFS AND PRE-WHITE DWARFS AND THE CLASSIFICATION OF THE DIFFERENT TYPES OF VARIABLES

An important characteristic of white dwarfs is that, along their evolution, all of them go through at least one phase of pulsational instability that converts white dwarfs into variable stars. As such, variable white dwarfs can be studied through *asteroseismology*, which allows for key information about the internal structure of pulsating stars to be extracted, through the study of their normal modes. In a sense, the global pulsations are something like "windows" that allow astronomers to "see" inside the stars (Cox, 1980; Unno et al., 1989; Aerts et al., 2010; Catelan and Smith, 2015). In the case of white dwarfs, the properties derived through asteroseismology for pulsating objects are likely valid for non-pulsating white dwarfs as well. On the other hand, this is a unique tool that makes it possible to delve inside the white dwarfs. Finally, and due to the fact that the equilibrium structures of white dwarfs are simple—by virtue of its degenerate nature—their pulsation properties are consequently simple and relatively easy to model to a meaningful precision. In particular, they can be treated within the context of the linear theory of stellar pulsations. These unique qualities explain why white-dwarf asteroseismology has, in recent years, become one of the most powerful tools to learn about their origin, evolution, and internal structure, complementing the traditional techniques of spectroscopy, photometry, and astrometry (Fontaine and Brassard, 2008; Winget and Kepler, 2008; Althaus et al., 2010; Córsico et al., 2019). As a matter of fact, white-dwarf asteroseismology has been a cornerstone of the field of asteroseismology (Brown and Gilliland, 1994). Below, we briefly describe the pulsational properties of white dwarfs along with their immediate precursors, the pre-white dwarfs, and the different classes of these compact pulsators known at the time of writing this review (March 2020).

Pulsations in white dwarfs manifest as brightness fluctuations in the optical, the ultraviolet (UV), and infrared (IR) regions of the electromagnetic spectrum, with amplitudes between 0.001 mmag and 0.4 mag. The variations are thought to be produced by changes in the surface temperature due to non-radial g modes (McGraw, 1979; Robinson et al., 1982) with low harmonic degree ($\ell = 1, 2$) and low and intermediate radial order (k). In particular, Robinson et al. (1982) showed that during pulsations, the changes of the stellar radius are fairly small ($\Delta R_{\star} \sim 10^{-5} R_{\star}$), and that the variations in surface temperature ($\Delta T_{\rm eff} \sim 200$ K) are the true cause of the variability of pulsating white dwarfs. Kepler (1984) investigated the effects of r-mode non-radial pulsations[2] on the lightcurves and line profiles of a slowly rotating star, and concluded that the observed variations of the prototype H-rich pulsating white dwarf, G117−B15A, are not caused by r-mode pulsations, but are consistent with g-mode pulsations. By virtue of the high electron degeneracy in the core of white dwarfs, the g-mode critical frequency—the "buoyancy" or Brunt-Väisälä frequency—is very low at the core regions. This forces g modes to probe, in particular, the regions of the envelope (see, for instance Brassard et al., 1991), although some low radial-order modes are generally sensitive to the central regions. In the case of hot pre-white dwarfs like PG1159 stars, degeneracy is not as important, and g modes can propagate throughout the star, including the core regions (Kawaler et al., 1985; Córsico and Althaus, 2006). The first pulsating white dwarf ever detected, HL Tau 76, was discovered unexpectedly by Landolt (1968). Since then, an increasing number of pulsating white dwarfs have been detected, either through observations from Earth—mainly for candidates identified from SDSS—and recently as a result of uninterrupted observations of space missions, such as *Kepler*/*K2* (Borucki et al., 2010; Howell et al., 2014). Prior to the era of observations from space, an important international collaborative tool called the Whole Earth Telescope (WET; Nather et al., 1990) was successfully used to observe pulsating white dwarfs and pre-white dwarfs for long intervals of time, without interruption. As a matter of fact, observations from this world-wide network of telescopes resulted in the most precise light curves ever obtained for any pulsating star at that time (see, for instance, Winget et al., 1991, 1994). The properties of the light curves of pulsating white dwarfs and pre-white dwarfs are varied, ranging from very simple and with low-amplitude variations (containing a single period) to complex and with high-amplitude fluctuations (usually harboring several periods). The first ones are usually associated with pulsating white dwarfs located at the hot edge of the specific instability domain, and the last ones are found generally for stars populating the cool boundary of that instability

[2] r modes are toroidal modes in presence of rotation (Papaloizou and Pringle, 1978).

TABLE 1 | Basic characteristics of the different types of pulsating white dwarfs and pre-white dwarfs, sorted by decreasing effective temperature.

Class	Year of disc. (#)	$T_{\rm eff}$ (× 1,000 K)	$\log g$ (C.G.S.)	Period range (s)	Amplitudes (mag)	Main surface composition
GW Vir (PNNV)	1984 (10)	100 – 180	5.5 – 7	420 – 6,000	0.01 – 0.15	He, C, O
GW Vir (DOV)	1979 (9)	80 – 100	7.3 – 7.7	300 – 2,600	0.02 – 0.1	He, C, O
V777 Her (DBV)	1982 (27)	22.4 – 32	7.5 – 8.3	120 – 1,080	0.05 – 0.3	He (H)
GW Lib	1998 (20)	10.5 – 16	8.35 – 8.7	100 – 1,900	0.007 – 0.07	H, He
ZZ Cet (DAV)	1968 (260)	10.4 – 12.4	7.5 – 9.1	100 – 1,400	0.01 – 0.3	H
pre-ELMV	2013 (7)	8 – 13	4 – 5	300 – 1,400	0.001 – 0.05	He, H
ELMV	2012 (11)	7.8 – 10	6 – 6.8	100 – 6,300	0.002 – 0.044	H

region—as the convection zone deepens, longer-period modes are excited. In the case of the complex lightcurves, that usually exhibit features of non-linearity, it is common to find harmonics and linear combinations of eigenfrequencies that are not related to real pulsation modes. Rather, they are likely connected with physical phenomena inherent to the outermost regions of the white dwarf, probably related to the outer convection zone. In the case of pulsating pre-white dwarfs, the effective temperatures are so high that these stars probably lack an extensive external convective zone. This may be the explanation for the fact that non-linearities are not detected in any pulsating hot pre-white dwarf star.

Currently, the number of known pulsating white dwarfs and pre-white dwarfs is about 350 (Córsico et al., 2019). They are distributed in six confirmed types, namely ZZ Ceti (or DAV) stars, GW Lib stars, V777 Her (or DBV) stars, GW Vir (or pulsating PG1159) stars, ELMV stars, and pre-ELMV stars. There are two additional claimed classes of pulsating white dwarfs, the hot DAV stars ($T_{\rm eff} \sim 30,000$ K, $7.3 \lesssim \log g \lesssim 7.8$; Kurtz et al., 2008, 2013) and the DQV stars (Montgomery et al., 2008). Pulsational instabilities in hot DAVs were predicted on theoretical grounds by Shibahashi (2005, 2007); the actual existence of pulsations in these stars must be confirmed by additional observations. On the other hand, DQVs are hot DQ (C- and He-rich atmospheres) white dwarfs with surface parameters $19,000$ K $\lesssim T_{\rm eff} \lesssim 22,000$ K and $8 \lesssim \log g \lesssim 9$. At present, there is a growing consensus that the variability of these objects could be due to other effects than global pulsations. The main characteristics of the confirmed classes of pulsating white dwarfs are listed in **Table 1** and the location in the $\log T_{\rm eff} - \log g$ is depicted in **Figure 1** (details can be found in Córsico et al., 2019). In **Table 1**, the second column indicates the discovery year of the first star of each type and the number of detected objects at the time of writing this review, the third column corresponds to the range of effective temperatures at which they are found (instability domain), the fourth column shows the range of surface gravity, the fifth column indicates the range of periods detected, the sixth column is the range of amplitudes of the fluctuations in the light curves, and the seventh column shows the surface chemical composition. Pulsation periods usually span the interval $\sim 100 - 1,400$ s; however PNNVs and ELMVs display longer periods, up to $\sim 6,300$ s. In **Figure 2** we show the periods detected in the different families of pulsating white dwarfs and pre-white dwarfs. Curiously, and due to the compactness of these objects, the periods of g modes in white dwarfs have magnitudes comparable to the values of the periods of p modes exhibited by non-degenerate pulsating stars, like the Sun.

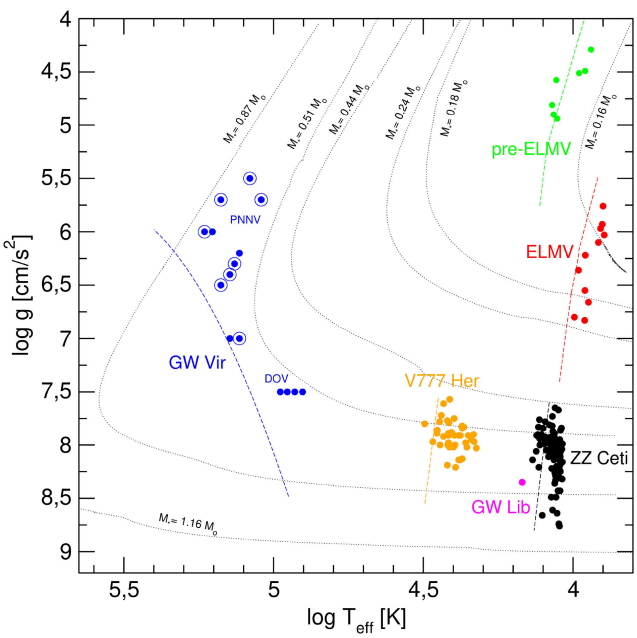

FIGURE 1 | The families of confirmed pulsating white dwarf and pre-white dwarf stars (circles of different colors) in the $\log T_{\rm eff} - \log g$ plane. This figure is an update of Figure 1 of Córsico et al. (2019). GW Vir stars indicated with blue circles surrounded by blue circumferences are PNNVs. Only the location of the prototypical object of GW Lib class, the star GW Librae, has been indicated (magenta dot). Two post-VLTP (Very Late Thermal Pulse) evolutionary tracks for H-deficient white dwarfs (0.51 and $0.87 M_\odot$; Miller Bertolami and Althaus, 2006), four evolutionary tracks of low-mass He-core H-rich white dwarfs (0.16, 0.18, 0.24, and $0.44 M_\odot$; Althaus et al., 2013), and one evolutionary track for ultra-massive H-rich white dwarfs ($1.16 M_\odot$; Camisassa et al., 2019) are included for reference. Dashed lines correspond to the location of the theoretical hot boundary of the different instabilities strips.

Pulsations in white dwarfs are self-excited, in contrast to the stochastic pulsations, which are forced oscillations driven by turbulent convection in the Sun, the solar-like, and red giant

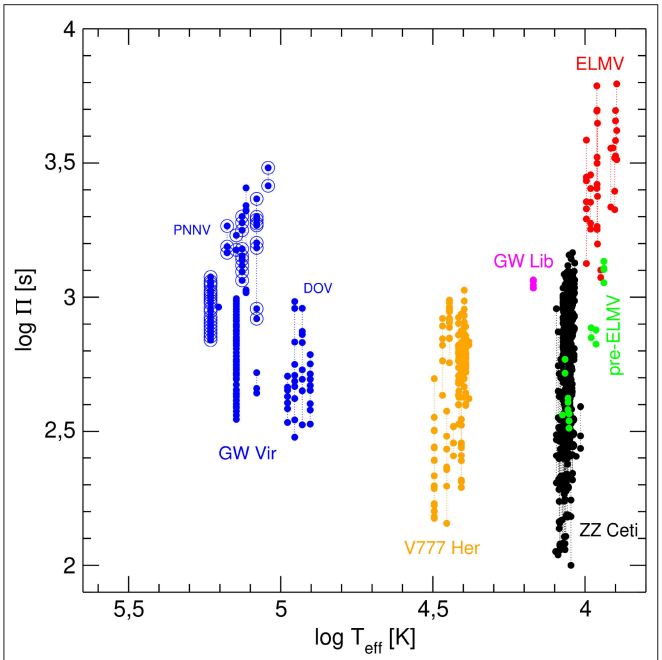

FIGURE 2 | The logarithm of the observed periods in terms of the logarithm of the effective temperature corresponding to the different families of confirmed pulsating white dwarf and pre-white dwarf stars (circles of different colors; see **Figure 1**). This figure is an update of Figure 2 of Saio (2013).

pulsating stars. The cause of the pulsations in white dwarfs appears to be a mechanism that begins to act when the star cools down to an effective temperature at which the dominant nuclear species becomes partially ionized near the stellar surface (that is, when there is a coexistence of neutral and ionized atoms of the same chemical element; "partial ionization zone"). At the partial ionization zones, the opacity increases at the compression phase of the oscillations, and this excites global pulsations with periods that are of the same order of magnitude as the thermal timescale at the driving region. The $\kappa - \gamma$ mechanism has been invoked to explain at least the onset of pulsations in all the categories of pulsating white dwarfs (see, for instance, Winget et al., 1982; Starrfield et al., 1984, for the case of the DAV and GW Vir stars, respectively). For DAVs and DBVs, the validity of the $\kappa - \gamma$ mechanism has been questioned. Instead, it has been proposed that the so-called "convective driving" mechanism (Brickhill, 1991; Goldreich and Wu, 1999), that becomes efficient when the base of the outer convective zone sinks, is the responsible mode of driving. For GW Vir stars, which do not have surface convection zones as a result of their very-high effective temperatures, the $\kappa - \gamma$ mechanism seems to be enough to destabilize high-order g-mode pulsations[3]. The proposed mechanisms are able to predict with decent precision the $T_{\rm eff}$ of the blue (hot) edge of the instability strips. However, in general, all theories fail in terms of the predicted effective temperature of the red (cool) boundary, where white dwarfs quench their pulsations. This is discouraging, since even detailed calculations that take into account the interaction between convection and pulsations (Van Grootel et al., 2012) fail to reproduce the location of the red edges in the cases of DAVs and DBVs. Recently, Luan and Goldreich (2018) proposed a theoretical framework that accounts for the existence of the red edge of the DAV instability strip.

Therefore, the physical processes that excite and quench pulsations in white dwarfs are not fully understood. This happens, in general, for all the classes of pulsating stars, aside from white dwarfs. However, this does not prevent us from extracting information from the pulsation periods through adiabatic asteroseismological analyses alone. In the case of white dwarfs, these analyses are based on the forward approximation, in which the measured periods are compared with the periods calculated on a huge set of white-dwarf models to obtain a representative asteroseismological solution of the star under study. The theoretical models can be the result of detailed computations that take into account the complete evolutionary history of the white-dwarf progenitor, the approach adopted by the La Plata Group[4] (see e.g., Córsico et al., 2008, 2012a), or instead, they can consist of static white-dwarf models with parameterized chemical composition profiles (see, for instance Giammichele et al., 2018). A variant of this last method is the use of evolutionary models with parameterized chemical profiles (see Bischoff-Kim et al., 2019). These approaches are complementary, among them (Córsico et al., 2019). In some cases, a large set of consecutive periods can be detected, and it is possible to make asteroseismological inferences of the stellar mass from the mean period of spacing. This is the case of several DBV and GW Vir stars.

3. PULSATING WHITE DWARFS MONITORED BY THE *KEPLER* SPACECRAFT

The primary goal of the *Kepler* spacecraft was to detect transiting planets, discovering by the end of the mission a total of more than 4,000 exoplanets (Thompson et al., 2018). As a byproduct of the planetary hunt, high-quality photometric data of variable stars was collected, allowing a rapid blooming of asteroseismology of many classes of pulsating stars, in particular solar-like and red giant pulsators. The initial survey of pulsating stars undertaken by the *Kepler* Asteroseismic Science Consortium (KASC) contained a total of 113 compact pulsator candidates (including subdwarfs and white dwarfs) which were checked for variability using *Kepler* short-cadence exposures. Unfortunately, none of the 17 white dwarfs contained in the sample turned out to be variable. In order not to miss the exceptional capacity of the *Kepler* mission, other candidate objects (not included in the

[3]There exist theoretical evidence of another mechanism that could excite global pulsations in white dwarfs and pre-white dwarfs, that is, the ϵ mechanism due to nuclear burning. This could be responsible for short-period g-mode pulsations in GW Vir stars (Córsico et al., 2009), ELMVs (Córsico and Althaus, 2014), ZZ Ceti stars coming from low-metalicity progenitors (Camisassa et al., 2016), and in very hot DA white dwarfs (Maeda and Shibahashi, 2014; Calcaferro et al., 2017). However, the predicted pulsations have not been detected, so far, in any case.

[4]http://evolgroup.fcaglp.unlp.edu.ar/

TABLE 2 | All the published pulsating white-dwarf stars observed with the *Kepler* spacecraft (*Kepler* and *K2* missions).

Star	Class	$T_{\rm eff}$ (K)	$\log g$	$M_\star$ ($M_\odot$)	$P_{\rm rot}$ (h)	Mission	References
KIC 4357037	DAV	12,650	8.01	0.62	22.0	*Kepler*	Hermes et al., 2017a
KIC 4552982‡	DAV	10,860	8.16	0.71	18.4	*Kepler*	Bell et al., 2015
KIC 7594781	DAV	11,730	8.11	0.67	26.8	*Kepler*	Hermes et al., 2017a
KIC 10132702	DAV	11,940	8.12	0.68	11.2	*Kepler*	Hermes et al., 2017a
KIC 11911480	DAV	11,580	7.96	0.58	74.7	*Kepler*	Greiss et al., 2014
EPIC 60017836	DAV	10,980	8.00	0.57	6.9	*K2*	Hermes et al., 2014
EPIC 201355934	DAV	11,770	7.97	0.59	...	*K2*	Hermes et al., 2017a
EPIC 201719578	DAV	11,070	7.94	0.57	26.8	*K2*	Hermes et al., 2017a
EPIC 201730811	DAV	12,480	7.96	0.68	2.6	*K2*	Hermes et al., 2015a
EPIC 201802933	DAV	12,330	8.11	0.68	31.3	*K2*	Hermes et al., 2017a
EPIC 201806008‡	DAV	10,910	8.02	0.61	31.3	*K2*	Hermes et al., 2017a
EPIC 206212611	DAV	10,830	8.00	0.60	...	*K2*	Hermes et al., 2017a
EPIC 210377280	DAV	11,590	7.94	0.57	...	*K2*	Bell et al., 2017b
EPIC 210397465	DAV	11,200	7.71	0.45	49.1	*K2*	Hermes et al., 2017a
EPIC 211596649	DAV	11,600	7.91	0.56	81.8	*K2*	Hermes et al., 2017a
EPIC 211629697‡	DAV	10,600	7.77	0.48	64.0	*K2*	Bell et al., 2016
EPIC 211891315§	DAV	11,310	8.03	...	...	*K2*	Bell, 2017
EPIC 211914185	DAV	13,590	8.43	0.88	1.1	*K2*	Hermes et al., 2017a
EPIC 211916160	DAV	11,510	7.96	0.58	...	*K2*	Hermes et al., 2017a
EPIC 211926430	DAV	11,420	7.98	0.59	25.4	*K2*	Hermes et al., 2017a
EPIC 220204626	DAV	11,620	8.17	0.71	24.3	*K2*	Hermes et al., 2017a
EPIC 220258806	DAV	12,800	8.09	0.66	30.0	*K2*	Hermes et al., 2017a
EPIC 220274129	DAV	11,810	8.03	0.62	12.7	*K2*	Bell et al., 2017b
EPIC 220329764‡	DAV	11,180	8.03	0.62	...	*K2*	Bell, 2017
EPIC 220347759	DAV	12,770	8.08	0.66	31.7	*K2*	Hermes et al., 2017a
EPIC 220453225‡	DAV	11,220	8.04	0.62	...	*K2*	Hermes et al., 2017a
EPIC 228682478	DAV	12,070	8.18	0.72	109.1	*K2*	Hermes et al., 2017a
EPIC 228952212‡	DAV	11,080	7.95	0.58	...	*K2*	Bell, 2017
EPIC 229227292‡	DAV	11,210	8.03	0.62	29.4	*K2*	Bell et al., 2016
EPIC 229228364‡	DAV	11,030	8.03	0.62	...	*K2*	Hermes et al., 2017a
EPIC 229228478	DAV	12,500	7.93	0.57	...	*K2*	Hermes et al., 2017a
EPIC 229228480	DAV	12,450	8.18	0.72	...	*K2*	Hermes et al., 2017a
KIC 8626021	DBV	29,700	7.890	0.56	43.0	*Kepler*	Østensen et al., 2011a
PG 0112+104	DBV	31,040	7.800	0.58	10.2	*K2*	Hermes et al., 2017b

The values of $T_{\rm eff}$, $\log g$, and $M_\star$ are those published in Córsico et al. (2019), except in the case of EPIC 211891315, EPIC 220329764, EPIC 220453225, and EPIC 228952212, for which the values are those of Bell (2017). The last column corresponds to the paper in which the pulsations were analyzed.
‡*Outbursting ZZ Ceti stars.* §*Probable outbursting ZZ Ceti star.*

initial survey; Østensen et al., 2011b) began to be monitored with *Kepler*. Fortunately, this search resulted in the first observations of pulsating white dwarfs by this space mission (Hermes et al., 2011; Østensen et al., 2011a; Greiss et al., 2014, 2015, 2016). Once it finished the nominal 4-years mission, the *Kepler* spacecraft lost two of its four reaction wheels (2013 May). The mission was then redirected to monitoring new fields along the ecliptic plane during uninterrupted time-intervals of $\sim$ 90 days (Howell et al., 2014). This extended *Kepler* mission was renamed as *K2* and operated from 2014 until the spacecraft ran out of fuel in 2018. The *K2* mission provided an exceptional chance to extend space-based monitoring for a lot of new white dwarfs. This extended mission was cleverly exploited by astronomers, and, at the end, many pulsating white dwarfs were discovered and studied.

In the following sections, we summarize the main findings achieved in white-dwarf asteroseismology thanks to the observations of *Kepler* and *K2*. In particular, we focus on several detailed asteroseismological studies performed on pulsating white dwarfs observed by this space mission, and also on selected outstanding discoveries that have been the result of uninterrupted observations from space. As a result of the *Kepler* and *K2* observations, 2 DBV and 29 DAV stars have been intensively studied, and the results of those analyses have been published. We have to add to this list three more DAV stars analyzed and published in a PhD Thesis (Bell, 2017). One of the

DBV stars, KIC 8626021, has been the focus of intense modeling by several independent groups of asteroseismologists, thanks to which, its internal structure is known with unprecedented precision. In **Table 2** we show the main characteristics of all the published pulsating white dwarfs observed with the *Kepler* spacecraft (in both the *Kepler* and *K2* missions). The first column corresponds to the name of the star, the second column is the class of pulsating white dwarf, the third and fourth columns correspond to the effective temperature and surface gravity values, the fifth column is the stellar mass, the sixth column corresponds to the rotation period determined using the observed splittings of frequencies, the seventh column gives the phase of the space mission (*Kepler* or *K2*), and the last column shows the reference to the paper in which the pulsational analysis has been presented.

The findings reported from here to the end of the article are associated with results already published (up to early 2020). However, we emphasize that there is still a large amount of reduced data from the *Kepler* and *K2* missions that have not yet been analyzed, and which could translate into future new discoveries about pulsating white-dwarf and pre-white-dwarf stars.

3.1. A V777 Her Star in the Nominal *Kepler* Mission Field: KIC 8626021

The DB white dwarf star GALEX J192904.6+444708 ($T_{\rm eff} = 24,900 \pm 750$ K and $\log g = 7.91 \pm 0.07$), identified with the name KIC 8626021 in the *Kepler* input catalog (also known as WD J1929+4447), was photometrically observed by Østensen et al. (2011a) to check for variability from the Earth. This star was part of a number of targets that had not been included in the original sample of 17 white dwarfs to be observed by *Kepler*. A 2-hr photometry run on this star clearly revealed the presence of variability with a period of 232 s and an additional period around 270 s. With ground-based photometry, the dataset was too short to perform any meaningful analysis on, but it clearly demonstrated the pulsational nature of KIC 8626021. After that, Østensen et al. (2011a) analyzed 1 month of short-cadence observations of this pulsating star by *Kepler*. The Fourier transform of the lightcurve is shown in the upper panel of **Figure 3**. The detected frequencies are depicted in the sub-panels, three of which show clear signals of triplet structures due to rotation. The periods detected appear to be associated to a sequence of $\ell = 1$ g modes with low radial order values. The period spacing is close to 36 s, typical of DBV stars. On the basis of the frequency splitting ($\delta\nu \sim 3.3$ μHz) it is possible to infer an estimate of the rotational period of $P_{\rm rot} \sim 1.7$ days. By using the grids of model atmospheres of Koester (2010), Østensen et al. (2011a) determined $T_{\rm eff} = 24,900 \pm 750$ K and $\log g = 7.91 \pm 0.07$, placing the star in the middle of the DBV instability strip.

Shortly after the discovery of pulsations in KIC 8626021, the first detailed asteroseismological analysis of the star was performed by Bischoff-Kim and Østensen (2011). They presented an analysis based on the five-mode pulsation spectrum detected by Østensen et al. (2011a) with *Kepler* data. The observed pulsational characteristics of the star and the asteroseismic analysis strongly suggested that KIC 8626021 was actually hotter than indicated by model-atmosphere fits to the low signal-to-noise electromagnetic spectrum of the object. Indeed, Bischoff-Kim and Østensen (2011) employed a large set of evolutionary models of DB white dwarfs with parameterized chemical profiles, and took three different avenues to determine the effective temperature of KIC 8626021: (i) by means of an inspection of the observed pulsation spectrum, noting that only short-period g modes were present; (ii) employing the average separation between consecutive periods; and (iii) by carrying out asteroseismological period-to-period fits of the pulsation spectrum. All three approaches pointed to an effective temperature of $T_{\rm eff} \sim 29,200$ K, in disagreement with the spectroscopic value derived by Østensen et al. (2011a) ($T_{\rm eff} = 24,900$ K). If true, since hot DBVs are thought to lose a large portion of their internal energy through the emission of plasmon neutrinos (Winget et al., 2004), this star could be an extremely important target to place limits on the plasmon-neutrino emission rate. However, the measurement of a rate of period change requires extremely stable (over many years) oscillation modes, a condition that is not perfectly met by KIC 8626021 (see at the end of this section).

As a sanity check for this important result, an independent asteroseismological analysis was crucial at that time. This did not take long. Córsico et al. (2012a) carried out a second asteroseismological analysis, which was based on a set of fully evolutionary/pulsational DB white-dwarf models constructed with the `LPCODE` evolutionary code (Althaus et al., 2005) and the `LP-PUL` pulsation code (Córsico and Althaus, 2006). By considering the mean period spacing of KIC 8626021, Córsico et al. (2012a) found that the star should be substantially more massive than suggested by spectroscopy. From period-to-period fits these authors found an asteroseismological model characterized by an effective temperature much higher than the spectroscopic estimate, in agreement with the results of Bischoff-Kim and Østensen (2011). So, this analysis was the second piece of evidence that KIC 8626021 should be located near the blue edge of the DBV instability strip. A very interesting and exciting point is that the DB white-dwarf models used by both groups were completely different, particularly regarding the composition profiles (see **Figure 4**), but nonetheless, similar conclusions were reached regarding the effective temperature of the star.

A subsequent asteroseismological analysis of KIC 8626021 was carried out by Bischoff-Kim et al. (2014) on the basis of an augmented set of observed pulsation periods and DB white-dwarf evolutionary models with parameterized chemical profiles, like in Bischoff-Kim and Østensen (2011). The analysis of Bischoff-Kim et al. (2014) was better constrained by the employment of a set of seven independent periods for this star—instead of the five original periods—resulting from 2-years long observations of *Kepler*. By exploiting the presence of the various triplets and doublets, the authors were able to constrain the value of ℓ and m, something that simplified the period-to-period fit and reduced the assumptions at the outset. The resulting asteroseismological model for KIC 8626021 is characterized by a thin pure-He envelope [$\log(1 - M_{\rm He}/M_\star = -7.90)$] and a high effective temperature ($T_{\rm eff} = 29,650$ K). This last result confirmed that

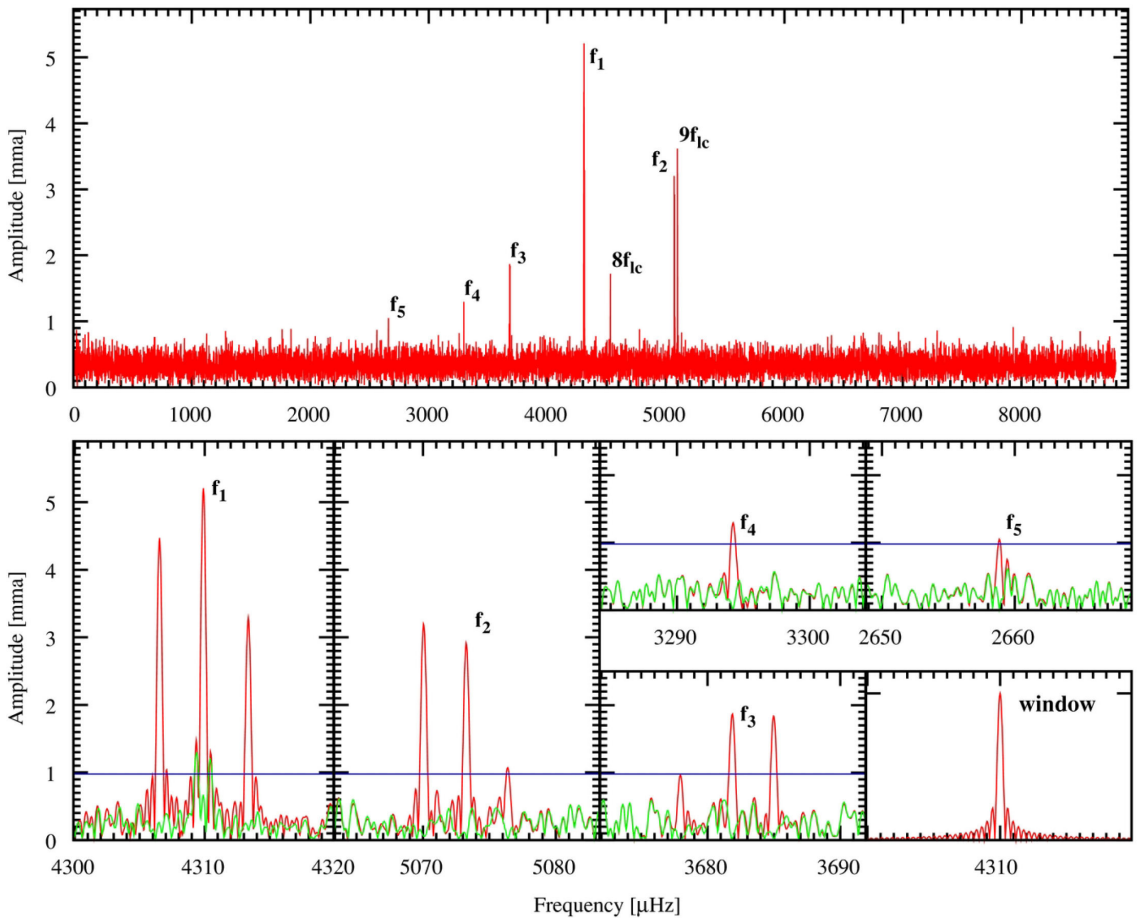

FIGURE 3 | Fourier Transform of the *Kepler* lightcurve of the DBV star KIC 8626021 (upper panel) derived from Østensen et al. (2011a). The peaks labeled as $8f_{lc}$ and $9f_{lc}$ are two long-cadence artifacts. The real frequencies are labeled as f_1 to f_5. Lower panels: Zoomed-in views of the five frequencies, including the spectral window of the *Kepler* data set (final panel). Reproduced with permission from the AAS.

the star is near the blue edge of the DBV instability strip, in line with the previous analyses. Furthermore, a thin pure-helium layer constituted evidence that the hotter the DB model, the thinner the pure-He layer, supporting the theory that as a DB cools and He diffuses outward, the pure-He layer becomes thicker (see Bischoff-Kim et al., 2014, and references therein).

The most detailed asteroseismological analysis on KIC 8626021 was presented by Giammichele et al. (2018). These authors considered a set of eight periods from the analysis of Zong et al. (2016b). The additional period comes from the alternative interpretation that the structure in the 3.677 − 3.686 μHz range of the spectrum, identified previously as a triplet of frequencies, is actually a doublet, and then the third component is actually an independent mode. Giammichele et al. (2018) presented a new method for parameterizing the chemical profiles in the core of static white-dwarf models, based on Akima splines. They derived an asteroseismological model characterized by a ^{16}O content and an extent of its core that clearly goes beyond the limits predicted by standard DB white dwarf models resulting from fully evolutionary computations. The asteroseismological model is characterized by $T_{\rm eff} = 29,968 \pm 200$ K and $\log g = 7.917 \pm 0.009$, which closely match the independent measurements obtained from spectroscopy by the same authors ($T_{\rm eff} = 29,360 \pm 780$ K and $\log g = 7.89 \pm 0.05$) using the DB white-dwarf model atmospheres of Bergeron et al. (2011). One point to note is that these results confirm the predictions of previous studies that this star is a hot DBV and is close to the blue edge of the V777 Her instability strip. On the other hand, with the new spectroscopic determination of $T_{\rm eff}$, the discrepancy between asteroseismology and spectroscopy is eliminated. But the most relevant conclusion of this work is that the star seems to have a ^{16}O core (and thus a ^{16}O content) much larger than what standard evolutionary calculations predict. The total ^{16}O content of the white-dwarf core reaches 78.0 ± 4.2%, large in excess when compared with the expected value of around 64% for a standard evolutionary DB white-dwarf model of the same stellar mass. This result constitutes a challenge for the theory of white-dwarf formation and has aroused the interest of several research groups to try to explain how an object of these characteristics could be formed. For example, De Gerónimo et al. (2019) find

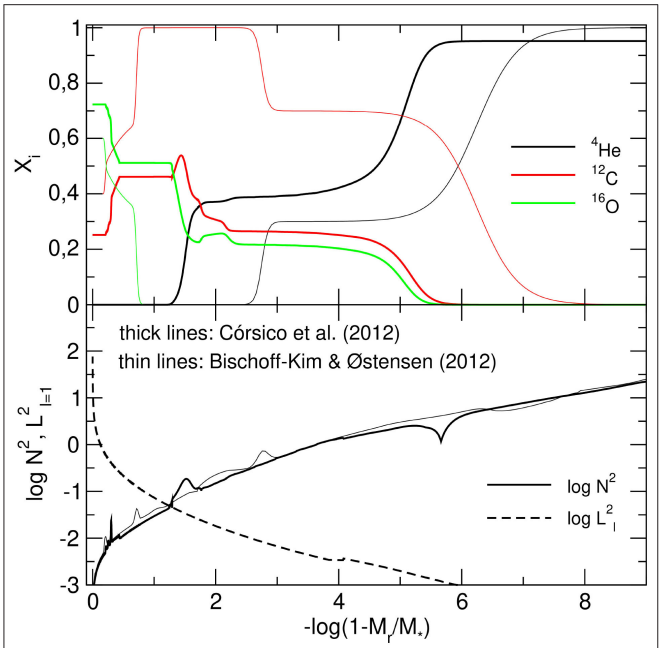

FIGURE 4 | Internal chemical profiles (upper panel), and the logarithm of the squared Brunt-Väisälä and Lamb frequencies for $\ell = 1$ (lower panel) corresponding to a template DB white-dwarf model of Córsico et al. (2012a) with a stellar mass of $M_\star = 0.565 M_\odot$, an effective temperature $T_{\rm eff} \sim 28,400$ K, and a He envelope mass of $M_{\rm He}/M_\star \sim 6.7 \times 10^{-3}$ (thick lines). For comparison, we show, using thin lines, the chemical profiles and the Brunt-Väisälä frequency of the best-fit model for KIC 8626021 found by Bischoff-Kim and Østensen (2011).

that, within our current understanding of white-dwarf formation and evolution, it is difficult (if not impossible) to replicate the most relevant features of the chemical structure of KIC 08626021 derived with asteroseismology. Timmes et al. (2018) have drawn attention to the impact that neutrino emission—a physical ingredient ignored in the DB white-dwarf modeling on which the Giammichele et al. (2018) analysis is based—should have on the pulsation periods of KIC 08626021. In order to assess the effect of neutrino emission on the asteroseismological solution of Giammichele et al. (2018), Charpinet et al. (2019) have redone the analysis on this star by incorporating the effects of neutrino cooling, and basically find the same asteroseismological model for KIC 08626021 than in Giammichele et al. (2018). A summary of all the asteroseismological analyses carried out until now for KIC 08626021 are given in **Table 3**.

We close this section by noting an interesting phenomenon discovered thanks to the continuous observations of KIC 08626021 with *Kepler*. Zong et al. (2016b) have detected amplitude and frequency modulations of the components of the triplets of frequencies due to a rotation present in the pulsation spectrum of KIC 08626021. Similar secular changes of oscillation frequencies and amplitudes have been measured with the *Kepler* mission in the subdwarf B star KIC 10139564 by Zong et al. (2016a). Since these frequency and amplitude changes occur with timescales that are several orders of magnitude shorter than the cooling timescale of a DB white dwarf, these modulations of frequencies and amplitudes have nothing to do with any evolutionary effect, such as, e.g., neutrino cooling. Also, it is not expected that these modulations are provoked by orbiting companions around the star, since different timescales for the different triplets are involved. A clue to clarify this behavior could be a the possible interaction between the components of the rotationally split triplets, that is, the presence of non-linear resonant mode coupling (see, for details, Buchler et al., 1997). If true, this star could constitute an excellent opportunity to study non-linear effects in pulsating white dwarfs. Note that, unfortunately, the presence of frequency modulations can make the measurement of the evolutionary (cooling) rate of period change of KIC 08626021 unrealizable, thus hampering any possibility of placing constraints on the plasmon-neutrino emission rate.

3.2. A V777 Her Star in the Field of the *K2* Mission: PG 0112+104

Hermes et al. (2017b) presented a pulsational analysis of the already known DBV star PG 0112+104. With $T_{\rm eff} \gtrsim 30,000$ K, this star is the hottest V777 Her star known, that defines the blue edge of the DBV instability strip. The star was analyzed on the basis of 78.7 days of nearly uninterrupted photometry from the *Kepler* space telescope—specifically the campaign eight of the *K2* extended mission. Hermes et al. (2017b) discovered nine additional periods apart from the two periods that were already known from ground-based observations. The pulsation spectrum of this star includes clear patterns of rotational splittings from consecutive sequences of $\ell = 1$ and $\ell = 2$ modes. In addition, a surface rotational period of 10.17 h has been measured using an apparent spot modulation. To summarize, this hot star is a promising candidate to derive the dependence of rotational angular velocity with depth, that is, the differential rotation of the star, through asteroseismology. The estimation of the surface rotation independently from the spot would constitute a strong test for the asteroseismological analysis. On the other hand, as PG 0112+104 is such a hot DBV star, it constitutes an excellent laboratory for studying plasmon neutrino production if the rate of period change for any mode is measured. Since the pulsation frequencies in PG 0112+104 are extremely stable in phase, the secular change of the periods could be detected and measured with additional—ground- or space-based—observations.

3.3. ZZ Ceti Stars in the Nominal *Kepler* Mission Field

Hermes et al. (2011) reported the discovery of the first identified DAV, WD J1916+3938 (Kepler ID 4552982), in the original field of the *Kepler* mission. This ZZ Ceti star was first identified through ground-based, time-series photometry. A follow-up spectroscopic analysis indicated that it is a DA white dwarf with $T_{\rm eff} = 11,129 \pm 115$ K and $\log g = 8.34 \pm 0.06$, situating it near the hot boundary of the ZZ Ceti instability domain. The object showed up to 0.5 % amplitude variability at several periods between 800 and 1,450 s (Bell et al., 2015). This star was submitted for *Kepler* short-cadence observations. These observations led

TABLE 3 | The main characteristics of KIC 08626021.

Quantity	ØEA11	BKØ11	CEA12	BKEA14	GEA18	CHEA19
$T_{\rm eff}$ (K)	$24,950 \pm 750$	29,200	27,263	29,650	29,968	30,114
$M_\star$ ($M_\odot$)	0.56 ± 0.03	0.570	0.664	0.550	0.570	0.562
$\log g$ (cm/s^2)	7.91 ± 0.07	—	8.099	—	7.917	7.905
$\log(L_\star/L_\odot)$	—	—	−1.14	—	−0.86	—
$\log(R_\star/R_\odot)$	—	—	−1.93	—	−1.86	−1.86
$X_{\rm O}$ (center)	—	0.60 – 0.65	0.65	0.55	0.86	0.84
$\log(1 - M_{\rm He}/M_\star)$	—	−6.30	−5.95	−7.90	−7.63	−7.83
$\log(1 - M_{\rm env}/M_\star)$	—	−2.80	−1.63	−3.10	−3.23	−3.48

*The second column corresponds to the spectroscopic results by ØEA11 (Østensen et al., 2011a), the third, fourth, fifth, sixth, and seventh columns present the results from the asteroseismological studies of BKØ11 (Bischoff-Kim and Østensen, 2011), CEA12 (Córsico et al., 2012a), BKEA14 (Bischoff-Kim et al., 2014), GEA18 (Giammichele et al., 2018), and CHEA19 (Charpinet et al., 2019), respectively. The last two rows correspond to the coordinate of the basis of the pure-He envelope, and the basis of the mixed zone containing ^{4}He, ^{12}C, and ^{16}O (see **Figure 4**).*

to the unexpected discovery of a new phenomenon: outburst-like events in DAV stars with effective temperatures near the cool edge of the instability strip (Bell et al., 2015, see section 3.5 for details).

The second DAV in the *Kepler* field, KIC 11911480, was discovered by Greiss et al. (2014) using the *Kepler*-INT Survey (KIS; Greiss et al., 2012) to select white-dwarf candidates with color-colors diagrams. The variable nature of KIC 11911480 was confirmed using ground-based time series photometry. This star is close to the blue edge of the ZZ Ceti instability strip ($T_{\rm eff} = 12,160 \pm 250$ K and $\log g = 7.94 \pm 0.10$). The star was scrutinized for 6 months with the short-cadence mode of the *Kepler* telescope, and a total of six independent pulsation periods in the range 172.9 − 324.5 s—typical of the hot ZZ Ceti stars—were detected. A preliminary analysis indicated that the star is rotating with a period of $\sim$ 3.5 days. Greiss et al. (2015) and Greiss et al. (2016) reported the pulsation properties of three additional DAV stars observed with *Kepler*: KIC 10132702 ($T_{\rm eff} = 11048 \pm 217$ K, $\log g = 8.07 \pm 0.08$), KIC 04357037 ($T_{\rm eff} = 11898 \pm 200$ K, $\log g = 8.03 \pm 0.08$), and KIC 07594781 ($T_{\rm eff} = 12217 \pm 1700$ K, $\log g = 7.54 \pm 0.22$). Using the frequency spacing in the triplets and doublets, these authors estimated the rotation periods of these stars, obtaining values in the range of (0.9 − 3.2) days.

3.4. ZZ Ceti Stars Monitored With the *K2* Mission

The first DAV star observed with the *K2* mission was GD 1212 (Hermes et al., 2014). This star, which was already known to be pulsating (Gianninas et al., 2006), is a cool DAV with $T_{\rm eff} = 10,970 \pm 170$ K and $\log g = 8.03 \pm 0.05$, corresponding to a mass of $0.62 \pm 0.03 M_\odot$. *K2* short-cadence observations revealed at least 19 independent pulsation modes, ranging from 828.2 to 1220.8 s, and at least 17 non-linear combination frequencies. This star also exhibits amplitude and frequency variations on timescales less than a week, reminiscent to the behavior detected by Zong et al. (2016b) in the DBV star KIC 08626021 (see at the end of section 3.1). This phenomenon makes a precise determination of the pulsation periods of GD 1,212 more complicated. Since this star is a cool ZZ Ceti, it would be expected to be characterized by high amplitudes. However, the independent modes detected, as well as the frequency combinations, show low amplitudes.

Another DAV star analyzed with the *K2* mission is SDSS J113655.17+040952.6 (hereafter SDSS J1136+0409), the first known pulsating DA white-dwarf in a post-common envelope binary system with a main-sequence (dM) companion star (Pyrzas et al., 2015). The ZZ Ceti component has $T_{\rm eff} = 12,330 \pm 260$ K and $M_\star = 0.601 \pm 0.036 M_\odot$. Nearly 78 days of *K2* observations allowed Hermes et al. (2015a) to detect seven independent pulsation modes, three of which are rotationally split multiplets compatible with a rotation period of 2.49 ± 0.53 h.

Usually, observations of pulsating white dwarfs with the *Kepler* space telescope have to be performed using the short-cadence mode of observations (1-min exposures) to sufficiently over-sample typical white-dwarf pulsation periods (3–20 min) for straightforward frequency measurement. However, Bell et al. (2017b) have demonstrated that it is possible to combine long-cadence *K2* data (30 min exposures) with high-speed follow-up ground-based observations, to derive accurate oscillation frequencies to a precision of $\sim 0.01 \mu$Hz. Using this approach, Bell et al. (2017b) have discovered two new ZZ Ceti variables from *K2* long-cadence data: EPIC 210377280 and EPIC 220274129. For EPIC 220274129, Bell et al. (2017b) inferred a stellar rotation period of 12.7 ± 1.3 h.

The most complete and detailed study of ZZ Ceti stars observed with the *Kepler* space telescope has been presented by Hermes et al. (2017a). This monumental work, based on the observations of 27 ZZ Ceti stars collected with the nominal *Kepler* mission and mostly with the extended *K2* mission, presents, in detail, the occurrence of outbursts in ZZ Ceti stars near the red edge of the DAV instability strip (see section 3.5), the discovery of a dichotomy of the widths of peaks in the Fourier spectrum (section 3.6), and a possible relationship between the rotation periods derived from frequency splittings for 20 of the 27 DAVs and their stellar mass (see section 3.7). In addition, Hermes et al. (2017a) have been able to characterize the DAV instability strip as observed by *Kepler* and *K2*. Indeed,

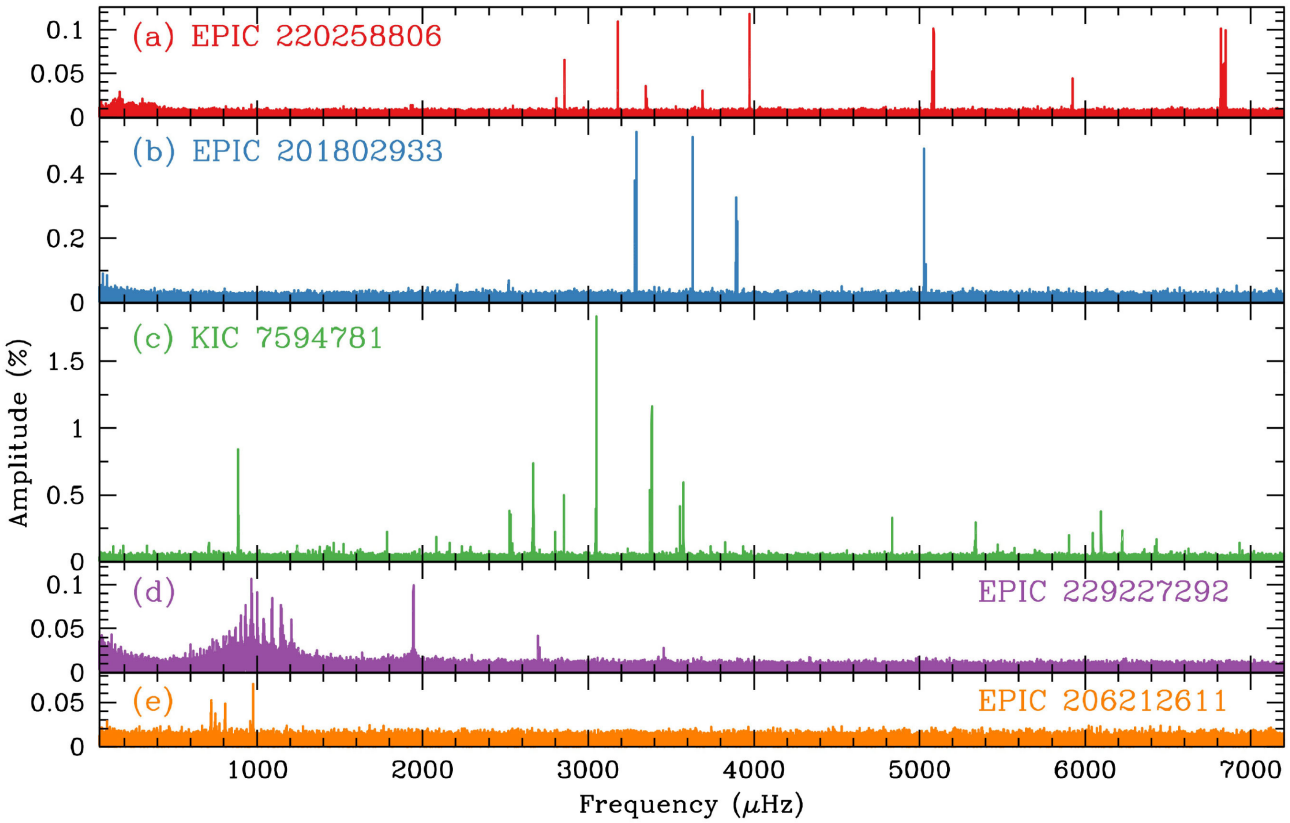

FIGURE 5 | The Fourier Transform corresponding to five representative ZZ Ceti stars observed with *K2*, with decreasing $T_{\rm eff}$ from the top to bottom panel (Hermes et al., 2017a). The figures highlight the different phases of DAV stars along the ZZ Ceti instability strip. Reproduced with permission from the AAS.

they show how the different trends regarding the length of the excited periods and the amplitude of the modes evolve as the effective temperature decreases along the instability strip. In particular, Hermes et al. (2017a) find that the excited periods are short and with low amplitude near the blue edge of the instability domain, but then the excited periods grow (modes of larger radial orders are excited) and the amplitude also increases with decreasing $T_{\rm eff}$. Toward effective temperatures near the cool boundary of the instability strip, some ZZ Ceti show outbursts. Finally, at the red edge, the excited modes of DAVs are the longest-period pulsations with relatively small amplitude. **Figure 5**, which displays the Fourier spectrum of ZZ Ceti stars at different effective temperatures, dramatically illustrates the described trend.

3.5. Outbursting ZZ Ceti Stars

The *Kepler* spacecraft observations of ZZ Ceti stars led to the discovery of a energetic phenomenon never observed before from the ground in this type of quiet pulsating stars: outburst-like events (Bell et al., 2017a). So far, this constitutes one of the most transcendent discoveries (perhaps the most transcendent) in relation to pulsations in white dwarfs observed with *Kepler*. An important aspect of these events is that they repeat chaotically, with no fixed period of recurrence. The first outbursting DAV, KIC4552982[5], which is located near the red edge of the ZZ Ceti instability strip ($T_{\rm eff} = 11,129 \pm 115$ K, log $= 8.34 \pm 0.06$), was observed during $\sim$ 20 months with the nominal *Kepler* mission, yielding the longest pseudo-continuous light curve of a ZZ Ceti ever obtained (Bell et al., 2015). These observations allowed the detection of 20 pulsation modes with periodicities commonly observed in ZZ Ceti stars, along with 178 increments of brightness typical of outburst phenomena, with peaks of up to 17% above the quiescent level. The outbursts involve very energetic events ($E \sim 10^{33}$ erg), with a mean recurrence period of about 2.7 days and 4–25 h of duration (Bell et al., 2015). The second outbursting star, the already known cool DAV PG 1149+057 ($T_{\rm eff} = 11,060 \pm 170$ K, log $= 8.06 \pm 0.05$), was analyzed by Hermes et al. (2015b) with nearly continuous *K2* observations for more than 78.8 days. This star shows outbursts with a typical recurrence time of $\sim$ 8 days and 15 h of duration, and very large flux enhancements of up to 45% above the quiescent level. For this star, the outbursts have a measurable impact on the spectrum of *g* modes (in amplitude and frequency), demonstrating that *outbursts are an intrinsic phenomenon of the (otherwise isolated) star*. In **Figure 6** we show

[5]This star was the first ZZ Ceti identified in the original *Kepler* mission field (Hermes et al., 2011, ; see section 3.3).

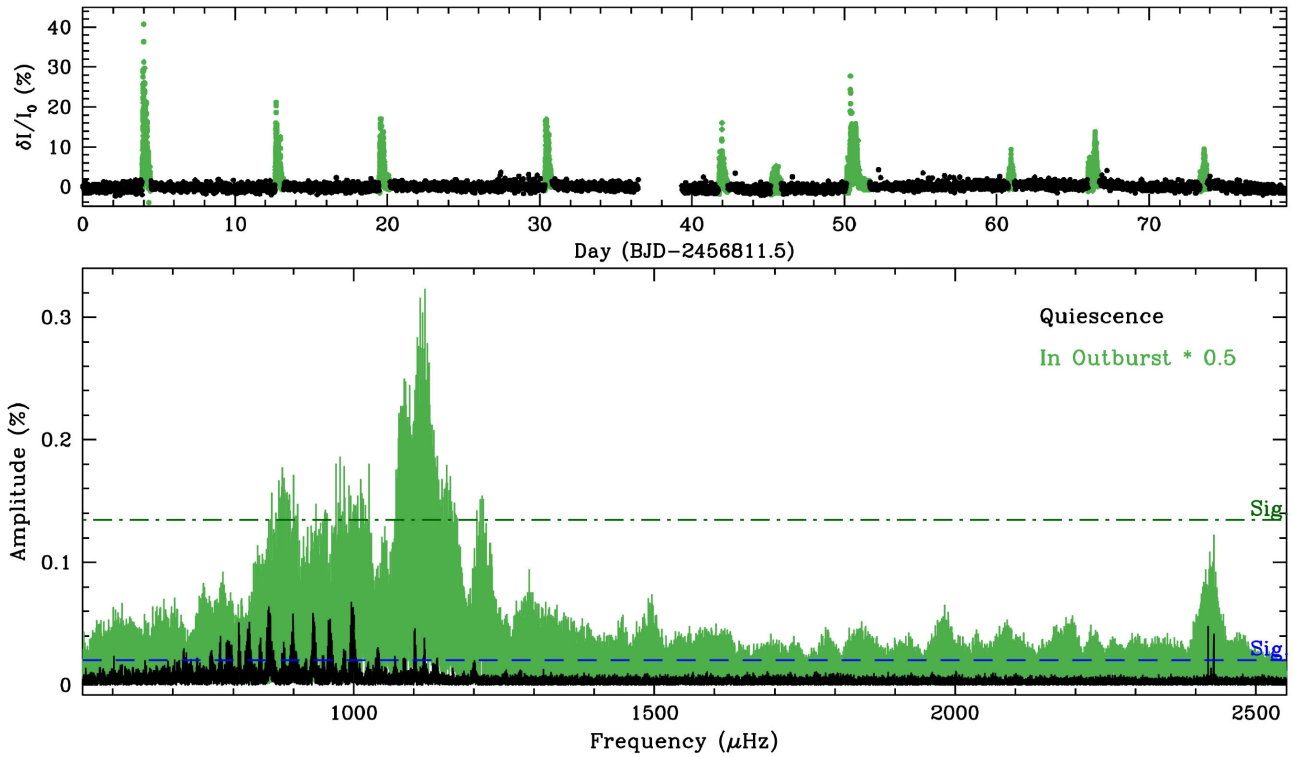

FIGURE 6 | Upper panel: the complete *K2* light curve of PG 1149+057 derived by Hermes et al. (2015b). The 10 outburst events are emphasized with green dots and the data in quiescence are marked with black dots. Bottom panel: the Fourier Transforms during and out of outburst (green and black). In both cases, pulsations have amplitudes larger than the corresponding significance thresholds, shown as dark green dashed–dotted and blue dashed lines. Note that normal-mode pulsations remain during the outbursts, but they have larger amplitudes and higher frequencies than in quiescence. Reproduced with permission from the AAS.

the complete *K2* light curve of PG 1149+057 (upper panel) and the Fourier Transforms for the case during and out of outburst (lower panels). At the time of writing this article, a total of eight outbursting (isolated) DAV stars have been discovered (Bell et al., 2016, 2017a), all of them populating the red edge of the ZZ Ceti instability strip (see Figure 12 of Córsico et al., 2019). This strongly suggests that outbursts could be related to the origin of the cool edge of the DAV instability domain, that is, the cessation of the *g*-mode pulsations (Bell et al., 2017a). A possible explanation for both the occurrence of outbursts and the origin of the cool edge of the ZZ Ceti instability strip, has been proposed by Luan and Goldreich (2018). It is connected with parametric instability through mode coupling of white-dwarf pulsations (Dziembowski, 1982; Wu and Goldreich, 2001; Luan and Goldreich, 2018).

3.6. Dichotomy of Mode-Line Widths in ZZ Ceti Stars

Another major observational result from the *Kepler* space telescope is the discovery by Hermes et al. (2017a) of a clear dichotomy of oscillation mode-line widths in the power spectrum of 27 DAVs observed from space. Indeed, *g* modes characterized by periods longer than roughly 800 s are generally incoherent (large line widths) over the length of observations, while *g* modes with periods $\lesssim$ 800 s are observed to be much more stable in phase and amplitude (smaller line width)[6]. We depict in **Figure 7** (extracted from Hermes et al., 2017a) the half-width at half-maximum (HWHM) of all significant peaks (excluding any non-linear combination frequencies) in the power spectra of 27 DAVs observed through *Kepler* and *K2*. The dichotomy of mode-line widths could be intimately linked to the oscillation of the outer convection zone of a DA white dwarf during pulsations. Specifically, the oscillation out of and in the base of the convection zone would affect the radial eigenfunction of certain *g* modes—those that have the outer turning point of oscillation located precisely at the base of the convection zone (Montgomery et al., 2020). This mechanism may be relevant for the limitation of pulsation amplitudes in pulsating white dwarfs for modes with periods above a threshold period.

3.7. White-Dwarf Rotation Rates From Asteroseismology of ZZ Ceti Stars

Hermes et al. (2017a) have also derived the rotation rates of 20 isolated DAVs observed with *Kepler* and *K2* using rotational splittings, doubling the number of pulsating white dwarfs with

[6]This phenomenon cannot be associated to stochastic mode driving, which for white dwarfs would excite pulsations with very short periods, of the order of $\sim$ 1 s (Saio, 2013).

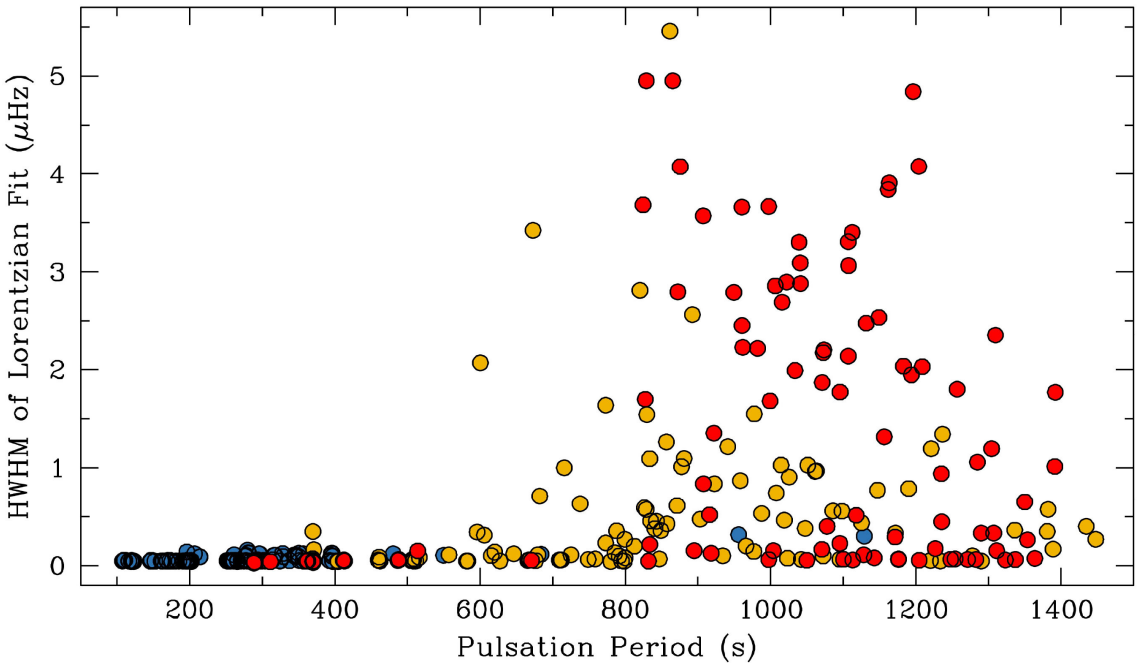

FIGURE 7 | Half-width at half-maximum (HWHM) of Lorentzian functions fit to all significant peaks (corresponding to genuine eigenmodes) in the power spectra of 27 DAVs observed through K2 (Hermes et al., 2017a). Blue circles are for objects with weighted mean period (WMP) <600 s, gold with WMP >600 s, and red are those with outbursts. A clear increase in HWHM at ∼800 s is present. Reproduced with permission from the AAS.

measured rotation rates via asteroseismology[7] (see **Table 2** of this article and Table 10 of Córsico et al., 2019). The results indicate that the average rotation period is $\sim 30-40$ h, although ZZ Ceti stars that rotate faster (with periods of $\sim 1-2$ h) have also been found. There is some evidence of the existence of a correlation between high mass and fast rotation, an idea reinforced by the fastest rotation ever measured in an isolated white dwarf[8], of 1.13 h, for the massive ZZ Ceti star SDSSJ0837+1856 ($M_\star = 0.87 M_\odot$) by Hermes et al. (2017c), although more high-mass white dwarfs are necessary to confirm this trend. Hermes et al. (2017a) find that most isolated descendants of $1.7-3.0 M_\odot$ ZAMS progenitors rotate at $\sim$ 1.5 days, instead of minutes, which would be expected if the angular momentum of a $3.0 M_\odot$ MS star with an initial rotation period of 10 h, were fully conserved (Kawaler, 2004). This fact strongly indicates that most internal angular momentum must be lost on the first-ascent giant branch.

3.8. Asteroseismology of *Kepler* ZZ Ceti Stars With Fully Evolutionary Models

In section 3.1 we described, in detail, the various asteroseismological analyses conducted to elucidate the internal structure of the *Kepler* DBV star KIC 8626021. Here, we briefly describe the asteroseismological analysis on ZZ Cetis observed with *Kepler* carried out by Romero et al. (2017). This analysis was based on evolutionary and pulsational white-dwarf models computed with the `LPCODE` and `LP-PUL` codes, adopting the La Plata Group's approach of white-dwarf asteroseismology (see at the end of section 2). Specifically, the first four published ZZ Ceti stars observed with the *Kepler* mission, that is, EPIC 60017836 (GD 1212), EPIC 201730811 (SDSS J113655.17+040952.6), KIC 11911480, and KIC 4552982, were studied. Currently, this remains the only detailed asteroseismological study of DAVs observed with the *Kepler* space telescope. A period-to-period fit analysis of the four target stars was carried out by employing a grid of full evolutionary models representative of C/O-core DA white-dwarf stars constructed with detailed and updated input physics. These models have consistent chemical profiles for both the core and the envelope for various stellar masses, particularly suitable for asteroseismological fits of ZZ Ceti stars. The chemical profiles of the models were computed considering the complete evolution of the progenitor stars from the ZAMS through the thermally pulsing and mass-loss phases on the asymptotic giant branch (AGB).

Apart from the observed periods, the analysis by Romero et al. (2017) incorporated the amplitude of the modes, rotational splitting multiplets, and period spacing data, as well as photometry and spectroscopy information. For each analyzed star, an asteroseismological model that closely reproduces observed properties, such as periods, stellar mass, and effective temperature was presented. In the particular case of KIC 11911480 and EPIC 201730811, the asteroseismological masses

[7]Note that rotation rates can sometimes also be measured from long-cadence data, as in Bell et al. (2017b).

[8]Except for the magnetic DA white dwarf RE J0317-853, with an apparent period of ∼725 s (Barstow et al., 1995), and SDSSJ125230.93?023417.72, which is the fastest-rotating apparently isolated white dwarf yet discovered, that rotates with a period of 317.278 ± 0.013 s (Reding et al., 2020).

are similar to each other, although the H envelope for EPIC 201730811 (that is part of a binary system and likely went through a common envelope phase) is 10 times thinner than that for KIC 11911480. This result confirms what was discussed in Hermes et al. (2015a) on the basis of a preliminary asteroseismological analysis, that the H-layer mass of EPIC 201730811 is roughly $10^{-5}M_{\star}$. In the case of KIC 4552982, which is a red-edge ZZ Ceti star, the asteroseismological model has a very thin H envelope mass ($M_{\rm H}/M_{\odot} = 4.7 \times 10^{-9}$), which could be related to the outburst nature of this star, as reported by Bell et al. (2015). Whether this is a common characteristic between all the outbursting DAVs or not is a very interesting topic that deserves further exploration. Finally, in the case of EPIC 60017836 (another red-edge DAV), an asteroseismological model was obtained with a stellar mass compatible with the atmospheric parameters from photometry combined with parallax and spectroscopy.

4. CONCLUSIONS

The *Kepler* space telescope—both the nominal *Kepler* mission and the extended mission *K2*—has been very successful in its search for extrasolar planets and has also meant a revolution in the area of asteroseismology for many classes of pulsating stars. In the particular case of pulsating white dwarfs, the numbers speak for themselves. In total, 2,166 white dwarfs were observed by *Kepler*/*K2*. There were 81 DAVs observed by *Kepler*/*K2*, with 75 of them obtaining short cadence data. Of them, analyses of 32 DAVs have been published (29 stars analyzed in journals and three objects analyzed in a PhD Thesis; see **Table 2**). Thanks to *Kepler*/*K2*, the number of ZZ Ceti stars that have a rotation period measured with asteroseismology has increased by a factor of 2. Regarding DBVs, seven stars were observed, although the analysis of only two of them have been published to date. Finally, two unique GW Vir stars were observed, including the prototypical star PG 1159−035, but no results have been published yet.

The story of the *Kepler* mission and the pulsating white dwarf stars does not end here. There is an immense amount of data waiting to be analyzed, and this will likely lead to new discoveries in the near future. In turn, this will drive new asteroseismological analyses, in addition to those already published. Altogether, the *Kepler* space telescope has had a strong impact (and will continue to have) on the area of white-dwarf asteroseismology. This first step will be multiplied by current and future space missions, such as the Transiting Exoplanet Survey Satellite (*TESS*; Ricker et al., 2015), which is already in full operation and is providing the first results on pulsating white dwarfs (Bell et al., 2019; Althaus et al., 2020; Bognár et al., 2020), and other space missions that will become operational in the coming years, such as Cheops (Moya et al., 2018) and Plato (Piotto, 2018).

AUTHOR CONTRIBUTIONS

The author confirms being the sole contributor of this work and has approved it for publication.

FUNDING

Part of this work was supported by AGENCIA through the Programa de Modernización Tecnológica BID 1728/OC-AR, by the PIP 112-200801-00940 grant from CONICET, and by the grant G149 from the University of La Plata.

ACKNOWLEDGMENTS

I thank the referees for their valuable suggestions that improved the content and presentation of the paper. I warmly thank Leandro G. Althaus, Keaton J. Bell, and J. J. Hermes for being so kind to read the manuscript and suggest relevant changes that greatly improved its content. This research has made intensive use of the NASA Astrophysics Data System.

REFERENCES

Aerts, C., Christensen-Dalsgaard, J., and Kurtz, D. W. (2010). *Asteroseismology*. Dordrecht; Heidelberg; London; New York, NY: Springer.

Althaus, L. G., Córsico, A. H., Isern, J., and García-Berro, E. (2010). Evolutionary and pulsational properties of white dwarf stars. *Astron. Astrophys. Rev.* 18, 471–566. doi: 10.1007/s00159-010-0033-1

Althaus, L. G., Córsico, A. H., Uzundag, M., Vučković, M., Baran, A. S., Bell, K. J., et al. (2020). About the existence of warm H-rich pulsating white dwarfs. *Astron. Astrophys.* 633:A20. doi: 10.1051/0004-6361/201936346

Althaus, L. G., Miller Bertolami, M. M., and Córsico, A. H. (2013). New evolutionary sequences for extremely low-mass white dwarfs. Homogeneous mass and age determinations and asteroseismic prospects. *Astron. Astrophys.* 557:A19. doi: 10.1051/0004-6361/201321868

Althaus, L. G., Miller Bertolami, M. M., Córsico, A. H., García-Berro, E., and Gil-Pons, P. (2005). The formation of DA white dwarfs with thin hydrogen envelopes. *Astron. Astrophys.* 440, L1–L4. doi: 10.1051/0004-6361:20050159

Barstow, M. A., Jordan, S., O'Donoghue, D., Burleigh, M. R., Napiwotzki, R., and Harrop-Allin, M. K. (1995). RE J0317-853: the hottest known highly magnetic DA white dwarf. *Mon. Not. R. Astron. Soc.* 277, 971–985. doi: 10.1093/mnras/277.3.971

Bedin, L. R., Salaris, M., Anderson, J., Cassisi, S., Milone, A. P., Piotto, G., et al. (2015). Hubble space telescope observations of the Kepler-field cluster NGC 6819–I. The bottom of the white dwarf cooling sequence. *Mon. Not. R. Astron. Soc.* 448, 1779–1788. doi: 10.1093/mnras/stv069

Bedin, L. R., Salaris, M., Piotto, G., Anderson, J., King, I. R., and Cassisi, S. (2009). The end of the white dwarf cooling sequence in M4: an efficient approach. *Astrophys. J.* 697, 965–979. doi: 10.1088/0004-637X/697/2/965

Bell, K. J. (2017). *Pulsational oddities at the extremes of the DA white dwarf instability strip* (Ph.D. thesis), University of Texas, Austin, TX, United States.

Bell, K. J., Córsico, A. H., Bischoff-Kim, A., Althaus, L. G., Bradley, P. A., Calcaferro, L. M., et al. (2019). TESS first look at evolved compact pulsators. Asteroseismology of the pulsating helium-atmosphere white dwarf TIC 257459955. *Astron. Astrophys.* 632:A42. doi: 10.1051/0004-6361/201936340

Bell, K. J., Hermes, J. J., Bischoff-Kim, A., Moorhead, S., Montgomery, M. H., Østensen, R., et al. (2015). KIC 4552982: outbursts and asteroseismology from the Longest pseudo-continuous light curve of a ZZ Ceti. *Astrophys. J.* 809:14. doi: 10.1088/0004-637X/809/1/14

Bell, K. J., Hermes, J. J., Montgomery, M. H., Gentile Fusillo, N. P., Raddi, R., Gänsicke, B. T., et al. (2016). Outbursts in two new cool pulsating DA white dwarfs. *Astrophys. J.* 829:82. doi: 10.3847/0004-637X/829/2/82

Bell, K. J., Hermes, J. J., Montgomery, M. H., Winget, D. E., Gentile Fusillo, N. P., Raddi, R., et al. (2017a). "The first six outbursting cool DA white dwarf pulsators," in *20th European White Dwarf Workshop, Volume 509 of Astronomical Society of the Pacific Conference Series*, eds P. E. Tremblay, B. Gaensicke, and T. Marsh (San Francisco, CA), 303.

Bell, K. J., Hermes, J. J., Vanderbosch, Z., Montgomery, M. H., Winget, D. E., Dennihy, E., et al. (2017b). Destroying aliases from the ground and space: super-nyquist ZZ Cetis in K2 long cadence data. *Astrophys. J.* 851:24. doi: 10.3847/1538-4357/aa9702

Bergeron, P., Wesemael, F., Dufour, P., Beauchamp, A., Hunter, C., Saffer, R. A., et al. (2011). A comprehensive spectroscopic analysis of DB white dwarfs. *Astrophys. J.* 737:28. doi: 10.1088/0004-637X/737/1/28

Bessel, F. W. (1844). On the variations of the proper motions of Procyon and Sirius. *Mon. Not. R. Astron. Soc.* 6, 136–141. doi: 10.1093/mnras/6.11.136a

Bischoff-Kim, A., and Østensen, R. H. (2011). Asteroseismology of the Kepler field DBV white dwarf. It is a hot one. *Astrophys. J. Lett.* 742:L16. doi: 10.1088/2041-8205/742/1/L16

Bischoff-Kim, A., Østensen, R. H., Hermes, J. J., and Provencal, J. L. (2014). Seven-period asteroseismic fit of the Kepler DBV. *Astrophys. J.* 794:39. doi: 10.1088/0004-637X/794/1/39

Bischoff-Kim, A., Provencal, J. L., Bradley, P. A., Montgomery, M. H., Shipman, H. L., Harrold, S. T., et al. (2019). GD358: three decades of observations for the in-depth asteroseismology of a DBV star. *Astrophys. J.* 871:13. doi: 10.3847/1538-4357/aae2b1

Bognár, Z., Kawaler, S. D., Bell, K. J., Schrand t, C., Baran, A. S., Bradley, P. A., et al. (2020). TESS first look at evolved compact pulsators: known ZZ Ceti stars of the southern ecliptic hemisphere as seen by TESS. *arXiv* arXiv:2003.11481.

Borucki, W. J., Koch, D., Basri, G., Batalha, N., Brown, T., Caldwell, D., et al. (2010). Kepler planet-detection mission: introduction and first results. *Science* 327:977. doi: 10.1126/science.1185402

Brassard, P., Fontaine, G., Wesemael, F., Kawaler, S. D., and Tassoul, M. (1991). Adiabatic properties of pulsating DA white dwarfs. I–the treatment of the Brunt-Vaisala frequency and the region of period formation. *Astrophys. J.* 367, 601–611. doi: 10.1086/169655

Brickhill, A. J. (1991). The pulsations of ZZ Ceti stars. III–the driving mechanism. *Mon. Not. R. Astron. Soc.* 251, 673–680. doi: 10.1093/mnras/251.4.673

Brown, T. M., and Gilliland, R. L. (1994). Asteroseismology. *ARA&A* 32, 37–82. doi: 10.1146/annurev.aa.32.090194.000345

Buchler, J. R., Goupil, M. J., and Hansen, C. J. (1997). On the role of resonances in nonradial pulsators. *Astron. Astrophys.* 321, 159–176.

Calcaferro, L. M., Córsico, A. H., Camisassa, M. E., Althaus, L. G., and Shibahashi, H. (2017). "Pulsational instability of high-luminosity H-rich pre-white dwarf star," in *European Physical Journal Web of Conferences, Volume 152 of European Physical Journal Web of Conferences* (Les Ulis), 06012.

Camisassa, M. E., Althaus, L. G., Córsico, A. H., De Gerónimo, F. C., Miller Bertolami, M. M., Novarino, M. L., et al. (2019). The evolution of ultra-massive white dwarfs. *Astron. Astrophys.* 625:A87. doi: 10.1051/0004-6361/201833822

Camisassa, M. E., Córsico, A. H., Althaus, L. G., and Shibahashi, H. (2016). Pulsations powered by hydrogen shell burning in white dwarfs. *Astron. Astrophys.* 595:A45. doi: 10.1051/0004-6361/201628857

Campos, F., Bergeron, P., Romero, A. D., Kepler, S. O., Ourique, G., Costa, J. E. S., et al. (2016). A comparative analysis of the observed white dwarf cooling sequence from globular clusters. *Mon. Not. R. Astron. Soc.* 456, 3729–3742. doi: 10.1093/mnras/stv2911

Campos, F., Kepler, S. O., Bonatto, C., and Ducati, J. R. (2013). Multichromatic colour-magnitude diagrams of the globular cluster NGC 6366. *Mon. Not. R. Astron. Soc.* 433, 243–250. doi: 10.1093/mnras/stt719

Catelan, M., and Smith, H. A. (2015). *Pulsating Stars*. Weinheim: Wiley-VCH Verlag GmbH & Co.

Chandrasekhar, S. (1939). *An Introduction to the Study of Stellar Structure*. Chicago, IL: University of Chicago Press.

Charpinet, S., Brassard, P., Giammichele, N., and Fontaine, G. (2019). Improved seismic model of the pulsating DB white dwarf KIC 08626021 corrected from the effects of neutrino cooling. *Astron. Astrophys.* 628:L2. doi: 10.1051/0004-6361/201935823

Córsico, A. H., and Althaus, L. G. (2006). Asteroseismic inferences on GW Virginis variable stars in the frame of new PG 1159 evolutionary models. *Astron. Astrophys.* 454, 863–881. doi: 10.1051/0004-6361:20054199

Córsico, A. H., and Althaus, L. G. (2014). Short-period G-mode pulsations in low-mass white dwarfs triggered by H-shell burning. *Astrophys. J. Lett.* 793:L17. doi: 10.1088/2041-8205/793/1/L17

Córsico, A. H., Althaus, L. G., García-Berro, E., and Romero, A. D. (2013). An independent constraint on the secular rate of variation of the gravitational constant from pulsating white dwarfs. *J. Cosmol. Astropart. Phys.* 2013:032. doi: 10.1088/1475-7516/2013/06/032

Córsico, A. H., Althaus, L. G., Kepler, S. O., Costa, J. E. S., and Miller Bertolami, M. M. (2008). Asteroseismological measurements on PG 1159-035, the prototype of the GW Virginis variable stars. *Astron. Astrophys.* 478, 869–881. doi: 10.1051/0004-6361:20078646

Córsico, A. H., Althaus, L. G., Miller Bertolami, M. M., and Bischoff-Kim, A. (2012a). Asteroseismology of the Kepler V777 Herculis variable white dwarf with fully evolutionary models. *Astron. Astrophys.* 541:A42. doi: 10.1051/0004-6361/201118736

Córsico, A. H., Althaus, L. G., Miller Bertolami, M. M., González Pérez, J. M., and Kepler, S. O. (2009). On the possible existence of short-period G-mode instabilities powered by nuclear-burning shells in post-asymptotic giant branch H-deficient (PG1159-type) stars. *Astrophys. J.* 701, 1008–1014. doi: 10.1088/0004-637X/701/2/1008

Córsico, A. H., Althaus, L. G., Miller Bertolami, M. M., and Kepler, S. O. (2019). Pulsating white dwarfs: new insights. *Astron. Astrophys. Rev.* 27:7. doi: 10.1007/s00159-019-0118-4

Córsico, A. H., Althaus, L. G., Miller Bertolami, M. M., Kepler, S. O., and García-Berro, E. (2014). Constraining the neutrino magnetic dipole moment from white dwarf pulsations. *J. Cosmol. Astropart. Phys.* 2014:054. doi: 10.1088/1475-7516/2014/08/054

Córsico, A. H., Althaus, L. G., Miller Bertolami, M. M., Romero, A. D., García-Berro, E., Isern, J., et al. (2012b). The rate of cooling of the pulsating white dwarf star G117-B15A: a new asteroseismological inference of the axion mass. *Mon. Not. R. Astron. Soc.* 424, 2792–2799. doi: 10.1111/j.1365-2966.2012.21401.x

Córsico, A. H., Benvenuto, O. G., Althaus, L. G., Isern, J., and García-Berro, E. (2001). The potential of the variable DA white dwarf G117-B15A as a tool for fundamental physics. *Nature* 6, 197–213. doi: 10.1016/S1384-1076(01)00055-0

Cox, J. P. (1980). *Theory of Stellar Pulsation*. Princeton, NJ: Princeton University Press.

De Gerónimo, F. C., Battich, T., Miller Bertolami, M. M., Althaus, L. G., and Córsico, A. H. (2019). On the recent parametric determination of an asteroseismological model for the DBV star KIC 08626021. *Astron. Astrophys.* 630:A100. doi: 10.1051/0004-6361/201834988

Dziembowski, W. (1982). Nonlinear mode coupling in oscillating stars. I–second order theory of the coherent mode coupling. *Acta Astron.* 32, 147–171.

Fields, C. E., Farmer, R., Petermann, I., Iliadis, C., and Timmes, F. X. (2016). Properties of carbon-oxygen white dwarfs from Monte Carlo stellar models. *Astrophys. J.* 823:46. doi: 10.3847/0004-637X/823/1/46

Fontaine, G., and Brassard, P. (2008). The pulsating white dwarf stars. *Publ. ASP* 120, 1043–1096. doi: 10.1086/592788

Fontaine, G., Brassard, P., and Bergeron, P. (2001). The potential of white dwarf cosmochronology. *Publ. ASP* 113, 409–435. doi: 10.1086/319535

Gänsicke, B. T., Koester, D., Farihi, J., Girven, J., Parsons, S. G., and Breedt, E. (2012). The chemical diversity of exo-terrestrial planetary debris around white dwarfs. *Mon. Not. R. Astron. Soc.* 424, 333–347. doi: 10.1111/j.1365-2966.2012.21201.x

Gänsicke, B. T., Koester, D., Girven, J., Marsh, T. R., and Steeghs, D. (2010). Two white dwarfs with oxygen-rich atmospheres. *Science* 327:188. doi: 10.1126/science.1180228

Gänsicke, B. T., Schreiber, M. R., Toloza, O., Fusillo, N. P. G., Koester, D., and Manser, C. J. (2019). Accretion of a giant planet onto a white dwarf star. *Nature* 576, 61–64. doi: 10.1038/s41586-019-1789-8

García-Berro, E., and Oswalt, T. D. (2016). The white dwarf luminosity function. *New Astron. Rev.* 72, 1–22. doi: 10.1016/j.newar.2016.08.001

García-Berro, E., Torres, S., Althaus, L. G., Renedo, I., Lorén-Aguilar, P., Córsico, A. H., et al. (2010). A white dwarf cooling age of 8Gyr for NGC 6791 from physical separation processes. *Nature* 465, 194–196. doi: 10.1038/nature09045

Gentile Fusillo, N. P., Tremblay, P.-E., Gänsicke, B. T., Manser, C. J., Cunningham, T., Cukanovaite, E., et al. (2019). A Gaia data release 2 catalogue of white dwarfs and a comparison with SDSS. *Mon. Not. R. Astron. Soc.* 482, 4570–4591. doi: 10.1093/mnras/sty3016

Giammichele, N., Charpinet, S., Fontaine, G., Brassard, P., Green, E. M., Van Grootel, V., et al. (2018). A large oxygen-dominated core from the seismic cartography of a pulsating white dwarf. *Nature* 554, 73–76. doi: 10.1038/nature25136

Gianninas, A., Bergeron, P., and Fontaine, G. (2006). Mapping the ZZ Ceti instability strip: discovery of six new pulsators. *Astron. J.* 132, 831–835. doi: 10.1086/506516

Goldreich, P., and Wu, Y. (1999). Gravity modes in ZZ Ceti stars. I. Quasi-adiabatic analysis of overstability. *Astrophys. J.* 511, 904–915. doi: 10.1086/306705

Greiss, S., Gänsicke, B. T., Hermes, J. J., Giammichele, N., Fontaine, G., Koester, D., et al. (2015). *White Dwarfs in the Kepler Field–What's New? Volume 493 of Astronomical Society of the Pacific Conference Series, 169*. San Francisco, CA: Astronomical Society of the Pacific.

Greiss, S., Gänsicke, B. T., Hermes, J. J., Steeghs, D., Koester, D., Ramsay, G., et al. (2014). KIC 11911480: the second ZZ Ceti in the Kepler field. *Mon. Not. R. Astron. Soc.* 438, 3086–3092. doi: 10.1093/mnras/stt2420

Greiss, S., Hermes, J. J., Gänsicke, B. T., Steeghs, D. T. H., Bell, K. J., Raddi, R., et al. (2016). The search for ZZ Ceti stars in the original Kepler mission. *Mon. Not. R. Astron. Soc.* 457, 2855–2863. doi: 10.1093/mnras/stw053

Greiss, S., Steeghs, D., Gänsicke, B. T., Martín, E. L., Groot, P. J., Irwin, M. J., et al. (2012). Initial data release of the Kepler-INT survey. *Astron. J.* 144:24. doi: 10.1088/0004-6256/144/1/24

Hermes, J. J., Charpinet, S., Barclay, T., Pakstiene, E., Mullally, F., Kawaler, S. D., et al. (2014). Precision asteroseismology of the pulsating white dwarf GD 1212 using a two-wheel-controlled Kepler spacecraft. *Astrophys. J.* 789:85. doi: 10.1088/0004-637X/789/1/85

Hermes, J. J., Gänsicke, B. T., Bischoff-Kim, A., Kawaler, S. D., Fuchs, J. T., Dunlap, B. H., et al. (2015a). Insights into internal effects of common-envelope evolution using the extended Kepler mission. *Mon. Not. R. Astron. Soc.* 451, 1701–1712. doi: 10.1093/mnras/stv1053

Hermes, J. J., Gänsicke, B. T., Kawaler, S. D., Greiss, S., Tremblay, P.-E., Gentile Fusillo, N. P., et al. (2017a). White dwarf rotation as a function of mass and a dichotomy of mode line widths: Kepler observations of 27 pulsating DA white dwarfs through K2 campaign 8. *Astrophys. J. Suppl.* 232:23. doi: 10.3847/1538-4365/aa8bb5

Hermes, J. J., Kawaler, S. D., Bischoff-Kim, A., Provencal, J. L., Dunlap, B. H., and Clemens, J. C. (2017b). A deep test of radial differential rotation in a helium-atmosphere white dwarf. I. Discovery of pulsations in PG 0112+104. *Astrophys. J.* 835:277. doi: 10.3847/1538-4357/835/2/277

Hermes, J. J., Kawaler, S. D., Romero, A. D., Kepler, S. O., Tremblay, P.-E., Bell, K. J., et al. (2017c). Evidence from K2 for rapid rotation in the descendant of an intermediate-mass star. *Astrophys. J. Lett.* 841:L2. doi: 10.3847/2041-8213/aa6ffc

Hermes, J. J., Montgomery, M. H., Bell, K. J., Chote, P., Gänsicke, B. T., Kawaler, S. D., et al. (2015b). A second case of outbursts in a pulsating white dwarf observed by Kepler. *Astrophys. J. Lett.* 810:L5. doi: 10.1088/2041-8205/810/1/L5

Hermes, J. J., Mullally, F., Østensen, R. H., Williams, K. A., Telting, J., Southworth, J., et al. (2011). Discovery of a ZZ Ceti in the Kepler mission field. *Astrophys. J. Lett.* 741:L16. doi: 10.1088/2041-8205/741/1/L16

Hollands, M. A., Gänsicke, B. T., and Koester, D. (2018). Cool DZ white dwarfs II: compositions and evolution of old remnant planetary systems. *Mon. Not. R. Astron. Soc.* 477, 93–111. doi: 10.1093/mnras/sty592

Hollands, M. A., Tremblay, P. E., Gänsicke, B. T., Camisassa, M. E., Koester, D., Aungwerojwit, A., et al. (2020). An ultra-massive white dwarf with a mixed hydrogen-carbon atmosphere as a likely merger remnant. *Nat. Astron.* 4, 663–669. doi: 10.1038/s41550-020-1028-0

Howell, S. B., Sobeck, C., Haas, M., Still, M., Barclay, T., Mullally, F., et al. (2014). The K2 mission: characterization and early results. *Publ. ASP* 126:398. doi: 10.1086/676406

Isern, J., García-Berro, E., Torres, S., and Catalán, S. (2008). Axions and the cooling of white dwarf stars. *Astrophys. J. Lett.* 682:L109. doi: 10.1086/591042

Isern, J., García-Berro, E., Torres, S., Cojocaru, R., and Catalán, S. (2018). Axions and the luminosity function of white dwarfs: the thin and thick discs, and the halo. *Mon. Not. R. Astron. Soc.* 478, 2569–2575. doi: 10.1093/mnras/sty1162

Isern, J., Hernanz, M., and Garcia-Berro, E. (1992). Axion cooling of white dwarfs. *Astrophys. J. Lett.* 392, L23–L25. doi: 10.1086/186416

Kawaler, S. D. (2004). "White dwarf rotation: observations and theory," in *Stellar Rotation, Volume 215 of IAU Symposium*, eds A. Maeder and P. Eenens (Paris), 561.

Kawaler, S. D., Winget, D. E., and Hansen, C. J. (1985). Evolution of the pulsation properties of hot pre-white dwarf stars. *Astrophys. J.* 295, 547–560. doi: 10.1086/163398

Kepler, S. O. (1984). Light and line profile variations die to r-mode pusations with an application to the ZZ Ceti star G 117-B15A. *Astrophys. J.* 286, 314–327. doi: 10.1086/162601

Kepler, S. O., Koester, D., and Ourique, G. (2016a). A white dwarf with an oxygen atmosphere. *Science* 352, 67–69. doi: 10.1126/science.aad6705

Kepler, S. O., Pelisoli, I., Koester, D., Ourique, G., Romero, A. D., Reindl, N., et al. (2016b). New white dwarf and subdwarf stars in the Sloan Digital Sky Survey data release 12. *Mon. Not. R. Astron. Soc.* 455, 3413–3423. doi: 10.1093/mnras/stv2526

Kepler, S. O., Pelisoli, I., Koester, D., Reindl, N., Geier, S., Romero, A. D., et al. (2019). White dwarf and subdwarf stars in the Sloan Digital Sky Survey data release 14. *Mon. Not. R. Astron. Soc.* 486, 2169–2183. doi: 10.1093/mnras/stz960

Kilic, M., Munn, J. A., Harris, H. C., von Hippel, T., Liebert, J. W., Williams, K. A., et al. (2017). The ages of the thin disk, thick disk, and the halo from nearby white dwarfs. *Astrophys. J.* 837:162. doi: 10.3847/1538-4357/aa62a5

Kleinman, S. J., Kepler, S. O., Koester, D., Pelisoli, I., Peçanha, V., Nitta, A., et al. (2013). SDSS DR7 white dwarf catalog. *Astrophys. J. Suppl.* 204:5. doi: 10.1088/0067-0049/204/1/5

Koester, D. (2010). White dwarf spectra and atmosphere models. *Mem. Soc. Astron. Ital.* 81, 921–931.

Koester, D., Gänsicke, B. T., and Farihi, J. (2014). The frequency of planetary debris around young white dwarfs. *Astron. Astrophys.* 566:A34. doi: 10.1051/0004-6361/201423691

Kunz, R., Fey, M., Jaeger, M., Mayer, A., Hammer, J. W., Staudt, G., et al. (2002). Astrophysical reaction rate of $^{12}C(\alpha, \gamma)^{16}O$. *Astrophys. J.* 567, 643–650. doi: 10.1086/338384

Kurtz, D. W., Shibahashi, H., Dhillon, V. S., Marsh, T. R., and Littlefair, S. P. (2008). A search for a new class of pulsating DA white dwarf stars in the DB gap. *Mon. Not. R. Astron. Soc.* 389, 1771–1779. doi: 10.1111/j.1365-2966.2008.13664.x

Kurtz, D. W., Shibahashi, H., Dhillon, V. S., Marsh, T. R., Littlefair, S. P., Copperwheat, et al. (2013). Hot DAVs: a probable new class of pulsating white dwarf stars. *Mon. Not. R. Astron. Soc.* 432, 1632–1639. doi: 10.1093/mnras/stt585

Landolt, A. U. (1968). A new short-period blue variable. *Astrophys. J.* 153:151. doi: 10.1086/149645

Luan, J., and Goldreich, P. (2018). DAVs: red edge and outbursts. *Astrophys. J.* 863:82. doi: 10.3847/1538-4357/aad0f4

Maeda, K., and Shibahashi, H. (2014). Pulsations of pre-white dwarfs with hydrogen-dominated atmospheres. *Publ. ASJ* 66:76. doi: 10.1093/pasj/psu051

Maoz, D., Mannucci, F., and Nelemans, G. (2014). Observational clues to the progenitors of type Ia supernovae. *Annu. Rev. Astron. Astrophys.* 52, 107–170. doi: 10.1146/annurev-astro-082812-141031

McGraw, J. T. (1979). The physical properties of the ZZ Ceti stars and their pulsations. *Astrophys. J.* 229, 203–211. doi: 10.1086/156946

Mestel, L. (1952). On the theory of white dwarf stars. I. The energy sources of white dwarfs. *Mon. Not. R. Astron. Soc.* 112:583. doi: 10.1093/mnras/112.6.583

Metcalfe, T. S. (2003). White dwarf asteroseismology and the $^{12}C(\alpha,\gamma)^{16}O$ rate. *Astrophys. J. Lett.* 587, L43–L46. doi: 10.1086/375044

Miller Bertolami, M. M. (2014). Limits on the neutrino magnetic dipole moment from the luminosity function of hot white dwarfs. *Astron. Astrophys.* 562:A123. doi: 10.1051/0004-6361/201322641

Miller Bertolami, M. M., and Althaus, L. G. (2006). Full evolutionary models for PG 1159 stars. Implications for the helium-rich O(He) stars. *Astron. Astrophys.* 454, 845–854. doi: 10.1051/0004-6361:20054723

Miller Bertolami, M. M., Melendez, B. E., Althaus, L. G., and Isern, J. (2014). Revisiting the axion bounds from the galactic white dwarf luminosity function. *J. Cosmol. Astropart. Phys.* 2014:069. doi: 10.1088/1475-7516/2014/10/069

Montgomery, M. H., Hermes, J. J., Winget, D. E., Dunlap, B. H., and Bell, K. J. (2020). Limits on mode coherence in pulsating DA white dwarfs due to a nonstatic convection zone. *Astrophys. J.* 890:11. doi: 10.3847/1538-4357/ab6a0e

Montgomery, M. H., Klumpe, E. W., Winget, D. E., and Wood, M. A. (1999). Evolutionary calculations of phase separation in crystallizing white dwarf stars. *Astrophys. J.* 525, 482–491. doi: 10.1086/307871

Montgomery, M. H., Williams, K. A., Winget, D. E., Dufour, P., DeGennaro, S., and Liebert, J. (2008). SDSS J142625.71+575218.3: a prototype for a new class of variable white dwarf. *Astrophys. J. Lett.* 678:L51. doi: 10.1086/588286

Montgomery, M. H., and Winget, D. E. (1999). The effect of crystallization on the pulsations of white dwarf stars. *Astrophys. J.* 526, 976–990. doi: 10.1086/308044

Moya, A., Barceló Forteza, S., Bonfanti, A., Salmon, S. J. A. J., Van Grootel, V., and Barrado, D. (2018). Asteroseismic potential of CHEOPS. *Astron. Astrophys.* 620:A203. doi: 10.1051/0004-6361/201833772

Nather, R. E., Winget, D. E., Clemens, J. C., Hansen, C. J., and Hine, B. P. (1990). The whole earth telescope–a new astronomical instrument. *Astrophys. J.* 361, 309–317. doi: 10.1086/169196

Østensen, R. H., Bloemen, S., Vučković, M., Aerts, C., Oreiro, R., Kinemuchi, K., et al. (2011a). At last A V777 Her pulsator in the Kepler field. *Astrophys. J. Lett.* 736:L39. doi: 10.1088/2041-8205/736/2/L39

Østensen, R. H., Silvotti, R., Charpinet, S., Oreiro, R., Bloemen, S., Baran, A. S., et al. (2011b). First Kepler results on compact pulsators–VI. Targets in the final half of the survey phase. *Mon. Not. R. Astron. Soc.* 414, 2860–2870. doi: 10.1111/j.1365-2966.2011.18405.x

Papaloizou, J., and Pringle, J. E. (1978). Non-radial oscillations of rotating stars and their relevance to the short-period oscillations of cataclysmic variables. *Mon. Not. R. Astron. Soc.* 182, 423–442. doi: 10.1093/mnras/182.3.423

Piotto, G. (2018). "PLATO science: main goals and expected achievements," in *European Planetary Science Congress, EPSC2018–969* (Berlin).

Pyrzas, S., Gänsicke, B. T., Hermes, J. J., Copperwheat, C. M., Rebassa-Mansergas, A., Dhillon, V. S., et al. (2015). Discovery of ZZ Cetis in detached white dwarf plus main-sequence binaries. *Mon. Not. R. Astron. Soc.* 447, 691–697. doi: 10.1093/mnras/stu2412

Reding, J. S., Hermes, J. J., Vanderbosch, Z., Dennihy, E., Kaiser, B. C., Mace, C. B., et al. (2020). An isolated white dwarf with 317 s rotation and magnetic emission. *Astrophys. J.* 894:19. doi: 10.3847/1538-4357/ab8239

Ricker, G. R., Winn, J. N., Vanderspek, R., Latham, D. W., Bakos, G. Á., Bean, J. L., et al. (2015). Transiting exoplanet survey satellite (TESS). *J. Astron. Telesc. Instr. Syst.* 1:014003. doi: 10.1117/1.JATIS.1.1.014003

Robinson, E. L., Kepler, S. O., and Nather, R. E. (1982). Multicolor variations of the ZZ Ceti stars. *Astrophys. J.* 259, 219–231. doi: 10.1086/160162

Romero, A. D., Córsico, A. H., Castanheira, B. G., De Gerónimo, F. C., Kepler, S. O., Koester, D., et al. (2017). Probing the structure of Kepler ZZ Ceti stars with full evolutionary models-based asteroseismology. *Astrophys. J.* 851:60. doi: 10.3847/1538-4357/aa9899

Saio, H. (2013). "Pulsations in white dwarfs: selected topics," in *European Physical Journal Web of Conferences, Volume 43 of European Physical Journal Web of Conferences* (Les Ulis), 05005.

Salaris, M., Serenelli, A., Weiss, A., and Miller Bertolami, M. (2009). Semi-empirical white dwarf initial-final mass relationships: a thorough analysis of systematic uncertainties due to stellar evolution models. *Astrophys. J.* 692, 1013–1032. doi: 10.1088/0004-637X/692/2/1013

Shibahashi, H. (2005). "The DB gap and pulsations of white dwarfs," in *EAS Publications Series, Volume 17 of EAS Publications Series*, eds G. Alecian, O. Richard, and S. Vauclair (Les Ulis), 143–148.

Shibahashi, H. (2007). "The DB gap and pulsations of white dwarfs," in *Unsolved Problems in Stellar Physics: A Conference in Honor of Douglas Gough, Volume 948 of American Institute of Physics Conference Series*, eds R. J. Stancliffe, G. Houdek, R. G. Martin, and C. A. Tout (College Park, MD), 35–42.

Starrfield, S., Cox, A. N., Kidman, R. B., and Pesnell, W. D. (1984). Nonradial instability strips based on carbon and oxygen partial ionization in hot, evolved stars. *Astrophys. J.* 281, 800–810. doi: 10.1086/162158

Straniero, O., Domínguez, I., Imbriani, G., and Piersanti, L. (2003). The chemical composition of white dwarfs as a test of convective efficiency during core helium burning. *Astrophys. J.* 583, 878–884. doi: 10.1086/345427

Thompson, S. E., Coughlin, J. L., Hoffman, K., Mullally, F., Christiansen, J. L., Burke, C. J., et al. (2018). Planetary candidates observed by Kepler. VIII. A fully automated catalog with measured completeness and reliability based on data release 25. *Astrophys. J. Suppl.* 235:38. doi: 10.3847/1538-4365/aab4f9

Timmes, F. X., Townsend, R. H. D., Bauer, E. B., Thoul, A., Fields, C. E., and Wolf, W. M. (2018). The impact of white dwarf luminosity profiles on oscillation frequencies. *Astrophys. J. Lett.* 867:L30. doi: 10.3847/2041-8213/aae70f

Tremblay, P.-E., Fontaine, G., Fusillo, N. P. G., Dunlap, B. H., Gänsicke, B. T., Hollands, M. A., et al. (2019). Core crystallization and pile-up in the cooling sequence of evolving white dwarfs. *Nature* 565, 202–205. doi: 10.1038/s41586-018-0791-x

Tremblay, P. E., Cummings, J., Kalirai, J. S., Gänsicke, B. T., Gentile-Fusillo, N., and Raddi, R. (2016). The field white dwarf mass distribution. *Mon. Not. R. Astron. Soc.* 461, 2100–2114. doi: 10.1093/mnras/stw1447

Unno, W., Osaki, Y., Ando, H., Saio, H., and Shibahashi, H. (1989). *Nonradial Oscillations of Stars*. Tokyo: University of Tokyop Press.

Van Grootel, V., Dupret, M.-A., Fontaine, G., Brassard, P., Grigahcène, A., and Quirion, P.-O. (2012). The instability strip of ZZ Ceti white dwarfs. I. Introduction of time-dependent convection. *Astron. Astrophys.* 539:A87. doi: 10.1051/0004-6361/201118371

Van Horn, H. M. (2015). *Unlocking the Secrets of White Dwarf Stars*. Cham; Heidelberg; New York, NY; Dordrecht; London: Springer.

Winget, D. E., and Kepler, S. O. (2008). Pulsating white dwarf stars and precision asteroseismology. *ARA&A* 46, 157–199. doi: 10.1146/annurev.astro.46.060407.145250

Winget, D. E., Kepler, S. O., Campos, F., Montgomery, M. H., Girardi, L., Bergeron, P., et al. (2009). The physics of crystallization from globular cluster white dwarf stars in NGC 6397. *Astrophys. J. Lett.* 693, L6–L10. doi: 10.1088/0004-637X/693/1/L6

Winget, D. E., Nather, R. E., Clemens, J. C., Provencal, J., Kleinman, S. J., Bradley, P. A., et al. (1991). Asteroseismology of the DOV star PG 1159-035 with the whole earth telescope. *Astrophys. J.* 378, 326–346. doi: 10.1086/170434

Winget, D. E., Nather, R. E., Clemens, J. C., Provencal, J. L., Kleinman, S. J., Bradley, P. A., et al. (1994). Whole earth telescope observations of the DBV white dwarf GD 358. *Astrophys. J.* 430, 839–849. doi: 10.1086/174455

Winget, D. E., Sullivan, D. J., Metcalfe, T. S., Kawaler, S. D., and Montgomery, M. H. (2004). A strong test of electroweak theory using pulsating DB white dwarf stars as plasmon neutrino detectors. *Astrophys. J. Lett.* 602, L109–L112. doi: 10.1086/382591

Winget, D. E., van Horn, H. M., Tassoul, M., Fontaine, G., Hansen, C. J., and Carroll, B. W. (1982). Hydrogen-driving and the blue edge of compositionally stratified ZZ ceti star models. *Astrophys. J. Lett.* 252, L65–L68. doi: 10.1086/183721

Wood, M. A. (1990). *Astero-archaeolgy reading the galactic history recorded in the white dwarf stars* (Ph.D. thesis), Texas University, Austin, TX, United States.

Woosley, S. E., and Heger, A. (2015). The remarkable deaths of 9-11 solar mass stars. *Astrophys. J.* 810:34. doi: 10.1088/0004-637X/810/1/34

Wu, Y., and Goldreich, P. (2001). Gravity modes in ZZ Ceti stars. IV. Amplitude saturation by parametric instability. *Astrophys. J.* 546, 469–483. doi: 10.1086/318234

York, D. G., Adelman, J., Anderson, J. E. Jr., Anderson, S. F., Annis, J., Bahcall, N. A., et al. (2000). The Sloan Digital Sky Survey: technical summary. *Astron. J.* 120, 1579–1587. doi: 10.1086/301513

Zong, W., Charpinet, S., and Vauclair, G. (2016a). Signatures of nonlinear mode interactions in the pulsating hot B subdwarf star KIC 10139564. *Astron. Astrophys.* 594:A46. doi: 10.1051/0004-6361/201629132

Zong, W., Charpinet, S., Vauclair, G., Giammichele, N., and Van Grootel, V. (2016b). Amplitude and frequency variations of oscillation modes in the pulsating DB white dwarf star KIC 08626021. The likely signature of nonlinear resonant mode coupling. *Astron. Astrophys.* 585:A22. doi: 10.1051/0004-6361/201526300

Conflict of Interest: The author declares that the research was conducted in the absence of any commercial or financial relationships that could be construed as a potential conflict of interest.

frontiers in Astronomy and Space Sciences

REVIEW
published: 19 October 2020
doi: 10.3389/fspas.2020.578584

Asteroseismology of High-Mass Stars: New Insights of Stellar Interiors With Space Telescopes

*Dominic M. Bowman**

Institute of Astronomy, KU Leuven, Leuven, Belgium

Massive stars are important metal factories in the Universe. They have short and energetic lives, and many of them inevitably explode as a supernova and become a neutron star or black hole. In turn, the formation, evolution and explosive deaths of massive stars impact the surrounding interstellar medium and shape the evolution of their host galaxies. Yet the chemical and dynamical evolution of a massive star, including the chemical yield of the ultimate supernova and the remnant mass of the compact object, strongly depend on the interior physics of the progenitor star. We currently lack empirically calibrated prescriptions for various physical processes at work within massive stars, but this is now being remedied by asteroseismology. The study of stellar structure and evolution using stellar oscillations—asteroseismology—has undergone a revolution in the last two decades thanks to high-precision time series photometry from space telescopes. In particular, the long-term light curves provided by the MOST, CoRoT, BRITE, Kepler/K2, and TESS missions provided invaluable data sets in terms of photometric precision, duration and frequency resolution to successfully apply asteroseismology to massive stars and probe their interior physics. The observation and subsequent modeling of stellar pulsations in massive stars has revealed key missing ingredients in stellar structure and evolution models of these stars. Thus, asteroseismology has opened a new window into calibrating stellar physics within a highly degenerate part of the Hertzsprung–Russell diagram. In this review, I provide a historical overview of the progress made using ground-based and early space missions, and discuss more recent advances and breakthroughs in our understanding of massive star interiors by means of asteroseismology with modern space telescopes.

Keywords: asteroseismology, stars: interiors, stars: oscillations, stars: evolution, stars: rotation, stars: massive, stars: early-type

OPEN ACCESS

Edited by:
Anthony Eugene Lynas-Gray, University College London, United Kingdom

Reviewed by:
Richard Townsend, University of Wisconsin-Madison, United States
Hideyuki Saio, Tohoku University, Japan

***Correspondence:**
Dominic M. Bowman
dominic.bowman@kuleuven.be

Specialty section:
This article was submitted to Stellar and Solar Physics, a section of the journal Frontiers in Astronomy and Space Sciences

Received: *30 June 2020*
Accepted: *24 August 2020*
Published: *19 October 2020*

Citation:
Bowman DM (2020) Asteroseismology of High-Mass Stars: New Insights of Stellar Interiors With Space Telescopes. Front. Astron. Space Sci. 7:578584. doi: 10.3389/fspas.2020.578584

1. INTRODUCTION

Stars are the essential building blocks of planetary systems, stellar clusters and galaxies. The lives and energetic deaths of massive stars, i.e., those with birth masses larger than ∼8 times that of the Sun (8 $M_{\odot}$)—play a pivotal role in shaping the Universe (Maeder and Meynet, 2000; Maeder, 2009; Kippenhahn et al., 2012; Langer, 2012). Massive stars were amongst the first stars in our Universe (Bromm and Larson, 2004; Bromm et al., 2009), and are progenitors of core-collapse supernovae and gamma-ray bursts (Heger et al., 2003; Smartt, 2009; Tanvir et al., 2009; Modjaz et al., 2019). The properties of massive stars allow them to be observed at large distances (see e.g., Stark, 2016),

hence allow us to study the early epochs of the Universe including the re-ionization of the Universe and the formation of the first galaxies (Bromm and Larson, 2004; Robertson et al., 2010).

Massive stars typically form in dense, cold and large molecular clouds with one of the important signatures of massive star formation being giant filament structures and powerful bi-polar outflows when they are embedded in such dense clouds—see the recent review by Rosen et al. (2020). After the formation phase, massive stars enter the so-called main sequence phase of stellar evolution, which is defined by the onset of hydrogen fusion in the core via the CNO cycle whilst maintaining hydrostatic equilibrium. The length of the main sequence is governed by the nuclear time scale, with more massive stars having shorter main sequence life times. During their lives, massive stars produce intense radiation fields from their high luminosities and experience line-driven winds, which together play major roles in the shaping of their environment (Kippenhahn et al., 2012; Langer, 2012). The majority of massive stars experience an explosive death as a supernova, which provides mechanical and chemical feedback to the interstellar environment (Mac Low and Klessen, 2004; de Rossi et al., 2010; Hopkins et al., 2014; Crowther et al., 2016; Stark, 2016) and can trigger a new generation of stars and planets. The exotic compact remnants of massive star evolution are neutron stars and black holes, with the latter being end products for many of the higher-mass progenitor stars. These remnants facilitate important tests of Einstein's theory of General Relativity and the study of the Universe using gravitational waves when they coalesce (Abbott et al., 2016, 2019). Hence, understanding the evolution of massive stars and their roles as supernovae and gravitational-wave progenitors represent fundamental questions in astronomy (Smartt, 2009; Langer, 2012). It is especially important to understand massive star evolution since there is a strong dependence of a supernova's chemical yield and the mass of the remnant on the interior physics of the progenitor star (Hirschi et al., 2005; Nomoto et al., 2006; Langer, 2012; Stark, 2016), and because of the large diversity in observed supernovae light curves (Dessart and Hillier, 2019).

Despite the importance of massive stars in our Universe, their physics is not yet fully understood. There are still many questions spanning all evolutionary phases, and specifically how their formation, evolution and inevitable deaths differ to those of the more common intermediate- and low-mass stars (Langer, 2012). A major shortcoming of current stellar evolution models is that they contain large theoretical uncertainties for massive stars, which is evident already during the earliest phases of stellar evolution including the main sequence. Consequently these uncertainties propagate and strongly impact the post-main sequence stage of stellar evolution (Maeder and Meynet, 2000; Ekström et al., 2012; Chieffi and Limongi, 2013). Hence the power of models for predicting if a massive star will explode as a supernova, the corresponding chemical yield and the mass of the compact remnant are limited by the accuracy of models reproducing the observed properties of stars prior to them exploding as supernovae.

Since massive stars have convective cores and radiative envelopes during the main sequence, the physics and numerical implementation of convection and convective-boundary mixing is crucial in determining their core masses and subsequent evolution (Gabriel et al., 2014; Georgy et al., 2014; Paxton et al., 2018, 2019). The mixing profile at the interface of convective and radiative regions, and the mixing profile within the envelope directly impact the amount of hydrogen available for nuclear burning. With more internal mixing, a massive star experiences a longer main sequence and produces a larger helium core mass at the end of the main sequence since fresh hydrogen from the envelope is readily supplied to the convective core (Miglio et al., 2008b; Kippenhahn et al., 2012; Pedersen et al., 2018; Michielsen et al., 2019). In the case of single, slowly rotating and non-magnetic massive stars, it is the internal mixing profile and helium core mass that dictates the evolution beyond the main sequence and determines the ultimate end state. However, probing the physical processes beneath the opaque surfaces of massive stars is practically impossible using standard methods and techniques in astronomy, such as spectroscopy.

Rotation plays a major role among massive stars, specifically because rotationally induced mixing is expected within their interiors (Zahn, 1992; Maeder and Meynet, 2000). Yet prescriptions for such mixing profiles are currently assumed in models and controlled by numerous free parameters that have yet to be empirically calibrated. This represents a large source of uncertainty within theoretical evolution models when estimating the masses and ages of high-mass stars (see e.g., Aerts, 2020 and Serenelli et al., 2020 for recent detailed reviews). The combined influence of various rotation rates, different metallicity regimes and mass loss through stellar winds also introduce strong degeneracies within evolutionary models of massive stars (Maeder and Meynet, 2000; Georgy et al., 2011, 2013; Ekström et al., 2012; Chieffi and Limongi, 2013; Groh et al., 2019). Furthermore, based on dedicated studies, such as MiMeS (Wade et al., 2016), the BOB campaign (Morel et al., 2015), and the BRITE spectropolarimetric survey (Neiner et al., 2017), ∼10% of massive stars are inferred to host a large-scale magnetic field with polar field strengths that range from ∼100 G up to a few kG. The degeneracies within evolutionary models are also more complex when dealing with the presence of magnetic fields in massive stars (Alecian et al., 2014; Shultz et al., 2018; Keszthelyi et al., 2019, 2020).

It is known that many massive stars are members of multiple systems, which interact over the course of their lifetimes, so theoretical uncertainties are further compounded by the effects of binarity and mass transfer (Podsiadlowski et al., 1992; Sana et al., 2012; de Mink et al., 2013; Duchêne and Kraus, 2013; Moe and Di Stefano, 2017). However, despite the complexities associated with rotation, metallicity, mass loss and magnetic fields, massive stars in multiple systems have proven extremely useful in probing and mitigating model parameter uncertainties (Guinan et al., 2000; Hilditch et al., 2005; Torres et al., 2010; Tkachenko et al., 2014, 2016; Almeida et al., 2015; Abdul-Masih et al., 2019; Johnston et al., 2019; Mahy et al., 2020a,b). This is primarily because binary studies have the potential to provide masses and radii from the stars' relative orbital motion around a common center of mass. Moreover, accurate, absolute and model-independent masses and radii are achievable in the case of eclipsing binary

systems (see e.g., Southworth et al., 2020 and Tkachenko et al., 2020) owing to the ability to simultaneously model spectroscopic radial velocities together with the eclipse depths in the light curve of a binary system.

To truly maximize the predictive power of evolutionary models for massive stars, it is essential to calibrate their physical prescriptions and parameters using stringent observational constraints on stellar interiors. One of the most successful and novel methodologies for this is called asteroseismology, which uses the resonant oscillation frequencies of stars to probe their structure—see the research monograph by Aerts et al. (2010). Until recently, most observational studies of massive stars have focused on the determination of global and/or average properties of these stars, such as the effective temperature and surface gravity derived from spectroscopy being used to estimate masses and ages. On the other hand, the recent space photometry revolution has truly brought asteroseismology to the forefront of astronomy as a means to calibrate stellar evolution theory across the Hertzsprung–Russell (HR) diagram (Chaplin and Miglio, 2013; Hekker and Christensen-Dalsgaard, 2017; García and Ballot, 2019; Aerts, 2020).

In this review, I discuss the progress that has been made in constraining the interiors of massive stars by means of asteroseismology and the space photometry revolution made possible thanks to modern space missions. In section 2, I provide a brief overview of asteroseismology, its methodology, and the types of pulsating massive stars it can be applied to. In section 3, an overview of the space telescopes that have led to the space photometry revolution is described. In section 4, I discuss the recent advances in massive star interiors made by means of asteroseismology, and section 5 describes the state-of-the-art of variability studies in some of the most massive stars. I finish by discussing the current challenges and future prospects for asteroseismology of high-mass stars in section 6.

2. ASTEROSEISMOLOGY

A powerful method for probing and constraining the physics of stellar interiors is asteroseismology, which uses stellar oscillations to probe the physics of stellar structure (Aerts et al., 2010). The pulsation modes of stars are standing waves exhibiting nodes and anti-nodes and are described by spherical harmonics. In the case of non-rotating and non-magnetic stars, the wavefunctions of stellar pulsations are separable into the radial and angular directions. The radial parts of the wavefunction solutions are characterized by the radial order n. Whereas, the angular dependence is characterized by the angular degree ℓ (number of surface nodes), and the azimuthal order m (where $|m|$ is the number of surface nodes that are lines of longitude). The simplest example of a pulsation mode is a radial mode for which $\{\ell, m\} = 0$ such that the surface of a star expands and contracts during a pulsation cycle. More complex examples of pulsation modes include non-radial modes (i.e., $\ell > 0$), for which the indices ℓ and m define the surface geometry of the oscillation. As an example, the axisymmetric dipole mode (i.e., $\{\ell, m\} = \{1, 0\}$) has the stellar equator as a node. Thus, the northern and southern hemispheres of a star expand and contract in anti-phase with one another.

Although they have a common structure comprising a convective core and a radiative envelope during the main sequence, there are different types of pulsations that can be excited in massive stars. In general, however, the excitation mechanism of pulsation modes has been shown to be the heat-engine mechanism operating in the local maximum of the Rosseland mean opacity caused by iron-group elements—the so-called Z-bump (Dziembowski and Pamyatnykh, 1993; Dziembowski et al., 1993; Gautschy and Saio, 1993; Pamyatnykh, 1999; Miglio et al., 2007). This κ-mechanism gives rise to pulsation modes with properties and excitation physics which depend on the host star's mass, age and chemical composition. There are two main types of pulsation modes excited by the κ-mechanism in massive stars, which are defined based on their respective restoring force: pressure (p) modes and gravity (g) modes.

2.1. Pressure Modes

Pressure (p) modes are standing waves for which the pressure force acts as a restoring force (Aerts et al., 2010). Typically, p modes have high frequencies (i.e., pulsation periods of order several hours in massive stars), can be radial or non-radial and are mostly sensitive to the radiative envelopes of massive stars. For radial p modes, the entire interior of the star acts as a pulsation cavity, with the center of a star being a node and its surface an anti-node. In the cases of non-radial p modes, the depth of the pulsation cavity from the surface is determined by the local adiabatic sound speed $c(r)$. A non-radial pulsation mode encounters an increasing $c(r)$ when traveling inward from the stellar surface, which causes it to travel faster and be refracted. The depth a non-radial p mode can reach is called its turning radius, r_t, which is proportional to $\sqrt{\ell(\ell+1)}$ and defined outwards from the center of the star (Aerts et al., 2010). Thus, higher degree p modes have smaller pulsation cavities that are more sensitive to the stellar surface. The power of asteroseismology is that each pulsation has a cavity defined by a star's structure, such that each pulsation mode can be used as a direct probe of the physical processes at work within its cavity.

If the radial orders of p modes are sufficiently large such that the modes satisfy $n \gg \ell$, which is called the asymptotic regime, the pulsations are approximately equally-spaced in frequency (Tassoul, 1980). Deviations from a constant frequency spacing are possible, and become more prevalent for more evolved stars. During the main sequence phase of evolution the radius of a massive star increases and the core contracts, which drives the g- and p-mode pulsation cavities closer to one another as a result of an increasing Brunt-Väisälä frequency (Aerts et al., 2010). Consequently, this can cause a form of pulsation mode interaction called avoided crossings, in which p and g modes can exchange character whilst retaining their identities if their frequencies approach one another (Osaki, 1975). In more evolved cases, such as post-main sequence stars, the evanescent region between the p- and g-mode cavities inside massive stars decreases. This can allow p and g modes to couple with each other and form mixed modes, which are modes with the character of

a p mode in the envelope and the character of a g mode in the deep interior (Aerts et al., 2010). The regularities of asymptotic p modes in the amplitude spectra of low- and intermediate-mass stars has greatly simplified the issue of mode identification and facilitated asteroseismology for low-mass stars (see e.g., Chaplin and Miglio, 2013; Hekker and Christensen-Dalsgaard, 2017; García and Ballot, 2019), but are rarely observed in massive stars (see e.g., Belkacem et al., 2010; Degroote et al., 2010b). Such high-radial order p modes are generally not expected for massive stars owing to the excitation physics of the κ-mechanism being inefficient in driving such modes in massive stars (Dziembowski and Pamyatnykh, 1993; Dziembowski et al., 1993; Gautschy and Saio, 1993; Pamyatnykh, 1999; Miglio et al., 2007).

In the presence of rotation the frequency degeneracy of non-radial pulsation modes with respect to m is lifted, which serves as a unique method of mode identification in certain pulsating stars. The simplest case is for stars that rotate (very) slowly and rigidly, i.e., with a uniform interior rotation angular frequency Ω—such that the splitting of non-radial pulsation frequency, $\omega_{n\ell m}$, is given by

$$\omega_{n\ell m} = \omega_{n\ell} + m\,(1 - C_{n\ell})\,\Omega, \tag{1}$$

where $C_{n\ell}$ is the Ledoux constant which sets the size of the splitting due to the Coriolis force. In this idealized example, the result of Equation (1) produces a multiplet of pulsation frequencies separated by the stellar rotation frequency in the amplitude spectrum for p modes of high radial order or high-angular degree since $C_{n\ell} \simeq 0$ in such cases (Aerts et al., 2010). An example of rotationally-split quadrupole p modes is shown in **Figure 1**, using the example of KIC 11145123 originally discovered by Kurtz et al. (2014). The amplitude spectrum of the resultant quintuplet split by rotation shown in **Figure 1** uses both 1 and 4-years light curves to emphasize the significant improvement in the resolving power of longer light curves for asteroseismic studies of rotation. Therefore, if the rotation rate is sufficiently slow, p-mode multiplets serve as a means of determining the interior rotation rates of stellar envelopes using an almost model-independent methodology.

Beyond the first-order perturbative approach for including the Coriolis force in slow and rigid rotators given in Equation (1), second- and third-order perturbative formalisms have been discussed by, for example, Dziembowski and Goode (1992), Daszyńska-Daszkiewicz et al. (2002), and Suárez et al. (2010). As described by Suárez et al. (2010), it is important to note that the first-order perturbative treatment of the Coriolis force applied to p modes is only applicable for stars with rotation velocities below ∼15% of their critical breakup velocity, with faster rotating stars requiring more complex formalisms.

2.2. Gravity Modes

Gravity (g) modes are standing waves for which buoyancy (i.e., gravity) acts as a restoring force (Aerts et al., 2010). Typically, g modes have low frequencies, can only be non-radial and are mostly sensitive to the deep interiors of massive stars near their convective cores. In the asymptotic regime, g modes are equally spaced in period (Tassoul, 1980), and exhibit a characteristic

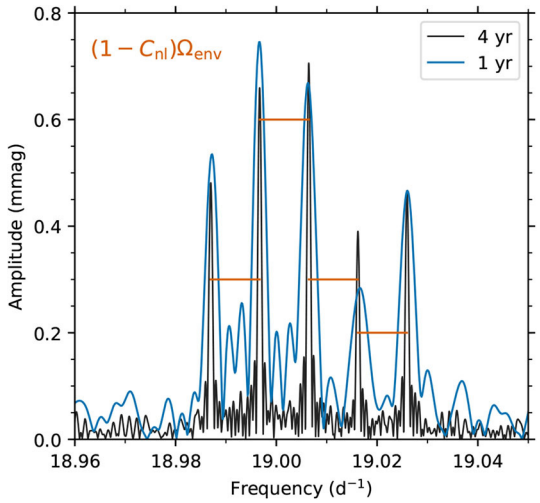

FIGURE 1 | Example of rotational splitting of quadrupole p modes into a quintuplet using both 1 and 4-years light curves of the star KIC 11145123 (Kurtz et al., 2014). Horizontal red lines correspond to the rotational splitting value of the modes.

period Π_0. In the case of a non-rotating and chemically-homogeneous star, Π_0 can be calculated from the individual g-mode periods, $P_{n,\ell}$, given by

$$P_{n\ell} = \frac{\Pi_0}{\sqrt{\ell\,(\ell+1)}}\,(|n| + \alpha)\,, \tag{2}$$

in which α is a phase term independent of the mode degree, ℓ, and

$$\Pi_0 = 2\pi^2 \left(\int_{r_1}^{r_2} N(r) \frac{\mathrm{d}r}{r} \right)^{-1}, \tag{3}$$

where r_1 and r_2 are the inner and outer boundaries of the g-mode pulsation cavity, and $N(r)$ is its Brunt-Väisälä frequency. Thus, Equation (2) defines a constant spacing in period for g modes of the same angular degree, ℓ, and consecutive radial order, n. Equation (3) demonstrates that the characteristic period, Π_0, is largely determined by the Brunt-Väisälä frequency, $N(r)$, which has a strong dependence on the mass of the convective core, and hence the mass and age of a star (Miglio et al., 2008a).

2.2.1. Interior Rotation

Since all massive stars rotate to some extent, the Coriolis force is also a dominant restoring force for g modes. Therefore, it is more appropriate to describe massive stars having gravito-inertial modes, for which both the Coriolis force and buoyancy are important. This is particularly true for pulsation modes with frequencies in the co-rotating frame below twice the rotation frequency (see Aerts et al., 2019a). As discussed in detail by Bouabid et al. (2013), the period spacing increases with period in the co-rotating frame for prograde modes, and decreases in the inertial frame. This is because in the co-rotating frame the effective $\ell(\ell + 1)$ (cf. Equation 2) for prograde sectoral

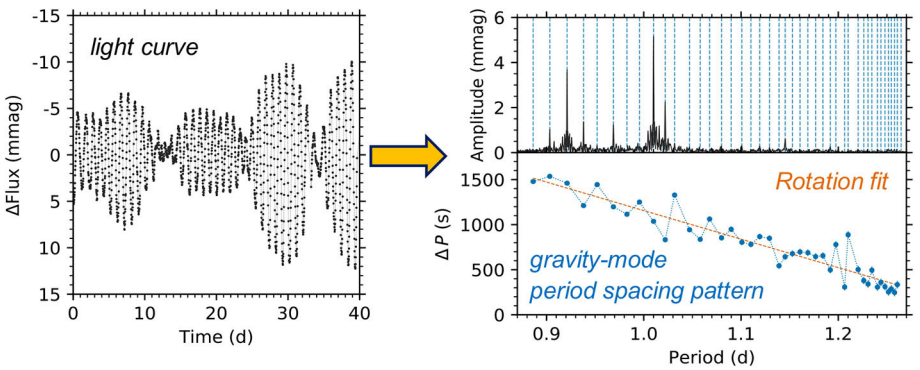

FIGURE 2 | Schematic of the methodology of constraining interior rotation using g modes. **(Left)** Light curve of the Slowly Pulsating B (SPB) star KIC 3459297 pulsating in low-frequency g modes (cf. Pápics et al., 2017). **(Right)** Amplitude spectrum and period-spacing pattern of the prograde g-mode pulsations in the light curve are shown as the top and bottom panels, respectively. Pápics et al. (2017) determined $f_{\rm rot} = 0.63 \pm 0.04$ d^{-1} from the g-mode period spacing pattern for KIC 3459297.

modes decreases with rotation due to the effect of Coriolis force. Whereas, in the inertial frame an increasing period spacing is caused by the frequency increase (i.e., period decrease) due to the effect of advection $|m|\Omega$. Therefore, for rotating stars as viewed in the inertial frame by an observer, one expects a decreasing period spacing for prograde g modes and an increasing period spacing for retrograde g modes.

Consequently, a powerful diagnostic in interpreting the oscillation spectrum of a rotating star pulsating in g modes is its period spacing pattern, which is defined as the period differences, ΔP, of consecutive radial order (n) gravity modes of the same angular degree (ℓ) and azimuthal order (m) as a function of the pulsation mode period, P. An example of an observed period spacing pattern for a series of prograde dipole g modes in the star KIC 3459297 (Pápics et al., 2017) is shown in **Figure 2**, in which a fit to the g-mode period spacing pattern reveals the near-core rotation rate—see Van Reeth et al. (2016), Ouazzani et al. (2017), and Pápics et al. (2017) for the application of this technique. Under the asymptotic approximation, g modes in a non-rotating, chemically homogenous star are equally spaced in period (cf. Equation 2), yet rotation and a chemical gradient left behind from nuclear burning within a receding convective core introduce perturbations in the form of a tilt and dips, respectively (Miglio et al., 2008a; Bouabid et al., 2013). Higher rotation rates induce a larger tilt with the gradient being negative for prograde modes and positive for retrograde modes in the inertial frame.

The commonly-used and mathematically appropriate approach to including rotation in the numerical computation of pulsation mode frequencies is the use of the Traditional Approximation for Rotation (TAR; Eckart, 1960; Lee and Saio, 1987a,b; Bildsten et al., 1996; Townsend, 2003b). Such a treatment of the Coriolis force is necessary for g-mode pulsators if $2\Omega/\omega \gtrsim 1$ (Aerts et al., 2018). This is because high-radial order g modes in moderately and rapidly-rotating stars are in the gravito-inertial regime (Aerts et al., 2019a). Within the formalism of the TAR, the horizontal component of the rotation vector is ignored, which is a reasonable assumption for gravito-inertial modes in main sequence stars given that the Lagrangian displacement vector is predominantly horizontal. The differential equations for non-radial pulsations in rotating stars are almost equivalent to those of non-rotating stars (using the Cowling approximation) if $\ell(\ell+1)$ is replaced by the eigenvalue of the Laplace tidal equation, λ. Hence, the mathematical framework of the TAR allows the asymptotic approximation to be used for high-radial g modes in rotating stars (see Lee and Saio, 1997, Townsend, 2003b and Townsend, 2003a). Today, the TAR has been used to probe the impact of rotation on g-mode period spacing patterns both theoretically (e.g., Bouabid et al., 2013) and observationally (e.g., Van Reeth et al., 2016), and has been extended by Mathis (2009) and Mathis and Prat (2019) to take into account differential rotation and the slight deformation of stars, respectively. The TAR is implemented within the state-of-the-art pulsation code GYRE (Townsend and Teitler, 2013; Townsend et al., 2018) and has been used by various observational studies to probe (differential) rotation inside g-mode pulsators (Van Reeth et al., 2016, 2018). We refer the reader to Aerts (2020) for a detailed discussion of the TAR and its application to pulsating stars.

2.2.2. Interior Mixing

Since massive stars have convective cores and radiative envelopes during the main sequence, the physics of convection and convective-boundary mixing is crucial in determining their core masses and evolution (Kippenhahn et al., 2012). The mixing profile at the interface of convective and radiative regions, and the mixing profile within the envelope directly impact the amount of hydrogen available for nuclear burning. Mixing at the boundary of convective regions, such as near the convective core in a main sequence star, is typically implemented as overshooting in numerical codes and expressed in terms of the local pressure scale height (Freytag et al., 1996; Herwig, 2000). This is predicated on the non-zero inertia of convective bubbles at a convective boundary causing them to overshoot into a radiative layer. In massive stars, the overshooting of the convective core (also known as convective-boundary mixing) entrains hydrogen from the envelope into the core resulting in a longer main sequence

lifetime and a larger helium core mass (Pedersen et al., 2018; Michielsen et al., 2019). This has a direct impact on the characteristic g-mode period, Π_0, of main-sequence stars with convective cores (Mombarg et al., 2019).

A non-zero amount of convective core overshooting is necessary when interpreting pulsations in massive stars using 1D stellar evolution codes (Dupret et al., 2004; Briquet et al., 2007; Daszyńska-Daszkiewicz et al., 2013b). Yet, the amount and shape of convective-boundary mixing remains largely unconstrained for such stars. Two examples of typical shapes of convective-boundary mixing profiles currently implemented in evolution codes include a step overshoot and an exponential overshoot (see e.g., Herwig, 2000; Paxton et al., 2015). Typically, these two prescriptions in the shape of convective core overshooting are referred to as $\alpha_{\rm ov}$ and $f_{\rm ov}$, respectively, in the literature and differ approximately by a factor of 10–12 (Moravveji et al., 2015). However, it is only recently that asteroseismology has demonstrated the potential to discriminate them in observations using g-mode period spacing patterns (Moravveji et al., 2015, 2016; Pedersen et al., 2018). Moreover, there is considerable ongoing work using 3D hydrodynamical simulations (Augustson and Mathis, 2019) and g-mode pulsations to probe the temperature gradient within an overshooting layer and ascertain if it is adiabatic, radiative, or intermediate between the two (Michielsen et al., 2019).

In addition to the need for convective-boundary mixing in massive stars, the origin of mixing within their radiative envelopes is also unconstrained within evolutionary models. Direct evidence for needing increased envelope mixing comes from enhanced surface nitrogen abundances in massive stars (Hunter et al., 2009; Brott et al., 2011). Since nitrogen is a by-product of the CNO cycle of nuclear fusion in a massive star (Kippenhahn et al., 2012), an efficient mixing mechanism in the stellar envelope must bring it to the surface. Rotationally-induced mixing has been proposed as a possible mechanism (Maeder and Meynet, 2000), but it is currently unable to explain observed surface nitrogen abundances in slowly-rotating massive stars in the Milky Way and low-metallicity Large Magellanic Cloud (LMC) galaxies (Hunter et al., 2008; Brott et al., 2011). Nor can rotational mixing fully explain surface abundances in massive overcontact systems (Abdul-Masih et al., 2019, 2020). Furthermore, there was no statistically-significant relationship between the observed rotation and surface nitrogen abundance in a sample of galactic massive stars studied by Aerts et al. (2014). In fact, the only robust correlation with surface nitrogen abundance in the sample was the dominant pulsation frequency (Aerts et al., 2014), which suggests that pulsations play a significant role in determining the mixing properties within the interiors of massive stars.

2.2.3. Period Spacing Patterns as Probes of Interior Rotation and Mixing

As previously illustrated in **Figure 2**, an observed g-mode period spacing pattern provides direct insight of the interior rotation rate of a star. Such patterns also allow the amount of interior mixing in terms of both convective core overshooting and envelope mixing to be determined. Since massive stars have a receding core whilst on the main sequence, they develop a chemical gradient in the near-core region as they evolve. Gravity modes are particularly sensitive to this molecular weight (μ) gradient and in the absence of large amounts of internal mixing this leads to mode trapping (Aerts, 2020). Thus, the g modes get trapped which leads to "dips" in the g-mode period spacing pattern on top of the overall "tilt" caused by rotation (cf. **Figure 2**).

An illustration of the effect of different amounts of interior mixing and rotation on the g-mode period spacing patterns of prograde dipole modes in a 12 $M_\odot$ star about halfway through the main sequence is shown in **Figure 3**. In the left column of **Figure 3**, the effect of increasing the amount of envelope mixing (denoted by $D_{\rm mix}$) is shown going from top to bottom. Whereas, in the right column, the effect of increasing the amount of convective core overshooting (denoted by $f_{\rm ov}$) is shown from top to bottom. Such values of $D_{\rm mix}$ and $f_{\rm ov}$ represent the range of values typically found by asteroseismic studies of stars with convective cores. Clearly, even for moderate values of envelope mixing (i.e., $D_{\rm mix} \simeq 10^4$ cm^2 s^{-1}), the presence of dips in the g-mode period spacing pattern are strongly diminished, as shown in the bottom-left panel of **Figure 3**. Thus, the observed presence of strong dips in g-mode period spacing patterns already places an upper limit on the amount of envelope mixing possible in such stars. In all panels of **Figure 3**, three different rotation rates are shown in green, blue and red, demonstrating the significant affect of rotation for g modes, which correspond approximately to rotation frequencies of 0.0, 0.1, and 0.2 d^{-1}, respectively. The effect of rotation was calculated assuming rigid rotation using the TAR implemented in the GYRE pulsation code (Townsend and Teitler, 2013; Townsend et al., 2018).

Yet, it is possible that only some, or even none, of the pulsation modes shown in **Figure 3** are observed in massive stars, since the excitation of a given pulsation mode depends on stellar parameters, including mass, age, metallicity. The example using a 12 $M_\odot$ shown in **Figure 3** does not include any predictions of mode excitation. Nevertheless, **Figure 3** serves as a schematic example of similar behavior for any main sequence star born with a convective core. In summary, the morphology of an observed g-mode period spacing pattern facilitates mode identification and offers a direct measurement of the near-core rotation and chemical mixing within a star. In practice, asteroseismology of g modes requires long-term and high-precision time series (space) photometry to extract g-mode period spacing patterns. These patterns consequently allows one to measure the interior rotation and constrain the envelope mixing of the host star, and the corresponding characteristic g-mode period, Π_0, which places constraints on its mass and age. From a large and multi-dimensional grid of stellar structure models covering the possible values of mass, age, and interior mixing parameterized by $f_{\rm ov}$ and $D_{\rm mix}$, a quantitative comparison of observed and theoretical g-mode period spacing patterns facilitates asteroseismology to derive the interior properties of massive stars (Aerts et al., 2018).

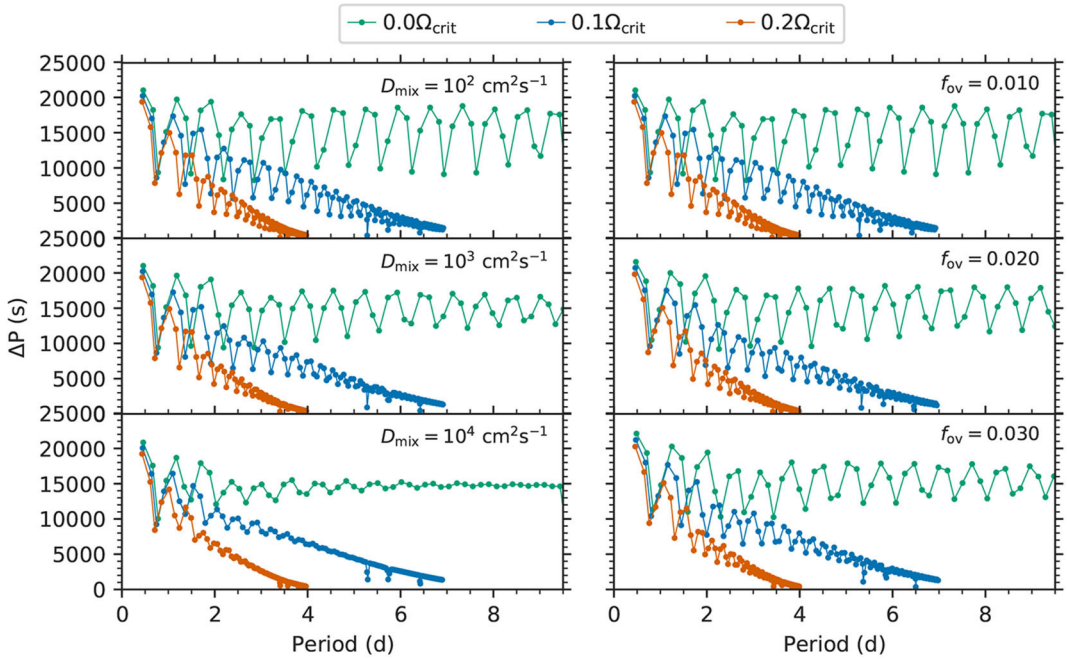

FIGURE 3 | Theoretical g-mode period spacing patterns for prograde dipole modes of a 12 $M_\odot$ star about halfway through the main sequence (i.e., $X_c = 0.4$). The left and right columns are for different envelope mixing (D_{mix}) in cm^2 s^{-1}, and exponential convective-boundary mixing (f_{ov}) expressed in local pressure scale heights, respectively, calculated using the MESA stellar evolution code (Paxton et al., 2019). For each panel, three different rotation rates expressed as a fraction of the critical rotation rate, Ω_{crit}, calculated using the Traditional Approximation for Rotation (TAR) using the GYRE pulsation code (Townsend and Teitler, 2013) are shown.

2.3. Instability Domains of High-Mass Stars

The common interior structures of massive stars includes a convective core and radiative envelope, with pulsations in these stars being driven by the κ-mechanism operating within the local opacity enhancements caused by the Z-bump associated with iron-peak elements in their near-surface layers (Dziembowski and Pamyatnykh, 1993; Dziembowski et al., 1993; Gautschy and Saio, 1993; Pamyatnykh, 1999; Miglio et al., 2007). The depth of the Z-bump at $T \simeq 200{,}000$ K depends on the effective temperature of the star and in turn defines an upper and lower temperature boundary for the instability region of the κ-mechanism in the HR diagram, which are sometimes referred to the blue and red edges of an instability region, respectively. In addition to the mass, radius and effective temperature of a star, which define its thermal structure, the metallicity and choice of opacity table in models are also important parameters (Dziembowski and Pamyatnykh, 2008; Paxton et al., 2015; Walczak et al., 2015; Daszyńska-Daszkiewicz et al., 2017). Since the κ-mechanism operates in the Z-bump, it requires a sufficiently-large opacity enhancement to block radiation and excite coherent pulsation modes. This is supported by theoretical models of pulsation excitation, and observations which indicate a dearth of massive pulsators in low-metallicity environments, such as the LMC galaxy with $Z \simeq 0.5\,Z_\odot$ (see e.g., Salmon et al., 2012).

Furthermore, rotation plays an important role in defining the instability regions of massive stars. From an observational perspective, moderate and fast rotation distorts the spherical symmetry of a star. This has significant implications for the spectroscopic determination of atmospheric parameters, such as the effective temperature and surface gravity, as these parameters are significantly affected by gravity darkening (von Zeipel, 1924; Townsend et al., 2004; Espinosa Lara and Rieutord, 2011). From a more theoretical perspective, the distorted spherical symmetry of rapidly-rotating stars impacts the applicability of using 1D models, and because phenomena associated with rapid rotation, such as rotationally-induced mixing, can significantly influence evolutionary tracks in the HR diagram (Maeder and Meynet, 2000; Maeder, 2009; Lovekin, 2020). Moreover, as discussed in section 2.2.1, the Coriolis force perturbs the pulsation frequencies of a rotating star and consequently also the expected parameter range of instability regions in the HR diagram (Townsend, 2005; Bouabid et al., 2013; Szewczuk and Daszyńska-Daszkiewicz, 2017).

The calculation of instability regions for stars requires non-adiabatic calculations, and specifically the calculation of a pulsation mode's growth rate (Unno et al., 1989; Aerts et al., 2010). Following the laws of thermodynamics, heat-driven pulsation modes require that heat is gained in phase with compression during a pulsation cycle. A non-adiabatic pulsation calculation yields a mode's eigenfrequency, and its imaginary component yields the growth rate. For heat-driven modes excited by the κ-mechanism, the growth rate is a positive quantity for modes that are effectively excited and negative for modes that are damped (Unno et al., 1989; Aerts et al., 2010). The instability regions of pulsations in massive stars for different masses, ages,

metallicities, and rotation rates can be readily calculated for early-type stars by means of stellar structure and evolution codes, such as MESA (Paxton et al., 2011, 2013, 2015, 2018, 2019), when coupled to non-adiabatic stellar pulsation codes, such as GYRE (Townsend and Teitler, 2013; Townsend et al., 2018). We refer the reader to Moravveji (2016), Godart et al. (2017), and Szewczuk and Daszyńska-Daszkiewicz (2017) for instability regions of main-sequence massive stars calculated with and without rotation, and to Daszyńska-Daszkiewicz et al. (2013a) and Ostrowski and Daszyńska-Daszkiewicz (2015) for instability calculations for post-main sequence massive stars.

Amongst the early-type stars, there are two main groups of stars that pulsate in coherent pulsation modes excited by the κ-mechanism: the β Cephei (β Cep) stars and the Slowly Pulsating B (SPB) stars, which together span the approximate mass range from 3 to 25 $M_\odot$. Although not traditionally classified as a distinct pulsator group amongst massive stars, the pulsating Be stars are also discussed in this section for completeness. Pulsations in more evolved and/or more massive stars have also been detected, such as those in periodically variable supergiant (PVSG) stars (Aerts et al., 2010). However, they are not included here since there are currently very few asteroseismic studies of these objects. The reader is referred to Saio et al. (2006) and Ostrowski et al. (2017) for insightful work on the variability of such stars.

2.3.1. β Cephei Stars

The β Cephei (β Cep) stars are Population I stars with spectral types ranging from late O to early B on the main sequence, and have birth masses larger than some 8 $M_\odot$ and up to 25 $M_\odot$. They pulsate in low-radial order g and p modes excited by the κ-mechanism operating in the Z-bump (Dziembowski and Pamyatnykh, 1993), and have pulsation periods that range between about 2 and 8 h (Stankov and Handler, 2005; Pigulski and Pojmański, 2008a,b; Aerts et al., 2010). Most β Cep stars are dwarf stars, making them likely main sequence stars, although a significant fraction are giants or supergiants. Our understanding of the driving of low-radial order g modes in high-mass β Cep stars remains somewhat elusive (Handler et al., 2004, 2017; Aerts et al., 2004a), since a substantial overabundance of iron and nickel in the Z-bump is typically needed for the κ-mechanism to be efficient at exciting g modes in such stars (Pamyatnykh et al., 2004; Moravveji, 2016; Daszyńska-Daszkiewicz et al., 2017). Moreover, in addition to the mode excitation by the κ-mechanism, β Cep stars have been shown to exhibit non-linear mode excitation (Degroote et al., 2009) and stochastically-excited pulsation modes (Belkacem et al., 2009, 2010; Degroote et al., 2010b), which demonstrate that multiple pulsation driving mechanisms exist in these stars.

2.3.2. Slowly Pulsating B Stars

The Slowly Pulsating B (SPB) stars are the lower-mass counterparts of the β Cep stars, with the original definition of this type of variable star made by Waelkens (1991) although individual examples of SPB stars were known previously (e.g., 53 Persei; Smith and McCall, 1978). The SPB stars are Population I stars with spectral types that range from B3 to B9 on the main sequence, thus they have birth masses between ∼3 and 8 $M_\odot$ (Aerts et al., 2010). They pulsate in high-radial order and predominantly prograde dipole g modes excited by the κ-mechanism operating in the Z-bump (Dziembowski et al., 1993; Gautschy and Saio, 1993) and have pulsation periods that range between a few days and several hours (Waelkens et al., 1998b; Aerts et al., 1999b; De Cat and Aerts, 2002).

2.3.3. Pulsating Be Stars

A subset of ∼20% of non-supergiant massive stars are classified as Be stars (Porter and Rivinius, 2003). This group comprises stars that have shown Balmer lines in emission on at least one occasion, since such emission lines are known to be transient (Zorec and Briot, 1997; Neiner et al., 2011; Rivinius et al., 2013). The Be stars are rapid rotators with circumstellar decretion disks, and their near-critical rotation rates are thought to be related to their evolutionary history. More specifically, Be stars may have accreted mass from a companion or are the result of a stellar merger, which is supported by the relative rarity of Be stars with main-sequence companions (Bodensteiner et al., 2020). Many Be stars show evidence of pulsations and experience outbursts of material thought to be driven by pulsations (Rivinius et al., 2003; Huat et al., 2009; Kurtz et al., 2015). The pulsational behavior of Be stars is quite diverse, with such stars showing coherent g modes and stochastically excited gravito-interial waves, with the amplitude of their pulsations being connected to whether the star is mid-outburst or in quiescence (Kambe et al., 1993; Porter and Rivinius, 2003; Neiner et al., 2009, 2012b; Baade et al., 2016). Given the diverse variability seen in Be stars, it remains unclear if a single excitation mechanism is unanimously responsible for exciting pulsations in Be stars, with their fast rotation being their main common characteristic (Porter and Rivinius, 2003; Townsend et al., 2004).

3. THE SPACE PHOTOMETRY REVOLUTION

The successful application of asteroseismology requires long-term, continuous and high-precision time series data to resolve individual pulsation mode frequencies, and perform unambiguous mode identification. As discussed in sections 2.1 and 2.2.3, mode identification using the continuous photometry provided by space telescopes can be readily achieved using rotationally-split modes and period spacing patterns, respectively. However, prior to space telescope missions different techniques were more common. Nevertheless, once mode identification has been achieved, a quantitative comparison of observed pulsation mode frequencies and those predicted by theoretical models in addition to atmospheric constraints, such as the effective temperature and metallicity from spectroscopy reveals the physics that best represents the observed star—a fitting process known as forward seismic modeling (Aerts et al., 2018).

3.1. Prior to Space Telescopes

Prior to the near-continuous photometry provided by space telescopes, pulsation modes in massive stars were identified by

means high-resolution and high-cadence spectroscopic and/or photometric time series data assembled using ground-based telescopes (e.g., Smith, 1977; Waelkens, 1991; De Cat et al., 2005). In the early days of massive star asteroseismology, mode identification via spectroscopic line profile variations (LPVs) targeted the silicon triplet at 4,560 Å in slowly-rotating β Cep stars (Gies and Kullavanijaya, 1988; Aerts et al., 1992, 1994a,b; Aerts and Waelkens, 1993; Telting and Schrijvers, 1997; Telting et al., 1997; Uytterhoeven et al., 2004, 2005), whereas for SPB stars the silicon doublet at 4,130 Å was also useful (Aerts et al., 1999a; Aerts and De Cat, 2003). A spectral resolving power of at least 50,000 and a very high signal-to-noise being preferable. In fast rotating B stars, such as Be stars, these silicon multiplets can be blended and one must target isolated lines, such as the helium I 6,678 Å line (e.g., Balona and Kambe, 1999; Balona et al., 1999; Maintz et al., 2003; Štefl et al., 2003). Balmer lines are not suitable for LPV studies as they are less sensitive to the radial and non-radial velocities of pulsations since they are dominated by intrinsic (i.e., Stark) broadening. For a complete discussion of mode identification using spectroscopic time series, we refer the reader to Aerts et al. (2010).

An alternative and complementary methodology to using LPVs in the identification of pulsation modes in massive stars is to use amplitude ratios from multi-color photometry. Originally devised by Watson (1988) and Heynderickx et al. (1994), this approach was particularly effective when applied to β Cep stars owing to their relatively high amplitude and short-period pulsations. We refer the reader to Shobbrook et al. (2006), Handler et al. (2012) and Handler et al. (2017) for examples of this technique. The analysis of ground-based photometry and/or spectroscopy has been successful in demonstrating the importance of constraining parameters, such as convective core overshooting, rotation and metallicity in massive star evolution (Aerts et al., 2003; Handler et al., 2004, 2006; Briquet et al., 2007; Daszyńska-Daszkiewicz et al., 2013b; Szewczuk and Daszyńska-Daszkiewicz, 2015).

3.2. Early Space Missions

When the era of space telescopes dawned, the revolution of asteroseismology for stars across the HR diagram truly began. Space telescopes not only provide long-term and near-continuous observations of multiple stars simultaneously, but the typical precision of space-based photometry is at least two orders of magnitude better than what is possible from the ground. Such early space missions, which were not designed for asteroseismic surveys but nonetheless were extremely useful, included the *Hipparcos* mission (van Leeuwen et al., 1997), which discovered hundreds of pulsating B stars (Waelkens et al., 1998a; Aerts et al., 2006c; Lefèvre et al., 2009). The drastically improved time series data allowed low-amplitude pulsation modes to be detected in stars previously believed to be constant, and yielded precise pulsation frequencies in multi-periodic pulsators that are dominated by complex beating patterns (Koen and Eyer, 2002).

The first space telescope dedicated to asteroseismology was the MOST mission, which was launched in 2003 (Walker et al., 2003). The MOST spacecraft may have been a small telescope, but it detected pulsations in a wide variety of different types of variable stars. Among the massive stars, MOST studied SPB, β Cep, and Be stars (Walker et al., 2005; Aerts et al., 2006a,b; Saio et al., 2007a,b; Cameron et al., 2008), including rare instances of β Cep stars in eclipsing binary systems (Desmet et al., 2009a,c). Simultaneous MOST photometry and ground-based spectroscopy proved vital in understanding and modeling the first massive star exhibiting hybrid p- and g-mode behavior, γ Peg (Handler et al., 2009; Walczak et al., 2013). Furthermore, MOST detected pulsations in blue supergiants, such as Rigel (Saio et al., 2006; Moravveji et al., 2012), and interestingly it also detected pulsations in some Wolf-Rayet stars (Lefèvre et al., 2005; Moffat et al., 2008a) but the absence of pulsations in others (Moffat et al., 2008b). Although the time series photometry assembled by the MOST mission was limited in length, it served as a valuable proof-of-concept exercise demonstrating the power of massive star asteroseismology using space telescopes compared to facilities on the ground.

The next major milestone in the space photometry revolution was the French-led CoRoT mission launched in 2006 (Auvergne et al., 2009). The CoRoT spacecraft was a combined planet hunting and asteroseismology focused mission, which delivered short-cadence (i.e., 32 s) time series photometry for different fields of view across the sky for up to 150 days (Baglin et al., 2009). Over the mission duration, CoRoT contributed a wealth of information concerning variability in massive stars, with some aspects remaining unchallenged in quality and impact more than a decade later. The CoRoT fields of view were optimized to contain hundreds of candidate pulsating B stars (Degroote et al., 2009), which included β Cep, SPB, and Be stars (Degroote et al., 2009; Aerts et al., 2011, 2019b; Briquet et al., 2011; Pápics et al., 2011; Neiner et al., 2012b; Degroote, 2013). The mission was a great success for massive star variability studies, with CoRoT detecting regular frequency spacings in the O8.5 V star HD 46149 (Degroote et al., 2010b), and providing firm confirmation that massive stars can pulsate in both p- and g-mode frequencies (Degroote et al., 2012). Furthermore, CoRoT led to the first discovery of deviations from a constant period spacing in the B3 V star HD 50230 (Degroote et al., 2010a). In addition to high-precision asteroseismology of targeted β Cep stars (Aerts et al., 2011, 2019a), CoRoT also discovered stochastic variability caused by pulsations in massive star photospheres. This includes stochastic non-radial pulsations in B stars (Belkacem et al., 2009; Neiner et al., 2012b) and stochastic low-frequency variability in the three O stars HD 46223, HD 46150, and HD 46966 (Blomme et al., 2011; Bowman et al., 2019a).

Of all the space photometry missions available for asteroseismology, the BRITE-constellation of nanosatellites is ranked amongst the highest for providing excellent asteroseismic returns considering its budget and etendue (Weiss et al., 2014; Pablo et al., 2016). The constellation of nanosatellites from the collaboration of Austria, Poland, and Canada, was originally launched in 2013 and have provided long-term time series photometry of some of the brightest stars in the sky. This includes β Cep, SPB and Be stars (Baade et al., 2016; Pigulski et al., 2016; Daszyńska-Daszkiewicz et al., 2017; Handler et al., 2017; Walczak et al., 2019), but also pulsating stars in multiple systems (Kallinger et al., 2017; Pablo et al., 2017, 2019) and

stochastic variability in O supergiants and Wolf-Rayet stars (Buysschaert et al., 2017b; Ramiaramanantsoa et al., 2018a,b, 2019). The multi-color and long-term photometry of BRITE and its observing strategy are naturally complementary to combing BRITE data with simultaneous ground-based photometry and/or spectroscopy (e.g., Handler et al., 2017).

3.3. The *Kepler* and K2 Missions

Perhaps the most famous of all space telescopes providing time series photometry, the *Kepler* space telescope was launched in 2009 and had a primary goal of finding Earth-like planets orbiting Sun-like stars (Borucki et al., 2010; Koch et al., 2010). Although by the end of the nominal *Kepler* mission, the 4-years light curves of more than 200,000 stars proved invaluable for asteroseismology as well as exoplanet studies. Massive stars ($> 8\ M_\odot$) were purposefully avoided by the *Kepler* mission since they are bright and typically saturated the CCDs, although dozens of SPB stars and rotationally-variable B stars were discovered (McNamara et al., 2012; Balona et al., 2015). Since the end of the nominal 4-years *Kepler* mission, the extremely high precision light curves have been used to discover and analyse rotationally-split modes and period spacing patterns of prograde dipole g modes in dozens of SPB stars (Pápics et al., 2014, 2015, 2017). Such asteroseismic studies have revealed the interior rotation rates, convective core overshooting and mixing in main-sequence B stars (Moravveji et al., 2015, 2016; Szewczuk and Daszyńska-Daszkiewicz, 2018). Despite massive stars not being included in the *Kepler* field of view, ingenious techniques to extract the light curves of nearby massive stars have been successful (Pope et al., 2016, 2019a), which includes the scattered-light variability of the O9.5 Iab star HD 188209 (Aerts et al., 2017).

After ∼4 years the *Kepler* spacecraft lost a second vital reaction wheel, which meant that the field of view could not be maintained without a significant expenditure of fuel. A new mission, K2: *Kepler*'s second light, was devised by NASA, which consisted of 80-days campaigns pointing in the direction of the ecliptic (Howell et al., 2014). Since the K2 campaign fields included young star-forming regions, a plethora of massive stars were available to study using K2 light curves. The first proof-of-concept of O-star asteroseismology was demonstrated by Buysschaert et al. (2015), which acted as an important demonstration of the feasibility of massive star asteroseismology with space photometry. The K2 mission allowed the rotation, pulsation, and binary properties of the seven sisters of the Pleiades to be studied in detail for the first time thanks to its long time base and high precision (White et al., 2017). Since the end of the K2 mission in 2018, these high-precision data have revealed dozens of previously unknown β Cep and SPB stars (Pope et al., 2016, 2019b; Burssens et al., 2019) and ubiquitous stochastic low-frequency variability in the photospheres of massive stars (Bowman et al., 2019b).

3.4. The TESS Mission

The ongoing Transiting Exoplanet Survey Satellite (TESS; Ricker et al., 2015) is currently providing high-precision and short cadence (i.e., 2 min) observations for hundreds of thousands of stars across the sky. Each ecliptic hemisphere ($|b| > 6°$) is divided into 13 sectors which are each observed for up to 28 days. However, there is overlap of the observational sectors near the ecliptic poles, such that stars within the TESS continuous viewing zones (CVZ) have uninterrupted light curves spanning 1 year. Such an observing strategy is optimized to find transiting exoplanets orbiting bright stars across the sky, but TESS data are also extremely valuable for massive star asteroseismology. Amongst the earliest studies of massive star variability as viewed by TESS are those by Handler et al. (2019), Bowman et al. (2019b) and Pedersen et al. (2019) in which the diverse variability of massive stars is demonstrated using a total sample of more than 200 massive stars. The study by Handler et al. (2019) considers one of the first β Cep stars observed by the TESS mission, which revealed it to be multi-periodic and subsequent asteroseismic modeling indicated it was a runaway star because of its inferred age.

Since the first 13 sectors of TESS data in the southern ecliptic hemisphere have become available, Burssens et al. (2020) have completed a census of massive star variability using TESS data, and coupled this to high-resolution spectroscopy from the IACOB (Simón-Díaz et al., 2011, 2015; Simón-Díaz and Herrero, 2014) and OWN (Barbá et al., 2010, 2014, 2017) surveys. This allowed them to place more than 100 pulsating massive stars in the spectroscopic HR diagram. A summary of the variability catalog by Burssens et al. (2020) is shown in the spectroscopic HR diagram in **Figure 4**, in which the observed stars are shown as green circles overlaid on top of evolutionary tracks (gray lines) and theoretical instability regions for p and g modes (blue and

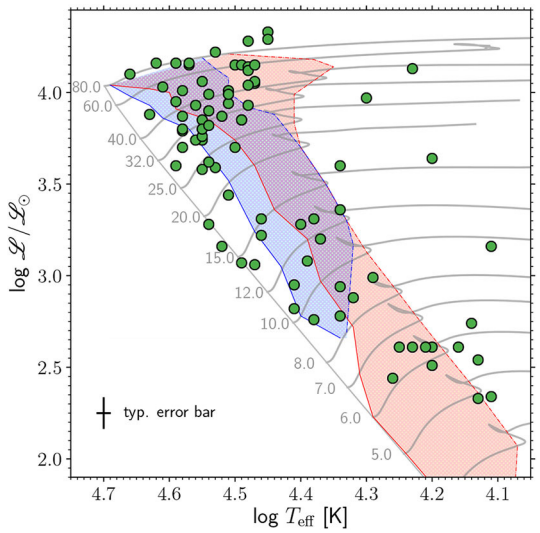

FIGURE 4 | Spectroscopic HR diagram of the pulsating massive stars observed by TESS in its sectors 1–13, which have spectroscopic parameters derived by high-resolution spectroscopy, are shown as green circles. Note that the ordinate axis shows spectroscopic luminosity such that $\mathscr{L} := T_{\rm eff}^4/g$ (Langer and Kudritzki, 2014). Red and blue hatched regions denote the theoretical instability regions of g and p modes, respectively, for main sequence stars. Non-rotating evolutionary tracks at solar metallicity (in units of $M_\odot$) are shown as solid gray lines, and a typical spectroscopic error bar is shown in the bottom-left corner. Figure adapted from Burssens et al. (2020), their Figure 3.

red hatched regions, respectively), which were calculated using the MESA evolution code (Paxton et al., 2019) and the GYRE pulsation code (Townsend and Teitler, 2013). Although there is general agreement between the observed location of pulsating stars and the predicted instability regions, the study by Burssens et al. (2020) clearly demonstrates that our understanding of the variability mechanisms in massive stars is far from complete given the overall distribution of stars within the HR diagram.

4. EMPIRICAL CONSTRAINTS ON MASSIVE STAR INTERIORS

In the previous section, it was described how early asteroseismic studies of massive star interiors were predominantly based on ground-based campaigns. The acquisition of these necessary data was painstakingly complex and required substantial dedication from all those involved, since it is non-trivial to collect and analyse such fragmented time series. However, despite the complications some aspects of these ground-based studies remain unrivaled to this day owing to the carefully-selected sample of stars and the relative exclusion of massive stars in later space missions. In particular, there remain only a handful of truly massive stars that have been undergone forward seismic modeling. In this section, some important case studies of pulsating massive stars that have studied using asteroseismology are presented. In particular the range of parameters that have been obtained via forward seismic modeling, where available, are summarized in **Table 1**, but we refer the reader to the individual studies for full details.

4.1. Ground-Based Studies

The first detailed study of the interior of a massive star using asteroseismology is arguably that of the slowly-rotating B3 V star V836 Cen (HD 129929) (Aerts et al., 2003, 2004b; Dupret et al., 2004). The analysis of the extensive ground-based data set consisting of multicolor Geneva photometry and high-resolution spectroscopy revealed HD 129929 to be a multiperiodic β Cep star pulsating in low-radial order g and p modes (Aerts et al., 2003, 2004b). The rotationally-split multiplets in HD 129929 yielded a non-rigid interior rotation rate where the near-core region was determined to be rotating a factor of $\sim$4 times faster than the envelope. This was the first measurement of the interior rotation rate of a main-sequence star. Subsequent forward seismic modeling allowed the best-fitting mass, age, metallicity, core hydrogen mass fraction, and convective core overshooting to be determined (Dupret et al., 2004), which are provided in **Table 1**.

An important example of extensive ground-based multicolor photometry and spectroscopy being used to probe the interior of a β Cep star is that of B2 III star ν Eri (HD 29248) (Handler and Aerts, 2002; Ausseloos et al., 2004; De Ridder et al., 2004; Handler et al., 2004; Pamyatnykh et al., 2004; Aerts et al., 2004a; Jerzykiewicz et al., 2005; Suárez et al., 2009; Daszyńska-Daszkiewicz and Walczak, 2010). At the time, and arguably still true today, ν Eri represents one of the best studied β Cep stars owing to the substantial data set having been assembled for the star. The spectroscopic and frequency analyses of this slowly-rotating ($\nu \sin i \lesssim 20$ km s^{-1}) star revealed rotationally-split low-radial order dipole g and p modes, and possibly high-radial order g modes (Handler et al., 2004; Aerts et al., 2004a). Forward seismic modeling of ν Eri was unable to find a satisfactory theoretical model unless an iron enhancement throughout the star, and in particular in the Z-bump, was included in the models to explain the mode excitation (Ausseloos et al., 2004; Pamyatnykh et al., 2004). The best-fitting parameters of ν Eri yielded a non-rigid interior rotation rate of $\sim$3–5 times faster in the near-core region compared to the envelope, although this is quite uncertain given the asymmetry of the small number of rotationally-split modes available (Ausseloos et al., 2004; Pamyatnykh et al., 2004). Later, Dziembowski and Pamyatnykh (2008), Suárez et al. (2009), and Daszyńska-Daszkiewicz and Walczak (2010) revisited the modeling of ν Eri and investigated its interior rotation, overshooting and mode excitation properties based on different opacity tables, specifically focusing on the relative abundance of iron in the Z-bump. In particular, these asteroseismic modeling studies were able to produce a better fit to the observed pulsation mode frequencies using larger overshooting values and an enhancement of iron in the Z-bump, albeit at the expense of not necessarily re-producing the inferred location of the star in the HR diagram. The best-fitting parameters from these studies are provided in **Table 1**, although the variance in the parameters can be understood as arising from the different metallicities and opacity tables being used.

A similarly famous β Cep star is 12 Lac (B1.5 III; HD 214993), which is comparable in mass to ν Eri although it is somewhat more rapidly rotating with a projected rotational velocity of $30 \lesssim \nu \sin i \lesssim 40$ km s^{-1} (Gies and Lambert, 1992; Abt et al., 2002). However, producing a satisfactory asteroseismic model for 12 Lac has been difficult owing to inconsistencies between observed and theoretically-predicted mode identifications, the consequential impact on the inferred interior rotation profile, and stellar opacity data being unable to explain the excitation of all observed pulsation mode frequencies (Aerts, 1996; Dziembowski and Jerzykiewicz, 1999; Handler et al., 2006; Dziembowski and Pamyatnykh, 2008; Desmet et al., 2009b). Despite these difficulties, Dziembowski and Pamyatnykh (2008) conclude based on the then-available observations of 12 Lac that it also exhibits an interior rotation rate of $\sim$4–5 times faster in the near-core region compared to the envelope. Desmet et al. (2009b) were able to constrain the parameters of 12 Lac, but the most advanced study of 12 Lac to date was performed by Daszyńska-Daszkiewicz et al. (2013b), who performed mode identification, asteroseismic modeling and studied how rotation, metallicity and opacity data significantly affect the modeling results.

The slowly-rotating ($\nu \sin i \simeq 30$ km s^{-1}) β Cep star θ Oph (B2 IV; HD 157056) was also subject to intense photometric campaigns to detect, extract and identify its variability (Briquet et al., 2005; Handler et al., 2005; Daszyńska-Daszkiewicz and Walczak, 2009). The frequency spectrum of θ Oph resembled that of V836 Cen in that it also contained a single radial mode and a handful of low-radial order rotationally-split multiplets, although one difference is that θ Oph is known to be a multiple system (Briquet et al., 2005). However, contrary to previous examples of

TABLE 1 | Best-fitting parameters of high-mass stars derived from forward seismic modeling of pulsations discussed in this review.

Star	Mass	Age	Z	X_c	Core overshooting		References
					α_{ov}	f_{ov}	
	($M_\odot$)	(Myr)					
V836 Cen (HD 129929)	9.35	16.3	0.0188	0.353	0.10 ± 0.05	–	Dupret et al., 2004
	9.23	–	0.0120	0.314	–	0.0365	Hendriks and Aerts, 2019
ν Eri (HD 29248)	9.0–9.9	16–20	0.0150	0.34–0.38	0.00–0.12	–	Pamyatnykh et al., 2004
	8.4	26.6	0.0115	–	0.21	–	Ausseloos et al., 2004
	7.13	14.82	0.019	0.139	0.28	–	Suárez et al., 2009
	8.01–9.77	16.2–29.1	0.014–0.018	0.247–0.279	0.03–0.35	–	Daszyńska-Daszkiewicz and Walczak, 2010
	9.0	–	0.015	–	0.163	–	Daszyńska-Daszkiewicz et al., 2017
	6.56	–	0.0195	0.275	–	0.0242	Hendriks and Aerts, 2019
θ Oph (HD 157056)	8.2 ± 0.3	–	0.009–0.015	0.38 ± 0.02	0.44 ± 0.07	–	Briquet et al., 2007
	8.00–8.81	7.20–7.38	0.01–0.02	0.35–0.42	0.07–0.39	–	Walczak et al., 2019
	7.21	–	0.0132	0.349	–	0.0402	Hendriks and Aerts, 2019
V2052 Oph (HD 163472)	8.2–9.6	16.9–23.7	0.010–0.016	0.25–0.32	0.00–0.15	–	Briquet et al., 2012
12 Lac (HD 214993)	10.2–14.4	11–23	0.015	0.13–0.21	0.0–0.4	–	Desmet et al., 2009b
	10.28	–	0.0115	–	0.39	–	Daszyńska-Daszkiewicz et al., 2013b
	12.80	–	0.0198	0.200	–	0.0187	Hendriks and Aerts, 2019
HD 50230	7–8	–	0.020	$\simeq 0.30$	0.2–0.3	–	Degroote et al., 2010a
	11.12	–	0.0200	0.045	–	0.0494	Hendriks and Aerts, 2019
	6.187 ± 0.025	$61.72^{+1.89}_{-0.21}$	0.0408 ± 0.0009	$0.3058^{+0.0006}_{-0.0007}$	–	0.0180 ± 0.0014	Wu and Li, 2019
HD 180642	11.4–11.8	12.4–13.0	0.008–0.014	0.21–0.25	< 0.05	–	Aerts et al., 2011
HD 46202	24.1 ± 0.8	4.3 ± 0.5	0.013–0.015	–	0.10 ± 0.05	–	Briquet et al., 2011
KIC 10526294	3.25	63	0.014	0.627	–	0.017	Moravveji et al., 2015
	5.25	–	0.0120	0.712	–	0.0348	Hendriks and Aerts, 2019
KIC 7760680	3.25 ± 0.05	202	0.020 ± 0.001	0.503 ± 0.001	–	0.024 ± 0.001	Moravveji et al., 2016
HD 43317	$5.8^{+0.2}_{-0.1}$			$0.54^{+0.01}_{-0.02}$	–	$0.004^{+0.014}_{-0.002}$	Buysschaert et al., 2018
KIC 3240411	6.25	–	0.006	0.612	–	0.02	Szewczuk and Daszyńska-Daszkiewicz, 2018

Note that not all studies listed here use the same evolution codes, opacity tables (e.g., standard vs. modified), nor necessarily the same numerical setup for selecting the statistically best-fitting asteroseismic model, so the reader is referred to each individual study for full details.

β Cep stars discussed in this section, forward seismic modeling of θ Oph by Briquet et al. (2007) revealed an approximately rigid interior rotation rate and a significantly larger amount of convective core overshooting with the best-fitting model yielding $\alpha_{ov} = 0.44 \pm 0.07$. Such a high value of convective core overshooting is rare in the context of modern asteroseismology of stars with convective cores (Aerts et al., 2019a), but does highlight the trend that stellar models typically underestimate the mass of the convective cores in high-mass main-sequence stars.

A final example case study of forward seismic modeling of a slowly-rotating β Cep star based on ground-based data is the B2 IV/V star V2052 Oph (HD 163472; Briquet et al., 2012). The importance of V2052 Oph in this context is that it is a known magnetic star (Neiner et al., 2003, 2012a). A large-scale magnetic field is thought to suppress the near-core mixing caused by convective core overshooting in massive stars. The data set of V2052 Oph assembled and analyzed by Briquet et al. (2012) included more than 1300 spectra from 10 different telescopes around the world, and the resultant frequency spectrum of included a radial mode and two prograde non-radial modes identified by means of spectroscopy. Forward seismic modeling of these identified pulsation modes yielded a relatively fast rotation rate with $v_{eq} \simeq 75$ km s^{-1}, and only a small amount of convective core overshooting with $\alpha_{ov} \in [0.00, 0.15]$, which was concluded to be low because of the star's magnetic field (Briquet et al., 2012).

4.2. Space-Based Studies

Early space missions, such as MOST (Walker et al., 2003) have targeted massive stars for the purposes of asteroseismology. However, in this review we focus on selected case studies from the BRITE, CoRoT and *Kepler* missions. This is because of their high photometric precision and their long observational base lines (Auvergne et al., 2009; Baglin et al., 2009; Borucki et al., 2010; Koch et al., 2010; Weiss et al., 2014), which are necessary for successful forward seismic modeling.

The CoRoT mission provided near-continuous light curves up to 150 days in length at a cadence of 32 s, which at the time was

a major revolution for asteroseismology. Early important results from the mission included the seismic modeling of the β Cep star HD 180642 (Aerts et al., 2011), and detection of the g-mode period spacing pattern in the B3 III SPB star HD 50230 (Degroote et al., 2010a). Such a g-mode period spacing pattern was a huge step forward in asteroseismology, as such patterns enable mode identification and allow interior rotation and mixing to be measured directly. Subsequent modeling of HD 50230 revealed it to be a mid-main sequence star with a mass of $\sim$7 $M_\odot$, and convective core overshooting of $0.2 \leq \alpha_{ov} \leq 0.3$ (Degroote et al., 2010a). Later, Degroote et al. (2012) discovered that HD 50230 is a wide-binary system, and confirmed its ultra-slow rotation rate of $v_{eq} \simeq 10$ km s^{-1} using spectroscopy, although they concluded that this does not impact the aforementioned g-mode period spacing pattern. More recently, Wu and Li (2019) have revisited the analysis of HD 50230 and conclude it to be a metal-rich hybrid pulsator with a modest amount of convective core overshooting.

Not long after the early studies by Degroote et al. (2010a) and Aerts et al. (2011), another important result for massive star asteroseismology from the CoRoT mission was made based on the O9 V star HD 46202 (Briquet et al., 2011). Spectroscopy of HD 46202 confirmed its literature spectral type and yielded a projected surface rotation rate of $v \sin i \simeq 25$ km s^{-1} and an effective temperature of $T_{eff} = 34{,}100 \pm 600$ K, which makes it amongst the hottest β Cep pulsators known (Briquet et al., 2011). Several radial and non-radial pulsation modes were identified using the CoRoT photometry of HD 46202. Forward seismic modeling of these identified modes yielded a precise mass and age for this massive pulsator, confirming it as the most massive modeled β Cep star to date. A significant amount of convective core overshooting was required to fit the observed pulsation frequencies and the best-fitting asteroseismic parameters from Briquet et al. (2011) are provided in **Table 1**.

A third pivotal study of a massive star using asteroseismology from CoRoT data is the magnetic and fast-rotating B3.5 V star HD 43317 (Pápics et al., 2012; Briquet et al., 2013; Buysschaert et al., 2017a, 2018). This star was originally studied by Pápics et al. (2012) using the 150-d CoRoT light curve and it was concluded to exhibit g and p modes based on its frequency spectrum, since it appeared to have independent pulsation modes in both high and low frequency regimes. High-resolution spectroscopy confirmed HD 43317 as an early-type star with an effective temperature of $T_{eff} = 17{,}350 \pm 750$ K, and as a fast rotator with a projected surface rotational velocity of $v \sin i = 115 \pm 9$ km s^{-1} (Pápics et al., 2012). Later, HD 43317 was detected to host a large-scale magnetic field with a polar field strength of $\sim$1.3 kG (Briquet et al., 2013; Buysschaert et al., 2017a). After revisiting the light curve with the knowledge of how such fast rotation perturbs the frequencies of g-mode pulsations in B stars (see e.g., Kurtz et al., 2015), Buysschaert et al. (2018) extracted all significant pulsation mode frequencies and performed forward seismic modeling of HD 43317 and determined its fundamental parameters, which are provided in **Table 1**. The small amount of convective core overshooting in the rapidly-rotating and magnetic star HD 43317 led Buysschaert et al. (2018) to a similar conclusion to that of Briquet et al. (2011) for the β Cep star V2052 Oph (cf. 4.1): the presence of a large-scale magnetic field is a plausible cause for the suppression of additional mixing (i.e., overshooting) in the near-core region.

As discussed in section 3.3, during the life time of the *Kepler* space mission, massive stars were avoided as targets in the field of view. Hence, whereas much of the asteroseismic inference of massive stars based on ground-based data were focused on β Cep stars, more recent asteroseismic results based on the 4-years light curves of the *Kepler* telescope are typically derived from SPB stars (Aerts et al., 2019a). Although not all SPB stars are "massive" stars, they do share a common interior structure whilst on the main sequence, so their discussion is relevant as part of this review.

Amongst the early days of *Kepler* asteroseismology, two SPB stars were identified as high priority targets: KIC 10526294 and KIC 7760680. A long series of rotationally-split g modes in the B8.3 V star KIC 10526294 allowed Pápics et al. (2014) to determine a near-core rotation period of $\sim$188 days. Later, Moravveji et al. (2015) performed the first in-depth asteroseismic modeling of this main-sequence B star, from which it was concluded that a modest amount of exponential diffusive overshooting (i.e., f_{ov}) fit the *Kepler* data significantly better than when using the step overshooting prescription (i.e., α_{ov}). Furthermore, a small but non-negligible amount of additional envelope mixing ($D_{mix} \simeq 100$ cm^2 s^{-1}) was needed despite KIC 10526294 being an ultra-slow rotator (Moravveji et al., 2015). The best-fitting asteroseismic modeling parameters, including the measured overshooting of $0.017 \leq f_{ov} \leq 0.018$, are included in **Table 1**. The exquisite *Kepler* data allowed Triana et al. (2015) to compute a near-rigid interior rotation profile through an asteroseismic inversion. Interestingly, at the 1-σ confidence level, the inversion by Triana et al. (2015) confirmed the ultra-slow rotation rate, but revealed that KIC 10526294 had a counter-rotating envelope compared to that of its core. Similar conclusions in terms of a non-negligible amount of convective core overshooting and envelope mixing were also reached for the B8 V SPB star KIC 7760680 based on the period spacing pattern of prograde dipole g modes by Moravveji et al. (2016). However, it should be noted that the uncertainties obtained by Moravveji et al. (2015) and Moravveji et al. (2016) are typically quoted as the step size within the computed grid of evolution models and may be unrealistically small, because they ignore degeneracies amongst the model parameters (see Aerts et al., 2018). There has been substantial development in the correct way to treat parameter correlations and degeneracies for asteroseismology of g-mode pulsators by moving away from the often-used χ^2 merit function and toward the use of the Mahalanobis distance which includes heteroscedasticity. We refer the reader to Aerts et al. (2018) for further details.

At somewhat higher masses, Szewczuk and Daszyńska-Daszkiewicz (2018) performed forward seismic modeling of the SPB star KIC 3240411 using its axisymmetric ($m = 0$) period spacing pattern extracted from *Kepler* data. KIC 3240411 was found to be a relatively young star near the zero-age main sequence with the upper limit on its convective core overshooting being $f_{ov} \leq 0.030$. The best-fitting model parameters (i.e., model #2 in Table 2 of Szewczuk and Daszyńska-Daszkiewicz, 2018)

are included in **Table 1**. Importantly, Szewczuk and Daszyńska-Daszkiewicz (2018) also studied the effect of rotation and opacity data within their modeling for the purposes of explaining mode excitation of high-radial order g modes in such stars. This is because the excitation of such a large number and radial order range for high-radial order g modes remains somewhat difficult to explain from a theoretical perspective.

Recently, the nanosatellites of the BRITE-constellation mission have been targeting pulsating massive stars with the aim of performing forward seismic modeling of the detected pulsation mode frequencies. Notable examples of the importance of the contribution of the BRITE mission in this aspect include ν Eri (Daszyńska-Daszkiewicz et al., 2017) and θ Oph (Walczak et al., 2019). The BRITE data marked the first time that these famous β Cep stars were observed from space, thus the first time an asteroseismic analysis of them benefitted from having near-continuous, short-cadence and long-term monitoring. Handler et al. (2017) discovered new g-mode pulsations in ν Eri using BRITE data, and Daszyńska-Daszkiewicz et al. (2017) used the extracted pulsation mode frequencies to perform forward seismic modeling. Daszyńska-Daszkiewicz et al. (2017) determined optimum parameters for ν Eri and emphasized the improvement of using modified opacity tables to explain all the observed pulsation mode frequencies. Moreover, the modified opacity data increases the efficiency of convection within the Z-bump, an effect also predicted when increasing the metallicity of the star (Cantiello et al., 2009) or increasing the rotation (Maeder et al., 2008). In the analysis of θ Oph using BRITE data, Walczak et al. (2019) discovered several g modes. From their forward seismic modeling, similar conclusions made by Daszyńska-Daszkiewicz et al. (2017) for ν Eri were made. Specifically that an increase in the mean opacity within the Z-bump is needed to explain all pulsation mode frequencies in θ Oph (Walczak et al., 2019). However, since θ Oph is a triple system with $\sim$ 8.5 and $\sim$ 5.5 $M_\odot$ primary and tertiary components, respectively, it was difficult to ascertain the origin of the g-mode frequencies (Walczak et al., 2019).

Recently, a new method of performing forward seismic modeling by means of a machine learning was developed by Hendriks and Aerts (2019). The authors trained a deep neural network using more than 62 million pulsation mode frequencies, which were calculated from a vast grid of stellar models covering main sequence intermediate- and high-mass stars spanning from 2 to 20 $M_\odot$. Optimum models were selected using a genetic algorithm making such an automated pipeline extremely quick compared to more conventional forward seismic modeling techniques. Hendriks and Aerts (2019) test their methodology using several well-studied massive stars to benchmark the accuracy of their technique and good agreement is found overall. However, as discussed in detail by Hendriks and Aerts (2019), the modeling results based on their deep neural network depend on the choice of hyperparameters, which affect the ability to find the global minimum in the solution space. In **Table 1** the model parameters resulting from the optimized tuning of these hyperparameters are provided (cf. gray points), but such values are claimed to be an "optimal starting point" for further complex modeling. We refer the reader to Hendriks and Aerts (2019) for full details.

Asteroseismology using *Kepler* data has also been applied to hundreds of intermediate-mass stars covering masses between $\sim$1 and 8 $M_\odot$, rotation rates up to 80% of critical, and evolutionary stages spanning from the main sequence through to the red giant branch. More specifically, g-mode period spacings have also been used to probe interior rotation in hundreds of intermediate-mass main-sequence stars, which are more commonly known as γ Dor stars (Van Reeth et al., 2015a,b, 2016, 2018; Ouazzani et al., 2017, 2019; Li et al., 2019a,b, 2020). An important conclusion from these works is that current angular momentum transport theory is erroneous by more than an order of magnitude (Aerts et al., 2019a). The situation is less clear for massive stars owing to the much smaller sample size currently available, but significant progress has already been made in recent years because of ground- and space-based data sets and asteroseismology.

The pioneering asteroseismic studies of massive stars using ground- and space-based data sets clearly demonstrate the importance of constraining the interior properties of massive stars and the effectiveness of using g-mode period spacing patterns in SPB stars and low-radial order g and p modes for β Cep stars. Thanks to the ongoing TESS mission (Ricker et al., 2015), the asteroseismic sample of pulsating massive stars has increased in size by at least two orders of magnitude (Pedersen et al., 2019; Burssens et al., 2020). Thus, detailed forward seismic modeling of many high-mass TESS targets are expected in the not-so-distant future. We refer the reader to Handler et al. (2019) for the first modeling study of a β Cep star using TESS data. Despite the relatively small sample size so far compared to intermediate-mass stars, asteroseismic studies of massive stars have demonstrated the need to include improved prescriptions for convective core overshooting and envelope mixing given that current evolution models underestimate the core masses of massive stars and consequently also their main-sequence lifetimes.

4.3. Implications of Mixing for the Post-Main Sequence

The majority of asteroseismic studies of massive stars have been of main sequence stars. Of course, based on evolutionary time scales, stars spend more than 90% of their lives in this phase (Kippenhahn et al., 2012). However, pulsating post-main sequence massive stars do exist (Saio et al., 2006; Aerts et al., 2010), and to truly understand their interior physics requires us to first understand the interiors of main-sequence stars. For example, the interplay of different mixing processes can cause some post-main sequence massive stars to undergo blue loops in the HR diagram. However, the exact nature of why some massive stars undergo blue loops and others do not remains unknown (Langer, 2012), especially given the differences in the physics and numerics in various stellar evolution codes (e.g., Martins and Palacios, 2013). It is known, however, that convection, mixing and mass loss all play significant roles in determining if stars undergo blue loops in the HR diagram and their pulsational

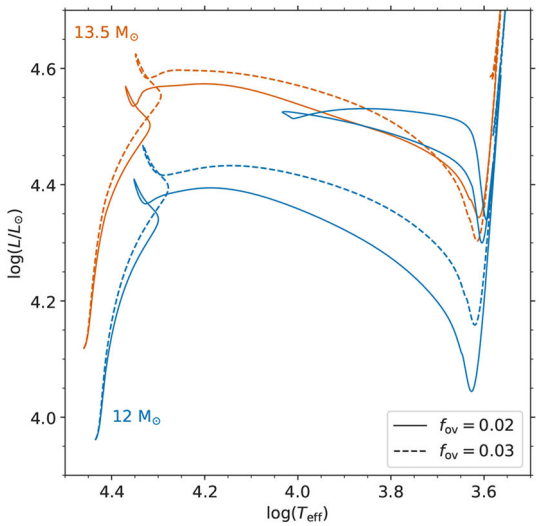

FIGURE 5 | HR diagram containing non-rotating evolutionary tracks starting from the zero-age main-sequence for stars of initial masses of 12- and 13.5-$M_\odot$ calculated using the MESA stellar evolution code (Paxton et al., 2019), using two different values for the diffusive exponential convective core-overshooting value (f_{ov}), which are expressed in pressure scale heights. With increased mixing in the near-core region, a massive star has a longer main-sequence lifetime and produces a larger convective core mass at the terminal age main-sequence. The increased core mass and interior mixing during the main sequence phase of evolution also impacts the post-main sequence evolution of a massive star, including whether it performs a "*blue loop*," which is demonstrated by the evolutionary track of the 12-$M_\odot$ star with $f_{ov} = 0.02$.

properties (Georgy, 2012; Saio et al., 2013; Georgy et al., 2014; Wagle et al., 2019). To demonstrate how the difference in the amount of the mixing at the boundary of a convective core within a massive main-sequence star drastically impacts its post-main sequence evolution, evolutionary tracks calculated with the MESA stellar evolution code (Paxton et al., 2011, 2013, 2015, 2018, 2019; r11554) for initial masses of 12- and 13.5-$M_\odot$ and two moderate values for their convective core-overshooting value using the diffusive exponential prescription (i.e., f_{ov}) are shown in **Figure 5**. The evolutionary tracks shown in **Figure 5** use initial hydrogen and metal mass fractions of $X = 0.71$ and $Z = 0.02$, respectively, OP opacity tables (Seaton, 2005), and the chemical mixture of Nieva and Przybilla (2012) and Przybilla et al. (2013) for cosmic B stars. As illustrated in **Figure 5**, only one of the four evolution tracks contains a blue loop in the post-main sequence stage of evolution.

Currently, there exists a knowledge gap concerning the interiors of blue supergiants yet to be filled by asteroseismology. This is primarily because until recently few pulsating blue supergiants had been found within the Hertzsprung gap in the HR diagram (Bowman et al., 2019b), despite theoretical models predicting such stars should pulsate (Saio et al., 2013; Daszyńska-Daszkiewicz et al., 2013a; Ostrowski and Daszyńska-Daszkiewicz, 2015). Asteroseismology of post-main sequence massive stars represents a major future goal for the community, especially since g-mode period spacing patterns and the presence of radial p modes have the capability to distinguish shell-hydrogen burning and core-helium burning massive stars (Saio et al., 2013; Bowman et al., 2019b). Furthermore, when coupled to spectroscopic surface abundances of core-processed material (e.g., C, N, and O), convection and mixing in massive stars can be significantly improved within stellar evolution codes, which has important consequences for stars that eventually explode as a supernova (e.g., Saio et al., 1988; Georgy et al., 2014; Wagle et al., 2019). In particular, the helium core masses of post-main sequence massive stars represent a critical deliverable to the wider astronomical community as it is a fundamental parameter for predicting the chemical properties of supernovae (Smartt, 2009; Langer, 2012).

5. DIVERSE PHOTOMETRIC VARIABILITY IN MASSIVE STARS

A recent discovery made using the CoRoT, K2, and TESS missions was that the vast majority of early-type stars have significant low-frequency variability in photometry (Bowman et al., 2019a,b). Such stochastic variability is not predicted from the κ-mechanism, but is expected from convectively-driven internal gravity waves (IGWs) excited by core convection (Rogers et al., 2013; Rogers, 2015; Edelmann et al., 2019; Horst et al., 2020). 2D and 3D hydrodynamical simulations predict that IGWs reach the surface with significant amplitudes and provide detectable perturbations in temperature and velocity (Edelmann et al., 2019), and that IGWs are also extremely efficient at transporting angular momentum and chemical elements (Rogers, 2015; Rogers and McElwaine, 2017). A snapshot of a 3D simulation of IGWs propagating within a 3-$M_\odot$ main-sequence star from Edelmann et al. (2019) is shown in **Figure 6**.

The morphology of the low-frequency variability in more than 160 massive stars was found to be similar across a large range of masses and ages for both metal-rich galactic and metal-poor LMC stars (Bowman et al., 2019b). The insensitivity of the stochastic variability to a star's metallicity together with the fact that evolutionary timescales predicted most stars were likely on the main sequence was concluded as strong evidence that the observed stochastic variability is likely caused by IGWs excited by core convection (Bowman et al., 2019b). More recently, Bowman et al. (2020) demonstrated that the morphology of the IGWs in the frequency spectrum probes the evolutionary properties of the star, such as mass and radius. Furthermore, the amplitudes of IGWs in photometry were found to correlate with the macroturbulent broadening in the spectral lines of dozens of massive stars observed by the TESS mission (Bowman et al., 2020), with macroturbulence also having been associated with pulsations (Aerts et al., 2009; Simón-Díaz et al., 2010, 2017). Thus, mixing and angular momentum transport caused by IGWs are important to take into account when studying massive star evolution (Aerts et al., 2019a), and are currently not implemented in most stellar evolution codes.

There are currently four known excitation mechanisms that can trigger variability in early-type stars: (i) coherent p and

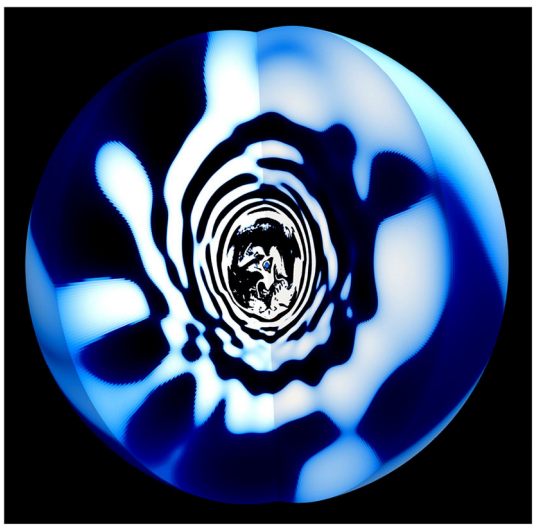

FIGURE 6 | Snapshot of a non-rotating 3D numerical simulation of gravity waves excited by core convection inside a main-sequence massive star, with a white-blue color scale indicating temperature fluctuations. Simulation courtesy of Edelmann et al. (2019).

g modes excited by the κ-mechanism (Dziembowski et al., 1993; Gautschy and Saio, 1993; Szewczuk and Daszyńska-Daszkiewicz, 2017); (ii) IGWs generated by turbulent core convection (Edelmann et al., 2019); (iii) IGWs generated by thin sub-surface convection zones (Cantiello et al., 2009); and (iv) waves generated from tides in binary systems (Fuller, 2017). Whereas, essentially all of the asteroseismic results discussed in section 4 are based on heat-driven modes, the other variability mechanisms in massive stars remain somewhat under-utilized despite having great probing power of stellar interiors. In the future, it is expected that binary asteroseismology in particular is going to play a more substantial role in providing excellent constraints of massive star interiors because recent space telescopes, such as BRITE and TESS are providing the necessary high-quality time-series observations (see e.g., Jerzykiewicz et al., 2020 and Southworth et al., 2020).

6. CONCLUSIONS AND FUTURE PROSPECTS

Our knowledge of the interior physics of massive stars has historically been based on a handful of asteroseismic studies using time series data obtained with ground-based telescopes. Such data sets are notoriously limited by their poor duty cycles which complicates mode identification (Aerts et al., 2003; Ausseloos et al., 2004; Dupret et al., 2004; Handler et al., 2004; Pamyatnykh et al., 2004; Briquet et al., 2007, 2012; Desmet et al., 2009b; Daszyńska-Daszkiewicz et al., 2013b, 2017). These initial asteroseismic studies, however, provided the first evidence of the interior rotation profiles of massive stars and that evolutionary models of such stars lacked calibrated prescriptions for interior processes, such as convective core overshooting. Consequently standard evolutionary models typically underestimate the mass of convective cores and hence the main sequence lifetimes of massive stars. Furthermore, ground-based studies yielded the first measurements of the interior rotation rates of main sequence stars (Aerts et al., 2003), with both rigid and non-rigid rotation rates being inferred for a handful of β Cep stars (Aerts et al., 2003; Ausseloos et al., 2004; Pamyatnykh et al., 2004; Briquet et al., 2007). More recently, the MOST (Walker et al., 2003), CoRoT (Auvergne et al., 2009), Kepler/K2 (Borucki et al., 2010; Howell et al., 2014), and the ongoing BRITE-Constellation (Weiss et al., 2014) missions have advanced asteroseismic studies beyond measuring only the masses, ages and metallicities of massive stars. More advanced forward seismic modeling techniques and improved observations have constrained both macroscopic and microscopic physical processes and mechanisms inside stars, such as the amount and shape of mixing in their radiative envelopes (Moravveji et al., 2015, 2016; Buysschaert et al., 2018; Szewczuk and Daszyńska-Daszkiewicz, 2018; Walczak et al., 2019) and angular momentum transport as a function of stellar evolution (Aerts et al., 2019a).

Today, thanks to the ongoing TESS mission (Ricker et al., 2015), there is huge asteroseismic potential for massive stars as we are no longer limited by the biases of having a small sample of pulsating massive stars. The long-term and high-photometric precision provided by space telescopes is unrivaled by ground-based telescopes, and the sample of massive stars has expanded to hundreds of stars because of the all-sky TESS mission (Pedersen et al., 2019; Burssens et al., 2020). Crucially, TESS is observing massive stars which span a large range in mass and age, but also massive stars in different metallicity regimes. This is because the southern CVZ of TESS includes the LMC galaxy, which allows pulsation excitation models to be tested for metal-rich and metal-poor stars (Bowman et al., 2019b). TESS also offers the opportunity to revisit "old friends" in terms of previously studied massive stars with high-precision photometry, which is particularly useful to probe the long-term stability in pulsation mode amplitudes and frequencies in relatively short-lived stars (e.g., Neilson and Ignace, 2015). The diverse variability of massive stars, which includes both coherent pulsation modes excited by the κ-mechanism and IGWs excited by core convection (Pedersen et al., 2019; Bowman et al., 2019b; Burssens et al., 2020), enables asteroseismology for a sample of massive stars larger by two orders of magnitude compared to any that came before.

The important future goals of asteroseismic studies based on the large and diverse TESS data set include constraining the helium core masses, near-core and envelope mixing processes, interior rotation profiles and angular momentum transport mechanisms inside massive stars. Insight of the physics in the near-core region of stars above $\sim$8 $M_\odot$ is currently lacking compared to intermediate- and low-mass stars (Aerts et al., 2019a). Moreover, HD 46202 remains the only massive star above 15 $M_\odot$ to have undergone forward seismic modeling (Briquet et al., 2011). In turn TESS data combined with high-resolution spectroscopy and asteroseismology will mitigate the currently large uncertainties in stellar evolution theory and lead to constraining why only some massive stars undergo blue

loops during the post-main sequence phase of evolution (e.g., Bowman et al., 2019b), and improved predictions of supernovae chemical yields and remnant masses. The future is very bright for massive stars, and the goal to calibrate stellar structure and evolution models of massive stars using asteroseismology is now within reach.

AUTHOR CONTRIBUTIONS

The author confirms being the sole contributor of this work and has approved it for publication.

FUNDING

DB gratefully acknowledges funding from the European Research Council (ERC) under the European Union's Horizon 2020 research and innovation programme (grant agreement No. 670519: MAMSIE), and a senior post-doctoral fellowship from the Research Foundation Flanders (FWO) with grant agreement No. 1286521N. The Kepler, K2 and TESS data presented in this paper were obtained from the Mikulski Archive for Space Telescopes (MAST) at the Space Telescope Science Institute (STScI), which is operated by the Association of Universities for Research in Astronomy, Inc., under NASA contract NAS5-26555. Support to MAST for these data is provided by the NASA Office of Space Science via grant NAG5-7584 and by other grants and contracts. Funding for the Kepler/K2 mission was provided by NASA's Science Mission Directorate. Funding for the TESS mission was provided by the NASA Explorer Program. Funding for the TESS Asteroseismic Science Operations Centre is provided by the Danish National Research Foundation (Grant agreement no.: DNRF106), ESA PRODEX (PEA 4000119301) and Stellar Astrophysics Centre (SAC) at Aarhus University. This research has made use of the SIMBAD database, operated at CDS, Strasbourg, France; the SAO/NASA Astrophysics Data System; and the VizieR catalog access tool, CDS, Strasbourg, France.

ACKNOWLEDGMENTS

DB was grateful to S. Burssens who graciously re-produced **Figure 4** and to P. V. F. Edelmann who made **Figure 6**. DB was grateful to the reviewers and Prof. C. Aerts for constructive feedback. DB was also grateful to the MESA and GYRE developers, in particular B. Paxton and R. H. D. Townsend, for continually supporting the development of state-of-the-art and open-source tools for modeling massive stars. This research has made use of the `PYTHON` library for publication quality graphics (`MATPLOTLIB`; Hunter 2007) and `Numpy` (van der Walt et al., 2011).

REFERENCES

Abbott, B. P., Abbott, R., Abbott, T. D., Abernathy, M. R., Acernese, F., Ackley, K., et al. (2016). Observation of gravitational waves from a binary black hole merger. *Phys. Rev. Lett.* 116:061102. doi: 10.1103/PhysRevLett.116.061102

Abbott, B. P., Abbott, R., Abbott, T. D., Abraham, S., Acernese, F., Ackley, K., et al. (2019). GWTC-1: a gravitational-wave transient catalog of compact binary mergers observed by LIGO and virgo during the first and second observing runs. *Phys. Rev. X* 9:031040. doi: 10.1103/PhysRevX.9.031040

Abdul-Masih, M., Sana, H., Conroy, K. E., Sundqvist, J., Prša, A., Kochoska, A., et al. (2020). Spectroscopic patch model for massive stars using PHOEBE II and FASTWIND. *Astron. Astrophys.* 636:A59. doi: 10.1051/0004-6361/201937341

Abdul-Masih, M., Sana, H., Sundqvist, J., Mahy, L., Menon, A., Almeida, L. A., et al. (2019). Clues on the origin and evolution of massive contact binaries: atmosphere analysis of VFTS 352. *Astrophys. J.* 880:115. doi: 10.3847/1538-4357/ab24d4

Abt, H. A., Levato, H., and Grosso, M. (2002). Rotational velocities of B stars. *Astrophys. J.* 573, 359–365. doi: 10.1086/340590

Aerts, C. (1996). Mode identification of pulsating stars from line-profile variations with the moment method: a more accurate discriminant. *Astron. Astrophys.* 314, 115–122.

Aerts, C. (2020). Probing the interior physics of stars through asteroseismology. *arXiv[Preprint].arXiv:1912.12300*.

Aerts, C., Briquet, M., Degroote, P., Thoul, A., and van Hoolst, T. (2011). Seismic modelling of the β Cephei star HD 180642 (V1449 Aquilae). *Astron. Astrophys.* 534:A98. doi: 10.1051/0004-6361/201117629

Aerts, C., Christensen-Dalsgaard, J., and Kurtz, D. W. (2010). *Asteroseismology*. Berlin: Springer.

Aerts, C., De Boeck, I., Malfait, K., and De Cat, P. (1999a). HD 42927 and HD 126341: two pulsating B stars surrounded by circumstellar dust. *Astron. Astrophys.* 347, 524–531.

Aerts, C., and De Cat, P. (2003). β Cep stars from a spectroscopic point of view. *Space Sci. Rev.* 105, 453–492. doi: 10.1023/A:1023983704925

Aerts, C., De Cat, P., Handler, G., Heiter, U., Balona, L. A., Krzesinski, J., et al. (2004a). Asteroseismology of the β Cephei star ν Eridani - II. Spectroscopic observations and pulsational frequency analysis. *Mon. Not. R. Astron. Soc.* 347, 463–470. doi: 10.1111/j.1365-2966.2004.07215.x

Aerts, C., De Cat, P., Kuschnig, R., Matthews, J. M., Guenther, D. B., Moffat, A. F. J., et al. (2006a). Discovery of the new slowly pulsating B star HD 163830 (B5 II/III) from MOST space-based photometry. *Astrophys. J. Letters* 642, L165–L168. doi: 10.1086/504634

Aerts, C., De Cat, P., Peeters, E., Decin, L., De Ridder, J., Kolenberg, K., et al. (1999b). Selection of a sample of bright southern Slowly Pulsating B Stars for long-term photometric and spectroscopic monitoring. *Astron. Astrophys.* 343, 872–882.

Aerts, C., de Pauw, M., and Waelkens, C. (1992). Mode identification of pulsating stars from line profile variations with the moment method. An example : the beta Cephei star delta Ceti. *Astron. Astrophys.* 266, 294–306.

Aerts, C., Marchenko, S. V., Matthews, J. M., Kuschnig, R., Guenther, D. B., Moffat, A. F. J., et al. (2006b). δ Ceti is not monoperiodic: seismic modeling of a β Cephei star from MOST space-based photometry. *Astrophys. J.* 642, 470–477. doi: 10.1086/500800

Aerts, C., Mathias, P., Gillet, D., and Waelkens, C. (1994a). Multiperiodicity and pulsation characteristics of β Cephei. *Astron. Astrophys.* 286, 109–120.

Aerts, C., Mathis, S., and Rogers, T. M. (2019a). Angular momentum transport in stellar interiors. *Ann. Rev. Astron. Astrophys.* 57, 35–78. doi: 10.1146/annurev-astro-091918-104359

Aerts, C., Molenberghs, G., Kenward, M. G., and Neiner, C. (2014). The surface nitrogen abundance of a massive star in relation to its oscillations, rotation, and magnetic field. *Astrophys. J.* 781:88. doi: 10.1088/0004-637X/781/2/88

Aerts, C., Molenberghs, G., Michielsen, M., Pedersen, M. G., Björklund, R., Johnston, C., et al. (2018). Forward asteroseismic modeling of stars with a convective core from gravity-mode oscillations: parameter estimation and stellar model selection. *Astrophys. J. Supp. Ser.* 237:15. doi: 10.3847/1538-4365/aaccfb

Aerts, C., Pedersen, M. G., Vermeyen, E., Hendriks, L., Johnston, C., Tkachenko, A., et al. (2019b). Combined asteroseismology, spectroscopy, and astrometry of the CoRoT B2V target HD 170580. *Astron. Astrophys.* 624:A75. doi: 10.1051/0004-6361/201834762

Aerts, C., Puls, J., Godart, M., and Dupret, M.-A. (2009). Collective pulsational velocity broadening due to gravity modes as a physical explanation for macroturbulence in hot massive stars. *Astron. Astrophys.* 508, 409–419. doi: 10.1051/0004-6361/200810471

Aerts, C., Símon-Díaz, S., Bloemen, S., Debosscher, J., Pápics, P. I., Bryson, S., et al. (2017). Kepler sheds new and unprecedented light on the variability of a blue supergiant: gravity waves in the O9.5Iab star HD 188209. *Astron. Astrophys.* 602:A32. doi: 10.1051/0004-6361/201730571

Aerts, C., Thoul, A., Daszyńska, J., Scuflaire, R., Waelkens, C., Dupret, M. A., et al. (2003). Asteroseismology of HD 129929: core overshooting and nonrigid rotation. *Science* 300, 1926–1928. doi: 10.1126/science.1084993

Aerts, C., and Waelkens, C. (1993). Line profile variations of rotating, pulsating stars. *Astron. Astrophys.* 273, 135–146.

Aerts, C., Waelkens, C., Daszyńska-Daszkiewicz, J., Dupret, M.-A., Thoul, A., Scuflaire, R., et al. (2004b). Asteroseismology of the β Cep star HD 129929. I. Observations, oscillation frequencies and stellar parameters. *Astron. Astrophys.* 415, 241–249. doi: 10.1051/0004-6361:20034142

Aerts, C., Waelkens, C., De Cat, P., Kolenberg, K., Kestens, E., Grenon, M., et al. (2006c). Pulsating B stars discovered by HIPPARCOS. *J. Am. Assoc. Var. Star Observ.* 35:58.

Aerts, C., Waelkens, C., and de Pauw, M. (1994b). Mode identification with the moment method in four multiperiodic β Cephei stars: KK Velorum, ν Eri, β CMa, and V348 Normae. *Astron. Astrophys.* 286, 136–148.

Alecian, E., Kochukhov, O., Petit, V., Grunhut, J., Landstreet, J., Oksala, M. E., et al. (2014). Discovery of new magnetic early-B stars within the MiMeS HARPSpol survey. *Astron. Astrophys.* 567:A28. doi: 10.1051/0004-6361/201323286

Almeida, L. A., Sana, H., de Mink, S. E., Tramper, F., Soszyński, I., Langer, N., et al. (2015). Discovery of the massive overcontact binary VFTS352: evidence for enhanced internal mixing. *Astrophys. J.* 812:102. doi: 10.1088/0004-637X/812/2/102

Augustson, K. C., and Mathis, S. (2019). A model of rotating convection in stellar and planetary interiors. I. Convective Penetration. *Astrophys. J.* 874:83. doi: 10.3847/1538-4357/ab0b3d

Ausseloos, M., Scuflaire, R., Thoul, A., and Aerts, C. (2004). Asteroseismology of the β Cephei star ν Eridani: massive exploration of standard and non-standard stellar models to fit the oscillation data. *Mon. Not. R. Astron. Soc.* 355, 352–358. doi: 10.1111/j.1365-2966.2004.08320.x

Auvergne, M., Bodin, P., Boisnard, L., Buey, J.-T., Chaintreuil, S., Epstein, G., et al. (2009). The CoRoT satellite in flight: description and performance. *Astron. Astrophys.* 506, 411–424. doi: 10.1051/0004-6361/200810860

Baade, D., Rivinius, T., Pigulski, A., Carciofi, A. C., Martayan, C., Moffat, A. F. J., et al. (2016). Short-term variability and mass loss in Be stars. I. BRITE satellite photometry of η and μ Centauri. *Astron. Astrophys.* 588:A56. doi: 10.1051/0004-6361/201528026

Baglin, A., Auvergne, M., Barge, P., Deleuil, M., Michel, E., and CoRoT Exoplanet Science Team (2009). "CoRoT: description of the mission and early results," In *Transiting Planets, Vol. 253 of IAU Symposium*, eds F. Pont, D. Sasselov, and M. J. Holman, 71–81. doi: 10.1017/S1743921308026252

Balona, L. A., Aerts, C., and Štefl, S. (1999). Simultaneous photometry and spectroscopy of the Be star 28 (omega) CMa–II. Line profile modelling. *Mon. Not. R. Astron. Soc.* 305, 519–526. doi: 10.1046/j.1365-8711.1999.02386.x

Balona, L. A., Baran, A. S., Daszyńska-Daszkiewicz, J., and De Cat, P. (2015). Analysis of Kepler B stars: rotational modulation and Maia variables. *Mon. Not. R. Astron. Soc.* 451, 1445–1459. doi: 10.1093/mnras/stv1017

Balona, L. A., and Kambe, E. (1999). On the moving subfeatures in the Be star ζ OPH. *Mon. Not. R. Astron. Soc.* 308, 1117–1125. doi: 10.1046/j.1365-8711.1999.02770.x

Barbá, R., Gamen, R., Arias, J. I., Morrell, N., Walborn, N. R., Maíz Apellániz, J., et al. (2014). "OWN survey: results after seven years of high-resolution spectroscopic monitoring of Southern O and WN stars," in *Revista Mexicana de Astronomia y Astrofisica Conference Series. Vol. 44 of Revista Mexicana de Astronomia y Astrofisica Conference Series*, 148–148.

Barbá, R. H., Gamen, R., Arias, J. I., Morrell, N., Maíz Apellániz, J., Alfaro, E., et al. (2010). "Spectroscopic survey of galactic O and WN stars. OWN survey: new binaries and trapezium-like systems," in *Revista Mexicana de Astronomia y Astrofisica Conference Series. Vol. 38 of Revista Mexicana de Astronomia y Astrofisica Conference Series*, 30–32.

Barbá, R. H., Gamen, R., Arias, J. I., and Morrell, N. I. (2017). "OWN survey: a spectroscopic monitoring of Southern Galactic O and WN-type stars," in *The Lives and Death-Throes of Massive Stars, Vol. 329 of IAU Symposium*, eds. J. J. Eldridge, J. C. Bray, L. A. S. McClelland, and L. Xiao, 89–96. doi: 10.1017/S1743921317003258

Belkacem, K., Dupret, M. A., and Noels, A. (2010). Solar-like oscillations in massive main-sequence stars. I. Asteroseismic signatures of the driving and damping regions. *Astron. Astrophys.* 510:A6. doi: 10.1051/0004-6361/200913221

Belkacem, K., Samadi, R., Goupil, M.-J., Lefèvre, L., Baudin, F., Deheuvels, S., et al. (2009). Solar-like oscillations in a massive star. *Science* 324:1540. doi: 10.1126/science.1171913

Bildsten, L., Ushomirsky, G., and Cutler, C. (1996). Ocean g-modes on rotating neutron stars. *Astrophys. J.* 460:827. doi: 10.1086/177012

Blomme, R., Mahy, L., Catala, C., Cuypers, J., Gosset, E., Godart, M., et al. (2011). Variability in the CoRoT photometry of three hot O-type stars. HD 46223, HD 46150, and HD 46966. *Astron. Astrophys.* 533:A4. doi: 10.1051/0004-6361/201116949

Bodensteiner, J., Shenar, T., and Sana, H. (2020). Investigating the lack of main-sequence companions to massive Be stars. *arXiv* 641, A42. doi: 10.1051/0004-6361/202037640

Borucki, W. J., Koch, D., Basri, G., Batalha, N., Brown, T., Caldwell, D., et al. (2010). Kepler planet-detection mission: introduction and first results. *Science* 327:977. doi: 10.1126/science.1185402

Bouabid, M.-P., Dupret, M.-A., Salmon, S., Montalbán, J., Miglio, A., and Noels, A. (2013). Effects of the Coriolis force on high-order g modes in γ Doradus stars. *Mon. Not. R. Astron. Soc.* 429, 2500–2514. doi: 10.1093/mnras/sts517

Bowman, D. M., Aerts, C., Johnston, C., Pedersen, M. G., Rogers, T. M., Edelmann, P. V. F., et al. (2019a). Photometric detection of internal gravity waves in upper main-sequence stars. I. Methodology and application to CoRoT targets. *Astron. Astrophys.* 621:A135. doi: 10.1051/0004-6361/201833662

Bowman, D. M., Burssens, S., Pedersen, M. G., Johnston, C., Aerts, C., Buysschaert, B., et al. (2019b). Low-frequency gravity waves in blue supergiants revealed by high-precision space photometry. *Nat. Astron.* 3, 760–765. doi: 10.1038/s41550-019-0768-1

Bowman, D. M., Burssens, S., Simón-Díaz, S., Edelmann, P. V. F., Rogers, T. M., Horst, L., et al. (2020). Photometric detection of internal gravity waves in upper main-sequence stars. II. Combined TESS photometry and high-resolution spectroscopy. *Astron. Astrophys.* 640:A36. doi: 10.1051/0004-6361/202038224

Briquet, M., Aerts, C., Baglin, A., Nieva, M. F., Degroote, P., Przybilla, N., et al. (2011). An asteroseismic study of the O9V star HD 46202 from CoRoT space-based photometry. *Astron. Astrophys.* 527:A112. doi: 10.1051/0004-6361/201015690

Briquet, M., Lefever, K., Uytterhoeven, K., and Aerts, C. (2005). An asteroseismic study of the β Cephei star θ Ophiuchi: spectroscopic results. *Mon. Not. R. Astron. Soc.* 362, 619–625. doi: 10.1111/j.1365-2966.2005.09287.x

Briquet, M., Morel, T., Thoul, A., Scuflaire, R., Miglio, A., Montalbán, J., et al. (2007). An asteroseismic study of the β Cephei star θ Ophiuchi: constraints on global stellar parameters and core overshooting. *Mon. Not. R. Astron. Soc.* 381, 1482–1488. doi: 10.1111/j.1365-2966.2007.12142.x

Briquet, M., Neiner, C., Aerts, C., Morel, T., Mathis, S., Reese, D. R., et al. (2012). Multisite spectroscopic seismic study of the β Cep star V2052 Ophiuchi: inhibition of mixing by its magnetic field. *Mon. Not. R. Astron. Soc.* 427, 483–493. doi: 10.1111/j.1365-2966.2012.21933.x

Briquet, M., Neiner, C., Leroy, B., Pápics, P. I., and MiMeS Collaboration (2013). Discovery of a magnetic field in the CoRoT hybrid B-type pulsator HD 43317. *Astron. Astrophys.* 557:L16. doi: 10.1051/0004-6361/201321779

Bromm, V., and Larson, R. B. (2004). The first stars. *Ann. Rev. Astron. Astrophys.* 42, 79–118. doi: 10.1146/annurev.astro.42.053102.134034

Bromm, V., Yoshida, N., Hernquist, L., and McKee, C. F. (2009). The formation of the first stars and galaxies. *Nature* 459, 49–54. doi: 10.1038/nature07990

Brott, I., Evans, C. J., Hunter, I., de Koter, A., Langer, N., Dufton, P. L., et al. (2011). Rotating massive main-sequence stars. II. Simulating a population of LMC early B-type stars as a test of rotational mixing. *Astron. Astrophys.* 530:A116. doi: 10.1051/0004-6361/201016114

Burssens, S., Bowman, D. M., Aerts, C., Pedersen, M. G., Moravveji, E., and Buysschaert, B. (2019). New β Cep pulsators discovered with K2 space photometry. *Mon. Not. R. Astron. Soc.* 489, 1304–1320. doi: 10.1093/mnras/stz2165

Burssens, S., Simón-Díaz, S., Bowman, D. M., Holgado, G., Michielsen, M., de Burgos, A., et al. (2020). Variability of OB stars from TESS southern Sectors 1-13 and high-resolution IACOB and OWN spectroscopy. *Astron. Astrophys.* 639:A81. doi: 10.1051/0004-6361/202037700

Buysschaert, B., Aerts, C., Bloemen, S., Debosscher, J., Neiner, C., Briquet, M., et al. (2015). Kepler's first view of O-star variability: K2 data of five O stars in Campaign 0 as a proof of concept for O-star asteroseismology. *Mon. Not. R. Astron. Soc.* 453, 89–100. doi: 10.1093/mnras/stv1572

Buysschaert, B., Aerts, C., Bowman, D. M., Johnston, C., Van Reeth, T., Pedersen, M. G., et al. (2018). Forward seismic modeling of the pulsating magnetic B-type star HD 43317. *Astron. Astrophys.* 616:A148. doi: 10.1051/0004-6361/201832642

Buysschaert, B., Neiner, C., Briquet, M., and Aerts, C. (2017a). Magnetic characterization of the SPB/β Cep hybrid pulsator HD 43317. *Astron. Astrophys.* 605:A104. doi: 10.1051/0004-6361/201731012

Buysschaert, B., Neiner, C., Richardson, N. D., Ramiaramanantsoa, T., David-Uraz, A., Pablo, H., et al. (2017b). Studying the photometric and spectroscopic variability of the magnetic hot supergiant ζ Orionis Aa. *Astron. Astrophys.* 602:A91. doi: 10.1051/0004-6361/201630318

Cameron, C., Saio, H., Kuschnig, R., Walker, G. A. H., Matthews, J. M., Guenther, D. B., et al. (2008). MOST detects SPBe pulsations in HD 127756 and HD 217543: asteroseismic rotation rates independent of v sin i. *Astrophys. J.* 685, 489–507. doi: 10.1086/590369

Cantiello, M., Langer, N., Brott, I., de Koter, A., Shore, S. N., Vink, J. S., et al. (2009). Sub-surface convection zones in hot massive stars and their observable consequences. *Astron. Astrophys.* 499, 279–290. doi: 10.1051/0004-6361/200911643

Chaplin, W. J., and Miglio, A. (2013). Asteroseismology of solar-type and red-giant stars. *Ann. Rev. Astron. Astrophys.* 51, 353–392. doi: 10.1146/annurev-astro-082812-140938

Chieffi, A., and Limongi, M. (2013). Pre-supernova evolution of rotating solar metallicity stars in the mass range 13-120 M $_{\odot}$ and their explosive yields. *Astrophys. J.* 764:21. doi: 10.1088/0004-637X/764/1/21

Crowther, P. A., Caballero-Nieves, S. M., Bostroem, K. A., Maíz Apellániz, J., Schneider, F. R. N., Walborn, N. R., et al. (2016). The R136 star cluster dissected with Hubble Space Telescope/STIS. I. Far-ultraviolet spectroscopic census and the origin of He II λ1640 in young star clusters. *Mon. Not. R. Astron. Soc.* 458, 624–659. doi: 10.1093/mnras/stw273

Daszyńska-Daszkiewicz, J., Dziembowski, W. A., Pamyatnykh, A. A., and Goupil, M. J. (2002). Photometric amplitudes and phases of nonradial oscillation in rotating stars. *Astron. Astrophys.* 392, 151–159. doi: 10.1051/0004-6361:20020911

Daszyńska-Daszkiewicz, J., Ostrowski, J., and Pamyatnykh, A. A. (2013a). Pulsational instability in B-type supergiant stars. *Mon. Not. R. Astron. Soc.* 432, 3153–3160. doi: 10.1093/mnras/stt670

Daszyńska-Daszkiewicz, J., Pamyatnykh, A. A., Walczak, P., Colgan, J., Fontes, C. J., and Kilcrease, D. P. (2017). Interpretation of the BRITE oscillation data of the hybrid pulsator ν Eridani: a call for the modification of stellar opacities. *Mon. Not. R. Astron. Soc.* 466, 2284–2293. doi: 10.1093/mnras/stw3315

Daszyńska-Daszkiewicz, J., Szewczuk, W., and Walczak, P. (2013b). The β Cep/SPB star 12 Lacertae: extended mode identification and complex seismic modelling. *Mon. Not. R. Astron. Soc.* 431, 3396–3407. doi: 10.1093/mnras/stt418

Daszyńska-Daszkiewicz, J., and Walczak, P. (2009). Constraints on opacities from complex asteroseismology of B-type pulsators: the β Cephei star θ Ophiuchi. *Mon. Not. R. Astron. Soc.* 398, 1961–1969. doi: 10.1111/j.1365-2966.2009.15229.x

Daszyńska-Daszkiewicz, J., and Walczak, P. (2010). Complex asteroseismology of the β Cep/slowly pulsating B-type pulsator ν Eridani: constraints on opacities. *Mon. Not. R. Astron. Soc.* 403, 496–504. doi: 10.1111/j.1365-2966.2009.16141.x

De Cat, P., and Aerts, C. (2002). A study of bright southern slowly pulsating B stars. II. The intrinsic frequencies. *Astron. Astrophys.* 393, 965–981. doi: 10.1051/0004-6361:20021068

De Cat, P., Briquet, M., Daszyńska-Daszkiewicz, J., Dupret, M. A., De Ridder, J., Scuflaire, R., et al. (2005). A study of bright southern slowly pulsating B stars. III. Mode identification for singly-periodic targets in spectroscopy. *Astron. Astrophys.* 432, 1013–1024. doi: 10.1051/0004-6361:20042103

de Mink, S. E., Langer, N., Izzard, R. G., Sana, H., and de Koter, A. (2013). The Rotation Rates of Massive Stars: The Role of Binary Interaction through Tides, Mass Transfer, and Mergers. *Astrophys. J.* 764:166. doi: 10.1088/0004-637X/764/2/166

De Ridder, J., Telting, J. H., Balona, L. A., Handler, G., Briquet, M., Daszyńska-Daszkiewicz, J., et al. (2004). Asteroseismology of the β Cephei star ν Eridani–III. Extended frequency analysis and mode identification. *Mon. Not. R. Astron. Soc.* 351, 324–332. doi: 10.1111/j.1365-2966.2004.07791.x

de Rossi, M. E., Tissera, P. B., and Pedrosa, S. E. (2010). Impact of supernova feedback on the Tully-Fisher relation. *Astron. Astrophys.* 519:A89. doi: 10.1051/0004-6361/201014058

Degroote, P. (2013). Chaos in large-amplitude pulsators: application to the β Cep star HD 180642. *Mon. Not. R. Astron. Soc.* 431, 2554–2559. doi: 10.1093/mnras/stt350

Degroote, P., Aerts, C., Baglin, A., Miglio, A., Briquet, M., Noels, A., et al. (2010a). Deviations from a uniform period spacing of gravity modes in a massive star. *Nature* 464, 259–261. doi: 10.1038/nature08864

Degroote, P., Aerts, C., Michel, E., Briquet, M., Pápics, P. I., Amado, P., et al. (2012). The CoRoT B-type binary HD 50230: a prototypical hybrid pulsator with g-mode period and p-mode frequency spacings. *Astron. Astrophys.* 542:A88. doi: 10.1051/0004-6361/201118548

Degroote, P., Briquet, M., Auvergne, M., Simón-Díaz, S., Aerts, C., Noels, A., et al. (2010b). Detection of frequency spacings in the young O-type binary HD 46149 from CoRoT photometry. *Astron. Astrophys.* 519:A38. doi: 10.1051/0004-6361/201014543

Degroote, P., Briquet, M., Catala, C., Uytterhoeven, K., Lefever, K., Morel, T., et al. (2009). Evidence for nonlinear resonant mode coupling in the β Cephei star HD 180642 (V1449 Aquilae) from CoRoT photometry. *Astron. Astrophys.* 506, 111–123. doi: 10.1051/0004-6361/200911782

Desmet, M., Aerts, C., Matthews, J. M., Cameron, C., Kuschnig, R., Walker, G. A. H., et al. (2009a). "MOST reveals spica as an eclipsing binary," inn *American Institute of Physics Conference Series, Vol. 1170 of American Institute of Physics Conference Series*, eds. J. A. Guzik and P. A. Bradley, 376–378. doi: 10.1063/1.3246517

Desmet, M., Briquet, M., Thoul, A., Zima, W., De Cat, P., Handler, G., et al. (2009b). An asteroseismic study of the β Cephei star 12 Lacertae: multisite spectroscopic observations, mode identification and seismic modelling. *Mon. Not. R. Astron. Soc.* 396, 1460–1472. doi: 10.1111/j.1365-2966.2009.14790.x

Desmet, M., Walker, G., Yang, S., Bohlender, D., Briquet, M., Østensen, R. H., et al. (2009c). Simultaneous MOST photometry and high-resolution spectroscopy of Spica, a binary system with a massive beta Cephei star component. *Commun. Asteroseismol.* 158:303. doi: 10.1063/1.3246517

Dessart, L., and Hillier, D. J. (2019). Supernovae from blue supergiant progenitors: What a mess! *Astron. Astrophys.* 622:A70. doi: 10.1051/0004-6361/201833966

Duchêne, G., and Kraus, A. (2013). Stellar multiplicity. *Ann. Rev. Astron. Astrophys.* 51, 269–310. doi: 10.1146/annurev-astro-081710-102602

Dupret, M.-A., Thoul, A., Scuflaire, R., Daszyńska-Daszkiewicz, J., Aerts, C., Bourge, P.-O., et al. (2004). Asteroseismology of the β Cep star HD 129929. II. Seismic constraints on core overshooting, internal rotation and stellar parameters. *Astron. Astrophys.* 415, 251–257. doi: 10.1051/0004-6361:20034143

Dziembowski, W. A., and Goode, P. R. (1992). Effects of differential rotation on stellar oscillations—a second-order theory. *Astrophys. J.* 394, 670–687. doi: 10.1086/171621

Dziembowski, W. A., and Jerzykiewicz, M. (1999). Asteroseismology of the beta Cephei stars. II. 12 (DD) Lacertae. *Astron. Astrophys.* 341, 480–486.

Dziembowski, W. A., Moskalik, P., and Pamyatnykh, A. A. (1993). The opacity mechanism in B-type stars–part two–excitation of high-order G-modes in main sequence stars. *Mon. Not. R. Astron. Soc.* 265:588.

Dziembowski, W. A., and Pamyatnykh, A. A. (1993). The opacity mechanism in B-type stars. I–unstable modes in beta Cephei star models. *Mon. Not. R. Astron. Soc.* 262, 204–212.

Dziembowski, W. A., and Pamyatnykh, A. A. (2008). The two hybrid B-type pulsators: ν Eridani and 12 Lacertae. *Mon. Not. R. Astron. Soc.* 385, 2061–2068. doi: 10.1111/j.1365-2966.2008.12964.x

Eckart, C. (1960). Variation principles of hydrodynamics. *Phys. Fluids* 3, 421–427. doi: 10.1063/1.1706053

Edelmann, P. V. F., Ratnasingam, R. P., Pedersen, M. G., Bowman, D. M., Prat, V., and Rogers, T. M. (2019). Three-dimensional simulations of massive stars. I. Wave generation and propagation. *Astrophys. J.* 876:4. doi: 10.3847/1538-4357/ab12df

Ekström, S., Georgy, C., Eggenberger, P., Meynet, G., Mowlavi, N., Wyttenbach, A., et al. (2012). Grids of stellar models with rotation. I. Models from 0.8 to 120 $M_{\odot}$ at solar metallicity (Z = 0.014). *Astron. Astrophys.* 537:A146. doi: 10.1051/0004-6361/201117751

Espinosa Lara, F., and Rieutord, M. (2011). Gravity darkening in rotating stars. *Astron. Astrophys.* 533:A43. doi: 10.1051/0004-6361/201117252

Freytag, B., Ludwig, H. G., and Steffen, M. (1996). Hydrodynamical models of stellar convection. The role of overshoot in DA white dwarfs, A-type stars, and the Sun. *Astron. Astrophys.* 313, 497–516.

Fuller, J. (2017). Heartbeat stars, tidally excited oscillations and resonance locking. *Mon. Not. R. Astron. Soc.* 472, 1538–1564. doi: 10.1093/mnras/stx2135

Gabriel, M., Noels, A., Montalbán, J., and Miglio, A. (2014). Proper use of Schwarzschild Ledoux criteria in stellar evolution computations. *Astron. Astrophys.* 569:A63. doi: 10.1051/0004-6361/201423442

García, R. A., and Ballot, J. (2019). Asteroseismology of solar-type stars. *Liv. Rev. Sol. Phys.* 16:4. doi: 10.1007/s41116-019-0020-1

Gautschy, A., and Saio, H. (1993). On non-radial oscillations of B-type stars. *Mon. Not. R. Astron. Soc.* 262, 213–219. doi: 10.1093/mnras/262.1.213

Georgy, C. (2012). Yellow supergiants as supernova progenitors: an indication of strong mass loss for red supergiants? *Astron. Astrophys.* 538:L8. doi: 10.1051/0004-6361/201118372

Georgy, C., Ekström, S., Eggenberger, P., Meynet, G., Haemmerlé, L., Maeder, A., et al. (2013). Grids of stellar models with rotation. III. Models from 0.8 to 120 $M_{\odot}$ at a metallicity Z = 0.002. *Astron. Astrophys.* 558:A103. doi: 10.1051/0004-6361/201322178

Georgy, C., Meynet, G., and Maeder, A. (2011). Effects of anisotropic winds on massive star evolution. *Astron. Astrophys.* 527:A52. doi: 10.1051/0004-6361/200913797

Georgy, C., Saio, H., and Meynet, G. (2014). The puzzle of the CNO abundances of α Cygni variables resolved by the Ledoux criterion. *Mon. Not. R. Astron. Soc.* 439, L6–L10. doi: 10.1093/mnrasl/slt165

Gies, D. R., and Kullavanijaya, A. (1988). The line profile variations of epsilon Persei. I. Evidence for multimode nonradial Pulsations. *Astrophys. J.* 326:813. doi: 10.1086/166140

Gies, D. R., and Lambert, D. L. (1992). Carbon, nitrogen, and oxygen abundances in early B-type stars. *Astrophys. J.* 387:673. doi: 10.1086/171116

Godart, M., Simón-Díaz, S., Herrero, A., Dupret, M. A., Grötsch-Noels, A., Salmon, S. J. A. J., et al. (2017). The IACOB project. IV. New predictions for high-degree non-radial mode instability domains in massive stars and their connection with macroturbulent broadening. *Astron. Astrophys.* 597:A23. doi: 10.1051/0004-6361/201628856

Groh, J. H., Ekström, S., Georgy, C., Meynet, G., Choplin, A., Eggenberger, P., et al. (2019). Grids of stellar models with rotation. IV. Models from 1.7 to 120 $M_{\odot}$ at a metallicity Z = 0.0004. *Astron. Astrophys.* 627:A24. doi: 10.1051/0004-6361/201833720

Guinan, E. F., Ribas, I., Fitzpatrick, E. L., Giménez, Á., Jordi, C., McCook, G. P., et al. (2000). Eclipsing binaries as astrophysical laboratories: internal structure, core convection, and evolution of the B-star components of V380 Cygni. *Astrophys. J.* 544, 409–422. doi: 10.1086/317211

Handler, G., and Aerts, C. (2002). A five-month multitechnique, multisite campaign on the Beta Cephei star Nu Eridani. *Commun. Asteroseismol.* 142, 20–24.

Handler, G., Jerzykiewicz, M., Rodríguez, E., Uytterhoeven, K., Amado, P. J., Dorokhova, T. N., et al. (2006). Asteroseismology of the β Cephei star 12 (DD) Lacertae: photometric observations, pulsational frequency analysis and mode identification. *Mon. Not. R. Astron. Soc.* 365, 327–338. doi: 10.1111/j.1365-2966.2005.09728.x

Handler, G., Matthews, J. M., Eaton, J. A., Daszyńska-Daszkiewicz, J., Kuschnig, R., Lehmann, H., et al. (2009). Asteroseismology of hybrid pulsators made possible: simultaneous MOST space photometry and ground-based spectroscopy of γ peg. *Astrophys. J. Letters* 698, L56–L59. doi: 10.1088/0004-637X/698/1/L56

Handler, G., Pigulski, A., Daszyńska-Daszkiewicz, J., Irrgang, A., Kilkenny, D., Guo, Z., et al. (2019). Asteroseismology of massive stars with the TESS mission: the runaway β Cep pulsator PHL 346 = HN Aqr. *Astrophys. J. Letters* 873:L4. doi: 10.3847/2041-8213/ab095f

Handler, G., Rybicka, M., Popowicz, A., Pigulski, A., Kuschnig, R., Zocłońska, E., et al. (2017). Combining BRITE and ground-based photometry for the β Cephei star ν Eridani: impact on photometric pulsation mode identification and detection of several g modes. *Mon. Not. R. Astron. Soc.* 464, 2249–2258. doi: 10.1093/mnras/stw2518

Handler, G., Shobbrook, R. R., Jerzykiewicz, M., Krisciunas, K., Tshenye, T., Rodríguez, E., et al. (2004). Asteroseismology of the β Cephei star ν Eridani–I. Photometric observations and pulsational frequency analysis. *Mon. Not. R. Astron. Soc.* 347, 454–462. doi: 10.1111/j.1365-2966.2004.07214.x

Handler, G., Shobbrook, R. R., and Mokgwetsi, T. (2005). An asteroseismic study of the β Cephei star θ Ophiuchi: photometric results. *Mon. Not. R. Astron. Soc.* 362, 612–618. doi: 10.1111/j.1365-2966.2005.09341.x

Handler, G., Shobbrook, R. R., Uytterhoeven, K., Briquet, M., Neiner, C., Tshenye, T., et al. (2012). A multisite photometric study of two unusual β Cep stars: the magnetic V2052 Oph and the massive rapid rotator V986 Oph. *Mon. Not. R. Astron. Soc.* 424, 2380–2391. doi: 10.1111/j.1365-2966.2012.21414.x

Heger, A., Fryer, C. L., Woosley, S. E., Langer, N., and Hartmann, D. H. (2003). How Massive Single Stars End Their Life. *Astrophys. J.* 591, 288–300. doi: 10.1086/375341

Hekker, S., and Christensen-Dalsgaard, J. (2017). Giant star seismology. *Astron. Astrophys. Rev.* 25:1. doi: 10.1007/s00159-017-0101-x

Hendriks, L., and Aerts, C. (2019). Deep learning applied to the asteroseismic modeling of stars with coherent oscillation modes. *Public. Astronom. Soc. Pac.* 131:108001. doi: 10.1088/1538-3873/aaeeec

Herwig, F. (2000). The evolution of AGB stars with convective overshoot. *Astron. Astrophys.* 360, 952–968.

Heynderickx, D., Waelkens, C., and Smeyers, P. (1994). A photometric study of β Cephei stars. II. Determination of the degrees L of pulsation modes. *Astron. Astrophys. Sup. Ser.* 105, 447–480.

Hilditch, R. W., Howarth, I. D., and Harries, T. J. (2005). Forty eclipsing binaries in the small magellanic cloud: fundamental parameters and cloud distance. *Mon. Not. R. Astron. Soc.* 357, 304–324. doi: 10.1111/j.1365-2966.2005.08653.x

Hirschi, R., Meynet, G., and Maeder, A. (2005). Stellar evolution with rotation. XIII. Predicted GRB rates at various Z. *arXiv* 443, 581–591. doi: 10.1051/0004-6361:20053329

Hopkins, P. F., Kereš, D., Oñorbe, J., Faucher-Giguère, C.-A., Quataert, E., Murray, N., et al. (2014). Galaxies on FIRE (feedback in realistic environments): stellar feedback explains cosmologically inefficient star formation. *Mon. Not. R. Astron. Soc.* 445, 581–603. doi: 10.1093/mnras/stu1738

Horst, L., Edelmann, P. V. F., Andrássy, R., Röpke, F. K., Bowman, D. M., Aerts, C., et al. (2020). Fully compressible simulations of waves and core convection in main-sequence stars. *Astron. Astrophys.* 641:A18. doi: 10.1051/0004-6361/202037531

Howell, S. B., Sobeck, C., Haas, M., Still, M., Barclay, T., Mullally, F., et al. (2014). The K2 mission: characterization and early results. *Public. Astronom. Soc. Pac.* 126, 398–408. doi: 10.1086/676406

Huat, A. L., Hubert, A. M., Baudin, F., Floquet, M., Neiner, C., Frémat, Y., et al. (2009). The B0.5IVe CoRoT target HD 49330. I. Photometric analysis from CoRoT data. *Astron. Astrophys.* 506, 95–101. doi: 10.1051/0004-6361/200911928

Hunter, I., Brott, I., Langer, N., Lennon, D. J., Dufton, P. L., Howarth, I. D., et al. (2009). The VLT-FLAMES survey of massive stars: constraints on stellar evolution from the chemical compositions of rapidly rotating Galactic and Magellanic Cloud B-type stars. *Astron. Astrophys.* 496, 841–853. doi: 10.1051/0004-6361/200809925

Hunter, I., Brott, I., Lennon, D. J., Langer, N., Dufton, P. L., Trundle, C., et al. (2008). The VLT FLAMES survey of massive stars: rotation and nitrogen enrichment as the key to understanding massive star evolution. *Astrophys. J. Letters* 676:L29. doi: 10.1086/587436

Hunter, J. D. (2007). Matplotlib: a 2D graphics environment. *Comput. Sci. Eng.* 9, 90-95. doi: 10.1109/MCSE.2007.55

Jerzykiewicz, M., Handler, G., Shobbrook, R. R., Pigulski, A., Medupe, R., Mokgwetsi, T., et al. (2005). Asteroseismology of the β Cephei star ν Eridani–IV. The 2003–2004 multisite photometric campaign and the combined 2002–2004 data. *Mon. Not. R. Astron. Soc.* 360, 619–630. doi: 10.1111/j.1365-2966.2005.09088.x

Jerzykiewicz, M., Pigulski, A., Handler, G., Moffat, A. F. J., Popowicz, A., Wade, G. A., et al. (2020). BRITE-constellation photometry of π^5 orionis, an ellipsoidal SPB variable. *Mon. Not. R. Astron. Soc.* 496, 2391–2401. doi: 10.1093/mnras/staa1665

Johnston, C., Pavlovski, K., and Tkachenko, A. (2019). Modelling of the B-type binaries CW Cephei and U Ophiuchi. A critical view on dynamical masses, core boundary mixing, and core mass. *Astron. Astrophys.* 628:A25. doi: 10.1051/0004-6361/201935235

Kallinger, T., Weiss, W. W., Beck, P. G., Pigulski, A., Kuschnig, R., Tkachenko, A., et al. (2017). Triple system HD 201433 with a SPB star component seen by BRITE–constellation: pulsation, differential rotation, and angular momentum transfer. *Astron. Astrophys.* 603:A13. doi: 10.1051/0004-6361/201730625

Kambe, E., Ando, H., and Hirata, R. (1993). Short-term line-profile variations and episodic mass loss in the Be star dzeta Ophiuchi. *Astron. Astrophys.* 273, 435–450.

Keszthelyi, Z., Meynet, G., Georgy, C., Wade, G. A., Petit, V., and David-Uraz, A. (2019). The effects of surface fossil magnetic fields on massive star evolution: I. Magnetic field evolution, mass-loss quenching, and magnetic braking. *Mon. Not. R. Astron. Soc.* 485, 5843–5860. doi: 10.1093/mnras/stz772

Keszthelyi, Z., Meynet, G., Shultz, M. E., David-Uraz, A., ud-Doula, A., Townsend, R. H. D., et al. (2020). The effects of surface fossil magnetic fields on massive star evolution - II. Implementation of magnetic braking in MESA and implications for the evolution of surface rotation in OB stars. *Mon. Not. R. Astron. Soc.* 493, 518–535. doi: 10.1093/mnras/staa237

Kippenhahn, R., Weigert, A., and Weiss, A. (2012). *Stellar Structure and Evolution*. Berlin: Springer. doi: 10.1007/978-3-642-30304-3

Koch, D. G., Borucki, W. J., Basri, G., Batalha, N. M., Brown, T. M., Caldwell, D., et al. (2010). Kepler mission design, realized photometric performance, and early science. *Astrophys. J. Letters* 713:L79. doi: 10.1088/2041-8205/713/2/L79

Koen, C., and Eyer, L. (2002). New periodic variables from the Hipparcos epoch photometry. *Mon. Not. R. Astron. Soc.* 331, 45–59. doi: 10.1046/j.1365-8711.2002.05150.x

Kurtz, D. W., Saio, H., Takata, M., Shibahashi, H., Murphy, S. J., and Sekii, T. (2014). Asteroseismic measurement of surface-to-core rotation in a main-sequence A star, KIC 11145123. *Mon. Not. R. Astron. Soc.* 444, 102–116. doi: 10.1093/mnras/stu1329

Kurtz, D. W., Shibahashi, H., Murphy, S. J., Bedding, T. R., and Bowman, D. M. (2015). A unifying explanation of complex frequency spectra of γ Dor, SPB and Be stars: combination frequencies and highly non-sinusoidal light curves. *Mon. Not. R. Astron. Soc.* 450, 3015–3029. doi: 10.1093/mnras/stv868

Langer, N. (2012). Presupernova evolution of massive single and binary stars. *Ann. Rev. Astron. Astrophys.* 50, 107–164. doi: 10.1146/annurev-astro-081811-125534

Langer, N., and Kudritzki, R. P. (2014). The spectroscopic Hertzsprung-Russell diagram. *Astron. Astrophys.* 564:A52. doi: 10.1051/0004-6361/201423374

Lee, U., and Saio, H. (1987a). Low-frequency oscillations of uniformly rotating stars. *Mon. Not. R. Astron. Soc.* 224, 513–526. doi: 10.1093/mnras/224.3.513

Lee, U., and Saio, H. (1987b). Non-adiabatic analysis of low-frequency oscillations of uniformly rotating stars. *Mon. Not. R. Astron. Soc.* 225, 643–651. doi: 10.1093/mnras/225.3.643

Lee, U., and Saio, H. (1997). Low-frequency nonradial oscillations in rotating stars. I. Angular dependence. *Astrophys. J.* 491, 839–845. doi: 10.1086/304980

Lefèvre, L., Marchenko, S. V., Moffat, A. F. J., and Acker, A. (2009). A systematic study of variability among OB-stars based on HIPPARCOS photometry. *Astron. Astrophys.* 507, 1141–1201. doi: 10.1051/0004-6361/200912304

Lefèvre, L., Marchenko, S. V., Moffat, A. F. J., Chené, A. N., Smith, S. R., St-Louis, N., et al. (2005). Oscillations in the massive Wolf-Rayet star WR 123 with the MOST satellite. *Astrophys. J. Letters* 634, L109–L112. doi: 10.1086/498393

Li, G., Bedding, T. R., Murphy, S. J., Van Reeth, T., Antoci, V., and Ouazzani, R.-M. (2019a). Period spacings of γ Doradus pulsators in the Kepler field: detection methods and application to 22 slow rotators. *Mon. Not. R. Astron. Soc.* 482, 1757–1785. doi: 10.1093/mnras/sty2743

Li, G., Van Reeth, T., Bedding, T. R., Murphy, S. J., and Antoci, V. (2019b). Period spacings of γ Doradus pulsators in the Kepler field: Rossby and gravity modes in 82 stars. *Mon. Not. R. Astron. Soc.* 487, 782–800. doi: 10.1093/mnras/stz1171

Li, G., Van Reeth, T., Bedding, T. R., Murphy, S. J., Antoci, V., Ouazzani, R.-M., et al. (2020). Gravity-mode period spacings and near-core rotation rates of 611 γ Doradus stars with Kepler. *Mon. Not. R. Astron. Soc.* 491, 3586–3605. doi: 10.1093/mnras/stz2906

Lovekin, C. C. (2020). Challenges in 2D stellar modelling. *Front. Astron. Space Sci.* 6:77. doi: 10.3389/fspas.2019.00077

Mac Low, M.-M., and Klessen, R. S. (2004). Control of star formation by supersonic turbulence. *Rev. Mod. Phys.* 76, 125–194. doi: 10.1103/RevModPhys.76.125

Maeder, A. (2009). *Physics, Formation and Evolution of Rotating Stars*. Berlin: Springer.

Maeder, A., Georgy, C., and Meynet, G. (2008). Convective envelopes in rotating OB stars. *Astron. Astrophys.* 479, L37–L40. doi: 10.1051/0004-6361:20079007

Maeder, A., and Meynet, G. (2000). The evolution of rotating stars. *Ann. Rev. Astron. Astrophys.* 38, 143–190. doi: 10.1146/annurev.astro.38.1.143

Mahy, L., Almeida, L. A., Sana, H., Clark, J. S., de Koter, A., de Mink, S. E., et al. (2020a). The Tarantula massive binary monitoring. IV. Double-lined photometric binaries. *Astron. Astrophys.* 634:A119. doi: 10.1051/0004-6361/201936152

Mahy, L., Sana, H., Abdul-Masih, M., Almeida, L. A., Langer, N., Shenar, T., et al. (2020b). The Tarantula massive binary monitoring. III. Atmosphere analysis of double-lined spectroscopic systems. *Astron. Astrophys.* 634:A118. doi: 10.1051/0004-6361/201936151

Maintz, M., Rivinius, T., Štefl, S., Baade, D., Wolf, B., and Townsend, R. H. D. (2003). Stellar and circumstellar activity of the Be star omega CMa. III. Multiline non-radial pulsation modeling. *Astron. Astrophys.* 411, 181–191. doi: 10.1051/0004-6361:20031375

Martins, F., and Palacios, A. (2013). A comparison of evolutionary tracks for single Galactic massive stars. *Astron. Astrophys.* 560:A16. doi: 10.1051/0004-6361/201322480

Mathis, S. (2009). Transport by gravito-inertial waves in differentially rotating stellar radiation zones. I–theoretical formulation. *Astron. Astrophys.* 506, 811–828. doi: 10.1051/0004-6361/200810544

Mathis, S., and Prat, V. (2019). The traditional approximation of rotation, including the centrifugal acceleration for slightly deformed stars. *Astron. Astrophys.* 631:A26. doi: 10.1051/0004-6361/201935639

McNamara, B. J., Jackiewicz, J., and McKeever, J. (2012). The classification of Kepler B-star variables. *Astrom. J.* 143:101. doi: 10.1088/0004-6256/143/4/101

Michielsen, M., Pedersen, M. G., Augustson, K. C., Mathis, S., and Aerts, C. (2019). Probing the shape of the mixing profile and of the thermal structure at the convective core boundary through asteroseismology. *Astron. Astrophys.* 628:A76. doi: 10.1051/0004-6361/201935754

Miglio, A., Montalbán, J., and Dupret, M.-A. (2007). Instability strips of slowly pulsating B stars and β Cephei stars: the effect of the updated OP opacities and of the metal mixture. *Mon. Not. R. Astron. Soc.* 375, L21–L25. doi: 10.1111/j.1745-3933.2006.00267.x

Miglio, A., Montalbán, J., Eggenberger, P., and Noels, A. (2008a). Gravity modes and mixed modes as probes of stellar cores in main-sequence stars: from solar-like to β Cep stars. *Astron. Nach.* 329, 529–534. doi: 10.1002/asna.200710991

Miglio, A., Montalbán, J., Noels, A., and Eggenberger, P. (2008b). Probing the properties of convective cores through g modes: high-order g modes in SPB and γ Doradus stars. *Mon. Not. R. Astron. Soc.* 386, 1487–1502. doi: 10.1111/j.1365-2966.2008.13112.x

Modjaz, M., Gutiérrez, C. P., and Arcavi, I. (2019). New regimes in the observation of core-collapse supernovae. *Nat. Astron.* 3, 717–724. doi: 10.1038/s41550-019-0856-2

Moe, M., and Di Stefano, R. (2017). Mind your Ps and Qs: the interrelation between period (P) and mass-ratio (Q) distributions of binary stars. *Astrophys. J. Supp. Ser.* 230:15. doi: 10.3847/1538-4365/aa6fb6

Moffat, A. F. J., Marchenko, S. V., Lefèvre, L., Chené, A.-N., St-Louis, N., Zhilyaev, B. E., et al. (2008a). "Pulsations beneath the winds: unique precise photometry from MOST," in *Mass Loss from Stars and the Evolution of Stellar Clusters, Vol. 388 of Astronomical Society of the Pacific Conference Series*, eds. A. de Koter, L. J. Smith, and L. B. F. M. Waters (Potsdam), 29.

Moffat, A. F. J., Marchenko, S. V., Zhilyaev, B. E., Rowe, J. F., Muntean, V., Chené, A.-N., et al. (2008b). MOST finds no coherent oscillations in the hot carbon-rich Wolf-Rayet star HD 165763 (WR 111). *Astrophys. J. Letters* 679:L45. doi: 10.1086/589237

Mombarg, J. S. G., Van Reeth, T., Pedersen, M. G., Molenberghs, G., Bowman, D. M., Johnston, C., et al. (2019). Asteroseismic masses, ages, and core properties of γ Doradus stars using gravito-inertial dipole modes and spectroscopy. *Mon. Not. R. Astron. Soc.* 485, 3248–3263. doi: 10.1093/mnras/stz501

Moravveji, E. (2016). The impact of enhanced iron opacity on massive star pulsations: updated instability strips. *Mon. Not. R. Astron. Soc.* 455, L67–L71. doi: 10.1093/mnrasl/slv142

Moravveji, E., Aerts, C., Pápics, P. I., Triana, S. A., and Vandoren, B. (2015). Tight asteroseismic constraints on core overshooting and diffusive mixing in the slowly rotating pulsating B8.3V star KIC 10526294. *Astron. Astrophys.* 580:A27. doi: 10.1051/0004-6361/201425290

Moravveji, E., Guinan, E. F., Shultz, M., Williamson, M. H., and Moya, A. (2012). Asteroseismology of the nearby SN-II progenitor: Rigel. I. The MOST high-precision photometry and radial velocity monitoring. *Astrophys. J.* 747:108. doi: 10.1088/0004-637X/747/2/108

Moravveji, E., Townsend, R. H. D., Aerts, C., and Mathis, S. (2016). Sub-inertial gravity modes in the B8V star KIC 7760680 reveal moderate core overshooting and low vertical diffusive mixing. *Astrophys. J.* 823:130. doi: 10.3847/0004-637X/823/2/130

Morel, T., Castro, N., Fossati, L., Hubrig, S., Langer, N., Przybilla, N., et al. (2015). "The B fields in OB stars (BOB) survey," in *New Windows on Massive Stars, Vol. 307 of IAU Symposium*, eds. G. Meynet, C. Georgy, J. Groh, and P. Stee (Geneva), 342–347. doi: 10.1017/S1743921314007054

Neilson, H. R., and Ignace, R. (2015). Period change and stellar evolution of β Cephei stars. *Astron. Astrophys.* 584:A58. doi: 10.1051/0004-6361/201526836

Neiner, C., Alecian, E., Briquet, M., Floquet, M., Frémat, Y., Martayan, C., et al. (2012a). Detecting and modelling the magnetic field of the β Cephei star V 2052 Ophiuchi. *Astron. Astrophys.* 537:A148. doi: 10.1051/0004-6361/201117941

Neiner, C., de Batz, B., Cochard, F., Floquet, M., Mekkas, A., and Desnoux, V. (2011). The Be star spectra (beSS) Database. *Astrom. J.* 142:149. doi: 10.1088/0004-6256/142/5/149

Neiner, C., Floquet, M., Samadi, R., Espinosa Lara, F., Frémat, Y., Mathis, S., et al. (2012b). Stochastic gravito-inertial modes discovered by CoRoT in the hot Be star HD 51452. *Astron. Astrophys.* 546:A47. doi: 10.1051/0004-6361/201219820

Neiner, C., Gutiérrez-Soto, J., Baudin, F., de Batz, B., Frémat, Y., Huat, A. L., et al. (2009). The pulsations of the B5IVe star HD 181231 observed with CoRoT and ground-based spectroscopy. *Astron. Astrophys.* 506, 143–151. doi: 10.1051/0004-6361/200911971

Neiner, C., Henrichs, H. F., Floquet, M., Frémat, Y., Preuss, O., Hubert, A. M., et al. (2003). Rotation, pulsations and magnetic field in <ASTROBJ>V 2052 Ophiuchi</ASTROBJ>: a new He-strong star. *Astron. Astrophys.* 411, 565–579. doi: 10.1051/0004-6361:20031342

Neiner, C., Wade, G. A., Marsden, S. C., and Blazère, A. (2017). "The BRITE spectropolarimetric program," in *Second BRITE-Constellation Science Conference: Small Satellites–Big Science, Proceedings of the Polish Astronomical Society Volume 5, Held 22–26 August, 2016 in Innsbruck, Austria* (Warsaw: Polish Astronomical Society), 86–93.

Nieva, M.-F., and Przybilla, N. (2012). Present-day cosmic abundances. A comprehensive study of nearby early B-type stars and implications for stellar and Galactic evolution and interstellar dust models. *Astron. Astrophys.* 539:A143. doi: 10.1051/0004-6361/201118158

Nomoto, K., Tominaga, N., Umeda, H., Kobayashi, C., and Maeda, K. (2006). Nucleosynthesis yields of core-collapse supernovae and hypernovae, and galactic chemical evolution. *Nucl. Phys. A* 777, 424–458. doi: 10.1016/j.nuclphysa.2006.05.008

Osaki, J. (1975). Nonradial oscillations of a 10 solar mass star in the main-sequence stage. *Public. Astronom. Soc. Jpn.* 27, 237–258.

Ostrowski, J., and Daszyńska-Daszkiewicz, J. (2015). Pulsations in B-type supergiants with masses $M<20\ M_{\odot}$ before and after core helium ignition. *Mon. Not. R. Astron. Soc.* 447, 2378–2386. doi: 10.1093/mnras/stu2605

Ostrowski, J., Daszyńska-Daszkiewicz, J., and Cugier, H. (2017). Revising the evolutionary stage of HD 163899: the effects of convective overshooting and rotation. *Astrophys. J.* 835:290. doi: 10.3847/1538-4357/835/2/290

Ouazzani, R.-M., Salmon, S. J. A. J., Antoci, V., Bedding, T. R., Murphy, S. J., and Roxburgh, I. W. (2017). A new asteroseismic diagnostic for internal rotation in γ Doradus stars. *Mon. Not. R. Astron. Soc.* 465, 2294–2309. doi: 10.1093/mnras/stw2717

Ouazzani, R. M., Marques, J. P., Goupil, M. J., Christophe, S., Antoci, V., Salmon, S. J. A. J., et al. (2019). γ Doradus stars as a test of angular momentum transport models. *Astron. Astrophys.* 626:A121. doi: 10.1051/0004-6361/201832607

Pablo, H., Richardson, N. D., Fuller, J., Rowe, J., Moffat, A. F. J., Kuschnig, R., et al. (2017). The most massive heartbeat: an in-depth analysis of ι Orionis. *Mon. Not. R. Astron. Soc.* 467, 2494–2503. doi: 10.1093/mnras/stx207

Pablo, H., Shultz, M., Fuller, J., Wade, G. A., Paunzen, E., Mathis, S., et al. (2019). $\in$ Lupi: measuring the heartbeat of a doubly magnetic massive binary with BRITE constellation. *Mon. Not. R. Astron. Soc.* 488, 64–77. doi: 10.1093/mnras/stz1661

Pablo, H., Whittaker, G. N., Popowicz, A., Mochnacki, S. M., Kuschnig, R., Grant, C. C., et al. (2016). The BRITE constellation nanosatellite mission: testing, commissioning, and operations. *Public. Astronom. Soc. Pac.* 128:125001. doi: 10.1088/1538-3873/128/970/125001

Pamyatnykh, A. A. (1999). Pulsational instability domains in the upper main sequence. *Astron. Nach.* 49, 119–148.

Pamyatnykh, A. A., Handler, G., and Dziembowski, W. A. (2004). Asteroseismology of the β Cephei star ν Eridani: interpretation and applications of the oscillation spectrum. *Mon. Not. R. Astron. Soc.* 350, 1022–1028. doi: 10.1111/j.1365-2966.2004.07721.x

Pápics, P. I., Briquet, M., Auvergne, M., Aerts, C., Degroote, P., Niemczura, E., et al. (2011). CoRoT high-precision photometry of the B0.5 IV star HD 51756. *Astron. Astrophys.* 528:A123. doi: 10.1051/0004-6361/201016131

Pápics, P. I., Briquet, M., Baglin, A., Poretti, E., Aerts, C., Degroote, P., et al. (2012). Gravito-inertial and pressure modes detected in the B3 IV CoRoT target HD 43317. *Astron. Astrophys.* 542:A55. doi: 10.1051/0004-6361/201218809

Pápics, P. I., Moravveji, E., Aerts, C., Tkachenko, A., Triana, S. A., Bloemen, S., et al. (2014). KIC 10526294: a slowly rotating B star with rotationally split, quasi-equally spaced gravity modes. *Astron. Astrophys.* 570:A8. doi: 10.1051/0004-6361/201424094

Pápics, P. I., Tkachenko, A., Aerts, C., Van Reeth, T., De Smedt, K., Hillen, M., et al. (2015). Asteroseismic fingerprints of rotation and mixing in the slowly pulsating B8 V star KIC 7760680. *Astrophys. J. Letters* 803:L25. doi: 10.1088/2041-8205/803/2/L25

Pápics, P. I., Tkachenko, A., Van Reeth, T., Aerts, C., Moravveji, E., Van de Sande, M., et al. (2017). Signatures of internal rotation discovered in the Kepler data of five slowly pulsating B stars. *Astron. Astrophys.* 598:A74. doi: 10.1051/0004-6361/201629814

Paxton, B., Bildsten, L., Dotter, A., Herwig, F., Lesaffre, P., and Timmes, F. (2011). Modules for experiments in stellar astrophysics (MESA). *Astrophys. J. Supp. Ser.* 192:3. doi: 10.1088/0067-0049/192/1/3

Paxton, B., Cantiello, M., Arras, P., Bildsten, L., Brown, E. F., Dotter, A., et al. (2013). Modules for experiments in stellar astrophysics (MESA): planets, oscillations, rotation, and massive stars. *Astrophys. J. Supp. Ser.* 208:4. doi: 10.1088/0067-0049/208/1/4

Paxton, B., Marchant, P., Schwab, J., Bauer, E. B., Bildsten, L., Cantiello, M., et al. (2015). Modules for experiments in stellar astrophysics (MESA): binaries, pulsations, and explosions. *Astrophys. J. Supp. Ser.* 220:15. doi: 10.1088/0067-0049/220/1/15

Paxton, B., Schwab, J., Bauer, E. B., Bildsten, L., Blinnikov, S., Duffell, P., et al. (2018). Modules for experiments in stellar astrophysics (MESA): convective boundaries, element diffusion, and massive star explosions. *Astrophys. J. Supp. Ser.* 234:34. doi: 10.3847/1538-4365/aaa5a8

Paxton, B., Smolec, R., Schwab, J., Gautschy, A., Bildsten, L., Cantiello, M., et al. (2019). Modules for experiments in stellar astrophysics (MESA): pulsating variable stars, rotation, convective boundaries, and energy conservation. *Astrophys. J. Supp. Ser.* 243:10. doi: 10.3847/1538-4365/ab2241

Pedersen, M. G., Aerts, C., Pápics, P. I., and Rogers, T. M. (2018). The shape of convective core overshooting from gravity-mode period spacings. *Astron. Astrophys.* 614:A128. doi: 10.1051/0004-6361/201732317

Pedersen, M. G., Chowdhury, S., Johnston, C., Bowman, D. M., Aerts, C., Handler, G., et al. (2019). Diverse variability of O and B stars revealed from 2-minute Cadence light curves in sectors 1 and 2 of the TESS mission: selection of an asteroseismic sample. *Astrophys. J. Letters* 872:L9. doi: 10.3847/2041-8213/ab01e1

Pigulski, A., Cugier, H., Popowicz, A., Kuschnig, R., Moffat, A. F. J., Rucinski, S. M., et al. (2016). Massive pulsating stars observed by BRITE-Constellation. I. The triple system β Centauri (Agena). *Astron. Astrophys.* 588:A55. doi: 10.1051/0004-6361/201527872

Pigulski, A., and Pojmański, G. (2008a). β Cephei stars in the ASAS-3 data. I. Long-term variations of periods and amplitudes. *Astron. Astrophys.* 477, 907–915. doi: 10.1051/0004-6361:20078580

Pigulski, A., and Pojmański, G. (2008b). β Cephei stars in the ASAS-3 data. II. 103 new β Cephei stars and a discussion of low-frequency modes. *Astron. Astrophys.* 477, 917–929. doi: 10.1051/0004-6361:20078581

Podsiadlowski, P., Joss, P. C., and Hsu, J. J. L. (1992). Presupernova evolution in massive interacting binaries. *Astrophys. J.* 391:246. doi: 10.1086/171341

Pope, B. J. S., Davies, G. R., Hawkins, K., White, T. R., Stokholm, A., Bieryla, A., et al. (2019a). The Kepler smear campaign: light curves for 102 very bright stars. *Astrophys. J. Supp. Ser.* 244:18. doi: 10.3847/1538-4365/ab2c04

Pope, B. J. S., White, T. R., Farr, W. M., Yu, J., Greklek-McKeon, M., Huber, D., et al. (2019b). The K2 bright star survey. I. Methodology and data release. *Astrophys. J. Supp. Ser.* 245:8. doi: 10.3847/1538-4365/ab3d29

Pope, B. J. S., White, T. R., Huber, D., Murphy, S. J., Bedding, T. R., Caldwell, D. A., et al. (2016). Photometry of very bright stars with Kepler and K2 smear data. *Mon. Not. R. Astron. Soc.* 455, L36–L40. doi: 10.1093/mnrasl/slv143

Porter, J. M., and Rivinius, T. (2003). Classical Be stars. *Public. Astronom. Soc. Pac.* 115, 1153–1170. doi: 10.1086/378307

Przybilla, N., Nieva, M. F., Irrgang, A., and Butler, K. (2013). "Hot stars and cosmic abundances," in *EAS Publications Series, Vol. 63 of EAS Publications Series*, eds. G. Alecian, Y. Lebreton, O. Richard, and G. Vauclair, 13–23. doi: 10.1051/eas/1363002

Ramiaramanantsoa, T., Ignace, R., Moffat, A. F. J., St-Louis, N., Shkolnik, E. L., Popowicz, A., et al. (2019). The chaotic wind of WR 40 as probed by BRITE. *Mon. Not. R. Astron. Soc.* 490, 5921–5930. doi: 10.1093/mnras/stz2895

Ramiaramanantsoa, T., Moffat, A. F. J., Harmon, R., Ignace, R., St-Louis, N., Vanbeveren, D., et al. (2018a). BRITE-Constellation high-precision time-dependent photometry of the early O-type supergiant ζ Puppis unveils the photospheric drivers of its small- and large-scale wind structures. *Mon. Not. R. Astron. Soc.* 473, 5532–5569. doi: 10.1093/mnras/stx2671

Ramiaramanantsoa, T., Ratnasingam, R., Shenar, T., Moffat, A. F. J., Rogers, T. M., Popowicz, A., et al. (2018b). A BRITE view on the massive O-type supergiant V973 Scorpii: hints towards internal gravity waves or sub-surface convection zones. *Mon. Not. R. Astron. Soc.* 480, 972–986. doi: 10.1093/mnras/sty1897

Ricker, G. R., Winn, J. N., Vanderspek, R., Latham, D. W., Bakos, G. Á., Bean, J. L., et al. (2015). Transiting exoplanet survey satellite (TESS). *J. Astron. Telesc. Instrum. Syst.* 1:014003. doi: 10.1117/1.JATIS.1.1.014003

Rivinius, T., Baade, D., and Štefl, S. (2003). Non-radially pulsating Be stars. *Astron. Astrophys.* 411, 229–247. doi: 10.1051/0004-6361:20031285

Rivinius, T., Carciofi, A. C., and Martayan, C. (2013). Classical Be stars. Rapidly rotating B stars with viscous Keplerian decretion disks. *Astron. Astrophys. Rev.* 21:69. doi: 10.1007/s00159-013-0069-0

Robertson, B. E., Ellis, R. S., Dunlop, J. S., McLure, R. J., and Stark, D. P. (2010). Early star-forming galaxies and the reionization of the universe. *Nature* 468, 49–55. doi: 10.1038/nature09527

Rogers, T. M. (2015). On the differential rotation of massive main-sequence stars. *Astrophys. J. Letters* 815:L30. doi: 10.1088/2041-8205/815/2/L30

Rogers, T. M., Lin, D. N. C., McElwaine, J. N., and Lau, H. H. B. (2013). Internal gravity waves in massive stars: angular momentum transport. *Astrophys. J.* 772:21. doi: 10.1088/0004-637X/772/1/21

Rogers, T. M., and McElwaine, J. N. (2017). On the chemical mixing induced by internal gravity waves. *Astrophys. J. Letters* 848:L1. doi: 10.3847/2041-8213/aa8d13

Rosen, A. L., Offner, S. S. R., Sadavoy, S. I., Bhandare, A., Vázquez-Semadeni, E., and Ginsburg, A. (2020). Zooming in on individual star formation: low- and high-mass stars. *Space Sci. Rev.* 216:62. doi: 10.1007/s11214-020-00688-5

Saio, H., Cameron, C., Kuschnig, R., Walker, G. A. H., Matthews, J. M., Rowe, J. F., et al. (2007a). g-modes in the late-type Be star β CMi detected by the MOST satellite. *Commun. Asteroseismol.* 150:215. doi: 10.1553/cia150s215

Saio, H., Cameron, C., Kuschnig, R., Walker, G. A. H., Matthews, J. M., Rowe, J. F., et al. (2007b). MOST detects g-modes in the late-type Be star β Canis Minoris (B8 Ve). *Astrophys. J.* 654, 544–550. doi: 10.1086/509315

Saio, H., Georgy, C., and Meynet, G. (2013). Evolution of blue supergiants and α Cygni variables: puzzling CNO surface abundances. *Mon. Not. R. Astron. Soc.* 433, 1246–1257. doi: 10.1093/mnras/stt796

Saio, H., Kato, M., and Nomoto, K. (1988). Why did the progenitor of SN 1987A undergo the blue-red-blue evolution? *Astrophys. J.* 331, 388–393. doi: 10.1086/166565

Saio, H., Kuschnig, R., Gautschy, A., Cameron, C., Walker, G. A. H., Matthews, J. M., et al. (2006). MOST detects g- and p-modes in the B supergiant HD 163899 (B2 Ib/II). *Astrophys. J.* 650, 1111–1118. doi: 10.1086/507409

Salmon, S., Montalbán, J., Morel, T., Miglio, A., Dupret, M.-A., and Noels, A. (2012). Testing the effects of opacity and the chemical mixture on the excitation of pulsations in B stars of the magellanic clouds. *Mon. Not. R. Astron. Soc.* 422, 3460–3474. doi: 10.1111/j.1365-2966.2012.20857.x

Sana, H., de Mink, S. E., de Koter, A., Langer, N., Evans, C. J., Gieles, M., et al. (2012). Binary interaction dominates the evolution of massive stars. *Science* 337:444. doi: 10.1126/science.1223344

Seaton, M. J. (2005). Opacity project data on CD for mean opacities and radiative accelerations. *Mon. Not. R. Astron. Soc.* 362, L1–L3. doi: 10.1111/j.1365-2966.2005.00019.x

Serenelli, A., Weiss, A., Aerts, C., Angelou, G. C., Baroch, D., Bastian, N., et al. (2020). Weighing stars from birth to death: mass determination methods across the HRD. *arXiv[Preprint].arXiv:2006.10868*.

Shobbrook, R. R., Handler, G., Lorenz, D., and Mogorosi, D. (2006). Photometric studies of three multiperiodic β Cephei stars: β CMa, 15 CMa and KZ Mus. *Mon. Not. R. Astron. Soc.* 369, 171–181. doi: 10.1111/j.1365-2966.2006.10289.x

Shultz, M. E., Wade, G. A., Rivinius, T., Neiner, C., Alecian, E., Bohlender, D., et al. (2018). The magnetic early B-type stars I: magnetometry and rotation. *Mon. Not. R. Astron. Soc.* 475, 5144–5178. doi: 10.1093/mnras/sty103

Simón-Díaz, S., Castro, N., Garcia, M., Herrero, A., and Markova, N. (2011). The IACOB spectroscopic database of Northern Galactic OB stars. *Bull. Soc. R. Sci. Liege* 80, 514–518.

Simón-Díaz, S., Godart, M., Castro, N., Herrero, A., Aerts, C., Puls, J., et al. (2017). The IACOB project. III. New observational clues to understand macroturbulent broadening in massive O- and B-type stars. *Astron. Astrophys.* 597:A22. doi: 10.1051/0004-6361/201628541

Simón-Díaz, S., and Herrero, A. (2014). The IACOB project. I. Rotational velocities in northern Galactic O- and early B-type stars revisited. The impact of other sources of line-broadening. *Astron. Astrophys.* 562:A135. doi: 10.1051/0004-6361/201322758

Simón-Díaz, S., Herrero, A., Uytterhoeven, K., Castro, N., Aerts, C., and Puls, J. (2010). Observational evidence for a correlation between macroturbulent broadening and line-profile variations in OB supergiants. *Astrophys. J. Letters* 720, L174–L178. doi: 10.1088/2041-8205/720/2/L174

Simón-Díaz, S., Negueruela, I., Maíz Apellániz, J., Castro, N., Herrero, A., Garcia, M., et al. (2015). "The IACOB spectroscopic database: recent updates and first data release," in *Highlights of Spanish Astrophysics VIII*, eds. A. J. Cenarro, F. Figueras, C. Hernández-Monteagudo, J. Trujillo Bueno, and L. Valdivielso (Teruel), 576–581.

Smartt, S. J. (2009). Progenitors of core-collapse supernovae. *Ann. Rev. Astron. Astrophys.* 47, 63–106. doi: 10.1146/annurev-astro-082708-101737

Smith, M. A. (1977). Nonradial pulsations in early to mid-B stars. *Astrophys. J.* 215, 574–583. doi: 10.1086/155391

Smith, M. A., and McCall, M. L. (1978). Undulations of a B-type star: 53 Persei. *Astrophys. J.* 223, 221–233. doi: 10.1086/156253

Southworth, J., Bowman, D. M., Tkachenko, A., and Pavlovski, K. (2020). Discovery of β Cep pulsations in the eclipsing binary V453 Cygni. *Mon. Not. R. Astron. Soc.* 497, L19–L23. doi: 10.1093/mnrasl/slaa091

Stankov, A., and Handler, G. (2005). Catalog of Galactic β Cephei stars. *Astrophys. J. Supp. Ser.* 158, 193–216. doi: 10.1086/429408

Stark, D. P. (2016). Galaxies in the first billion years after the big bang. *Ann. Rev. Astron. Astrophys.* 54, 761–803. doi: 10.1146/annurev-astro-081915-023417

Štefl, S., Baade, D., Rivinius, T., Stahl, O., Budovičová, A., Kaufer, A., et al. (2003). Stellar and circumstellar activity of the Be star omega CMa. II. Periodic line-profile variability. *Astron. Astrophys.* 411, 167–180. doi: 10.1051/0004-6361:20031179

Suárez, J. C., Goupil, M. J., Reese, D. R., Samadi, R., Lignières, F., Rieutord, M., et al. (2010). On the interpretation of Echelle diagrams for solar-like oscillations effect of centrifugal distortion. *Astrophys. J.* 721, 537–546. doi: 10.1088/0004-637X/721/1/537

Suárez, J. C., Moya, A., Amado, P. J., Martín-Ruiz, S., Rodríguez-López, C., and Garrido, R. (2009). Seismology of β Cephei stars: differentially rotating models for interpreting the oscillation spectrum of ν Eridani. *Astrophys. J.* 690, 1401–1411. doi: 10.1088/0004-637X/690/2/1401

Szewczuk, W., and Daszyńska-Daszkiewicz, J. (2015). Seismic modelling of the rotating, slowly pulsating B-type star HD 21071. *Mon. Not. R. Astron. Soc.* 453, 277–286. doi: 10.1093/mnras/stv1589

Szewczuk, W., and Daszyńska-Daszkiewicz, J. (2017). Domains of pulsational instability of low-frequency modes in rotating upper main sequence stars. *Mon. Not. R. Astron. Soc.* 469, 13–46. doi: 10.1093/mnras/stx738

Szewczuk, W., and Daszyńska-Daszkiewicz, J. (2018). KIC 3240411–the hottest known SPB star with the asymptotic g-mode period spacing. *Mon. Not. R. Astron. Soc.* 478, 2243–2256. doi: 10.1093/mnras/sty1126

Tanvir, N. R., Fox, D. B., Levan, A. J., Berger, E., Wiersema, K., Fynbo, J. P. U., et al. (2009). A γ-ray burst at a redshift of z$\sim$8.2. *Nature* 461, 1254–1257. doi: 10.1038/nature08459

Tassoul, M. (1980). Asymptotic approximations for stellar nonradial pulsations. *Astrophys. J. Supp. Ser.* 43, 469–490. doi: 10.1086/190678

Telting, J. H., Aerts, C., and Mathias, P. (1997). A period analysis of the optical line variability of β Cephei: evidence for multi-mode pulsation and rotational modulation. *Astron. Astrophys.* 322, 493–506.

Telting, J. H., and Schrijvers, C. (1997). Line-profile variations of non-radial adiabatic pulsations of rotating stars. II. The diagnostic value of amplitude and phase diagrams derived from time series of spectra. *Astron. Astrophys.* 317, 723–741.

Tkachenko, A., Degroote, P., Aerts, C., Pavlovski, K., Southworth, J., Pápics, P. I., et al. (2014). The eccentric massive binary V380 Cyg: revised orbital elements and interpretation of the intrinsic variability of the primary component. *Mon. Not. R. Astron. Soc.* 438, 3093–3110. doi: 10.1093/mnras/stt2421

Tkachenko, A., Matthews, J. M., Aerts, C., Pavlovski, K., Pápics, P. I., Zwintz, K., et al. (2016). Stellar modelling of Spica, a high-mass spectroscopic binary with a β Cep variable primary component. *Mon. Not. R. Astron. Soc.* 458, 1964–1976. doi: 10.1093/mnras/stw255

Tkachenko, A., Pavlovski, K., Johnston, C., Pedersen, M. G., Michielsen, M., Bowman, D. M., et al. (2020). The mass discrepancy in intermediate- and high-mass eclipsing binaries: the need for higher convective core masses. *Astron. Astrophys.* 637:A60. doi: 10.1051/0004-6361/202037452

Torres, G., Andersen, J., and Giménez, A. (2010). Accurate masses and radii of normal stars: modern results and applications. *Astron. Astrophys. Rev.* 18, 67–126. doi: 10.1007/s00159-009-0025-1

Townsend, R. H. D. (2003a). A semi-analytical formula for the light variations due to low-frequency g modes in rotating stars. *Mon. Not. R. Astron. Soc.* 343, 125–136. doi: 10.1046/j.1365-8711.2003.06640.x

Townsend, R. H. D. (2003b). Asymptotic expressions for the angular dependence of low-frequency pulsation modes in rotating stars. *Mon. Not. R. Astron. Soc.* 340, 1020–1030. doi: 10.1046/j.1365-8711.2003.06379.x

Townsend, R. H. D. (2005). Influence of the Coriolis force on the instability of slowly pulsating B stars. *Mon. Not. R. Astron. Soc.* 360, 465–476. doi: 10.1111/j.1365-2966.2005.09002.x

Townsend, R. H. D., Goldstein, J., and Zweibel, E. G. (2018). Angular momentum transport by heat-driven g-modes in slowly pulsating B stars. *Mon. Not. R. Astron. Soc.* 475, 879–893. doi: 10.1093/mnras/stx3142

Townsend, R. H. D., Owocki, S. P., and Howarth, I. D. (2004). Be-star rotation: how close to critical? *Mon. Not. R. Astron. Soc.* 350, 189–195. doi: 10.1111/j.1365-2966.2004.07627.x

Townsend, R. H. D., and Teitler, S. A. (2013). GYRE: an open-source stellar oscillation code based on a new Magnus Multiple Shooting scheme. *Mon. Not. R. Astron. Soc.* 435, 3406–3418. doi: 10.1093/mnras/stt1533

Triana, S. A., Moravveji, E., Pápics, P. I., Aerts, C., Kawaler, S. D., and Christensen-Dalsgaard, J. (2015). The internal rotation profile of the B-type star KIC 10526294 from frequency inversion of its dipole gravity modes. *Astrophys. J.* 810:16. doi: 10.1088/0004-637X/810/1/16

Unno, W., Osaki, Y., Ando, H., Saio, H., and Shibahashi, H. (1989). *Nonradial Oscillations of Stars*. Tokyo: University of Tokyo Press.

Uytterhoeven, K., Briquet, M., Aerts, C., Telting, J. H., Harmanec, P., Lefever, K., et al. (2005). Disentangling component spectra of κ Scorpii, a spectroscopic binary with a pulsating primary. II. Interpretation of the line-profile variability. *Astron. Astrophys.* 432, 955–967. doi: 10.1051/0004-6361:20041444

Uytterhoeven, K., Telting, J. H., Aerts, C., and Willems, B. (2004). Interpretation of the variability of the β Cephei star λ Scorpii. II. The line-profile diagnostics. *Astron. Astrophys.* 427, 593–605. doi: 10.1051/0004-6361:20041224

van der Walt, S., Colbert, S. C., and Varoquaux, G. (2011). The NumPy Array: a structure for efficient numerical computation. *Comput. Sci. Eng.* 13, 22–30.

van Leeuwen, F., Evans, D. W., Grenon, M., Grossmann, V., Mignard, F., and Perryman, M. A. C. (1997). The HIPPARCOS mission: photometric data. *Astron. Astrophys.* 323, L61–L64.

Van Reeth, T., Mombarg, J. S. G., Mathis, S., Tkachenko, A., Fuller, J., Bowman, D. M., et al. (2018). Sensitivity of gravito-inertial modes to differential rotation in intermediate-mass main-sequence stars. *Astron. Astrophys.* 618:A24. doi: 10.1051/0004-6361/201832718

Van Reeth, T., Tkachenko, A., and Aerts, C. (2016). Interior rotation of a sample of γ Doradus stars from ensemble modelling of their gravity-mode period spacings. *Astron. Astrophys.* 593:A120. doi: 10.1051/0004-6361/201628616

Van Reeth, T., Tkachenko, A., Aerts, C., Pápics, P. I., Degroote, P., Debosscher, J., et al. (2015a). Detecting non-uniform period spacings in the Kepler photometry of γ Doradus stars: methodology and case studies. *Astron. Astrophys.* 574:A17. doi: 10.1051/0004-6361/201424585

Van Reeth, T., Tkachenko, A., Aerts, C., Pápics, P. I., Triana, S. A., Zwintz, K., et al. (2015b). Gravity-mode period spacings as a seismic diagnostic for a sample of γ Doradus stars from Kepler space photometry and high-resolution ground-based spectroscopy. *Astrophys. J. Supp. Ser.* 218:27. doi: 10.1088/0067-0049/218/2/27

von Zeipel, H. (1924). The radiative equilibrium of a rotating system of gaseous masses. *Mon. Not. R. Astron. Soc.* 84, 665–683. doi: 10.1093/mnras/84.9.665

Wade, G. A., Neiner, C., Alecian, E., Grunhut, J. H., Petit, V., Batz, B. d., et al. (2016). The MiMeS survey of magnetism in massive stars: introduction and overview. *Mon. Not. R. Astron. Soc.* 456, 2–22. doi: 10.1093/mnras/stv2568

Waelkens, C. (1991). Slowly pulsating B stars. *Astron. Astrophys.* 246, 453–468.

Waelkens, C., Aerts, C., Grenon, M., and Eyer, L. (1998a). "Pulsating B stars discovered by HIPPARCOS," in *A Half Century of Stellar Pulsation Interpretation, Vol. 135 of Astronomical Society of the Pacific Conference Series*, eds. P. A. Bradley and J. A. Guzik (Los Alamos, NM), 375.

Waelkens, C., Aerts, C., Kestens, E., Grenon, M., and Eyer, L. (1998b). Study of an unbiased sample of B stars observed with Hipparcos: the discovery of a large amount of new slowly pulsating B stars. *Astron. Astrophys.* 330, 215–221.

Wagle, G. A., Ray, A., Dev, A., and Raghu, A. (2019). Type IIP supernova progenitors and their explodability. I. Convective overshoot, blue loops, and surface composition. *Astrophys. J.* 886:27. doi: 10.3847/1538-4357/ab4a19

Walczak, P., Daszyńska-Daszkiewicz, J., Pamyatnykh, A. A., and Zdravkov, T. (2013). The hybrid B-type pulsator γ Pegasi: mode identification and complex seismic modelling. *Mon. Not. R. Astron. Soc.* 432, 822–831. doi: 10.1093/mnras/stt492

Walczak, P., Daszyńska-Daszkiewicz, J., Pigulski, A., Pamyatnykh, A., Moffat, A. F. J., Handler, G., et al. (2019). Seismic modelling of early B-type pulsators observed by BRITE–I. θ Ophiuchi. *Mon. Not. R. Astron. Soc.* 485, 3544–3557. doi: 10.1093/mnras/stz639

Walczak, P., Fontes, C. J., Colgan, J., Kilcrease, D. P., and Guzik, J. A. (2015). Wider pulsation instability regions for β Cephei and SPB stars calculated using new Los Alamos opacities. *Astron. Astrophys.* 580:L9. doi: 10.1051/0004-6361/201526824

Walker, G., Matthews, J., Kuschnig, R., Johnson, R., Rucinski, S., Pazder, J., et al. (2003). The MOST asteroseismology mission: ultraprecise photometry from space. *Public. Astronom. Soc. Pac.* 115, 1023–1035. doi: 10.1086/377358

Walker, G. A. H., Kuschnig, R., Matthews, J. M., Cameron, C., Saio, H., Lee, U., et al. (2005). MOST detects g-modes in the Be star HD 163868. *Astrophys. J. Letters* 635, L77–L80. doi: 10.1086/499362

Watson, R. D. (1988). Contributing factors to flux changes in nonradial stellar pulsations. *Astrophys. Space Sci.* 140, 255–290. doi: 10.1007/BF00638984

Weiss, W. W., Rucinski, S. M., Moffat, A. F. J., Schwarzenberg-Czerny, A., Koudelka, O. F., Grant, C. C., et al. (2014). BRITE-constellation: nanosatellites for precision photometry of bright stars. *Public. Astronom. Soc. Pac.* 126:573. doi: 10.1086/677236

White, T. R., Pope, B. J. S., Antoci, V., Pápics, P. I., Aerts, C., Gies, D. R., et al. (2017). Beyond the Kepler/K2 bright limit: variability in the seven brightest members of the Pleiades. *Mon. Not. R. Astron. Soc.* 471, 2882–2901. doi: 10.1093/mnras/stx1050

Wu, T., and Li, Y. (2019). High-precision asteroseismology in a slowly pulsating B star: HD 50230. *Astrophys. J.* 881:86. doi: 10.3847/1538-4357/ab2ad8

Zahn, J.-P. (1992). Circulation and turbulence in rotating stars. *Astron. Astrophys.* 265, 115–132.

Zorec, J., and Briot, D. (1997). Critical study of the frequency of Be stars taking into account their outstanding characteristics. *Astron. Astrophys.* 318, 443–460.

Conflict of Interest: The author declares that the research was conducted in the absence of any commercial or financial relationships that could be construed as a potential conflict of interest.

frontiers in Astronomy and Space Sciences

ORIGINAL RESEARCH
published: 29 October 2020
doi: 10.3389/fspas.2020.529025

The Hot Limit of Solar-like Oscillations From *Kepler* Photometry

Luis A. Balona *

South African Astronomical Observatory, Cape Town, South Africa

Kepler short-cadence photometry of 2,347 stars with effective temperatures in the range 6,000–10,000 K was used to search for the presence of solar-like oscillations. The aim is to establish the location of the hot end of the stochastic convective excitation mechanism and to what extent it may overlap the δ Scuti/γ Doradus instability region. A simple but effective autocorrelation method is described which is capable of detecting low-amplitude solar-like oscillations, but with significant risk of a false detection. The location of the frequency of maximum oscillation power, $\nu_{\max}$, and the large frequency separation, $\Delta\nu$, is determined for 167 stars hotter than 6,000 K, of which 70 are new detections. Results indicate that the hot edge of excitation of solar-like oscillations does not appear to extend into the δ Scuti/γ Doradus instability strip.

Keywords: solar-like oscillations, stellar pulsation, asteroseismology, δ Scuti stars, γ Doradus stars, asteroseismology

OPEN ACCESS

Edited by:
Antony Eugene Lynas-Gray, University College London, United Kingdom

Reviewed by:
Tiago Campante, Instituto de Astrofísica e Ciências do Espaço (IA), Portugal
Andrzej S. Baran, Pedagogical University of Kraków, Poland

***Correspondence:**
Luis A. Balona
lab@saao.ac.za

Specialty section:
This article was submitted to Frontiers in Astronomy and Space Sciences, a section of the journal Frontiers in Astronomy and Space Sciences

Received: *22 January 2020*
Accepted: *24 September 2020*
Published: *29 October 2020*

Citation:
Balona LA (2020) The Hot Limit of Solar-like Oscillations From Kepler Photometry. Front. Astron. Space Sci. 7:529025. doi: 10.3389/fspas.2020.529025

INTRODUCTION

Convective eddies in the outermost layers of a star have characteristic turn-over time scales. If the turn-over time scale matches a global pulsational period, energy is transferred from convective cell motion to drive the global pulsation mode at that period; destructive interference filters out all but the resonant frequencies. Thus random convective noise is transformed into distinct p-mode pulsations with a wide range of spherical harmonics. Stochastic oscillations driven in this way are called solar-like oscillations. Such oscillations were first detected in the Sun by Leighton et al. (1962) as quasi-periodic intensity and radial velocity variations with a period of about 5 min.

Owing to their very small amplitudes, detection from the ground of solar-like oscillations in other stars had to await advances in spectroscopic detectors. The first unambiguous detection may perhaps be attributed to Kjeldsen et al. (1995) for the G0IV star η Boo. The advent of space photometry, first with the *CoRoT* (Fridlund et al., 2006) and later the *Kepler* spacecrafts (Borucki et al., 2010), led to the discovery of solar-like oscillations in thousands of stars. Most of these are red giants where the oscillations have the highest amplitudes.

The individual modes in solar-like oscillations form a distinctive frequency pattern which is well-described by the asymptotic relation for p modes (Tassoul, 1980). Successive radial overtones, n, of modes with the same spherical harmonic number, l, are spaced at a nearly constant frequency interval, $\Delta\nu$, which is known as the large separation. The large separation depends on the mean density of the star and increases as the square root of the mean density. The mode amplitudes form a distinctive bell-shaped envelope with maximum frequency, $\nu_{\max}$. This frequency depends on surface gravity and effective temperature and is related to the critical acoustic frequency (Brown et al., 1991). If $\nu_{\max}$ and $\Delta\nu$ can be measured and the effective temperature is known, the stellar radius and mass can be determined (Stello et al., 2008; Kallinger et al., 2010).

The δ Scuti stars are A and early F dwarfs and giants with multiple frequencies higher than 5 days^{-1} while γ Doradus stars are F dwarfs and giants pulsating in multiple frequencies in the range

0.3–3 days^{-1}. It was originally thought that the δ Sct stars do not pulsate with frequencies lower than about 5 days^{-1}, but photometry from the *Kepler* satellite has shown that low frequencies occur in practically all δ Sct stars (Balona, 2018). Furthermore, the γ Dor stars should probably not be considered as a separate class of variable (Xiong et al., 2016; Balona, 2018). There are, in fact, more δ Sct stars than γ Dor stars in the γ Dor instability region. It seems that the γ Dor stars are δ Sct stars in which the high frequencies are damped for some unknown reason.

Samadi et al. (2002) computed models of δ Sct stars located in the vicinity of the cool edge of the classical instability strip and suggested that the amplitudes of solar-like oscillations in these stars may be detectable even with ground-based instruments, provided they can be distinguished from the large-amplitude pulsations. This is an interesting prospect because it would allow the stellar parameters to be determined and greatly simplify mode identification. Antoci et al. (2011) reported detection of solar-like oscillations in the δ Sct star HD 187547 observed by *Kepler*, but further data failed to confirm this identification (see Antoci et al., 2014; Bedding et al., 2020). Another attempt to search for solar-like oscillations, this time on the δ Sct star ρ Pup, also failed (Antoci et al., 2013). Since then, no further searches have been published.

Huber et al. (2011) discussed the location in the H–R diagram of stars with solar-like oscillations relative to the observed and theoretical cool edges of the δ Sct instability strip. They do not arrive at any conclusion as to whether stars with solar-like oscillations are present within the δ Sct instability strip.

The main purpose of this investigation is to determine the location of the hot edge of solar-like oscillations. This is important because it places a constraint on any theory seeking to explain these oscillations and because it gives information on convection at the interface between radiative and convective atmospheres. For this purpose, all stars with short-cadence *Kepler* observations in the temperature range $6,000 < T_{\rm eff} < 10,000$ K were examined for solar-like oscillations. As a consequence, many new hot solar-like variables were discovered. The hot limit of these stars is a good estimate of the hot edge of excitation of solar-like oscillations and places a limit on the likely amplitudes of solar-like oscillations which might be present in δ Sct or γ Dor stars.

THE DATA

Kepler observations consist of almost continuous photometry of many thousands of stars over a four-year period with micromagnitude precision. The vast majority of stars were observed in long-cadence mode with a sampling cadence of 29.4 min. A few thousand stars were also observed in short-cadence mode (sampling cadence of 1 min), but typically only for a few months. The *Kepler* light curves used here are those with pre-search data conditioning in which instrumental effects are removed (Smith et al., 2012; Stumpe et al., 2012). In main sequence stars with solar-like oscillations, the frequency of maximum amplitude, $\nu_{\rm max}$, is always larger than the Nyquist frequency of 24 days^{-1} of *Kepler* long-cadence mode. Hence only short-cadence data are used. The sample consists of 2,347 stars with $6,000 < T_{\rm eff} < 10,000$ K.

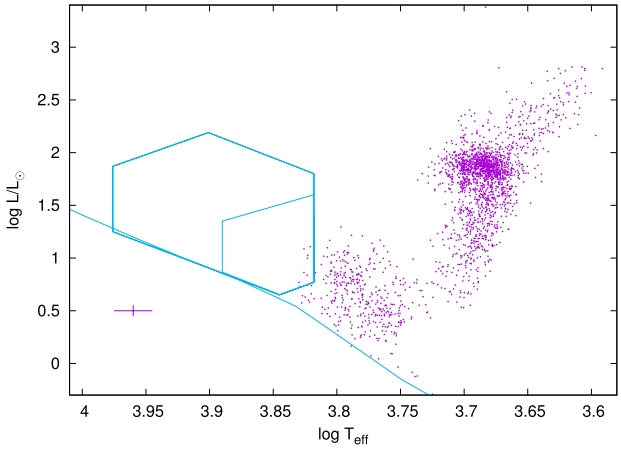

FIGURE 1 | The location of stars with solar-like oscillations from Huber et al. (2017) in the H-R diagram. The zero-age main sequence for models of solar abundance from Bertelli et al. (2008) is shown (solid line). The large polygonal region shows the location of δ Sct stars from Balona (2018). The smaller polygon shows the location of the γ Dor stars. The cross at bottom left indicates 1 – σ error bars in effective temperature and luminosity.

Most stars in the *Kepler* field have been observed by multicolour photometry, from which effective temperatures, surface gravities, metal abundances and stellar radii can be estimated. These stellar parameters are listed in the *Kepler Input Catalog* (KIC, Brown et al., 2011). The effective temperatures, $T_{\rm eff}$, of *Kepler* stars cooler than about 6,500 K were revised by Mathur et al. (2017). For hotter stars, Balona et al. (2015) found that adding 144 K to the *Kepler Input Catalog* $T_{\rm eff}$ reproduced the spectroscopic effective temperatures very well. These revisions in $T_{\rm eff}$ have been used in this paper.

Huber et al. (2017) lists 2,236 *Kepler* stars with solar-like oscillations compiled from various catalogs giving $\nu_{\rm max}$ and $\Delta\nu$ for each star. Other compilations of *Kepler* stars with solar-like oscillations are those of Chaplin et al. (2014) and Serenelli et al. (2017). **Figure 1** shows the Huber et al. (2017) stars in the Hertzprung-Russel (H-R) diagram together with the δ Sct and γ Dor instability regions from Balona (2018). The luminosities of these stars were obtained from *Gaia DR2* parallaxes (Gaia Collaboration et al., 2016, Gaia Collaboration et al., 2018) using a table of bolometric corrections in the Sloan photometric system by Castelli and Kurucz (2003). Corrections for interstellar extinction were derived using the 3D Galactic reddening model by Gontcharov (2017).

It is intriguing that the hot edge of solar-like oscillations seems to coincide with the cool edge of the δ Sct/γ Dor instability regions. Very few stars having solar-like oscillations are hotter than 6,500 K and none exceed 7,000 K.

DETECTION METHOD

Solar-like oscillations are usually detected by searching for the typical bell-shaped amplitude envelope in the power spectrum of the light curve. Most methods use a smoothed power spectrum to

obtain the global parameters of the Gaussian envelope. A model consisting of the background, which includes a contribution from granulation, and a Gaussian is then fitted to the data and tested for significance. The peak of the Gaussian gives $\nu_{\max}$ while $\Delta\nu$ is estimated by autocorrelation. This procedure and variants are described in, for example, Gilliland et al. (1993); Mosser and Appourchaux (2009); Huber et al. (2009); Mathur et al. (2010); Benomar et al. (2012); Lund et al. (2012).

All methods make use of the well-known asymptotic formula for p modes (Tassoul, 1980):

$$\nu_{nl} \approx \Delta\nu\left(n + \frac{1}{2}l + \varepsilon\right) - l(l+1)D_0,$$

where l is the spherical harmonic number of the mode and n is its radial order. The constant ϵ is sensitive to the surface layers and D_0 is sensitive to the sound speed gradient near the core. This equation is valid for non-rotating stars and leads to an approximately repetitive frequency pattern with characteristic frequency of $(1/2)\Delta\nu$. The factor of half comes from the fact that the $l = 1$ frequency peaks are approximately midway between consecutive radial ($l = 0$) peaks. In a star with solar-like oscillations one would expect to find a regular frequency spacing of $(1/2)\Delta\nu$ within a restricted frequency range corresponding to the location of bell-shaped amplitude distribution centered at $\nu_{\max}$. Several reviews on solar-like oscillations are available (Chaplin and Miglio, 2013; Aerts, 2019; García and Ballot, 2019).

Rotation will introduce splitting of each mode into $2l + 1$ multiplets. However, axisymmetric modes will only be slightly affected for small to moderate rotation, so the repetitive frequency pattern will still be preserved, though degraded somewhat. Because hotter stars tend to be more rapid rotators, the difficulty of detecting solar-like oscillations is expected to increase with increasing effective temperature. In addition, the shorter mode lifetimes lead to broader frequency peaks and lower amplitudes.

The detection of a regular frequency spacing is commonly achieved using the power spectrum of the power spectrum of the light curve or by autocorrelation. The autocorrelation, $R(k)$, is the correlation of a signal with a delayed copy of itself with lag k: $R_k = \sum y(n)y(n-k)$. The autocorrelation can be obtained from this summation, but for computational purposes it is faster to calculate R_k from the inverse FFT of the power spectrum of the power spectrum of the light curve.

The method used here most closely resembles that of Mathur et al. (2010) in that the presence of equally-spaced frequencies in some region of the power spectrum of the light curve is detected. A suitably small region of the power spectrum of the light curve is selected and the autocorrelation function is calculated. If a pattern of equally-spaced frequencies exists in this region, the autocorrelation function will display a periodic variation with period equal to the frequency separation. The amplitude of the periodic variation depends on the strength of the correlation and follows the bell shape seen in the amplitude envelope of the solar-like oscillations in the power spectrum of the light curve.

The frequency range, $\delta\nu$, of the portion of the power spectrum of the light curve used to calculate the autocorrelation needs careful consideration. We know that $\Delta\nu$ is roughly proportional to $\nu_{\max}$ (more accurately, $\Delta\nu \propto \nu_{\max}^{s}$ where $s \approx 0.8$, Stello et al., 2009). At high frequencies $\delta\nu$ needs to be large enough to include a few periods in the autocorrelation function. Thus $\delta\nu$ should be at least 2 or 3 times $\Delta\nu$. At low frequencies $\Delta\nu$ will be smaller and hence $\delta\nu$

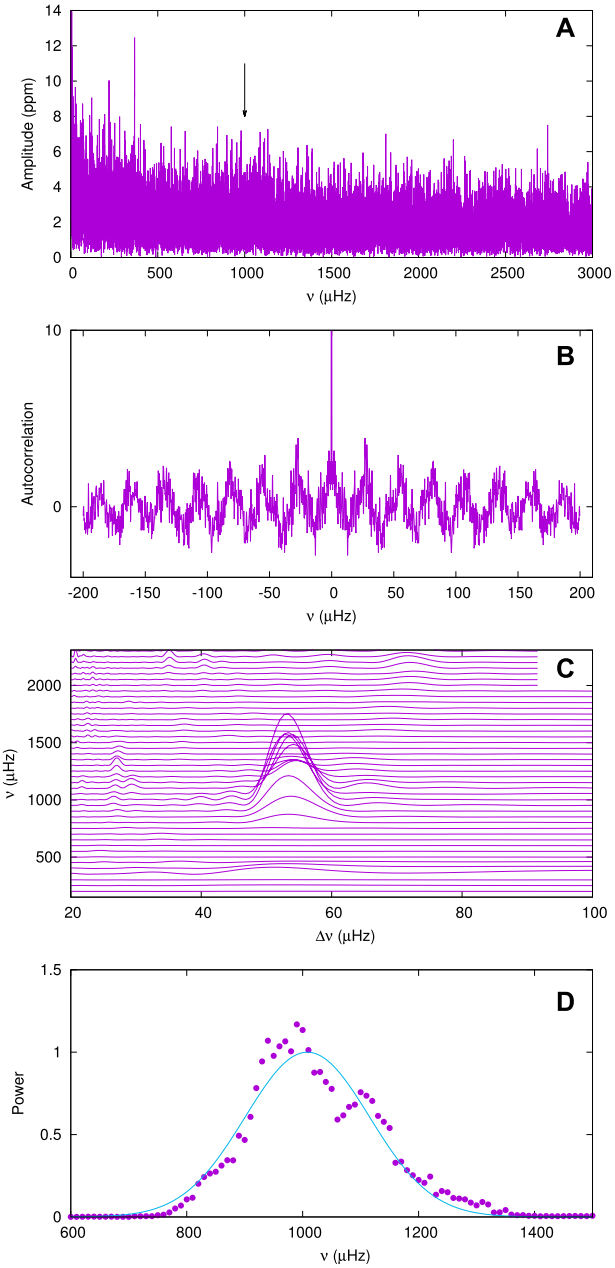

FIGURE 2 | Panel **(A)** shows the amplitude periodogram for KIC 3219634, the arrow indicating $\nu_{\max}$. Panel **(B)** shows the autocorrelation at a frequency of 1,000 μHz showing a period of about $(1/2)\Delta\nu \approx 27$ μHz. Panel **(C)** shows power spectra of the autocorrelation (after removing the central peak) plotted against frequency (the ν–$\Delta\nu$ diagram). Panel **(D)** shows the maximum autocorrelation power as a function of frequency within a 10% range of the approximate $\Delta\nu$. The curve is a fitted Gaussian with a maximum at $\nu_{\max} = 1,008.1 \pm 2.8$ μHz. The average $\Delta\nu$ within $\pm$ (1/2)FWHM of the maximum is 54.06 ± 0.18 μHz.

can be made correspondingly smaller. In other words, the frequency range to be sampled for autocorrelation should be roughly proportional to the frequency, ν, that is being sampled, i.e., $\delta\nu = \alpha\nu$. A value of $\alpha = 0.2$–0.4 was found to be suitable.

To measure the period of the autocorrelation function, it is convenient to calculate the power spectrum of the autocorrelation. This is actually the same as the power spectrum of the power spectrum of the light curve. However, it was found that removing the large maximum at zero lag, which is always present in the autocorrelation, leads to a cleaner power spectrum. The period of variation in the autocorrelation, if any exists, is given by the inverse of the frequency of the highest peak in the power spectrum of the modified autocorrelation. Its amplitude measures the significance of the period.

In the method used here, the autocorrelation is calculated at equal frequency steps in the power spectrum of the light curve. Let ν be the central frequency at which the autocorrelation is calculated. The power spectrum of the autocorrelation function is plotted at this frequency. If a solar-like oscillation is present, a significant peak will occur in this power spectrum at a period

TABLE 1 | Table of known stars with solar-like oscillations. The first column is the KIC number. The values of $\nu_{\max}$ (μHz) and $\Delta\nu$ (μHz) (together with their $1-\sigma$ errors) follows. The effective temperature, $T_{\rm eff}$ (K), from the literature and the luminosity, $\log L/L_\odot$, from the *Gaia DR2* parallax, are shown. Note that for stars with $T_{\rm eff} > 6,500$ K, values are from the calibration of Balona et al. (2015).

KIC	$\nu_{\max}$	$\Delta\nu$	$T_{\rm eff}$	$\log(L/L_\odot)$	KIC	$\nu_{\max}$	$\Delta\nu$	$T_{\rm eff}$	$\log(L/L_\odot)$
1430163	1,829.0 ± 3.6	86.39 ± 0.21	6,588	0.64	8367710	1,107.1 ± 1.2	56.40 ± 0.25	6,364	0.88
1435467	1,464.6 ± 1.5	71.38 ± 0.40	6,306	0.66	8377423	1,023.0 ± 2.3	52.46 ± 0.23	6,141	0.84
1725815	1,009.0 ± 1.7	51.96 ± 0.15	6,196	0.85	8408931	594.3 ± 1.8	34.20 ± 0.69	6,143	1.12
2837475	1,633.5 ± 1.1	76.80 ± 0.12	6,641	0.74	8420801	1,361.1 ± 3.1	67.20 ± 0.38	6,245	0.69
3123191	2,092.3 ± 6.7	91.16 ± 0.60	6,450	0.60	8494142	1,174.9 ± 0.7	62.77 ± 0.23	6,070	0.69
3236382	1,643.5 ± 3.9	75.33 ± 0.65	6,715	0.74	8579578	946.8 ± 1.2	50.64 ± 0.08	6,339	0.91
3344897	835.0 ± 1.8	47.35 ± 0.12	6,434	0.95	8866102	2,118.0 ± 1.4	95.57 ± 0.30	6,264	0.51
3424541	754.0 ± 1.0	41.94 ± 0.07	6,123	1.06	8940939	1,535.1 ± 3.3	78.91 ± 0.25	6,342	0.77
3456181	1,005.9 ± 1.1	52.93 ± 0.29	6,381	0.88	8956017	1,254.5 ± 4.1	62.87 ± 0.58	6,397	0.80
3547794	1,327.7 ± 4.5	68.37 ± 0.54	6,462	0.77	9116461	2,452.2 ± 3.7	106.13 ± 0.39	6,429	0.47
3633889	2,113.0 ± 4.3	96.35 ± 0.60	6,328	0.48	9139151	2,735.7 ± 2.6	118.47 ± 0.17	6,114	0.30
3733735	2,075.7 ± 1.9	93.47 ± 0.13	6,726	0.66	9139163	1,757.8 ± 1.3	81.90 ± 0.40	6,403	0.68
3967430	1,981.1 ± 2.9	89.30 ± 0.39	6,682	0.63	9163769	1,753.3 ± 4.1	80.97 ± 1.47	6,410	0.65
4465529	1,546.7 ± 3.0	71.96 ± 0.87	6,344	0.70	9206432	1,953.0 ± 1.6	85.69 ± 0.21	6,531	0.67
4586099	1,229.6 ± 1.3	62.47 ± 0.46	6,378	0.76	9226926	1,480.3 ± 1.6	74.71 ± 0.57	6,736	0.77
4638884	1,231.3 ± 1.1	61.44 ± 0.14	6,448	0.82	9287845	1,034.7 ± 3.5	49.60 ± 0.43	6,309	0.97
4646780	1,074.5 ± 3.2	60.85 ± 0.57	6,628	0.84	9328372	1,406.0 ± 5.4	67.59 ± 0.56	6,390	0.84
4931390	2,080.4 ± 1.2	93.73 ± 0.12	6,703	0.60	9455860	1,534.3 ± 3.4	71.05 ± 0.93	6,579	0.74
5095850	750.6 ± 7.5	46.59 ± 0.59	6,759	1.09	9457728	1,114.4 ± 1.9	59.97 ± 0.49	6,284	0.78
5214711	1,310.9 ± 1.7	60.78 ± 0.43	6,302	0.73	9542776	823.8 ± 3.6	41.42 ± 0.51	6,435	1.10
5431016	917.8 ± 0.9	49.97 ± 0.26	6,594	0.96	9697131	1,204.2 ± 2.0	61.25 ± 0.29	6,337	0.84
5516982	1,827.7 ± 1.4	85.02 ± 0.47	6,386	0.57	9812850	1,292.9 ± 1.3	65.70 ± 0.39	6,458	0.71
5636956	1,056.8 ± 2.0	55.30 ± 0.14	6,436	0.88	9821513	1,230.8 ± 1.7	60.66 ± 0.12	6,335	0.77
5773345	1,156.7 ± 1.0	58.19 ± 0.28	6,179	0.80	10003270	792.3 ± 2.5	43.07 ± 0.15	6,395	1.02
5961597	1,206.5 ± 1.9	60.94 ± 0.11	6,573	0.86	10016239	2,326.8 ± 1.8	102.98 ± 0.40	6,277	0.51
6064910	828.9 ± 1.5	44.53 ± 0.23	6,370	0.96	10024648	1,084.7 ± 1.6	57.46 ± 0.39	6,258	0.78
6225718	2,410.3 ± 1.4	106.89 ± 0.12	6,223	0.36	10070754	2,320.4 ± 3.1	102.62 ± 0.38	6,437	0.48
6232600	2,178.2 ± 2.0	96.68 ± 0.32	6,447	0.51	10081026	745.0 ± 2.8	44.21 ± 0.08	6,368	1.03
6508366	998.0 ± 0.9	52.31 ± 0.24	6,343	0.87	10273246	903.6 ± 1.2	49.07 ± 0.38	6,155	0.81
6530901	1,639.1 ± 3.2	79.79 ± 0.71	6,233	0.63	10351059	1,382.1 ± 3.4	66.13 ± 0.27	6,435	0.83
6612225	1,167.1 ± 1.4	60.12 ± 0.12	6,309	0.78	10355856	1,366.9 ± 1.7	68.06 ± 0.22	6,438	0.76
6679371	976.1 ± 0.8	51.42 ± 0.07	6,302	0.96	10454113	2,428.7 ± 1.3	106.34 ± 0.24	6,155	0.51
7103006	1,199.5 ± 1.0	60.34 ± 0.26	6,420	0.81	10491771	1,773.9 ± 6.6	83.50 ± 0.96	6,491	0.62
7106245	2,448.9 ± 2.3	112.73 ± 0.21	6,082	0.21	10709834	1,416.2 ± 1.5	68.70 ± 0.11	6,453	0.83
7133688	1,172.7 ± 3.5	59.09 8 0.23	6,383	0.85	10730618	1,343.2 ± 1.1	67.11 ± 0.34	6,401	0.81
7206837	1,742.7 ± 1.3	80.14 ± 0.42	6,340	0.60	10972252	863.4 ± 1.9	45.05 ± 0.27	6,202	0.93
7218053	707.0 ± 1.9	40.70 ± 0.46	6,366	1.03	11070918	1,253.2 ± 1.5	68.04 ± 0.49	6,642	1.22
7282890	852.0 ± 1.4	45.67 ± 0.12	6,345	0.99	11081729	2,009.0 ± 1.8	91.10 ± 0.50	6,530	0.61
7465072	1,534.2 ± 3.9	69.77 ± 1.35	6,309	0.67	11189107	992.2 ± 4.8	46.47 ± 0.46	6,513	1.03
7529180	1,963.7 ± 2.0	86.56 ± 0.20	6,657	0.68	11229052	1,867.5 ± 2.9	84.82 ± 0.17	6,376	0.65
7530690	2,027.9 ± 4.4	98.02 ± 0.57	6,568	0.61	11253226	1,647.5 ± 1.2	78.01 ± 0.15	6,642	0.75
7622208	1,254.0 ± 6.9	59.60 ± 0.69	6,396	0.82	11453915	2,486.2 ± 4.5	109.58 ± 1.01	6,331	0.33
7670943	1,927.8 ± 1.4	90.13 ± 0.20	6,315	0.53	11460626	839.8 ± 1.9	48.39 ± 0.28	6,065	0.81
7800289	599.0 ± 3.8	32.89 ± 0.42	6,455	1.17	11467550	1,023.0 ± 2.9	54.89 ± 0.35	6,202	0.76
7938112	1,218.4 ± 4.5	63.12 ± 1.03	6,337	0.76	11757831	1,256.3 ± 2.7	64.35 ± 0.43	6,468	0.86
8150065	1,933.7 ± 1.6	89.76 ± 0.17	6,263	0.49	11919192	866.2 ± 1.8	47.82 ± 0.33	6,448	1.00
8179536	2,138.5 ± 1.6	96.27 ± 0.28	6,347	0.47	12156916	1,523.4 ± 1.9	77.53 ± 0.24	6,438	0.58
8216936	1,110.1 ± 2.6	57.61 ± 0.38	6,419	1.01	12317678	1,254.3 ± 1.3	64.42 ± 0.11	6,589	0.83
8298626	2,050.9 ± 3.3	91.81 ± 0.20	6,200	0.46	—	—	—	—	—

TABLE 2 | Newly-discovered stars with solar-like oscillations. The columns are the same as **Table 1**.

KIC	ν_{max}	$\Delta\nu$	T_{eff}	$\log(L/L_\odot)$	KIC	ν_{max}	$\Delta\nu$	T_{eff}	$\log(L/L_\odot)$
3102595	1,074.9 ± 3.3	52.65 ± 0.18	6,183	0.79	8279146	1,366.7 ± 3.2	70.69 ± 0.34	6,650	0.77
3219634	1,008.1 ± 2.7	54.06 ± 0.18	6,286	0.81	8346342	915.8 ± 0.8	49.37 ± 0.30	6,316	0.89
3241299	1,117.6 ± 3.0	57.80 ± 0.18	6,316	1.10	8737094	887.5 ± 2.0	45.72 ± 0.18	6,541	1.08
3850086	989.9 ± 2.5	52.09 ± 0.58	6,461	0.92	8801316	1,111.4 ± 2.4	59.37 ± 0.11	6,489	0.93
3852594	1,006.4 ± 2.2	53.64 ± 0.21	6,417	0.85	8806223	1,729.0 ± 2.9	83.09 ± 0.28	6,480	0.62
3936993	1,195.3 ± 4.4	61.89 ± 1.33	6,225	0.73	8914779	1,492.6 ± 4.1	74.05 ± 0.59	6,258	0.64
4484238	2,080.2 ± 2.1	92.80 ± 0.07	6,043	0.56	9109988	2,255.5 ± 5.6	98.22 ± 0.23	6,127	0.44
5105070	1,154.8 ± 2.2	61.93 ± 0.47	6,090	0.62	9209245	1,092.0 ± 3.4	54.61 ± 0.31	6,235	0.77
5183581	1,017.8 ± 1.7	53.81 ± 0.19	6,387	0.87	9221678	1,746.4 ± 5.1	80.81 ± 0.75	6,281	0.62
5597743	1,060.7 ± 3.3	55.07 ± 0.59	6,014	0.84	9412514	823.3 ± 2.4	47.93 ± 0.19	6,075	0.92
5696625	704.9 ± 2.7	39.29 ± 0.18	6,402	1.48	9426660	1,491.9 ± 2.5	75.43 ± 0.39	6,157	0.54
5771915	1,420.6 ± 5.3	70.55 ± 0.74	6,230	0.68	9529969	1,581.8 ± 3.2	73.75 ± 1.50	6,021	0.48
5791521	669.0 ± 2.7	34.45 ± 0.26	6,398	1.35	9715099	741.9 ± 1.1	40.93 ± 0.17	6,217	1.04
5856836	2,104.9 ± 5.0	91.87 ± 0.59	6,233	0.48	9837454	782.9 ± 2.0	46.62 ± 0.29	5,912	0.78
5871558	862.6 ± 2.4	47.23 ± 0.28	6,239	0.88	9898385	1,269.3 ± 5.4	69.58 ± 0.35	6,257	0.75
5905822	1,686.0 ± 1.7	82.86 ± 0.10	6,057	0.50	9959494	1,856.8 ± 3.2	88.99 ± 0.17	6,638	0.51
5982353	940.9 ± 3.3	47.77 ± 0.16	6,208	1.04	10010623	952.3 ± 3.6	57.17 ± 0.95	6,532	1.01
6048403	1,039.9 ± 2.0	53.58 ± 0.15	6,444	0.89	10208303	1,254.4 ± 2.0	63.35 ± 0.43	6,303	0.84
6062024	1,060.7 ± 2.2	57.59 ± 0.17	6,166	0.81	10340511	1,957.4 ± 2.9	91.73 ± 0.21	5,822	0.36
6268607	789.7 ± 3.3	41.71 ± 0.63	6,208	0.95	10448382	825.8 ± 1.8	45.79 ± 0.23	5,969	0.94
6359801	1,309.2 ± 6.8	64.85 ± 1.11	6,463	0.78	10514274	1,098.6 ± 3.5	53.47 ± 0.41	6,190	0.84
6761569	1,057.4 ± 1.3	58.27 ± 0.34	6,271	0.83	10557075	1,794.6 ± 2.7	80.11 ± 0.16	5,825	0.52
6777146	2,090.3 ± 4.9	92.55 ± 0.66	6,103	0.47	10775748	1,195.6 ± 1.6	61.25 ± 0.29	6,393	0.82
6784857	1,241.9 ± 1.8	63.70 ± 0.39	6,172	0.71	10813660	1,846.0 ± 3.0	84.82 ± 0.70	6,170	0.50
6881330	1,790.1 ± 3.8	84.03 ± 0.26	6,092	0.49	10864215	478.4 ± 1.6	32.16 ± 0.42	6,348	1.21
7205315	1,345.9 ± 5.3	66.59 ± 0.50	6,051	0.75	10920182	1,354.1 ± 1.9	67.24 ± 0.12	5,957	0.62
7215603	1,790.2 ± 1.9	83.65 ± 0.26	6,230	0.54	11137841	667.2 ± 2.2	39.90 ± 0.32	6,406	1.12
7272437	—	63.62 ± 0.39	6,078	0.70	11230757	1,079.2 ± 2.5	59.51 ± 0.41	6,158	0.86
7418476	1,241.8 ± 4.0	63.95 ± 0.28	6,725	0.74	11245074	420.4 ± 1.0	23.23 ± 0.34	6,073	1.29
7439300	809.6 ± 1.6	42.15 ± 0.17	6,121	1.03	11255615	1,340.9 ± 1.2	70.55 ± 0.19	6,194	0.59
7500061	1,307.3 ± 2.9	63.50 ± 0.15	6,265	0.73	11337566	958.3 ± 1.4	50.52 ± 0.40	6,238	0.91
7669332	503.9 ± 1.8	43.87 ± 1.08	6,183	1.13	11769801	880.9 ± 3.2	45.23 ± 0.56	6,389	1.06
7833587	1,302.9 ± 3.0	64.91 ± 0.22	6,236	0.72	11862497	2,072.7 ± 3.4	90.68 ± 0.39	6,426	0.58
8165738	1,622.5 ± 4.3	82.40 ± 1.25	6,331	0.53	11970698	1,324.0 ± 2.3	67.54 ± 0.22	5,841	0.62
8243381	879.8 ± 3.6	50.26 ± 1.51	6,101	0.81	12600459	2,019.1 ± 3.5	91.33 ± 0.26	6,284	0.48

given by $(1/2)\Delta\nu$. By plotting the power spectra at each sampled frequency, ν, a solar oscillation that may be present will be revealed because the maxima of the power spectra will occur at approximately the same period in the power spectrum. It is convenient to plot $\Delta\nu$ itself instead of the period. This ν–$\Delta\nu$ plot is central to detection of solar-like oscillations.

The value of ν_{max} will be the value of ν at which the peak attains maximum amplitude. This can be obtained by sampling the power spectrum of the light curve with smaller frequency steps on a second pass. At each frequency step, the maximum power of the autocorrelation is plotted as a function of ν. This relationship is very close to a Gaussian in most cases, so ν_{max} may be obtained by fitting a Gaussian to this curve. The uncertainty in ν_{max} is taken to be the standard deviation of the location of the Gaussian peak obtained from the least-squares fit. Since $\Delta\nu$ is only approximately constant, a best estimate of $\Delta\nu$ is found by taking the mean value within the full-width at half maximum of the Gaussian centered on ν_{max}. The uncertainty in $\Delta\nu$ is taken as the standard deviation of these values.

After a suitable list of candidate stars is compiled and the Lomb-Scargle power spectra calculated, the power spectrum of the modified correlation is plotted as a function of $\Delta\nu$ (the ν–$\Delta\nu$ plot) using a relatively large frequency step in ν. This plot is examined for the possible presence of a significant peak. As an example, **Figure 2A** shows the amplitude periodogram of the light curve of KIC 3219634, which is a previously undiscovered solar-like pulsator. The solar-like oscillations are hardly detectable by visual inspection of the periodogram. **Figure 2B** shows the autocorrelation function near ν_{max}. The periodicity is clearly seen. **Figure 2C** shows part of the ν–$\Delta\nu$ diagram calculated with a step size of 50 μHz in ν. It is clear that equally-spaced frequencies are present at about $\Delta\nu \approx 55\,\mu$Hz and $\nu_{max} \approx 1{,}000\,\mu$Hz. In a second pass, the step size in ν has been reduced to 10 μHz and at each frequency step the maximum power in the modified autocorrelation is measured within a restricted range of $\Delta\nu$. The range was taken to be $\pm 0.1\Delta\nu$. A Gaussian fitted to the larger peak gives the best estimate of ν_{max}.

The detection of the "humps" which represent a region of high autocorrelation is never a problem as they always have high signal-to-noise. The example of **Figure 2C** is fairly typical. The main problem is that for some stars many similar humps and/or ridges are visible. For example, eclipsing binaries have significant power at large harmonics which appear as ridges in the ν–$\Delta\nu$ diagram. Although these cannot be mistaken for the hump characteristic of solar-like oscillations, it interferes with detection of such a hump. Pulsating stars, such as δ Sct/γ Dor

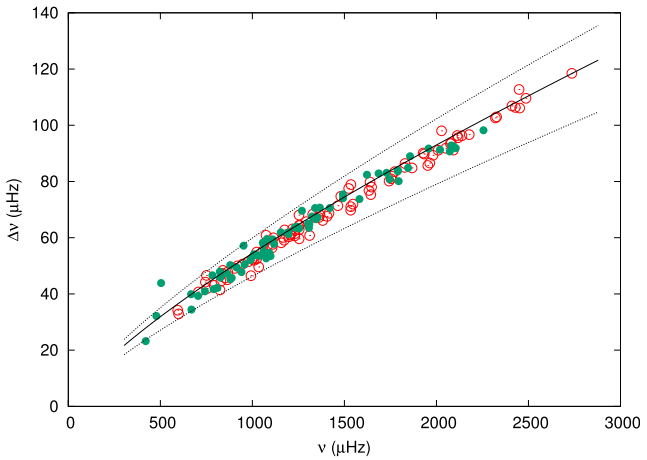

FIGURE 3 | The large separation, $\Delta\nu$, as a function of ν_{max} for 167 stars. Stars known from the literature are shown by open circles (red), newly detected stars by filled circles (green). The solid line is the relation from Stello et al. (2009) and dotted lines show +10 and −15 per cent deviations.

variables also have ridges in the diagram which tend to confuse the detection of solar-like oscillations. This is the case for HD 187547, the δ Sct star previously thought to contain solar-like oscillations (Antoci et al., 2011). This means that any solar-like oscillations in δ Sct stars, if they exist, may be obscured by the ridges created by δ Sct pulsation in the ν–$\Delta\nu$ diagram. If a hump lies close to the expected location in (ν_{max}, $\Delta\nu$), it may represent a true oscillation, but one cannot be certain. The method is aimed at finding oscillations with very low amplitudes. This, of course, is what is needed to extend the region where these oscillations are to be found to higher effective temperatures. The price to be paid is that there is a significant risk of a false detection.

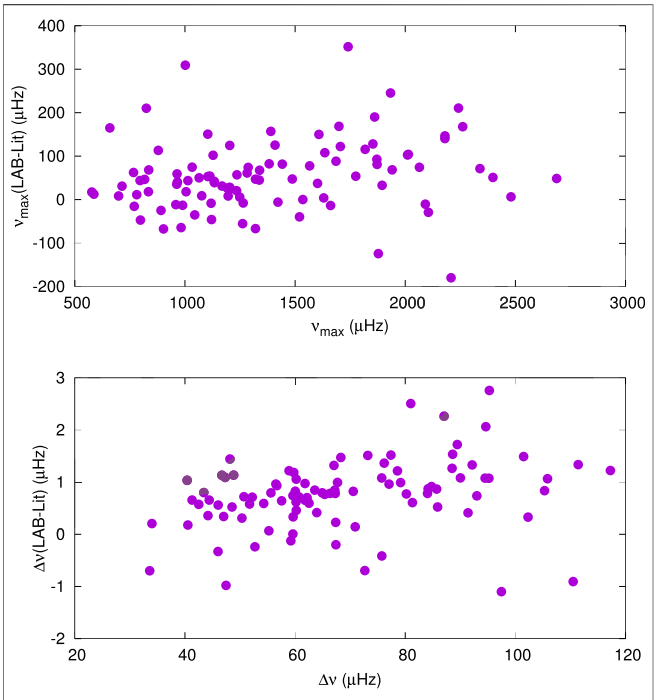

FIGURE 4 | Comparison of ν_{max} (top panel) and $\Delta\nu$ (bottom panel) obtained in this paper with those in the literature.

RESULTS

Of the 2,347 stars with $6,000 < T_{\rm eff} < 10,000$ K observed in short-cadence mode, solar-like oscillations were detected in 167 stars. This includes the 97 stars in **Table 1** which were already known to have solar-like oscillations. The fact that all stars with $T_{\rm eff} > 6,000$ K and with known solar-like oscillations were quite easily detected, lends confidence to the method described above. In addition, **Table 2** lists 70 stars with newly-found solar-like oscillations. For all 167 stars, there is no difficulty in locating the hump as it is the only one with significant visibility. The tables

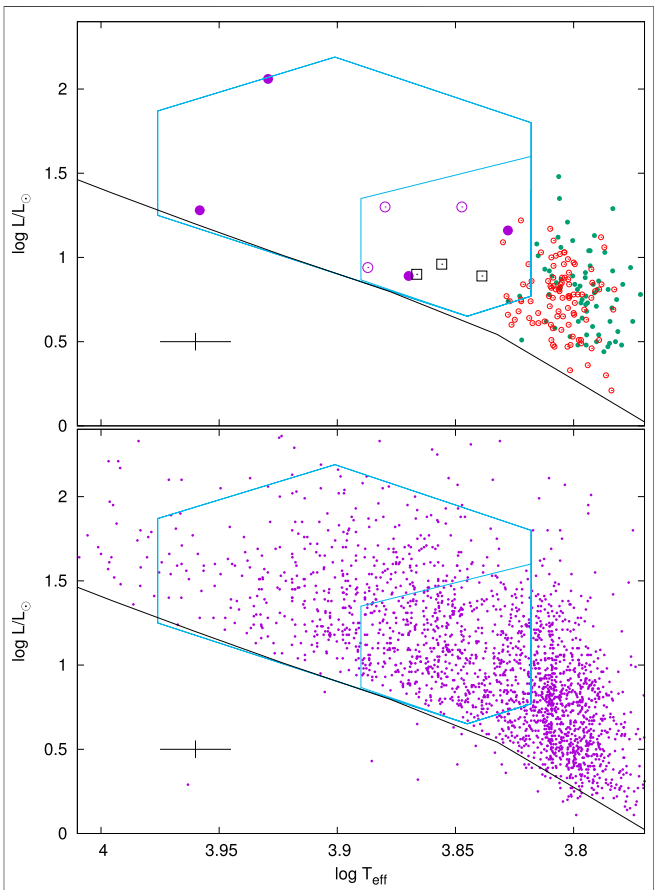

FIGURE 5 | Top panel: the location in the H–R diagram of stars in **Tables 1–3**. Newly detected stars are shown by the small filled green circles and known stars by small open red circles. The large symbols are stars with possible solar-like oscillations: violet filled circles—non-variable stars; violet open circles: δ Sct; black squares—γ Dor stars. Bottom panel: the small filled circles are from the sample of 2,347 stars used to search for solar-like oscillations. The zero-age main sequence for models of solar abundance from Bertelli et al. (2008) is shown (black solid line). The large polygonal region shows the location of δ Sct stars from Balona (2018). The smaller polygon shows the location of the γ Dor stars. The cross at bottom left shows 1 – σ error bars.

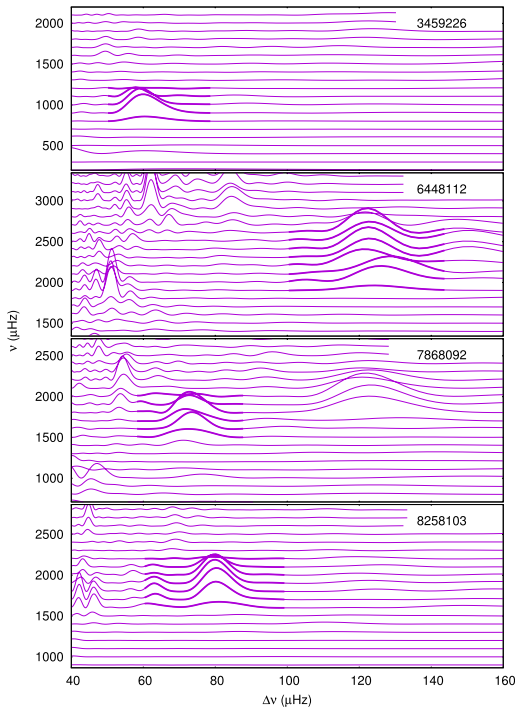

FIGURE 6 | The ν–$\Delta\nu$ diagrams for the four hottest non-pulsating stars. The thicker solid lines indicate the region which might be a result of solar-like oscillations.

give the oscillation parameters as well as the adopted effective temperatures and luminosities derived from *Gaia DR2* parallaxes as mentioned above. The median rms error is 1.95 μHz in $\nu_{\max}$ and 0.31 μHz in $\Delta\nu$.

Figure 3 shows the large separation, $\Delta\nu$, as a function of $\nu_{\max}$ for the 167 stars. The 70 newly discovered stars follow the same relationship as the 97 stars in which solar-like oscillations are known to be present. This is a strong indication that the detected oscillations are real.

Figure 4 compares the values of $\nu_{\max}$ and $\Delta\nu$ obtained here with those in the literature. In both cases, the difference increases with $\nu_{\max}$. Neither $\nu_{\max}$ or $\Delta\nu$ are well-defined quantities. $\nu_{\max}$ is usually estimated by fitting a Gaussian to the envelope of the peaks. $\Delta\nu$ varies slightly with ν and is normally measured at $\nu_{\max}$. In both cases the trend shown in **Figure 4** may be related to the fact that the frequency range, $\delta\nu$, which is sampled to derive the autocorrelation increases with $\nu_{\max}$, as described above. In short, the method described here is suited to the detection of low-amplitude signals but is not optimized for a strict evaluation of $\nu_{\max}$ and $\Delta\nu$. This clearly requires individual peaks to be resolved.

The top panel in **Figure 5** shows the location of the 167 stars with solar-like oscillations in the H-R diagram as well as the δ Sct and γ Dor region of instability from Balona (2018). The bottom panel shows the location of the 2,347 stars in our sample. This is to show that there is a uniform decrease of density of stars with increasing $T_{\rm eff}$. There is no abrupt change in stellar density which might be responsible for a sharp decrease in number of stars with solar-like oscillations. In the effective temperature range 6,000–6,500 K about 17 percent of stars in our sample are solar-like oscillators. If this fraction remains the same for hotter stars, at least 80 solar-like oscillators may be expected just within the δ Sct instability strip in the temperature range 6,500–7,000 K.

Two apparently non-pulsating stars KIC 6448112 ($T_{\rm eff}$ = 8, 498 K) and KIC 8258103 ($T_{\rm eff}$ = 9, 082 K) seem to have a hump in the ν–$\Delta\nu$ diagram which might be a result of solar-like oscillations. KIC 7868092 ($T_{\rm eff}$ = 6, 726 K) and KIC 3459226 ($T_{\rm eff}$ = 7, 410 K) are somewhat cooler non-pulsating stars in which a hump is also visible. In all these stars, no indication of periodogram peaks are seen at $\nu_{\max}$.

The ν–$\Delta\nu$ diagrams for these stars are shown in **Figure 6**. In every case the detection of possible solar-like oscillations is very tentative because of the presence of similar hump-like features. For this reason, it is not certain that solar-like oscillations are present, even though the measured $\nu_{\max}$ and $\Delta\nu$ are consistent with solar-like oscillations.

Indications of solar like oscillations were also detected in three δ Sct stars (KIC 7212040, KIC5476495, KIC 9347095), and three γ Dor stars (KIC 9696853, KIC 8264254, KIC 5608334). Once again, many other hump-like features are present as well as ridges in the ν–$\Delta\nu$ diagram. As before, this greatly reduces the confidence that solar-like oscillations are present. For the sake of completeness, oscillation parameters of these ten stars are given in **Table 3**.

DISCUSSION AND CONCLUSION

In this study an attempt is made to detect solar-like oscillating stars hotter than 6,000 K in order to determine the hot edge of the excitation of solar-like oscillations in main sequence stars. The temperature region examined includes the δ Sct/γ Dor instability strip. Discovery of solar-like oscillations in δ Sct stars would, of course, be of great interest. There are also large numbers of non-pulsating stars within the δ Sct/γ Dor instability strip. Detecting solar-like oscillations in these stars would be much easier than in δ Sct or γ Dor stars because the low-amplitude of solar-like

TABLE 3 | Stars discussed in the text with possible solar-like oscillations. The columns are the same as in **Table 1**.

KIC	$\nu_{\max}$	$\Delta\nu$	$T_{\rm eff}$	$\log(L/L_\odot)$	KIC	$\nu_{\max}$	$\Delta\nu$	$T_{\rm eff}$	$\log(L/L_\odot)$
3459226	964.8 ± 4.2	60.17 ± 1.44	7,410	0.89	7868092	1,709.9 ± 7.6	73.31 ± 1.39	6,726	1.16
5476495	954.7 ± 3.1	52.09 ± 0.92	7,582	1.30	8258103	1,866.5 ± 3.3	80.83 ± 0.40	9,082	1.28
5608334	2,099.4 ± 12.2	97.97 ± 3.61	6,900	0.89	8264254	1,534.6 ± 11.0	72.33 ± 3.65	7,174	0.96
6448112	2,343.3 ± 8.4	122.80 ± 2.25	8,498	2.06	9347095	762.2 ± 1.6	35.23 ± 0.44	7,035	1.30
7212040	1,313.9 ± 4.4	57.29 ± 0.60	7,710	0.94	9696853	1,297.9 ± 8.0	66.71 ± 1.78	7,352	0.90

oscillations is likely to be swamped by the much higher amplitudes of self-driven modes.

In order to improve the detection probability, a simple method of detecting solar-like oscillations of low amplitudes (well below the level of detection by inspection of the periodogram) was devised. However, the method does have a significant risk of a false detection. The method does not require smoothing of the periodogram or fitting of a granulation model. In this method, a search is made for equal frequency spacings using autocorrelation. It is found that the power spectrum of the autocorrelation is a powerful tool which easily allows detection of very low-amplitude solar-like oscillations. This is accomplished by inspecting a plot of the power spectrum as a function of frequency (the ν–$\Delta\nu$ diagram). In this way, all known solar-like oscillating stars hotter than 6,000 K were independently detected without difficulty.

Application of this method to stars with $6,000 < T_{\rm eff} < 10,000$ K led to the detection of 70 previously unknown solar-like oscillating stars. None of these stars are located within the δ Sct/γ Dor instability strip. If the fraction of stars with solar-like oscillations is the same on either side of the cool edge of the δ Sct instability strip, then several dozen such stars should have been detected. There are 77 stars within the δ Sct instability strip with no apparent variability. These would be the best candidates as there is no interference from self-driven pulsations. Yet solar-like oscillations are not found with certainty in any of these stars.

Some uncertain indication of solar like oscillations were detected in four non-variable stars and six pulsating stars inside the δ Sct instability strip. However, the detections are not sufficiently convincing. None of these ten stars constitute sufficient proof that the hot edge of solar-like oscillations extends to within the δ Sct/γ Dor instability strip.

It should be noted that the line-widths in the periodogram of main sequence stars with solar-like oscillations increases with effective temperature (White et al., 2012; Lund et al., 2017; Compton et al., 2019). This is a consequence of the shorter stochastic mode lifetimes. Increase of line broadening results in a decrease of line amplitude for oscillations of the same energy. In addition, the rotation rate increases with $T_{\rm eff}$, further complicating the frequency spectrum. As a result, detection of individual modes in these stars becomes increasingly more difficult with increasing $T_{\rm eff}$. However, the characteristic bell-shaped envelope of solar-like oscillations should still be visible. The author has inspected the periodograms of many thousands of δ Sct stars, but no indication of such a feature has ever been seen.

Results presented in the present paper demonstrate, as is already well-known, and as Antoci (2014) **Figure 1** nicely illustrates, that the hot edge of solar-like oscillations probably coincides with the cool edge of the δ Sct/γ Dor instability strip. The question arises as to whether physical factors giving rise to self-driven pulsations also act to damp solar-like oscillations. Further study of this problem would require the precision and time span matching that of the *Kepler* photometry. Hopefully, this may be attained in the not too distant future.

DATA AVAILABILITY STATEMENT

All datasets generated for this study are included in the article.

AUTHOR CONTRIBUTIONS

The author confirms being the sole contributor of this work and has approved it for publication.

FUNDING

This paper includes data collected by the Kepler mission. Funding for the Kepler mission is provided by the NASA Science Mission directorate. This work also used data from the European Space Agency (ESA) mission Gaia (https://www.cosmos.esa.int/gaia), processed by the Gaia Data Processing and Analysis Consortium (DPAC, https://www.cosmos.esa.int/web/gaia/dpac/consortium). Funding for the DPAC has been provided by national institutions, in particular the institutions participating in the Gaia Multilateral Agreement.

ACKNOWLEDGMENTS

LB wishes to thank the National Research Foundation of South Africa for financial support.

REFERENCES

Aerts, C. (2019). Probing the interior physics of stars through asteroseismology. *arXiv e-prints*, arXiv:1912.12300

Antoci, V., Cunha, M., Houdek, G., Kjeldsen, H., Trampedach, R., Handler, G., et al. (2014). The role of turbulent pressure as a coherent pulsational driving mechanism: the case of the δ Scuti star HD 187547. *Astrophys. J.* 796, 118. doi:10.1088/0004-637X/796/2/118

Antoci, V., Handler, G., Campante, T. L., Thygesen, A. O., Moya, A., and Kallinger, T., et al. (2011). The excitation of solar-like oscillations in a δ sct star by efficient envelope convection. *Nature* 477, 570–573. doi:10.1038/nature10389

Antoci, V., Handler, G., Grundahl, F., Carrier, F., Brugamyer, E. J., Robertson, P., et al. (2013). Searching for solar-like oscillations in the δ Scuti star ρ Puppis. *Mon. Not. R. Astron. Soc.* 435, 1563–1575. doi:10.1093/mnras/stt1397

Antoci, V. (2014). "Stochastically excited oscillations in the upper main sequence," in IAU symposium, Wroclaw, Poland, August 19–23, 2013 Precision asteroseismology (Cambridge University Press). Editors J. A. Guzik, W. J. Chaplin, G. Handler, and A. Pigulski, Vol. 301, 333–340. doi:10.1017/S1743921313014543

Balona, L. A. (2018). Gaia luminosities of pulsating A-F stars in the Kepler field. *Mon. Not. R. Astron. Soc.* 479, 183–191. doi:10.1093/mnras/sty1511

Balona, L. A., Daszyńska-Daszkiewicz, J., and Pamyatnykh, A. A. (2015). Pulsation frequency distribution in δ Scuti stars. *Mon. Not. R. Astron. Soc.* 452, 3073–3084. doi:10.1093/mnras/stv1513

Bedding, T. R., Murphy, S. J., Hey, D. R., Huber, D., Li, T., Smalley, B., et al. (2020). Very regular high-frequency pulsation modes in young intermediate-mass stars. *Nature* 581, 147–151. doi:10.1038/s41586-020-2226-8

Benomar, O., Baudin, F., Chaplin, W. J., Elsworth, Y., and Appourchaux, T. (2012). Acoustic spectrum fitting for a large set of solar-like pulsators. *Mon. Not. R. Astron. Soc.* 420, 2178–2189. doi:10.1111/j.1365-2966.2011.20184.x

Bertelli, G., Girardi, L., Marigo, P., and Nasi, E. (2008). Scaled solar tracks and isochrones in a large region of the Z–Y plane. *Astron. Astrophys.* 484, 815–830. doi:10.1051/0004-6361:20079165

Borucki, W. J., Koch, D., Basri, G., Batalha, N., Brown, T., Caldwell, D., et al. (2010). Kepler planet-detection mission: introduction and first results. *Science* 327, 977. doi:10.1126/science.1185402

Brown, T. M., Gilliland, R. L., Noyes, R. W., and Ramsey, L. W. (1991). Detection of possible p-mode oscillations on Procyon. *Astrophys. J.* 368, 599. doi:10.1086/169725

Brown, T. M., Latham, D. W., Everett, M. E., and Esquerdo, G. A. (2011). Keplerinput catalog: photometric calibration and stellar classification. *Astron. J.* 142, 112. doi:10.1088/0004-6256/142/4/112

Castelli, F., and Kurucz, R. L. (2003). "New grids of ATLAS9 model atmospheres," in Modelling of stellar atmospheres, IAU symposium. Editors N. Piskunov, W. W. Weiss, and D. F. Gray, Vol. 210, A20.

Chaplin, W. J., Basu, S., Huber, D., Serenelli, A., Casagrande, L., Silva Aguirre, V., et al. (2014). Asteroseismic fundamental properties of solar-type stars observed by the NASA kepler mission. *Astrophys. J. Suppl. Ser.* 210, 1. doi:10.1088/0067-0049/210/1/1

Chaplin, W. J., and Miglio, A. (2013). Asteroseismology of solar-type and red-giant stars. *Annu. Rev. Astron. Astrophys.* 51, 353–392. doi:10.1146/annurev-astro-082812-140938

Compton, D. L., Bedding, T. R., and Stello, D. (2019). Asteroseismology of main-sequence F stars with Kepler: overcoming short mode lifetimes. *Mon. Not. R. Astron. Soc.* 485, 560–569. doi:10.1093/mnras/stz432

Fridlund, M., Roxburgh, I., Favata, F., and Volonté, S. (2006). "The European space agency's science program and CoRoT," in *The CoRoT mission pre-launch status—stellar seismology and planet finding*. Editors M. Fridlund, A. Baglin, J. Lochard, and L. Conroy, Noordwijk, The Netherlands (New York City, NY: ESA Special Publication), Vol. 1306, 135

Gaia CollaborationBrown, A. G. A., Vallenari, A., Prusti, T., de Bruijne, J. H. J., Babusiaux, C., et al. (2018). Gaia data release 2. Summary of the contents and survey properties. *Astron. Astrophys.* 616, 22. doi:10.1051/0004-6361/201833051

Gaia CollaborationPrusti, T., de Bruijne, J. H. J., Brown, A. G. A., Vallenari, A., Babusiaux, C., et al. (2016). The Gaia mission. *Astron. Astrophys.* 595, A1. doi:10.1051/0004-6361/201629272

García, R. A., and Ballot, J. (2019). Asteroseismology of solar-type stars. *Living Rev. Sol. Phys.* 16, 4. doi:10.1007/s41116-019-0020-1

Gilliland, R. L., Brown, T. M., Kjeldsen, H., McCarthy, J. K., Peri, M. L., Belmonte, J. A., et al. (1993). A search for solar-like oscillations in the stars of M67 with CCD ensemble photometry on a network of 4 M telescopes. *Astron. J.* 106, 2441–2476. doi:10.1086/116814

Gontcharov, G. A. (2017). 3D stellar reddening map from 2MASS photometry: an improved version. *Astron. Lett.* 43, 472–488. doi:10.1134/S1063773717070039

Huber, D., Bedding, T. R., Stello, D., Hekker, S., Mathur, S., Mosser, B., et al. (2011). Testing scaling relations for solar-like oscillations from the main sequence to red giants usingkeplerdata. *Astrophys. J.* 743, 143. doi:10.1088/0004-637X/743/2/143

Huber, D., Stello, D., Bedding, T. R., Chaplin, W. J., Arentoft, T., Quirion, P.-O., et al. (2009). Automated extraction of oscillation parameters for Kepler observations of solar-type stars. *Commun. Asteroseismol.* 160, 74

Huber, D., Zinn, J., Bojsen-Hansen, M., Pinsonneault, M., Sahlholdt, C., Serenelli, A., et al. (2017). Asteroseismology and Gaia: testing scaling relations using 2200KeplerStars with TGAS parallaxes. *Astrophys. J.* 844, 102. doi:10.3847/1538-4357/aa75ca

Kallinger, T., Mosser, B., Hekker, S., Huber, D., Stello, D., Mathur, S., et al. (2010). Asteroseismology of red giants from the first four months of Keplerdata: fundamental stellar parameters. *Astron. Astrophys.* 522, A1. doi:10.1051/0004-6361/201015263

Kjeldsen, H., Bedding, T. R., Viskum, M., and Frandsen, S. (1995). Solarlike oscillations in eta Boo. *Astron. J.* 109, 1313–1319. doi:10.1086/117363

Leighton, R. B., Noyes, R. W., and Simon, G. W. (1962). Velocity fields in the solar atmosphere. I. Preliminary report. *Astrophys. J.* 135, 474. doi:10.1086/147285

Lund, M. N., Aguirre, V. S., Davies, G. R., Chaplin, W. J., Christensen-Dalsgaard, J., Houdek, G., et al. (2017). Standing on the shoulders of dwarfs: the Kepler Asteroseismic LEGACY sample. I. Oscillation mode parameters. *Astrophys. J.* 835, 172. doi:10.3847/1538-4357/835/2/172

Lund, M. N., Chaplin, W. J., and Kjeldsen, H. (2012). A new method to detect solar-like oscillations at very low S/N using statistical significance testing. *Mon. Not. R. Astron. Soc.* 427, 1784–1792. doi:10.1111/j.1365-2966.2012.22098.x

Mathur, S., García, R. A., Régulo, C., Creevey, O. L., Ballot, J., Salabert, D., et al. (2010). Determining global parameters of the oscillations of solar-like stars. *Astron. Astrophys.* 511, A46. doi:10.1051/0004-6361/200913266

Mathur, S., Huber, D., Batalha, N. M., Ciardi, D. R., Bastien, F. A., Bieryla, A., et al. (2017). Revised stellar properties of kepler targets for the Q1-17 (DR25) transit detection run. *Astrophys. J. Suppl. Ser.* 229, 30. doi:10.3847/1538-4365/229/2/30

Mosser, B., and Appourchaux, T. (2009). On detecting the large separation in the autocorrelation of stellar oscillation times series. *Astron. Astrophys.* 508, 877–887. doi:10.1051/0004-6361/200912944

Samadi, R., Goupil, M.-J., and Houdek, G. (2002). Solar-like oscillations inδ Scuti stars. *Astron. Astrophys.* 395, 563–571. doi:10.1051/0004-6361:20021322

Serenelli, A., Johnson, J., Huber, D., Pinsonneault, M., Ball, W. H., Tayar, J., et al. (2017). The first APOKASC catalog of kepler dwarf and subgiant stars. *Astrophys. J. Suppl. Ser.* 233, 23. doi:10.3847/1538-4365/aa97df

Smith, J. C., Stumpe, M. C., Van Cleve, J. E., Jenkins, J. M., Barclay, T. S., Fanelli, M. N., et al. (2012). Kepler Presearch data conditioning II—A Bayesian approach to systematic error correction. *PASP* 124, 1000–1014. doi:10.1086/667697

Stello, D., Bruntt, H., Preston, H., and Buzasi, D. (2008). Oscillating K giants with the WIRE satellite: determination of their asteroseismic masses. *Astrophys. J.* 674, L53. doi:10.1086/528936

Stello, D., Chaplin, W. J., Basu, S., Elsworth, Y., and Bedding, T. R. (2009). The relation between $\Delta\nu$ and $\nu_{\max}$ for solar-like oscillations. *Mon. Not. R. Astron. Soc.* 400, L80–L84. doi:10.1111/j.1745-3933.2009.00767.x

Stumpe, M. C., Smith, J. C., Van Cleve, J. E., Twicken, J. D., Barclay, T. S., Fanelli, M. N., et al. (2012). Kepler presearch data conditioning I-architecture and algorithms for error correction in kepler light curves. *Publ. Astron. Soc. Pac.* 124, 985–999. doi:10.1086/667698

Tassoul, M. (1980). Asymptotic approximations for stellar nonradial pulsations. *Astrophys. J. Suppl. Ser.* 43, 469–490. doi:10.1086/190678

White, T. R., Bedding, T. R., Gruberbauer, M., Benomar, O., Stello, D., Appourchaux, T., et al. (2012). Solving the mode identification problem in asteroseismology of F stars observed with kepler. *Astrophys. J.* 751, L36. doi:10.1088/2041-8205/751/2/L36

Xiong, D. R., Deng, L., Zhang, C., and Wang, K. (2016). Turbulent convection and pulsation stability of stars - II. Theoretical instability strip for δ Scuti and γ Doradus stars. *Mon. Not. Roy. Astron. Soc.* 457, 3163–3177. doi:10.1093/mnras/stw047

Conflict of Interest: The author declares that the research was conducted in the absence of any commercial or financial relationships that could be construed as a potential conflict of interest.

frontiers in Astronomy and Space Sciences

REVIEW
published: 15 February 2021
doi: 10.3389/fspas.2020.577695

RR Lyrae Stars as Seen by the *Kepler* Space Telescope

Emese Plachy[1,2,3] *and Róbert Szabó*[1,2,3]*

[1]Konkoly Observatory, Research Centre for Astronomy and Earth Sciences, Budapest, Hungary, [2]MTA CSFK Lendület Near-Field Cosmology Research Group, Budapest, Hungary, [3]ELTE Eötvös Loránd University, Institute of Physics, Budapest, Hungary

The unprecedented photometric precision along with the quasi-continuous sampling provided by the *Kepler* space telescope revealed new and unpredicted phenomena that reformed and invigorated RR Lyrae star research. The discovery of period doubling and the wealth of low-amplitude modes enlightened the complexity of the pulsation behavior and guided us toward nonlinear and nonradial studies. Searching and providing theoretical explanation for these newly found phenomena became a central question, as well as understanding their connection to the oldest enigma of RR Lyrae stars, the Blazhko effect. We attempt to summarize the highest impact RR Lyrae results based on or inspired by the data of the *Kepler* space telescope both from the nominal and from the K2 missions. Besides the three most intriguing topics, the period doubling, the low-amplitude modes, and the Blazhko effect, we also discuss the challenges of *Kepler* photometry that played a crucial role in the results. The secrets of these amazing variables, uncovered by *Kepler*, keep the theoretical, ground-based, and space-based research inspired in the post-*Kepler* era, since light variation of RR Lyrae stars is still not completely understood.

Keywords: RR Lyrae stars, Kepler spacecraft, Blazhko effect, pulsating variable stars, horizontal-branch stars, pulsation, asteroseismology, nonradial oscillations

OPEN ACCESS

Edited by:
Karen Kinemuchi,
New Mexico State University,
United States

Reviewed by:
Charles Kuehn,
University of Northern Colorado,
United States
Marcella Di Criscienzo,
National Institute of Astrophysics (INAF), Italy

***Correspondence:**
Róbert Szabó
szabo.robert@csfk.mta.hu

Specialty section:
This article was submitted to Stellar and Solar Physics, a section of the journal Frontiers in Astronomy and Space Sciences

Received: *29 June 2020*
Accepted: *22 September 2020*
Published: *15 February 2021*

Citation:
Plachy E and Szabó R (2021) RR Lyrae Stars as Seen by the Kepler Space Telescope. Front. Astron. Space Sci. 7:577695. doi: 10.3389/fspas.2020.577695

1. INTRODUCTION

RR Lyrae stars are large-amplitude, horizontal-branch pulsating stars which serve as tracers and distance indicators of old stellar populations in the Milky Way and neighboring galaxies. They are also essential laboratories for testing evolutionary and pulsation models. Due to their importance and their large numbers among pulsating variables, they have been the subject of extensive research even before the era of space-based missions. Those studies had special interest in the properties of globular clusters, the pulsation period changes, and the long-standing mystery of the Blazhko effect (Blažko, 1907). The Blazhko phenomenon is a quasiperiodic modulation of the pulsation amplitude and phase along with a prominent change of the light curve shape, which can be seen in a significant fraction of RR Lyrae stars. In spite of the enormous efforts from both theoretical and observational sides, the Blazhko effect is still not fully explained. However, except for this problem, RR Lyrae stars were thought to be a well-studied and well-understood class of pulsating variables before the launch of *Kepler*. New phenomena hiding in the fine details were not expected.

The dominant component of RR Lyrae light variation is the radial pulsation (with 0.2–1 day long periods) that can be either fundamental or first overtone mode, and in rarer cases these two modes appear simultaneously. The types are called RRab, RRc, and RRd, respectively, following the tradition of Solon Bailey's original nomenclature (Bailey, 1902). The light curve shape itself is an excellent classifier of the pulsation mode and it is also useful to estimate physical parameters that make

RR Lyrae stars extremely valuable objects for asteroseismology [see the recent study of Bellinger et al. (2020) and references therein]. By achieving the millimagnitude level in precision via space-based photometry in the last 20 years, it became clear that RR Lyrae pulsation is more complex than previously assumed, in which nonradial pulsation and nonlinear dynamics also play important roles.

Low-amplitude additional frequencies were first detected by the MOST space telescope (Matthews et al., 2000) in the light curve of an RRd type star, AQ Leo (Gruberbauer et al., 2007). No ground-based survey could compete with the continuity of space-based data that were eventually crucial in the discovery of the wealth of low-amplitude features in RR Lyrae stars. The CoRoT (Convection Rotation and planetary Transits) space mission (Baglin et al., 2009) was launched almost three years before *Kepler*, but by the time of the publication of the first RR Lyrae results, *Kepler* had already been routinely delivering quarterly data. The first additional frequency in a CoRoT light curve was found by Chadid et al. (2010) in the Blazhko star V1127 Aql, with a period ratio of ~ 0.69 with the fundamental mode, which they also suggested to be a nonradial mode. This short prehistory of additional modes in RR Lyrae stars was then followed by the first *Kepler* results and with these, a new era has begun.

In this paper we present a summary of the most intriguing and defining discoveries in RR Lyrae stars achieved with or inspired by the *Kepler* space telescope. We start with the 4-year-long nominal mission and continue with the K2 mission which, in spite of technical difficulties, became surprisingly successful and equally important for RR Lyrae investigations. At the time of this writing, *Kepler* and especially K2 data of RR Lyrae stars are far from being fully exploited, but two years after the official retirement of the telescope the time is ripe to review the major results obtained so far.

2. THE NOMINAL *KEPLER* MISSION

Kepler was designed to find Earth-sized exoplanets around solar-like stars in the habitable zone with the transit method; hence at the core of its mission lies high-precision photometry of a large number of stars (on the order of 10^5) for extended periods of time (originally planned for 3.5 years). Despite some minor difficulties (larger stellar noise than originally planned, unexpected safe-modes lasting for a few days to three weeks, and the failure of one CCD module and later that of one of the reaction wheels), the mission was tremendously successful, providing an extraordinary wealth of planets and exotic planetary systems orbiting around a large variety of host stars.

The strategy in the original mission was to monitor one particular field of view (10^5 deg^2) close to the plane of the northern Milky Way that contains a large number of stars. In the telescope tube of the 95 cm effective-diameter Schmidt telescope a 42-CCD mosaic was collecting stellar light, slightly defocused to shift the saturation limit and enable higher signal-to-noise ratio per exposure. The individual exposures were approximately 6 s long and were stacked to provide 1-min (called short cadence, for a small number of stars) and 30-min integrations (referred to as long cadence observations, the default observing mode for the vast majority of *Kepler* targets). The cadence rate, along with the photometric precision and continuous nature of data, played an important role in *Kepler*'s ability to improve on ground-based observations.

In March 2009, *Kepler* was launched to an Earth-trailing orbit around the Sun, with a period of 372.5 days. This ensured that the same part of the sky could be monitored continuously, as opposed to MOST, CoRoT, and the BRITE Constellation (Weiss et al., 2014), all moving on Earth-bound orbits.

In order to ensure optimal illumination of the solar panels of the spacecraft, a 90-degree rotation of the spacecraft was employed every 90–95 days (a quarter of the *Kepler* year). The first two quarters (Q0, an engineering run lasting for 10 days, and Q1, an incomplete, 33-day-long run) were performed keeping the same orientation, and after the first roll, Q2 was the first full-length quarter. The last quarter (Q17) meant a premature end of the original mission which was caused by the failure of a second reaction wheel. Reaction wheels were providing the stable and precise orientation of the spacecraft that played a crucial role in collecting close-to-micromagnitude precision light curves.

Once every month during the mission (and eight times within 1.5 days at the beginning) full frame images (FFIs) were also taken. These were rarely used for scientific exploitation, although a few exceptions do exist (Montet and Simon, 2016; Hippke and Angerhausen, 2018; Molnár et al., 2018). All *Kepler* data, including raw RR Lyrae light curves and full frame images, are available at the MAST database.[a]

Due to bandwidth limitations, only a small fraction of all pixels (typically 5–6%) could be downloaded of *Kepler*'s images. It meant that only preselected targets were observed; hence target selection prior to the main mission was crucial for the exoplanetary and also for the stellar astrophysics communities, although later on additional targets could be added through the Guest Observer opportunities. A thorough study to select main-sequence stars instead of giants was performed to help with the achievement of the main mission goal, that is, finding transiting exoplanets. The first and most important exoplanet results were announced by the core *Kepler* team (Borucki et al., 2010).

However, a smaller number (6,000) of targets were dedicated to stellar characterization by the *Kepler* Asteroseismic Science Consortium (KASC). Members of the KASC Working Group #13 which focused on RR Lyrae stars [later combined with WG#7 for Cepheids, since the original *Kepler* field contained only one classical Cepheid, V1154 Cyg (Szabó et al., 2011)] made sure that *Kepler* observed all known RR Lyrae stars in the field. Therefore, all available variability catalogs were used for the preselection process. In total, roughly 50 RR Lyrae stars were found in the field prior to *Kepler*'s launch. All targets that were found to be close to other targets were excluded; hence large contamination was expected. Specifically, the KASC RR Lyrae Working Group submitted 57 targets of which 21 were RRab stars (period range: 0.47–0.69 days, apparent *Kepler* magnitudes ranging between 11.4 and 16.7), 2 were RRc stars (V

[a]http://archive.stsci.edu/kepler/data_search/search.php

magnitude of 13.0 and 13.5 mag periods: 0.2485 and 0.3658 days), and all the rest were candidate RR Lyrae stars gathered from various ground-based variability surveys. It is worth noting that essentially no metallicity information was available for these targets. The situation was later remedied by Nemec et al. (2011) and Nemec et al. (2013).

In addition, ground-based photometric measurements were also scheduled to find stars showing the Blazhko effect. Interestingly, only one of the targets among the RR Lyrae stars in the *Kepler* field, namely, RR Lyr itself, had been known to be modulated, although at the time of launch we already knew that close to half of the RRab stars should show the phenomenon. The incidence rate was determined by a systematic survey of the Blazhko effect in a galactic sample consisting of 30 RRab stars (Jurcsik et al., 2009) and later was indeed confirmed by the *Kepler* observations (Benkő et al., 2010). This dramatic improvement in our knowledge of RR Lyrae stars just after a few weeks to months of *Kepler* observations demonstrated the power of space photometric observations excellently.

The quarterly roll of the spacecraft, however, caused discontinuities in the observations that led to the problem of data stitching. The position of the stars in the CCD changed with every roll, and the differences in pixel sensitivity appeared as mean brightness deviations as well as a bias in the pulsation amplitudes. This was complicated by the orbital motion of the satellite, the so-called *Kepler* year that manifests itself in the differential velocity aberration, causing slow positional shifts of the targets on the CCDs. The extent of the shift is dependent on the positions in the field of view. To correct for these effects the type of the brightness variability had to also be taken into account. The larger the difference between the timescales of systematics and the intrinsic brightness variation, the easier to correct for them.

The light curves could be detrended within the quarters by fitting and subtracting either a linear or polynomial fit, followed by a shift (addition) along with a stretch or a compression (multiplication) of the data. The zero-point differences and the scaling factors with respect to the reference quarter (for that Q4 was often chosen) were straightforward to calculate for the non-Blazhko stars, but not so simple for the Blazhko stars. Proper stitching of the modulated amplitudes needed special care, and the need to collect all the flux as accurately as possible became essential. Therefore, tailor-made apertures were created for each target star and each quarter. These apertures contained all pixels that contained the signal of the star. This way the quarterly differences in the pulsation amplitudes were hoped to practically disappear, leaving solely zero-point shifts between the quarters. That could be not fully achieved, because the downloaded pixel 'stamps' sometimes turned out to be too tight, creating inevitable flux loss. In these cases a few percent of scaling was applied to normalize the amplitudes from quarter to quarter (Benkő et al., 2014).

The prototype star, RR Lyr, was an important target of the mission. This star is not only the eponym of the type, but by far the brightest representative of its class; thus it saturated the *Kepler* CCDs. With RR Lyr we learned an important lesson about how to collect all available flux and restore the full pulsation amplitude. High-amplitude variables can suffer significant flux loss at maximum light, if inadequate number of pixels are used in the photometry, and flux spilling along the pixel columns exceeds the aperture, which then distorts the measured light curve shape. The situation, when the central saturation column bleeds out from the aperture, could be handled with a clever trick: the ratio of the central column flux to the adjacent column fluxes can be determined, and we can predict the flux when the central column is not fully captured. The light curve of RR Lyr was restored this way for quarters Q1–Q2 (Kolenberg et al., 2011).

2.1. The Discovery of Period Doubling and Additional Modes

The light curves of the first quarter (Q1) were analyzed soon after they were obtained (Kolenberg et al., 2010). The unprecedentedly precise and continuous data were not only impressive, but clearly revealed that a much more complex pulsation is going on in RR Lyrae stars than we ever thought and that the Fourier spectra displayed low-amplitude additional frequencies. The most surprising discovery among them was undoubtedly the half-integer (subharmonic) frequencies being present in some Blazhko RRab stars (at $0.5f$, $1.5f$, $2.5f$, etc., where f is the fundamental mode frequency). **Figure 1** illustrates the differences between the spectra of a non-Blazhko RRab, a Blazhko RRab, and a Blazhko star with period doubling. It is important to mention here that only Blazhko RRab stars showed half-integer frequencies; RRc and non-Blazhko RRab variables did not, notwithstanding that the *Kepler* sample size was limited. Namely, in Q1 42 RR Lyrae candidates were observed by *Kepler* altogether: 17 Blazhko-modulated RRab, 17 nonmodulated RRab, 4 RRc stars, and 4 candidates turned out to be non-RR Lyraes.

The half-integer frequencies were immediately recognized as the sign of period doubling bifurcation, a nonlinear phenomenon, where the singly periodic oscillation is destabilized by a resonance and turns into a two-period oscillation. The doubled period is visible in the light curves in the form of alternating low- and high-amplitude cycles of the original pulsation period (see **Figure 2**). This again showed the benefit of uninterrupted observations, since ground-based observations were inadequate to detect the period doubling with a characteristic timescale of close to one day, since on consecutive nights only every second pulsation cycle can be observed in a typical 0.5-day-period RRab star.

By a fortunate coincidence, at about the same time period doubling was discovered in new RR Lyrae hydrodynamic simulations, providing an explanation and identifying the resonance that can be responsible for it (Szabó et al., 2010; Kolláth et al., 2011). High-order radial overtones were investigated in detail and it was found that the ninth overtone can lock into a 9:2 resonance with the fundamental mode in a wide temperature range. Such high overtone modes are normally heavily damped and were thought to have no effect on the pulsation, but in RR Lyrae models this mode is trapped between the partial ionization zone and the stellar surface (this type of mode is called a "strange mode"). The left panel of **Figure 3** shows the period ratios of the first eleven radial

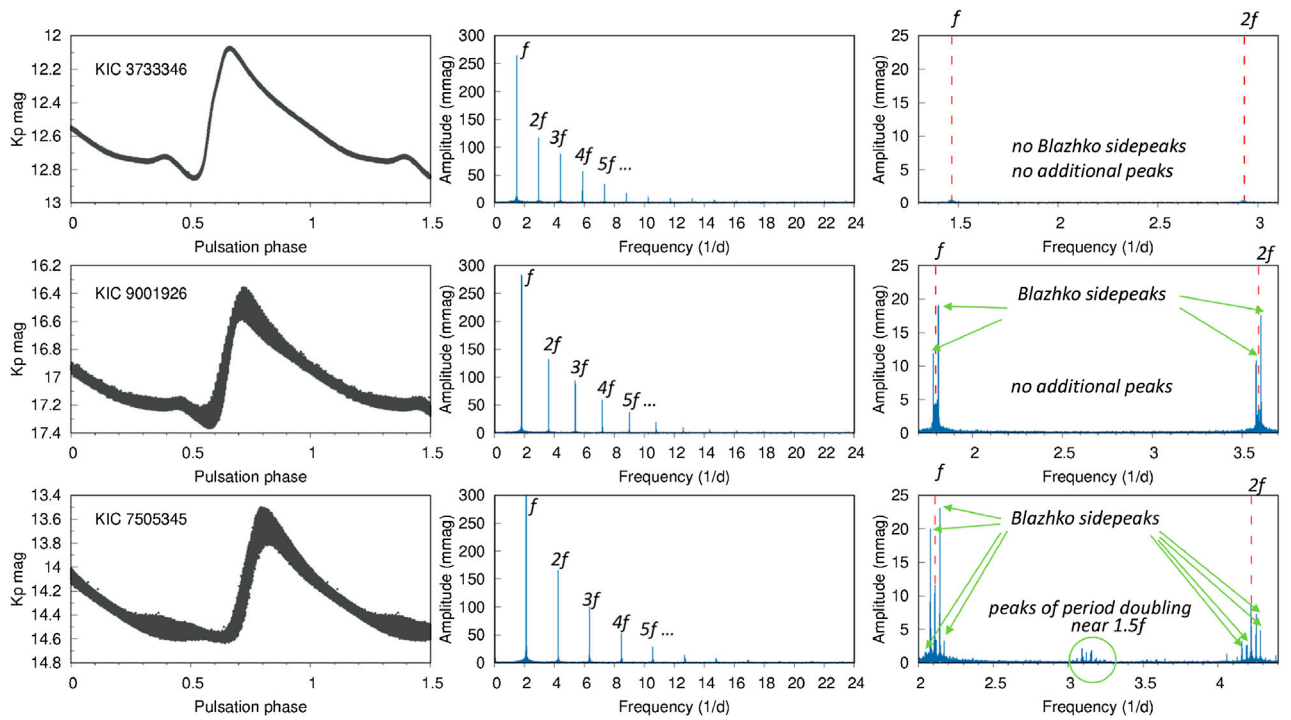

FIGURE 1 | Examples of non-Blazhko, Blazhko, and period doubled Blazhko RRab stars of the *Kepler* field. Panels show folded light curves, Fourier spectra, and zooms of residual spectra (after prewhitening with the pulsation frequency series: $f, 2f, 3f \ldots$), respectively. Based on the light curves published by Benkő et al. (2014).

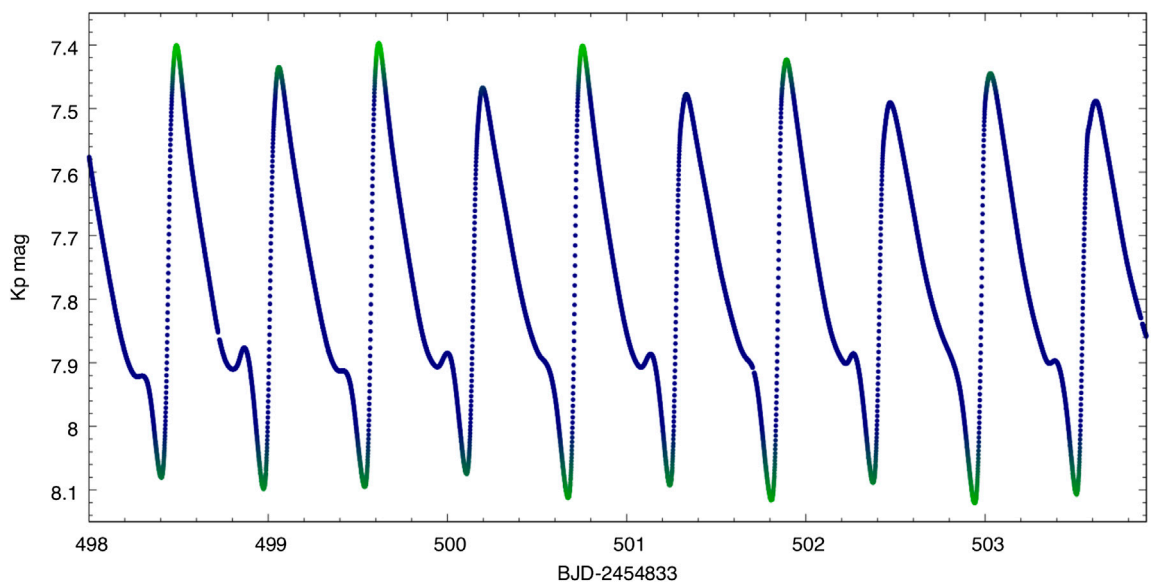

FIGURE 2 | Alternation of the pulsation amplitudes of RR Lyr, the brightest representative of its class, as observed by *Kepler*. The observed fluxes were transformed to K_p magnitude, which is *Kepler*'s photometric system. Colors change with brightness for better visibility of the alternation. Data downloaded from the MAST.

modes of an RR Lyrae model as a function of the effective temperature. Periods are scaled with the fundamental mode. Deviations in the nonadiabatic period ratios are most pronounced around 4.5, indicating the presence of strange modes. The right panel shows the linear growth rates of the same radial modes along with that of the fundamental mode. Instead of damping one finds excitation around the 9th and 10th radial overtones. To find out which high overtone is coupled to

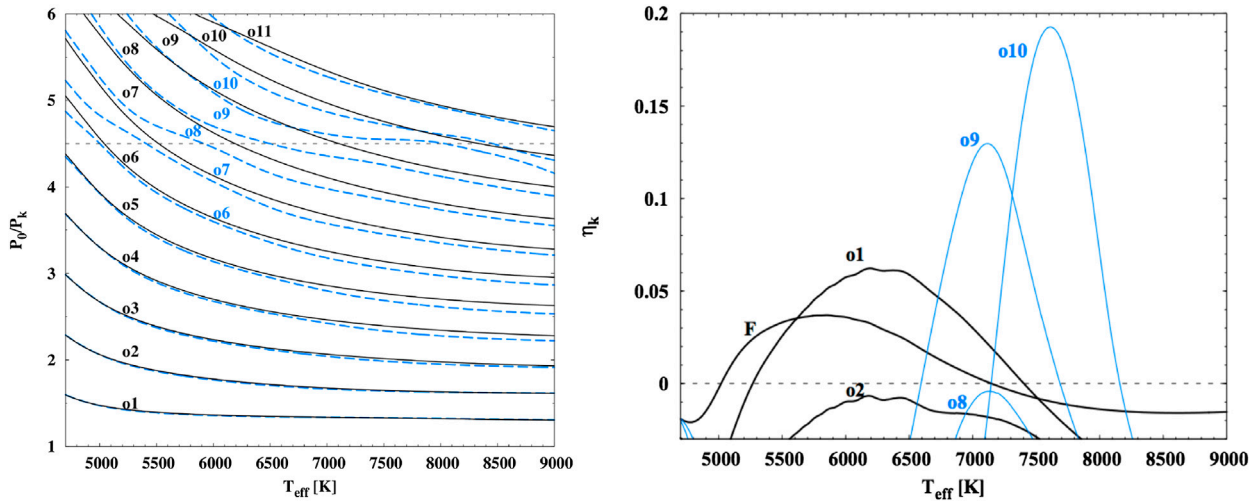

FIGURE 3 | Left: Modal diagram of an RR Lyrae model sequence (Kolláth et al., 2011). Period ratios of adiabatic modes (black lines) and nonadiabatic modes (blue dashed lines). The 9/2 period ratio is indicated with the horizontal dashed line. **Right:** Linear growth rates of radial modes. Overtones nine and ten could become excited. Figure reproduced from **Figures 3** and **4** of Kolláth et al. (2011).

the fundamental mode a thorough nonlinear model search was performed in Kolláth et al. (2011), which resulted in the unambiguous detection of the 9:2 resonance between the fundamental mode and the ninth radial overtone. Note that the ninth overtone being locked in a 9:2 resonance is a pure numerical coincidence. The ability of inducing period doubling and maybe modulation (see later) by a high radial overtone is a strong effect that was completely unexpected prior to *Kepler*.

The unexpected discovery of period doubling was followed by the exploration of oscillations in the low-amplitude regime. Benkő et al. (2010) analyzed 29 RR Lyrae stars observed during the first 138 days of the mission (quarters Q0–Q2). Fourteen of them showed the Blazhko effect with modulation periods ranging from 28 days to much longer than the observing period. Beyond the usual ingredients of an RR Lyrae Fourier spectrum, namely, the fundamental mode frequency and its harmonics plus the modulation multiplets around them, and the Blazhko frequency (occasionally along with its harmonics), new, low-amplitude periodicities were discovered at the millimag level and below. In four RRab stars these new frequencies fall close to the expected first or second (in some cases both) overtone pulsation frequencies. Three of these stars were identified as Blazhko-modulated ones, and one of them, V350 Lyr, was later recognized as the record-holder RRab with the smallest detected multiperiodic Blazhko modulation ever (0.6 and 0.8 mmag, respectively, see Benkő and Szabó, 2015).

Interestingly, linear hydrodynamic pulsation model computations (presented in Benkő et al., 2010) demonstrated that the fundamental mode and the second overtone can be simultaneously excited in these stars, so these observational results can be interpreted as the second radial overtone mode being excited with unusually low amplitudes, that is, much lower than amplitudes of secondary frequencies in canonical double-mode RR Lyrae stars, where the amplitudes of the primary and secondary modes are comparable. Here there is a difference of two to three orders of magnitude. A confirmation of this hypothesis can come from nonlinear pulsation simulations, but nonlinear effects both affect the mode selection process and shift the linear periods, and multimode pulsations are notoriously hard to reproduce.

In fact, such a help from the modeling side seems to be inevitable, since theory suggests that periodicities close to radial overtone mode frequencies may arise from not only the radial modes themselves, but also the dense spectrum of nonradial modes, that are preferentially excited close to the radial ones (Dziembowski, 1977; Van Hoolst et al., 1998). It is extremely interesting in this context that, based on *Kepler* observations, Molnár et al. (2012) found the first overtone to be excited with (very) small amplitude (at the 2-mmag level) in RR Lyrae, the prototype of the class. In fact, since RR Lyr is a Blazhko RRab, showing the period doubling phenomenon as well, one may assume that this star pulsates in three radial modes: fundamental mode, ninth radial overtone, and the first overtone. This was clearly demonstrated with the use of nonlinear hydrodynamical calculations, since the three-mode state showed up in the models as a stable state. Such model calculations, however, do not exist for the second radial overtone yet.

2.2. The Blazhko Effect Seen in the *Kepler* Field

The first analysis of the *Kepler* data of RR Lyr was presented by Kolenberg et al. (2011). The early data contained three Blazhko cycles only but still clearly showed that the repetition was not strict. A slow shortening of the Blazhko period was documented before *Kepler* (Kolenberg et al., 2006), but the new *Kepler* data revealed that the Blazhko effect was variable on an even shorter

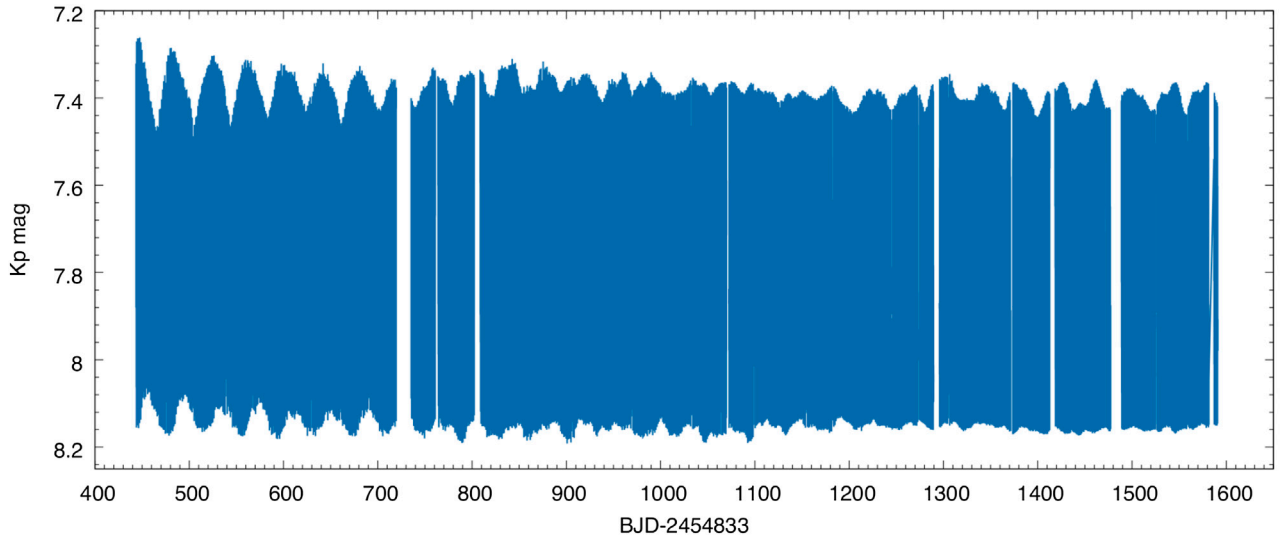

FIGURE 4 | The *Kepler* Q5-Q17 short cadence data light curve of RR Lyr, the eponym of its class. Data downloaded from the MAST. Note that individual pulsation cycles are not discernible on this scale. Gaps are present in the data due to safe mode events and other occasional technical problems.

time scale. At the same time, period doubling was also detected in RR Lyr.

RR Lyr was not observed in quarters Q3 and Q4, due to its underestimated brightness in the standard aperture assignment algorithms. Fortunately, the problem was fixed, new custom apertures were set, and RR Lyr was observed until the end of the mission in short cadence mode (**Figure 4**). This rich data set witnessed a vanishing Blazhko effect (Stellingwerf et al., 2013; Le Borgne et al., 2014). The Blazhko amplitude variation was 40% of the pulsation amplitude in its strongest phase but then decreased below 10%, while the Blazhko period showed a 2% decrease. This intriguing feature requires continuous monitoring, and RR Lyr provides a unique laboratory to study drastic changes in the pulsation state within human lifetime.

The value of amplitude-independent methods is especially high for the analysis of the Blazhko modulation, due to the uncertainties in the pulsation amplitudes caused by the potential flux loss. The continuity and cadence of *Kepler* data allow us to construct precise O–C diagrams that not only provide us with spectacular visualizations for the phase modulation, but can also be the subject of Fourier analysis themselves.

Fifteen Blazhko stars were found in the *Kepler* field and analyzed by Benkő et al. (2014). An unprecedentedly high percentage (80%) of this sample was found to be multiperiodically modulated. Moreover, some of these stars showed different modulation periods to be dominant in the phase and in the amplitude variations. The ratio between the primary and secondary modulation periods was also investigated and found to be close to small integer numbers in almost all cases, suggesting that undiscovered resonances may play role in the modulation.

The Blazhko stars with monoperiodic modulation also showed some kind of irregularity. The nature of the irregularity (i.e., chaotic or stochastic) provides constraints for the theoretical models of the Blazhko effect; therefore V783 Cyg was investigated with nonlinear dynamical methods (Plachy et al., 2014a). This star was the most promising candidate for that sensitive analysis, since it has the shortest modulation period; thus the number of observed modulation cycles during the *Kepler* mission was the highest. The nonlinear dynamical analysis has strict requirements; only precise, continuous, and long input data (preferably of hundreds of cycles) will give reliable results. We were never able to collect such data for the Blazhko modulation in the pre-*Kepler* era. The phase-space reconstruction applied to V783 Cyg revealed low-dimensional deterministic chaos in the dynamics behind the Blazhko modulation. However, the effect of instrumental issues was also tested, and it was found that the technical problems of the data stitching, the detrending, and the sparse sampling may lead to apparent cycle-to-cycle variations in the modulation that could mimic the chaotic behavior. Thus the intrinsic origin of the irregularity in the Blazhko effect could not be proven for V783 Cyg, showing the limitations of *Kepler* data.

Studying the relation between the phase modulation and the amplitude modulation we can discover various morphology types. In **Figure 5**, we present three examples (KIC 7257008, KIC 4484128, and KIC 7671081) where instantaneous amplitudes of the $f_0\,(t)$ pulsation frequency are plotted as the function of the instantaneous phase. These trajectories show very different routes, for which no explanation or connection to other pulsation properties has been found yet.

The connection between the Blazhko effect and the period doubling phenomenon is also an important question that needs to be investigated since only the Blazhko stars show the period doubling. Nine out of the 15 Blazhko stars of the *Kepler* field show half-integer frequencies, while the others do not. The half-integer frequency series appears with the highest peak typically at $1.5f$, which is very often a noncoherent peak suggesting temporal variability. Indeed, the alternation of the pulsation cycles in the

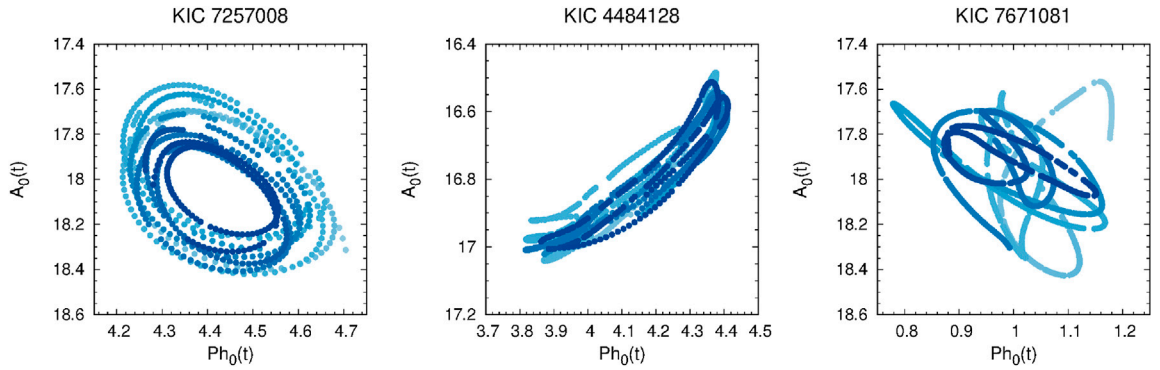

FIGURE 5 | Examples of the relation between the variations of the amplitude and phase of the pulsation frequency f_0 over time in three Blazhko stars. Color represents the progression of time, from light blue toward dark blue. Based on the light curves published by Benkő et al. (2014).

light curves sometimes disappears or decreases to a very low amplitude. The order of the low- and high-amplitude cycles also changes; this feature was visualized by Molnár et al. (2014) who connected every second maxima for the even and for the odd cycles with separate lines. The interchanges in the order occur when these lines cross each other. Similar interchanges were observed in the pulsation of RV Tau stars by Plachy et al. (2014b).

2.3. The Wealth of Low-Amplitude Frequencies

The detailed Fourier analysis of the Blazhko RRab stars recovered different groups of low-amplitude additional frequencies (Benkő et al., 2014). The expected regions of the first (f_1) and the second overtone (f_2) are positioned at the two sides of the 1.5f frequency group in the Fourier spectra. Frequencies at millimagnitude level

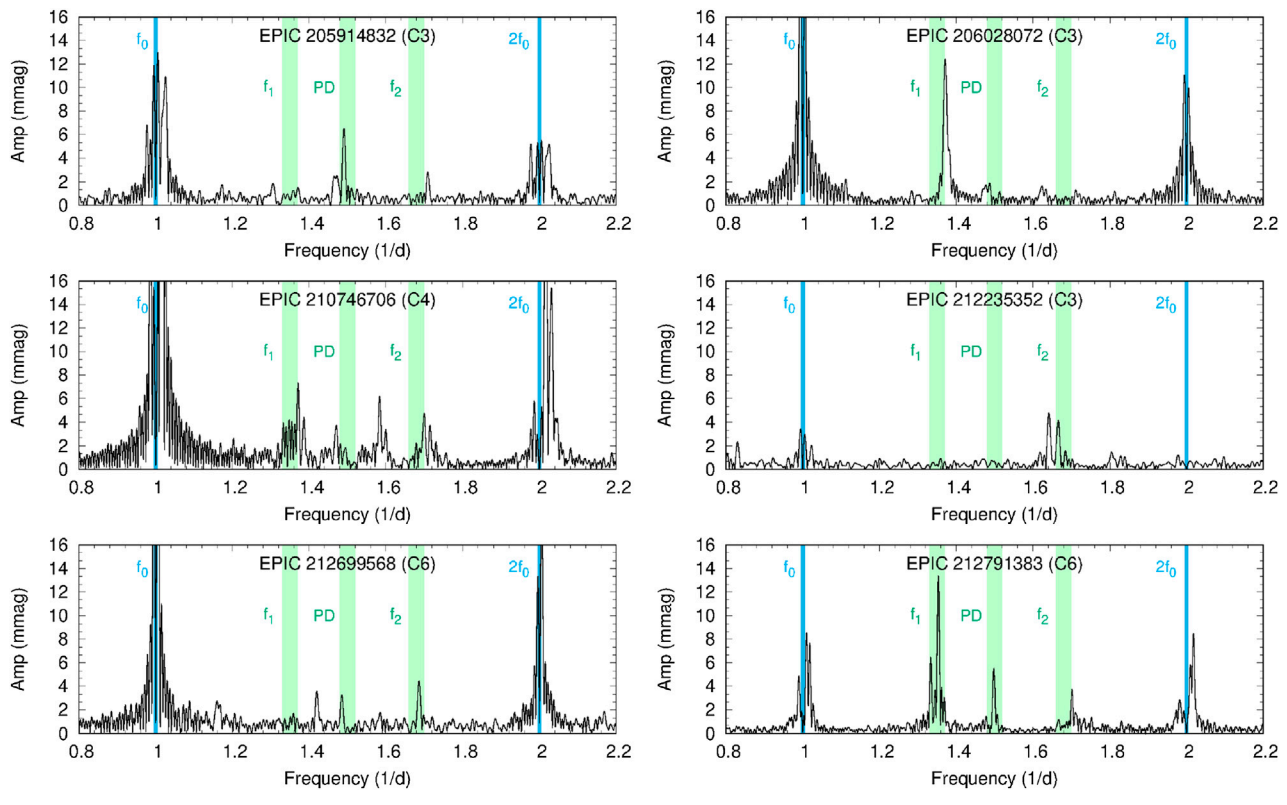

FIGURE 6 | Examples of residual Fourier spectra of K2 RR Lyrae stars showing low-amplitude additional peaks (after removing the frequency series of the main pulsation). Green areas are the expected frequency regions of the first radial overtone, period doubling (PD), and the second radial overtone, respectively. Based on the light curves published by Plachy et al. (2019).

appear within these regions, but sometimes also between them. We demonstrate this on examples from the K2 mission in **Figure 6**. The origin of frequency peaks outside the expected frequency regions is unclear.

A rich frequency spectrum of additional modes was observed in V445 Lyr, a Blazhko star showing extreme strong modulation (Guggenberger et al., 2012). The peaks belonging to the period doubling, the first and second overtones, all appeared, the latter with a clearly variable amplitude that was not connected to the Blazhko phase. A fourth peak was interpreted as a nonradial mode. Altogether 80 combination frequencies have been identified in this star.

The analysis of the four *Kepler* RRc stars resulted in the clear detection of low-amplitude oscillations with period ratio of P/P_1 = 0.612–0.632 with the dominant first overtone mode (Moskalik et al., 2015). Subharmonics of these $f_{0.61}$ frequencies at $0.5f_{0.61}$ and $1.5f_{0.61}$ have also been detected. This type of low-amplitude modes was identified in Cepheid stars in the Large Magellanic Cloud, all within similar period ratios (0.6–0.64) relative to the overtone mode (Moskalik and Kolaczkowski, 2008). Nonradial oscillation was immediately proposed as the origin. This discovery was made possible by the OGLE (Optical Gravitational Lensing Experiment) survey that became a fundamental source of high-quality ground-based photometry of radial pulsators in the last decade. Modes with similar period ratios were first seen in the RRc type by Olech and Moskalik (2009) among the RR Lyraes of the ω Centauri. Since then, it became clear that these stars form similar sequences in the Petersen diagram as overtone Cepheids do (Smolec et al., 2017). A model explaining the nature of these additional periodicities has been proposed by Dziembowski (2016), in which strongly trapped, unstable nonradial modes (ℓ = 7, 8, and 9 degrees in classical Cepheids and ℓ = 8 and 9 in RR Lyr stars) are excited. In this model the nonradial mode is actually at the $0.5f_{0.61}$ frequency, while its first harmonic signal can reach higher amplitudes due to geometric and nonlinear effects.

Nineteen nonmodulated RR Lyrae stars were analyzed by Nemec et al. (2011). None of these stars shows the period doubling phenomenon that strongly suggests its connection to the Blazhko effect. Empirical photometric metal abundances were also derived for these stars and compared to spectroscopic metallicities. The so-derived metallicities of most of the stars were found to be similar to those of intermediate-metallicity globular clusters ([Fe/H] ∼ –1.6). However, the lowest-amplitude stars turned out to be metal-rich with [Fe/H] between –0.55 and +0.07. Spectroscopic observations of the *Kepler* field RR Lyrae stars were performed by the Canada–France–Hawaii 3.6-m telescope (CFHT) and the Keck-I 10-m telescope (W. M. Keck Observatory) (Nemec et al., 2013), and these measurements confirmed the photometric [Fe/H] results for the non-Blazhko and most Blazhko RRab stars.

The reanalysis of the non-Blazhko stars revealed cycle-to-cycle light curve variations in stars which are brighter than K_p ∼ 15.4 mag (Benkő et al., 2019). Scattered short cadence observations that have been obtained for a few quarters for non-Blazhko *Kepler* RR Lyrae stars were crucial in this discovery. The amplitude differences between the light curve maxima were found to be in the range of 5–8 mmag. Additional modes identified as the first and the second overtone modes have also been recovered at several non-Blazhko stars with extremely low amplitude ratios with the fundamental mode. Moreover, the amplitude of the additional modes shows changes over time, while in some cases they appear only temporarily. Their linear combinations with the fundamental mode were also detectable, sometimes with much higher amplitude than the low-amplitude additional modes themselves. This again suggests the nonradial origin of these modes, since a scenario was found only in case of nonradial modes. In **Table 1**, we summarized the identification of low-amplitude additional frequencies in the *Kepler* RR Lyrae stars for which detailed Fourier analysis has already been performed.

The *Kepler* data of non-Blazhko stars provide opportunity to search for binarity too. The variation of the O–C diagrams of two RRab stars could be fitted with the light time effect caused by a low-mass companion, likely a substellar object (giant planet or brown dwarf) (Li and Qian, 2014). Comparing the high number of RR Lyrae stars and the few binary candidate systems that have been found so far (Hajdu et al., 2015; Prudil et al., 2019), we may conclude that RR Lyrae close-in companions are very rare, in accord with (binary) stellar evolution theory predictions of stars that are past the red giant phase.

2.4. Studies Inspired by *Kepler* RR Lyrae Results

The *Kepler* RR Lyrae results entirely reformed the research field of classical pulsators. Searching for more examples of period doubling and nonradial modes in hydrodynamical models and high-quality ground- and space-based photometry became the most relevant.

The discovery of period doubling revitalized the theoretical side of the radial stellar pulsation field. Hydrodynamic models of the 90s already predicted that period doubling can naturally occur in Cepheids (Moskalik and Buchler, 1990). Cepheids are radially pulsating siblings of RR Lyrae stars showing pulsation behavior similar in several aspects, most prominently in the shape of the light curve. These stars, however, are more massive and cross the classical instability strip at different evolutionary phases. The two main types are distinguished based on their Population I or II membership, and this also determines the nonlinear phenomena they can exhibit. The weakly dissipative Population I Cepheid models showed only period doubling, whereas models of the strongly dissipative Population II Cepheids followed a cascade of period doubling bifurcation that eventually led to chaos. The destabilization was caused by low-order half-integer resonances at both types (3:2 and 5:2, respectively).

As the period doubling appeared in the RR Lyrae models (Kolláth et al., 2011), the suspicion that resonant interaction between the fundamental mode and ninth overtone might also be the key in the Blazhko immediately arose. The hydrodynamical simulations, however, did not produce modulation. Only the amplitude equation formalism provided a demonstration that amplitude modulations may occur as a result of nonlinear, resonant mode coupling between these two modes (Buchler

TABLE 1 | Additional modes in the *Kepler* RR Lyrae stars.

KIC number	GCVS name	Subtype	Period	Additional frequencies
3864443	V2178 Cyg	RRab-BL	0.486947	f_2, PD (Benkő et al., 2010)
4484128	V808 Cyg	RRab-BL	0.5478635	PD (Benkő et al., 2010), f_2 (Benkő et al., 2014)
5559631	V783 Cyg	RRab-BL	0.6207001	—
6183128	V354 Lyr	RRab-BL	0.5616892	f_1, f_2, PD (Benkő et al., 2010), (no f_1) (Benkő et al., 2014)
6186029	V445 Lyr	RRab-BL	0.5130907	f_1, f_2, PD (Benkő et al., 2010)
7198959	RR Lyr	RRab-BL	0.566788	PD (Benkő et al., 2010), f_1 (Molnár et al., 2012)
7505345	V355 Lyr	RRab-BL	0.4736995	PD (Benkő et al., 2010), f_2 (Benkő et al., 2014)
7671081	V450 Lyr	RRab-BL	0.5046198	f_2 (Benkő et al., 2014)
9001926	V353 Lyr	RRab-BL	0.5567997	—
9578833	V366 Lyr	RRab-BL	0.5270284	f_2 (Benkő et al., 2014)
9697825	V360 Lyr	RRab-BL	0.5575755	f_1, PD (Benkő et al., 2010), f_2 (no f_1) (Benkő et al., 2014)
11125706	—	RRab-BL	0.61322	—
12155928	V1104 Cyg	RRab-BL	0.4363851	—
7257008	—	RRab-BL	0.511787	f_2, PD (Benkő et al., 2014)
9973633	—	RRab-BL	0.510783	f_2, PD (Benkő et al., 2014)
10789273	V838 Cyg	RRab-BL	0.48028	f_2, PD (Benkő et al., 2014)
9508655	V350 Lyr	RRab-BL	0.59424	f_2 (Benkő et al., 2010)
7021124	—	RRab-BL	0.6224925	f_2 (Nemec et al., 2011)
3733346	NR Lyr	RRab	0.6820264	—
3866709	V715 Cyg	RRab	0.47070609	—
5299596	V782 Cyg	RRab	0.5236377	—
6070714	V784 Cyg	RRab	0.5340941	—
6100702	—	RRab	0.4881457	—
6763132	NQ Lyr	RRab	0.5877887	f_1 (Benkő et al., 2019)
6936115	FN Lyr	RRab	0.52739847	—
7030715	—	RRab	0.68361247	—
7176080	V349 Lyr	RRab	0.507074	—
7742534	V368 Lyr	RRab	0.4564851	—
7988343	V1510 Cyg	RRab	0.5811436	$f_2 - f_0$ (Benkő et al., 2019)
8344381	V346 Lyr	RRab	0.5768288	$f_2 - f_0$ (Benkő et al., 2019)
9591503	V894 Lyr	RRab	0.5713866	$f_2 - f_0$ (Benkő et al., 2019)
9658012	—	RRab	0.533206	f_2 (Benkő et al., 2019)
9717032	—	RRab	0.5569092	—
9947026	V2470 Cyg	RRab	0.5485905	f_1 (Benkő et al., 2019)
10136240	V1107 Cyg	RRab	0.5657781	—
10136603	V839 Cyg	RRab	0.4337747	—
11802860	AW Dra	RRab	0.687216	—
8832417	—	RRc	0.2485464	$f_{0.61}$ (Moskalik et al., 2015)
5520878	—	RRc	0.2691699	$f_{0.61}$ (Moskalik et al., 2015)
4064484	—	RRc	0.3370019	$f_{0.61}$ (Moskalik et al., 2015)
9453114	—	RRc	0.3660809	$f_{0.61}$, $f_{0.68}$ (Moskalik et al., 2015)

and Kolláth, 2011). This new theory of the Blazhko effect predicts both types of modulations: periodic and chaotic.

The resonant mode coupling mechanism is also supported by BL Her hydrodynamical calculations (Smolec and Moskalik, 2012). The models of these short-period Type II Cepheids exhibited periodic and quasiperiodic modulation of the pulsation amplitudes and phases. Moreover, some models showed period doubling with or without modulation. A 3:2 resonance was identified behind the phenomenon. This theoretical work was then further improved and two period doubling domains were recovered, one within 2–6.5 days and one above 9.5 days, in the regime of W Vir-type stars (Smolec, 2016).

The luminous siblings of RR Lyrae stars, the classical Cepheids, are the primary standard candles in extragalactic distance measurements, and they were believed to be clockwork-precision pulsators before the era of ultraprecise measurements. The only exception was the unique case of V473 Lyrae, the only known Cepheid displaying strong Blazhko effect (Burki and Mayor, 1980). The pulsation of this star is multiply modulated and the measurement by the MOST space telescope also revealed period doubling in it (Molnár et al., 2017a).

Regarding Type II Cepheids, cycle-to-cycle variations were known to be common among W Vir stars and toward the longer periods (P > 20 days). The RV Tau phenomenon was recognized as period doubling, caused most likely by a 2:1 resonance (Fokin, 1994). Nevertheless, the first detection of period doubling in W Vir stars has only been achieved with the *Kepler* space telescope in the K2 mission (Plachy et al., 2017). In this new context it was also recognized that the amplitude alternation seen by Templeton and Henden (2007) in multicolor observations of W Vir, the eponym of the class, is actually period doubling. Thanks to the extensive analysis of Cepheids in the galactic bulge by the OGLE survey, we know that period doubling is common for periods above 15 days and the transition toward the RV Tau regime is a smooth process

(Smolec et al., 2018). Period doubling at shorter periods has also been discovered in OGLE BL Her stars (Smolec et al., 2012), but only three such stars are known so far, suggesting that period doubling is a rare phenomenon in that class.

Based on the *Kepler* findings the CoRoT RR Lyrae data were revisited to look for phenomena that might be overlooked before (Szabó et al., 2014). The most important result was the discovery of period doubling in modulated CoRoT RRab stars. Short sections of alternating maxima, typical of the period doubling effect, were found in four CoRoT RR Lyrae stars out of six modulated RRab stars. Given the usually brief time intervals where the phenomenon is detectable, occurrence can be even higher. This result corroborates with the previous claims about the strong correlation of the occurrence of period doubling and the Blazhko phenomenon, since no period doubling was found in nonmodulated RRab or RRc/RRd stars in the CoRoT sample. It also became clear that additional modes are ubiquitous in all RR Lyrae subtypes except for the nonmodulated RRab pulsators. In these stars no additional periodicities were found down to the precision of CoRoT and *Kepler*. In addition, noncoherence (temporal variability) of the additional modes in RRc, RRd, and modulated RRab stars were found to be dominant. While in the latter group the Blazhko modulation itself might be a clue, some other mechanism should be at work in the overtone and classical double-mode pulsators.

3. THE K2 MISSION

Kepler was only barely able to extend its original mission. By May of 2013 only two functioning reaction wheels remained on the spacecraft out of four; thus triaxial stabilization was lost. It became clear that the original mission could not be continued without significant deterioration in data quality. NASA called for ideas and methods for a new observational strategy in the two-wheel mode. The scientific community reacted fast to save the mission; 42 white papers have been submitted including two that considered potential RR Lyrae observations. One suggested a continued observation of the *Kepler* field of view with extended number of high cadence targets among the large-amplitude pulsators (Molnár et al., 2013). Beside many advantages, the longer time span would have been allowed to study the Blazhko effect in more detail. The other white paper proposed to turn the telescope to the South Ecliptic Pole to monitor the largest possible sample of well classified large-amplitude pulsating and eclipsing variables (Szabó et al., 2013). That would have meant synergy with the OGLE survey and the TESS mission.

The final concept opted for a solution that maximizes the photometric performance by minimizing the roll of the spacecraft. This was possible with target fields placed along the ecliptic plane. Each field could be monitored for about 80 days, and before changing fields the telescope had to turn sideways to keep the fixed solar panels aimed at the Sun. These periods were called "Campaigns." The design of the mission opened new opportunities for RR Lyrae investigations, as well as many other fields of astronomy. With the changing fields of view, massive continuous space photometry became accessible for a variety of stellar objects the first time. The new mission was named K2 (Howell et al., 2014).

The observation started with an 8.9-day-long Two-Wheel Engineering Test in February of 2014, which targeted nearly two thousand stars. The K2-E2 sample contained 33 RR Lyrae stars, members from each subtypes (RRab, RRc, and RRd). This short run demonstrated that all new low-amplitude phenomena seen in the *Kepler* mission can be recovered from K2 data too (Molnár et al., 2015b). Period doubling was detected in two RRab stars, and nonradial modes were detected in two RRd and the three nonmodulated RRc stars. The first space-based photometry of a Blazhko-RRc star was also provided by K2 Engineering Test.

With K2 we lost the chance to study stars showing long-period Blazhko effect, but in exchange we got a large sample of RR Lyrae stars from different regions of the galaxy, providing us with a basis for population studies and statistical investigations. Careful target selection therefore became a new important task for the KASC Working Group #7. The *Kepler* Guest Observer Office developed the K2FoV tool to check the visibility of targets in each Campaign. Proposals could be submitted through the NASA NSPIRES System starting from Campaign 3. The existing large ground-based surveys, such as the Catalina Sky Survey (Drake et al., 2014), the Lincoln Near Earth Asteroid Research (Sesar et al., 2013), the All Sky Automated Survey (Pojmanski, 2002), and the Northern Sky Variability Survey (Woźniak et al., 2004), offered photometric data of a great number of RR Lyrae candidates that we subsequently used in the target selection (Plachy et al., 2016). RR Lyrae proposals prioritized the less common double-mode and overtone RR Lyrae stars and those RRab stars that looked special in some sense, like having extreme Blazhko modulation or an unusually long pulsation period. A few of the most interesting targets were also proposed for 1-min cadence. The observable targets in the K2 mission were limited by the telemetry; 10 to 20 thousand long cadence targets and 50 to 100 short cadence targets were available per Campaign. Nevertheless, most of the proposed RR Lyrae targets have been approved during the K2 mission (except for the first Campaigns), altogether reaching about 4000 RR Lyrae stars. At the time of writing this paper, only a small fraction of this huge sample has been analyzed, leaving the better part of it for future studies. The major problem that slows down the massive analysis is the pointing jitter of the space telescope. No comprehensive correction solution could be invented so far for this problem, which would work well also for RR Lyrae stars. The EVEREST pipeline comes close but even that one removes the pulsation signal from a significant fraction of RR Lyrae stars (Luger et al., 2018). The instrumental signal is similar to RR Lyrae light curves in periodicity and shape, which makes its elimination challenging. We report the discoveries based on early K2 RR Lyrae data in the following sections.

3.1. The Challenges of K2 RR Lyrae Photometry

The two-wheel mode of the K2 mission made attitude control maneuvers of the satellite necessary in about every 6 h (occasionally 12 h). These maneuvers corrected the torque caused by the radiation pressure that distributed unevenly on

the spacecraft. As a consequence, sudden drifts and jumps occurred in the positions of the field of view that reached as much as two pixels at the edges of the detector. Therefore, the sensitivity variation within and between the pixels caused a systematic variation in the light curves. In worse cases they were contaminated by the flux from nearby stars as well. Besides the Simple Aperture Photometry (SAP) and Presearch Data Conditioned SAP (PDCSAP) data products provided by the mission (Van Cleve et al., 2016), several other pipelines have been developed to fix or at least minimize the instrumental effects. These pipelines used different approaches to find general solution to all variables, but most of them failed on RR Lyrae stars for two main reasons. Apertures were too tight to capture the ~ 1 magnitude variability and/or the correction methods could not distinguish between the sharp features of systematics and RR Lyrae variation that occurs on the same timescale. A comparison analysis of various photometry outputs has been carried out by Plachy et al. (2019), who suggested a method optimized for the detection of RR Lyrae light variation. The main idea for the EAP (Extended Aperture Photometry) method was the extension of the apertures to contain the star in the maximum brightness phases. This alone improved the light curve significantly and applying the K2SC (K2 Systematics Correction) pipeline (Aigrain et al., 2016) on EAP solutions, light curves improved even more. Over four hundred such RR Lyrae light curves have been prepared and analyzed so far from Campaigns 3 to 6.

Anomalous Cepheids constitute a rare type of pulsating stars. They are 2–3 times more massive than RR Lyrae stars and pulsate with periods ranging from 0.3 to 2 days either in the fundamental or in the first overtone. Their origin is not fully clear; probably both single-star and binary evolution channels contribute to the production of these objects (Bono et al., 1997; Gautschy and Saio, 2017). RR Lyrae stars and anomalous Cepheids can be distinguished based on their light curve shapes, but only precise photometry can show their slightly distinct location in the Fourier parameter plane of $\log(p) - \phi_{21}$ and $\log(p) - \phi_{31}$. A useful byproduct of K2 RR Lyrae analysis was the discovery of four new anomalous Cepheid candidates (Plachy et al., 2019). All four candidates found among K2 RR Lyrae stars are fundamental mode pulsators, and they also provide the first detection of Blazhko modulation in this variable type.

Campaign 1 pointed to the North Galactic Cap containing the dwarf spheroidal galaxy Leo IV in the field of view. Leo IV is one among the ultra-faint satellites of the Milky Way discovered by the Sloan Digital Sky Survey (Belokurov et al., 2007). Three fundamental mode RR Lyraes have been identified in Leo IV by Moretti et al. (2009) at brightness ~ 21.5 mag in V band. All three RRab were detectable in K2 images, which made them the faintest pulsating stars measured with *Kepler* ever (Molnár et al., 2015a). To obtain accurate photometry for such faint objects, image subtraction techniques had to be involved. That was performed with the open source FITSH software package (Pál, 2012). The individual frames had to be adjusted to the same reference system to compensate for the pointing motions. Additional neighboring K2 stamps were used beside the target frames to determine the precise transformations and background level. This technique ensured light curve precision in the order of 50–100 mmag, and that was adequate to detect the farthest Blazhko modulation from Earth, as well as the first clear detection of Blazhko effect beyond the Milky Way and the Magellanic Clouds (**Figure 7**). The existence of Blazhko effect in such a metal poor galaxy as Leo IV ($\langle [F/H] \rangle = \sim -2.3$) also provides constraints for the theoretic models, while the experience collected with this study will be useful for future investigations of faint and/or extragalactic objects of the K2 mission.

3.2. Characterization of the Low-Amplitude Modes

A short cadence RRd target of Campaign 1, EPIC 201585823, has been analyzed by Kurtz et al. (2016). This star provided a new space-based detection of low-amplitude modes in double-mode RR Lyraes, in addition to AQ Leo (Gruberbauer et al., 2007), CoRoT ID 0101368812 (Chadid, 2012), and two more from the K2-E2 data (Molnár et al., 2015b). Although the interpretation of these modes differs in the aforementioned publications, they all belong to the same group of modes with $P/P_0 \sim 0.61$ period ratio. Kurtz et al. (2016) also reported the first comparison of photometric pipelines in the case of an RR Lyrae and concluded that the careful choice of photometric mask was essential. Double-mode RR Lyrae stars observed during the K2 mission have been studied by Moskalik et al. (2018). 39 RRd stars were investigated from Campaigns 0 to 13 in this preliminary study. The major parts of these stars show the typical period ratios that form a well-defined arc in the Petersen diagram and are denoted as "classical" RRd stars (Soszyński et al., 2019). Three stars, in turn, have lower period ratios belonging to the newly identified subgroups: two of them to the anomalous RRd stars (Soszyński et al., 2016a) and one to the group identified by Prudil et al. (2017). The pulsation modes of both anomalous RRd stars, as most of the members of the subgroup, show modulations. Similarly, the detected strong dominance of the fundamental mode is typical for anomalous RRd stars. The "Prudil" stars are a mysterious group where the mode of shorter period cannot be the radial first overtone. Returning to the classical RRd sample of K2, the $f_{0.61}$ mode has been detected in many of them at the millimagnitude level. Sometimes these modes seem to be nonstationary, while the dominant radial modes are stable. The additional modes of RRc stars populate two different regions in the Petersen diagram (**Figure 8**): three sequences of $f_{0.61}$ modes (which according to Dziembowski (2016) might correspond to nonradial modes of moderate degree $\ell = 8$, 9 and the middle sequence due to their linear combination) and the coherent frequency group of $f_{0.68}$ modes recently studied in detail by Netzel and Smolec (2019). Theoretical explanation for the latter group is still in question. Only one star has been found so far in which $f_{0.61}$ and $f_{0.68}$ modes coexist: KIC 9453114 in the *Kepler* field (Moskalik et al., 2015).

Low-amplitude modes of RRab stars from the early Campaigns of the K2 mission have been investigated by Molnár et al. (2017b). The Petersen diagram of period ratios of these new findings traced out the new groups of RRab low-amplitude modes. In **Figure 8** we present a Petersen diagram for

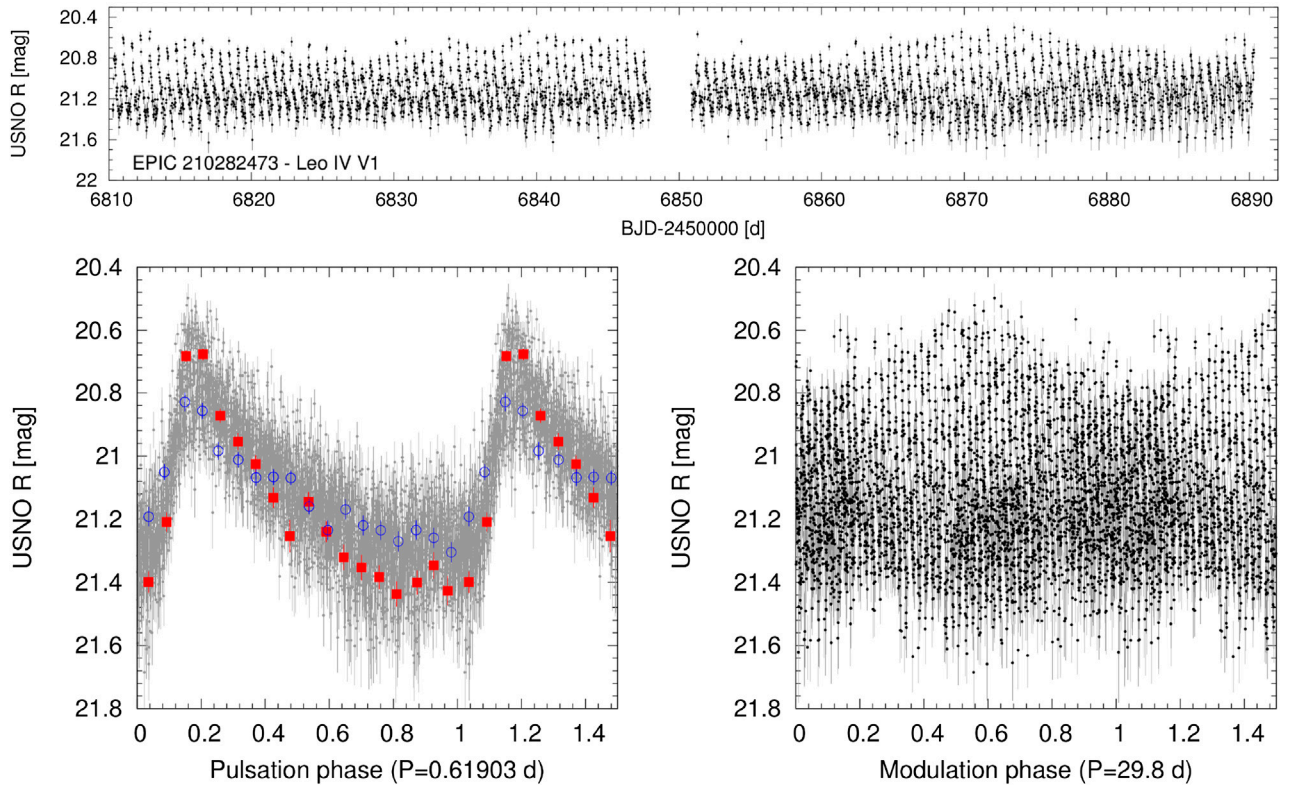

FIGURE 7 | The faintest Blazhko star from the K2 mission , EPIC 210282473 (Leo IV V1). **Upper panel:** the K2 light curve. **Lower left panel:** phase curve folded by the pulsation period, 2-day binned data from the maximum-amplitude phase (red) and minimum-amplitude phase (blue) are marked. **Lower right panel:** phase curve folded with the modulation period. Figure reproduced from **Figures 3** and **5** in Molnár et al. (2015) copyright AAS. Reproduced with permission.

the various multimode RR Lyrae stars of all subtypes, based on the OGLE and the *Kepler*/K2 data. The most unambiguous new group is the f_2 group, which shows a much lower scatter in frequencies than the group near f_1. Many stars exhibit low-amplitude peaks at slightly longer frequencies than $1.5f_0$ (i.e., above the period doubling line at ~ 0.666 period ratio in the Petersen diagram); the transition toward the f_1 regime is almost continuous. It is unclear what causes this incredible variety of low-amplitude modes, and the origin of stars outside the main groups is also mysterious.

As we mentioned, only a small fraction of the K2 RR Lyrae sample is processed so far. Additional frequencies from the whole K2 survey will populate the Petersen diagram even more and may provide us better understanding of the mode selection mechanism.

3.3. Studying the Blazhko Effect With K2

The high-quality massive photometry of K2 RR Lyrae stars offers a basis to investigate the incidence rate of the Blazhko effect. To recover modulation, not only could the modulation triplets be searched in the Fourier spectra, but it is possible to construct proper amplitude and phase variation curves by a template fitting method (Plachy et al., 2019). This kind of analysis resulted in 44.7% for the incidence rate of Blazhko effect that is in agreement with the widely excepted value of around fifty percent. These incidence rates have been questioned by Kovács (2018, 2020) who proposed all RR Lyrae stars to be modulated based on his analysis of K2 data produced with the SAP pipeline. However, the estimation of the incidence rate strongly depends on the time span and the data quality, and as we mentioned earlier SAP light curves are of inferior quality compared to EAP light curves; therefore in our opinion it is highly unlikely that a thorough analysis would return close 90% percent occurrence. The literature values of the RRab Blazhko incidence rate range between 5% and 60% (see Kovács, 2016). The analysis of the most extended sample over 8,000 RRab in the galactic bulge by OGLE IV put the minimum value just above $\sim 40\%$ (Prudil and Skarka, 2017).

Not only can the incidence rate be studied with K2, but the fine details of the Blazhko effect at the shortest modulation periods can be studied as well. The K2 Blazhko sample shows a large variety of modulations; some examples are displayed in **Figure 9**.

The simultaneous appearance of the Blazhko effect and period doubling in some stars supports the theory of their common origin (Buchler and Kolláth, 2011). However, K2 Blazhko stars show a very low fraction of period doubled cases: only 7 stars out of 166 display clear subharmonics in their Fourier spectra. This is

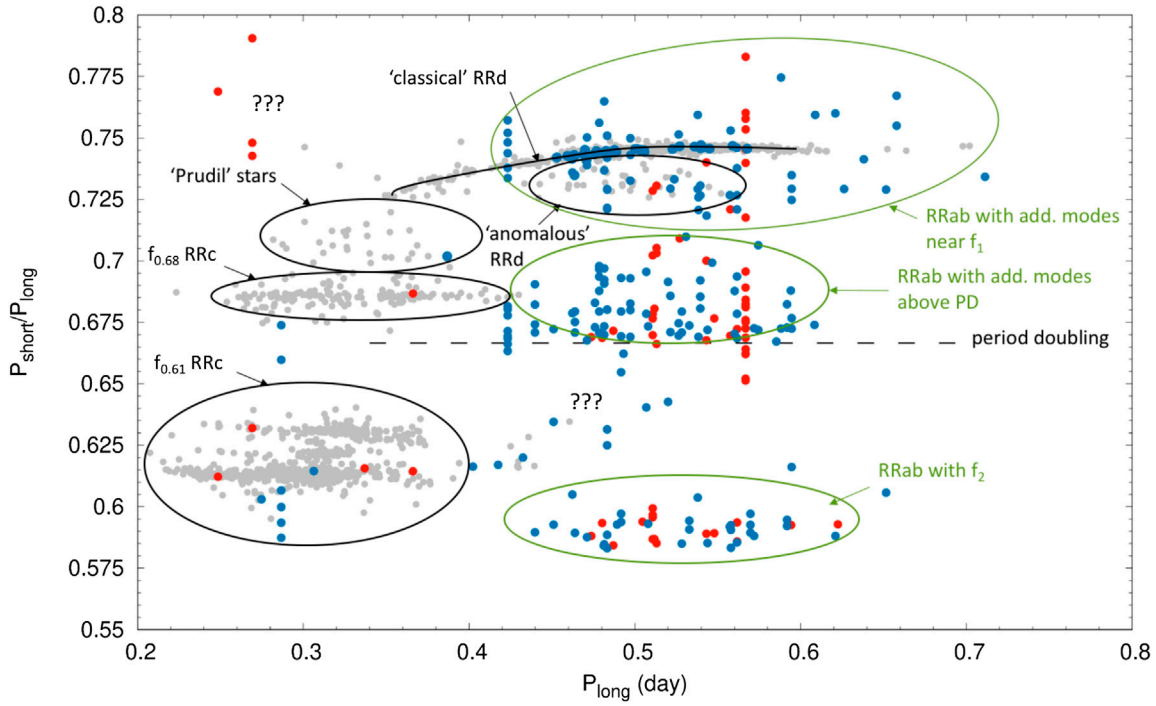

FIGURE 8 | Petersen diagram of multimode RR Lyrae stars. The gray points denote OGLE discoveries collected (Soszyński et al., 2016a; Soszyński et al., 2016b; Prudil et al., 2017; Netzel and Smolec, 2019; Soszyński et al., 2019). Red points are results from the *Kepler* field (Benkő et al., 2014; Moskalik et al., 2015) and blue points from the K2 mission (Molnár et al., 2017b; Moskalik et al., 2018; Plachy et al., 2019).

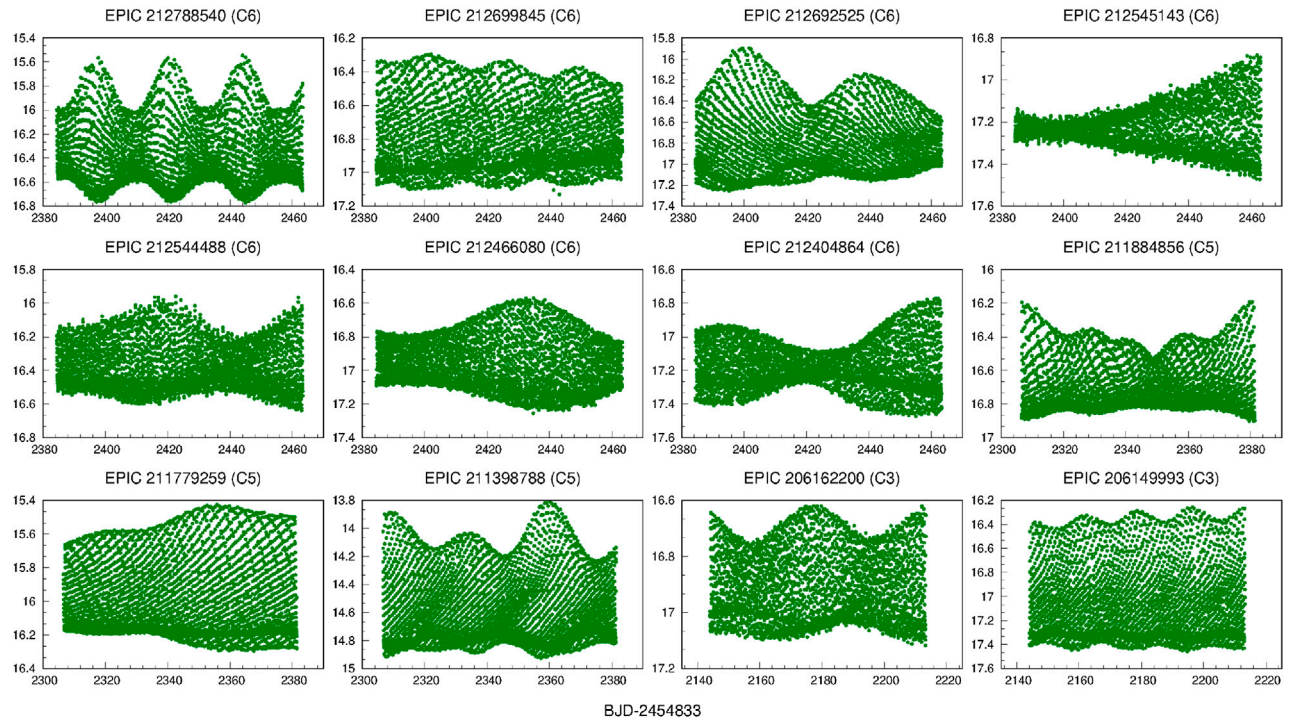

FIGURE 9 | Blazhko stars in the K2 mission. Based on the light curves published by Plachy et al. (2019).

a much lower incidence rate that we experienced in the original *Kepler* field (9 out of 15).

4. OUTLOOK

After nine years of operation *Kepler* ran out of fuel and officially retired on 30 October 2018 leaving us with an unprecedented amount of space photometric data. Ongoing and upcoming missions, like NASA's original and extended TESS mission (Ricker et al., 2015) and the PLATO mission of the European Space Agency (Rauer et al., 2014) scheduled for launch in 2026, will provide hundreds to thousands of continuous RR Lyrae light curves spanning from a few weeks to several months and to years of coverage.

TESS observes brighter targets than *Kepler* did, partly because of its smaller apertures and larger pixel size (4″ for *Kepler* and 21″ for TESS), and its observation length provides shorter (27 days) light curves than K2 did, for most of the targets. But even with these short observations ∼ 30–130 RR Lyrae pulsation cycles can be monitored, adequate to explore the low-amplitude mode content. One year of quasi-continuous coverage is also possible close to the ecliptic poles, lending opportunity to study the Blazhko effect in this regions. In addition, large parts of the sky will be reobserved by TESS during its extended mission(s); hence altogether 90% of the sky will be covered. PLATO will also cover much larger areas of the sky than the *Kepler* and K2 missions: it will have long observing runs (up to 1–2 years) complemented by shorter (2–3 months) so-called step-and-stare runs; thus altogether nearly 50% of the sky will be covered.

Similarly, Gaia (Gaia Collaboration et al., 2018) and the Legacy Survey of Space and Time (LSST) of the Vera Rubin Observatory (LSST Science Collaboration et al., 2009) are and will be game-changers in the field. Gaia provides parallax and proper motion information for more than 1.3 billion stars down to 21 magnitude complemented by variability information, basic color measurements, and low-resolution spectroscopy in Data Release 2, and the numbers will increase in the later releases. Tens of thousands of new RR Lyrae stars will be discovered providing a homogeneous all-sky catalog which is not possible by either of the aforementioned missions. Coincidentally, Gaia will provide distances down to the faint end of TESS's RR Lyrae sample. LSST will monitor the sky visible from Chile in six photometric bands every 3 days with a 3.5 Gpixel camera for 10 years, thus providing on average 800–1,000 photometric data points (i.e., OGLE-like cadence) for each target down to 23.5 mag (reaching 25 mag in coadded images). This capability will allow the discovery of tens of thousands of new RR Lyrae stars out to a large distance (400 kpc) providing excellent opportunities to use RR Lyrae stars to trace halo structures in the galactic halos and discover faint surface brightness dwarf galaxies in the Local Group.

All these prospective data sets from upcoming missions will shed new light on the occurrence of the Blazhko effect (including long-period and multiperiod modulations), period doubling, additional radial and nonradial modes, chaotic behavior, and other dynamical phenomena as a function of a broad range of stellar parameters and galactic and extragalactic environments. In light of these prospects, we are witnessing a golden era of classical pulsating variables, including RR Lyrae stars.

AUTHOR CONTRIBUTIONS

EP contributed the review of the scientific results and prepared the figures. RSz provided the historical and technical description of the mission.

FUNDING

This project has been supported by the Lendület Program of the Hungarian Academy of Sciences, projects No. LP2014–17 and LP2018–7/2020, and the MW-Gaia COST Action (CA-18104). This paper includes data collected by the *Kepler* mission and obtained from the MAST data archive at the Space Telescope Science Institute (STScI). EP acknowledges the financial support of the Hungarian National Research, Development and Innovation Office (NKFI), grant KH_18 130405, and the János Bolyai Research Scholarship of the Hungarian Academy of Sciences. This research has made use of NASA's Astrophysics Data System. Funding for the *Kepler* mission is provided by the NASA Science Mission Directorate. STScI is operated by the Association of Universities for Research in Astronomy, Inc., under NASA contract NAS 5–26555.

ACKNOWLEDGMENTS

The authors thank the reviewers for their valuable comments and suggestions that helped to improve this paper. The authors gratefully acknowledge the entire *Kepler* team, whose outstanding efforts have made these results possible. Fruitful discussions with László Molnár and Zoltán Kolláth are also acknowledged.

REFERENCES

Aigrain, S., Parviainen, H., and Pope, B. J. S. (2016). K2SC: flexible systematics correction and detrending of K2 light curves using Gaussian process regression. *Mon. Not. Roy. Astron. Soc.* 459, 2408–2419. doi:10.1093/mnras/stw706

Baglin, A., Auvergne, M., Barge, P., Deleuil, M., and Michel, E., and CoRoT Exoplanet Science Team (2009). "CoRoT: description of the mission and early results," in *Transiting planets*. F. Pont, D. Sasselov, and M. J. Holman (Editors). Vol. 253, 71–81. doi:10.1017/S1743921308026252

Bailey, S. I. (1902). A discussion of variable stars in the cluster ω Centauri. *Ann. Harvard Coll. Observatory* 38, 1.

Bellinger, E. P., Kanbur, S. M., Bhardwaj, A., and Marconi, M. (2020). When a period is not a full stop: light-curve structure reveals fundamental parameters of Cepheid and RR Lyrae stars. *Mon. Not. Roy. Astron. Soc.* 491, 4752–4767. doi:10.1093/mnras/stz3292

Belokurov, V., Zucker, D. B., Evans, N. W., Kleyna, J. T., Koposov, S., and Hodgkin, S. T. (2007). Cats and dogs, hair and a hero: a quintet of new Milky way companions. *Astrophys. J.* 654, 897–906. doi:10.1086/509718

Benkő, J. M., and Szabó, R. (2015). The Blazhko effect and additional excited modes in RR Lyrae stars. *Astrophys. J. Lett.* 809, L19. doi:10.1088/2041-8205/809/2/L19

Benkő, J. M., Kolenberg, K., Szabó, R., Kurtz, D. W., Bryson, S., and Bregman, J. (2010). Flavours of variability: 29 RR Lyrae stars observed with Kepler. *Mon. Not. Roy. Astron. Soc.* 409, 1585–1593. doi:10.1111/j.1365-2966.2010.17401.x

Benkő, J. M., Plachy, E., Szabó, R., Molnár, L., and Kolláth, Z. (2014). Long-timescale behavior of the Blazhko effect from rectified kepler data. *Astrophys. J. Suppl.* 213, 31. doi:10.1088/0067-0049/213/2/31

Benkő, J. M., Jurcsik, J., and Derekas, A. (2019). Revisiting the Kepler non-Blazhko RR Lyrae sample: cycle-to-cycle variations and additional modes. *Mon. Not. Roy. Astron. Soc.* 485, 5897–5913. doi:10.1093/mnras/stz833

Blažko, S. (1907). Mitteilung über veränderliche Sterne. *Astron. Nachr.* 175, 325. doi:10.1002/asna.19071752002

Bono, G., Caputo, F., Santolamazza, P., Cassisi, S., and Piersimoni, A. (1997). Evolutionary scenario for metal-poor pulsating stars. II. Anomalous cepheids. *Astron. J.* 113, 2209. doi:10.1086/118431

Borucki, W. J., Koch, D., Basri, G., Batalha, N., Brown, T., and Caldwell, D. (2010). Kepler planet-detection mission: introduction and first results. *Science* 327, 977. doi:10.1126/science.1185402

Buchler, J. R., and Kolláth, Z. (2011). On the Blazhko effect in RR Lyrae stars. *Astrophys. J.* 731, 24. doi:10.1088/0004-637X/731/1/24

Burki, G., and Mayor, M. (1980). HR 7308, a new cepheid with variable amplitude and very-short period (1.5d). *Astron. Astrophys.* 91, 115–121.

Chadid, M., Benkő, J. M., Szabó, R., Paparó, M., Chapellier, E., and Kolenberg, K. (2010). First CoRoT light curves of RR Lyrae stars. Complex multiplet structure and non-radial pulsation detections in V1127 Aquilae. *Astron. Astrophys.* 510, A39. doi:10.1051/0004-6361/200913345

Chadid, M. (2012). Detection of multiple modes in a new double-mode RR Lyrae star. *Astron. Astrophys.* 540, A68. doi:10.1051/0004-6361/201117408

Drake, A. J., Graham, M. J., Djorgovski, S. G., Catelan, M., Mahabal, A. A., and Torrealba, G. (2014). The Catalina surveys periodic variable star catalog. *Astrophys. J. Suppl.* 213, 9. doi:10.1088/0067-0049/213/1/9

Dziembowski, W. (1977). Oscillations of giants and supergiants. *Acta Astronom.* 27, 95–126.

Dziembowski, W. A. (2016). Nonradial oscillations in classical pulsating stars. Predictions and discoveries. *Commun. Konkoly Observatory Hungary* 105, 23–30.

Fokin, A. B. (1994). Nonlinear pulsations of the RV Tauri stars. *Astron. Astrophys.* 292, 133–151.

Gaia Collaboration, Brown, A. G. A., Vallenari, A., Prusti, T., de Bruijne, J. H. J., and Babusiaux, C. (2018). Gaia Data Release 2. Summary of the contents and survey properties. *Astron. Astrophys.* 616, A1. doi:10.1051/0004-6361/201833051

Gautschy, A., and Saio, H. (2017). On binary channels to anomalous Cepheids. *Mon. Not. Roy. Astron. Soc.* 468, 4419–4428. doi:10.1093/mnras/stx811

Gruberbauer, M., Kolenberg, K., Rowe, J. F., Huber, D., Matthews, J. M., and Reegen, P. (2007). MOST photometry of the RRdLyrae variable AQLeo: two radial modes, 32 combination frequencies and beyond. *Mon. Not. Roy. Astron. Soc.* 379, 1498–1506. doi:10.1111/j.1365-2966.2007.12042.x

Guggenberger, E., Kolenberg, K., Nemec, J. M., Smolec, R., Benkő, J. M., and Ngeow, C. C. (2012). The complex case of V445 Lyr observed with Kepler: two Blazhko modulations, a non-radial mode, possible triple mode RR Lyrae pulsation, and more. *Mon. Not. Roy. Astron. Soc.* 424, 649–665. doi:10.1111/j.1365-2966.2012.21244.x

Hajdu, G., Catelan, M., Jurcsik, J., Dekany, I., Drake, A. J., and Marquette, J. B. (2015). New RR Lyrae variables in binary systems. *Mon. Not. Roy. Astron. Soc.* 449, L113–L117. doi:10.1093/mnrasl/slv024

Hippke, M., and Angerhausen, D. (2018). The year-long flux variations in Boyajian's star are asymmetric or aperiodic. *Astrophys. J. Lett.* 854, L11. doi:10.3847/2041-8213/aaab44

Howell, S. B., Sobeck, C., Haas, M., Still, M., Barclay, T., and Mullally, F. (2014). The K2 mission: characterization and early results. *Publ. Astron. Soc. Pac.* 126, 398. doi:10.1086/676406

Jurcsik, J., Sódor, Á., Szeidl, B., Hurta, Z., Váradi, M., and Posztobányi, K. (2009). The Konkoly Blazhko Survey: is light-curve modulation a common property of RRab stars? *Mon. Not. Roy. Astron. Soc.* 400, 1006–1018. doi:10.1111/j.1365-2966.2009.15515.x

Kolenberg, K., Smith, H. A., Gazeas, K. D., Elmaslı, A., Breger, M., and Guggenberger, E. (2006). The Blazhko effect of RR Lyrae in 2003-2004. *Astron. Astrophys.* 459, 577–588. doi:10.1051/0004-6361:20054415

Kolenberg, K., Szabó, R., Kurtz, D. W., Gilliland, R. L., Christensen-Dalsgaard, J., and Kjeldsen, H. (2010). First kepler results on RR Lyrae stars. *Astrophys. J. Lett.* 713, L198–L203. doi:10.1088/2041-8205/713/2/L198

Kolenberg, K., Bryson, S., Szabó, R., Kurtz, D. W., Smolec, R., and Nemec, J. M. (2011). Kepler photometry of the prototypical Blazhko star RR Lyr: an old friend seen in a new light. *Mon. Not. Roy. Astron. Soc.* 411, 878–890. doi:10.1111/j.1365-2966.2010.17728.x

Kolláth, Z., Molnár, L., and Szabó, R. (2011). Period-doubling bifurcation and high-order resonances in RR Lyrae hydrodynamical models. *Mon. Not. Roy. Astron. Soc.* 414, 1111–1118. doi:10.1111/j.1365-2966.2011.18451.x

Kovács, G. (2016). The Blazhko phenomenon. *Commun. Konkoly Observatory Hungary* 105, 61–68.

Kovács, G. (2018). Are all RR Lyrae stars modulated? *Astron. Astrophys.* 614, L4. doi:10.1051/0004-6361/201833181

Kovács, G. (2020). On the incidence rate of Blazhko stars. arXiv e-prints, arXiv:2004.06452.

Kurtz, D. W., Bowman, D. M., Ebo, S. J., Moskalik, P., Handberg, R., and Lund, M. N. (2016). EPIC 201585823, a rare triple-mode RR Lyrae star discovered in K2 mission data. *Mon. Not. Roy. Astron. Soc.* 455, 1237–1245. doi:10.1093/mnras/stv2377

Le Borgne, J. F., Poretti, E., Klotz, A., Denoux, E., Smith, H. A., and Kolenberg, K. (2014). Historical vanishing of the Blazhko effect of RR Lyr from the GEOS and Kepler surveys. *Mon. Not. Roy. Astron. Soc.* 441, 1435–1443. doi:10.1093/mnras/stu671

Li, L. J., and Qian, S. B. (2014). Period analysis of two non-Blazhko RRab stars, FN Lyr and V894 Cyg, based on Kepler photometry: evidence of low-mass companions on wider orbits. *Mon. Not. Roy. Astron. Soc.* 444, 600–605. doi:10.1093/mnras/stu1344

LSST Science Collaboration, Abell, P. A., Allison, J., Anderson, S. F., Andrew, J. R., Angel, J. R. P., et al. (2009). *LSST science book*, Version 2.0. Tucson, AZ: LSST Corporation.

Luger, R., Kruse, E., Foreman-Mackey, D., Agol, E., and Saunders, N. (2018). An update to the EVEREST K2 pipeline: short cadence, saturated stars, and kepler-like photometry down to Kp = 15. *Astron. J.* 156, 99. doi:10.3847/1538-3881/aad230

Matthews, J. M., Kuschnig, R., Walker, G. A. H., Pazder, J., Johnson, R., and Skaret, K. (2000). "Ultraprecise photometry from space: the MOST microsat mission," in Astronomical Society of the Pacific Conference Series, Astronomical Society of the Pacific. San Francisco CA: Budapest, Hungary, August 8-12, 1999 Vol. 203, 74–75.

Molnár, L., Kolláth, Z., Szabó, R., Bryson, S., Kolenberg, K., and Mullally, F. (2012). Nonlinear asteroseismology of RR Lyrae. *Astrophys. J. Lett.* 757, L13. doi:10.1088/2041-8205/757/1/L13

Molnár, L., Szabó, R., Kolenberg, K., Borkovits, T., Antoci, V., and Vida, K. (2013). The Kep-Cont Mission: continuing the observation of high-amplitude variable stars in the Kepler field of view. arXiv e-prints, arXiv:1309.0740.

Molnár, L., Benkő, J. M., Szabó, R., and Kolláth, Z. (2014). "Kepler RR Lyrae stars: beyond period doubling," in *Precision asteroseismology*. J. A. Guzik, W. J. Chaplin, G. Handler, and A. Pigulski (Editors). Vol. 301, 459–460. doi:10.1017/S1743921313015044

Molnár, L., Pál, A., Plachy, E., Ripepi, V., Moretti, M. I., and Szabó, R. (2015a). Pushing the limits, episode 2: K2 observations of extragalactic RR Lyrae stars in the dwarf galaxy Leo IV. *Astrophys. J.* 812, 2. doi:10.1088/0004-637X/812/1/2

Molnár, L., Szabó, R., Moskalik, P. A., Nemec, J. M., Guggenberger, E., and Smolec, R. (2015b). An RR Lyrae family portrait: 33 stars observed in Pisces with K2-E2. *Mon. Not. Roy. Astron. Soc.* 452, 4283–4296. doi:10.1093/mnras/stv1638

Molnár, L., Derekas, A., Szabó, R., Matthews, J. M., Cameron, C., and Moffat, A. F. J. (2017a). V473 Lyr, a modulated, period-doubled Cepheid, and U TrA, a double-mode Cepheid, observed by MOST. *Mon. Not. Roy. Astron. Soc.* 466, 4009–4020. doi:10.1093/mnras/stw3345

Molnár, L., Plachy, E., Klagyivik, P., Juhász, Á. L., Szabó, R., and D'Alessandro, Z. (2017b). "The additional-mode garden of RR Lyrae stars," in *European physical journal web of conferences*. Vol. 160, 04008. doi:10.1051/epjconf/201716004008

Molnár, L., Plachy, E., Juhász, Á. L., and Rimoldini, L. (2018). Gaia data Release 2. Validating the classification of RR Lyrae and Cepheid variables with the Kepler and K2 missions. *Astron. Astrophys.* 620, A127. doi:10.1051/0004-6361/201833514

Montet, B. T., and Simon, J. D. (2016). KIC 8462852 faded throughout the Kepler mission. *Astrophys. J. Lett.* 830, L39. doi:10.3847/2041-8205/830/2/L39

Moretti, M. I., Dall'Ora, M., Ripepi, V., Clementini, G., Di Fabrizio, L., and Smith, H. A. (2009). The Leo IV dwarf spheroidal galaxy: color-magnitude diagram and pulsating stars. *Astrophys. J. Lett.* 699, L125–L129. doi:10.1088/0004-637X/699/2/L125

Moskalik, P., and Buchler, J. R. (1990). Resonances and period doubling in the pulsations of stellar models. *Astrophys. J.* 355, 590. doi:10.1086/168792

Moskalik, P., and Kolaczkowski, Z. (2008). Nonradial modes in classical cepheids. *Commun. Asteroseismol.* 157, 343–344.

Moskalik, P., Smolec, R., Kolenberg, K., Molnár, L., Kurtz, D. W., and Szabó, R. (2015). Kepler photometry of RRc stars: peculiar double-mode pulsations and period doubling. *Mon. Not. Roy. Astron. Soc.* 447, 2348–2366. doi:10.1093/mnras/stu2561

Moskalik, P., Nemec, J., Molnár, L., Plachy, E., Szabó, R., and Kolenberg, K. (2018). "K2 observations of double-mode RR Lyrae stars," in *The RR Lyrae 2017 conference. Revival of the classical pulsators: from galactic structure to stellar interior diagnostics*. R. Smolec, K. Kinemuchi, and R. I. Anderson. Vol. 6, 162–166.

Nemec, J. M., Smolec, R., Benkő, J. M., Moskalik, P., Kolenberg, K., and Szabó, R. (2011). Fourier analysis of non-Blazhko ab-type RR Lyrae stars observed with the Kepler space telescope. *Mon. Not. Roy. Astron. Soc.* 417, 1022–1053. doi:10.1111/j.1365-2966.2011.19317.x

Nemec, J. M., Cohen, J. G., Ripepi, V., Derekas, A., Moskalik, P., and Sesar, B. (2013). Metal abundances, radial velocities, and other physical characteristics for the RR Lyrae stars in the Kepler field. *Astrophys. J.* 773, 181. doi:10.1088/0004-637X/773/2/181

Netzel, H., and Smolec, R. (2019). The census of non-radial pulsation in first-overtone RR Lyrae stars of the OGLE Galactic bulge collection. *Mon. Not. Roy. Astron. Soc.* 487, 5584–5592. doi:10.1093/mnras/stz1626

Olech, A., and Moskalik, P. (2009). Double mode RR Lyrae stars in Omega Centauri. *Astron. Astrophys.* 494, L17–L20. doi:10.1051/0004-6361:200811441

Pál, A. (2012). FITSH- a software package for image processing. *Mon. Not. Roy. Astron. Soc.* 421, 1825–1837. doi:10.1111/j.1365-2966.2011.19813.x

Plachy, E., Benkő, J. M., Kolláth, Z., Molnár, L., and Szabó, R. (2014a). Non-linear dynamical analysis of the Blazhko effect with the Kepler space telescope: the case of V783 Cyg. *Mon. Not. Roy. Astron. Soc.* 445, 2810–2817. doi:10.1093/mnras/stu1943

Plachy, E., Molnár, L., Kolláth, Z., Benkő, J. M., and Kolenberg, K. (2014b). "On the interchange of alternating-amplitude pulsation cycles," in *Precision asteroseismology*. J. A. Guzik, W. J. Chaplin, G. Handler, and A. Pigulski (Editors). Vol. 301, 473–474. doi:10.1017/S1743921313015111

Plachy, E., Molnar, L., Szabo, R., Kolenberg, K., and Banyai, E. (2016). Target selection of classical pulsating variables for space-based photometry. *Commun. Konkoly Observatory Hungary* 105, 19–22.

Plachy, E., Molnár, L., Jurkovic, M. I., Smolec, R., Moskalik, P. A., and Pál, A. (2017). First observations of W Virginis stars with K2: detection of period doubling. *Mon. Not. Roy. Astron. Soc.* 465, 173–179. doi:10.1093/mnras/stw2703

Plachy, E., Molnár, L., Bódi, A., Skarka, M., Szabó, P., and Szabó, R. (2019). Extended aperture photometry of K2 RR Lyrae stars. *Astrophys. J. Suppl.* 244, 32. doi:10.3847/1538-4365/ab4132

Pojmanski, G. (2002). The all sky automated survey. Catalog of variable stars. I. 0 h - 6 hQuarter of the southern hemisphere. *Acta Astronom.* 52, 397–427.

Prudil, Z., and Skarka, M. (2017). Blazhko effect in the Galactic bulge fundamental mode RR Lyrae stars - I. Incidence rate and differences between modulated and non-modulated stars. *Mon. Not. Roy. Astron. Soc.* 466, 2602–2613. doi:10.1093/mnras/stw3231

Prudil, Z., Smolec, R., Skarka, M., and Netzel, H. (2017). Peculiar double-periodic pulsation in RR Lyrae stars of the OGLE collection - II. Short-period stars with a dominant radial fundamental mode. *Mon. Not. Roy. Astron. Soc.* 465, 4074–4084. doi:10.1093/mnras/stw3010

Prudil, Z., Skarka, M., Liška, J., Grebel, E. K., and Lee, C. U. (2019). Candidates for RR Lyrae in binary systems from the OGLE Galactic bulge survey. *Mon. Not. Roy. Astron. Soc.* 487, L1–L6. doi:10.1093/mnrasl/slz069

Rauer, H., Catala, C., Aerts, C., Appourchaux, T., Benz, W., and Brandeker, A. (2014). The PLATO 2.0 mission. *Exp. Astron.* 38, 249–330. doi:10.1007/s10686-014-9383-4

Ricker, G. R., Winn, J. N., Vanderspek, R., Latham, D. W., Bakos, G. Á., and Bean, J. L. (2015). Transiting exoplanet survey satellite (TESS). *J. Astronomical Telesc. Instrum. Syst.* 1, 014003. doi:10.1117/1.JATIS.1.1.014003

Sesar, B., Ivezić, Ż., Stuart, J. S., Morgan, D. M., Becker, A. C., and Sharma, S. (2013). Exploring the variable sky with LINEAR. II. Halo structure and substructure traced by RR Lyrae stars to 30 kpc. *Astron. J.* 146, 21. doi:10.1088/0004-6256/146/2/21

Smolec, R., and Moskalik, P. (2012). Period doubling and Blazhko modulation in BL Herculis hydrodynamic models. *Mon. Not. Roy. Astron. Soc.* 426, 108–119. doi:10.1111/j.1365-2966.2012.21678.x

Smolec, R., Soszyński, I., Moskalik, P., Udalski, A., Szymański, M. K., and Kubiak, M. (2012). Discovery of period doubling in BL Herculis stars of the OGLE survey. Observations and theoretical models. *Mon. Not. Roy. Astron. Soc.* 419, 2407–2423. doi:10.1111/j.1365-2966.2011.19891.x

Smolec, R., Dziembowski, W., Moskalik, P., Netzel, H., Prudil, Z., and Skarka, M. (2017). "Petersen diagram revolution," in European physical journal web of conferences. San Pedro de Atacama, Chile, Nov 28 – Dec 2, 2016 Vol. 152, 06003. doi:10.1051/epjconf/201715206003

Smolec, R., Moskalik, P., Plachy, E., Soszyński, I., and Udalski, A. (2018). Diversity of dynamical phenomena in type II Cepheids of the OGLE collection. *Mon. Not. Roy. Astron. Soc.* 481, 3724–3749. doi:10.1093/mnras/sty2452

Smolec, R. (2016). Survey of non-linear hydrodynamic models of type-II Cepheids. *Mon. Not. Roy. Astron. Soc.* 456, 3475–3493. doi:10.1093/mnras/stv2868

Soszyński, I., Smolec, R., Dziembowski, W. A., Udalski, A., Szymański, M. K., and Wyrzykowski, Ł. (2016a). Anomalous double-mode RR Lyrae stars in the magellanic Clouds. *Mon. Not. Roy. Astron. Soc.* 463, 1332–1341. doi:10.1093/mnras/stw1933

Soszyński, I., Udalski, A., Szymański, M. K., Wyrzykowski, Ł., Ulaczyk, K., and Poleski, R. (2016b). The OGLE collection of variable stars. Over 45 000 RR Lyrae stars in the magellanic system. *Acta Astronom.* 66, 131–147.

Soszyński, I., Udalski, A., Wrona, M., Szymański, M. K., Pietrukowicz, P., and Skowron, J. (2019). Over 78 000 RR Lyrae stars in the galactic bulge and disk from the OGLE survey. *Acta Astronom.* 69, 321–337. doi:10.32023/0001-5237/69.4.2

Stellingwerf, R. F., Nemec, J. M., and Moskalik, P. (2013). The Kepler RR Lyrae SC data set: period variation and Blazhko effect. in 40 years of variable stars: a celebration of contributions by Horace A. Smith conference proceedings of the regional variable star conference, East Lansing, MI, May 30-31. 2013, Editor K. Kinemuchi, C.A. Kuehn, N. De Lee, and H. A. Smith.

Szabó, R., Kolláth, Z., Molnár, L., Kolenberg, K., Kurtz, D. W., and Bryson, S. T. (2010). Does Kepler unveil the mystery of the Blazhko effect? First detection of period doubling in Kepler Blazhko RR Lyrae stars. *Mon. Not. Roy. Astron. Soc.* 409, 1244–1252. doi:10.1111/j.1365-2966.2010.17386.x

Szabó, R., Szabados, L., Ngeow, C. C., Smolec, R., Derekas, A., and Moskalik, P. (2011). Cepheid investigations using the Kepler space telescope. *Mon. Not. Roy. Astron. Soc.* 413, 2709–2720. doi:10.1111/j.1365-2966.2011.18342.x

Szabó, R., Molnár, L., Kołaczkowski, Z., Moskalik, P., Ivezić, Ž., and Udalski, A. (2013). The Kepler-SEP mission: harvesting the south ecliptic pole large-amplitude variables with Kepler. arXiv e-prints, arXiv:1309.0741.

Szabó, R., Benkő, J. M., Paparó, M., Chapellier, E., Poretti, E., and Baglin, A. (2014). Revisiting CoRoT RR Lyrae stars: detection of period doubling and temporal variation of additional frequencies. *Astron. Astrophys.* 570, A100. doi:10.1051/0004-6361/201424522

Templeton, M. R., and Henden, A. A. (2007). Multicolor photometry of the type II cepheid prototype W virginis. *Astron. J.* 134, 1999. doi:10.1086/522945

Van Cleve, J. E., Howell, S. B., Smith, J. C., Clarke, B. D., Thompson, S. E., and Bryson, S. T. (2016). That's how we roll: the NASA K2 mission science products and their performance metrics. *Publ. Astron. Soc. Pac.* 128, 075002. doi:10.1088/1538-3873/128/965/075002

Van Hoolst, T., Dziembowski, W. A., and Kawaler, S. D. (1998). Unstable non-radial modes in radial pulsators: theory and an example. *Mon. Not. Roy. Astron. Soc.* 297, 536–544. doi:10.1046/j.1365-8711.1998.01540.x

Weiss, W. W., Rucinski, S. M., Moffat, A. F. J., Schwarzenberg-Czerny, A., Koudelka, O. F., and Grant, C. C. (2014). BRITE-constellation: nanosatellites for precision photometry of bright stars. *Publ. Astron. Soc. Pac.* 126, 573. doi:10.1086/677236

Woźniak, P. R., Vestrand, W. T., Akerlof, C. W., Balsano, R., Bloch, J., and Casperson, D. (2004). Northern sky variability survey: public data release. *Astron. J.* 127, 2436–2449. doi:10.1086/382719

Conflict of Interest: The authors declare that the research was conducted in the absence of any commercial or financial relationships that could be construed as a potential conflict of interest.

frontiers in Astronomy and Space Sciences

REVIEW
published: 24 March 2021
doi: 10.3389/fspas.2020.595017

Solar-Like Oscillators in the *Kepler* Era: A Review

*Jason Jackiewicz**

Department of Astronomy, New Mexico State University, Las Cruces, NM, United States

Many late-type stars across the Milky Way exhibit observable pulsations similar to our Sun that open up a window into stellar interiors. The NASA *Kepler* mission, a space-based photometric telescope, measured the micro-magnitude luminosity fluctuations caused by solar-like oscillations of tens of thousands of stars for almost 10 years. Detailed stellar structure, evolution, and oscillation theoretical work established in the decades before, such as predictions about mode mixing in the interior of red-giant stars, among many others, now had voluminous precision data against which it could be tested. The overwhelming result is the general validation of the theory of stellar oscillations as well as stellar-structure models; however, important gaps in our understanding of interior physics was also revealed by *Kepler*. For example, interior rotation, convection, and mixing processes are complex phenomena not fully captured by standard models. This review explores some of the important impacts *Kepler* observations of solar-like oscillations across the cool end of the H-R diagram has had on stellar astrophysics through the use of asteroseismology.

Keywords: stars, solar-like oscillations, asteroseismology, stellar parameters, convection, kepler

OPEN ACCESS

Edited by:
Andrzej S. Baran, Pedagogical University of Kraków, Poland

Reviewed by:
Paul G. Beck, University of Graz, Austria
Tiago Campante, Instituto de Astrofísica e Ciências do Espaço, Portugal
Saskia Hekker, Heidelberg Institute for Theoretical Studies, Germany

***Correspondence:**
Jason Jackiewicz
jasonj@nmsu.edu

Specialty section:
This article was submitted to Stellar and Solar Physics, a section of the journal Frontiers in Astronomy and Space Sciences

Received: *14 August 2020*
Accepted: *17 November 2020*
Published: *24 March 2021*

Citation:
Jackiewicz J (2021) Solar-Like Oscillators in the Kepler Era: A Review. Front. Astron. Space Sci. 7:595017. doi: 10.3389/fspas.2020.595017

1 INTRODUCTION

The NASA *Kepler* spacecraft was launched in 2009 and spent the next four years staring at a fixed region of the sky toward the *Cygnus* and Lyra constellations (Borucki et al., 2010; Koch et al., 2010). After the loss of a couple of reactions wheels, the mission was revamped to carry out a series of observing campaigns in fields along the ecliptic plane, where pointing accuracy could be more easily controlled (Howell et al., 2014). The K2 mission successfully lasted for another five years. The most significant scientific objective for *Kepler* and K2 was the detection and characterization of terrestrial extrasolar planets by transit photometry. To accomplish this, approximately a half-million stars were monitored.

Apart from discovering new planets, a tremendous value-added benefit to these types of observations is the potential for stellar astrophysics. Almost continuous monitoring of starlight at high temporal cadence (1 or 30 min) and high precision (several tens of parts-per-million) has been a goldmine for the study of variable stars. In particular, a vast research effort has been focused on stars that are variable due to pulsations, which are present for stars across the H-R diagram, and revolutionizing the field of asteroseismology.

This review will focus on stars that pulsate in ways similar to our Sun, commonly known as "solar-like" oscillators. Such stars may not necessarily be "solar-type" main-sequence objects like the Sun; for example, red giants display solar-like oscillations. These oscillations are due to acoustic (pressure) standing waves. In most cases, they are excited to small, yet observable amplitudes, which are stochastically driven and damped by near-surface turbulent convection (Goldreich and Keeley, 1977). Classical pulsators, such as Cepheids, RR Lyrae, δ Scuti, γ Doradus, white dwarfs, etc., typically

have opacity-driven oscillations and will not be discussed here, nor will systems with oscillations driven by tidal forcings in multi-star configurations.

For any star to potentially exhibit solar-like oscillations, it must be cool enough to have an outer convection zone. Therefore, the effective (surface) temperature is important, and needs to be below about 7000 K, corresponding to an upper mass of approximately 1.5 $M_\odot$ on the main sequence, and to spectral types later than mid-F, to G and K dwarf stars. For evolved stars, this temperature limit is above much of the subgiant branch and red-giant (G, K, and M) stars, whose mass can be greater than 1.5 $M_\odot$.

Kepler and K2 observed thousands of stars with detectable solar-like oscillations, and the main question this review hopes to address, is what new stellar astrophysics have we learned from stars that pulsate like the Sun? To that end, exciting asteroseismic results in the *Kepler* era include progress on interior rotation, mixing processes, precise mass and radius measurements, ages and evolutionary state determinations, stellar populations, binarity, granulation, magnetic fields, and interior discontinuities of structure or composition. It is difficult to overemphasize the revolution that *Kepler* has had on the field of asteroseismology of solar-type stars, particularly in terms of the precision with which stellar parameters can now be computed. To keep the review focused on important results, topics such as new analysis and data-reduction techniques (of which many have been developed in the past decade of *Kepler* science), complementary ground-based observations, new theoretical modeling tools, etc., will not be covered. Other excellent reviews have a much broader focus (Chaplin and Miglio, 2013; Hekker, 2013; García and Ballot, 2019).

In **Section 2**, the properties and diagnostic potential of solar-like oscillations are briefly discussed, followed by **Section 3** on the most exciting asteroseismic results on different classes of stars. **Section 4** present conclusions and future prospects in the field.

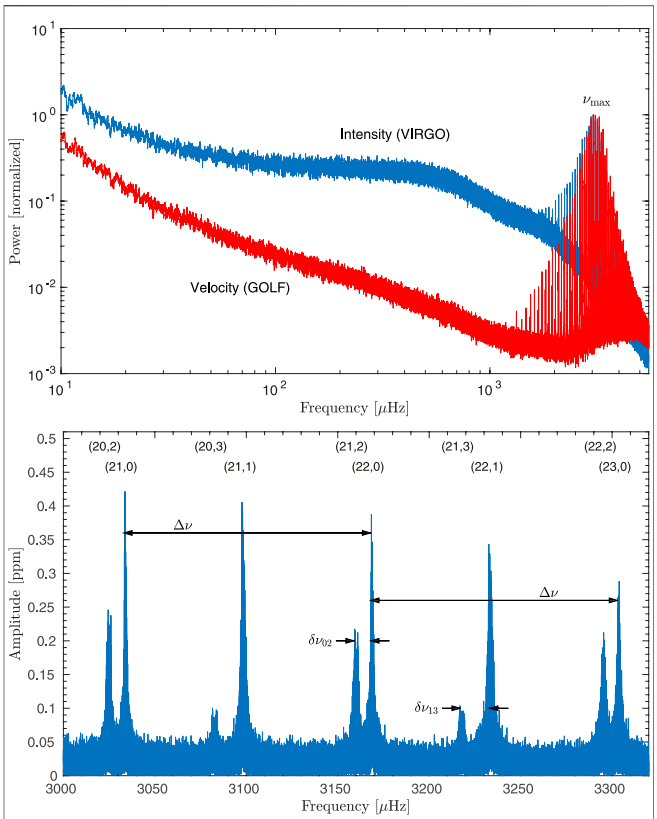

FIGURE 1 | *Top panel:* Solar power spectra computed from almost 20 years of data from the VIRGO and GOLF instruments on board the SOHO satellite. The VIRGO observations are from the green channel at 500 nm. The power spectra have been smoothed by a boxcar function of 0.17 μHz width, and are normalized such that the amplitudes are equal near the frequency of maximum amplitude of the acoustic modes $\nu_{max} \approx 3100\,\mu$Hz. *Bottom panel:* Amplitude spectrum computed from the VIRGO photometric data near ν_{max} (note the non-logarithmic scale). The peaks are labeled by their radial order n and angular degree ℓ as (n, ℓ). A few characteristic large and small frequency spacing examples are labeled with $\Delta\nu$ and $\delta\nu$, respectively.

2 SOLAR-LIKE OSCILLATIONS IN A NUTSHELL

First, we look at what observations of solar-type stars look like, using the best prototype - the Sun.

2.1 Observations of Solar-like Oscillators

Pulsations excited by near-surface turbulent convection can set up standing, global modes in a star. The pulsations distort the stellar surface with a spatial pattern that can usually be described by spherical harmonics. These distortions result in small luminosity fluctuations, as well as radial-velocity variations. For distant stars, only the large-scale spatial variations can be observed in integrated light due to cancellation effects, corresponding to only the lowest spherical harmonic degrees ($\ell = 0 - 3$). A very detailed discussion of all aspects of asteroseismology can be found in Aerts et al. (Aerts et al., 2010).

Synoptic observations of the Sun for seismic studies have been ongoing for decades from the ground using networks of dedicated telescopes, such as the Birmingham Solar Oscillation Network [BISON, (Chaplin et al., 1996)], and the Global Oscillations Network Group [GONG, (Harvey et al., 1996)]. From space, the ESA/NASA SOHO satellite, launched in 1995, had instrumentation to observe the Sun as a star both photometrically and spectroscopically, namely VIRGO (Fröhlich et al., 1995; Frohlich et al., 1997; Jiménez et al., 2002) and GOLF (Gabriel et al., 1995), respectively. Time series of luminosity or velocity fluctuations are best analyzed in the Fourier domain to search for various mode properties. The typical quantity is an amplitude or power spectrum. Power spectra of an approximately 20-years time series from VIRGO and GOLF data are shown in **Figure 1**. The figure shows a representative comb-like structure near 3000 μHz where the acoustic $p-$ mode envelope has the largest amplitude, whose frequency is known as ν_{max}. At low frequencies, there are contributions in the spectrum from rotational signals (spots and other activity) and convection (granulation and supergranulation). At high frequencies, one finds the contribution from photon noise. One of the important

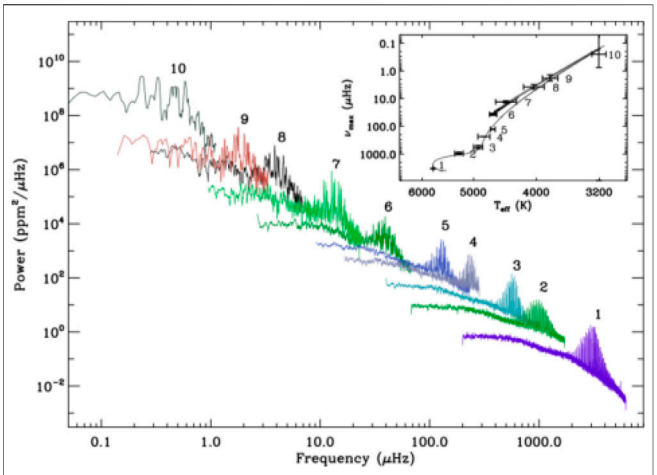

FIGURE 2 | Samples of power spectral density for *Kepler* solar-like oscillators at different evolutionary stages. The Sun's spectrum is labeled #1 (purple). The inset shows model tracks of a 1 $M_\odot$ star and the corresponding power spectra labels approximately related to each evolutionary state. Figure from Garcia and Stello (Garcia and Stello, 2018).

differences between photometric and Doppler velocity measurements is the signal-to-noize ratio (SNR), which is about an order of magnitude larger in velocity near $\nu_{\max}$. The photometric SNR is lower because background convection has a larger signal in temperature fluctuations than in the velocity fluctuations measured with spectroscopy [e.g., 8]. The higher SNR allows for better measurements of lower-frequency modes using velocity, as **Figure 1** demonstrates.

Noting that *Kepler* is a photometric instrument, the bottom panel of **Figure 1** shows an amplitude spectrum of the photometric VIRGO data near $\nu_{\max}$. The comb-like pattern is evidently the result of modes very evenly spaced in frequency, at least for large radial orders n. As is the case for distant stars, this type of solar observation is only sensitive to radial ($\ell = 0$) and the first few nonradial ($\ell = 1, 2, 3$) modes. The frequency difference between modes of consecutive radial order and the same spherical degree is known as the large frequency spacing $\Delta\nu$. The frequency difference between modes of consecutive radial order and degrees different by two is the small frequency spacing $\delta\nu$. Their diagnostic potential is described in the next section. It's worth pointing out the small amplitude of solar-like oscillations, particularly for main-sequence stars, which lies in the parts-per-million range. *Kepler*'s unprecedented sensitivity was necessary for similar quality observations of distant stars.

Kepler observed the photometric variations of many pulsating stars at cadences of 1 min or 30 min. Main-sequence solar-like stars show a $\nu_{\max}$ of a few thousand μHz, corresponding to periods of about 5 min. Therefore, a faster sampling such as 1 min is required. Evolved red-giant stars, on the other hand, who also show solar-like oscillations, have frequencies as low as $\sim 20\,\mu$ Hz, or periods of about half a day, so 30-min sampling is sufficient. Power spectra of several pulsating *Kepler* stars in different evolutionary states are shown in **Figure 2**. Each star is approximately one solar mass. Note the different amplitude and frequency range of the p-modes. While not completely evident from this figure, the *Kepler* data are of extremely high quality, and in some cases comparable to what exists for the Sun, which is shown as the rightmost spectrum.

2.2 Properties and Diagnostic Potential of the Oscillations

A detailed review of the physics of solar-like oscillations can be found in many places [e.g., 16]. Here, we only provide a quick overview and focus on the major properties discernable from stellar oscillations.

The sequence of spectra in **Figure 2** already provides hints of the utility of solar-like oscillations for probing stellar interiors. At a given mass, as stars evolve their intrinsic frequencies shift, resulting in a decreasing value of $\nu_{\max}$. As discussed below, this quantity is related most closely to a star's surface gravity. Since radii increase with time, this is the expected and observed behavior. So at zeroth order, for stars of similar masses and composition, $\nu_{\max}$ acts as a relative clock.

Zooming in on a solar-like spectrum, as in the lower panel of **Figure 1**, the dominant features are peaks that are arranged according to the large and small frequency spacings. The oscillation peaks are typically high-order (large n), radial and non-radial oscillations. In this case, asymptotic theory of stellar oscillations (Tassoul, 1980) shows that the expected frequencies of such modes are well described to second order by

$$\nu_{n\ell} \simeq \Delta\nu \left(n + \frac{\ell}{2} + \epsilon \right) - \ell\,(\ell+1) D_0, \tag{1}$$

where ε is a frequency-dependent offset term that is mostly dependent on near-surface effects (Christensen-Dalsgaard and Perez Hernandez, 1992; Kjeldsen et al., 2008; Mosser et al., 2013b), and D_0 is described below. The large-frequency separation $\Delta\nu$ is precisely the quantity depicted in **Figure 1**, and is related to the sound crossing time of an acoustic wave across the star

$$\Delta\nu = \nu_{n\ell} - \nu_{n-1\,\ell} = \left(2 \int_0^R \frac{\mathrm{d}r}{c} \right)^{-1}, \tag{2}$$

where c is the adiabatic sound speed. Since the sound speed scales as $c^2 \propto M\,R^{-1}$, **Eq. 2** implies that $\Delta\nu \propto \sqrt{M\,R^{-3}} \propto \sqrt{\overline{\rho}}$, or the root of the mean stellar density, a quantity that also decreases as stars evolve (at least up until the tip of the red-giant branch).

Given this physically-motivated relationship for the large frequency spacing, and an empirically-motivated one for the frequency at maximum amplitude [but see (Belkacem et al., 2011)], $\nu_{\max} \propto \nu_{\rm ac} \propto g T_{\rm eff}^{-1/2}$, where $\nu_{\rm ac}$ is the atmospheric acoustic cut-off frequency, one can identify the asteroseismic scaling relations (Brown et al., 1991; Kjeldsen and Bedding, 1995; Kallinger et al., 2010) as

$$\begin{aligned} \frac{M}{M_\odot} &= \left(\frac{\nu_{\max}}{\nu_{\max,\odot}} \right)^3 \left(\frac{\Delta\nu}{\Delta\nu_\odot} \right)^{-4} \left(\frac{T_{\rm eff}}{T_{\rm eff,\odot}} \right)^{3/2}, \\ \frac{R}{R_\odot} &= \left(\frac{\nu_{\max}}{\nu_{\max,\odot}} \right) \left(\frac{\Delta\nu}{\Delta\nu_\odot} \right)^{-2} \left(\frac{T_{\rm eff}}{T_{\rm eff,\odot}} \right)^{1/2}. \end{aligned} \tag{3}$$

These relations assume homology with the Sun and thus are scaled to solar reference values (⊙ symbols), and comprise the most common tool for obtaining stellar parameters from two rather straightforward asteroseismic measurements, as well as an estimate of the effective temperature, usually easily available. Note, however, in this form the lack of dependence on stellar composition, for example. Much recent effort has gone into calibrating these relations for a broad range of evolutionary states and other stellar properties [see 25, for an extensive review]. Even new data-driven scaling relations for stellar age on the main sequence and red-giant branch are now available (Bellinger, 2019; Bellinger, 2020).

The small frequency separation that appears as the other obvious feature in power spectra can be obtained from **Eq. 1**:

$$\delta\nu_{n\ell} = \nu_{n\ell} - \nu_{n-1\,\ell+2} = (4\ell + 6)D_0 \simeq -\frac{\Delta\nu}{4\pi^2\nu_{n\ell}}\int_0^R \frac{\mathrm{d}c}{\mathrm{d}r}\frac{\mathrm{d}r}{r}. \quad (4)$$

The small frequency separation is a useful quantity since its weighting by the sound-speed gradient makes it sensitive to the core and its composition. Thus, it can be used to measure stellar ages in some cases, notably on the main sequence, particularly when used in an asteroseismic "C-D" diagram (Christensen-Dalsgaard, 1988; White et al., 2011). All of the above is the theoretical framework in the asymptotic limit, which describes high-frequency modes of large radial orders. In some cases, particularly for evolved stars where the observed low-degree modes do not correspond to large radial orders, the asymptotic limit is not strictly satisfied. In such instances, however, the departure from this limit is small enough that higher-order corrections and empirical calibrations are commonly adopted to retain the accuracy of this formalism. A detailed discussion can be found in Mosser et al. (Mosser et al., 2013b).

Apart from the large and small separations and the location of the mode power envelope, higher-order effects are additionally seen. One such effect is due to gravity modes in a star, which are excited in convectively stable regions where buoyancy is the restoring force. For solar-like stars, these modes are not visible at the surface like pressure modes, as their propagation cavity is in the deep radiative interior. However, if their frequencies become commensurate to those of the *p*-modes, they can "mix" and interact with non-radial *p*-modes and impart new information in the *p*-mode frequency spectrum. This can be interpreted as a mode having the character of acoustic modes in the outer layers, and having the character of gravity modes in the deeper layers. Asymptotic theory applied to (gravity) *g*-modes predicts that they will be evenly spaced, not in frequency as for the *p*-modes, but in wave period. The period spacing is given by

$$\Delta\Pi = 2\pi^2\left(\int_{r_1}^{r_2} N\frac{\mathrm{d}r}{r}\right)^{-1}, \quad (5)$$

where N is the Brunt-Väisälä buoyancy frequency, and the integration is over the internal *g*-mode cavity. The buoyancy frequency is approximately related to the local gravitational acceleration, which increases in radiative cores as stars evolve, allowing for this mixing to occur. Gravity-mode period spacings can be measured in the spectrum of *p*-modes, providing a very powerful diagnostic of the core regions of evolved stars, as discussed in **Section 3.1**.

Another feature in power spectra is the splitting of mode frequencies into multiplets due to rotation. Such an effect has been exploited in the Sun to determine its latitudinal and radial differential rotation profile to a very high precision (Thompson et al., 1996). In stars, *p*-mode frequencies can be split by somewhat rapid rotation, but even more interesting, is that the mixed modes themselves can be split by core rotation. In the evolved stars where this situation most often arises, the effects due to rotation are smaller than those due to mode mixing since such stars are typically slow rotators. There are exceptions, however, which can make the interpretation of such effects challenging. The measurement of these frequency shifts, and their amplitudes, is further affected by the inclination of the rotation axis with respect to the observer (Gizon and Solanki, 2003).

Beyond all of the observables mentioned to this point, powerful inferences can be made by measuring the frequencies of many individual modes and then using numerical models to match the expected frequencies to the observed ones. If successful, and the modes can be correctly identified, the interior model then gives *all* relevant stellar properties and the evolutionary state. These studies can be computationally intensive when large grids in parameter space of stellar models are required. Furthermore, to make the most robust inferences and assess theoretical uncertainties, multiple evolutionary codes are often employed for the same problem, each one with various differences in the physical prescriptions and numerical solvers [e.g., (Silva Aguirre et al., 2017; Nsamba et al., 2018)]. Powerful statistical methods are also becoming common to constrain models from observations (Rendle et al., 2019). Some examples of these efforts are provided in the following sections.

Finally, it is known from theory that interior radial discontinuities or boundaries lead to sharp variations in the local sound speed (Gough, 1990) known as "glitches." The mode eigenfrequences then show an oscillatory behavior that departs from the regular pattern seen above, whose period is related to the depth location of the glitch. Possible sources of the glitch are the base of the stellar convection zone, where structure varies quickly, and the second helium ionization zone. These quantities are indirectly related to other interesting properties such as abundances of helium and metals. Only the best seismic data are amenable to these inferences, however.

3 WHAT HAVE WE LEARNED FROM *KEPLER*?

These are the main tools in the hands of the asteroseismologist to gain better understanding of stellar interiors, evolution, and populations. The *Kepler* mission has been able to exploit these asteroseismic tools more successfully than any other experiment so far for stellar astrophysics.

Since solar-like oscillations are only found in late-type stars, the discussion will be limited to stars on the main sequence (MS), subgiant (SG) branch, red-giant branch (RGB), the red clump

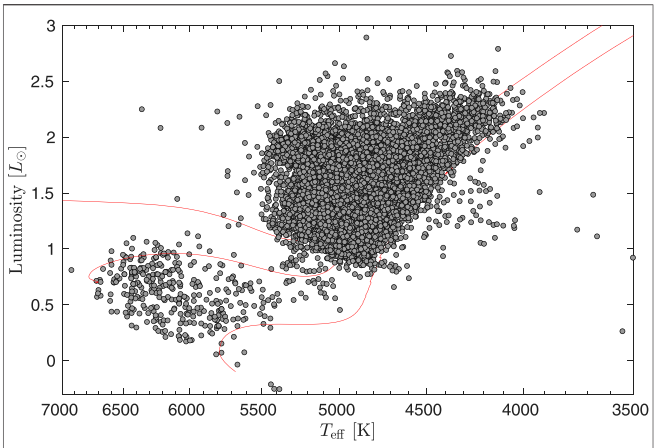

FIGURE 3 | H-R diagram showing a representative sample of *Kepler* stars with detected solar-like oscillations. These stars comprise the main sequence, subgiant branch, red-giant branch, and red clump. Also shown in red are nominal evolution tracks for 1, 1.5, and 2 $M_\odot$ stellar models. Parameters obtained from Serenelli et al. (Serenelli et al., 2017) and Yu et al. (Yu et al., 2018).

(RC), sometimes referred to as the cool horizontal branch, and the secondary red clump (RC2), the population of higher-mass clump stars that do not experience a helium flash on the RGB. A sample of about 16,500 oscillators are shown in **Figure 3**. These are the main phases of evolution that *Kepler* data has addressed. The results presented are by no means exhaustive or final, as new analysis techniques and modeling improvements will help exploit *Kepler* data well into the future. This should only be considered a taste of the success so far.

3.1 Mass, Radius, Age, and Evolutionary State

As already remarked, one of the most straightforward, yet powerful applications of asteroseismology is to use the scaling relations (**Eq. 3**) to estimate a star's mass and radius. This has led to the idea of ensemble asteroseismology.

Ensemble asteroseismology seeks to analyze a large, statistical sample of stars in one homogeneous fashion to obtain these general stellar parameters, and does not require these stars to be in clusters. One of the first attempts with *Kepler* main-sequence and subgiant stars was described in Chaplin et al. (Chaplin et al., 2011), where 500 stars that are mostly hotter and more massive than the Sun were observed to have detectable solar-like oscillations from only one month of short-cadence *Kepler* data. With reasonably good estimates of mass and radius available from the scaling relations for the first time for a large sample, it was possible to compare this cohort to predictions of galactic population synthesis models. The *Kepler* sample was distributed more broadly in mass, as well as peaked at a lower mass, than predictions from models (Chaplin et al., 2011). Even at this early stage of *Kepler* analysis, implications for models regarding the initial mass function, star-formation rate, and interior mixing processes were brought into the spotlight from the precise seismic inferences.

A subset of 87 of these stars that had spectroscopic temperatures and metallicities were studied in Chaplin et al. (Chaplin et al., 2014) in a grid-based modeling approach. This comprises computing a large number of numerical stellar models from a dense grid of initial parameters (mass, composition, etc.,). The global seismic and spectroscopic parameters of each star are then matched to a model to yield, among other things, a stellar age. The models including the spectroscopic constraints resulted in surprising precision, at the levels of ~ 5.4 % in mass, ~ 2.2 % in radius, ~ 0.01 dex in $\log(g)$, ~ 2.8 % in density, and ~ 25 % in age. Over the subsequent lifetime of *Kepler*, and using some of the best-observed main-sequence stars (Bellinger, 2019; Bellinger et al., 2019), the mean precision is approximately 11%, 3.5%, and 1.5% on stellar ages, masses, and radii, respectively. The level

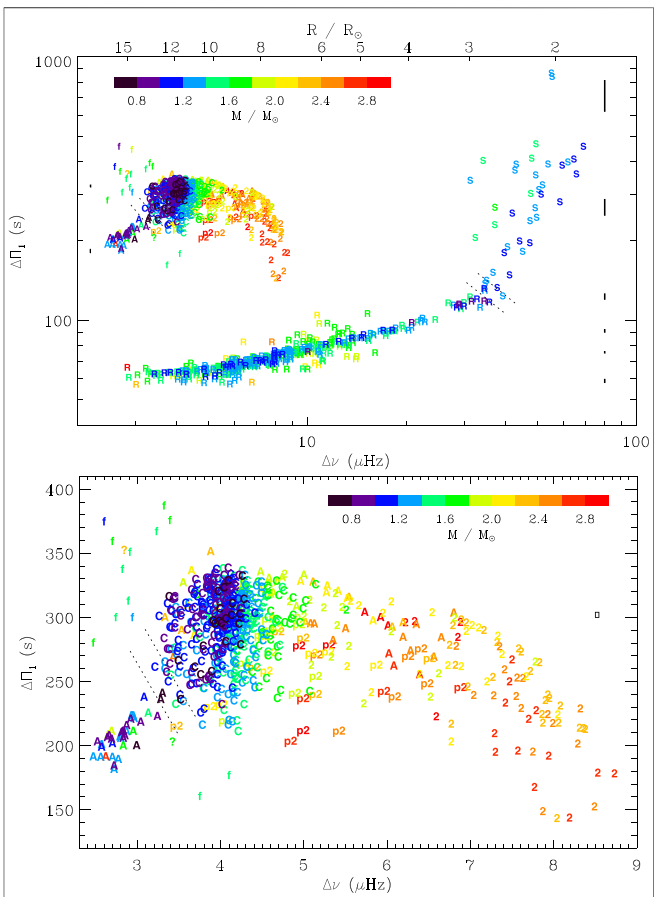

FIGURE 4 | Mixed-mode period spacing ($\Delta\Pi$) vs. the large frequency spacing ($\Delta\nu$) for a large sample of *Kepler* solar-like pulsators. Top: the seismic proxy for the stellar mass is indicated by the color code. The evolutionary states are indicated by *S* (subgiants), *R* (RGB), *f* (helium subflash stage), *C* (red clump), p2 (pre-secondary clump), 2 (secondary clump), and A (stars leaving the red clump moving toward the AGB). The error boxes on the right side indicate the mean uncertainties, as a function of, for stars on the RGB; for clump stars, uncertainties are indicated on the left side. Dotted lines indicate the boundaries between evolutionary stages. Bottom: zoom in the red-clump region. From Mosser et al. (Mosser et al., 2014).

of precision on age is about at the level of isochrone fitting in clusters.

All of these studies used global seismic parameters, such as frequency spacings or frequency differences and ratios. To do better, a powerful inference tool is to accurately measure and model *individual* eigenfrequencies, in addition to any other global seismic properties and any spectroscopic and photometric constraints. Metcalfe et al. (Metcalfe et al., 2014) did just that with 42 stars collected from earlier asteroseismic measurements by Appourchaux et al. (Appourchaux et al., 2012). A stellar model pipeline was used with a large amount of automatization, yielding median uncertainties of 7.9 % on the age, 2.8 % on the mass, and 1.2 % on the radius–improving on the other approach, but more computationally expensive.

Solar-like oscillations have been found at later evolution stages of cool stars in much greater numbers, since long-cadence *Kepler* data, the primary mode of operation, are sufficient for sampling the longer periods. It had been thought that non-radial modes would be strongly damped in red-giant stars (Dziembowski et al., 2001; Christensen-Dalsgaard, 2004), however De Ridder et al. (De Ridder et al., 2009) convincingly reported the first detected non-radial oscillations in several hundred giants. Over a decade later, the sample has now grown to a few tens of thousands (Yu et al., 2018).

Red giants have a "universal pattern" of modes in the frequency spectrum (Mosser et al., 2011), allowing for fast and reliable measurements of the large frequency spacing and $\nu_{\max}$, and therefore, mass and radius measurements. Perhaps the most exciting discovery in this area from *Kepler* is signatures of gravity-modes (Beck et al., 2011) and their associated period spacings that almost unambiguously reveal if red-giant stars are burning hydrogen in a shell around the core only (on the RGB) or have transitioned onto the RC by igniting helium burning in the core (Bedding et al., 2011; Mosser et al., 2012b).

An example of classification of the evolutionary state of hundreds of stars is shown in **Figure 4**, where the period spacings of mixed modes ($\Delta\Pi$) is plotted against the large frequency separation. The stars above $\sim 40\,\mu$Hz are subgiants, while main-sequence stars are beyond that and do not show mixed modes. As stars evolve onto and up the giant branch, the large frequency separation continues to decrease along with the period spacing of mixed modes. Once He is ignited, the period spacing increases to over 200 s. This happens because along the RGB the inert He core increases in density due to the overlying H-burning shell dropping its ashes onto it, which results in smaller period spacings (increasing N in **Eq. 5**). Once helium is ignited, the core becomes convective and expands, density decreases locally, N does too, and the period spacing increases. Stars on the red clump are therefore of larger period spacings. Massive stars around 2 $M_{\odot}$ ignite He without a flash, and occupy a slightly different region in the diagram as the lower panel highlights, offering a way to distinguish these two regions of the cool horizontal branch.

These measurements are now ubiquitous tools for determining evolutionary states. Thousands of evolved stars can be analyzed using consistent pipeline methods (Stello et al., 2013; Yu et al., 2018). For giants, the scaling relations yield typical median uncertainties of approximately $7-10$ % in mass, $2-4$ % in radius, and about 0.01 dex in seismic $\log(g)$. A thorough review of asteroseismology of evolved giant stars is given in Hekker and Christensen-Dalsgaard (Hekker and Christensen-Dalsgaard, 2017) and Basu and Hekker (Basu and Hekker, 2020).

Given the large size of the *Kepler* data set, a rapid area of growth in asteroseismic analysis is data-driven methods with machine learning. For example, intelligent regression algorithms can reveal subtle relationships among model quantities of stars to connect them to traditional observables very quickly (Bellinger et al., 2016). The results are similar to the grid-based approach, but with significant computational efficiency. Neural networks are being applied to well-studied power spectra of solar-like oscillators to predict stellar properties and evolutionary states of stars with less distinct spectra (Hon et al., 2017; Hon et al., 2018; Hon et al., 2020), or even from the fundamental light curves themselves (Blancato et al., 2020). The coming decade will likely see such approaches applied more frequently as the amount of available data continues to increase and the community pushes forward with open-source software initiatives (Tollerud, 2020).

As a final note, while the precision of the scalings for mass and radius estimates for large numbers of stars is greater than any other methods, what about the accuracy? While it is difficult to find "ground truth" values of these quantities to compare to, there are a few avenues beyond using models (Huber et al., 2011). One direction is with eclipsing-binary star systems. Binaries with (at least) one oscillating component and photometrically measured eclipses are extremely useful for stellar astrophysics, since stellar parameters, such as mass, can be measured in two independent ways once radial-velocity measurements are obtained. The first such system detected by *Kepler* was a red-giant oscillator in orbit with a main-sequence F star (Hekker et al., 2010). Since then, a catalog of a dozen or so oscillating red giants have been found in eclipsing binaries with mass and radius derived seismically and dynamically (Frandsen et al., 2013; Gaulme et al., 2013; Gaulme et al., 2016; Benbakoura et al., 2017). While different studies use various small corrections to the scaling relations, in general the masses and radii of the giants are systematically overestimated compared to the dynamical solutions, by about 10 % and 5 %, respectively. On the other hand, a few other analyses using more detailed corrections to the scaling relations and different reference values, find much better agreement (Brogaard et al., 2018; Kallinger et al., 2018; Themeßl et al., 2018).

Another absolute measurement of stellar radii comes from interferometric observations of bright targets. Huber et al. (Huber et al., 2012) used the CHARA array to measure angular radii of 10 solar-like pulsators. They found agreement between seismic and interferometric radii, with an accuracy better than about 4% for main-sequence stars and no obvious systematic offset. Similarly, a comparison of radii estimated from Gaia parallax measurements with seismic radii was carried out in Huber et al. (Huber et al., 2017). Overall, for a wide range of stars of 0.8–8 R⊙, seismology and Gaia agree to within 5%. On the subgiant branch only (1.5–3 R⊙), the seismic radii are *underestimated* by about 5%. Zinn et al. (Zinn et al., 2019) found better radii agreement with Gaia for a few thousand stars, mostly on the giant branch.

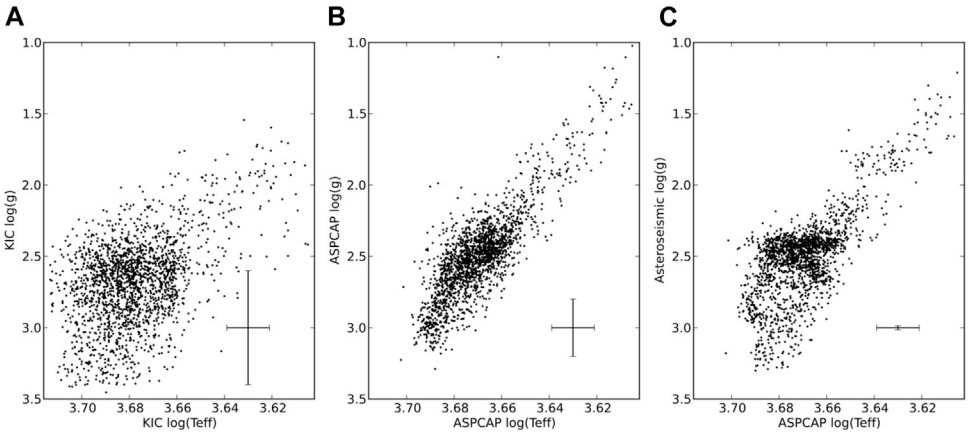

FIGURE 5 | Evolved APOKASC catalog stars plotted from different sources. The left panel are parameters from the photometric *Kepler* Input Catalog. The middle panel uses APOGEE's pipeline-derived spectroscopic values. The right panel uses the more precise asteroseismic surface gravity. The red clump is significantly enhanced, as is the RGB bump. Median uncertainties are given by the crosses in the lower part of each panel. From Pinsonneault et al. (Pinsonneault et al., 2014).

On the other hand, for almost 100 dwarf pulsators, Sahlholdt and Silva Aguirre (Sahlholdt & Silva Aguirre, 2018) found seismic radii overestimated by about 5% compared to Gaia using the basic scaling relations. These studies give a good overall picture of the level of departure from the simple scalings, which is surprisingly low given all the potential sources of uncertainty: $T_{\rm eff}$, metallicity, reddening, parallax, and the homology assumption itself. Clearly, while some improvements are needed, the scaling relations are powerful and rather simple tools. A review of how the scaling relations have been "tuned" to provide more consistent results is found in Hekker (Hekker, 2020).

3.2 Galactic Archaeology

Galactic Archaeology is a term used to describe efforts to trace the structure and past chemical and physical evolution of the Milky Way by interpreting its current stellar populations. Key stellar parameters are age, evolutionary state, composition, kinematics, and distance. During *Kepler*'s early operations, the Apache Point Observatory Galactic Evolution Experiment (APOGEE) came online as part of the Sloan Digital Sky Survey (SDSS-III and IV) (Majewski et al., 2010). The APOGEE instrument is an IR (H-band) multi-fiber spectrograph, optimized to survey tens of thousands of red giants across the galaxy for "archaeological" purposes.

Traditional stellar population studies have used photometric and/or limited spectroscopic observations (Zhao et al., 2006; Gilmore et al., 2012), which can provide some of the required parameters, but with large uncertainties on masses and age. *Kepler* seismology adds new and more precise observables to the mix, particularly masses and evolutionary state, and is particularly powerful when considering red-giant stars, which are bright, ubiquitous, and almost always pulsating. However, on the red-giant branch, a precise mass alone is not sufficient to determine an age without composition information (Salaris et al., 2015; Martig et al., 2016; Ness et al., 2016). APOGEE provides effective temperature, surface gravity, metallicity, and a dozen individual abundances to high precision (García Pérez et al., 2016). Recognizing the tremendous synergy between APOGEE and *Kepler*, the APOGEE *Kepler* Asteroseismic Consortium (APOKASC) was spearheaded to coordinate APOGEE observations of the *Kepler* fields. Complementary large asteroseismic and spectroscopic surveys can yield precious new information on galactic stellar populations (clusters *and* field stars), stellar atmospheres, and stellar interiors.

The main product of the APOKASC effort has been a catalog containing a number of internally calibrated stellar parameters, including mass, radius, evolutionary state, surface gravity, and age, for almost 7,000 giants and about 500 main-sequence and subgiants stars (Pinsonneault et al., 2014; Serenelli et al., 2017; Pinsonneault et al., 2018). An example of how seismology and spectroscopy can work in tandem is shown in **Figure 5**. The H-R diagram of giants on the left is from purely photometric observables from the *Kepler* Input Catalog (KIC). Since surface gravity is a much more natural spectroscopic observable, the middle panel shows the APOGEE observations of the same stars, which presents a tighter red-giant branch as well as a red clump. Surface gravity is an even more precise asteroseismic observable, and is substituted in for the right panel, which now shows a secondary red clump of more massive giants, and evidence of the RGB bump. Remarkably, it is important to note that these stars are not in a cluster.

The APOKASC catalog has been the foundation for a number of important studies, and likely will be well into the future. One interesting example is in Silva Aguirre et al. (Silva Aguirre et al., 2018), who use a subset of the APOKASC catalog, combining precise ages and chemical information to dissect the Milky Way disk. It has been known from spectroscopic surveys and isochrone fitting that the disk contains stars with enhanced α abundances and low metallicity that are old, and young ones with lower-α abundances and high metallicity. But Silva Aguirre et al. (Silva Aguirre et al., 2018) find many older stars in the disk with low-α and high metallicity, not observed before, and which are more consistent with chemical evolution models. Without the

level of precision of asteroseismic ages for large numbers of stars, this result would not have been possible.

Solar-like oscillators are improving our picture of the galaxy. Distances are also a key observable, and one can compute precise radii for far-away red giants to get distances to place stars throughout the Milky Way (Miglio et al., 2013) in 3D. Period-luminosity relations for pulsating M giants have been studied, which could be a new way to give access to distances to other galaxies (Mosser et al., 2013a; Stello et al., 2014). Seismology has even been of use to the Gaia mission to help correct parallax biases and offsets (Davies et al., 2017).

Other notable photometric and spectroscopic surveys that target the *Kepler* fields to exploit solar-like pulsators and study the structure of the Milky Way are the Strömgren Survey for Asteroseismology and Galactic Archaeology [SAGA, (Casagrande et al., 2014; Casagrande et al., 2016)], the Large Sky Area Multi-Object Fiber Spectroscopic Telescope [LAMOST, (Ren et al., 2016; Wang et al., 2016)], and the Galactic Archaeology with HERMES [GALAH, (De Silva et al., 2015; Martell et al., 2020)] survey, as well as some fortuitous projects such as the Asteroid Terrestrial-impact Last Alert System (ATLAS) and the All-Sky Automated Survey for Supernovae [ASAS-SN, (Auge et al., 2020)].

3.3 Stellar Clusters

A similar focus is the application of asteroseismology to clusters, which are critical astrophysical objects. The *Kepler* field contained four open clusters bright enough to be well observed, while K2 observed almost 20 globular and open clusters. Trusting the simple assumptions that one can ignore variations in cluster members' age, (initial) composition, and distance, potentially stringent constraints can be placed on cluster properties. This, in turn, allows for improvements in theoretical modeling regarding isochrones, as well as for interpreting disparate observational data sets.

NGC 6791 and NGC 6819 are two well-studied open clusters observed by *Kepler*. Basu et al. (Basu et al., 2011) used solar-like pulsators to estimate masses, seismic distances, and ages of the clusters' members. Adding in a third *Kepler* cluster, NGC 6811, Stello et al. (Stello et al., 2011) used seismology to assess membership. Consider the seismic scaling relations when $T_{\rm eff}$ and L are substituted in for the radius. This allows the global seismic parameters to then be expressed as the dependent variables in the form $\Delta\nu(M, T_{\rm eff}, L)$ and $\nu_{\rm max}(M, T_{\rm eff}, L)$. On the red-giant branch of a cluster, L is expected to vary more strongly than either M or $T_{\rm eff}$. In other words, two stars of similar luminosity should have similar values of $\Delta\nu$ and $\nu_{\rm max}$. If they don't, it likely means the star is a foreground or background object. In a cluster with minimal distance variations, therefore, one should expect a strong correlation between either $\Delta\nu$ or $\nu_{\rm max}$ and a good proxy for the luminosity–the apparent magnitude–a quantity readily available. Indeed, this is what was found, and the membership of the clusters was improved by the simple removal of outliers to this tight relationship.

Seismology also gives a way to constrain mass loss on the RGB, a historically difficult quantity to predict theoretically, as well to observe quantitatively. Imagine a cluster with a populated RGB and RC. If one could measure the average mass of giants in the RC, and compare to the average mass of giants on the RGB at or below the luminosity of the RC, then any difference could potentially be explained by mass loss as stars climbed the RGB above that luminosity level before arriving on the clump. This is the clever strategy employed by Miglio et al. (Miglio et al., 2012) for NGC 6791 and NGC 6819. As an older high-metallicity cluster, NGC 6791 is a strong candidate to exhibit strong mass loss on the RGB. However, using several dozen stars, the authors find that the difference in average mass between the clump and branch stars is $\Delta M = 0.09 \pm 0.03$ (random) ± 0.04 (systematic), which is statistically significant, but not extreme, as other works had suggested. NGC 6819, on the other hand, did not show evidence of mass loss, which was subsequently reconfirmed (Handberg et al., 2017).

The effects of compositional variations among stars on seismic observables is not precisely known, and clusters offer great laboratories. Using shell-burning giants, McKeever et al. (McKeever et al., 2019) modeled individual p-mode frequencies to determine that NGC 6791 is rich in helium, which consequently helps constrain the age to within 300 million years. The old globular cluster M4 allows for metal-poor asteroseismology to be attempted, and (Miglio et al., 2016) found preliminary evidence that the scaling relations still give reasonable masses in this regime. The future is bright for cluster seismology as new oscillators are being discovered. Lund et al. (Lund et al., 2016) found main-sequence pulsators for the first time in an open cluster–the young Hyades cluster. Pulsating giants have also been observed in the solar metallicity cluster M67 (Stello et al., 2016).

3.4 Precision Stellar Interior Physics

Kepler pulsators with the highest-quality light curves allow for very precise experiments, particularly bright targets with long-baseline observations and/or short-cadence data. These are excellent candidates for constraining physics that are not standardized across stellar models, such as mixing length properties, convective overshooting, and microscopic diffusion of helium and metals. Many of the best candidates have also been targeted for ground-based follow up.

Perhaps the best studied and modeled stars (apart from the Sun) so far have been those in the solar analog binary system, 16 Cyg A and B (Metcalfe et al., 2012; Metcalfe et al., 2003), whose age of ~ 7 Gyr is now precise to less than 6% (Bazot, 2020). Over 50 global modes have been observed and identified in each star at sub-microhertz precision. Using the oscillatory "glitch" signature of the eigenfrequencies (**Section 2.2**), Verma et al. (Verma et al., 2014) measured the current He abundance in the outer envelope of both stars, which of course is less than the BBN value due to gravitational settling.

A sample of 66 main-sequence pulsating stars has been collated and called the *Kepler* seismic LEGACY project [(Lund et al., 2017; Silva Aguirre et al., 2017), which includes (Christensen-Dalsgaard, 2004) Cyg A and B]. Their global properties have been well characterized, as has the locations of the He II ionization zones (Verma et al., 2017). The signature of the bottom of the convective zones is less constrained, however. A few dozen LEGACY stars have surface helium abundance

measurements (Verma et al., 2019), again showing that atomic diffusion does occur in solar-type stars.

Main-sequence stars slightly more massive than the Sun have convective cores rather than radiative ones. Silva Aguirre et al. (Silva Aguirre et al., 2013) found strong evidence in a main-sequence pulsator, very near the transition mass value, for convective core overshooting. Such processes mix extra material in the fusion region and asteroseismic constraints helped select the best models. Montalbán et al. (Montalbán et al., 2013) found evidence of extra mixing from core convective overshooting for red clump stars, while Deheuvels et al. (Deheuvels et al., 2016) were able to do the same for eight main-sequence stars. These studies crucially show that models without an extended core from overshooting cannot match the seismic data, and that new model calibrations of this effect for low-mass stars are now available, which will lead to improvements in modeling other stellar properties.

The mixing-length parameter in the outer convection zone of stars is also an important model ingredient, and most studies have used the calibrated solar value, regardless of the type of star. Bonaca et al. (Bonaca et al., 2012), using *Kepler* seismic constraints, calibrated this parameters for a range of stars and found that its value is generally lower than solar, with a clear metallicity dependence. Similar findings for a larger number of main-sequence stars (Creevey et al., 2017), and APOKASC stars along the red-giant branch were measured by Tayar et al. (Tayar et al., 2017), where the mixing length parameter takes on super-solar values. That work emphasized that this effect needs to be taken into account if Gaia is indeed to be used to give isochrone ages for giants. Confirmation of the need for larger model values of this parameter from a sample of red giants in eclipsing binaries is discussed in Li et al. (Li et al., 2018). Until we develop a more complete theoretical understanding of near-surface convection in the context of 1D models, or until fully 3D models are routinely employed, these mixing-length calibrations need to be taken into account.

As mentioned in **Section 3.1**, binary systems where one or both stars are oscillating have been crucial for independent assessment of the accuracy of the scaling relations. A host of other experiments can be carried out with such valuable objects to learn very detailed evolutionary physics. One obvious example is testing tidal interaction theories [e.g., (Remus et al., 2012)]. Beck et al. (Beck et al., 2018a) used a sample of binaries with at least one red-giant star to show that the equilibrium tide is sufficient to explain the distribution of the measured orbital eccentricities and periods. As another important example, a prediction of stellar evolution theory is that stars climbing the red-giant branch will "dredge-up" nuclear-processed material as the surface convection zone deepens, potentially altering the surface composition. Beck et al. (2018b) studied a double-lined spectroscopic binary system of two oscillating giants observed by *Kepler*. The mass ratio of the stars was found to be about 1%. This relatively small difference, however, translated into a drastic disparity in surface lithium abundance between the stars, indicating that each star was in a different stage of the dredge-up event. Since the interior rotation was also estimated from the oscillation frequencies, these observations place tight contraints on interior mixing processes in this dynamic evolutionary phase.

3.5 Rotation

As mentioned earlier, rotation shifts the stellar eigenfrequencies, which can be used to estimate surface and interior rotation depending on which modes are available. A consistency check is sometimes available if photometic modulations due to surface magnetic activity, presumably with the same average periodicity as the rotation, can be measured and compared to the value obtained from asteroseismology. The bright stars 16 Cyg A and B again have shown to be good candidates in this regard. From seismology, their inclination angles and surface rotation rates were measured using evidence that the internal differential rotation is weak (weaker than the Sun's), due to their evolved state (Davies et al., 2015).

Differential rotation across latitudes is another important quantity of solar-like stars, as it can provide information about stellar activity cycles. Selecting promising targets from the *Kepler* LEGACY sample, Benomar et al. (Benomar et al., 2018) found strong evidence for latitudinal differential rotation in 13 stars. Motivated by this, Bazot et al. (Bazot et al., 2019) did a detailed analysis of 16 Cyg A and B, including inversions of the frequencies, and found solar-like latitudinal differential profiles, i.e., the equators rotate more rapidly than the polar regions.

Interior rotation is a powerful measure of how angular momentum evolves in a star (Pinsonneault et al., 1990). After the main sequence to the tip of the red-giant branch, in principle the stellar core is shrinking and should spin up, decoupling from the envelope. Some of the first evidence from *Kepler* of radial differential rotation in red-giants stars was shown in Beck et al. (2012), where the core rotation in a few stars was found to be about 10 times faster than the surface value by exploiting rotationally-split mixed modes. This was achieved because some of the mixed modes have more *g*-mode character and confined to the core, and some have more *p*-mode character confined to the outer envelope. The faster core rotation was then deduced by comparing the relative frequency shifts of such modes.

As a confirmation of this result, some of the first formal seismic inversions were carried out on frequency shifts from a low luminosity red-giant star to show a rapidly rotation core (Deheuvels et al., 2012). These results are in tension with models of angular momentum transfer (Ceillier et al., 2012), which predict cores should be rotating even *more rapidly* than what was found, suggesting that there may be mechanisms that transport angular momentum away from the deep interior that current models do not taking into account. Nonetheless, from large samples of evolved stars, it is generally found that core rotation decreases up the RGB Gehan et al. (Gehan et al., 2018), and continues to slow down on the red clump (Mosser et al., 2012a; Deheuvels et al., 2015).

On the subgiant branch, Deheuvels et al. (Deheuvels et al., 2014) and Eggenberger et al. (Eggenberger et al., 2019) measure rather slow core rotation. When they employed standard stellar models with rotation calibrated to match the measured surface

values, the models' core region still spins an order of magntidue faster. By introducing an artificial viscosity to the models, they were able to better reproduce the core rotation found in the seismic measurements. They also found that the efficiency of the unknown transport process actually decreases along the subgiant branch, but must then increase again on the giant branch to explain the observations there. Finally, for main-sequence solar-like stars, even those 50% more massive than the Sun, minimal internal differential rotation was measured (Benomar et al., 2015), again suggesting some efficient angular momentum transport process.

All in all, angular momentum transport on the main sequence, subgiant phase, and red-giant branch is complicated and a very active area of research. Suggested mechanisms for transferring angular momentum across the stars are mixed modes and internal gravity waves [(Belkacem et al., 2015), particularly for more evolved giants], meridional circulation, dynamos, and, most convincingly, magnetic instabilities (Fuller et al., 2019).

In terms of global rotation, solar-type, main-sequence F, G, and K stars with outer convection zones are born with relatively rapid rotation, but then should spin down as they evolve due to angular momentum loss from stellar winds entrained in magnetic fields. This torquing effect is called magnetic braking. Since ages of field stars are difficult to obtain, the rotation-age-mass relation is potentially a powerful inference tool, known as gyrochronology (Barnes, 2003). Indeed, before *Kepler*, the Sun was the oldest star that had a reliable age. The goal of gyrochronology in general is to provide a means of predicting the age of a star given observations of its color (or proxies like mass, or temperature) and rotation period. Empirical relationships have been calibrated successfully, but only constrained by the Sun and young clusters where ages are obtainable.

In the *Kepler* era, such theories can be extended outside of clusters, since age can be measured in a reasonably accurate way from seismology, and stellar rotation can be measured from seismology, or the modulation from spots of the light curves themselves, or from spectroscopy. Indeed, tight rotation-age relationships were found in early *Kepler* analysis (do Nascimento et al., 2014; García et al., 2014). In addition, Ceillier et al. (Ceillier et al., 2016) studied 11 planet-hosting stars with asteroseismic ages and photometric rotation periods, compared to a sample without planets, and found similar age-rotation-mass relationships.

However, using a larger sample of a few hundred field stars with asteroseismic ages, Angus et al. (Angus et al., 2015) found that many of the older stars did not obey the relation, in the sense that the older stars were rotating faster than expected. Since gyrochronology is intimately tied to magnetic fields generated through a dynamo mechanism in solar-type stars, the mismatch with current theory explored in Angus et al. (Angus et al., 2015) suggests a new complication. van Saders et al. (van Saders et al., 2016) studied a subset of 21 *Kepler* stars with high-precision asteroseismic measurements that are near or beyond the age of the Sun and found shorter rotation periods than gyrochronology predicts. The authors speculate that angular momentum loss from magnetic breaking depends sensitively on the global magnetic field configuration, suggesting a possible change in the dynamo mechanism as stars evolve. One common way of describing this from a modeling point of view is through the Rossby number, which describes the ratio of the rotational period to the convective turnover time. Efficient dynamo regimes are characterized by small Rossby number, typically below unity. By including a new prescription in models that has a Rossby number threshold, van Saders et al. (van Saders et al., 2016) were able to show that angular momentum loss stops abruptly in stars when their rotation slows down and Rossby numbers reach a value of about 2. The magnetic activity and rotation essentially decouple at some age, roughly corresponding to the middle age on the main sequence.

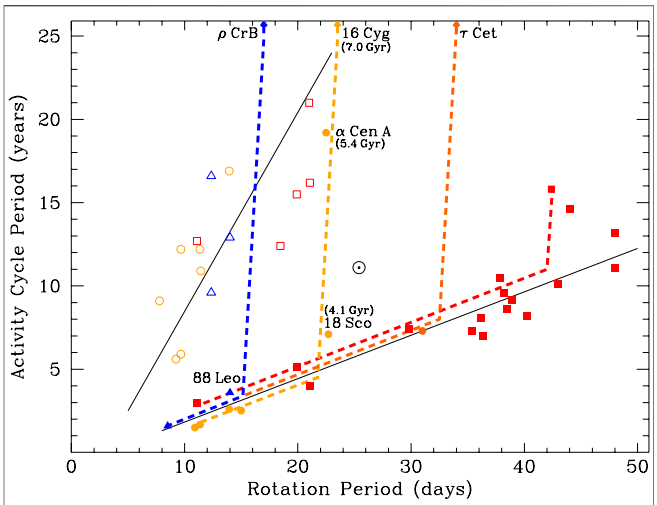

FIGURE 6 | Stellar activity cycle length vs. rotation period for stars with measured cycles. The solid lines denote two different sequences that had been studied before *Kepler*, with the Sun (⊙) being a perplexing outlier (or midlier). Symbols are colored by spectral type, *F* (blue triangles), early *G* (yellow circles), late *G* (orange circles), and *K* (red squares). The dashed lines are schematic evolutionary tracks, which advance in time to the right and upwards. Some well known stars are labeled. Adapted from Metcalfe et al. (Metcalfe et al., 2019).

This was validated in Metcalfe et al. (Metcalfe et al., 2016) by comparing stellar activity cycles with rotation periods. An illustration is given in **Figure 6** (Metcalfe & van Saders, 2017; Metcalfe et al., 2019), showing the empirical relationship between stellar magnetic activity cycles and rotation periods. The lower, flatter solid line represents a sequence whereby stars' rotation slows down and cycles lengthen, and had been thought to continue on throughout a star's lifetime. The new picture is that when the critical Rossby number ~ 2 is approached, the star's rotation does not decrease rapidly anymore, due to an altered magnetic field configuration and less braking. The star stays at the same rotation period and moves upward on the plot. The changing global magnetic field is weakening, thus causing a lengthening of the stellar cycle. The slowest rotators with measured cycles are K-type stars, since magnetic braking stops in more massive stars before they reach such slow rotation rates. Most K stars have not had time to reach this transition yet.

A star like the Sun, therefore, may be in a transition phase that occurs in all middle-aged stars whereby the rotation and

magnetic-field topology are changing (likely becoming smaller scale), the solar cycle is lengthening, and will some day disappear altogether. Therefore, after their middle-age on the main sequence, stellar ages cannot reliably be predicted from their rotation. Without precise asteroseismic ages from *Kepler*, this discovery would not have been possible.

3.6 Magnetic Fields

Magnetic fields in other stars are very difficult to measure unless the stars are bright and the fields are strong enough to allow Zeeman observations. Perhaps the easiest seismological measurement of magnetism is based on lessons from the Sun, which have shown that the solar cycle and the variable surface magnetic fields affect the *p*-mode eigenfrequencies. Two potential effects are observable: the amplitude of modes can be suppressed, and the frequencies can be shifted (Howe et al., 2002). The Sun has provided an excellent test star for these behaviors, showing us that as the magnetic cycle progresses, frequencies become larger, and mode amplitudes decrease due to the absorption of acoustic energy. Importantly, the frequency shifts are smooth functions of frequency only, as larger frequencies show larger shifts (Basu, 2016). This suggests that the structural changes induced by the activity cycle are mostly confined to the near-surface region where the modes are excited.

It was noticed early on that some *Kepler* solar-like oscillators had heavily damped modes, likely due to some kind of magnetic activity (Chaplin et al., 2011; Campante et al., 2014; García et al., 2014; Gaulme et al., 2014). Frequency shifts with time have also been measured [e.g. (Kiefer et al., 2017)], suggesting magnetic variability. Using the entire 4-years *Kepler* data, however, is necessary to have any hope to detect periodicities resulting from a possible stellar cycle. With an 87-star sample, Santos et al. (Santos et al., 2018) find that 60 to 70 percent show indications of magnetic activity over time from frequency shifts, mode heights, and even a varying stellar granulation timescale. Salabert et al. (Salabert et al., 2018), using a similar sample of main-sequence solar-like oscillators, find cycle-related frequency shifts that are not smooth like Sun. They conclude that there may be other sources of frequency perturbations associated with magnetic variability that are not present in the Sun. Using oscillations to estimate differential rotation, Bazot et al. (Bazot et al., 2018) find the first evidence for a butterfly-type diagram in a distant star.

These are all likely near-surface manifestations of the magnetic fields. Evidence of potential core magnetic fields of evolved stars became possible with the connection of suppressed dipole ($\ell = 1$) modes to a leaking of mode energy in the core due to interaction of the internal gravity waves with magnetic fields (Fuller et al., 2015; Stello et al., 2016). This became known as the magnetic "greenhouse effect." The predicted core fields are on the order of a million gauss and above. One may wonder how a star with a radiative core could harbor such strong fields. The key observation is that the suppression only occurs for giants with a mass above about 1.2 $M_{\odot}$ (measured with seismology). This is the approximate lower limit for stars that have convective cores on the main sequence, suggesting that a dynamo mechanism generated the fields at that time and which survive into the giant phase. However, if the observed suppressed modes are mixed dipole modes rather than pure acoustic modes, this theoretical interpretation will need to be modified, as discussed in Mosser et al. (Mosser et al., 2017).

3.7 Exoplanet Host Stars

Knowing the planet requires knowing the star, as is often pointed out. If a planet host is oscillating and seismic observables can be determined, planetary properties with unmatched precision can be obtained. Asteroseismic and exoplanetary research communities have a natural synergy (Campante et al., 2018; Lundkvist et al., 2018). For example, transit observations give estimates of the ratio of the planetary and stellar radius, but there are degeneracies that are often difficult to disentangle due to other orbital parameters. However, under common conditions, the ratio of the orbital semi-major axis to the stellar radius ($a/R_{\star}$) can be shown to be (Seager & Mallén-Ornelas, 2003; Huber, 2018)

$$\rho_{\star} = \frac{3\pi}{GP^2}\left(\frac{a}{R_{\star}}\right)^3, \tag{6}$$

where $\rho_{\star}$ is the stellar density. A similar expression relating the mean stellar density to the orbital eccentricity can also be derived (Kipping, 2010). Eccentricity is a difficult measurement for small planets, yet a crucial one for understanding formation and habitability. Since asteroseismic observations can provide the stellar density to high precision, these expressions allow for a complementary way of measuring and constraining these important transit parameters (and without requiring radial-velocity data). This is sometimes known as asterodensity profiling (Kipping, 2014).

Using seismically-determined stellar parameters for 66 host stars, Huber et al. (Huber et al., 2013) rederived planet and orbital properties and found significant differences with previous studies that relied on transit and spectroscopic observations only. Remarkably, *Kepler*-93b's radius was measured to an uncertainty of 120 km using *Kepler* and Spitzer Space Telescope observations by Ballard et al. (Ballard et al., 2014). Using 4 years of *Kepler* observations of 33 solar-like host stars and a wide array of seismic and evolutionary modeling tools, Silva Aguirre et al. (Silva Aguirre et al., 2015) were able to add the critical age dimension to planetary studies at a precision of better than 15%. No large trends were found in the distributions of planet radius or period with age. As for age, Campante et al. (Campante et al., 2015) estimated the seismic age of metal-poor *Kepler*-444 to be about 11.2 Gyr, making its five terrestrial planets the oldest known system of its type so far discovered.

The asterodensity profiling method to determine eccentricities was used by Sliski and Kipping (Sliski and Kipping, 2014). Interestingly, a very high false-positive rate was determined for *Kepler* planet candidates with red-giant host stars, nearing 70%. Van Eylen and Albrecht (Van Eylen and Albrecht, 2015) also employed seismic asterodensity profiling to measure eccentricities of 28 stars with multiple planets (mostly below about 10 Earth masses), and, like in our Solar System, found low eccentricities. The distribution of eccentricities was distinctly different from those obtained from radial-velocity measurements (of mostly higher-mass planets). Van Eylen

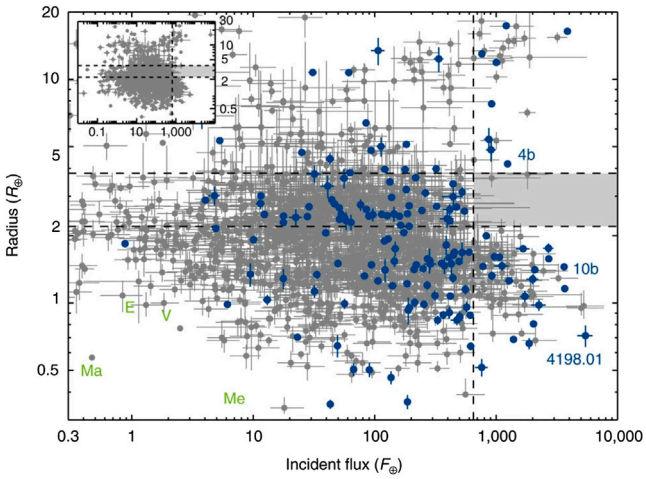

FIGURE 7 | Exoplanet radius as a function of incident flux for a large sample of *Kepler* Objects of Interest (gray filled circles). The blue filled circles are 157 of those planets whose hosts have seismic measurements. The key point is the high level of precision on both the radius and incident flux of the seismic sample (< 10 %). The gray shaded region is the hot super Earth desert, which receives at least 650 times the amount of incident flux as Earth and gets clearly delineated due to the seismic measurements. The inset shows a larger non-seismic sample. The four terrestrial planets are shown for reference. Figure from Lundkvist et al. (Lundkvist et al., 2016).

et al. (Van Eylen et al., 2019) subsequently constrained the eccentricity of 51 small, single-transiting *Kepler* planets. They find a very different distribution, peaking at moderate eccentricities ~ 0.3. These reults, based almost solely on eccentricity estimations, suggest different formation and evolutionary pathways for single- and multi-planet sytems that models will need to reconcile.

In another interesting planetary population study, Lundkvist et al. (Lundkvist et al., 2016) used precise seismic stellar radii to show there is a "desert" of hot super Earths with radii between 2.2 and 3.8 Earth radii in ultra short period orbits, shown in **Figure 7**. Such exoplanets are ubiquitous at longer periods in *Kepler* data. These observations confirmed models that such planets' volatile-rich atmospheres are photo-evaporated due to the intense incident flux they receive from their host star.

Stellar rotation can split solar-like oscillation modes into multiplets (**Section 2.2**), and the relative amplitude of the split modes depends on the viewing angle relative to the stellar rotation axis (Gizon and Solanki, 2003). Transit and radial-velocity observations (Rossiter-McLaughlin effect) provide the planet orbital axis inclination and the sky-project spin-orbit angle. A measurement of all three angles gives the absolute spin-orbit angle, or obliquity, of the system. This property is crucial for understanding the formation history and dynamical evolution of planetary systems.

Kepler transit and seismic data have allowed for the determination of the obliquity of dozens of exoplanetary systems. In cases where there is evidence for multiple exoplanets, most systems are highly aligned (low obliquity) [e.g., (Chaplin et al., 2013; Van Eylen et al., 2014; Quinn et al., 2015; Campante et al., 2016)]. Note that our Solar System has an obliquity of about 7%.

However, a large obliquity was found in *Kepler*-56, which is a red giant pulsator with two transiting planets (Huber et al., 2013). The misalignment (>37°) is likely caused by a third, non-transiting planet that tidally torques the system (Li et al., 2014). In general, the hot Jupiters have been found to be consistently misaligned (Albrecht et al., 2013; Winn and Fabrycky, 2015), begging the question as to why? Possible scenarios include the channels through which hot Jupiters migrated or the formation history as the star and protoplanetary disk evolved (Albrecht et al., 2013). Larger statistical samples will hopefully lead to a clearer picture (Winn et al., 2017).

Clearly, the use of pulsating stars to study their exoplanets adds a promising new avenue for understanding these distant worlds.

4 CONCLUSION

Asteroseismology of stars that oscillate like the Sun has experienced a paradigm shift as a result of the *Kepler* mission, yielding data of unprecedented quality. To fully exploit these data, one of the key developments that is needed is the improvement of 1D stellar models as discussed above. Subtle effects due to rotation, angular momentum evolution, mixing processes, meridional circulation, magnetic fields, and convection at boundaries are still not understood fully enough for the robust interpretation of *Kepler* data. However, tremendous progress is being made in this area, and the MESA 1D stellar evolution open-source software instrument is helping a large number of scientists to delve into theoretical modeling [see (Paxton et al., 2019), for the most recent instrument paper]. In the near future, we can expect increased implementation of 3D simulations that capture more of the physics, particularly in the outer layers of stars (Mosumgaard et al., 2020).

Solar-like oscillations are not only powerful probes of stellar interiors, but by providing precise stellar parameters, become an indispensible tool for galactic studies, particularly as large ground-based surveys scan the skies. *Kepler*, as well as NASA's current Transiting Exoplanet Survey Satellite [(TESS) (Ricker et al., 2015)], have even shown that these oscillations may exist in

intermediate-mass main-sequence stars that had never been considered before (Antoci et al., 2011; Bedding et al., 2020).

The legacy of revolutionary missions with dual goals of exoplanetary and stellar astrophysics, such as CoRoT (Convection Rotation and Planetary Transits), *Kepler*, and TESS, will be carried forward with the European Space Agency's PLATO (PLanetary Transits and Oscillations of stars) mission, set to launch in 2026. Just as importantly, asteroseismic efforts on solar-like pulsators will be enhanced from ground-based telescopes, the most promising of which is the Stellar Oscillations Network Group [SONG, (Grundahl et al., 2007)]. This initiative follows the lead that GONG has shown for the Sun, whereby a network of small telescopes will target bright stars with high-resolution spectroscopy. The goal is for telescopes that are spread around the Earth in longitude to allow for nearly-continuous observations that permit detailed seismic investigations. As of this article, there are SONG nodes in the Canary Islands (the Hertzsprung SONG telescope), Australia, and China. Even with this initial distribution, there has tremendous success [e.g., (Grundahl et al., 2017; Arentoft et al., 2019; Fredslund Andersen et al., 2019; Li et al., 2019)], showing that dedicated asteroseismic observations from the ground can lead to an understanding of a sample of stars at the level near to that of our Sun.

AUTHOR CONTRIBUTIONS

The author confirms being the sole contributor of this work and has approved it for publication.

FUNDING

National Science Foundation under Grant Number 1351311.

ACKNOWLEDGMENTS

The author gratefully acknowledges support from the National Science Foundation under Grant Number 1351311. The VIRGO instrument onboard SoHO is a cooperative effort of scientists, engineers, and technicians, to whom we are indebted. SoHO is a project of international collaboration between ESA and NASA. Funding for the *Kepler* mission is provided by the NASA Science Mission Directorate. The author benefitted greatly from the *Kepler* Guest Observer publication database https://keplerscience.arc.nasa.gov/kpub-astrophysics.html. Three anonymous referees are also acknowledged for their very astute recommendations that have substantially improved the manuscript.

REFERENCES

Aerts, C., Christensen-Dalsgaard, J., and Kurtz, DW. (2010). *Asteroseismology*. Cham, Switzerland: Springer.

Albrecht, S., Winn, J. N., Marcy, G. W., Howard, A. W., Isaacson, H., and Johnson, J. A. (2013). Low stellar obliquities in compact multiplanet systems. *Astrophys. J* 771, 11. doi:10.1088/0004-637X/771/1/11

Angus, R., Aigrain, S., Foreman-Mackey, D., and McQuillan, A. (2015). Calibrating gyrochronology using Kepler asteroseismic targets. *Mon. Not. Roy. Astron. Soc.* 450, 1787–1798. doi:10.1093/mnras/stv423

Antoci, V., Handler, G., Campante, T. L., Thygesen, A. O., Moya, A., Kallinger, T., et al. (2011). The excitation of solar-like oscillations in a δSct star by efficient envelope convection. *Nature* 477, 570–573. doi:10.1038/nature10389

Appourchaux, T., Chaplin, W. J., García, R. A., Gruberbauer, M., Verner, G. A., Antia, H. M., et al. (2012). Oscillation mode frequencies of 61 main-sequence and subgiant stars observed by Kepler. *Astron. Astrophys*. 543, A54. doi:10.1051/0004-6361/201218948

Arentoft, T., Grundahl, F., White, T. R., Slumstrup, D., Handberg, R., Lund, M. N., et al. (2019). Asteroseismology of the Hyades red giant and planet host Tauri. *Astron. Astrophys*. 622, A190. doi:10.1051/0004-6361/201834690

Auge, C., Huber, D., Heinze, A., Shappee, B. J., Tonry, J., Chakrabarti, S., et al. (2020). Beyond Gaia: asteroseismic distances of M giants using ground-based transient surveys. *Astron. J.* 160, 18. doi:10.3847/1538-3881/ab91bf

Ballard, S., Chaplin, W. J., Charbonneau, D., Désert, J. M., Fressin, F., Zeng, L., et al. (2014). Kepler-93b: a terrestrial world measured to within 120 km, and a test case for a new spitzer observing mode. *Astrophys. J.* 790, 12. doi:10.1088/0004-637X/790/1/12

Barnes, S. A. (2003). On the rotational evolution of solar- and late-type stars, its magnetic origins, and the possibility of stellar gyrochronology. *Astrophys. J* 586, 464–479. doi:10.1086/367639

Basu, S. (2016). Global seismology of the Sun. *Living Rev. Sol. Phys*. 13, 2. doi:10.1007/s41116-016-0003-4

Basu, S., Grundahl, F., Stello, D., Kallinger, T., Hekker, S., Mosser, B., et al. (2011). Sounding open clusters: asteroseismic constraints from kepler on the properties of NGC 6791 and NGC 6819. *Astrophys. J. Lett*. 729, L10. doi:10.1088/2041-8205/729/1/L10

Basu, S., and Hekker, S. (2020). Unveiling the structure and dynamics of red giants with asteroseismology. *Frontiers in Astronomy and Space Sciences* 7, 44. doi:10.3389/fspas.2020.00044

Bazot, M., Benomar, O., Christensen-Dalsgaard, J., Gizon, L., Hanasoge, S., Nielsen, M., et al. (2019). Latitudinal differential rotation in the solar analogues 16 Cygni A and B. *Astron. Astrophys.* 623, A125. doi:10.1051/0004-6361/201834594

Bazot, M., Nielsen, M. B., Mary, D., Christensen-Dalsgaard, J., Benomar, O., Petit, P., et al. (2018). Butterfly diagram of a Sun-like star observed using asteroseismology. *Astron. Astrophys.* 619, L9. doi:10.1051/0004-6361/201834251

Bazot, M. (2020). Uncertainties and biases in modelling 16 Cygni A and B. *Astron. Astrophys*. 635, A26. doi:10.1051/0004-6361/201935565

Beck, P. G., Bedding, T. R., Mosser, B., Stello, D., Garcia, R. A., Kallinger, T., et al. (2011). Kepler detected gravity-mode period spacings in a red giant star. *Science* 332, 205. doi:10.1126/science.1201939

Beck, P. G., Kallinger, T., Pavlovski, K., Palacios, A., Tkachenko, A., Mathis, S., et al. (2018a). Seismic probing of the first dredge-up event through the eccentric red-giant and red-giant spectroscopic binary KIC 9163796. How different are red-giant stars with a mass ratio of 1.015?. *Astron. Astrophys.* 612, A22. doi:10.1051/0004-6361/201731269

Beck, P. G., Mathis, S., Gallet, F., Charbonnel, C., Benbakoura, M., García, R. A., et al. (2018b). Testing tidal theory for evolved stars by using red giant binaries observed by Kepler. *Mon. Not. Roy. Astron. Soc.* 479, L123–L128. doi:10.1093/mnrasl/sly114

Beck, P. G., Montalban, J., Kallinger, T., De Ridder, J., Aerts, C., García, R. A., et al. (2012). Fast core rotation in red-giant stars as revealed by gravity-dominated mixed modes. *Nature.* 481, 55–57. doi:10.1038/nature10612

Bedding, T. R., Mosser, B., Huber, D., Montalbán, J., Beck, P., Christensen-Dalsgaard, J., et al. (2011). Gravity modes as a way to distinguish between hydrogen- and helium-burning red giant stars. *Nature.* 471, 608–611. doi:10.1038/nature09935

Bedding, T. R., Murphy, S. J., Hey, D. R., Huber, D., Li, T., Smalley, B., et al. (2020). Very regular high-frequency pulsation modes in young intermediate-mass stars. *Nature*. 581, 147–151. doi:10.1038/s41586-020-2226-8

Belkacem, K., Goupil, M. J., Dupret, M. A., Samadi, R., Baudin, F., Noels, A., et al. (2011). The underlying physical meaning of the ν - ν_c relation. *Astron. Astrophys.* 530, A142. doi:10.1051/0004-6361/201116490

Belkacem, K., Marques, J. P., Goupil, M. J., Mosser, B., Sonoi, T., Ouazzani, R. M., et al. (2015). Angular momentum redistribution by mixed modes in evolved

low-mass stars. II. Spin-down of the core of red giants induced by mixed modes. *Astron. Astrophys.* 579, A31. doi:10.1051/0004-6361/201526043

Bellinger, E. P. (2019). A seismic scaling relation for stellar age. *Mon. Not. Roy. Astron. Soc.* 486, 4612–4621. doi:10.1093/mnras/stz714

Bellinger, E. P. (2020). A seismic scaling relation for stellar age II: the red giant branch. *Mon. Not. Roy. Astron. Soc.* 492, L50–L55. doi:10.1093/mnrasl/slz178

Bellinger, E. P., Angelou, G. C., Hekker, S., Basu, S., Ball, W. H., and Guggenberger, E. (2016). Fundamental parameters of main-sequence stars in an instant with machine learning. *Astrophys. J.* 830, 31. doi:10.3847/0004-637X/830/1/31

Bellinger, E. P., Hekker, S., Angelou, G. C., Stokholm, A., and Basu, S. (2019). Stellar ages, masses, and radii from asteroseismic modeling are robust to systematic errors in spectroscopy. *Astron. Astrophys.* 622, A130. doi:10.1051/0004-6361/201834461

Benbakoura, M., Gaulme, P., McKeever, J., Beck, P. G., Jackiewicz, J., and García, R. A. (2017). Modeling radial velocities and eclipse photometry of the kepler target KIC 4054905: an oscillating red giant in an eclipsing binary. Available at: https://arxiv.org/pdf/1712.01082.pdf.

Benomar, O., Bazot, M., Nielsen, M. B., Gizon, L., Sekii, T., Takata, M., et al. (2018). Asteroseismic detection of latitudinal differential rotation in 13 Sun-like stars. *Science.* 361, 1231–1234. doi:10.1126/science.aao6571

Benomar, O., Takata, M., Shibahashi, H., Ceillier, T., and García, R. A. (2015). Nearly uniform internal rotation of solar-like main-sequence stars revealed by space-based asteroseismology and spectroscopic measurements. *Mon. Not. Roy. Astron. Soc.* 452, 2654–2674. doi:10.1093/mnras/stv1493

Blancato, K., Ness, M., Huber, D., Lu, Y., and Angus, R. (2020). Data-driven derivation of stellar properties from photometric time series data using convolutional neural networks. Available at: https://arxiv.org/abs/2005.09682.

Bonaca, A., Tanner, J. D., Basu, S., Chaplin, W. J., Metcalfe, T. S., Monteiro, M. J. P. F. G., et al. (2012). Calibrating convective properties of solar-like stars in the kepler field of view. *Astrophys. J. Lett.* 755, L12. doi:10.1088/2041-8205/755/1/L12

Borucki, W. J., Koch, D., Basri, G., Batalha, N., Brown, T., Caldwell, D., et al. (2010). Kepler planet-detection mission: introduction and first results. *Science.* 327, 977. doi:10.1126/science.1185402

Brogaard, K., Hansen, C. J., Miglio, A., Slumstrup, D., Frandsen, S., Jessen-Hansen, J., et al. (2018). Establishing the accuracy of asteroseismic mass and radius estimates of giant stars - I. Three eclipsing systems at [Fe/H] -0.3 and the need for a large high-precision sample. *Mon. Not. Roy. Astron. Soc.* 476, 3729–3743. doi:10.1093/mnras/sty268

Brown, T. M., Gilliland, R. L., Noyes, R. W., and Ramsey, L. W. (1991). Detection of possible p-mode oscillations on Procyon. *Astrophys. J.* 368, 599. doi:10.1086/169725

Campante, T. L., Barclay, T., Swift, J. J., Huber, D., Adibekyan, V. Z., Cochran, W., et al. (2015). An ancient extrasolar system with five sub-earth-size planets. *Astrophys. J.* 799, 170. doi:10.1088/0004-637X/799/2/170

Campante, T. L., Chaplin, W. J., Lund, M. N., Huber, D., Hekker, S., García, R. A., et al. (2014). Limits on surface gravities of kepler planet-candidate host stars from non-detection of solar-like oscillations. *Astrophys. J.* 783, 123. doi:10.1088/0004-637X/783/2/123

Campante, T. L., Lund, M. N., Kuszlewicz, J. S., Davies, G. R., Chaplin, W. J., Albrecht, S., et al. (2016). Spin-orbit alignment of exoplanet systems: ensemble analysis using asteroseismology. *Astrophys. J.* 819, 85. doi:10.3847/0004-637X/819/1/85

Campante, T. L., Santos, N. C., and Monteiro, M. J. P. F. G. (2018). *Asteroseismology and exoplanets: listening to the stars and searching for new worlds.* Cham, Switzerland: Springer.

Casagrande, L., Silva Aguirre, V., Schlesinger, K. J., Stello, D., Huber, D., Serenelli, A. M., et al. (2016). Measuring the vertical age structure of the Galactic disc using asteroseismology and SAGA. *Mon. Not. Roy. Astron. Soc.* 455, 987–1007. doi:10.1093/mnras/stv2320

Casagrande, L., Silva Aguirre, V., Stello, D., Huber, D., Serenelli, A. M., Cassisi, S., et al. (2014). Strömgren survey for asteroseismology and galactic archaeology: let the SAGA begin. *Astrophys. J.* 787, 110. doi:10.1088/0004-637X/787/2/110

Ceillier, T., Eggenberger, P., García, R. A., and Mathis, S. (2012). Attempts to reproduce the rotation profile of the red giant KIC 7341231 observed by Kepler. *Astron. Nachr.* 333, 971. doi:10.1002/asna.201211806

Ceillier, T., van Saders, J., García, R. A., Metcalfe, T. S., Creevey, O., Mathis, S., et al. (2016). Rotation periods and seismic ages of KOIs - comparison with stars without detected planets from Kepler observations. *Mon. Not. Roy. Astron. Soc.* 456, 119–125. doi:10.1093/mnras/stv2622

Chaplin, W. J., Basu, S., Huber, D., Serenelli, A., Casagrande, L., Silva Aguirre, V., et al. (2014). Asteroseismic fundamental properties of solar-type stars observed by the NASA kepler mission. *Astrophys. J. Supp.* 210, 1. doi:10.1088/0067-0049/210/1/1

Chaplin, W. J., Bedding, T. R., Bonanno, A., Broomhall, A. M., García, R. A., Hekker, S., et al. (2011). Evidence for the impact of stellar activity on the detectability of solar-like oscillations observed by kepler. *Astrophys. J. Lett.* 732, L5. doi:10.1088/2041-8205/732/1/L5

Chaplin, W. J., Elsworth, Y., Howe, R., Isaak, G. R., McLeod, C. P., Miller, B. A., et al. (1996). BiSON performance. *Sol. Phys.* 168, 1–18. doi:10.1007/BF00145821

Chaplin, W. J., Kjeldsen, H., Christensen-Dalsgaard, J., Basu, S., Miglio, A., Appourchaux, T., et al. (2011). Ensemble asteroseismology of solar-type stars with the NASA kepler mission. *Science.* 332, 213. doi:10.1126/science.1201827

Chaplin, W. J., and Miglio, A. (2013). Asteroseismology of solar-type and red-giant stars. *Annu. Rev. Astron. Astrophys.* 51, 353–392. doi:10.1146/annurev-astro-082812-140938

Chaplin, W. J., Sanchis-Ojeda, R., Campante, T. L., Hand berg, R., Stello, D., Winn, J. N., et al. (2013). Asteroseismic determination of obliquities of the exoplanet systems kepler-50 and kepler-65. *Astrophys. J.* 766, 101. doi:10.1088/0004-637X/766/2/101

Christensen-Dalsgaard, J. (1988). "A hertzsprung-russell diagram for stellar oscillations," in Advances in helio- and asteroseismology, Aarhus, Denmark, July 11–17, 1986. Editors J. Christensen-Dalsgaard and S. Frandsen (Dordrecht, Netherlands: D. Reidel Publishing Co.), 295.

Christensen-Dalsgaard, J., and Perez Hernandez, F. (1992). The phase function for stellar acoustic oscillations. I - Theory. *Mon. Not. Roy. Astron. Soc.* 257, 62–88. doi:10.1093/mnras/257.1.62

Christensen-Dalsgaard, J. (2004). Physics of solar-like oscillations. *Sol. Phys.* 220, 137–168. doi:10.1023/B:SOLA.0000031392.43227.7d

Creevey, O. L., Metcalfe, T. S., Schultheis, M., Salabert, D., Bazot, M., Thévenin, F., et al. (2017). Characterizing solar-type stars from full-length Kepler data sets using the Asteroseismic Modeling Portal. *Astron. Astrophys.* 601, A67. doi:10.1051/0004-6361/201629496

Davies, G. R., Chaplin, W. J., Farr, W. M., García, R. A., Lund, M. N., Mathis, S., et al. (2015). Asteroseismic inference on rotation, gyrochronology and planetary system dynamics of 16 Cygni. *Mon. Not. Roy. Astron. Soc.* 446, 2959–2966. doi:10.1093/mnras/stu2331

Davies, G. R., Lund, M. N., Miglio, A., Elsworth, Y., Kuszlewicz, J. S., North, T. S. H., et al. (2017). Using red clump stars to correct the Gaia DR1 parallaxes. *Astron. Astrophys.* 598, L4. doi:10.1051/0004-6361/201630066

De Ridder, J., Barban, C., Baudin, F., Carrier, F., Hatzes, A. P., Hekker, S., et al. (2009). Non-radial oscillation modes with long lifetimes in giant stars. *Nature.* 459, 398–400. doi:10.1038/nature08022

De Silva, G. M., Freeman, K. C., Bland-Hawthorn, J., Martell, S., de Boer, E. W., Asplund, M., et al. (2015). The GALAH survey: scientific motivation. *Mon. Not. Roy. Astron. Soc.* 449, 2604–2617. doi:10.1093/mnras/stv327

Deheuvels, S., Ballot, J., Beck, P. G., Mosser, B., Østensen, R., García, R. A., et al. (2015). Seismic evidence for a weak radial differential rotation in intermediate-mass core helium burning stars. *Astron. Astrophys.* 580, A96. doi:10.1051/0004-6361/201526449

Deheuvels, S., Brandão, I., Silva Aguirre, V., Ballot, J., Michel, E., Cunha, M. S., et al. (2016). Measuring the extent of convective cores in low-mass stars using Kepler data: toward a calibration of core overshooting. *Astron. Astrophys.* 589, A93. doi:10.1051/0004-6361/201527967

Deheuvels, S., Doğan, G., Goupil, M. J., Appourchaux, T., Benomar, O., Bruntt, H., et al. (2014). Seismic constraints on the radial dependence of the internal rotation profiles of six Kepler subgiants and young red giants. *Astron. Astrophys.* 564, A27. doi:10.1051/0004-6361/201322779

Deheuvels, S., García, R. A., Chaplin, W. J., Basu, S., Antia, H. M., Appourchaux, T., et al. (2012). Seismic evidence for a rapidly rotating core in a lower-giant-branch star observed with kepler. *Astrophys. J.* 756, 19. doi:10.1088/0004-637X/756/1/19

do Nascimento, J. J. D., García, R. A., Mathur, S., Anthony, F., Barnes, S. A., Meibom, S., et al. (2014). Rotation periods and ages of solar analogs and solar twins revealed by the kepler mission. *Astrophys. J. Lett.* 790, L23. doi:10.1088/2041-8205/790/2/L23

Dziembowski, W. A., Gough, D. O., Houdek, G., and Sienkiewicz, R. (2001). Oscillations of α UMa and other red giants. *Mon. Not. Roy. Astron. Soc.* 328, 601–610. doi:10.1046/j.1365-8711.2001.04894.x

Eggenberger, P., Deheuvels, S., Miglio, A., Ekström, S., Georgy, C., Meynet, G., et al. (2019). Asteroseismology of evolved stars to constrain the internal transport of angular momentum. I. Efficiency of transport during the subgiant phase. *Astron. Astrophys.* 621, A66. doi:10.1051/0004-6361/201833447

Frandsen, S., Lehmann, H., Hekker, S., Southworth, J., Debosscher, J., Beck, P., et al. (2013). KIC 8410637: a 408-day period eclipsing binary containing a pulsating giant star. *Astron. Astrophys.* 556, A138. doi:10.1051/0004-6361/201321817

Fredslund Andersen, M., Pallé, P., Jessen-Hansen, J., Wang, K., Grundahl, F., Bedding, T. R., et al. (2019). Oscillations in the Sun with SONG: setting the scale for asteroseismic investigations. *Astron. Astrophys.* 623, L9. doi:10.1051/0004-6361/201935175

Frohlich, C., Andersen, B. N., Appourchaux, T., Berthomieu, G., Crommelynck, D. A., Domingo, V., et al. (1997). First results from VIRGO, the experiment for helioseismology and solar irradiance monitoring on SOHO. *Sol. Phys.* 170, 1–25. doi:10.1023/A:1004969622753

Fröhlich, C., Romero, J., Roth, H., Wehrli, C., Andersen, B. N., Appourchaux, T., et al. (1995). VIRGO: experiment for helioseismology and solar irradiance monitoring. *Sol. Phys.* 162, 101–128. doi:10.1007/BF00733428

Fuller, J., Cantiello, M., Stello, D., Garcia, R. A., and Bildsten, L. (2015). Asteroseismology can reveal strong internal magnetic fields in red giant stars. *Science*. 350, 423–426. doi:10.1126/science.aac6933

Fuller, J., Piro, A. L., and Jermyn, A. S. (2019). Slowing the spins of stellar cores. *Mon. Not. Roy. Astron. Soc.* 485, 3661–3680. doi:10.1093/mnras/stz514

Gabriel, A. H., Grec, G., Charra, J., Robillot, J. M., Roca Cortés, T., Turck-Chièze, S., et al. (1995). Global oscillations at low frequency from the SOHO mission (GOLF). *Sol. Phys.* 162, 61–99. doi:10.1007/BF00733427

García Pérez, A. E., Allende Prieto, C., Holtzman, J. A., Shetrone, M., Mészáros, S., Bizyaev, D., et al. (2016). ASPCAP: the APOGEE stellar parameter and chemical abundances pipeline. *Astron. J.* 151, 144. doi:10.3847/0004-6256/151/6/144

García, R. A., and Ballot, J. (2019). Asteroseismology of solar-type stars. *Living Rev. Sol. Phys.* 16, 4. doi:10.1007/s41116-019-0020-1

García, R. A., Ceillier, T., Salabert, D., Mathur, S., van Saders, J. L., Pinsonneault, M., et al. (2014). Rotation and magnetism of Kepler pulsating solar-like stars. Towards asteroseismically calibrated age-rotation relations. *Astron. Astrophys.* 572, A34. doi:10.1051/0004-6361/201423888

García, R. A., Pérez Hernández, F., Benomar, O., Silva Aguirre, V., Ballot, J., Davies, G. R., et al. (2014). Study of KIC 8561221 observed by Kepler: an early red giant showing depressed dipolar modes. *Astron. Astrophys.* 563, A84. doi:10.1051/0004-6361/201322823

Garcia, R. A., and Stello, D. (2018). Asteroseismology of red giant stars. Available at: https://arxiv.org/abs/1801.08377.

Gaulme, P., Jackiewicz, J., Appourchaux, T., and Mosser, B. (2014). Surface activity and oscillation amplitudes of red giants in eclipsing binaries. *Astrophys. J.* 785, 5. doi:10.1088/0004-637X/785/1/5

Gaulme, P., McKeever, J., Jackiewicz, J., Rawls, M. L., Corsaro, E., Mosser, B., et al. (2016). Testing the asteroseismic scaling relations for red giants with eclipsing binaries observed by kepler. *Astrophys. J.* 832, 121. doi:10.3847/0004-637X/832/2/121

Gaulme, P., McKeever, J., Rawls, M. L., Jackiewicz, J., Mosser, B., and Guzik, J. A. (2013). Red giants in eclipsing binary and multiple-star systems: modeling and asteroseismic analysis of 70 candidates from kepler data. *Astrophys. J.* 767, 82. doi:10.1088/0004-637X/767/1/82

Gehan, C., Mosser, B., Michel, E., Samadi, R., and Kallinger, T. (2018). Core rotation braking on the red giant branch for various mass ranges. *Astron. Astrophys.* 616, A24. doi:10.1051/0004-6361/201832822

Gilmore, G., Randich, S., Asplund, M., Binney, J., Bonifacio, P., Drew, J., et al. (2012). The gaia-ESO public spectroscopic survey. *Messenger.* 147, 25–31.

Gizon, L., and Solanki, S. K. (2003). Determining the inclination of the rotation Axis of a sun-like star. *Astrophys. J.* 589, 1009–1019. doi:10.1086/374715

Goldreich, P., and Keeley, D. A. (1977). Solar seismology. II. The stochastic excitation of the solar p-modes by turbulent convection. *Astrophys. J.* 212, 243–251. doi:10.1086/155043

Gough, D. O. (1990). "Comments on helioseismic inference,"in *Progress of seismology of the sun and stars*. Editors Y. Osaki and H. Shibahashi (Berlin, Germany: Springer), 283.

Grundahl, F., Fredslund Andersen, M., Christensen-Dalsgaard, J., Antoci, V., Kjeldsen, H., Hand berg, R., et al. (2017). First results from the Hertzsprung SONG telescope: asteroseismology of the G5 subgiant star μ herculis. *Astrophys. J.* 836, 142. doi:10.3847/1538-4357/836/1/142

Grundahl, F., Kjeldsen, H., Christensen-Dalsgaard, J., Arentoft, T., and Frandsen, S. (2007). Stellar oscillations network Group. *Commun. Asteroseismol.* 150, 300. doi:10.1553/cia150s300

Handberg, R., Brogaard, K., Miglio, A., Bossini, D., Elsworth, Y., Slumstrup, D., et al. (2017). NGC 6819: testing the asteroseismic mass scale, mass loss and evidence for products of non-standard evolution. *Mon. Not. Roy. Astron. Soc.* 472, 979–997. doi:10.1093/mnras/stx1929

Harvey, J. W., Hill, F., Hubbard, R. P., Kennedy, J. R., Leibacher, J. W., Pintar, J. A., et al. (1996). The global oscillation network Group (GONG) project. *Science*. 272, 1284–1286. doi:10.1126/science.272.5266.1284

Hekker, S., and Christensen-Dalsgaard, J. (2017). Giant star seismology. *Astron. AstroPhys. Rev.* 25, 1. doi:10.1007/s00159-017-0101-x

Hekker, S. (2013). CoRoT and kepler results: solar-like oscillators. *Adv. Space Res.* 52, 1581–1592. doi:10.1016/j.asr.2013.08.005

Hekker, S., Debosscher, J., Huber, D., Hidas, M. G., De Ridder, J., Aerts, C., et al. (2010). Discovery of a red giant with solar-like oscillations in an eclipsing binary system from kepler space-based photometry. *Astrophys. J. Lett.* 713, L187–L191. doi:10.1088/2041-8205/713/2/L187

Hekker, S. (2020). Scaling relations for solar-like oscillations: a review. *Frontiers in Astron. Space Sci.* 7, 3. doi:10.3389/fspas.2020.00003

Hon, M., Bellinger, E. P., Hekker, S., Stello, D., and Kuszlewicz, J. S. (2020). Asteroseismic inference of subgiant evolutionary parameters with deep learning. *Mon. Not. Roy. Astron. Soc.* 499, 2445–2461. doi:10.1093/mnras/staa2853

Hon, M., Stello, D., and Yu, J. (2017). Deep learning classification in asteroseismology. *Mon. Not. Roy. Astron. Soc.* 469, 4578–4583. doi:10.1093/mnras/stx1174

Hon, M., Stello, D., and Zinn, J. C. (2018). Detecting solar-like oscillations in red giants with deep learning. *Astrophys. J.* 859, 64. doi:10.3847/1538-4357/aabfdb

Howe, R., Komm, R. W., and Hill, F. (2002). Localizing the solar cycle frequency shifts in global p-modes. *Astrophys. J.* 580, 1172–1187. doi:10.1086/343892

Howell, S. B., Sobeck, C., Haas, M., Still, M., Barclay, T., Mullally, F., et al. (2014). The K2 mission: characterization and early results. *Publ. Astron. Soc. Pac.* 126, 398. doi:10.1086/676406

Huber, D., Bedding, T. R., Stello, D., Hekker, S., Mathur, S., Mosser, B., et al. (2011). Testing scaling relations for solar-like oscillations from the main sequence to red giants using kepler data. *Astrophys. J.* 743, 143. doi:10.1088/0004-637X/743/2/143

Huber, D., Carter, J. A., Barbieri, M., Miglio, A., Deck, K. M., Fabrycky, D. C., et al. (2013). Stellar spin-orbit misalignment in a multiplanet system. *Science*. 342, 331–334. doi:10.1126/science.1242066

Huber, D., Chaplin, W. J., Christensen-Dalsgaard, J., Gilliland, R. L., Kjeldsen, H., Buchhave, L. A., et al. (2013). Fundamental properties of kepler planet-candidate host stars using asteroseismology. *Astrophys. J.* 767, 127. doi:10.1088/0004-637X/767/2/127

Huber, D., Ireland, M. J., Bedding, T. R., Brand ão, I. M., Piau, L., Maestro, V., et al. (2012). Fundamental properties of stars using asteroseismology from kepler and CoRoT and interferometry from the CHARA array. *Astrophys. J.* 760, 32. doi:10.1088/0004-637X/760/1/32

Huber, D., Zinn, J., Bojsen-Hansen, M., Pinsonneault, M., Sahlholdt, C., Serenelli, A., et al. (2017). Asteroseismology and Gaia: testing scaling relations using 2200 kepler stars with TGAS parallaxes. *Astrophys. J.* 844, 102. doi:10.3847/1538-4357/aa75ca

Huber, D. (2018). "Synergies between asteroseismology and exoplanetary science," in *Asteroseismology and exoplanets: listening to the stars and searching for new worlds*. Editors T. L. Campante, N. C. Santos, and M. J. P. F. G. Monteiro (Cham, Switzerland: Springer International Publishing), 119–135.

Jiménez, A., Roca Cortés, T., and Jiménez-Reyes, S. J. (2002). Variation of the low-degree solar acoustic mode parameters over the solar cycle. *Sol. Phys.* 209, 247–263. doi:10.1023/A:1021226503589

Kallinger, T., Beck, P. G., Stello, D., and Garcia, R. A. (2018). Non-linear seismic scaling relations. *Astron. Astrophys*. 616, A104. doi:10.1051/0004-6361/201832831

Kallinger, T., Weiss, W. W., Barban, C., Baudin, F., Cameron, C., Carrier, F., et al. (2010). Oscillating red giants in the CoRoT exofield: asteroseismic mass and radius determination. *Astron. Astrophys*. 509, A77. doi:10.1051/0004-6361/200811437

Kiefer, R., Schad, A., Davies, G., and Roth, M. (2017). Stellar magnetic activity and variability of oscillation parameters: an investigation of 24 solar-like stars observed by Kepler. *Astron. Astrophys*. 598, A77. doi:10.1051/0004-6361/201628469

Kipping, D. M. (2014). Characterizing distant worlds with asterodensity profiling. *Mon. Not. Roy. Astron. Soc*. 440, 2164–2184. doi:10.1093/mnras/stu318

Kipping, D. M. (2010). Investigations of approximate expressions for the transit duration. *Mon. Not. Roy. Astron. Soc*. 407, 301–313. doi:10.1111/j.1365-2966.2010.16894.x

Kjeldsen, H., and Bedding, T. R. (1995). Amplitudes of stellar oscillations: the implications for asteroseismology. *Astron. Astrophys*. 293, 87–106.

Kjeldsen, H., Bedding, T. R., and Christensen-Dalsgaard, J. (2008). Correcting stellar oscillation frequencies for near-surface effects. *Astrophys. J. Lett*. 683, L175. doi:10.1086/591667

Koch, D. G., Borucki, W. J., Basri, G., Batalha, N. M., Brown, T. M., Caldwell, D., et al. (2010). Kepler mission design, realized photometric performance, and early science. *Astrophys. J. Lett*. 713, L79–L86. doi:10.1088/2041-8205/713/2/L79

Li, G., Naoz, S., Valsecchi, F., Johnson, J. A., and Rasio, F. A. (2014). The dynamics of the multi-planet system orbiting kepler-56. *Astrophys. J*. 794, 131. doi:10.1088/0004-637X/794/2/13

Li, T., Bedding, T. R., Huber, D., Ball, W. H., Stello, D., Murphy, S. J., et al. (2018). Modelling Kepler red giants in eclipsing binaries: calibrating the mixing-length parameter with asteroseismology. *Mon. Not. Roy. Astron. Soc*. 475, 981–998. doi:10.1093/mnras/stx3079

Li, T., Bedding, T. R., Kjeldsen, H., Stello, D., Christensen-Dalsgaard, J., and Deng, L. (2019). Asteroseismic modelling of the subgiant μ Herculis using SONG data: lifting the degeneracy between age and model input parameters. *Mon. Not. Roy. Astron. Soc*. 483, 780–789. doi:10.1093/mnras/sty3000

Lund, M. N., Basu, S., Silva Aguirre, V., Chaplin, W. J., Serenelli, A. M., García, R. A., et al. (2016). Asteroseismology of the Hyades with K2: first detection of main-sequence solar-like oscillations in an open cluster. *Mon. Not. Roy. Astron. Soc*. 463, 2600–2611. doi:10.1093/mnras/stw2160

Lund, M. N., Silva Aguirre, V., Davies, G. R., Chaplin, W. J., Christensen-Dalsgaard, J., Houdek, G., et al. (2017). Standing on the shoulders of dwarfs: the kepler asteroseismic LEGACY sample. I. Oscillation mode parameters. *Astrophys. J*. 835, 172. doi:10.3847/1538-4357/835/2/172

Lundkvist, M. S., Huber, D., Aguirre, V. S., and Chaplin, W. J. (2018). "Characterizing host stars using asteroseismology," in *Handbook of Exoplanets*. Editors H. Deeg and J. Belmonte (Cham, Switzerland: Springer International Publishing), 117. doi:10.1007/978-3-319-55333-7_177

Lundkvist, M. S., Kjeldsen, H., Albrecht, S., Davies, G. R., Basu, S., Huber, D., et al. (2016). Hot super-Earths stripped by their host stars. *Nat. Commun*. 7, 11201. doi:10.1038/ncomms11201

Majewski, S. R., Wilson, J. C., Hearty, F., Schiavon, R. R., and Skrutskie, M. F. (2010). "The Apache point observatory galactic evolution experiment (APOGEE) in sloan digital sky survey III (SDSS-III)," in Chemical abundances in the universe: connecting first stars to planets, Paris, France, August 2009. Editors K. Cunha, M. Spite, and B. Barbuy (Paris, France: International Astronomical Union), 480–481.

Martell, S., Simpson, J., Balasubramaniam, A., Buder, S., Sharma, S., Hon, M., et al. (2020). The GALAH survey: lithium-rich giant stars require multiple formation channels. Available at: https://arxiver.moonhats.com/2020/06/04/the-galah-survey-lithium-rich-giant-stars-require-multiple-formation-channels-ssa/.

Martig, M., Fouesneau, M., Rix, H. W., Ness, M., Mészáros, S., García-Hernández, D. A., et al. (2016). Red giant masses and ages derived from carbon and nitrogen abundances. *Mon. Not. Roy. Astron. Soc*. 456, 3655–3670. doi:10.1093/mnras/stv2830

McKeever, J. M., Basu, S., and Corsaro, E. (2019). The helium abundance of NGC 6791 from modeling of stellar oscillations. *Astrophys. J*. 874, 180. doi:10.3847/1538-4357/ab0c04

Metcalfe, T. S., Chaplin, W. J., Appourchaux, T., García, R. A., Basu, S., Brandão, I., et al. (2012). Asteroseismology of the solar analogs 16 Cyg A and B from kepler observations. *Astrophys. J. Lett*. 748, L10. doi:10.1088/2041-8205/748/1/L10

Metcalfe, T. S., Creevey, O. L., and Davies, G. R. (2015). Asteroseismic modeling of 16 Cyg A & B using the complete kepler data set. *Astrophys. J. Lett*. 811, L37. doi:10.1088/2041-8205/811/2/L37

Metcalfe, T. S., Creevey, O. L., Doğan, G., Mathur, S., Xu, H., Bedding, T. R., et al. (2014). Properties of 42 solar-type kepler targets from the asteroseismic modeling portal. *Astrophys. J. Supp*. 214, 27. doi:10.1088/0067-0049/214/2/27

Metcalfe, T. S., Egeland, R., and van Saders, J. (2016). Stellar evidence that the solar dynamo may Be in transition. *Astrophys. J. Lett*. 826, L2. doi:10.3847/2041-8205/826/1/L2

Metcalfe, T. S., Kochukhov, O., Ilyin, I. V., Strassmeier, K. G., Godoy-Rivera, D., and Pinsonneault, M. H. (2019). LBT/PEPSI spectropolarimetry of a magnetic morphology shift in old solar-type stars. *Astrophys. J. Lett*. 887, L38. doi:10.3847/2041-8213/ab5e48

Metcalfe, T. S., and van Saders, J. (2017). Magnetic evolution and the disappearance of sun-like activity cycles. *Sol. Phys*. 292, 126. doi:10.1007/s11207-017-1157-5

Miglio, A., Brogaard, K., Stello, D., Chaplin, W. J., D'Antona, F., Montalbán, J., et al. (2012). Asteroseismology of old open clusters with Kepler: direct estimate of the integrated red giant branch mass-loss in NGC 6791 and 6819. *Mon. Not. Roy. Astron. Soc*. 419, 2077–2088. doi:10.1111/j.1365-2966.2011.19859.x

Miglio, A., Chaplin, W. J., Brogaard, K., Lund, M. N., Mosser, B., Davies, G. R., et al. (2016). Detection of solar-like oscillations in relics of the Milky Way: asteroseismology of K giants in M4 using data from the NASA K2 mission. *Mon. Not. Roy. Astron. Soc*. 461, 760–765. doi:10.1093/mnras/stw1555

Miglio, A., Chiappini, C., Morel, T., Barbieri, M., Chaplin, W. J., Girardi, L., et al. (2013). Galactic archaeology: mapping and dating stellar populations with asteroseismology of red-giant stars. *Mon. Not. Roy. Astron. Soc*. 429, 423–428. doi:10.1093/mnras/sts345

Montalbán, J., Miglio, A., Noels, A., Dupret, M. A., Scuflaire, R., and Ventura, P. (2013). Testing convective-core overshooting using period spacings of dipole modes in red giants. *Astrophys. J*. 766, 118. doi:10.1088/0004-637X/766/2/118

Mosser, B., Belkacem, K., Goupil, M. J., Michel, E., Elsworth, Y., Barban, C., et al. (2011). The universal red-giant oscillation pattern. An automated determination with CoRoT data. *Astron. Astrophys*. 525, L9. doi:10.1051/0004-6361/201015440

Mosser, B., Belkacem, K., Pinçon, C., Takata, M., Vrard, M., Barban, C., et al. (2017). Dipole modes with depressed amplitudes in red giants are mixed modes. *Astron. Astrophys*. 598, A62. doi:10.1051/0004-6361/201629494

Mosser, B., Benomar, O., Belkacem, K., Goupil, M. J., Lagarde, N., Michel, E., et al. (2014). Mixed modes in red giants: a window on stellar evolution. *Astron. Astrophys*. 572, L5. doi:10.1051/0004-6361/201425039

Mosser, B., Dziembowski, W. A., Belkacem, K., Goupil, M. J., Michel, E., Samadi, R., et al. (2013a). Period-luminosity relations in evolved red giants explained by solar-like oscillations. *Astron. Astrophys*. 559, A137. doi:10.1051/0004-6361/201322243

Mosser, B., Goupil, M. J., Belkacem, K., Marques, J. P., Beck, P. G., Bloemen, S., et al. (2012a). Spin down of the core rotation in red giants. *Astron. Astrophys*. 548, A10. doi:10.1051/0004-6361/201220106

Mosser, B., Goupil, M. J., Belkacem, K., Michel, E., Stello, D., Marques, J. P., et al. (2012b). Probing the core structure and evolution of red giants using gravity-dominated mixed modes observed with Kepler. *Astron. Astrophys*. 540, A143. doi:10.1051/0004-6361/201118519

Mosser, B., Michel, E., Belkacem, K., Goupil, M. J., Baglin, A., Barban, C., et al. (2013b). Asymptotic and measured large frequency separations. *Astron. Astrophys*. 550, A126. doi:10.1051/0004-6361/201220435

Mosumgaard, J. R., Jørgensen, A. C. S., Weiss, A., Silva Aguirre, V., and Christensen-Dalsgaard, J. (2020). Coupling 1D stellar evolution with 3D-hydrodynamical simulations on-the-fly II: stellar evolution and asteroseismic applications. *Mon. Not. Roy. Astron. Soc*. 491, 1160–1173. doi:10.1093/mnras/stz2979

Ness, M., Hogg, D. W., Rix, H. W., Martig, M., Pinsonneault, M. H., and Ho, A. Y. Q. (2016). Spectroscopic determination of masses (and implied ages) for red giants. *Astrophys. J*. 823, 114. doi:10.3847/0004-637X/823/2/114

Nsamba, B., Campante, T. L., Monteiro, M. J. P. F. G., Cunha, M. S., Rendle, B. M., Reese, D. R., et al. (2018). Asteroseismic modelling of solar-type stars: internal

systematics from input physics and surface correction methods. *Mon. Not. Roy. Astron. Soc.* 477, 5052–5063. doi:10.1093/mnras/sty948

Paxton, B., Smolec, R., Schwab, J., Gautschy, A., Bildsten, L., Cantiello, M., et al. (2019). Modules for experiments in stellar astrophysics (MESA): pulsating variable stars, rotation, convective boundaries, and energy conservation. *Astrophys. J. Supp.* 243, 10. doi:10.3847/1538-4365/ab2241

Pinsonneault, M. H., Elsworth, Y., Epstein, C., Hekker, S., Mészáros, S., Chaplin, W. J., et al. (2014). The APOKASC catalog: an asteroseismic and spectroscopic joint survey of targets in the kepler fields. *Astrophys. J. Supp.* 215, 19. doi:10.1088/0067-0049/215/2/19

Pinsonneault, M. H., Elsworth, Y. P., Tayar, J., Serenelli, A., Stello, D., Zinn, J., et al. (2018). The second APOKASC catalog: the empirical approach. *Astrophys. J. Supp.* 239, 32. doi:10.3847/1538-4365/aaebfd

Pinsonneault, M. H., Kawaler, S. D., and Demarque, P. (1990). Rotation of low-mass stars: a new probe of stellar evolution. *Astrophys. J. Supp.* 74, 501. doi:10.1086/191507

Quinn, S. N., White, T. R., Latham, D. W., Chaplin, W. J., Handberg, R., Huber, D., et al. (2015). Kepler-432: a red giant interacting with one of its two long-period giant planets. *Astrophys. J.* 803, 49. doi:10.1088/0004-637X/803/2/49

Remus, F., Mathis, S., and Zahn, J. P. (2012). The equilibrium tide in stars and giant planets. I. The coplanar case. *Astron. Astrophys.* 544, A132. doi:10.1051/0004-6361/201118160

Ren, A., Fu, J., De Cat, P., Wu, Y., Yang, X., Shi, J., et al. (2016). LAMOST observations in the kepler field. Analysis of the stellar parameters measured with LASP based on low-resolution spectra. *Astrophys. J. Supp.* 225, 28. doi:10.3847/0067-0049/225/2/28

Rendle, B. M., Buldgen, G., Miglio, A., Reese, D., Noels, A., Davies, G. R., et al. (2019). AIMS - a new tool for stellar parameter determinations using asteroseismic constraints. *Mon. Not. Roy. Astron. Soc.* 484, 771–786. doi:10.1093/mnras/stz031

Ricker, G. R., Winn, J. N., Vanderspek, R., Latham, D. W., Bakos, G. Á., Bean, J. L., et al. (2015). Transiting exoplanet survey satellite (TESS). *J. Astronomical Telesc. Instrum. Syst.* 1, 014003. doi:10.1117/1.JATIS.1.1.01400

Sahlholdt, C. L., and Silva Aguirre, V. (2018). Asteroseismic radii of dwarfs: new accuracy constraints from Gaia DR2 parallaxes. *Mon. Not. Roy. Astron. Soc.* 481, L125–L129. doi:10.1093/mnrasl/sly173

Salabert, D., Régulo, C., Pérez Hernández, F., and García, R. A. (2018). Frequency dependence of p-mode frequency shifts induced by magnetic activity in Kepler solar-like stars. *Astron. Astrophys.* 611, A84. doi:10.1051/0004-6361/201731714

Salaris, M., Pietrinferni, A., Piersimoni, A. M., and Cassisi, S. (2015). Post first dredge-up [C/N] ratio as age indicator. Theoretical calibration. *Astron. Astrophys.* 583, A87. doi:10.1051/0004-6361/201526951

Santos, A. R. G., Campante, T. L., Chaplin, W. J., Cunha, M. S., Lund, M. N., Kiefer, R., et al. (2018). Signatures of magnetic activity in the seismic data of solar-type stars observed by kepler. *Astrophys. J. Supp.* 237, 17. doi:10.3847/1538-4365/aac9b6

Seager, S., and Mallén-Ornelas, G. (2003). A unique solution of planet and star parameters from an extrasolar planet transit light curve. *Astrophys. J.* 585, 1038–1055. doi:10.1086/346105

Serenelli, A., Johnson, J., Huber, D., Pinsonneault, M., Ball, W. H., Tayar, J., et al. (2017). The first APOKASC catalog of kepler dwarf and subgiant stars. *Astrophys. J. Supp.* 233, 23. doi:10.3847/1538-4365/aa97df

Silva Aguirre, V., Basu, S., Brandão, I. M., Christensen-Dalsgaard, J., Deheuvels, S., Doğan, G., et al. (2013). Stellar ages and convective cores in field main-sequence stars: first asteroseismic application to two kepler targets. *Astrophys. J.* 769, 141. doi:10.1088/0004-637X/769/2/141

Silva Aguirre, V., Bojsen-Hansen, M., Slumstrup, D., Casagrande, L., Kawata, D., Ciucă, I., et al. (2018). Confirming chemical clocks: asteroseismic age dissection of the Milky Way disc(s). *Mon. Not. Roy. Astron. Soc.* 475, 5487–5500. doi:10.1093/mnras/sty150

Silva Aguirre, V., Davies, G. R., Basu, S., Christensen-Dalsgaard, J., Creevey, O., Metcalfe, T. S., et al. (2015). Ages and fundamental properties of Kepler exoplanet host stars from asteroseismology. *Mon. Not. Roy. Astron. Soc.* 452, 2127–2148. doi:10.1093/mnras/stv1388

Silva Aguirre, V., Lund, M. N., Antia, H. M., Ball, W. H., Basu, S., Christensen-Dalsgaard, J., et al. (2017). Standing on the shoulders of dwarfs: the kepler asteroseismic LEGACY sample. II.Radii, masses, and ages. *Astrophys. J.* 835, 173. doi:10.3847/1538-4357/835/2/173

Sliski, D. H., and Kipping, D. M. (2014). A high false positive rate for kepler planetary candidates of giant stars using asterodensity profiling. *Astrophys. J.* 788, 148. doi:10.1088/0004-637X/788/2/148

Stello, D., Cantiello, M., Fuller, J., Huber, D., García, R. A., Bedding, T. R., et al. (2016). A prevalence of dynamo-generated magnetic fields in the cores of intermediate-mass stars. *Nature*. 529, 364–367. doi:10.1038/nature16171

Stello, D., Compton, D. L., Bedding, T. R., Christensen-Dalsgaard, J., Kiss, L. L., Kjeldsen, H., et al. (2014). Non-radial oscillations in M-giant semi-regular variables: stellar models and kepler observations. *Astrophys. J. Lett.* 788, L10. doi:10.1088/2041-8205/788/1/L10

Stello, D., Huber, D., Bedding, T. R., Benomar, O., Bildsten, L., Elsworth, Y. P., et al. (2013). Asteroseismic classification of stellar populations among 13,000 red giants observed by kepler. *Astrophys. J. Lett.* 765, L41. doi:10.1088/2041-8205/765/2/L41

Stello, D., Huber, D., Kallinger, T., Basu, S., Mosser, B., Hekker, S., et al. (2011). Amplitudes of solar-like oscillations: constraints from red giants in open clusters observed by kepler. *Astrophys. J. Lett.* 737, L10. doi:10.1088/2041-8205/737/1/L10

Stello, D., Vanderburg, A., Casagrande, L., Gilliland, R., Silva Aguirre, V., Sandquist, E., et al. (2016). The K2 M67 study: revisiting old friends with K2 reveals oscillating red giants in the open cluster M67. *Astrophys. J.* 832, 133. doi:10.3847/0004-637X/832/2/133

Tassoul, M. (1980). Asymptotic approximations for stellar nonradial pulsations. *Astrophys. J. Supp.* 43, 469–490. doi:10.1086/190678

Tayar, J., Somers, G., Pinsonneault, M. H., Stello, D., Mints, A., Johnson, J. A., et al. (2017). The correlation between mixing length and metallicity on the giant branch: implications for ages in the Gaia era. *Astrophys. J.* 840, 17. doi:10.3847/1538-4357/aa6a1e

Themeßl, N., Hekker, S., Southworth, J., Beck, P. G., Pavlovski, K., Tkachenko, A., et al. (2018). Oscillating red giants in eclipsing binary systems: empirical reference value for asteroseismic scaling relation. *Mon. Not. Roy. Astron. Soc.* 478, 4669–4696. doi:10.1093/mnras/sty1113

Thompson, M. J., Toomre, J., Anderson, E. R., Antia, H. M., Berthomieu, G., Burtonclay, D., et al. (1996). Differential rotation and dynamics of the solar interior. *Science*. 272, 1300–1305. doi:10.1126/science.272.5266.1300

Tollerud, E. J. (2020). "Community-oriented programming in Astronomy: astropy as a case study," in Astronomical data analysis software and systems XXVII, Santiago de Chile, Chile, October 22–26, 2017. Editors P. Ballester, J. Ibsen, M. Solar, and K. Shortridge (San Francisco, CA: Astronomical Society of the Pacific Conference Series), 491.

Van Eylen, V., and Albrecht, S. (2015). Eccentricity from transit photometry: small planets in kepler multi-planet systems have low eccentricities. *Astrophys. J.* 808, 126. doi:10.1088/0004-637X/808/2/126

Van Eylen, V., Albrecht, S., Huang, X., MacDonald, M. G., Dawson, R. I., Cai, M. X., et al. (2019). The orbital eccentricity of small planet systems. *Astron. J.* 157, 61. doi:10.3847/1538-3881/aaf22f

Van Eylen, V., Lund, M. N., Silva Aguirre, V., Arentoft, T., Kjeldsen, H., Albrecht, S., et al. (2014). What asteroseismology can do for exoplanets: kepler-410a b is a small neptune around a bright star, in an eccentric orbit consistent with low obliquity. *Astrophys. J.* 782, 14. doi:10.1088/0004-637X/782/1/14

van Saders, J. L., Ceillier, T., Metcalfe, T. S., Aguirre, V. S., Pinsonneault, M. H., García, R. A., et al. (2016). Weakened magnetic braking as the origin of anomalously rapid rotation in old field stars. *Nature*. 529, 181–184. doi:10.1038/nature16168

Verma, K., Faria, J. P., Antia, H. M., Basu, S., Mazumdar, A., Monteiro, M. J. P. F. G., et al. (2014). Asteroseismic estimate of helium abundance of a solar analog binary system. *Astrophys. J.* 790, 138. doi:10.1088/0004-637X/790/2/138

Verma, K., Raodeo, K., Antia, H. M., Mazumdar, A., Basu, S., Lund, M. N., et al. (2017). Seismic measurement of the locations of the base of convection zone and helium ionization zone for stars in the kepler seismic LEGACY sample. *Astrophys. J.* 837, 47. doi:10.3847/1538-4357/aa5da7

Verma, K., Raodeo, K., Basu, S., Silva Aguirre, V., Mazumdar, A., Mosumgaard, J. R., et al. (2019). Helium abundance in a sample of cool stars: measurements from asteroseismology. *Mon. Not. Roy. Astron. Soc.* 483, 4678–4694. doi:10.1093/mnras/sty3374

Wang, L., Wang, W., Wu, Y., Zhao, G., Li, Y., Luo, A., et al. (2016). Calibration of LAMOST stellar surface gravities using the kepler asteroseismic data. *Astron. J.* 152, 6. doi:10.3847/0004-6256/152/1/6

White, T. R., Bedding, T. R., Stello, D., Appourchaux, T., Ballot, J., Benomar, O., et al. (2011). Asteroseismic diagrams from a survey of solar-like oscillations with kepler. *Astrophys. J. Lett*. 742, L3. doi:10.1088/2041-8205/742/1/L3

Winn, J. N., and Fabrycky, D. C. (2015). The occurrence and architecture of exoplanetary systems. *Annu. Rev. Astron. Astrophys*. 53, 409–447. doi:10.1146/annurev-astro-082214-122246

Winn, J. N., Petigura, E. A., Morton, T. D., Weiss, L. M., Dai, F., Schlaufman, K. C., et al. (2017). Constraints on the obliquities of kepler planet-hosting stars. *Astron. J*. 154, 270. doi:10.3847/1538-3881/aa93e3

Yu, J., Huber, D., Bedding, T. R., Stello, D., Hon, M., Murphy, S. J., et al. (2018). Asteroseismology of 16,000 kepler red giants: global oscillation parameters, masses, and radii. *Astrophys. J. Supp*. 236, 42. doi:10.3847/1538-4365/aaaf74

Zhao, G., Chen, Y. Q., Shi, J. R., Liang, Y. C., Hou, J. L., Chen, L., et al. (2006). Stellar abundance and galactic chemical evolution through LAMOST spectroscopic survey. *Chin. J. Astron. Astrophys*. 6, 265–280. doi:10.1088/1009-9271/6/3/01

Zinn, J. C., Pinsonneault, M. H., Huber, D., Stello, D., Stassun, K., and Serenelli, A. (2019). Testing the radius scaling relation with Gaia DR2 in the kepler field. *Astrophys. J*. 885, 166. doi:10.3847/1538-4357/ab44a9

Conflict of Interest: The author declares that the research was conducted in the absence of any commercial or financial relationships that could be construed as a potential conflict of interest.

frontiers in Astronomy and Space Sciences

ORIGINAL RESEARCH
published: 15 April 2021
doi: 10.3389/fspas.2021.626398

The roAp Stars Observed by the *Kepler* Space Telescope

*Daniel L. Holdsworth**

Jeremiah Horrocks Institute, University of Central Lancashire, Preston, United Kingdom

Before the launch of the *Kepler* Space Telescope, most studies of the rapidly oscillating Ap (roAp) stars were conducted with ground-based photometric *B* observations, supplemented with high-resolution time-resolved spectroscopy and some space observations with the WIRE, MOST, and BRITE satellites. These modes of observation often only provided information on a single star at a time, however, *Kepler* provided the opportunity to observe hundreds of thousands of stars simultaneously. Over the duration of the primary 4 year *Kepler* mission, and its 4 year reconfigured K2 mission, the telescope observed at least 14 new and known roAp stars. This paper provides a summary the results of these observations, including a first look at the entire data sets, and provides a look forward to NASA's *TESS* mission.

Keywords: asteroseimology, techniques: photometry, stars: oscillations, stars: chemical peculiar, stars-variable

OPEN ACCESS

Edited by:
Anthony Eugene Lynas-Gray, University College London, United Kingdom

Reviewed by:
Joyce Ann Guzik, Los Alamos National Laboratory (DOE), United States
Abhishek Kumar Srivastava, Indian Institute of Technology (BHU), India
Hiromoto Shibahashi, The University of Tokyo, Japan

***Correspondence:**
Daniel L. Holdsworth
dlholdsworth@uclan.ac.uk

Specialty section:
This article was submitted to Stellar and Solar Physics, a section of the journal Frontiers in Astronomy and Space Sciences

Received: *05 November 2020*
Accepted: *22 February 2021*
Published: *15 April 2021*

Citation:
Holdsworth DL (2021) The roAp Stars Observed by the Kepler Space Telescope. Front. Astron. Space Sci. 8:626398. doi: 10.3389/fspas.2021.626398

1. INTRODUCTION

The rapidly oscillating, chemically peculiar A (roAp) stars are found at the base of the classical instability strip, where it intersects the main-sequence. They provide the opportunity to study the interactions between strong magnetic fields, pulsation, rotation, and chemical stratification. Due to these properties, the roAp stars provide a unique insight to stellar atmospheres in 3D.

The Ap stars as a class are characterized by spectroscopic signatures of Sr, Eu, Cr, and/or Si in low-resolution classification spectroscopy (e.g., Gray and Corbally, 2009). In high-resolution spectroscopy, abundances of rare earth elements can be measured to be over a million times that observed in the Sun (e.g., Lüftinger et al., 2010). They are permeated by a strong, global, magnetic field that can be up to about 35 kG in strength (Elkin et al., 2010). It is the presence of the magnetic field which gives rise to the chemical peculiarities in the Ap stars; convection is suppressed by the magnetic field allowing for the radiative levitation of, most notably the rare earth elements, and the gravitational settling of others. The origin of the magnetic field is not conclusively known, but is suspected to be the result of the merger of close binary stars in the pre-main sequence phase of evolution where at least one star is still on the Henyey track (Ferrario et al., 2009; Tutukov and Fedorova, 2010). This scenario provides an explanation for the lack of Ap stars in close binary systems, and why the magnetic axis is inclined to the rotation axis.

The rapid oscillations in Ap stars were first discovered through the targeted observations of these stars by Kurtz (1978), with the seminal paper following a few years later (Kurtz, 1982). Since their discovery, over 75 roAp stars have been identified through ground- and space-based observations (e.g., Martinez and Kurtz, 1994a; Kochukhov et al., 2013; Holdsworth et al., 2014a; Joshi et al., 2016; Cunha et al., 2019; Hey et al., 2019). They show pulsational variability in the range 5–24 min and pulsate in low degree ($\ell \leq 3$), high-overtone ($n > 15$) modes that are thought to be driven by the κ-mechanism acting on the H I ionization zone (e.g., Balmforth et al., 2001; Saio, 2005). However, this mechanism is unable to explain all of the observed pulsation frequencies in the roAp stars,

leading Cunha et al. (2013) to postulate that turbulent pressure may play a role in the excitation of some observed modes.

Given the κ-mechanism is the most likely driving mechanism for *most* of the pulsations in roAp stars the frequencies should be stable, unlike the stochastically excited modes that are seen in the solar-like and red giant stars. Some of the roAp stars show very stable pulsation modes over the entire data spans. Others, however, do not. The most well-studied case of frequency variability in an roAp star is HR 3831 where 16 year of ground-based data are available (Kurtz et al., 1994, 1997), with 8 other stars showing frequency variability identified by Martinez et al. (1994). The cause of the frequency variability is unknown, but is postulated to have two possible origins. The first is frequency perturbation by an external body. In this instance, the Doppler shift of the roAp star is imparted on the arrival time, at the observer, of the pulsation signal. For a circular orbit, this would induce a sinusoidal change in the frequency. Much work has been done on this aspect in recent years, with the development of the Frequency Modulation (FM) theory (Shibahashi and Kurtz, 2012; Shibahashi et al., 2015), with an extension to Phase Modulation (PM; Murphy et al., 2014; Murphy and Shibahashi, 2015). Since, when fitting a sinusoidal function to a pulsation mode, the frequency and phase are inextricably intertwined, so the discussion of frequency and phase modulation is one and the same. In the reminder of this work, frequency variability is discussed in the *Kepler* roAp stars, but plots showing phase changes are produced since this is the directly observed changing feature.

The second interpretation of frequency variability in roAp stars is a change in the cavity in which the mode propagates. This could be due to an evolutionary change as the star evolves off the main-sequence. In this scenario, one would expect a monotonic decrease in the frequency (as is seen in solar-like pulsators; e.g., Chaplin and Miglio, 2013). Alternately, Kurtz et al. (1994) suggested that cyclic variability could be an indication of a stellar magnetic cycle analogous to the 11 year solar cycle. For non-cyclic and non-monotonic frequency variability small changes in the internal magnetic field configuration may be responsible. There could, of course, be a combination of many of these possibilities at work. With the ever increasing precision, and growing time base of observations, frequency variability is becoming a common observed feature of the roAp stars.

In fact, there is evidence for frequency variability in most pulsating stars. Stochastically excited modes in, for example, solar-like pulsators are incoherent which results in a natural variation in the pulsation frequency (or phase) over time. However, the classically pulsating stars are driven by a coherent force resulting in stable frequencies. Despite this, frequency variability is still observed. Neilson et al. (2016) discussed the observed frequency changes in a variety of classical pulsators in the context of evolutionary changes in the star. While some observations were accurately modeled by evolutionary changes alone, there was evidence for further physical processes altering the pulsation frequency. Whether these physical processes involve rotation, mass loss, magnetic fields, small changes in local chemical composition, or a combination of these factors is currently unclear. The identification and analysis of frequency changes in pulsating stars will pave the way for detailed stellar modeling to try and solve this problem.

The pulsations in roAp stars have overtones significantly greater than the degree, meaning the modes are in the asymptotic regime (Shibahashi, 1979; Tassoul, 1980, 1990). In this case, p modes become regularly spaced in frequency with alternating odd and even degree modes (see e.g., Aerts et al., 2010). The spacing between two consecutive modes of the same degree is the large frequency separation, $\Delta\nu$, while the frequency difference between two odd or even degree modes (e.g., $\ell = 0$ and $\ell = 2$ or $\ell = 1$ and $\ell = 3$) that have a radial overtone difference of one is the small frequency separation, $\delta\nu$. The value of the large frequency separation is dependent on stellar global properties, changing in proportion to the square root of the mean density, and can be scaled with reference to the Sun. The small frequency separation is sensitive to the core concentration of the star, and hence is an age indicator.

In the case of the roAp stars, the presence of a strong, global, magnetic field causes significant deviation from spherical symmetry and as such breaks the regular pattern of p modes. This "glitch" in the regular spacing changes $\Delta\nu$ for a single spacing, and may cause a change in the odd-even-odd pattern of the mode degree depending on the magnetic field geometry. The most well-studied case of this phenomenon is HR 1217 (Cunha, 2001; Kurtz et al., 2005).

From the early observations of roAp stars, it was seen that the pulsation mode in an amplitude spectrum is often accompanied by sidelobes that are split by the rotation frequency of the star. Kurtz (1982) interpreted this as oblique pulsation. It is well-known that the magnetic field axis in the Ap stars is misaligned with the rotation axis, leading to the oblique rotator model (Stibbs, 1950). This configuration results in a variable light curve over the rotation period of an Ap star, as chemical spots often form at the magnetic poles and provide a brightness contrast against the photosphere. The pulsation axis in a star is the axis of greatest deformation; in most stars it is the rotation axis that serves to break spherical symmetry, and in some binary stars it is the line of apsides (Handler et al., 2020; Kurtz et al., 2020). In the case of the Ap stars, it is the magnetic field, which can be of order 30 kG (e.g., Babcock, 1960; Freyhammer et al., 2008; Mathys, 2017), that causes the most significant deviation from spherical symmetry, and so the pulsation axis is closely aligned to the magnetic one (e.g., Shibahashi and Saio, 1985a; Shibahashi and Takata, 1993; Bigot and Dziembowski, 2002; Bigot and Kurtz, 2011).

This misalignment of the pulsation axis with the rotation one serves to provide an observer with a varying view of the pulsation, leading to amplitude modulation of the observed pulsation(s). In a Fourier spectrum of a light curve, one expects to see a multiplet of $2\ell + 1$ components for a *pure* mode, that is to say a mode that is described by a single spherical harmonic. For a *distorted* mode, the highest number of multiplet components so far observed is 14 (see the discussion of HD 24355 below). To detect these multiplet components, observations are required to cover at least 1.5 rotation cycles of the star, with a greater number being preferable. With the presence of the sidelobes, it is possible, through the analysis of their amplitude ratios, to provide

constraints on the geometry of the star. The stellar inclination value, i, and the angle between the rotation axis and the pulsation axis, β, can be either constrained or determined through the relations provided by Kurtz (1992).

The rotation periods of the Ap stars are, on the whole, significantly longer than their non-magnetic, chemically normal, counterparts likely due to magnetic braking (Stępień, 2000). It is common to find A stars with $v \sin i$ values $>120\,\mathrm{km\,s^{-1}}$ (Adelman, 2004), whereas the Ap stars are considerably lower (up to $40\,\mathrm{km\,s^{-1}}$; Abt and Morrell, 1995). Indeed, the rotation periods for some Ap stars are thought to be as long as centuries (Mathys, 2017). This serves as a problem when trying to apply the oblique pulsator model to determine the mode geometry. Although there is not yet a causal link established, over half of the known roAp stars have undetermined rotation periods, implying they are much longer than the observations cover (Mathys et al., 2020). It is hoped that the ongoing Transiting Exoplanet Survey Satellite (*TESS*) mission (Ricker et al., 2015) will provide insight to this.

2. *KEPLER* OBSERVATIONS OF ROAP STARS

The *Kepler* Space Telescope (Koch et al., 2010) was launched in 2009 to a 372.5 d Earth-trailing heliocentric orbit. The mission collected data in two cadences: the Long Cadence (LC) mode of 29.43 min and the Short Cadence (SC) mode of 58.85 s (Gilliland et al., 2010).

The pulsation mode frequencies in roAp stars are significantly greater than the Nyquist frequency of the LC data ($24.469\,\mathrm{d^{-1}}$). This causes an attenuation of the mode amplitude due to the length of the integration—the signal is effectively smeared out over the course of the 30 min observation. Furthermore, with exactly equally split data, Nyquist reflections of the true mode all have the same amplitude. However, Murphy et al. (2013) showed that although the exposures triggered by the on-board clock are at set intervals, when the time stamps are corrected to Barycentric time, the regularity of the exposures is broken, allowing for the development of Super-Nyquist asteroseismology. As such, pulsations with frequencies above the LC Nyquist frequency can be observed, and distinguished from aliases. The optimal way of observing roAp stars with *Kepler* was with the SC mode, where the sampling is much greater than the pulsation period. However, for each month only 512 stars could be observed in SC mode, thus limiting the target selection for roAp stars.

The following sections will review the roAp stars observed during both the primary *Kepler* mission and the subsequent K2 mission. In total, *Kepler* observed 14 roAp stars in its primary and K2 configurations. These stars are plotted as red stars on a HR diagram in **Figure 1**, where they are shown alongside other roAp stars (black pluses) and Ap stars that do not show detectable pulsations (black dots). As demonstrated by this figure, the rapid oscillations are predominantly found in the cooler Ap stars, despite the theoretical instability strip (calculated under the assumption that the magnetic field suppresses convection in some region of the stellar envelope; Cunha 2002) for these stars extending to about 10,000 K. This uneven distribution may be a result of the targeted ground-based observation campaigns from which many roAp stars were discovered (e.g., Martinez et al., 1991; Paunzen et al., 2012; Joshi et al., 2016).

2.1. Primary Mission

At the time of the launch of *Kepler* there were no known roAp stars in the proposed field of view, and few known Ap stars. However, during the 4 year primary mission, at least 11 roAp stars were observed. These stars were identified from the first 10-d commissioning run, up to using the full 4 year data set to search for pulsations above the LC Nyquist frequency.

2.1.1. Long Cadence Observations

Seven roAp stars were observed by *Kepler* in LC mode only. The first, KIC 7582608, was identified in SuperWASP photometry, with the *Kepler* data subsequently analyzed by Holdsworth et al. (2014b). The other 6 stars were identified as roAp stars by Hey et al. (2019) via a search of the 4-yr data set in the super-Nyquist regime.

The study of KIC 7582608 in the super-Nyquist regime was aided by the knowledge of the pulsation frequency from ground-based observations. Although it is possible to identify the correct pulsation frequency from aliases, prior knowledge removes any ambiguity. The analysis of this star was further aided by its intrinsically large amplitude, such that the signal was not suppressed to a non-detectable level. The data for this star showed a single mode that was split into a quintuplet by oblique pulsation. However, the peaks of the quintuplet were not "clean" but described as "ragged," i.e., they are partially resolved into many closely spaced peaks. This is shown in **Figure 2**. Such an observation implies frequency and/or amplitude variability in a star such that a single frequency cannot describe the variability. This variability was investigated by fitting a fixed frequency to short sections of the data, and observing how the pulsation amplitude and phase changed. The amplitude was constant, after accounting for the variability caused by oblique pulsation, but the phase showed a significant change over the length of the observations.

There are two main interpretations of this observed phenomenon: intrinsic frequency variability caused by changes in the pulsation cavity, or an external body causing positional changes in the star which leads to frequency modulation (FM) in a pulsation mode (Shibahashi and Kurtz, 2012). Given the length of the data set, and the almost cyclic nature of the phase variability, Holdsworth et al. (2014b) proposed that binary motion was the cause of the changes observed in KIC 7582608. By converting the pulsation frequency measured at discrete times into velocities, the authors showed a photometric RV curve. From these measurements, a binary model suggested a orbital period of about 1,200 d and a minimum mass of a companion of $1\,\mathrm{M_\odot}$. Subsequent spectroscopic RV measurements are currently inconclusive on the presence of a companion.

It was unfortunate that this star was not observed in SC mode at all during the *Kepler* mission, as high-precision, time-resolved observations may have provided the opportunity to resolve the binary/intrinsic variability conundrum in this star.

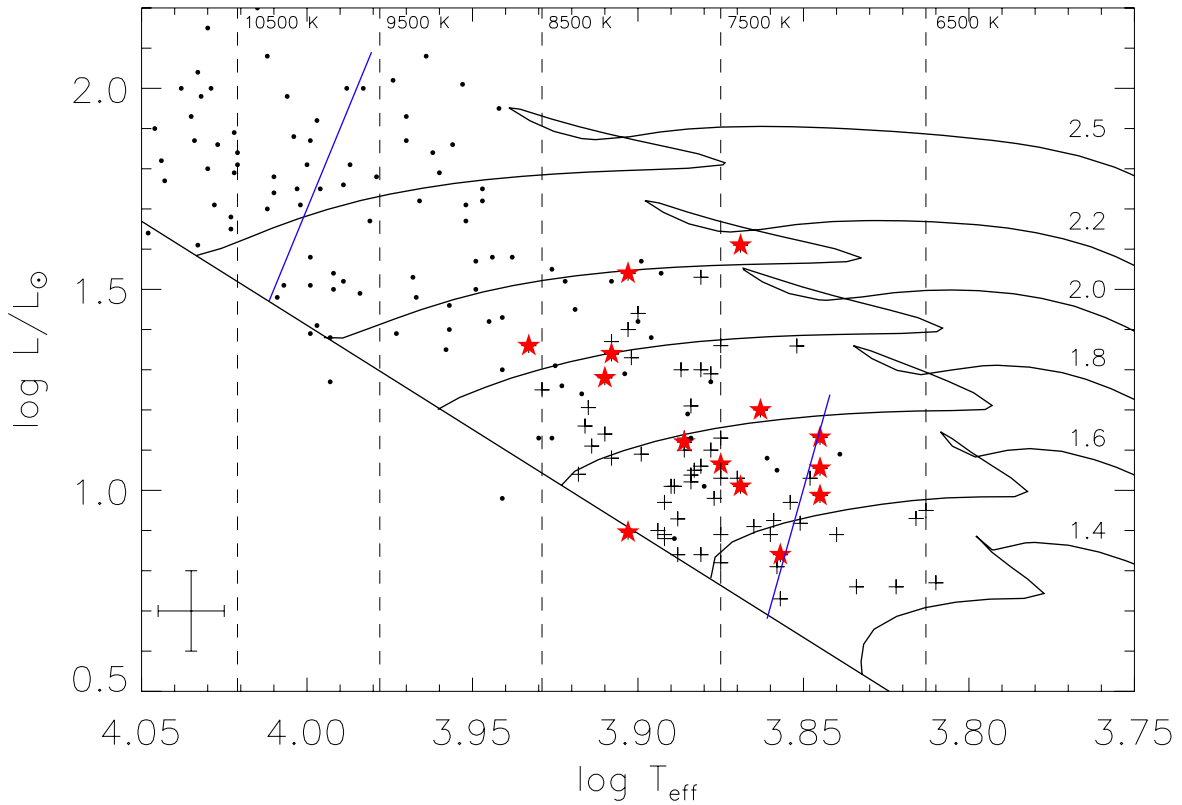

FIGURE 1 | HR diagram showing the location of the roAp stars where T_{eff} and luminosity estimates are available. The stars discussed here, which have been observed by *Kepler*, are shown by the red stars. The blue lines mark the extent of the theoretical instability strip as calculated by Cunha (2002). A selection of non-oscillating Ap stars are shown by dots. The evolutionary tracks, in solar masses, are from Bertelli et al. (2008). A representative error bar is shown in the lower left corner.

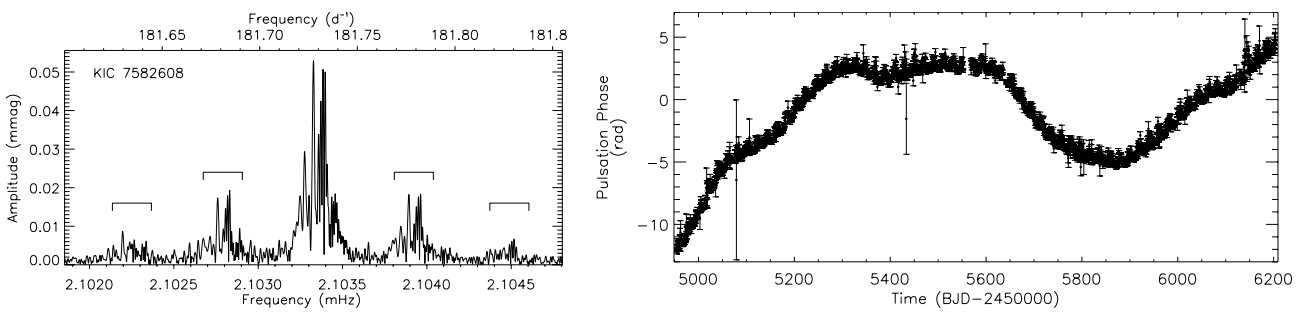

FIGURE 2 | (Left) Amplitude spectrum of the LC 4-year light curve of KIC 7582608 showing the "ragged" structure discussed in the text. The five broad peaks, the central peak and those under the brackets, are split by the rotation frequency of the star (0.566 μHz, $P = 20.4499$ d), indicating a quadrupole mode. **(Right)** Phase variation of the pulsation mode indicating significant frequency variability in this star.

For example, the identification of further, low-amplitude modes which behaved in the same way as the principal mode would suggest an external driving for the variability, otherwise a likely conclusion would be changes within the star which affect different modes differently.

The other six roAp stars observed with *Kepler* in LC mode were KIC 6631188, KIC 7018170, KIC 10685175, KIC 11031749, KIC 11296437, and KIC 11409673 (**Figure 3**). These stars were identified in a novel way by Hey et al. (2019). By selecting all stars in the *Kepler* data set with $T_{eff} > 6,000$ K, they identified variable stars by calculating the skewness of high-pass filtered light curves, and searching for non-aliased peaks. This technique is sensitive to most pulsation frequencies apart from those close to integer multiples of the sampling frequency, and the very highest frequencies (above about 3,500 μHz; 300 d^{-1}) in the *Kepler* LC data.

Although these stars pulsate above the Nyquist frequency, as does KIC 7582608, Hey et al. (2019) was able to apply the oblique

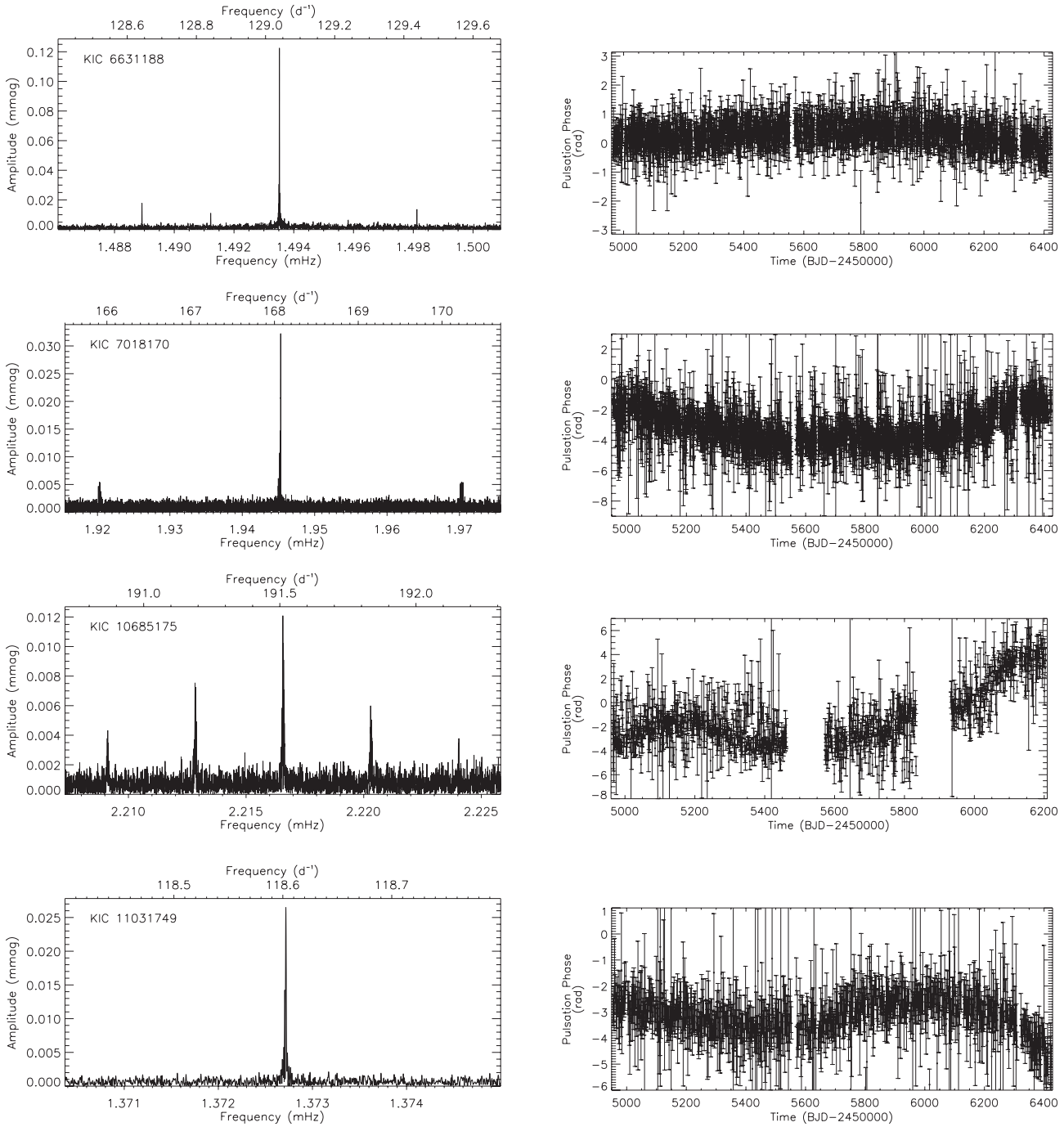

FIGURE 3 | Continued.

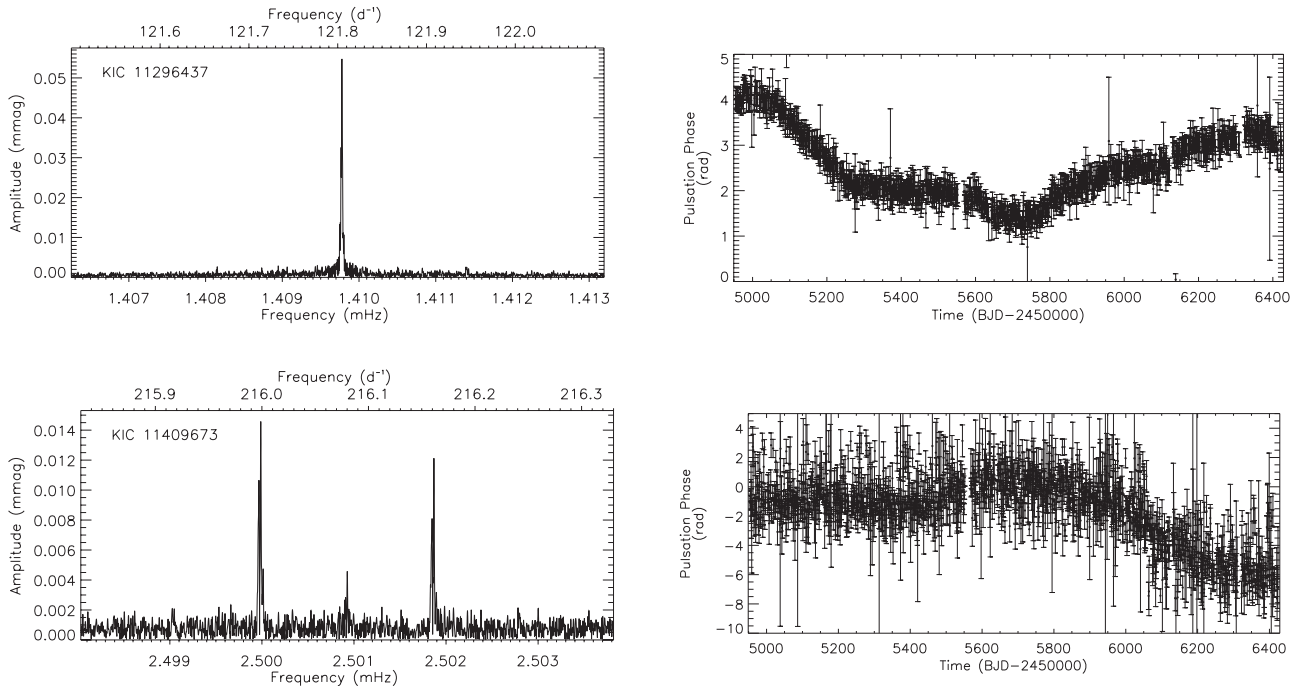

FIGURE 3 | Each row in the figure corresponds to a different star. From top to bottom: KIC 6631188, KIC 7018170, KIC 10685175, and KIC 11031749. **(Left)** Amplitude spectra of the LC light curve. **(Right)** Phase variability of the principal mode in the star, as shown in the left column. The top panels show KIC 11296437 and the bottom panel shows KIC 11409673.

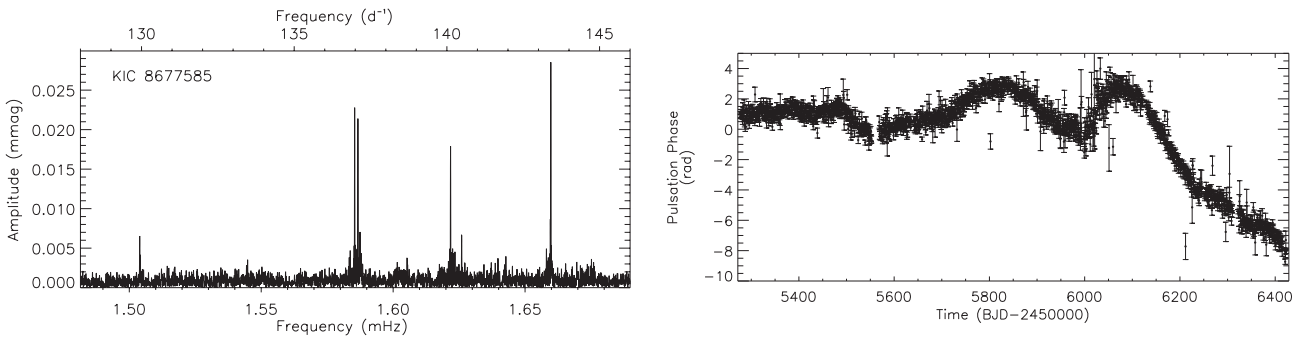

FIGURE 4 | (Left) The pulsations seen in KIC 8677585 in the high-frequency range. **(Right)** The phase variation of the principal mode in the left panels. There is significant frequency variability present in this mode.

pulsator model to four of the six stars and found significant frequency variability in three of them. However, it seems that all six stars show a degree of frequency variability, as evidenced in the right column of **Figure 3**. Again, the source of the frequency variability is unclear in these stars, but for KIC 11031749 the change seems to be cyclic, but on the order of the length of the *Kepler* data set, making conclusions uncertain. Given the stellar parameters derived by Hey et al. (2019), two of the roAp stars show pulsations above the theoretical cut-off limit, an upper frequency limit where pulsations are not driven in models of non-magnetic stars of the same fundamental parameters (e.g., Shibahashi and Saio, 1985b; Gautschy et al., 1998; Sousa and Cunha, 2011), thus providing more examples to challenge the theoretical models of these stars.

The objects discussed in this section will benefit from observations obtained with the ongoing *TESS* mission. Although data sets will be short, 2 min cadence observations will remove any alias ambiguities, as has been done for KIC 10685175 (Shi et al., 2020), and amplitude suppression, potentially allowing for the detection of further modes in these stars, and thus a full asterosismic analysis. Furthermore, new, well-separated in time, observations have the potential to shed light on the causes of the observed frequency/amplitude modulations observed by *Kepler*.

2.1.2. Short Cadence Observations

There were four confirmed roAp stars observed in SC by the primary *Kepler* mission: KIC 8677585, KIC 10483436, KIC 10195926, and KIC 4768731. The initial publications on three of these stars were compiled with only a short section of the now complete 4 year *Kepler* data, with KIC 4768731 being the exception.

Balona et al. (2011b) published the first results of an roAp star observed by *Kepler*, namely KIC 8677585, and provided a follow up study with more data in Balona et al. (2013). The authors showed this star to be variable in two distinct frequency ranges through the identification of modes at 3.141 and 6.423 d^{-1} and many modes in the range $125 - 145\,d^{-1}$, with harmonic and combination frequencies of the high-frequency group present.

This star is among the group of roAp stars that show significant frequency and amplitude variability, as shown in **Figure 4**, so precise mode identification becomes difficult. However, Balona et al. (2013) were able to measure the value of $\Delta\nu$ in this star to be 37.3 μHz which is close to the frequency of the long-period variation. Also linked to the low frequency modes, amplitude variability of some of the high-frequency modes occur with the same frequency, implying that these two phenomena are related. It was speculated that the low-frequency modes are g modes, but perhaps they are manifestations of the amplitude variations of the high-frequency modes, or a signature of beating.

The frequency variability for each of the observed modes in this star is also unique to each given mode. This is confirmation that the variability is intrinsic to the star, and not driven by an external body. This does then mean that all the pulsation cavities are changing over the observation period. Over the ∼ 830 d of observations analyzed by Balona et al. (2013), none of the variability seems cyclic, as was suggested for HR 3831 (Kurtz et al., 1994). Are we then observing evolutionary changes in the star? Will revisiting this star in the future lead to a different $\Delta\nu$ determination? It is unclear at this point as to what can be inferred from these precise observations.

The second star to be published from the *Kepler* data was KIC 10483436 by Balona et al. (2011a), with the analysis of a 27-d light curve. The number of harmonics of the rotation signature observed in this star was quite striking, indicating that with precise *Kepler* photometry, it is possible to observed small scale inhomogenities on the surface of stars, something that can later be investigated with high-resolution Doppler Imaging.

This star is clearly pulsating with a quadrupole mode with significant amplitude, and further modes at lower amplitude as shown in **Figure 5**. Although the discovery paper cites only two modes in this star, it is clear from an investigation using the full *Kepler* data set for this star, that many more modes are present, forming a clump around the low-amplitude mode previously reported. The identification of the number of modes in this star is hampered by the rotation sidelobes caused by oblique pulsation, causing modes and sidelobes to overlap in frequency. An independent determination of the rotation frequency, maybe with ground-based multicolor data since the amplitude is dependent on color (e.g., Kurtz et al., 1996; Drury et al., 2017), could allow this to be untangled.

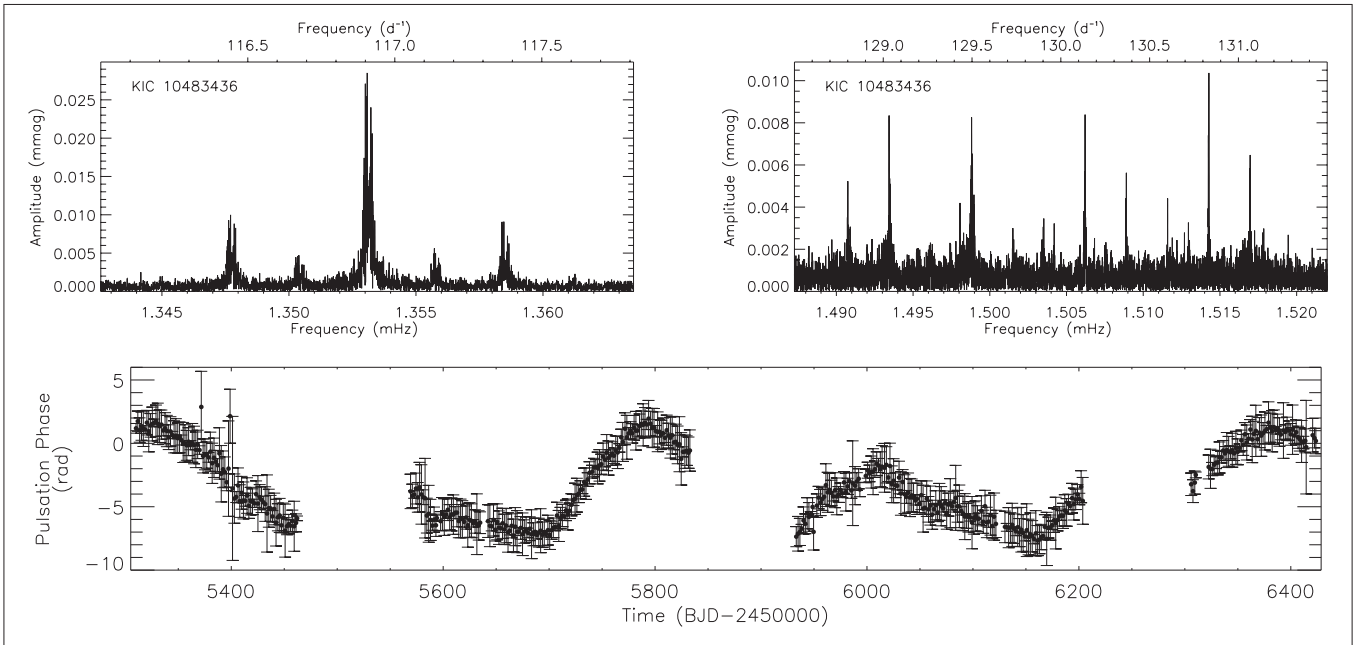

FIGURE 5 | (Top) Amplitude spectra of KIC 10483436 showing the pulsation frequencies in this star. The left plot shows a quadrupole quintuplet with the peaks separated by the rotation frequency (2.670 μHz,$P = 4.303$ d). The right panel shows many modes with rotational sidelobes, making mode identification less straightforward. **(Bottom)** The phase variation of the principal mode in this star (∼ 1.353 μHz).

Although not reported in the discovery paper, with the additional data available, it is evident that there is significant frequency variability in the principal pulsation mode in this star, with indications also in the low-amplitude modes. This variability is non-cyclic and shows sudden changes, implying that the changes are caused by internal phenomena rather than an external source such a companion which would introduce regular, smooth changes in the pulsation phase (see examples in Murphy et al., 2018) . This is therefore another example that the precise, long-term, monitoring by *Kepler* has revealed information that would otherwise have gone undetected.

KIC 10195926 was reported as an roAp star by Kurtz et al. (2011), with the analysis of 25 d of SC data. In the low-frequency regime, they identified a sub-harmonic of the rotation frequency which has an unknown origin. That feature is still present in the longer data set now available, but the source is still not explained. Spectroscopic observations of the star would be needed to determine if this frequency is related to a binary companion. However, a more likely suggestion by Kurtz et al. (2011) is that the sub-harmonic signature is that of an r mode—a global Rossby wave that is driven by the radial component of vorticity interacting with the Coriolis force (for a detailed discussion of r modes; see Saio et al., 2018). This is the first roAp star, and indeed Ap star, that is thought to host an r-mode oscillation. The visibility of r modes is dependent on inclination, spot size and contrast ratio and stellar rotation rate, with slow rotation posing significant visibility issues. The availability of high-precision, long time-base *Kepler* observations has the power to enable the detection of these signatures. Now, with more data, a full investigation into this possibility is possible.

There were two pulsation modes identified in KIC 10195926, one mode split into a septuplet and one into a triplet by oblique pulsation and distortion (**Figure 6**). From the analysis of the phase variations of the pulsations over the rotation cycle, it was concluded that both modes are $\ell = 1$ dipole modes; the triplet arises from a pure mode dipole mode, while the septuplet represents a distorted mode. However, since the relative sidelobe amplitudes for each mode differed, it was proposed that there are two pulsation axes in this star, and thus the geometry of the modes is different. The cause of this is proposed to be the interaction of the magnetic field and rotation on the pulsations. It has been shown by Bigot and Dziembowski (2002) that the difference in obliquity angle between two consecutive modes should be small in most cases, with Cunha and Gough (2000) and Saio and Gautschy (2004) showing that at specific frequencies, the magnetic field can greatly affect the modes. Now, with more data available, the low frequency mode is actually split into a quintuplet, thus the problem of the multiple axes in this star should be revisited.

Furthermore, in light of new results, we propose another interpretation of these different relative amplitudes. Recent observations by the *TESS* mission of HD 6532 show a distinctly different multiplet shape than the *B*-photometric observations presented by Kurtz et al. (1996) [see Kurtz and Holdsworth (2020) for comparison plots]. New ground-based multicolor

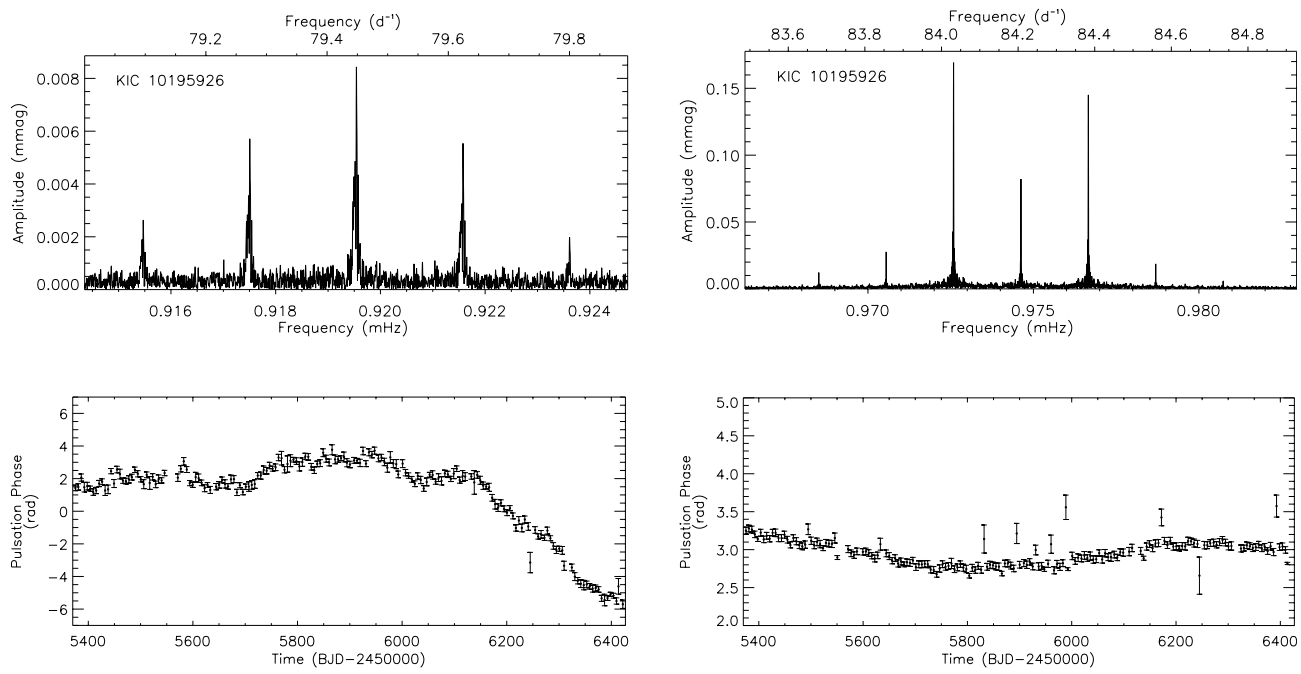

FIGURE 6 | (Top) Amplitude spectra of the two pulsation modes in KIC 10195926. The left plot shows that the lowest frequency mode is split into a quintuplet with the extra data from later *Kepler* quarters. In both cases, the sidelobes are split by the rotation frequency (2.036 μHz, $P = 5.685$ d). **(Bottom)** Corresponding phase variations of the pulsation modes in the top row. The high-frequency mode on the right has a fairly stable frequency over 4 years, but the low-frequency mode has a significant phase change.

observations confirm this difference in mode multiplet structure over five filters (Holdsworth et al., in prep.). Since each filter probes a different atmospheric depth, a simple comparison of data from different filters cannot be made, and strong conclusions about the mode geometry cannot be drawn. With KIC 10195926, the wide *Kepler* passband that probes a wide range of atmospheric layers, coupled with the significantly stratified atmospheres in Ap stars and potentially different mode sensitivities at a certain atmospheric depth, may result in the different mode structures seen in the two modes in KIC 10195926, rather than the presence of two distinct pulsation axes. This, however, is conjecture with a detailed theoretical study required to definitively solve this conundrum.

A preliminary look at this much longer data set reveals KIC 10195926 to be yet another frequency variable star. Interestingly in this case, the principal mode is only slightly variable, and perhaps in a cyclic way, but the low-amplitude mode has a very different, and more significant, variation in its frequency. With this different variability for each mode, it further complicates the physical interpretation of this star.

The final star to be observed in SC mode in the primary *Kepler* mission was KIC 4768731. This star was discovered to be an Ap star by Niemczura et al. (2015), with Smalley et al. (2015) providing an analysis of the pulsation behavior. Unfortunately, KIC 4768731 was only observed for a single month in SC mode, but does have a full set of LC observations. The SC data allowed for the discovery of a rotationally split triplet in this star, which is understood to be a dipole mode under the oblique pulsator model. As with many of the roAp stars discussed here, KIC 4768731 shows signs of frequency variability in the LC data set (**Figure 7**).

Given the lack of SC data for this star, not much further information could be gained from its light curve. Spectroscopically though, this star shows only weak over abundances of rare earth elements. When considering the numbers of Ap stars in clusters, Abt (2009) was able to estimate the age when peculiarities in Ap stars become strong; for a star the mass of KIC 4768731, this age is about 12% of its total main sequence life time. Therefore, KIC 4768731 may provide an opportunity to revisit the links between age, chemical peculiarities and pulsation in the roAp stars.

2.2. K2 Mission

With the failing of a second reaction wheel needed for precise pointing, the *Kepler* Space Telescope was reconfigured into the K2 mission (Howell et al., 2014). With only two functioning reaction wheels, the spacecraft was balanced against the solar radiation pressure with thruster firings. This configuration provided the opportunity to observe new parts of the sky in high-precision and short cadence and was a welcome change for the observations of roAp stars. Despite the 6 h occurrence of the thruster firings required to maintain precision pointing, these K2 data allowed the detailed analysis of three previously known roAp stars. Despite searches of the K2 data (e.g., Bowman et al., 2018), no new roAp stars have yet been confirmed in the K2 data.

2.2.1. Long Cadence Observations

Only one roAp star was observed in LC mode in the K2 mission: HD 177765. This star was identified as an roAp star through the analysis of time-resolved UVES spectroscopic observations (Alentiev et al., 2012), after a null detection in ground based photometric *B* observations (Martinez and Kurtz, 1994b). At the time of discovery, this star showed the longest period pulsation mode, at 23.6 min.

HD 177765 was observed in campaign 7 in LC mode. The data were analyzed by Holdsworth (2016), where it was found that the star is a multi-periodic roAp star, with three independent modes. The separation of the modes is not consistent with theoretical predictions of the large frequency separation, so an in-depth study could not be presented for this star. The largest separation, at $\sim$ 1.3 d^{-1}, also explains the reporting by Alentiev et al. (2012) of only a single mode, given their short data set.

In the white-light *Kepler* data, the highest amplitude mode has an amplitude of 11.0 ± 0.8 μmag. This is much below the ground-based detection limit, even when considering the amplitude when converting to the *B*-band. It is understandable that Martinez and Kurtz (1994b) did not detect the variability in this star. Given the low amplitude and the short data set for this star, it is not possible to draw any conclusions in the search for frequency variability in this star.

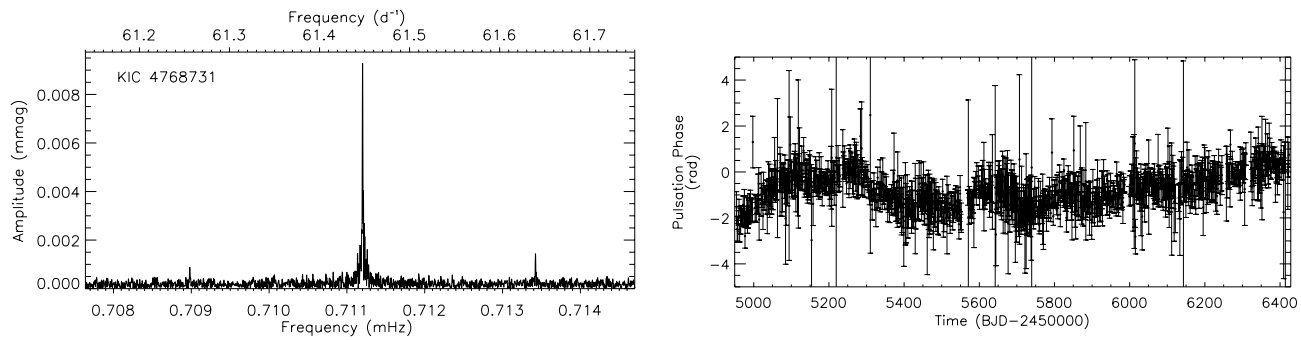

FIGURE 7 | (Left) Amplitude spectrum of the LC data for KIC 4768731. The pulsation mode and two rotationally split, by 2.2218 μHz (5.209 d), sidelobes are evident. **(Right)** Phase variation of the pulsation mode, showing frequency variation in this star.

2.2.2. Short Cadence Observations

Two roAp stars were observed in SC mode by K2: HD 24355 and 33 Lib (HD 137949). HD 24355 had only ground-based photometric survey data available prior to the K2 observations (Holdsworth et al., 2014a), while 33 Lib had been extensively studied with both ground-based photometry and spectroscopy (e.g., Kurtz, 1991; Sachkov et al., 2011, and references therein).

HD 24355 was observed in campaign 4, with the data analyzed by Holdsworth et al. (2016). They found just a single pulsation mode in the star, but with *13* rotationally split sidelobes. The presence of so many sidelobes is a result of significant distortion of the pulsation mode. With the presence of four high-amplitude sidelobes, the authors concluded that the star was pulsating in a quadrupole mode, and were able to model the amplitude variation to that effect.

The pulsation frequency in HD 24355 is much higher that the theoretical upper limit, given the spectroscopic constraints. The observed frequency is $224.304\,\mathrm{d}^{-1}$ whereas the cut-off

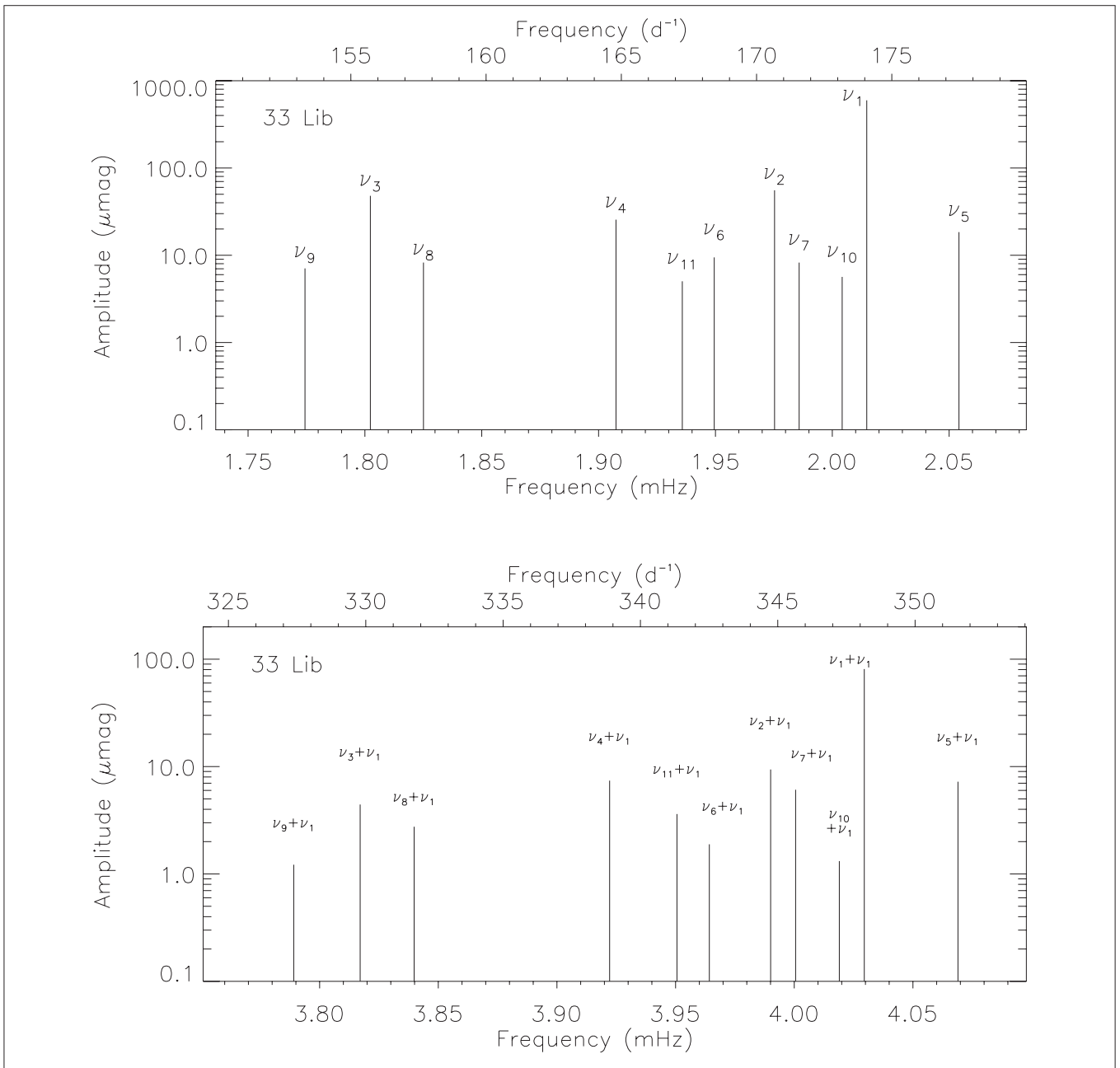

FIGURE 8 | (Top) Schematic view of the pulsations in 33 Lib. Note the logarithmic amplitude scale. **(Bottom)** schematic view of the pulsations around the harmonic. Note that the separation between the modes is the same in the two plots, and not twice in the bottom plot as one would expect.

frequency is about 164 d^{-1}. This brings into question the driving mechanism for this star. It is unclear whether the significant distortion of the mode is related to its super-critical nature. Without the K2 observations, the distortion would probably not have been detected, given that the amplitudes of the extended sidelobes do not exceed 40 μmag in the *Kepler* passband.

33 Lib was observed during campaign 15 of the K2 mission. These data, analyzed by Holdsworth et al. (2018), revealed a much more complex pulsation signature than was previously seen in either photometric or spectroscopic observations. The K2 data confirmed the presence of three modes as detected from the ground, but allowed for the detection of 11 independent modes. However, beyond these 11 modes, there are still signatures of variability in the light curve, as evidenced by excess power in an amplitude spectrum of the residuals. The source of the excess power was not investigated by the authors, but given that the pulsation mode frequencies in 33 Lib are close to the theoretical cut-off frequency, there may be some excitation of short-lived modes by turbulent pressure. However, this is conjecture, and requires investigation.

The main findings of the K2 observations of 33 Lib is the presence of unique non-linear interactions (**Figure 8**). It is common in roAp stars to observe harmonics of the pulsation modes, since they are non-linear in nature. However, rather than a series of harmonics of the 11 modes in 33 Lib, the authors reported the first harmonic of the principal (plus others) was accompanied by 10 peaks with frequencies of the original pulsation frequencies plus the frequency of the principal mode. This is an indication of mode coupling, i.e., frequency mixing due to non-linear effects predominately in the outer portions of the stellar envelope (e.g., Breger and Montgomery, 2014) between the principal mode and the 10 surrounding modes. This was the first time this phenomenon was observed in an roAp star, something that would not have been possible without the *Kepler* mission.

There was no clear frequency variability in 33 Lib during the K2 observations (Holdsworth et al., 2018), however Kurtz (1991) showed a significant change in the pulsation frequency between observations in 1981 and 1987. The K2 observations provide a third epoch where the frequency is different from both the aforementioned data sets. Literature values of the principal pulsation frequency of 33 Lib which cover over 36 year indicate significant frequency variability in this star, as shown in **Figure 9**. However, a careful re-analysis of all available data is needed since there are further epochs of data where either an independent frequency determination and/or error measurement has not been made. These epochs have been omitted from **Figure 9**.

3. SUMMARY

Although *Kepler* did not find the "holy grail" of the roAp stars, i.e., a multi-periodic pulsator with a series of modes in the asymptotic regime, it has provided high-quality data on new and well known roAp stars, and has provided new insights into the pulsation behavior of this class of variable star. From different pulsation axes, to potential low-frequency pulsation, binarity, non-linear interactions, and significant mode distortion, *Kepler* observations have perhaps posed more questions on the fundamental understanding of these stars than they have answered.

In the cases where the full 4 year data sets are available, it seems that all stars show a degree of frequency variability in their

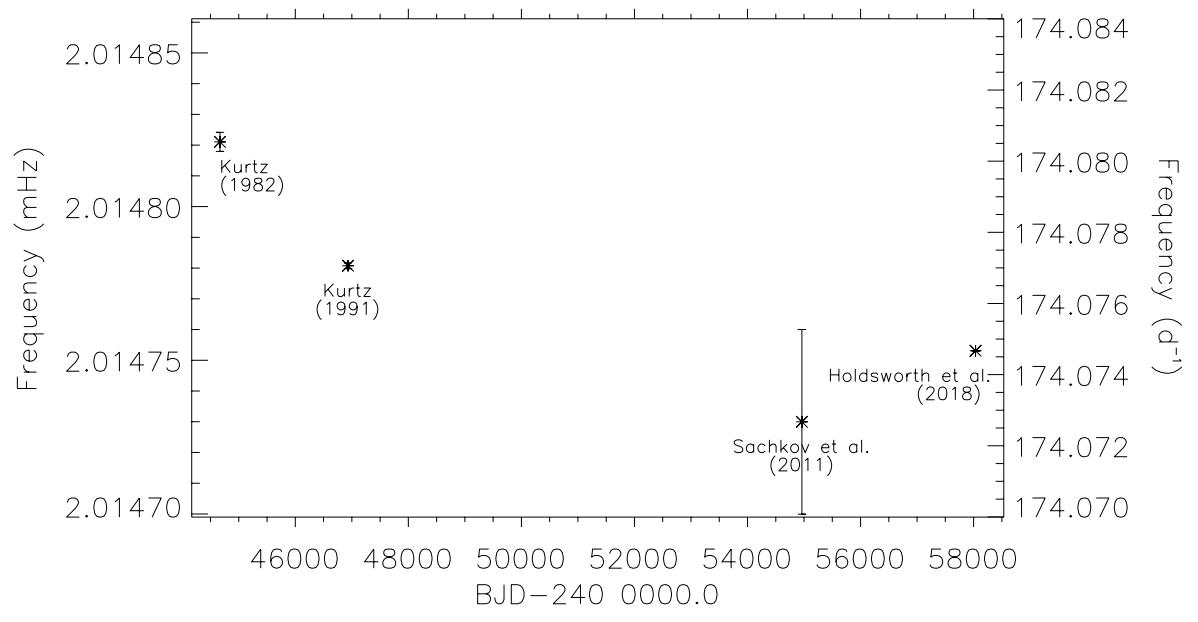

FIGURE 9 | Comparison of the main pulsation frequency reported in 33 Lib over 36 year. There is indication that the pulsation frequency, and thus phase, is variable over the observation period. The references for the data are: Kurtz (1982), Kurtz (1991), Sachkov et al. (2011), and Holdsworth et al. (2018).

modes, a variability that can be different for different modes in a given star. Is this phenomenon present in all roAp stars, or indeed all pulsating stars? This has been observed before from the ground, for example in the roAp star HR 3831 (Kurtz et al., 1994, 1997), although with significant gaps, but with the precision and time-space of the *Kepler* data, physical insight may now be possible. This also poses the question as to whether all roAp stars exhibit such variation, but it is only detected in the most obvious cases, or where data cover a significant time span.

It is possible that these phase variations are the first observations of stochastic perturbations of classical pulsators as discussed by Avelino et al. (2020) and Cunha et al. (2020). In those works, the authors considered models of a damped harmonic oscillator subjected to internal or external forces, and noise, and were able to show that, given a sufficient amount of time, a random phase variation is expected. It is also expected that these random variations are different for different modes in the same star, as was discussed above in the cases of KIC 10195926, for example. This demonstrates the continued legacy of the *Kepler* data set.

It is expected that NASA's next generation planet hunting mission, the Transiting Exoplanet Survey Satellite *TESS* (Ricker et al., 2015) will revisit all of the *Kepler* observed roAp stars, and indeed all roAp stars providing a homogeneous sample to draw statistical inference from. However, with observations as short as 27-d, with a maximum of almost 1-yr of (almost) uninterrupted data, the *TESS* observations will not provide the precision that *Kepler* did. This, coupled with the less favorable (for roAp stars) redder passband of *TESS*, means that the *Kepler* data on the roAp stars will be the definitive data for precise studies of the roAp stars.

DATA AVAILABILITY STATEMENT

Publicly available datasets were analyzed in this study. This data can be found at: *Kepler*; https://archive.stsci.edu.

AUTHOR CONTRIBUTIONS

The author confirms being the sole contributor of this work and has approved it for publication.

FUNDING

DH acknowledges financial support from the Science and Technology Facilities Council (STFC) via grant ST/M000877/1.

ACKNOWLEDGMENTS

I thank the referees for constructive comments and suggestions on the manuscript. This paper includes data collected by the Kepler mission. Funding for the Kepler mission is provided by the NASA Science Mission directorate. The author gratefully acknowledge the Kepler Science Team and all those who have contributed to making the Kepler mission possible.

REFERENCES

Abt, H. A. (2009). Why are there normal slow rotators among A-type stars? *Astron. J.* 138, 28–32. doi: 10.1088/0004-6256/138/1/28

Abt, H. A., and Morrell, N. I. (1995). The relation between rotational velocities and spectral peculiarities among A-type stars. *Astrophys. J. Suppl. Ser.* 99:135. doi: 10.1086/192182

Adelman, S. J. (2004). "The physical properties of normal A stars," in *The A-Star Puzzle, Vol. 224 of IAU Symposium*, eds J. Zverko, J. Ziznovsky, S. J. Adelman, and W. W. Weiss (Cambridge, UK), 1–11. doi: 10.1017/S1743921304004314

Aerts, C., Christensen-Dalsgaard, J., and Kurtz, D. W. (2010). *Asteroseismology*. Berlin: Springer. doi: 10.1007/978-1-4020-5803-5

Alentiev, D., Kochukhov, O., Ryabchikova, T., Cunha, M., Tsymbal, V., and Weiss, W. (2012). Discovery of the longest period rapidly oscillating Ap star HD 177765. *Mon. Not. R. Astron. Soc.* 421, L82–L86. doi: 10.1111/j.1745-3933.2011.01211.x

Avelino, P. P., Cunha, M. S., and Chaplin, W. J. (2020). Modelling stochastic signatures in classical pulsators. *Mon. Not. R. Astron. Soc.* 492, 4477–4483. doi: 10.1093/mnras/staa125

Babcock, H. W. (1960). The 34-KILOGAUSS magnetic field of HD 215441. *Astrophys. J.* 132:521. doi: 10.1086/146960

Balmforth, N. J., Cunha, M. S., Dolez, N., Gough, D. O., and Vauclair, S. (2001). On the excitation mechanism in roAp stars. *Mon. Not. R. Astron. Soc.* 323, 362–372. doi: 10.1046/j.1365-8711.2001.04182.x

Balona, L. A., Catanzaro, G., Crause, L., Cunha, M. S., Gandolfi, D., Hatzes, A., et al. (2013). The unusual roAp star KIC 8677585. *Mon. Not. R. Astron. Soc.* 432, 2808–2817. doi: 10.1093/mnras/stt636

Balona, L. A., Cunha, M. S., Gruberbauer, M., Kurtz, D. W., Saio, H., White, T. R., et al. (2011a). Rotation and oblique pulsation in Kepler observations of the roAp star KIC 10483436. *Mon. Not. R. Astron. Soc.* 413, 2651–2657. doi: 10.1111/j.1365-2966.2011.18334.x

Balona, L. A., Cunha, M. S., Kurtz, D. W., Brandão, I. M., Gruberbauer, M., Saio, H., et al. (2011b). Kepler observations of rapidly oscillating Ap, δScuti and γDoradus pulsations in Ap stars. *Mon. Not. R. Astron. Soc.* 410, 517–524. doi: 10.1111/j.1365-2966.2010.17461.x

Bertelli, G., Girardi, L., Marigo, P., and Nasi, E. (2008). Scaled solar tracks and isochrones in a large region of the Z-Y plane. I. From the ZAMS to the TP-AGB end for 0.15-2.5 $M_{\odot}$ stars. *Astron. Astrophys.* 484, 815–830. doi: 10.1051/0004-6361:20079165

Bigot, L., and Dziembowski, W. A. (2002). The oblique pulsator model revisited. *Astron. Astrophys.* 391, 235–245. doi: 10.1051/0004-6361:20020824

Bigot, L., and Kurtz, D. W. (2011). Theoretical light curves of dipole oscillations in roAp stars. *Astron. Astrophys.* 536:A73. doi: 10.1051/0004-6361/201116981

Bowman, D. M., Buysschaert, B., Neiner, C., Pápics, P. I., Oksala, M. E., and Aerts, C. (2018). K2 space photometry reveals rotational modulation and stellar pulsations in chemically peculiar A and B stars. *Astron. Astrophys.* 616:A77. doi: 10.1051/0004-6361/201833037

Breger, M., and Montgomery, M. H. (2014). Evidence of resonant mode coupling and the relationship between low and high frequencies in a rapidly rotating a star. *Astrophys. J.* 783:89. doi: 10.1088/0004-637X/783/2/89

Chaplin, W. J., and Miglio, A. (2013). Asteroseismology of solar-type and red-giant stars. *Annu. Rev. Astron. Astrophys.* 51, 353–392. doi: 10.1146/annurev-astro-082812-140938

Cunha, M. S. (2001). The sixth frequency of roAp star HR 1217. *Mon. Not. R. Astron. Soc.* 325, 373–378. doi: 10.1046/j.1365-8711.2001.04434.x

Cunha, M. S. (2002). A theoretical instability strip for rapidly oscillating Ap stars. *Mon. Not. R. Astron. Soc.* 333, 47–54. doi: 10.1046/j.1365-8711.2002.05377.x

Cunha, M. S., Alentiev, D., Brand ao, I. M., and Perraut, K. (2013). Testing excitation models of rapidly oscillating Ap stars with interferometry. *Mon. Not. R. Astron. Soc.* 436, 1639–1647. doi: 10.1093/mnras/stt1679

Cunha, M. S., Antoci, V., Holdsworth, D. L., Kurtz, D. W., Balona, L. A., Bognár, Z., et al. (2019). Rotation and pulsation in Ap stars: first light results from TESS sectors 1 and 2. *Mon. Not. R. Astron. Soc.* 487, 3523–3549. doi: 10.1093/mnras/stz1332

Cunha, M. S., Avelino, P. P., and Chaplin, W. J. (2020). From Solar-like to Mira stars: a unifying description of stellar pulsators in the presence of stochastic noise. *Mon. Not. R. Astron. Soc.* 499, 4687–4697. doi: 10.1093/mnras/staa2932

Cunha, M. S., and Gough, D. (2000). Magnetic perturbations to the acoustic modes of roAp stars. *Mon. Not. R. Astron. Soc.* 319, 1020–1038. doi: 10.1046/j.1365-8711.2000.03896.x

Drury, J. A., Murphy, S. J., Derekas, A., Sódor, Á., Stello, D., Kuehn, C. A., et al. (2017). Large amplitude change in spot-induced rotational modulation of the Kepler Ap star KIC 2569073. *Mon. Not. R. Astron. Soc.* 471, 3193–3199. doi: 10.1093/mnras/stx1722

Elkin, V. G., Mathys, G., Kurtz, D. W., Hubrig, S., and Freyhammer, L. M. (2010). A rival for Babcock's star: the extreme 30-kG variable magnetic field in the Ap star HD75049. *Mon. Not. R. Astron. Soc.* 402, 1883–1891. doi: 10.1111/j.1365-2966.2009.16015.x

Ferrario, L., Pringle, J. E., Tout, C. A., and Wickramasinghe, D. T. (2009). The origin of magnetism on the upper main sequence. *Mon. Not. R. Astron. Soc.* 400, L71–L74. doi: 10.1111/j.1745-3933.2009.00765.x

Freyhammer, L. M., Elkin, V. G., Kurtz, D. W., Mathys, G., and Martinez, P. (2008). Discovery of 17 new sharp-lined Ap stars with magnetically resolved lines. *Mon. Not. R. Astron. Soc.* 389, 441–460. doi: 10.1111/j.1365-2966.2008.13595.x

Gautschy, A., Saio, H., and Harzenmoser, H. (1998). How to drive roAp stars. *Mon. Not. R. Astron. Soc.* 301, 31–41. doi: 10.1046/j.1365-8711.1998.01960.x

Gilliland, R. L., Brown, T. M., Christensen-Dalsgaard, J., Kjeldsen, H., Aerts, C., Appourchaux, T., et al. (2010). Kepler asteroseismology program: introduction and first results. *Publ. Astron. Soc. Pac.* 122:131. doi: 10.1086/650399

Gray, R. O., and Corbally, C. J. (2009). *Stellar Spectral Classification*. Princeton, NJ: Princeton University Press.

Handler, G., Kurtz, D. W., Rappaport, S. A., Saio, H., Fuller, J., Jones, D., et al. (2020). Tidally trapped pulsations in a close binary star system discovered by TESS. *Nat. Astron.* 4, 684–689. doi: 10.1038/s41550-020-1035-1

Hey, D. R., Holdsworth, D. L., Bedding, T. R., Murphy, S. J., Cunha, M. S., Kurtz, D. W., et al. (2019). Six new rapidly oscillating Ap stars in the Kepler long-cadence data using super-Nyquist asteroseismology. *Mon. Not. R. Astron. Soc.* 488, 18–36. doi: 10.1093/mnras/stz1633

Holdsworth, D. L. (2016). Detection of new pulsations in the roAp star HD 177765. *Inform. Bull. Var. Stars* 6185:1. doi: 10.22444/IBVS.6185

Holdsworth, D. L., Cunha, M. S., Shibahashi, H., Kurtz, D. W., and Bowman, D. M. (2018). K2 observations of the rapidly oscillating Ap star 33 Lib (HD 137949): new frequencies and unique non-linear interactions. *Mon. Not. R. Astron. Soc.* 480, 2976–2984. doi: 10.1093/mnras/sty2053

Holdsworth, D. L., Kurtz, D. W., Smalley, B., Saio, H., Handler, G., Murphy, S. J., et al. (2016). HD 24355 observed by the Kepler K2 mission: a rapidly oscillating Ap star pulsating in a distorted quadrupole mode. *Mon. Not. R. Astron. Soc.* 462, 876–892. doi: 10.1093/mnras/stw1711

Holdsworth, D. L., Smalley, B., Gillon, M., Clubb, K. I., Southworth, J., Maxted, P. F. L., et al. (2014a). High-frequency A-type pulsators discovered using SuperWASP. *Mon. Not. R. Astron. Soc.* 439, 2078–2095. doi: 10.1093/mnras/stu094

Holdsworth, D. L., Smalley, B., Kurtz, D. W., Southworth, J., Cunha, M. S., and Clubb, K. I. (2014b). KIC 7582608: a new Kepler roAp star with frequency variability. *Mon. Not. R. Astron. Soc.* 443, 2049–2062. doi: 10.1093/mnras/stu1303

Howell, S. B., Sobeck, C., Haas, M., Still, M., Barclay, T., Mullally, F., et al. (2014). The K2 Mission: Characterization and Early Results. *Publ. Astron. Soc. Pac.* 126:398. doi: 10.1086/676406

Joshi, S., Martinez, P., Chowdhury, S., Chakradhari, N. K., Joshi, Y. C., van Heerden, P., et al. (2016). The Nainital-Cape Survey. IV. A search for pulsational variability in 108 chemically peculiar stars. *Astron. Astrophys.* 590:A116. doi: 10.1051/0004-6361/201527242

Koch, D. G., Borucki, W. J., Basri, G., Batalha, N. M., Brown, T. M., Caldwell, D., et al. (2010). Kepler mission design, realized photometric performance, and early science. *Astrophys. J. Lett.* 713, L79–L86. doi: 10.1088/2041-8205/713/2/L79

Kochukhov, O., Alentiev, D., Ryabchikova, T., Boyko, S., Cunha, M., Tsymbal, V., et al. (2013). Discovery of new rapidly oscillating Ap pulsators in the UVES survey of cool magnetic Ap stars. *Mon. Not. R. Astron. Soc.* 431, 2808–2819. doi: 10.1093/mnras/stt377

Kurtz, D. W. (1978). 12.15 Minute Light Variations in Przybylski's Star, HD 101065. *Inform. Bull. Var. Stars* 1436:1.

Kurtz, D. W. (1982). Rapidly oscillating AP stars. *Mon. Not. R. Astron. Soc.* 200, 807–859. doi: 10.1093/mnras/200.3.807

Kurtz, D. W. (1991). Afrequency analysis of new observations of the rapidly oscillating AP star (HD 137949) 33 Lib : an apparent change of frequency and detection of the first harmonic. *Mon. Not. R. Astron. Soc.* 249:468. doi: 10.1093/mnras/249.3.468

Kurtz, D. W. (1992). Axisymmetric spherical harmonic decomposition of the pulsation modes in rapidly oscillating AP stars. *Mon. Not. R. Astron. Soc.* 259, 701–708. doi: 10.1093/mnras/259.4.701

Kurtz, D. W., Cameron, C., Cunha, M. S., Dolez, N., Vauclair, G., Pallier, E., et al. (2005). Pushing the ground-based limit: 14-μmag photometric precision with the definitive Whole Earth Telescope asteroseismic data set for the rapidly oscillating Ap star HR1217. *Mon. Not. R. Astron. Soc.* 358, 651–664. doi: 10.1111/j.1365-2966.2005.08807.x

Kurtz, D. W., Cunha, M. S., Saio, H., Bigot, L., Balona, L. A., Elkin, V. G., et al. (2011). The first evidence for multiple pulsation axes: a new rapidly oscillating Ap star in the Kepler field, KIC 10195926. *Mon. Not. R. Astron. Soc.* 414, 2550–2566. doi: 10.1111/j.1365-2966.2011.18572.x

Kurtz, D. W., Handler, G., Rappaport, S. A., Saio, H., Fuller, J., Jacobs, T., et al. (2020). The single-sided pulsator CO Camelopardalis. *Mon. Not. R. Astron.* Soc. 494, 5118–5133. doi: 10.1093/mnras/staa989

Kurtz, D. W., and Holdsworth, D. L. (2020). Oblique pulsation: new, challenging observations with TESS data. *Astrophys. Space Sci. Proc.* 57, 313–319. doi: 10.1007/978-3-030-55336-4_43

Kurtz, D. W., Marang, F., van Wyk, F., and Roberts, G. (1996). The determination of the rotational periods of the rapidly oscillating AP stars from their mean light variations - V. an improved rotation period for the dipole pulsator HD 6532. *Mon. Not. R. Astron. Soc.* 280, 1–5. doi: 10.1093/mnras/280.1.1

Kurtz, D. W., Martinez, P., van Wyk, F., Marang, F., and Roberts, G. (1994). Cyclic frequency variability in the rapidly oscillating Ap-star HD3831. *Mon. Not. R. Astron. Soc.* 268:641. doi: 10.1093/mnras/268.3.641

Kurtz, D. W., van Wyk, F., Roberts, G., Marang, F., Handler, G., Medupe, R., et al. (1997). Frequency variability in the rapidly oscillating AP star HR 3831: three more years of monitoring. *Mon. Not. R. Astron. Soc.* 287, 69–78. doi: 10.1093/mnras/287.1.69

Lüftinger, T., Kochukhov, O., Ryabchikova, T., Piskunov, N., Weiss, W. W., and Ilyin, I. (2010). Magnetic Doppler imaging of the roAp star HD 24712. *Astron. Astrophys.* 509:A71. doi: 10.1051/0004-6361/200811545

Martinez, P., and Kurtz, D. W. (1994a). The Cape rapidly oscillating Ap star survey. II. Discovery of another six new roAp stars. *Mon. Not. R. Astron. Soc.* 271, 118–128. doi: 10.1093/mnras/271.1.118

Martinez, P., and Kurtz, D. W. (1994b). The Cape rapidly oscillating Ap star survey. III. Null results of searches for high-overtone pulsation. *Mon. Not. R. Astron. Soc.* 271, 129–154. doi: 10.1093/mnras/271.1.129

Martinez, P., Kurtz, D. W., and Kauffmann, G. M. (1991). The Cape rapidly oscillating star survey-I. First results. *Mon. Not. R. Astron. Soc.* 250:666. doi: 10.1093/mnras/250.4.666

Martinez, P., Kurtz, D. W., and van Wyk, F. (1994). The discovery of frequency variability in the pulsations of the rapidly oscillating Ap star HD 12932. *Mon. Not. R. Astron. Soc.* 271, 305–316. doi: 10.1093/mnras/271.2.305

Mathys, G. (2017). Ap stars with resolved magnetically split lines: Magnetic field determinations from Stokes I and V spectra⋆. *Astron. Astrophys.* 601:A14. doi: 10.1051/0004-6361/201628429

Mathys, G., Kurtz, D. W., and Holdsworth, D. L. (2020). Long period Ap stars discovered with TESS data. *arXiv e-prints arXiv:2003.14144*. doi: 10.1051/0004-6361/202038007

Murphy, S. J., Bedding, T. R., Shibahashi, H., Kurtz, D. W., and Kjeldsen, H. (2014). Finding binaries among Kepler pulsating stars from phase modulation of their pulsations. *Mon. Not. R. Astron. Soc.* 441, 2515–2527. doi: 10.1093/mnras/stu765

Murphy, S. J., Moe, M., Kurtz, D. W., Bedding, T. R., Shibahashi, H., and Boffin, H. M. J. (2018). Finding binaries from phase modulation of pulsating stars with Kepler: V. Orbital parameters, with eccentricity and mass-ratio distributions of 341 new binaries. *Mon. Not. R. Astron. Soc.* 474, 4322–4346. doi: 10.1093/mnras/stx3049

Murphy, S. J., and Shibahashi, H. (2015). Deriving the orbital properties of pulsators in binary systems through their light arrival time delays. *Mon. Not. R. Astron. Soc.* 450, 4475–4485. doi: 10.1093/mnras/stv884

Murphy, S. J., Shibahashi, H., and Kurtz, D. W. (2013). Super-Nyquist asteroseismology with the Kepler Space Telescope. *Mon. Not. R. Astron. Soc.* 430, 2986–2998. doi: 10.1093/mnras/stt105

Neilson, H. R., Percy, J. R., and Smith, H. A. (2016). Period changes and evolution in pulsating variable stars. *J. Am. Assoc. Var. Star Observ.* 44:179.

Niemczura, E., Murphy, S. J., Smalley, B., Uytterhoeven, K., Pigulski, A., Lehmann, H., et al. (2015). Spectroscopic survey of Kepler stars. I. HERMES/Mercator observations of A- and F-type stars. *Mon. Not. R. Astron. Soc.* 450, 2764–2783. doi: 10.1093/mnras/stv528

Paunzen, E., Netopil, M., Rode-Paunzen, M., Handler, G., Božić, H., Ruždjak, D., et al. (2012). The Hvar survey for roAp stars. I. The survey observations. *Astron. Astrophys.* 542:A89. doi: 10.1051/0004-6361/201118752

Ricker, G. R., Winn, J. N., Vanderspek, R., Latham, D. W., Bakos, G. Á., Bean, J. L., et al. (2015). Transiting exoplanet survey satellite (TESS). *J. Astron. Telesc. Instrum. Syst.* 1:014003. doi: 10.1117/1.JATIS.1.1.014003

Sachkov, M., Hareter, M., Ryabchikova, T., Wade, G., Kochukhov, O., Shulyak, D., et al. (2011). Pulsations in the atmosphere of the rapidly oscillating star 33 Lib. *Mon. Not. R. Astron. Soc.* 416, 2669–2677. doi: 10.1111/j.1365-2966.2011.19219.x

Saio, H. (2005). A non-adiabatic analysis for axisymmetric pulsations of magnetic stars. *Mon. Not. R. Astron. Soc.* 360, 1022–1032. doi: 10.1111/j.1365-2966.2005.09091.x

Saio, H., and Gautschy, A. (2004). Axisymmetric p-mode pulsations of stars with dipole magnetic fields. *Mon. Not. R. Astron. Soc.* 350, 485–505. doi: 10.1111/j.1365-2966.2004.07659.x

Saio, H., Kurtz, D. W., Murphy, S. J., Antoci, V. L., and Lee, U. (2018). Theory and evidence of global Rossby waves in upper main-sequence stars: r-mode oscillations in many Kepler stars. *Mon. Not. R. Astron. Soc.* 474, 2774–2786. doi: 10.1093/mnras/stx2962

Shi, F., Kurtz, D., Saio, H., Fu, J., and Zhang, H. (2020). Pulsations of the rapidly oscillating Ap Star KIC 10685175 revisited by TESS. *Astrophys. J.* 901:15. doi: 10.3847/1538-4357/abae59

Shibahashi, H. (1979). Modal analysis of stellar nonradial oscillations by an asymptotic method. *Publ. Astron. Soc. Jpn.* 31, 87–104.

Shibahashi, H., and Kurtz, D. W. (2012). FM stars: a Fourier view of pulsating binary stars, a new technique for measuring radial velocities photometrically. *Mon. Not. R. Astron. Soc.* 422, 738–752. doi: 10.1111/j.1365-2966.2012.20654.x

Shibahashi, H., Kurtz, D. W., and Murphy, S. J. (2015). FM stars II: a Fourier view of pulsating binary stars - determining binary orbital parameters photometrically for highly eccentric cases. *Mon. Not. R. Astron. Soc.* 450, 3999–4015. doi: 10.1093/mnras/stv875

Shibahashi, H., and Saio, H. (1985a). On the rotational frequency splitting in oblique pulsators. *Publ. Astron. Soc. Jpn.* 37, 601–607.

Shibahashi, H., and Saio, H. (1985b). Rapid oscillations of AP stars. *Publ. Astron. Soc. Jpn.* 37, 245–259.

Shibahashi, H., and Takata, M. (1993). Theory for the distorted dipole modes of the rapidly oscillating AP stars: a refinement of the oblique pulsator model. *Publ. Astron. Soc. Jpn.* 45, 617–641.

Smalley, B., Niemczura, E., Murphy, S. J., Lehmann, H., Kurtz, D. W., Holdsworth, D. L., et al. (2015). KIC 4768731: a bright long-period roAp star in the Kepler field. *Mon. Not. R. Astron. Soc.* 452, 3334–3345. doi: 10.1093/mnras/stv1515

Sousa, J. C., and Cunha, M. S. (2011). On the understanding of pulsations in the atmosphere of roAp stars: phase diversity and false nodes. *Mon. Not. R. Astron. Soc.* 414, 2576–2593. doi: 10.1111/j.1365-2966.2011.18573.x

Stępień, K. (2000). Loss of angular momentum of magnetic Ap stars in the pre-main sequence phase. *Astron. Astrophys.* 353, 227–238.

Stibbs, D. W. N. (1950). A study of the spectrum and magnetic variable star HD 125248. *Mon. Not. R. Astron. Soc.* 110:395. doi: 10.1093/mnras/110.4.395

Tassoul, M. (1980). Asymptotic approximations for stellar nonradial pulsations. *Astrophys. J. Suppl. Ser.* 43, 469–490. doi: 10.1086/190678

Tassoul, M. (1990). Second-order asymptotic approximations for stellar nonradial acoustic modes. *Astrophys. J.* 358:313. doi: 10.1086/168988

Tutukov, A. V., and Fedorova, A. V. (2010). Possible scenarios for the formation of Ap/Bp stars. *Astron. Rep.* 54, 156–162. doi: 10.1134/S1063772910020083

Conflict of Interest: The author declares that the research was conducted in the absence of any commercial or financial relationships that could be construed as a potential conflict of interest.

frontiers in Astronomy and Space Sciences

REVIEW
published: 20 April 2021
doi: 10.3389/fspas.2021.653558

Highlights of Discoveries for δ Scuti Variable Stars From the *Kepler* Era

*Joyce Ann Guzik**

Los Alamos National Laboratory, Los Alamos, NM, United States

The NASA *Kepler* and follow-on K2 mission (2009–2018) left a legacy of data and discoveries, finding thousands of exoplanets, and also obtaining high-precision long time-series data for hundreds of thousands of stars, including many types of pulsating variables. Here we highlight a few of the ongoing discoveries from *Kepler* data on δ Scuti pulsating variables, which are core hydrogen-burning stars of about twice the mass of the Sun. We discuss many unsolved problems surrounding the properties of the variability in these stars, and the progress enabled by *Kepler* data in using pulsations to infer their interior structure, a field of research known as asteroseismology.

Keywords: stars: δ Scuti, stars: γ Doradus, NASA *Kepler* mission, asteroseismology, stellar pulsation

OPEN ACCESS

Edited by:
Karen Kinemuchi,
New Mexico State University,
United States

Reviewed by:
Dominic Bowman,
KU Leuven, Belgium
Mike Reed,
Missouri State University,
United States

***Correspondence:**
Joyce Ann Guzik
joy@lanl.gov

Specialty section:
This article was submitted to Stellar and Solar Physics, a section of the journal Frontiers in Astronomy and Space Sciences

Received: *14 January 2021*
Accepted: *22 March 2021*
Published: *20 April 2021*

Citation:
Guzik JA (2021) Highlights of Discoveries for δ Scuti Variable Stars From the Kepler Era. Front. Astron. Space Sci. 8:653558. doi: 10.3389/fspas.2021.653558

1. INTRODUCTION

The long time-series, high-cadence, high-precision photometric observations of the NASA *Kepler* (2009-2013) (Borucki et al., 2010; Gilliland et al., 2010; Koch et al., 2010) and follow-on K2 (2014-2018) (Howell et al., 2014) missions have revolutionized the study of stellar variability. The amount and quality of data provided by *Kepler* is nearly overwhelming, and will motivate follow-on observations and generate new discoveries for decades to come.

Here we review some highlights of discoveries for δ Scuti (abbreviated as δ Sct) variable stars from the *Kepler* mission. The δ Sct variables are pre-main-sequence, main-sequence (core hydrogen-burning), or post-main-sequence (undergoing core contraction after core hydrogen-burning, and beginning shell hydrogen-burning) stars with spectral types A through mid-F, and masses around two solar masses. They pulsate in one or more radial and non-radial modes with periods of around 2 h. The pulsations are driven mainly by the "κ-effect" (opacity-valving) mechanism in the region of the second ionization of helium at temperatures around 50,000 K in the stellar envelope (Aerts et al., 2010).

Several reviews on *Kepler* findings for δ Sct variables have already been written (see, e.g., Balona, 2018; Bowman and Kurtz, 2018), and a comprehensive review of the *Kepler* legacy for these stars is premature. Prior to *Kepler*, one of the best compilations of the state-of-the-art of research on δ Sct variables was the Handbook and Conference Proceedings volume *δ Scuti and Related Stars* (Breger and Montgomery, 2000). New catalogs and lists of variable stars, including δ Sct stars observed and first discovered by the *Kepler*/K2 missions, have begun to appear [e.g., Bradley et al., 2015, 2016, 84 δ Sct and 32 hybrid (see section 2.1) candidates from *Kepler* Guest Observer Program Cycle 1–5 observations; Murphy et al., 2019, 1988 δ Sct stars from *Kepler* observations; Guzik et al., 2019, 249 δ Sct candidates from K2 observations].

After the successes of asteroseismology to infer the interior structure of the Sun and properties of sun-like stars, studying the slightly more massive δ Sct stars appeared to be a promising next direction for asteroseismology. Before the space observations of *Kepler*, CoRoT (see, e.g., Poretti et al., 2009), and MOST (see, e.g., Matthews, 2007), there existed only around a dozen δ Sct stars

with long time-series observations from ground-based networks allowing the detection of a large number of pulsation modes [e.g., FG Vir (Breger et al., 2005) or 4 CVn (Breger et al., 2017)] that could be used to constrain stellar models. The field of δ Sct asteroseismology has been impeded by the problem of mode identification for several reasons. Unlike for the Sun, the disks of distant stars cannot be highly resolved, so only low-degree ($\ell \lesssim 3$) mode variations that do not average out over the disk can be detected photometrically. Furthermore, most of these stars rotate more rapidly than the Sun, resulting in large and uneven rotational splittings, such that multiplets of adjacent modes can overlap. In addition, not all of the modes expected by non-adiabatic pulsation calculations are found in the observations. Finally, the modes are of low radial order n, and therefore the spacing pattern is not expected to show regular large separations seen for the higher-order stochastically excited solar-like modes where $n \sim 20$ and the modes can be described using asymptotic theory ($n \gg \ell$; see, e.g., García and Ballot, 2019). Unlike for the Sun, fundamental properties of a single δ Sct variable (mass, radius, age, detailed element abundances) cannot be derived from complementary or independent observations (e.g., meteorites, Earth, or planetary orbits). δ Sct stars in clusters, binaries, or having planetary systems are therefore useful to provide additional constraints for modeling.

The A-F main-sequence stars occupy a small region in the center of the H-R diagram, but have been differentiated into not only δ Sct and γ Doradus (abbreviated as γ Dor) variables (Pollard, 2009; Balona et al., 2011a), but also metallic-line A (Am) (Smalley et al., 2017), peculiar abundance A (Ap) (Mathys et al., 2020), rapidly-oscillating Ap (roAp) (Holdsworth, 2021) stars, α^2 CVn variables (Sikora et al., 2019), λ Boo stars (Murphy and Paunzen, 2017), the High Amplitude δ Sct (HADS) (McNamara, 2000) and SX Phe (Nemec et al., 2017) stars, blue stragglers (Rain et al., 2021), and the maybe "mythical"[1] Maia variables (Breger, 1980; Cox, 1983; Daszyńska-Daszkiewicz et al., 2017; White et al., 2017; Balona, 2018). *Kepler* observations have revealed overlap and commonalities among these types, pointing the way to a more fundamental understanding of the origins of the diverse phenomena seen in these stars.

While these stars were expected at first to be the next straightforward step beyond the solar-like oscillators for applications of asteroseismology, this goal has turned out to be more difficult to achieve than expected. However, the many complexities of these stars make this field of variable star research rich in potential discoveries.

[1]This term was coined by Breger (1980) re. reports of pulsating variables between the main-sequence δ Sct and Slowly-Pulsating B-type stars in the H-R diagram. There has been debate in the literature about whether these variables actually exist, what drives their pulsations, and whether they should be considered a separate class of variable stars. The prototype Maia, a member of the Pleiades, has been shown not to pulsate (see, e.g., White et al., 2017). Other proposed members of the class may be rapidly rotating SPB stars, or be slowly rotating, but have pulsations driven by the κ effect with enhanced opacity around 125,000 K (Daszyńska-Daszkiewicz et al., 2017).

2. DISCOVERY HIGHLIGHTS

2.1. Pre- and Post-*Kepler* View–Hybrids Everywhere!

Before *Kepler*, the δ Sct and γ Dor stars and their hybrids were found in the instability regions expected by theory. The δ Sct p-mode pulsations are driven by the κ mechanism in their radiative envelopes, but the longer period (1–3 day) γ Dor g-mode pulsations are proposed to be driven by the "convective blocking" mechanism operating at the base of their convective envelope around 300,000 K (Guzik et al., 2000). Using a time-dependent convection treatment, hybrid stars pulsating in both p and g modes were expected and found in a small region of the H-R diagram where these two instability regions overlapped (Dupret et al., 2005).

Just after the first *Kepler* light curves were received, it became apparent that this picture would be shattered. δ Sct and γ Dor variables and their hybrids were found throughout and even somewhat beyond the edges of the combined instability regions (Grigahcène et al., 2010; Uytterhoeven et al., 2011) (see **Figure 1**). Low-frequency pulsation modes identified using the long (30-min) cadence *Kepler* data could have been mis-identified as γ Dor g modes, but actually may be Nyquist reflections of frequencies above 24.5 d^{-1}. However, the low frequencies are also found using short (1-min) cadence data, and Nyquist reflection frequencies can be distinguished using a long-enough series (near one *Kepler* orbital period of 375.2 d) of long-cadence data (Murphy et al., 2013). Some low frequencies could possibly be caused by rotation/starspots, undetected binary companions, rotational perturbations of higher frequency modes, combination frequencies, a background star or nearby bright star in the field of view contaminating the light curve, or Rossby or Kelvin waves. However, Balona (2014), using only short-cadence data, ruled out most of these explanations, and arrives at the bold conclusion that "all δ Sct stars are essentially δ Sct/γ Dor hybrids."

On the other hand, there exist examples of δ Sct stars that do not show g-mode pulsations in the *Kepler* data. Bowman (2017) comments on Balona's claim, and discusses an example of a "pure" δ Sct star KIC 5617488, which has no low-frequency peaks with S/N $\geq$ 4. The few low-frequency peaks visible in the amplitude spectrum have amplitude less a few μmag. It is possible that g modes with angular degree $\ell \gtrsim 3$ are undetected in many stars photometrically, but may be discovered spectroscopically. Such modes have been identified in γ Dor variables (Pollard et al., 2013), but usually are also accompanied by higher amplitude $\ell = 1$ modes.

New pulsation driving mechanisms are being investigated. For example, Balona et al. (2015b) find that an opacity increase of about a factor of two near temperatures of 115,000 K ($\log T = 5.06$) in the stellar envelope can result in instability of some low-frequency modes, but this opacity bump also reduces the range of unstable high-frequency modes. Balona (2018) highlights theoretical and computational work by Xiong et al. (2016) with a new treatment of time-dependent convection that allows δ Sct stars to pulsate in low-frequency modes.

2.2. The "Superstar" and a New Pulsation Driving Mechanism

A δ Sct star that attracted early excitement was HD 187547 (KIC 7548479), known as the "superstar," observed by *Kepler* in short cadence. This star shows not only the expected δ Sct pulsation modes, but also some additional modes of somewhat higher frequency superimposed (**Figure 2**). Antoci et al. (2011) suggested that convection was stochastically exciting these modes, despite the fact that δ Sct star models do not have large efficient envelope convection zones, making this star the first δ Sct/solar-like oscillator discovered. However, continued *Kepler* observations showed that the mode lifetimes were quite long, longer than 960 days, and may in fact be "coherent," i.e., not stochastically excited. Antoci et al. (2014) proposed a new pulsation driving mechanism for these higher-frequency modes, the 'turbulent pressure' mechanism, operating in the outer convective layers of these stars. They illustrated this mechanism using models including a time-dependent convection treatment applied to radial modes. This discovery was one of several from the *Kepler* data resulting in a suggested new pulsation driving mechanism.

2.3. "Constant" Stars in the δ Sct Instability Region

While the *Kepler* data confused the picture of the instability regions for δ Sct and γ Dor stars and their hybrids, these data

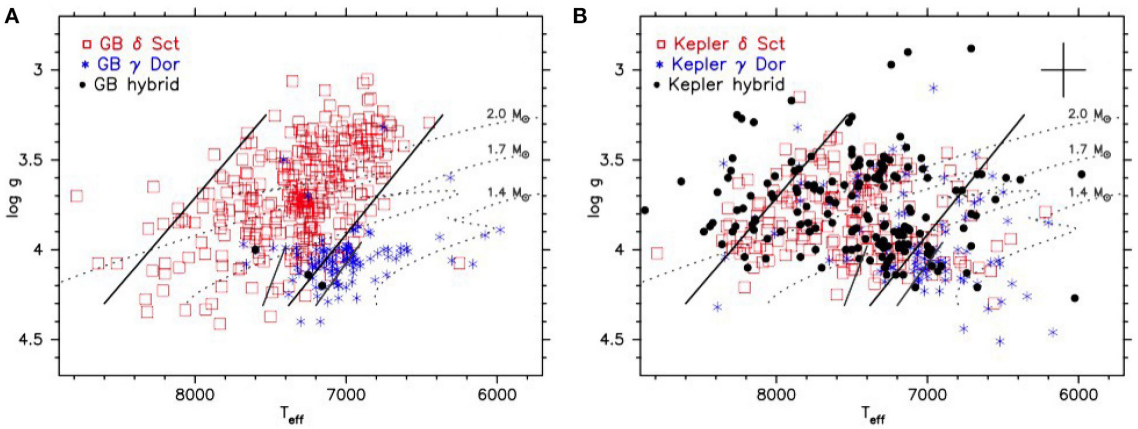

FIGURE 1 | Figure 10 from Uytterhoeven et al. (2011): **(A)** Log surface gravity vs. $T_{\rm eff}$ for the δ Sct, γ Dor, and hybrid stars detected from the ground (parameters taken from the literature). **(B)** Log surface gravity vs. $T_{\rm eff}$ for *Kepler* stars classified as δ Sct, γ Dor, and hybrid stars by Uytterhoeven et al. (2011). Open red squares represent δ Sct stars, blue asterisks indicate γ Dor stars, and hybrid stars are marked by black bullets. The black cross in the right top corner shows typical errors on the values. Evolutionary tracks for main-sequence stars with masses 1.4, 1.7, and 2.0 $M_{\odot}$ are plotted with gray dotted lines. The solid thick black and light gray lines mark the blue and red edge of the observed instability strips of δ Sct and γ Dor stars, as described by Rodríguez and Breger (2001) and Handler and Shobbrook (2002), respectively. Reproduced with permission © ESO.

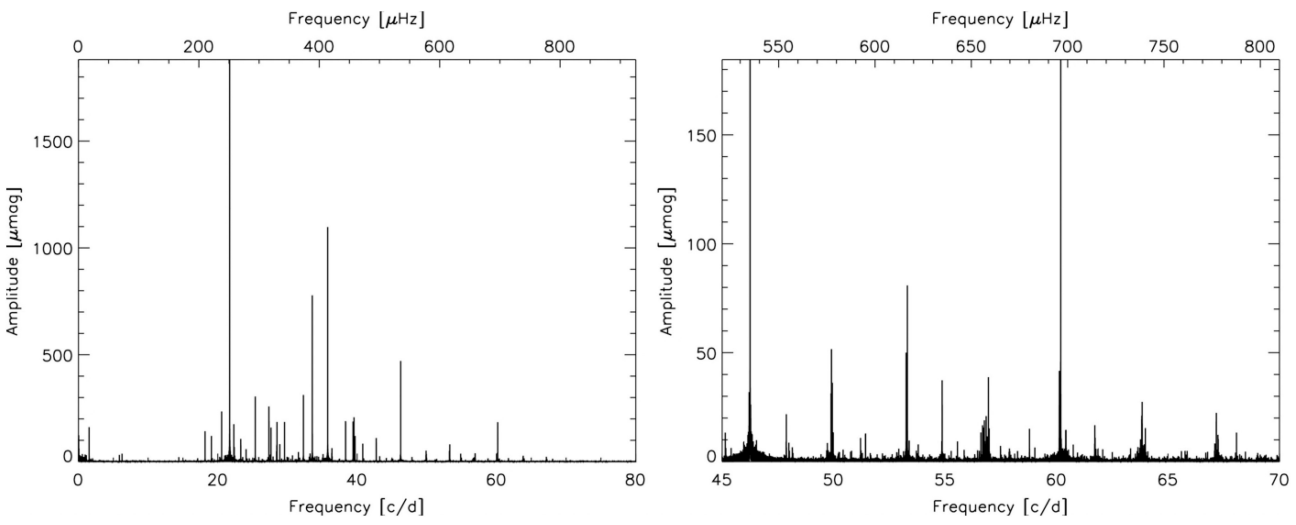

FIGURE 2 | Figure 1 from Antoci et al. (2014). **(Left)** Fourier spectra of the *Kepler* short-cadence data. **(Right)** Close-up in the frequency region interpreted by Antoci et al. (2011) to be stochastically excited. © AAS. Reproduced with permission.

also affirmed that many of the stars in the δ Sct instability region of the H-R diagram are "constant," i.e., not pulsating, at least not at levels detectable by *Kepler* (Guzik et al., 2013, 2014, 2015a,b; Balona et al., 2015b; Murphy et al., 2015).

Balona et al. (2015b) found that 1,165 out of 2,839 stars (41%) in the δ Sct temperature region are not pulsating according to *Kepler* photometry. Murphy et al. (2019) use Gaia DR2 (Gaia Collaboration et al., 2018) data to derive luminosities and to investigate the pulsator fraction in the instability strip as a function of effective temperature and luminosity, finding that the pulsator fraction peaks at around 70% in the middle of the instability strip.

Guzik et al. (2013, 2014, 2015a,b) studied two collections (633 and 2,100+ stars, respectively) of mostly faint stars in the original *Kepler* field, using long-cadence observations requested to search for δ Sct and γ Dor candidates. They find many constant stars, showing no variability at the 20 ppm level for frequencies between 0.2 and 24.5 d^{-1}. Most are outside the γ Dor and δ Sct instability regions, but they find six stars in their sample for Quarters 6–13 (Guzik et al., 2013, 2014), and 15-52 stars, depending on the uncertainty and systematic errors adopted for the *Kepler* Input Catalog effective temperature and surface gravity, for Quarters 14–17 (Guzik et al., 2015a,b) that lie within the pulsation instability regions (see **Figure 3**).

Murphy et al. (2015) use high-resolution spectroscopy to investigate constant stars (defined as showing no δ Sct *p*-mode variations above 50 μmag amplitude) within the δ Sct instability strip. They find that most of these stars have peculiar element abundances with enhancements and deficiencies of certain elements compared to solar abundances, and are classified as metallic-line A (Am) stars. The diffusive settling and radiative levitation believed to cause the abundance anomalies in Am stars would also be expected to deplete helium from the δ Sct pulsation driving region, and could explain why these stars are not pulsating. Setting aside the chemically-peculiar stars, Murphy et al. (2015) find that the remaining stars not pulsating in δ Sct *p* modes are near the edges of the instability regions (**Figure 4**). Murphy et al. (2015) propose that some of these stars may be in undetected binaries, and therefore have inaccurate effective temperatures and actually may lie outside the instability strip; it is also possible that a binary companion could inhibit pulsations. Additional investigation is needed to determine whether these explanations apply for all of the "constant" stars.

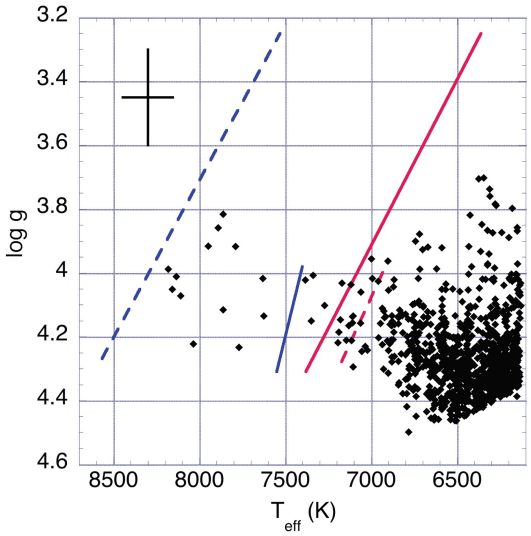

FIGURE 3 | Figure 1 from Guzik et al. (2015b): Location of stars that are "constant" in the log surface gravity-T_{eff} diagram, along with δ Sct (dashed lines) and γ Dor (solid lines) instability strip boundaries established from pre-*Kepler* ground-based observations (Rodríguez and Breger, 2001; Handler and Shobbrook, 2002). The T_{eff} of the sample stars has been shifted by +229 K to account for the systematic offset between T_{eff} of the *Kepler* Input Catalog and SDSS photometry for this temperature range as determined by Pinsonneault et al. (2012, 2013). The black cross shows an error bar on log g (0.3 dex) and T_{eff} (290 K) established by comparisons of KIC values and values derived from ground-based spectroscopy for brighter *Kepler* targets (Uytterhoeven et al., 2011). In this figure, 34 "constant" stars lie within the instability strip boundaries. Without the +229 K offset, 17 "constant" stars would fall within the instability strip boundaries.

2.4. Spots and Flares

Balona (2012, 2013, 2015, 2017, 2019) found that around 40% of A-type stars observed by *Kepler*, including many δ Sct stars, show modulations in their light curves attributed to magnetic activity and starspots, and 1.5% even show flares. This behavior is surprising, because hotter stars, including A-type stars, are believed to have thin and inefficient envelope convection layers instead of a larger convective envelope as found in the Sun and cooler stars, and so are not expected to have convection+differential-rotation driven dynamos and magnetic cycles as found in solar-like stars. Balona (2019) published a paper titled "Evidence for spots on hot stars suggests major revision of stellar physics," conveying the significance of these findings. It is possible that these stars retained a fossil field from their formation. It is also possible that a dynamo mechanism is operating in the convective core, if a way can be found for the field to diffuse through the overlying radiative layers quickly enough to reach the stellar surface (Brun et al., 2005; Featherstone et al., 2009).

Further investigations into A-type flaring stars have been conducted by Pedersen et al. (2017). They performed new analyses of the photometry of 33 flaring A-type stars listed by Balona (2012, 2013), verifying flares in 27 of these objects. In fourteen cases, an overlapping object in the *Kepler* pixel data may be responsible for the flares; in five other cases, the light curves are contaminated by nearby objects in the field. They also obtained new high-resolution spectroscopic observations of 22 of these stars, finding that eleven are spectroscopic binary systems, so that an unresolved low-mass companion may actually be producing the flares. Therefore, they have found possible alternative explanations for all but nine of these stars, six of them without high-resolution spectroscopy, casting some doubt on the A-star flare hypothesis.

Concerning the A-type stars, Balona (2013, 2017) attributed a broad unresolved hump of peaks with a higher amplitude sharp peak at the higher frequency edge in *Kepler* amplitude spectra to multiple star spots with finite lifetimes and differential rotation.

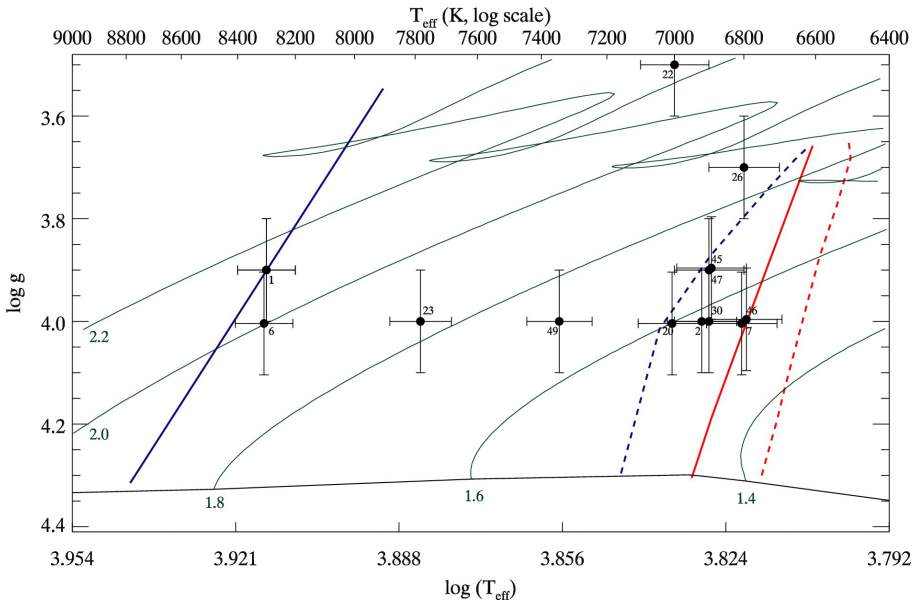

FIGURE 4 | Figure 2 from Murphy et al. (2015). Positions of chemically normal, non-δ Sct stars with 1σ error bars. Solid blue and red lines are the blue and red edges of the δ Sct instability strip, while dashed lines indicate the γ Dor instability strip. Green lines are evolutionary tracks, with masses in $M_{\odot}$ written beneath the ZAMS (black). The non-pulsators generally lie near the edges of the δ Sct instability strip, with exceptions discussed in Murphy et al. (2015).

This broad hump has been explained by Saio et al. (2018) as r modes (global Rossby waves). Saio et al. (2018) suggest that the resolved higher amplitude peak, usually accompanied by a few smaller peaks, is produced by one or a few long-lived star spots that could emerge in weakly magnetic A-type stars.

2.5. Chemically Peculiar Stars

The chemically peculiar A-type stars further challenge stellar pulsation and evolution theory. Diffusive settling of helium from the pulsation-driving region is expected to turn off the κ-effect mechanism and δ Sct pulsations in Am stars. However, some Am stars are observed to pulsate in δ Sct modes (Guzik et al., 2020; Murphy et al., 2020). Figure 5 from Murphy et al. (2020) shows the location of many Am stars including δ Sct pulsators, along with the blue edge of the δ Sct instability region calculated including diffusive settling of helium from the driving region. Murphy et al. (2020) find that pulsation driving from a Rosseland mean opacity bump at 50,000 K caused by the discontinuous H-ionization edge in bound-free opacity explains the observation of δ Sct pulsations in Am stars. Smalley et al. (2017) propose that δ Sct pulsations in Am stars are driven by the turbulent-pressure mechanism.

Balona et al. (2011b) find that the observed location of pulsating Am stars in the H-R diagram does not agree with the location predicted from diffusion calculations. Balona et al. (2015a) state: "The fact that so many Am stars are δ Sct variables is also at odds with the prediction of diffusion theory," and even suggest that accretion could be the origin of the metal enhancements.

Bowman et al. (2018) review magnetic chemically peculiar A-type (Ap) stars, including those that pulsate, observed during the *Kepler* K2 mission. Buysschaert et al. (2018) use spectro-polarimetry to detect large-scale kilogauss magnetic fields in several chemically peculiar stars observed during the K2 mission. In Ap stars,"chemical spots" form at the magnetic poles that cause brightness contrasts that show up as light curve variations as the star rotates; these variables are also called α^2 CVn variables.

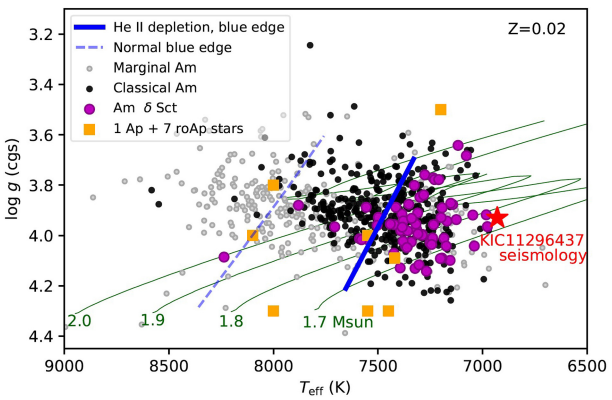

FIGURE 5 | Figure 10 from Murphy et al. (2020). The solid blue line marks the fundamental-mode blue edge for stars depleted of helium to the second He ionization zone. Similar depletion is expected from gravitational settling in Am stars, which are shown according to their degree of peculiarity (from Smalley et al., 2017). The pulsating Am stars are highlighted as magenta circles. Evolutionary tracks of helium depleted models with Z = 0.02 are shown, with their masses written beneath the ZAMS. Orange squares show the positions of seven comparison roAp stars, and the post-main-sequence δ Sct star with Ap-like abundances. The red star is the seismic result for KIC11296437.

Misalignment of the dipole magnetic field axis and rotation axis is the preferred explanation for properties of high-frequency *p* modes of the rapidly-oscillating Ap (roAp) stars (see Kurtz, 1982 and review by Holdsworth, 2021, this collection).

Strong magnetic fields, as are found in the Ap stars, are expected to suppress the low-overtone pulsations found in δ Sct stars. However, Murphy et al. (2020), using *Kepler* data, report the first δ Sct-roAp hybrid, KIC 11296437, having mean magnetic field modulus of 2.8 ± 0.5 kilogauss, and estimated polar magnetic field strength of 3.0–5.2 kilogauss. **Figure 5** shows the location of this star on the H-R diagram based on asteroseismic models.

2.6. HADS and SX Phe Stars

Other A to mid-F spectral type pulsators are further divided into the high-amplitude δ Sct stars (HADS), and the related SX Phe stars. The *Kepler* data show that there may not be any physical distinction between SX Phe and HADS, or really between HADS and normal δ Sct stars.

The SX Phe stars are defined as Population II (low-metallicity) high-amplitude δ Sct stars, with one or two high-amplitude modes, and are usually found in globular clusters and in dwarf galaxies of the Local Group. They are bluer and brighter than the cluster turnoffs, and so are called "blue stragglers," which may have been formed by binary mergers. Balona and Nemec (2012) identified 34 blue straggler candidates in the original *Kepler* field based on their high tangential velocities (distance × proper motion), which indicate that they belong to a thick disk or halo population (**Figure 6**). Nemec et al. (2017) supplemented the *Kepler* light curves with new spectroscopic observations to determine metallicity, temperatures, radial velocities, and projected rotational velocity $v \sin i$. They found that nearly all of these candidates had near-solar metallicities (**Figure 7**). Moreover, the *Kepler* light curves were not distinguishable from normal δ Sct stars, as they show complex spectra and even low frequencies as often seen in *Kepler* δ Sct light curves. It may turn out that the defining characteristic of field SX Phe stars, namely showing only one or two high-amplitude modes, is just a selection effect. There are also low-amplitude multi-periodic SX Phe stars found in globular clusters, lending support to the position that these stars should not be considered a separate class of pulsator from the normal δ Sct stars.

There is room for debate about whether SX Phe stars should be retained as a class of variables, and if so, how to define them and separate them from HADS or normal δ Sct stars. There are questions of cluster vs. field identification, metallicity (Pop. I or II), whether they have undergone mass transfer or merger, whether they are "blue stragglers," i.e., should have evolved off of the main sequence given their metallicity, age, and spectral type. It may be easiest to identify stars as SX Phe stars if they are found in globular clusters and are blue stragglers located on/near the main sequence above the turnoff. However, it is more difficult to distinguish them observationally if they are field stars. As discussed above, for the field stars, a high proper motion does not guarantee metallicity below solar, and so if one were to adopt the criteria of Pop. II metallicity and high proper motion, most of the *Kepler* SX Phe candidates would fail this test. Asteroseismic analysis of the prototype SX Phe (Daszyńska-Daszkiewicz et al., 2020a,b) shows that it is in the core contraction phase or shell H-burning phase, has age ∼4 Gyr, and has a low mass (M ∼ 1.05 $M_\odot$) compared to HADS and δ Sct stars. The best-fit models have metallicity Z = 0.0014–0.002, and favor a low hydrogen (high helium) abundance X = 0.67 (Daszyńska-Daszkiewicz et al., 2020b). One could consider adopting a mass plus age criterion to make the distinction, but these properties are not directly observable and would rely on asteroseismic analyses. Asteroseismic analyses fortunately show promise to constrain intrinsic metallicity and helium abundance,

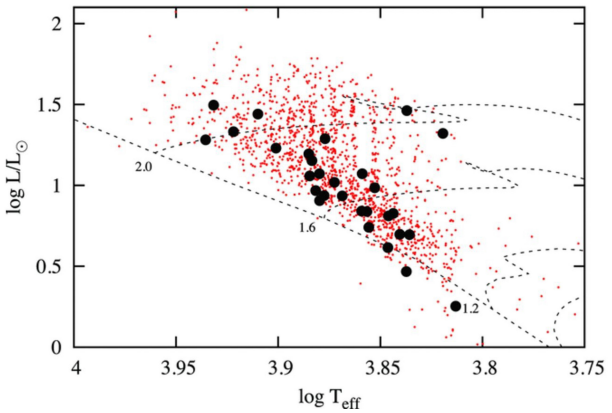

FIGURE 6 | Figure 2 from Balona and Nemec (2012). The theoretical H-R diagram for *Kepler* δ Sct stars (small filled circles). The large filled circles are δ Sct stars which have large proper motions and large tangential velocities (i.e., SX Phe candidates). Evolutionary tracks are shown and labeled with the solar mass.

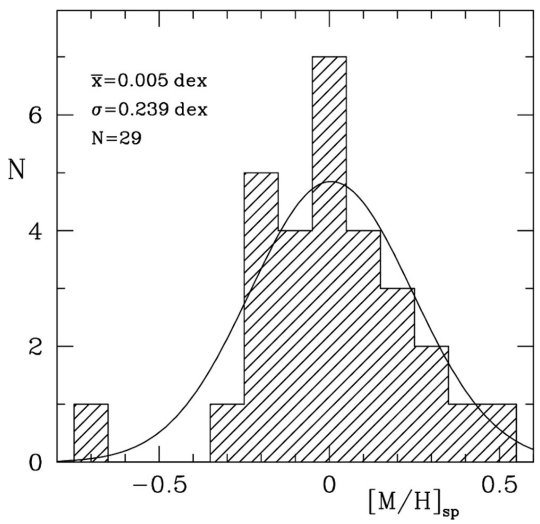

FIGURE 7 | Figure 13 from Nemec et al. (2017). Histogram of spectroscopic metal abundances, $[M/H]_{sp}$, for 29 of Balona and Nemec (2012) SX Phe candidates, fitted with a Gaussian of mean 0.005 dex and standard deviation 0.239 dex; note that KIC 11754974 is off-scale at $[M/H]_{sp} = -1.2 \pm 0.3$ dex.

and possibly whether the star has experienced mass transfer from a binary companion or is the product of a binary merger, either of which could enhance the helium abundance. Should pulsation mode amplitude or the presence of only one or a few modes be retained as defining criteria? These questions will require further discussion.

2.7. "Heartbeat" Stars and Tidally Excited Modes

A new variable type categorized as a result of *Kepler* data are the "heartbeat" stars (Thompson et al., 2012; Fuller, 2017; Hambleton et al., 2018; Cheng et al., 2020; Guo et al., 2020), with KOI-54 (Welsh et al., 2011) being the first dramatic example observed by *Kepler*. These stars are binaries in highly eccentric ($\epsilon \gtrsim 0.3$) orbits with orbital periods between 1 day and 1 year that show tidally induced oscillations (Fuller, 2017). These stars are so-named because their light curves resemble an electrocardiogram, with a brightness dip followed immediately by a sharp rise at periastron. This feature is caused by increased tidal distortion of the components and viewing them at different angles at they orbit each other at periastron, and is also enhanced by light reflecting from the companion star and Doppler boosting at close approach. These binaries show tidally excited oscillations that can be identified because they are exact multiples of the binary orbital frequency. Some have one or more components that also show intrinsic pulsations, and some also show eclipses. Before *Kepler*, only a few such systems had been identified, but 17 systems were quickly discovered and characterized from *Kepler* data (Thompson et al., 2012), motivating their grouping as a new class of variables. It is interesting that Kirk et al. (2016b) catalog 176 heartbeat systems in the original *Kepler* field, but most have not been closely studied, and only around 20% actually show the expected tidally excited oscillations (Cheng et al., 2020).

One such *Kepler* eclipsing heartbeat star is KIC 4544587, studied by Hambleton et al. (2013), with eccentricity 0.28, showing both high- and low-frequency modes typical of δ Sct and γ Dor pulsations, as well as modes that are orbital frequency harmonics that may be excited by tidal resonances (See light curve excerpt in **Figure 8**). The masses of the two stars derived from binary modeling are 1.98 and 1.6 $M_\odot$.

An attempt was made to evolve models for each star with a common initial abundance and age, and using the same mixing length parameter, which best fit the constraints from binary orbits and pulsation modeling (**Figure 9**). Pulsation calculations for the stars matching the derived constraints point to the 1.6 $M_\odot$ star as most likely being the δ Sct pulsator. This exercise illustrated the potential of additional constraints from binaries to assist asteroseismic investigations.

2.8. Amplitude Variations

Most δ Sct asteroseismic studies have focused on periods and period spacings, but few have made use of the amplitudes of the pulsations. The study of amplitudes requires non-linear, non-radial, multidimensional hydrodynamic models which have not advanced far enough to predict mode selection and amplitudes of δ Sct stars. While the frequency content, amplitudes, and phases of some δ Sct stars have been documented to change with time over many years, these phenomena were not investigated comprehensively until the project of Bowman et al. (2016) using *Kepler* data from 983 δ Sct stars observed continuously for 4 years. Bowman et al. found that 61.3% of stars in the sample showed amplitude variation in at least one pulsation mode during the 4 years. One star, KIC 7106205, showed a remarkable amplitude decrease for a single frequency over the first 2 years of the *Kepler* mission from 5 to <1 mmag (Bowman and Kurtz, 2014) (**Figure 10**). The amplitude of this same mode was found from WASP data to have decreased from 11 to 5 mmag during the 2 years prior to the *Kepler* mission (Bowman et al., 2015). Bowman and Kurtz (2014) suggest that this dramatic decrease might be explained by non-linear mode coupling with energy transfer from the *p* mode to low-frequency high-degree *g* modes that are not visible because their light variations average out over the stellar disk.

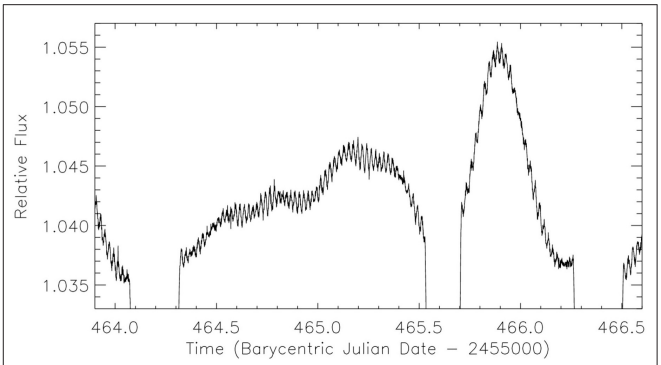

FIGURE 8 | Figure 2 from Hambleton et al. (2013). An amplified image of the out-of-eclipse phase of the *Kepler* Quarter 7 short-cadence light curve. Both the *p*-mode (periods in the range 30 min to 1 h) and the *g*-mode pulsations (∼1 d) are clearly visible. The pronounced periastron brightening can also be seen at approximately BJD 245 5466.

2.9. Finding and Interpreting Frequency (Period) Spacing Patterns–The Key to Asteroseismology

Because δ Sct stars have modes of low radial order *n*, these modes cannot be treated using asymptotic pulsation theory and are not expected to show regular frequency spacings, such as the equal spacings between modes of consecutive radial order that are evident in, e.g., solar-like oscillators. This lack of obvious regular frequency patterns, plus the more rapid rotation in these stars compared to the Sun, leading to asymmetric splitting of the modes into overlapping multiplets, has made it nearly impossible to identify the pulsation modes with certainty. In addition, not all modes that are predicted by non-adiabatic pulsation calculations are seen in the amplitude spectrum. Nevertheless, Suárez et al. (2014), using a grid of stellar models and calculating average frequency separations for degree $\ell = 1$ through 3 modes, show that an average large frequency spacing ($\Delta\nu$) can be determined and used to derive the mean stellar density (**Figure 11**). García Hernández et al. (2015) subsequently

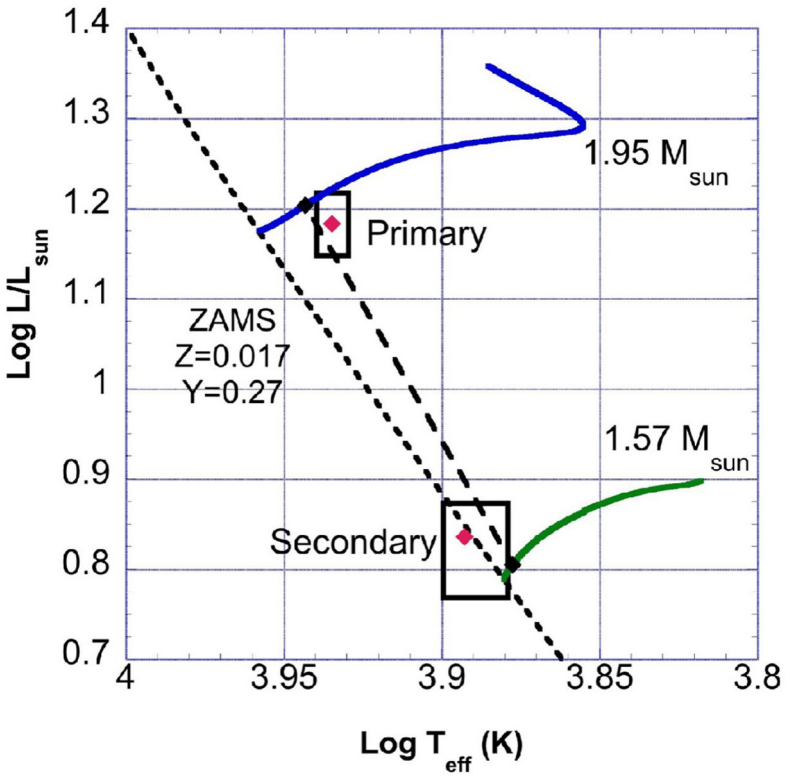

FIGURE 9 | Figure 13 from Hambleton et al. (2013). An H-R diagram for stellar models of components of KIC 4544587. The boxes outline the parameter space for the observationally derived primary and secondary components. The short-dashed line is zero-age main-sequence position for stellar models with Z = 0.017, Y = 0.27. Also shown are evolutionary tracks for a 1.95-$M_{\odot}$ (blue) and 1.57-$M_{\odot}$ (green) model. The two models with the same age and composition closest to the observational constraints are connected by the long-dashed line. The red diamonds mark the best-fitting models for each star that do not have exactly the same age and composition.

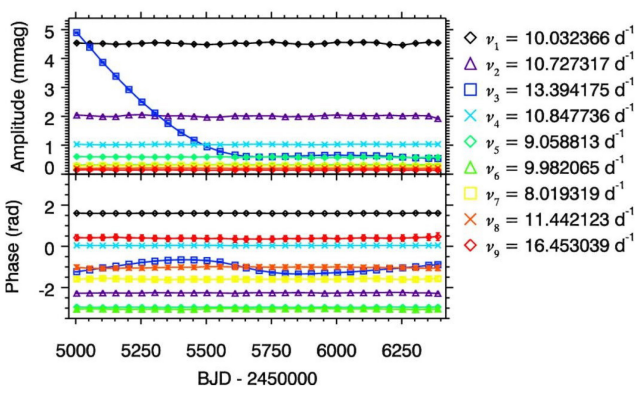

FIGURE 10 | Figure 8 from Bowman et al. (2016). KIC 7106205 amplitude and phase tracking plot showing variability in pulsation mode amplitudes and phases over time.

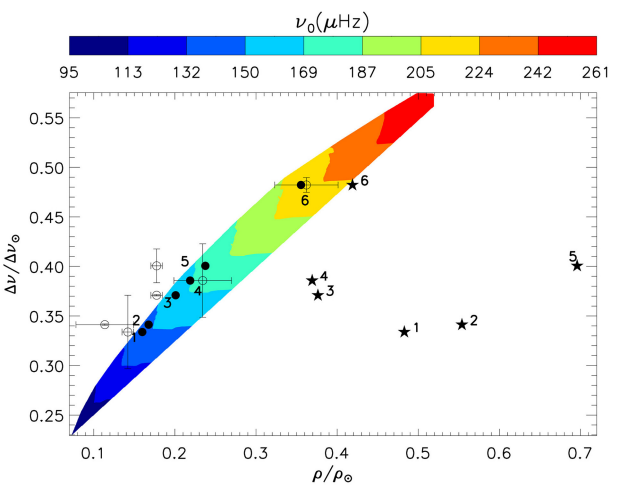

FIGURE 11 | Figure 2 from Suárez et al. (2014). Predicted large separation as a function of the mean density of the star, normalized to their solar values 134.8 μHz and 1.48 g cm^{-3}, respectively. Color contours indicate the predicted frequency of the fundamental radial mode. Filled dots, empty dots, and star symbols represent mean densities found in Suárez et al. (2014), in the literature, and using the calibration of Tingley et al. (2011), respectively. For the sake of clarity, the error bars in star symbol estimates are omitted, since they are larger than the abscissa range. Reproduced with permission © ESO.

calibrated an observational frequency spacing – mean density relationship using eclipsing binaries with a δ Sct component observed by CoRoT and *Kepler* to determine independently the mean density (**Figure 12**).

Paparó et al. (2016a,b) noticed by eye, and then confirmed by algorithm, that one or more sequences of characteristic spacings

could be found in a sample of 90 δ Sct stars observed by CoRoT (**Figures 13**, **14**). It is not always easy to determine, however, whether these characteristic frequency spacings are between successive radial order modes of the same angular degree (i.e., represent $\Delta\nu$) or are instead a combination of $\Delta\nu$ and the rotational splitting frequency.

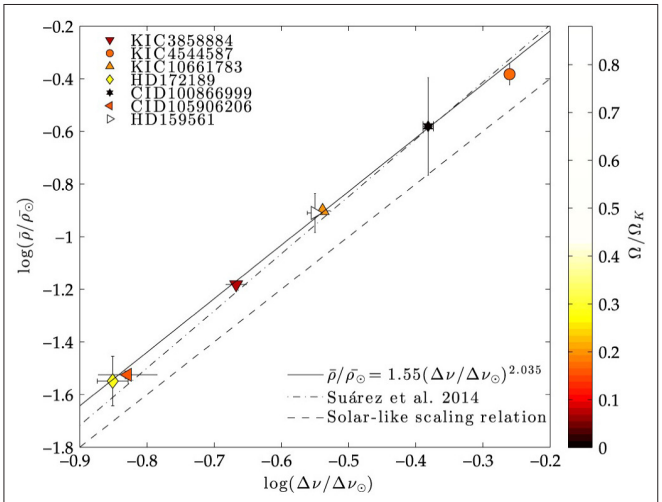

FIGURE 12 | Figure 1 from García Hernández et al. (2015). Large separation — mean density relation obtained for seven binary systems. A linear fit to the points is also depicted, as well as the solar-like scaling relation from Tassoul (1980), and the theoretical scaling relation for non-rotating models of δ Sct stars from Suárez et al. (2014). Symbols are plotted with a gradient color scale to account for the different rotation rates. © AAS. Reproduced with permission.

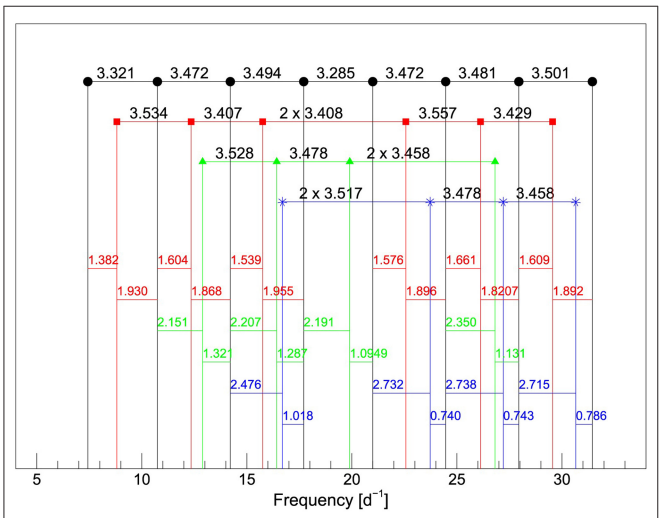

FIGURE 13 | Figure 1 from Paparó et al. (2016a). Sequences with quasi-equal spacing, and shifts of the sequences for CoRoT 102675756. First–black dots, average spacing 2.292 ± 0.138 d^{-1}; Second–red squares, 2.290 ± 0.068 d^{-1}; Third–green triangles, 2.265 ± 0.057 d^{-1}; Fourth–blue stars, 2.242 ± 0.051 d^{-1}. The mean spacing of the star is 2.277 ± 0.088 d^{-1}. The shifts of the second, third, and fourth sequences relative to the first one are also given in the same color as the sequences. © AAS. Reproduced with permission.

While these methods allow one to use δ Sct frequencies to determine a characteristic spacing and mean density, and point toward mode identifications, i.e., being able to identify sequences of modes of the same angular degree, they fall short of finishing the goal of detailed mode identification for asteroseismology.

Fortunately, δ Sct stars early in their main-sequence lifetime have simpler patterns as their cores are less perturbed by changes in composition gradient at the convective core boundary that lead to "avoided crossings" and modes with mixed *p*- and *g*-mode character. Bedding et al. (2020) found complete very regular sequences of *p* modes among 60 young δ Sct variables observed by *Kepler* and TESS (see section 4) and was able to use these to identify the modes, with an assumption that the highest amplitude mode in about 1/3 of the sample stars at frequency 18–23 d^{-1} likely is the radial fundamental ($n = 1$, $\ell = 0$) *p* mode, finally opening a window for δ Sct asteroseismology. This task may have been made easier by many stars in the sample having relatively slow rotation or possibly being observed pole-on, so that large rotational splittings did not confuse the sequence (Benkő and Paparó, 2020).

2.10. γ Doradus Breakthroughs

A similar breakthrough for asteroseismology of γ Doradus variables was enabled by the *Kepler* data. The γ Dor *g*-mode periods are of high radial order, and should obey asymptotic period spacing relations. These modes are sensitive to conditions at the convective core boundary, where a composition gradient from hydrogen burning forms. This gradient is altered by mixing from convective overshooting and differential rotation. This composition gradient perturbs the expected even asymptotic period spacing, and causes mode trapping that shifts pulsation frequencies. These deviations from even period spacing can

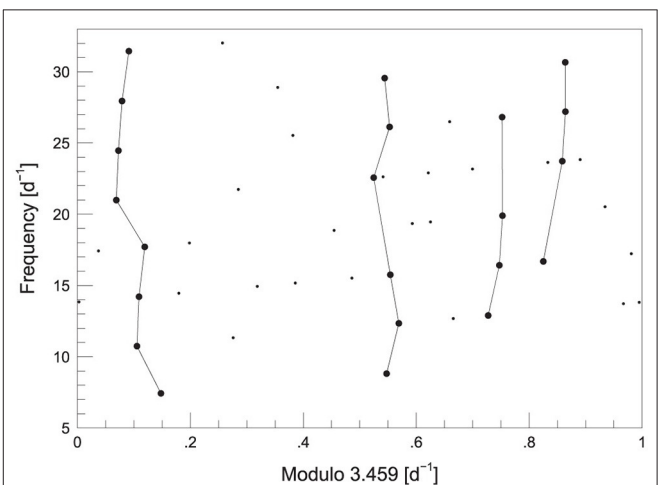

FIGURE 14 | Figure 2 from Paparó et al. (2016a). Echelle diagram for CoRoT 102675756, consistent with the sequences of the **Figure 13** result from visual inspection. The mean spacing of the star was used as a modulo frequency. The whole frequency content of the star is plotted (small and large dots). The larger dots show the vertical representation of the sequences, the echelle ridges. © AAS. Reproduced with permission.

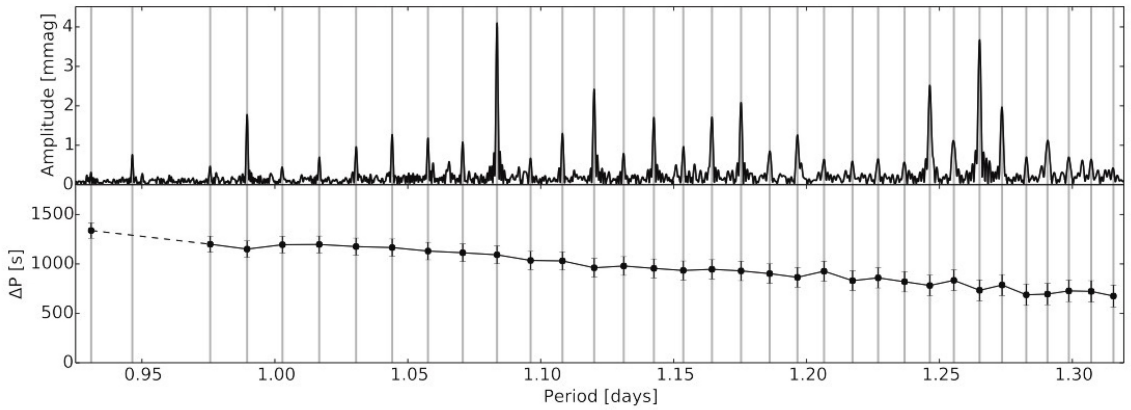

FIGURE 15 | Figure 11 from Van Reeth et al. (2015a). **(Top)** Close-up of part of the Fourier spectrum of KIC 11721304 (black). All the marked frequencies are accepted following the criterion described in Van Reeth et al. (2015a). **(Bottom)** The period spacing as computed from the accepted frequencies. The black markers and gray lines indicate the frequencies for which a smooth spacing pattern was found. Reproduced with permission © ESO.

be used to probe the region of the convective-core boundary, constrain mixing profiles, and measure interior rotation rates (See theoretical and modeling papers predicting and explaining these effects by Miglio et al., 2008 and Bouabid et al., 2013).

Despite the expectation that rapid rotation and overlapping non-equidistant rotationally split multiplets would make it difficult to find a period-spacing pattern, Van Reeth et al. (2015a,b) were able to develop a period-spacing detection algorithm and successfully identify period spacings in several γ Dor stars (**Figure 15**). As is the situation for the δ Sct frequency spacings, this method by itself does not allow one to identify the radial order n, angular degree ℓ or azimuthal order m of the modes. Nevertheless, these techniques have been subsequently developed and applied for studies of γ Dor stars observed by *Kepler* and CoRoT (see, e.g., Ouazzani et al., 2017, 2020; Li et al., 2019a,b).

In the γ Dor literature, the gravity or g modes are also referred to as gravito-inertial modes, as they are subject to both buoyancy and Coriolis forces because of rotation in the star (see, e.g., Mombarg et al., 2019). A key recent development for γ Dor stars was the detection and exploitation of the r modes, or global Rossby waves, (see, e.g., Saio et al., 2018) in many γ Dor stars observed by *Kepler*. These modes consist of predominantly toroidal motions that do not have a restoring force or cause light variation in a non-rotating star because they cause no compression or expansion. However, in a rotating star, the toroidal motion couples with spheroidal motion caused by the Coriolis force, resulting in temperature perturbations that are visible. In γ Dor stars, the r modes of a given azimuthal order m appear in groups with slightly lower frequency than m times the rotation frequency. These modes can be excited by the κ mechanism.

Gravity mode and inertial (r) mode period spacing patterns found in *Kepler* γ Dor stars, in some cases supplemented by δ Sct p modes for the hybrid pulsators, have since been used by many groups to determine core and envelope rotation profiles in these stars (see, e.g., Van Reeth et al., 2016, 2018; Ouazzani et al., 2017; Li et al., 2019b, 2020). Interior differential rotation has also been studied and confirmed in γ Dor stars using the mode spacing patterns by, e.g., Aerts et al. (2017), Christophe et al. (2018), and Van Reeth et al. (2018).

Many important modeling advances for γ Dor stars have resulted from the *Kepler* observations, among these models of individual targets (e.g., Kurtz et al., 2014; Saio et al., 2015; Schmid and Aerts, 2016). Mombarg et al. (2019, 2020) have developed comprehensive model grids to interpret mode spacing patterns for ensembles of γ Dor stars and evaluate the effects of including diffusive settling and radiative levitation.

2.11. δ Sct Discoveries in Binaries and Clusters

While not discussed in detail here, the *Kepler* mission discovered many eclipsing binary systems. As mentioned earlier, the stellar properties derived independently from the binary system modeling can be used to calibrate asteroseismic techniques and supplement constraints for detailed asteroseismic models. A catalog of such systems discovered or observed by *Kepler* and K2 is maintained by Villanova University, with links to the Mikulski Archive for Space Telescopes (MAST), and the VizieR On-line Data Catalog (see, e.g., Kirk et al., 2016a,b). As of this writing, the Third Edition of this catalog lists 2,922 binaries observed during the original *Kepler* mission[2] and 664 binaries from K2[3].

Many of these binaries have potential δ Sct (or hybrid) components. For example, Liakos and Niarchos (2016, 2017) catalog properties of 199 systems, many from *Kepler* observations, and Gaulme and Guzik (2019) find 149 such systems in the *Kepler* data. See also Kahraman Aliçavuş et al. (2017) who discuss spectroscopic observations of 92 eclipsing binaries with a δ Sct component apart from the *Kepler* data. We can add to this list 341 *Kepler* non-eclipsing A/F star binaries discovered from pulsation phase modulation by Murphy et al.

[2]http://keplerebs.villanova.edu
[3]http://keplerebs.villanova.edu/k2

(2018a,b), and the 176 *Kepler* heartbeat stars mentioned earlier (Kirk et al., 2016b). There are a few dozen *Kepler* binary systems containing a δ Sct component that have been studied in detail to date. A search on the ADS abstract service with terms "binary" and "δ Sct" in the abstract, and "KIC" (Kepler Input Catalog) in the title gives 42 results, and shows a trend of increasing number of publications from two to ten per year over the past decade. Searching for publications on binary *Kepler* objects with "γ Dor" in the abstract yields 28 results, with many of the objects studied being hybrid pulsators. This search does not include papers that are likely to appear soon studying binaries observed during the K2 mission.

δ Sct stars found in clusters have similar advantages to those in binaries, as the common age and metallicity of the cluster members offer independent constraints. For example, a comprehensive paper by Sandquist et al. (2016) compares the age and distance modulus of the open cluster NGC 6811 derived using a variety of methods. This cluster was observed during the original *Kepler* mission, and found to contain an eclipsing binary with an Am star and γ Dor component, many pulsating stars near the cluster turnoff, including 28 δ Sct, 15 γ Dor, and 5 hybrid stars, and many giant stars, some on the asymptotic giant branch and some in the "red clump" core helium-burning phase. They model the binary to determine component masses and compare with isochrones, finding inconsistent ages between the components of 1.05 Gyr for the Am star primary, and 1.21 Gyr for the γ Dor secondary; the younger Am star age is more consistent with the 1.0 Gyr age derived from the main-sequence turnoff in the color-magnitude diagram. However, the Am star abundance peculiarities are not properly taken into account in stellar models, so the Am star age may be more suspect. In addition, the (near-solar) metallicity of the stars in the cluster is uncertain and the ages would be less discrepant with a slightly lower metallicity than adopted. Applying asteroseismic $\Delta\nu$ vs. $\nu_{\rm max}$ relations for the core helium-burning stars to determine their radii and masses, they find that the derived masses of these stars appear to be larger (or their radii smaller) than expected for the cluster age(s) derived from the binary. These stars are more consistent with a 0.9 Gyr age. They derive the distance modulus using the period-luminosity relationship of high-amplitude δ Sct stars, finding $(m - M)_V = 10.37 \pm 0.03$, which is lower than the value derived using the eclipsing binary, $(m - M)_V = 10.47 \pm 0.05$. This example shows the possibilities for combining multiple constraints from clusters to check for consistency in inferences, and to identify discrepancies in modeling or asteroseismic analysis techniques for a particular star class.

3. SUCCESSES, UNRESOLVED PROBLEMS, AND QUESTIONS

In summary, it would not be an understatement to conclude that the *Kepler* mission has revolutionized the field of asteroseismology, in particular for δ Sct stars, and given researchers a wealth of data for analyses, modeling efforts, and motivating future long-term observations. A non-exhaustive list of successes includes:

- Unprecedented long time-series (months to years), high-cadence (1 or 30 min), high-precision photometry for thousands of δ Sct, γ Dor, and hybrid variables, many newly discovered using the *Kepler* data.
- Interpretation and application of frequency and period spacings and patterns to inform mode identification, exploiting these to determine interior structure, extent of mixing, and rotation profiles.
- More definitive quantification of the pervasiveness and range of amplitude variations that await explanation.
- Large expansion in the number of binaries showing tidally excited modes, establishing a new class of variable stars.
- Motivation for exploration of additional pulsation driving mechanisms, advancing stellar pulsation theory.
- More definitive data to quantify the role of magnetic fields in pulsation.
- More definitive constraints for quantifying the effects of element diffusive settling and radiative levitation and accurately including these processes in stellar models.

There are many problems and questions motivated or amplified by the *Kepler* data, among these:

- Why are many of the pulsation modes predicted by linear pulsation theory not observed?
- What is the origin of the low frequencies found in many δ Sct stars?
- Can observed frequency spacings and patterns be interpreted and used for mode identification?
- What determines the amplitudes of δ Sct modes, and what causes amplitude variations?
- Why are some stars in the δ Sct (and γ Dor) instability regions "constant," i.e., not pulsating?
- Why are some chemically peculiar stars pulsating?
- Are HADS or SX Phe stars different from each other or from normal δ Sct stars?
- What is the origin of blue stragglers?
- What is the origin of magnetic activity, spots, and flares in hot stars?
- What is the origin of the abundance peculiarities in λ Boo, Am, and Ap stars?
- Can new proposed pulsation driving mechanisms explain the unexpected frequencies observed in some δ Sct stars?

Answering these questions will require long-term monitoring, directed campaigns, high-resolution spectroscopy, multicolor photometry, interferometry, and other observations, in addition to advances in stellar evolution and pulsation theory and modeling.

4. THE NEAR FUTURE AND TESS

While the *Kepler* spacecraft ended its K2 mission in November 2018, the NASA TESS spacecraft (Ricker et al., 2015) was launched in April 2018. The TESS spacecraft has some advantages and some disadvantages compared to *Kepler* for asteroseismology. The TESS mission is surveying more of the sky over its mission lifetime, while *Kepler* covered a single field of view in the Cygnus and Lyra constellations during its

original mission, and 18 fields along the ecliptic during the extended K2 mission. However, TESS observes a sector of the sky continuously for only 27 days, compared to the possibility of obtaining up to 4 years of nearly continuous data during the original *Kepler* mission, or nearly 3 months continuously during K2. TESS is collecting full-frame images every 30 min (every 10 min starting in Cycle 3), and also has the possibility for 2-min and even 20-s cadence observations for selected targets. The pixel size for the TESS cameras is larger, making crowding and contamination from nearby stars in the field an issue that must be taken into account in data analyses. The redder TESS bandpass reduces the observed amplitudes of δ Sct pulsations by about 25% compared to the amplitudes of the *Kepler* mission (Antoci et al., 2019).

The TESS first-light papers have been published, including a first view of δ Sct and γ Dor stars with the TESS mission (Antoci et al., 2019). This paper contains up-to-date descriptions of δ Sct and related stars, including pre-main-sequence δ Sct stars that were not studied in detail using *Kepler* observations, λ Boo stars not discussed in this review, TESS observations of very bright stars such as α Pic, and the pulsation class prototypes SX Phe (see also Daszyńska-Daszkiewicz et al., 2020a,b) and γ Dor that were not targeted by *Kepler*. The paper also has an extensive explanation of the role of turbulent pressure in the hydrogen ionization zone in driving δ Sct pulsations, especially in the context of Am stars that are expected to have helium depleted from diffusive settling, inhibiting the classical κ-effect pulsation driving mechanism. TESS observations will extend and enhance the *Kepler* legacy.

What can we expect for the future of *Kepler* and TESS observations? Asteroseismic analyses will be conducted using data from individual stars or ensembles of stars with common properties, binaries, and δ Sct stars in clusters. K2 has observed many open clusters on the ecliptic that contain δ Sct stars (e.g., Hyades, Praesepe, Pleiades, and M67). Studies of clusters show promise to finally understand the nature of blue stragglers, and the development of abundance peculiarities in Am and λ Boo stars. There were no pre-main-sequence δ Sct stars in the original *Kepler* field, but discoveries for these stars may await using K2 or TESS data. It is hoped that these data will help disentangle or systematize the picture for stellar interior and evolution modeling from the pre-main-sequence through the shell H-burning stage, for example, the roles of processes such as convective overshooting, differential rotation, angular momentum transport, element levitation and settling, magnetic fields, mixing from internal gravity waves, etc. It is hoped that advances in theory and multidimensional stellar modeling, e.g., non-radial, non-linear, non-adiabatic pulsation modeling including turbulent and magnetic pressure and energy or rapid differential rotation, will lead to explanations for pulsation mode driving, mode selection, and amplitudes, and will better define instability strip boundaries.

AUTHOR CONTRIBUTIONS

JG was the sole author of this article that reviews the contributions of many authors to the field of δ Sct asteroseismology using *Kepler* data.

FUNDING

JG's research was supported at Los Alamos National Laboratory (LANL), managed by Triad National Security, LLC for the U.S. Department of Energy's NNSA, Contract #89233218CNA000001. JG also gratefully acknowledges a Los Alamos National Laboratory Center for Space and Earth Sciences Rapid Response grant for Summer 2020.

ACKNOWLEDGMENTS

JG thanks editors K. Kinemuchi and A. Baran for the opportunity to write this review, and for their careful reading and suggestions. JG also thanks many colleagues who have made important contributions to this field. In addition, JG thanks the two reviewers, and also Simon Murphy, who have provided extensive suggestions for additional literature to take into account, and for sharing their perspectives on the developments in this field. JG thanks colleagues J. Jackiewicz and P. Bradley for advice and help with the *Kepler* data over many years. Finally, JG thanks the authors and journals for granting permission to reproduce the figures used in this paper.

REFERENCES

Aerts, C., Christensen-Dalsgaard, J., and Kurtz, D. W. (2010). *Asteroseismology*. Dordrecht: Springer Astronomy and Astrophysics Library. doi: 10.1007/978-1-4020-5803-5

Aerts, C., Van Reeth, T., and Tkachenko, A. (2017). The interior angular momentum of core hydrogen burning stars from gravity-mode oscillations. *Astrophys. J. Lett*. 847:L7. doi: 10.3847/2041-8213/aa8a62

Antoci, V., Cunha, M., Houdek, G., Kjeldsen, H., Trampedach, R., Handler, G., et al. (2014). The role of turbulent pressure as a coherent pulsational driving mechanism: the case of the δ Scuti Star HD 187547. *Astrophys. J.* 796:118. doi: 10.1088/0004-637X/796/2/118

Antoci, V., Cunha, M. S., Bowman, D. M., Murphy, S. J., Kurtz, D. W., Bedding, T. R., et al. (2019). The first view of δ Scuti and γ Doradus stars with the TESS mission. *Mon. Not. RAS* 490, 4040–4059. doi: 10.1093/mnras/stz2787

Antoci, V., Handler, G., Campante, T. L., Thygesen, A. O., Moya, A., Kallinger, T., et al. (2011). The excitation of solar-like oscillations in a δ Sct star by efficient envelope convection. *Nature* 477, 570–573. doi: 10.1038/nature10389

Balona, L. A. (2012). Kepler observations of flaring in A-F type stars. *Mon. Not. RAS* 423, 3420–3429. doi: 10.1111/j.1365-2966.2012.21135.x

Balona, L. A. (2013). Activity in A-type stars. *Mon. Not. RAS* 431, 2240–2252. doi: 10.1093/mnras/stt322

Balona, L. A. (2014). Low frequencies in Kepler δ Scuti stars. *Mon. Not. RAS* 437, 1476–1484. doi: 10.1093/mnras/stt1981

Balona, L. A. (2015). Flare stars across the H-R diagram. *Mon. Not. RAS* 447, 2714–2725. doi: 10.1093/mnras/stu2651

Balona, L. A. (2017). Starspots on A stars. *Mon. Not. RAS* 467, 1830–1837. doi: 10.1093/mnras/stx265

Balona, L. A. (2018). Pulsation in intermediate-mass stars. *Front. Astron. Space Sci.* 5:43. doi: 10.3389/fspas.2018.00043

Balona, L. A. (2019). Evidence for spots on hot stars suggests major revision of stellar physics. *Mon. Not. RAS* 490, 2112–2116. doi: 10.1093/mnras/stz2808

Balona, L. A., Catanzaro, G., Abedigamba, O. P., Ripepi, V., and Smalley, B. (2015a). Spots on Am stars. *Mon. Not. RAS* 448, 1378–1388. doi: 10.1093/mnras/stv076

Balona, L. A., Daszyńska-Daszkiewicz, J., and Pamyatnykh, A. A. (2015b). Pulsation frequency distribution in δ Scuti stars. *Mon. Not. RAS* 452, 3073–3084. doi: 10.1093/mnras/stv1513

Balona, L. A., Guzik, J. A., Uytterhoeven, K., Smith, J. C., Tenenbaum, P., and Twicken, J. D. (2011a). The Kepler view of γ Doradus stars. *Mon. Not. RAS* 415, 3531–3538. doi: 10.1111/j.1365-2966.2011.18973.x

Balona, L. A., and Nemec, J. M. (2012). A search for SX Phe stars among Kepler δ Scuti stars. *Mon. Not. RAS* 426, 2413–2418. doi: 10.1111/j.1365-2966.2012.21957.x

Balona, L. A., Ripepi, V., Catanzaro, G., Kurtz, D. W., Smalley, B., De Cat, P., et al. (2011b). Kepler observations of Am stars. *Mon. Not. RAS* 414, 792–800. doi: 10.1111/j.1365-2966.2011.18454.x

Bedding, T. R., Murphy, S. J., Hey, D. R., Huber, D., Li, T., Smalley, B., et al. (2020). Very regular high-frequency pulsation modes in young intermediate-mass stars. *Nature* 581, 147–151. doi: 10.1038/s41586-020-2226-8

Benkő, J. M., and Paparó, M. (2020). A glimpse inside δ Scuti stars. *Nature* 581, 141–142. doi: 10.1038/d41586-020-01169-z

Borucki, W. J., Koch, D., Basri, G., Batalha, N., Brown, T., Caldwell, D., et al. (2010). Kepler planet-detection mission: introduction and first results. *Science* 327:977. doi: 10.1126/science.1185402

Bouabid, M. P., Dupret, M. A., Salmon, S., Montalbán, J., Miglio, A., and Noels, A. (2013). Effects of the Coriolis force on high-order g modes in γ Doradus stars. *Mon. Not. RAS* 429, 2500–2514. doi: 10.1093/mnras/sts517

Bowman, D. M. (2017). *Amplitude Modulation of Pulsation Modes in Delta Scuti Stars*. Springer Theses. Cham: Springer International Publishing AG doi: 10.1007/978-3-319-66649-5

Bowman, D. M., Buysschaert, B., Neiner, C., Pápics, P. I., Oksala, M. E., and Aerts, C. (2018). K2 space photometry reveals rotational modulation and stellar pulsations in chemically peculiar A and B stars. *Astron. Astrophys.* 616:A77. doi: 10.1051/0004-6361/201833037

Bowman, D. M., Holdsworth, D. L., and Kurtz, D. W. (2015). Combining WASP and Kepler data: the case of the δ Sct star KIC 7106205. *Mon. Not. RAS* 449, 1004–1010. doi: 10.1093/mnras/stv364

Bowman, D. M., and Kurtz, D. W. (2014). Pulsational frequency and amplitude modulation in the δ Sct star KIC 7106205. *Mon. Not. RAS* 444, 1909–1918. doi: 10.1093/mnras/stu1583

Bowman, D. M., and Kurtz, D. W. (2018). Characterizing the observational properties of δ Sct stars in the era of space photometry from the Kepler mission. *Mon. Not. RAS* 476:3169–3184. doi: 10.1093/mnras/sty449

Bowman, D. M., Kurtz, D. W., Breger, M., Murphy, S. J., and Holdsworth, D. L. (2016). Amplitude modulation in δ Sct stars: statistics from an ensemble study of Kepler targets. *Mon. Not. RAS* 460, 1970–1989. doi: 10.1093/mnras/stw1153

Bradley, P. A., Guzik, J. A., Miles, L. F., Uytterhoeven, K., Jackiewicz, J., and Kinemuchi, K. (2015). Results of a search for γ Dor and δ Sct stars with the Kepler spacecraft. *Astron. J.* 149:68. doi: 10.1088/0004-6256/149/2/68

Bradley, P. A., Guzik, J. A., Miles, L. F., Uytterhoeven, K., Jackiewicz, J., and Kinemuchi, K. (2016). Erratum: "Results of a search for γ Dor and δ Sct stars with the Kepler spacecraft" (2015, AJ 149:68). *Astron. J.* 151:86. doi: 10.3847/0004-6256/151/3/86

Breger, M. (1980). Delta-Scuti stars and Swarf Cepheids–review and pulsation modes. *Space Sci. Rev.* 27, 361–370. doi: 10.1017/S025292110008177X

Breger, M., Lenz, P., Antoci, V., Guggenberger, E., Shobbrook, R. R., Handler, G., et al. (2005). Detection of 75+ pulsation frequencies in the δ Scuti star FG Virginis. *Astron. Astrophys.* 435, 955–965. doi: 10.1051/0004-6361:20042480

Breger, M., and Montgomery, M. (Eds.). (2000). *Delta Scuti and Related Stars, Volume 210 of Astronomical Society of the Pacific Conference Series*. San Francisco, CA: Astronomical Society of the Pacific.

Breger, M., Montgomery, M. H., Lenz, P., and Pamyatnykh, A. A. (2017). Nonradial and radial period changes of the δ Scuti star 4 CVn. II. Systematic behavior over 40 years. *Astron. Astrophys.* 599:A116. doi: 10.1051/0004-6361/201629797

Brun, A. S., Browning, M. K., and Toomre, J. (2005). Simulations of core convection in rotating A-type stars: magnetic dynamo action. *Astrophys. J.* 629, 461–481. doi: 10.1086/430430

Buysschaert, B., Neiner, C., Martin, A. J., Aerts, C., Bowman, D. M., Oksala, M. E., et al. (2018). Detection of magnetic fields in chemically peculiar stars observed with the K2 space mission. *Mon. Not. RAS* 478, 2777–2793. doi: 10.1093/mnras/sty1190

Cheng, S. J., Fuller, J., Guo, Z., Lehman, H., and Hambleton, K. (2020). Detailed characterization of heartbeat stars and their tidally excited oscillations. *Astrophys. J.* 903:122. doi: 10.3847/1538-4357/abb46d

Christophe, S., Ballot, J., Ouazzani, R. M., Antoci, V., and Salmon, S. J. A. J. (2018). Deciphering the oscillation spectrum of γ Doradus and SPB stars. *Astron. Astrophys.* 618:A47. doi: 10.1051/0004-6361/201832782

Cox, A. N. (1983). "Stability problems with an application to early-type stars," in *Saas-Fee Advanced Course 13: Astrophysical Processes in Upper Main Sequence Stars*, eds A. N. Cox, S. Vauclair, and J. P. Zahn (Geneva: Geneva Observatory), 1.

Daszyńska-Daszkiewicz, J., Pamyatnykh, A. A., Walczak, P., and Szewczuk, W. (2020a). Seismic analysis of the double-mode radial pulsator SX Phoenicis. *Mon. Not. RAS* 499, 3034–3045. doi: 10.1093/mnras/staa3056

Daszyńska-Daszkiewicz, J., Walczak, P., and Pamyatnykh, A. (2017). "On possible explanations of pulsations in Maia stars," in *European Physical Journal Web of Conferences, Volume 160 of European Physical Journal Web of Conferences* (Vienna), 03013. doi: 10.1051/epjconf/201716003013

Daszyńska-Daszkiewicz, J., Walczak, P., Pamyatnykh, A., Szewczuk, W., and Dziembowski, W. (2020b). "The complex asteroseismology of SX Phoenicis," in *Stars and Their Variability Observed From Space*, eds C. Neiner, W. W. Weiss, D. Baade, R. E. Griffin, C. C. Lovekin, and A. F. J. Moffat (San Francisco, CA: Astronomical Society of the Pacific), 81–85.

Dupret, M. A., Grigahcène, A., Garrido, R., Gabriel, M., and Scuflaire, R. (2005). Convection-pulsation coupling. II. Excitation and stabilization mechanisms in δ Sct and γ Dor stars. *Astron. Astrophys.* 435, 927–939. doi: 10.1051/0004-6361:20041817

Featherstone, N. A., Browning, M. K., Brun, A. S., and Toomre, J. (2009). Effects of fossil magnetic fields on convective core dynamos in A-type stars. *Astrophys. J.* 705, 1000–1018. doi: 10.1088/0004-637X/705/1/1000

Fuller, J. (2017). Heartbeat stars, tidally excited oscillations and resonance locking. *Mon. Not. RAS* 472, 1538–1564. doi: 10.1093/mnras/stx2135

Gaia Collaboration, Brown, A. G. A., Vallenari, A., Prusti, T., de Bruijne, J. H. J., Babusiaux, C., et al. (2018). Gaia Data Release 2. Summary of the contents and survey properties. *Astron. Astrophys.* 616:A1. doi: 10.1051/0004-6361/201833051

García Hernández, A., Martín-Ruiz, S., Monteiro, M. J. P. F. G., Suárez, J. C., Reese, D. R., Pascual-Granado, J., et al. (2015). Observational $\delta\nu - \rho$ relation for δ Sct stars using eclipsing binaries and space photometry. *Astrophys. J. Lett.* 811:L29. doi: 10.1088/2041-8205/811/2/L29

García, R. A., and Ballot, J. (2019). Asteroseismology of solar-type stars. *Liv. Rev. Sol. Phys.* 16:4. doi: 10.1007/s41116-019-0020-1

Gaulme, P., and Guzik, J. A. (2019). Systematic search for stellar pulsators in the eclipsing binaries observed by Kepler. *Astron. Astrophys.* 630:A106. doi: 10.1051/0004-6361/201935821

Gilliland, R. L., Brown, T. M., Christensen-Dalsgaard, J., Kjeldsen, H., Aerts, C., Appourchaux, T., et al. (2010). Kepler asteroseismology program: introduction and first results. *Publ. ASP* 122:131. doi: 10.1086/650399

Grigahcène, A., Antoci, V., Balona, L., Catanzaro, G., Daszyńska-Daszkiewicz, J., Guzik, J. A., et al. (2010). Hybrid γ Doradus-δ Scuti pulsators: new insights into the physics of the oscillations from Kepler observations. *Astrophys. J. Lett.* 713, L192–L197. doi: 10.1088/2041-8205/713/2/L192

Guo, Z., Shporer, A., Hambleton, K., and Isaacson, H. (2020). Tidally excited oscillations in heartbeat binary stars: pulsation phases and mode identification. *Astrophys. J.* 888:95. doi: 10.3847/1538-4357/ab58c2

Guzik, J. A., Bradley, P. A., Jackiewicz, J., Molenda-Zakowicz, J., Uytterhoeven, K., and Kinemuchi, K. (2015a). The occurrence of non-pulsating stars in the γ Dor and δ Sct pulsation instability regions: results from Kepler quarter 14–17 data. *Astron. Rev.* 11, 1–24. doi: 10.1080/21672857.2015.1023120

Guzik, J. A., Bradley, P. A., Jackiewicz, J., Molenda-Zakowicz, J., Uytterhoeven, K., and Kinemuchi, K. (2015b). The occurrence of non-pulsating stars in the

gamma Dor and delta Sct pulsation instability regions: results from Kepler quarter 14–17 data. *arXiv* 1502.00175.

Guzik, J. A., Bradley, P. A., Jackiewiecz, J., Uytterhoeven, K., and Kinemuchi, K. (2013). The occurrence of non-pulsating stars in the gamma Doradus/delta Scuti pulsation instability region. *Astron. Rev.* 8, 83–107. doi: 10.1080/21672857.2013.11519724

Guzik, J. A., Bradley, P. A., Jackiewiecz, J., Uytterhoeven, K., and Kinemuchi, K. (2014). The occurrence of non-pulsating stars in the gamma Doradus/delta Scuti pulsation instability region. *Astron. Rev.* 9, 41–65. doi: 10.1080/21672857.2014.11519730

Guzik, J. A., Garcia, J. A., and Jackiewicz, J. (2019). Properties of 249 delta Scuti variable star candidates observed during the NASA K2 mission. *Front. Astron. Space Sci.* 6:40. doi: 10.3389/fspas.2019.00040

Guzik, J. A., Jackiewicz, J., Pigulski, A., Catanzaro, G., Soukup, M. S., Gaulme, P., et al. (2020). Data analysis of bright main-sequence A- and B-type stars observed using the TESS and BRITE spacecraft. *arXiv*.

Guzik, J. A., Kaye, A. B., Bradley, P. A., Cox, A. N., and Neuforge, C. (2000). Driving the gravity-mode pulsations in γ Doradus variables. *Astrophys. J. Lett.* 542, L57–L60. doi: 10.1086/312908

Hambleton, K., Fuller, J., Thompson, S., Prša, A., Kurtz, D. W., Shporer, A., et al. (2018). KIC 8164262: a heartbeat star showing tidally induced pulsations with resonant locking. *Mon. Not. RAS* 473, 5165–5176. doi: 10.1093/mnras/stx2673

Hambleton, K. M., Kurtz, D. W., Prša, A., Guzik, J. A., Pavlovski, K., Bloemen, S., et al. (2013). KIC 4544587: an eccentric, short-period binary system with δ Sct pulsations and tidally excited modes. *Mon. Not. RAS* 434, 925–940. doi: 10.1093/mnras/stt886

Handler, G., and Shobbrook, R. R. (2002). On the relationship between the δ Scuti and γ Doradus pulsators. *Mon. Not. RAS* 333, 251–262. doi: 10.1046/j.1365-8711.2002.05401.x

Holdsworth, D. L. (2021). The roAp stars observed by the Kepler space telescope. *Front. Astron. Space Sci.* doi: 10.3389/fspas.2021.626398

Howell, S. B., Sobeck, C., Haas, M., Still, M., Barclay, T., Mullally, F., et al. (2014). The K2 mission: characterization and early results. *Publ. ASP* 126:398. doi: 10.1086/676406

Kahraman Aliçavuş, F., Soydugan, E., Smalley, B., and Kubát, J. (2017). Eclipsing binary stars with a δ Scuti component. *Mon. Not. RAS* 470, 915–931. doi: 10.1093/mnras/stx1241

Kirk, B., Conroy, K., Prsa, A., Abdul-Masih, M., Kochoska, A., Matijevic, G., et al. (2016a). *VizieR Online Data Catalog: Kepler Mission. VII. Eclipsing Binaries in DR3 (Kirk+ 2016)*. Strasbourg: VizieR Online Data Catalog.

Kirk, B., Conroy, K., Prša, A., Abdul-Masih, M., Kochoska, A., Matijevič, G., et al. (2016b). Kepler eclipsing binary stars. VII. The catalog of eclipsing binaries found in the entire Kepler data set. *Astron. J.* 151:68. doi: 10.3847/0004-6256/151/3/68

Koch, D. G., Borucki, W. J., Basri, G., Batalha, N. M., Brown, T. M., Caldwell, D., et al. (2010). Kepler mission design, realized photometric performance, and early science. *Astrophys. J. Lett.* 713, L79–L86. doi: 10.1088/2041-8205/713/2/L79

Kurtz, D. W. (1982). Rapidly oscillating AP stars. *Mon. Not. RAS* 200, 807–859. doi: 10.1093/mnras/200.3.807

Kurtz, D. W., Saio, H., Takata, M., Shibahashi, H., Murphy, S. J., and Sekii, T. (2014). Asteroseismic measurement of surface-to-core rotation in a main-sequence A star, KIC 11145123. *Mon. Not. RAS* 444, 102–116. doi: 10.1093/mnras/stu1329

Li, G., Bedding, T. R., Murphy, S. J., Van Reeth, T., Antoci, V., and Ouazzani, R.-M. (2019a). Period spacings of γ Doradus pulsators in the Kepler field: detection methods and application to 22 slow rotators. *Mon. Not. RAS* 482, 1757–1785. doi: 10.1093/mnras/sty2743

Li, G., Van Reeth, T., Bedding, T. R., Murphy, S. J., and Antoci, V. (2019b). Period spacings of γ Doradus pulsators in the Kepler field: Rossby and gravity modes in 82 stars. *Mon. Not. RAS* 487, 782–800. doi: 10.1093/mnras/stz1171

Li, G., Van Reeth, T., Bedding, T. R., Murphy, S. J., Antoci, V., Ouazzani, R.-M., et al. (2020). Gravity-mode period spacings and near-core rotation rates of 611 γ Doradus stars with Kepler. *Mon. Not. RAS* 491, 3586–3605. doi: 10.1093/mnras/stz2906

Liakos, A., and Niarchos, P. (2016). Poetry in motion: asteroseismology of delta Scuti stars in binaries using Kepler data. *arXiv* 1606.08638.

Liakos, A., and Niarchos, P. (2017). Catalogue and properties of δ Scuti stars in binaries. *Mon. Not. RAS* 465, 1181–1200. doi: 10.1093/mnras/stw2756

Mathys, G., Kurtz, D. W., and Holdsworth, D. L. (2020). Long-period Ap stars discovered with TESS data. *Astron. Astrophys.* 639:A31. doi: 10.1051/0004-6361/202038007

Matthews, J. M. (2007). One small satellite, so many light curves: Examples of δ Scuti asteroseismology from the MOST space mission. *Commun. Asteroseismol.* 150:333. doi: 10.1553/cia150s333

McNamara, D. H. (2000). "The high-amplitude δ Scuti stars," in *Delta Scuti and Related Stars, Volume 210 of Astronomical Society of the Pacific Conference Series*, eds M. Breger, and M. Montgomery (San Francisco, CA), 373.

Miglio, A., Montalbán, J., Noels, A., and Eggenberger, P. (2008). Probing the properties of convective cores through g modes: high-order G modes in SPB and γ Doradus stars. *Mon. Not. RAS* 386, 1487–1502. doi: 10.1111/j.1365-2966.2008.13112.x

Mombarg, J. S. G., Dotter, A., Van Reeth, T., Tkachenko, A., Gebruers, S., and Aerts, C. (2020). Asteroseismic modeling of gravity modes in slowly rotating A/F stars with radiative levitation. *Astrophys. J.* 895:51. doi: 10.3847/1538-4357/ab8d36

Mombarg, J. S. G., Van Reeth, T., Pedersen, M. G., Molenberghs, G., Bowman, D. M., Johnston, C., et al. (2019). Asteroseismic masses, ages, and core properties of γ Doradus stars using gravito-inertial dipole modes and spectroscopy. *Mon. Not. RAS* 485, 3248–3263. doi: 10.1093/mnras/stz501

Murphy, S. J., Bedding, T. R., Niemczura, E., Kurtz, D. W., and Smalley, B. (2015). A search for non-pulsating, chemically normal stars in the δ Scuti instability strip using Kepler data. *Mon. Not. RAS* 447, 3948–3959. doi: 10.1093/mnras/stu2749

Murphy, S. J., Hey, D., Van Reeth, T., and Bedding, T. R. (2019). Gaia-derived luminosities of Kepler A/F stars and the pulsator fraction across the δ Scuti instability strip. *Mon. Not. RAS* 485, 2380–2400. doi: 10.1093/mnras/stz590

Murphy, S. J., Moe, M., Kurtz, D. W., Bedding, T., Shibahashi, H., and Boffin, H. M. J. (2018a). *VizieR Online Data Catalog: Orbital Parameters of 341 New Binaries (Murphy+ 2018)*. Strasbourg: VizieR Online Data Catalog.

Murphy, S. J., Moe, M., Kurtz, D. W., Bedding, T. R., Shibahashi, H., and Boffin, H. M. J. (2018b). Finding binaries from phase modulation of pulsating stars with Kepler: V. Orbital parameters, with eccentricity and mass-ratio distributions of 341 new binaries. *Mon. Not. RAS* 474, 4322–4346. doi: 10.1093/mnras/stx3049

Murphy, S. J., and Paunzen, E. (2017). Gaia's view of the λ Boo star puzzle. *Mon. Not. RAS* 466, 546–555. doi: 10.1093/mnras/stw3141

Murphy, S. J., Saio, H., Takada-Hidai, M., Kurtz, D. W., Shibahashi, H., Takata, M., et al. (2020). On the first δ Sct-roAp hybrid pulsator and the stability of P and G modes in chemically peculiar A/F stars. *Mon. Not. RAS* 498, 4272–4286. doi: 10.1093/mnras/staa2667

Murphy, S. J., Shibahashi, H., and Kurtz, D. W. (2013). Super-Nyquist asteroseismology with the Kepler space telescope. *Mon. Not. RAS* 430:2986–2998. doi: 10.1093/mnras/stt105

Nemec, J. M., Balona, L. A., Murphy, S. J., Kinemuchi, K., and Jeon, Y.-B. (2017). Metal-rich SX Phe stars in the Kepler field. *Mon. Not. RAS* 466, 1290–1329. doi: 10.1093/mnras/stw3072

Ouazzani, R.-M., Salmon, S. J. A. J., Antoci, V., Bedding, T. R., Murphy, S. J., and Roxburgh, I. W. (2017). A new asteroseismic diagnostic for internal rotation in γ Doradus stars. *Mon. Not. RAS* 465, 2294–2309. doi: 10.1093/mnras/stw2717

Ouazzani, R. M., Lignières, F., Dupret, M. A., Salmon, S. J. A. J., Ballot, J., Christophe, S., et al. (2020). First evidence of inertial modes in γ Doradus stars: the core rotation revealed. *Astron. Astrophys.* 640:A49. doi: 10.1051/0004-6361/201936653

Paparó, M., Benkő, J. M., Hareter, M., and Guzik, J. A. (2016a). Unexpected series of regular frequency spacing of δ Scuti stars in the non-asymptotic regime. I. The methodology. *Astrophys. J.* 822:100. doi: 10.3847/0004-637X/822/2/100

Paparó, M., Benkő, J. M., Hareter, M., and Guzik, J. A. (2016b). Unexpected series of regular frequency spacing of δ Scuti stars in the non-asymptotic regime. II. Sample-Echelle diagrams and rotation. *Astrophys. J. Suppl.* 224:41. doi: 10.3847/0067-0049/224/2/41

Pedersen, M. G., Antoci, V., Korhonen, H., White, T. R., Jessen-Hansen, J., Lehtinen, J., et al. (2017). Do A-type stars flare? *Mon. Not. RAS* 466, 3060–3076. doi: 10.1093/mnras/stw3226

Pinsonneault, M. H., An, D., Molenda-Żakowicz, J., Chaplin, W. J., Metcalfe, T. S., and Bruntt, H. (2012). A revised effective temperature scale for the Kepler input catalog. *Astrophys. J. Suppl.* 199:30. doi: 10.1088/0067-0049/199/2/30

Pinsonneault, M. H., An, D., Molenda-Żakowicz, J., Chaplin, W. J., Metcalfe, T. S., and Bruntt, H. (2013). Erratum: "A Revised Effective Temperature Scale for the Kepler Input Catalog" (2012, ApJS 199:30). *Astrophys. J. Suppl.* 208:12. doi: 10.1088/0067-0049/208/1/12

Pollard, K. R. (2009). "A review of γ Doradus variables," in *Stellar Pulsation: Challenges for Theory and Observation, Volume 1170 of American Institute of Physics Conference Series*, eds J. A. Guzik and P. A. Bradley (New York, NY: American Institute of Physics, Melville), 455–466.

Pollard, K. R., Brunsden, E. J., Cottrell, P. L., Davie, M. W., Greenwood, A., and Kilmartin, P. M. (2013). "Spectroscopic mode identification in γ Doradus stars," in *Progress in Physics of the Sun and Stars: A New Era in Helio- and Asteroseismology, Volume 479 of Astronomical Society of the Pacific Conference Series*, eds H. Shibahashi and A. E. Lynas-Gray (San Francisco, CA), 105.

Poretti, E., Michel, E., Garrido, R., Lefèvre, L., Mantegazza, L., Rainer, M., et al. (2009). HD 50844: a new look at δ Scuti stars from CoRoT space photometry. *Astron. Astrophys.* 506, 85–93. doi: 10.1051/0004-6361/200912039

Rain, M. J., Ahumada, J., and Carraro, G. (2021). A new, Gaia based, catalogue of blue straggler stars in open clusters. *arXiv* 2103.06004. doi: 10.1051/0004-6361/202040072

Ricker, G. R., Winn, J. N., Vanderspek, R., Latham, D. W., Bakos, G. Á., Bean, J. L., et al. (2015). Transiting exoplanet survey satellite (TESS). *J. Astron. Telesc. Instr. Syst.* 1:014003. doi: 10.1117/1.JATIS.1.1.014003

Rodríguez, E., and Breger, M. (2001). Delta Scuti and related stars: analysis of the R00 catalogue. *Astron. Astrophys.* 366, 178–196. doi: 10.1051/0004-6361:20000205

Saio, H., Kurtz, D. W., Murphy, S. J., Antoci, V. L., and Lee, U. (2018). Theory and evidence of global Rossby waves in upper main-sequence stars: R-mode oscillations in many Kepler stars. *Mon. Not. RAS* 474, 2774–2786. doi: 10.1093/mnras/stx2962

Saio, H., Kurtz, D. W., Takata, M., Shibahashi, H., Murphy, S. J., Sekii, T., et al. (2015). Asteroseismic measurement of slow, nearly uniform surface-to-core rotation in the main-sequence F star KIC 9244992. *Mon. Not. RAS* 447, 3264–3277. doi: 10.1093/mnras/stu2696

Sandquist, E. L., Jessen-Hansen, J., Shetrone, M. D., Brogaard, K., Meibom, S., Leitner, M., et al. (2016). The age and distance of the Kepler open cluster NGC 6811 from an eclipsing binary, turnoff star pulsation, and giant asteroseismology. *Astrophys. J.* 831:11. doi: 10.3847/0004-637X/831/1/11

Schmid, V. S., and Aerts, C. (2016). Asteroseismic modelling of the two F-type hybrid pulsators KIC 10080943A and KIC 10080943B. *Astron. Astrophys.* 592:A116. doi: 10.1051/0004-6361/201628617

Sikora, J., David-Uraz, A., Chowdhury, S., Bowman, D. M., Wade, G. A., Khalack, V., et al. (2019). MOBSTER–II. Identification of rotationally variable A stars observed with TESS in sectors 1–4. *Mon. Not. RAS* 487, 4695–4710. doi: 10.1093/mnras/stz1581

Smalley, B., Antoci, V., Holdsworth, D. L., Kurtz, D. W., Murphy, S. J., De Cat, P., et al. (2017). Pulsation versus metallicism in Am stars as revealed by LAMOST and WASP. *Mon. Not. RAS* 465, 2662–2670. doi: 10.1093/mnras/stw2903

Suárez, J. C., García Hernández, A., Moya, A., Rodrigo, C., Solano, E., Garrido, R., et al. (2014). Measuring mean densities of δ Scuti stars with asteroseismology. Theoretical properties of large separations using TOUCAN. *Astron. Astrophys.* 563:A7. doi: 10.1051/0004-6361/201322270

Tassoul, M. (1980). Asymptotic approximations for stellar nonradial pulsations. *Astrophys. J. Suppl.* 43, 469–490. doi: 10.1086/190678

Thompson, S. E., Everett, M., Mullally, F., Barclay, T., Howell, S. B., Still, M., et al. (2012). A class of eccentric binaries with dynamic tidal distortions discovered with Kepler. *Astrophys. J.* 753:86. doi: 10.1088/0004-637X/753/1/86

Tingley, B., Bonomo, A. S., and Deeg, H. J. (2011). Using stellar densities to evaluate transiting exoplanetary candidates. *Astrophys. J.* 726:112. doi: 10.1088/0004-637X/726/2/112

Uytterhoeven, K., Moya, A., Grigahcène, A., Guzik, J. A., Gutiérrez-Soto, J., Smalley, B., et al. (2011). The Kepler characterization of the variability among A- and F-type stars. I. General overview. *Astron. Astrophys.* 534:A125. doi: 10.1051/0004-6361/201117368

Van Reeth, T., Mombarg, J. S. G., Mathis, S., Tkachenko, A., Fuller, J., Bowman, D. M., et al. (2018). Sensitivity of gravito-inertial modes to differential rotation in intermediate-mass main-sequence stars. *Astron. Astrophys.* 618:A24. doi: 10.1051/0004-6361/201832718

Van Reeth, T., Tkachenko, A., and Aerts, C. (2016). Interior rotation of a sample of γ Doradus stars from ensemble modelling of their gravity-mode period spacings. *Astron. Astrophys.* 593:A120. doi: 10.1051/0004-6361/201628616

Van Reeth, T., Tkachenko, A., Aerts, C., Pápics, P. I., Degroote, P., Debosscher, J., et al. (2015a). Detecting non-uniform period spacings in the Kepler photometry of γ Doradus stars: methodology and case studies. *Astron. Astrophys.* 574:A17. doi: 10.1051/0004-6361/201424585

Van Reeth, T., Tkachenko, A., Aerts, C., Pápics, P. I., Triana, S. A., Zwintz, K., et al. (2015b). Gravity-mode period spacings as a seismic diagnostic for a sample of γ Doradus stars from Kepler space photometry and high-resolution ground-based spectroscopy. *Astrophys. J. Suppl.* 218:27. doi: 10.1088/0067-0049/218/2/27

Welsh, W. F., Orosz, J. A., Aerts, C., Brown, T. M., Brugamyer, E., Cochran, W. D., et al. (2011). KOI-54: The Kepler discovery of tidally excited pulsations and brightenings in a highly eccentric binary. *Astrophys. J. Suppl.* 197:4. doi: 10.1088/0067-0049/197/1/4

White, T. R., Pope, B. J. S., Antoci, V., Pápics, P. I., Aerts, C., Gies, D. R., et al. (2017). Beyond the Kepler/K2 bright limit: variability in the seven brightest members of the Pleiades. *Mon. Not. RAS* 471, 2882–2901. doi: 10.1093/mnras/stx1050

Xiong, D. R., Deng, L., Zhang, C., and Wang, K. (2016). Turbulent convection and pulsation stability of stars–II. Theoretical instability strip for δ Scuti and γ Doradus stars. *Mon. Not. RAS* 457, 3163–3177. doi: 10.1093/mnras/stw047

Conflict of Interest: The author declares that the research was conducted in the absence of any commercial or financial relationships that could be construed as a potential conflict of interest.

frontiers in Astronomy and Space Sciences

MINI REVIEW
published: 22 April 2021
doi: 10.3389/fspas.2021.576623

Asteroseismic Observations of Hot Subdwarfs

A. E. Lynas-Gray[1,2,3]*

[1]Department of Physics and Astronomy, University College London, London, United Kingdom, [2]Department of Physics, University of Oxford, Oxford, United Kingdom, [3]Department of Physics and Astronomy, University of the Western Cape, Bellville, South Africa

There are a number of reasons for studying hot subdwarf pulsation; the most obvious being that these stars remain a poorly understood late-stage of stellar evolution and knowledge of their interior structure, which pulsation studies reveal, constrains evolution models. Of particular interest are the red giant progenitors as in looking at a hot subdwarf we are seeing a stripped-down red giant as it would have been just before the Helium Flash. Moreover, hot subdwarfs may have formed through the merger of two helium white dwarfs and their study gives insight into how such a merger may have happened. A less obvious reason for studying pulsation in hot subdwarfs is that they provide a critical test of stellar envelope opacities and the atomic physics upon which they depend.

Keywords: stars: subdwarfs, stars: oscillations, stars: evolution, stars: binaries: general, stars: rotation

OPEN ACCESS

Edited by:
Jaymie Matthews,
University of British Columbia, Canada

Reviewed by:
Mkrtichian Egishe David,
National Astronomical Research Institute of Thailand, Thailand
Joyce Ann Guzik,
Los Alamos National Laboratory (DOE), United States

****Correspondence:***
A. E. Lynas-Gray
tony.lynas-gray@physics.ox.ac.uk

Specialty section:
This article was submitted to Stellar and Solar Physics, a section of the journal Frontiers in Astronomy and Space Sciences

Received: *26 June 2020*
Accepted: *01 February 2021*
Published: *22 April 2021*

Citation:
Lynas-Gray AE (2021) Asteroseismic Observations of Hot Subdwarfs. Front. Astron. Space Sci. 8:576623. doi: 10.3389/fspas.2021.576623

1 INTRODUCTION

Hot subdwarfs are understood (Heber, 2009; Heber, 2016) to be core-helium burning stars, having masses of $\sim 0.5 M_{\odot}$ and retaining only thin hydrogen envelopes ($\sim 10^{-4} M_{\odot}$); they form blue extensions of Horizontal Branches seen in Hertzsprung-Russell Diagrams. Some hot subdwarfs appear to be single stars and many exist in binary systems. Two broad categories of binary system are found to host hot subdwarfs: those with short (~ 0.1 days) orbital periods (Kupfer et al., 2015) where the companion is typically a M-dwarf or a white dwarf and those with long (~ 1000 days) orbital periods (Vos et al., 2019) where the companion is a F, G or K Main Sequence star.

Binary population synthesis calculations (Han et al., 2002; Han et al., 2003) show how single hot subdwarfs may form through the merger of two helium white dwarfs, while those in binary systems have red giant progenitors whose hydrogen envelope is almost completely removed at or just before the Helium Flash. Longer period binaries are understood to be a consequence of stable Roche Lobe overflow whereas the shorter period binaries form through common envelope evolution. Clausen and Wade (2011) and Clausen et al. (2012) propose another singleton hot-subdwarf formation channel involving the merger of a helium white dwarf and a low-mass hydrogen-burning star.

Most known hot subdwarfs have effective temperatures ($T_{\rm eff}$) of less than 40000K; these are referred to as subdwarf-B (sdB) stars to distinguish them from the hotter subdwarf-O stars. Greenstein (1957) argues that pulsational instability may be found in hot subdwarfs but some forty years were to elapse before this important discovery was made. The Edinburgh-Cape Survey (Stobie et al., 1997b, EC) includes photometric monitoring of sdB stars, finding $\sim 3\%$ to pulsate with periods typically between 100 and 500 s; the first pulsators identified being V361 Hya (EC 14026–2647, Kilkenny et al., 1997), EO Cet (PB 8783, Koen et al., 1997), UX Sex (EC 10228–0905, Stobie et al., 1997a) and V4640 Sgr (EC 20117–4014, O'Donoghue et al., 1997). The discovery of pulsation in a few sdB stars rejuvenated theoretical and observational hot subdwarf research, fields which had been largely dormant for the preceding two decades; there was now some

prospect of studying the internal structure of stars in a poorly-understood late stage of stellar evolution.

A subsequent survey (Green et al., 2003) finds longer period (~ 1 hour) sdB pulsators which are now referred to as V1093 Her (PG 1716 + 426) stars. Further observations (Oreiro et al., 2004; Baran et al., 2005; Oreiro et al., 2005; Schuh et al., 2005) identify DW Lyn (Ballon 090100001) as a hybrid sdB pulsator, having both short and long period pulsations. Long period pulsators have $T_{\rm eff} < 30000$ K, and for those having short periods $T_{\rm eff} > 30000$ K; hybrid pulsators being found to have $T_{\rm eff} \simeq 30000$ K.

While Greenstein (1957) advocates photometric monitoring of hot subdwarfs, Charpinet et al. (1996) model pulsation instability and so anticipate the publication of pulsation having been discovered in the following year; he and his co-authors then identify (Charpinet et al., 1997) the V361 Hya stars, as they came to be known, as p-mode pulsators driven by the κ-mechanism. V361 Hya star pulsation is driven by the κ-mechanism through a metal (mostly iron) ionisation zone which OPAL (Rogers and Iglesias, 1992a; Rogers and Iglesias, 1992b) and Opacity Project (OP, Seaton et al., 1994) stellar envelope opacity revisions identify. The metal ionisation zone results in an increased opacity (known as the "Z-Bump") and Charpinet et al. (1997) argue, in the case of sdB stars, that this is enhanced through the condition of diffusive equilibrium between gravitational settling and radiative levitation.

The discovery of p-mode pulsation in V361 Hya stars prompts Charpinet et al. (2000), Charpinet et al. (2002a), Charpinet et al. (2002b) to conduct an in-depth adiabatic survey of sdB star oscillations. Basic results are provided in Paper I (Charpinet et al., 2000) of the series in which pulsational properties of a representative evolutionary model are discussed. Essential guidance in understanding pulsation mode period behaviours as functions of sdB star stellar parameters is provided in the subsequent papers; the effects of model parameters being discussed in Paper II (Charpinet et al., 2002a) and Extreme Horizontal Branch evolutionary effects in Paper III (Charpinet et al., 2002b).

Pulsations in the longer period V1093 Her stars are also driven through the κ-mechanism, although in this case they are identified as g-mode pulsators (Fontaine et al., 2003). Jeffery and Saio (2006) resolve a 5,000 K discrepancy between the observed and theoretical blue edges of the V1093 Her instability domain through the use of updated OP opacities (Badnell et al., 2005), and considering an enhancement of nickel as well as iron in the driving zone; this arises because OP predicts iron and nickel contributions to the "Z-Bump" to occur at higher temperatures. Applied to sdB star pulsation more generally, Jeffery and Saio (2007) note that κ-mechanism driving of sdB star pulsation can occur through smaller increases in the iron and nickel concentrations in the driving-zone. Bloemen et al. (2014) show in a further study that iron and nickel enhancements occur naturally in the metal-ionisation zone, without the need for artificial enhancements.

Mode identification is a further crucial step in any asteroseismic analysis. One option is to secure a photometric time-series using multi-colour photometry which ideally is longer than the longest pulsation period of interest by a large factor, the larger the better. Randall et al. (2005a) present the theoretical basis for a multi-colour photometric technique, based on the frequency dependence of an oscillation amplitude and phase being related to the degree index ℓ and other factors which may be eliminated through the amplitude ratios and phase differences arising from the brightness variation in different wavebands. Time-series spectroscopy is another technique which Schoenaers and Lynas-Gray (2006, 2008), discuss, as does Telting (2008) more generally; this has yet to be widely applied to sdB stars as short cadence high dispersion spectra, at an adequate signal-to-noise are challenging to obtain over a long enough time-interval, even with modern instrumentation.

Eclipse mapping may be used for mode identifcation when a pulsating star is in an eclipsing binary, as Reed et al. (2005) and Nuspl (2011) demonstrate. The essential idea is to model observed power spectra at selected orbital phases as their amplitudes vary in a mode-dependent way determined by pulsation and rotation axes inclinations. Given observed power spectra with an adequate signal-to-noise and frequency resolution, simulations show that low-order ($\ell \lesssim 3$) modes may be identified and radial modes ($\ell = 0$) found easily, as in the latter case power spectrum amplitudes are not dependent on orbital phase.

It quickly became clear that an adequate frequency resolution in power spectra could not be achieved with ground-based observations made at a single site; this was most obvious in the case of the longer period g-mode pulsators. Kilkenny (2010) reporting of amplitude variations in pulsating sdB stars provides further emphasis on the importance of achieving a higher frequency resolution in power spectra, because these amplitude variations could conceivably be due to beating between very close unresolved frequencies. Hot subdwarfs in the Kepler (Borucki et al., 2010) field were observed almost continuously for more than three years and the purpose of the present paper is to review this work, in the context of earlier studies with the Whole Earth Telescope (WET, Nather et al., 1990) and CoRoT (Baglin et al., 2006), as well as subsequent observations with K2 (Howell et al., 2014) and TESS (Ricker et al., 2015). The intention was to complement and update earlier reviews of sdB asteroseismology by Fontaine et al. (2008), Østensen (2010), Reed (2016), Reed et al. (2018b)

Aerts (2019) summarises the use of asteroseismology to probe stellar interiors; her figure 1 shows the positions of many known types of pulsating star, including sdB pulsators, in a Hertzsprung-Russell Diagram. Pulsating sdB stars reviewed in the present paper have been listed in **Table 1**. Left-hand columns give equatorial and galactic coordinates. A sample of the names or designations used in the literature are provided in the central three columns. The column on the extreme right identifies the type of sdB pulsator, following the scheme Kilkenny (2010) suggest with a minor adaptation.

As discussed below, observations identify some g-mode pulsators as also showing weak p-modes in their power spectra; I have identified these in **Table 1** as "sdBV$_{(sr)}$" to distinguish them from the Kilkenny classification "sdBV$_{rs}$" for

TABLE 1 | Reviewed Pulsating sdB Stars.

Equatorial Coordinates		Galactic Coordinates		Designation(s)	PG/EC/KPD/		Space Mission		Pulsator
α (J2000)	δ (J2000)	ℓ^{II}	b^{II}	Commonly Used	KUV Catalogue		Input Catalogue		Type
00 16 54.27	+07 04 30.0	107.958740	−54.789659	EK Psc (PHL 766)	PG	0014 + 068	TIC	405212419	sdBV$_r$
00 47 29.22	+09 58 55.7	121.319967	−52.877245	HD 4539 (PHL 830)	PG	0044 + 097	EPIC	220641886	sdBV$_{(sr)}$
00 51 26.94	+09 21 32.9	122.936506	−53.512614	SDSS JJ005126.93 + 092132.9	PG	0048 + 091	EPIC	220614972	sdBV$_{(rs)}$ + F
01 04 21.67	+04 13 37.1	129.105414	−58.489796	Feige 11 (PB 6252)	PG	0101 + 039	EPIC	220376019	sdBV$_s$
01 08 26.78	−32 43 11.6	270.584263	−83.304895	CD −33° 417 (SB 459)			TIC	67584818	sdBV$_s$
01 23 43.25	−05 05 45.8	143.603685	−66.663360	EO Cet (PB 8783)			TIC	248949857	sdBV$_r$
01 56 31.90	−13 54 26.5	175.134253	−69.864921	GD 1053	EC	01541–1409	TIC	62381958	sdBV$_r$
03 45 34.58	+02 47 52.7	184.426667	−38.475269		PG	0342 + 026	TIC	457168745	sdBV$_s$
04 44 56.90	+14 21 50.2	184.190561	−19.811676	V1405 Ori	KUV	04421 + 1416	EPIC	246683636	sdBV$_{(rs)}$ + M?
05 07 20.23	−28 02 25.3	229.886388	−33.987631	CD −28° 1974	EC	05053–2806	TIC	13145616	sdBV$_{rs}$ + F/G
06 31 53.82	−00 19 13.1	210.985775	−04.493128	SDSS J063153.81–001913.0	KPD	0629–0016	TIC	36995993	sdBV$_s$
07 07 09.80	+60 38 50.2	155.677776	+25.299771	DW Lyn (Balloon 090100001)			TIC	88565376	sdBV$_{rs}$
08 20 03.36	+17 39 14.2	206.080058	+27.264486	SDSS J082003.35 + 173914.2			EPIC	211823779	sdBV$_r$ + F
08 28 32.87	+14 52 02.5	209.868554	+28.077860	UVO 0825 + 15			EPIC	211623711	He-sdBV
08 36 03.99	+15 52 16.4	209.614847	+30.137822	SDSS J083603.98 + 155216.4			EPIC	211696659	sdBV$_s$ + WD
08 36 12.03	+19 17 56.1	205.918128	+31.428427	LB 378 (EGGR 266)			EPIC	211938328	sdBV$_r$ + F
08 56 49.27	+17 01 14.7	210.568732	+35.181583	SDSS J083612.03 + 191755.9			EPIC	211779126	sdBV$_{rs}$
10 25 17.34	−09 20 40.6	253.673072	+39.164600	UX Sex	EC	10228–0905	TIC	36879659	sdBV$_r$
10 50 02.83	−00 00 36.9	250.855810	+50.170702	UY Sex	PG	1047 + 003	EPIC	248411044	sdBV$_r$
11 44 57.24	−03 56 53.3	273.077621	+55.023043		PG	1142–037	EPIC	201206621	sdBV$_s$ + WD?
12 44 20.24	−08 40 16.8	299.934029	+54.159064	HW Vir (BD −07° 3477)	PG	1241–084	TIC	156618553	sdBV$_{(sr)}$
13 17 39.21	−12 32 52.4	312.874993	+49.817059		PG	1315–123	EPIC	212508753	sdBV$_{(rs)}$ + F
13 27 48.56	+09 54 51.0	331.134760	+70.767330	QQ Vir	PG	1325 + 102	TIC	404505165	sdBV$_r$
13 38 48.15	−02 01 49.2	326.172422	+58.687745	NY Vir	PG	1336–018	TIC	175402069	sdBV$_r$ (EB)
13 40 08.83	+47 51 51.9	101.523443	+67.188615	SDSS J134008.83 + 475151.8	PG	1338 + 481	TIC	458452988	sdBV$_s$
13 55 44.72	−08 03 54.5	329.072625	+51.512995	SDSS J135544.71–080354.3			EPIC	212707862	sdBV$_s$
14 05 33.00	−27 01 34.1	322.655708	+32.991261	V361 Hya	EC	14026–2647	TIC	60793020	sdBV$_r$
16 08 03.69	+07 04 28.7	018.992818	+39.329833	V338 Ser	PG	1605 + 072	TIC	291032641	sdBV$_r$
16 19 26.60	+56 05 58.6	085.877991	+43.162539	SDSS J161926.58 + 560558.6	PG	1618 + 563B	TIC	207440585	sdBV$_r$
16 29 35.30	+01 38 18.8	016.572779	+31.949416	V2579 Oph	PG	1627 + 017	TIC	281269725	sdBV$_s$ + WD
16 49 56.23	−24 17 34.4	356.694762	+12.861245				EPIC	203948264	sdBV$_s$
17 17 22.06	+58 05 58.7	086.623052	+35.084435	V366 Dra			TIC	198412771	sdBV$_r$
17 18 03.86	+42 34 12.6	067.678153	+34.623301	V1093 Her	PG	1716 + 426	TIC	334901449	sdBV$_s$
18 24 52.41	+57 47 23.5	086.788792	+26.146641	LS Dra			TIC	353735596	sdBV$_r$
18 56 07.04	+43 19 19.3	073.257018	+17.435408				KIC	07664467	sdBV$_{(sr)}$ + WD?
19 02 21.94	+48 50 52.2	079.089792	+18.386459				KIC	11179657	sdBV$_s$ + M
19 03 37.03	+38 36 12.6	069.278167	+14.333026	SDSS J190337.02 + 383612.6			KIC	03527751	sdBV$_{sr}$
19 05 06.38	+43 18 31.2	073.878723	+15.912657				KIC	07668647	sdBV$_s$
19 09 07.15	+37 56 14.2	069.101928	+13.075789	SDSS J190907.14 + 375614.2			KIC	02697388	sdBV$_{(sr)}$
19 09 33.41	+46 59 04.1	077.730419	+16.585795				KIC	10001893	sdBV$_{(sr)}$
19 24 58.15	+47 07 53.7	078.954543	+14.236736				KIC	10139564	sdBV$_r$
19 26 34.11	+49 30 29.6	081.302431	+14.983279				KIC	11558725	sdBV$_s$
19 27 09.15	+38 10 26.4	070.883271	+09.975824	SDSS J192709.14 + 381026.3			KIC	02991276	sdBV$_{(sr)}$
19 27 15.88	+38 08 08.3	070.858605	+09.938826	SDSS J192715.88 + 380808.2			KIC	02991403	sdBV$_s$ + M
19 31 03.38	+44 13 25.5	076.730534	+12.024358				KIC	08302197	sdBV$_s$ + M?
19 32 14.81	+27 58 35.4	062.285531	+04.283443	V2214 Cyg	KPD	1930 + 2752	KIC	284692897	sdBV$_r$ + WD
19 34 39.94	+47 58 11.5	080.456691	+13.119129				KIC	10670103	sdBV$_{(sr)}$
19 38 28.03	+58 24 15.8	090.483610	+17.060368				TIC	1883989109	sdBV$_r$
19 38 32.61	+46 03 59.1	079.018765	+11.674294	2M 1938 + 4603			KIC	9472174	sdBV$_{(sr)}$ (EB)
19 45 25.47	+41 05 33.9	075.161197	+08.231124		KPD	1943 + 4058	KIC	5807616	sdBV$_{(sr)}$
19 53 08.39	+47 43 00.2	081.700956	+10.258111				KIC	10553698	sdBV$_s$ + WD
20 15 04.79	−40 05 44.1	000.805816	−32.457367	V4640 Sgr (CD −40°13747)	EC	20117–4014	TIC	355058528	sdBV$_r$
21 53 41.25	−70 04 31.4	321.130100	−40.184030	EC 21494–7018			TIC	278659026	sdBV$_s$
23 19 24.43	−08 52 37.9	068.617247	−61.611625	GD 1110 (PHL 457)			TIC	49590066	sdBV$_s$ + M
23 34 34.63	−01 19 36.9	084.174720	−58.292251	EQ Psc (PB 5450)			KIC	060018081	sdBV$_s$ + M
23 44 22.01	−34 27 00.4	001.845773	−73.871649	CD −35° 15910 (SB 815)			TIC	169285097	sdBV$_{(sr)}$

DW Lyn stars. Similarly, some p-mode pulsators have been identified as "sdBV$_{(rs)}$" because they are found to have weak g-modes in their power spectra. A qualifying upper case letter or "WD" was used to indicate an approximate companion spectral type and "(EB)" to indicate that the pulsating sdB star resides in an eclipsing binary.

2 MULTI-SITE AND WHOLE EARTH TELESCOPE OBSERVATIONS

Koen et al. (1998) identify V338 Ser (PG 1605 + 072) as an apparently single V361 Hya star with low surface gravity (log*g*) and high amplitude pulsation frequencies; these and the comparatively long period of the dominant frequency (480 s), when compared with other V361 Hya stars known at the time, made it the first V361 Hya candidate for a multi-site campaign. Kilkenny et al. (1999) observe V338 Ser over a 2 week period from five sites, well distributed in longitude, and obtain ~ 180 hours of useable photometry. Twenty frequencies are found to agree with those Koen et al. find if possible aliases of up to three-cycles per day are taken into account; these and pulsation amplitude changes emphasise the importance of multi-site observations and for the need to repeat V361 Hya star monitoring at a sequence of epochs.

O'Toole et al. (2005), Tillich et al. (2007) conduct further multi-site campaigns on V338 Ser, involving photometry and contemporaneous spectroscopy. Line profile variations are detected and measured in about 9,000 spectra from which $T_{\rm eff}$ and log*g* are determined by quantitative spectral analysis based on model stellar atmospheres and line formation calculations, made assuming a static atmosphere. $T_{\rm eff}$ and log*g* are obtained for eight modes with semi-amplitudes ranging from $\Delta T_{\rm eff}$ = 880 K to as little as $\Delta T_{\rm eff}$ = 88 K, and $\Delta \log g$ = 0.08 dex to as low as $\Delta \log g$ = 0.008 dex. Gravity and temperature vary almost in phase, whereas phase lags are found between temperature and radial velocity.

UY Sex (PG 1047 + 003) is another apparently single V361 Hya star (Billères et al., 1997; O'Donoghue et al., 1998) for which Kilkenny et al. (2002) conduct a multi-site photometric campaign over a two-week period and obtain ~ 98 hours of useful data. Eighteen frequencies are recovered with some evidence of 1 day aliasing in frequencies which the discovery data (Billères et al., 1997; O'Donoghue et al., 1998) identify, again demonstrating the value of multi-site observations which allow monitoring over an extended period. Kilkenny et al. note that four pairs of the frequencies they identify are closely spaced, separated on average by 1.05 μHz which would correspond to a rotation period of about 11.0 days; this could be the first indication that V361 Hya stars are slow rotators.

NY Vir (PG 1336–018) is a very short-period (0.101 days) eclipsing binary with a V361 Hya star primary, the secondary being a late-type dwarf of type ~ M5 (Kilkenny et al., 1998). NY Vir was arguably one of the more important V361 Hya stars to have been discovered because stellar parameters inferred from an asteroseismic analysis could be directly compared with those from analyses of light and radial velocity curves, although in this case pulsation frequency aliasing is provided by the orbital period. Kilkenny et al. (2003) therefore observe NY Vir with WET, obtaining photometry over ~172 hours; they find substantial pulsation frequency changes to have occurred since discovery with amplitude changes occurring, at least in the dominant three frequencies, on a time-scale of order one day. Power spectra based on data obtained during eclipses to eliminate aliases these cause, recover the three main pulsation frequencies although these are not adequate for mode identification. An eclipse mapping application by Reed (2006) for NY Vir, based on WET data, attempts pulsation mode identification with the pulsation axis assumed to lie in the direction of the companion, but ≃20 low amplitude frequencies remain unidentified.

QQ Vir (PG 1325 + 101) is seen (Silvotti et al., 2002) to be a particularly interesting V361 Hya star having large pulsation amplitudes and showing an harmonic of the main pulsation frequency; 215 hours of multi-site photometry are obtained by Silvotti et al. (2006) and fifteen pulsation frequencies identified. Charpinet et al. (2006) use the Silvotti et al. observations for an asteroseismic study; observed periods correspond to low order acoustic modes, defining a band of unstable modes in agreement with non-adiabatic pulsation theory. The hydrogen envelope mass is found to be $10^{-4.18 \pm 0.1}$ of the stellar mass of $0.50 \pm 0.01 M_{\odot}$. The rotation period is 1.6 ± 0.2 days which makes QQ Vir a slow rotator.

Multi-site campaigns are carried out for PG 1618 + 563B and PG 0048 + 091, two V361 Hya class sdB pulsators, from which Reed et al. (2007) present interesting results for both stars. Some observations of PG 1618 + 563B show a small number of stable (in amplitude) frequencies with a closely spaced pair, as would be typical for a V361 Hya star. In contrast, other data show PG 1618 + 563B to be a complex pulsator with four "regions" of power showing amplitude and phase variability; it is an obvious target for further observation, over a longer time-interval, with the view to examining its long-term frequency stability.

Reed et al. (2007) find PG 0048 + 091 to be a more complex pulsator than PG 1618 + 563B as it shows wildly variable amplitudes, while from discovery observations Koen et al. (2004) find stable pulsation amplitudes. Although an extremely rich pulsator with at least twenty-eight independent frequencies, many modes are only occasionally excited to amplitudes above the noise, often for very short lengths of time. Stochastically excited oscillations are inferred although these are not expected in a V361 Hya star where pulsations are understood to be driven by the κ-mechanism as described above.

In a later paper, Reed et al. (2012) report multi-site observations of EC 01541–1409; it turns out to be similar to PG 0048 + 091 in that both stars oscillate over a large frequency range. Thirty-four pulsation frequencies are identified in the case of EC 01541–1409, most of which are unstable in amplitude or phase. EC 01541–1409 differs from PG 0048 + 091 in that it has one high-amplitude phase-stable oscillation and, as the other frequencies are less variable in phase, stochastic excitation is not inferred in this case.

Billéres et al. (2000) find forty-four oscillations in the light curve of V2214 Cyg (KPD 1930 + 2752); it therefore has a rich frequency spectrum similar to those subsequently found in the cases of PG 0048 + 091 and EC 01541–1409 discussed above. V2214 Cyg is also found to be an ellipsoidal variable having a white dwarf as a binary companion, the binary period being 2.3 hours. Maxted et al. (2000) stimulate further interest in the system; their spectra suggest a total mass for the system of $1.47 M_{\odot}$, if the sdB star has the canonical $0.5 M_{\odot}$, making it a candidate Type Ia Supernova Progenitor as gravitational radiation will eventually result in binary component merger.

Reed et al. (2011b) report photometric observations of V2214 Cyg they make during 2003 with WET, and a smaller multisite campaign made in 2002. Sixty-eight pulsation frequencies are found in 355 hours of WET data, these showing many of the stochastic characteristics seen in PG 0048 + 091. Amplitude variations are compared with simulated stochastic data, and the binary nature of V2214 Cyg used for identifying pulsation modes using multiplet structure and a tidally induced pulsation geometry. Results suggest a complicated pulsation structure which includes a sixteen-hour amplitude variability, rotationally split and tidally induced modes, as well as some pulsations which are geometrically limited to the sdB star. Satellite observations of V2214 Cyg would have provided further insight but it lies just outside the Kepler field.

Vučković et al. (2006) highlight the pulsating sdB star EK Psc (PG 0014 + 067) as a promising candidate for a future seismic analysis, as it has a rich pulsation spectrum. As the frequency spectrum is too complex to be explained with low-degree ($\ell < 3$) p-modes without rotational splittings, a fundamental challenge to understanding its pulsation was immediately obvious. While assigning a high degree ($\ell \geq 3$) to some modes remains a possibilty, theoretical models (Kawaler and Hostler, 2005) suggest that sdB stars may retain rapidly rotating cores, resulting in the presence a few rotationally split triplet ($\ell = 1$) and quintuplet ($\ell = 2$) modes, along with radial ($\ell = 0$) p-modes. The need for a better frequency resolution to help distinguish among possible pulsation models persuades Vučković et al. to obtain WET observations of EK Psc; they find frequencies which do not appear to fit any theoretical model then available although they suggest a simple empirical relation which does match all well-determined frequencies in this star.

Baran et al. (2009) present results from a multi-site photometric campaign on the prototype hybrid sdB pulsator DW Lyn (Balloon 090100001) noted above. Forty-eight nights of data give a temporal resolution of 0.36 μHz, with a detection threshold of about 0.2 mmag in a B-filter; the subsequent analysis finds 114 frequencies, of these ninety-seven are independent and seventeen are combinations. Most of the twenty-four g-mode frequencies lie between 0.1 and 0.4 mHz; the remainder (presumably p-modes) are in four distinct groups near 2.8, 3.8, 4.7, and 5.5 mHz. The density of frequencies requires some modes to have $\ell > 2$.

Modes in the 2.8 mHz region found by Baran et al. (2009) have the largest amplitudes, the strongest is understood to be a radial mode while others in this region form two nearly symmetric multiplets: a triplet and quintuplet with rotational splitting. Splitting in both multiplets increases by $\sim 15\%$ between 2004 and 2005, implying a rotation rate dependent on latitude and highest on the equator. Torsional oscillations seem to be the only plausible explanation, though this needs to be verified by modelling. The amplitudes of almost all modes are found to vary, even within a single season.

In the case of V1093 Her stars, longer periods mean that any ground-based observations must almost necessarily be multi-site if a sufficient number of pulsation cycles are to be observed to allow a periodogram analysis. Among the V1093 Her stars, Randall et al. (2006a), Randall et al. (2006b) select V2579 Oph (PG 1627 + 017) and PG 1338 + 481 for their campaigns. V2579 Oph is a binary, the companion understood to be a white dwarf, with an orbital period ~0.83 days; Randall et al. (2006a) select it because it is relatively bright (V = 12.9), has a large pulsation amplitude and can be observed from either hemisphere. By contrast, Randall et al. (2006b) select PG 1338 + 481 for their second campaign because it is a more typical V1093 Her star understood, from spectroscopy, to be a single star.

Randall et al. (2006a) extract twenty-three pulsation frequencies for V2579 Oph, with periods between 4500 and 9,000 s, from 300 hours of useful R-band and fifty hours of simultaneous U/R differential photometry. Rotation synchronous with the binary orbit is understood to produce splitting in the highest amplitude frequencies which cluster in the period range 6300–7050 seconds. Nonadiabatic pulsation models reproduce V2579 Oph pulsation frequencies for $\ell =$ 2, 3 or 4 if $T_{\rm eff}$ is near the lower bound its error bars indicate. But period spacing, rotational splitting and U/R photometry suggest $\ell = 1$ for at least the four highest amplitude peaks in the power spectrum, suggesting non-adiabatic effects as not being fully accounted for in adopted pulsation models.

Seven continuous weeks of observing PG 1338 + 481 at Mount Bigelow and Kitt Peak provide Randall et al. (2006b) ~250 hours of simultaneous U/R time-series photometry, as well as a further ~70 hours of R-band only data. Thirteen frequencies are extracted in the 2100–7200 second range, with amplitudes up to $\sim 0.3\%$ and $\sim 0.2\%$ in U and R respectively. An amplitude ratio comparison in the two wave-bands with those predicted by non-adiabatic pulsation theory suggests the presence of dipole modes, consistent with the highest amplitude peak period spacing. Randall et al. fix $T_{\rm eff}$ and log$g$ to the spectroscopic estimates and isolate a family of optimal models reproducing measured periods to better than 1%. Preliminary stellar parameters inferred include an uncharacteristically high mass of $0.616 M_{\odot}$ and a thicker residual hydrogen envelope than those found in V361 Hya stars; this latter result is not surprising and is predicted for cooler sdB stars.

I have summarised sdB star WET and multi-site campaigns that I am aware of. Of particular note was the selection of PG 1618 + 563B, PG 0048 + 091, EC 01541–1409, V2214 Cyg, EK Psc and DW Lyn as targets for multi-site and WET observing programmes. In each case, I understood selection to have been based in part on the target being known beforehand to have a "rich pulsation spectrum", providing the hope that higher frequency resolution achievable through multi-site and WET observations would provide a high quality power spectrum from which a definitive asteroseismic analysis could follow. WET and multi-site observations showed, however, for each target in turn, that V361 Hya and DW Lyn star power spectra are highly variable and that asteroseismic analyses will be much more challenging than originally supposed.

3 MOST AND COROT OBSERVATIONS

Randall et al. (2005b) pioneer the use of spacecraft to obtain high-precision photometry of sdB stars; they monitor Feige 11 (PG

0101 + 039) for ~400 hours with the MOST Satellite (Walker et al., 2003) and identify periods of 7235, 5227, and 2650 seconds. Pulsation amplitudes which Randall et al. find are between 0.03 and 0.06% of the mean brightness, an observation which would be challenging for ground-based observers. The detection of pulsations in Feige 11 meant that the theoretical instability strip blue-edge for V1093 Her stars, as it was then understood, had to lie at higher effective temperatures as Jeffery and Saio (2006) subsequently demonstrate.

Three frequencies are, however, insufficient for a thorough asteroseismic analyis and Charpinet et al. (2010) circumvent this limitation by using CoRoT to identify seventeen pulsation frequencies in KPD 0629–0016. Longer period g-modes in sdB pulsators penetrate the deeper stellar interior, as far as the core, and asteroseismic analyses potentially reveal core masses and compositions. Van Grootel et al. (2010b) perform the second (the first being described below) asteroseismic analyses of a g-mode sdB pulsator using Charpinet et al. observations of KPD 0629–0016; they derive a core-mass and composition corresponding to an age of 42.6 ± 1.0 Myr relative to the Zero Age Horizontal Branch (ZAHB).

4 KEPLER OBSERVATIONS

Given the success of asteroseismic observations of pulsating sdB stars with multi-site ground based facilities and spacecraft, the launch of the Kepler satellite was accompanied with an understanding that further advances were about to be achieved. Østensen et al. (2010b) present results from the first two quarters of the Kepler survey, identifying nine sdB pulsators of which one is a V361 Hya star, another a DW Lyn star and seven V1093 Her stars. Below the $T_{\rm eff}$ boundary region where DW Lyn stars are found, all sdB targets are found to pulsate; with only a fraction (< 10%) of sdB stars with higher $T_{\rm eff}$ being pulsators. Østensen et al. also note that the V361 Hya pulsator (KIC 10139564) shows a low-amplitude mode in the long-period region, while several V1093 Her pulsators show low-amplitude modes in the short period region; this suggests that hybrid behaviour may be a common feature observable in many if not all sdB star pulsators.

The identification of KIC 10139564 as the only V361 Hya pulsator, among a sample of hot subdwarfs in the Kepler field, prompts Kawaler et al. (2010b) to present a more detailed analyis of the 30.5 days of nearly continuous time-series photometry they obtain with the Kepler spacecraft. Most of the ten independent pulsation frequencies they identify appear to be stable in phase and amplitude, providing an initial estimate for the rotation period of 2–3 weeks. With a further fifteen months of Kepler photometry, Baran et al. (2012) detect fifty-seven periodicities including several multiplets they attribute to stellar rotation, indicating a rotation period of 25.6 ± 1.8 days for KIC 10139564. A further interesting result (Baran and Østensen, 2013) is that two regions of the KIC 10139564 amplitude spectrum contain modes of degree $\ell = 3$ and $\ell = 4$. Based on thirty-eight months of almost continuous Kepler photometry of KIC 10139564, Zong et al. (2016) identify frequency and amplitude modulations as a first signature of non-linear resonant coupling occurring in V361 Hya stars which appear to follow more complicated patterns than simple predictions from current non-linear theory.

Reed et al. (2010) provide more details on the discovery of non-radial pulsations in five apparently single V1093 Her stars, based on 27 days of nearly continuous Kepler satellite photometry which Østensen et al. (2010b) report. Every sdB star cooler than $T_{\rm eff} \leq 27500$ K observed by Kepler (seven at that time) is found to be a V1093 Her or a DW Lyn pulsator. Periods range from 1 to 4.5 hours and are associated with g-mode pulsations. Three stars (KIC 02697388, KIC 03527751 and KPD 1943 + 4058 (KIC 05807616)) also exhibit short 2–5 min periods indicative of p-modes, as well as periods of 15–45 min, intermediate between the two classes. Reed et al. also find KIC 10670103 to be the longest-period V1093 Her star known and to have the lowest $T_{\rm eff}$ of 20900 K. Equally remarkable is KIC 02697388, a suspected hybrid pulsator, for which $T_{\rm eff} = 23900$ K; this turns out to have g-modes with amplitudes larger than those of its p-modes.

KPD 1943 + 4058 is one of three V1093 Her stars in which Reed et al. (2010) identify at least one short-period oscillation. Van Grootel et al. (2010a) retain eighteen pulsations in early Kepler data for their analysis, identifying these as low-degree ($\ell = 1$ and 2) intermediate-order (k = −9 through −58) g-modes. Pulsation models reproduce observed frequencies at the 0.22% level, comparable with the best results achieved in analyses of p-mode V361 Hya pulsators. Structural parameters Van Grootel et al. infer are: the sdB star mass $M = 0.496 \pm 0.002 M_{\odot}$, the mass of the residaul hydrogen envelope $\log(M_{env}/M) = -2.55 \pm 0.07$, the mass of the carbon-oxygen (C + O) core $\log(1 - M_{\rm core}/M) = -0.37 \pm 0.01$, and the core mass fraction $X_{\rm core}(C + O) = 0.261 \pm 0.008$; relative to the ZAHB, these correspond to an age of 18.4 ± 1.0 Myr. The Van Grootel et al. results suggest overshooting as an important process shaping the helium burning core. Further consideration of convective overshooting beyond the boundary of the helium core is discussed further below in the context of confirmed mode trapping in KIC 10553698A.

Charpinet et al. (2011a) find two very weak modulations in the low frequency range of the KPD 1943 + 4058 *Kepler* power spectrum which Van Grootel et al. use. The timescales involved are 5.7625 ± 0.0001 hours (F_1, with an amplitude of 52 ± 6 parts per million) and 8.2293 ± 0.0003 hours (F_2, with an amplitude of ~ 47 parts per million). Phase folding shows F_1 and F_2 to repeat at coherent phases throughout the entire light curve; Charpinet et al. therefore interpret these to be orbital periods of two planets orbiting KPD 1943 + 4058 at distances of 0.0060 and 0.0076 AU. The two orbiting bodies must have survived deep immersion in the envelope of any former red giant progenitor, and Charpinet et al. suggest that they could be residual dense cores of evaporated giant planets that became closer to the star during the red giant expansion phase, triggering the mass-loss necessary for sdB star formation.

KIC 02697388 is another of the V1093 Her stars in which Reed et al. (2010) identify at least one short-period oscillation and for which Charpinet et al. (2011b) make an asteroseismic analysis,

following the approach Van Grootel et al. (2010a) adopt in the case of KPD 1943 + 4058. New high signal-to-noise spectra of KIC 02697388 are obtained and fitted using appropriate non-LTE model atmosphere and line-formation calculations to derive $T_{\rm eff}$ = 25395 ± 227 K, log$g$ = 5.500 ± 0.031 and log$N$(He)/N(H) = −2.767 ± 0.122. Forty-three frequencies are identified in the early *Kepler* light curve, all modulations corresponding to g-mode pulsations except one high-frequency signal, typical of a p-mode oscillation. Although the presence of a p-mode is surprising considering atmospheric parameters they derive, Charpinet et al. show that it is particularly well accounted for by optimal seismic models, both in terms of frequency match and nonadiabatic properties. The seismic analysis leads to two model solutions which account for observed pulsation properties of KIC 02697388 and correspond to structural parameters similar to those Van Grootel et al. find for KPD 1943 + 4058.

Using data from the first two quarters of the *Kepler* satellite mission, Kawaler et al. (2010a) analyse two V1093 Her stars (KIC 02991403 and KIC 11179657) found to be g-mode pulsators; these also display the distinct irradiation (reflection) effect typical of sdB stars in short-period binaries with a close M-dwarf companion. Tidal locking has frequently been assumed for sdB binaries with periods less than 0.5 days and, if this has occurred, the sdB star should rotate synchronously with the orbital motion. However, Preece et al. (2018) find synchronisation time-scales to be longer than sdB lifetimes in all cases. In power spectra for KIC 02991403 and KIC 11179657 based on early *Kepler* data, Kawaler et al. find no clear evidence of the rotational splitting that would be expected if the sdB star rotation had become synchronised with orbital motion. With later *Kepler* data, obtained between 2010 March and 2011 March, Pablo et al. (2012) obtain further seismic evidence for non-synchronisation of sdB star rotation in both KIC 02991403 and KIC 11179657, strongly supporting the Kawaler et al. conclusion.

Østensen et al. (2011) identify five V1093 Her pulsators (KIC 07668647, KIC 08302197, KIC 10001893, KIC 10553698, KIC 11558725) in the second half of the *Kepler* survey phase; they also find and list (their table 7) fourteen binaries and other long-period variables which have a hot subdwarf or white dwarf as a component. Baran et al. (2011) perform time-series analyses for the five V1093 Her pulsators Østensen et al. identify, using the nearly continuous month-long *Kepler* data sets they obtain in Q3 and Q4; these data sets provide nearly alias-free photometry at unprecedented precision. Frequencies and amplitudes turn out to be typical of g-mode pulsators of the V1093 Her type, with no evidence of binarity being seen in their pulsation frequencies. Average period spacings may indicate ℓ = 1 and ℓ = 2 modes and possible evidence of rotational splitting needs further investigation.

Reed et al. (2011a) investigate period spacing in twelve V1093 Her stars (KIC 02991403, KIC 03527751, KIC 05807616, KPD 1943 + 4058 (KIC 05807616), KIC 07664467, KIC 07668647, KIC 08302197, KIC 09472174, KIC 10001893, KIC 10553698, KIC 10670103, KIC 11179657, KIC 11558725) and one possible DW Lyn star (KIC 02697388) they observe with the *Kepler* satellite as already referenced (Østensen et al., 2010b); in addition, they include KPD 0629–016 which Charpinet et al. (2010) observe with CoRoT. Relationships between equal-period spacings of modes with differing degrees ℓ, and periods of the same radial order n but differing degrees ℓ, are provided by asymptotic limits for g-mode pulsations; Reed et al. use these to associate observed periods of variability with pulsation modes for ℓ = 1 and 2. A ℓ = 1 or ℓ = 2 constant period spacing is detected at a confidence of 95% or better for all stars except in the cases of KIC 09472174, where the power spectrum is complicated by the presence of a binary companion, and KPD 1943 + 4058 for which more subtle mode trapping in the model may be needed.

2M 1938 + 4603 (KIC 09472174) is an eclipsing binary consisting of a pulsating V1093 Her star and a cool M-dwarf companion in an effectively circular three-hour orbit; it attracts attention (Østensen et al., 2010a; Barlow et al., 2012; Baran et al., 2015b) for the same reason as NY Vir as it allows a direct comparison between asteroseismic and orbital solutions. The *Kepler* satellite light curve is dominated by a strong reflection effect. Østensen et al. (2010a) use a phase-folded *Kepler* light curve to detrend orbital effects, obtaining an amplitude spectrum of the residual light curve which reveals a rich collection of pulsation peaks spanning frequencies from ~ 50 to ~4500 μHz. Østensen et al. present a first analysis based on the 9.7 days commissioning light curve, augmented by ground-based photometry and spectroscopy, allowing them to derive a radial-velocity amplitude $K_1 = 65.7 \pm 0.6\,\mathrm{kms}^{-1}$, an inclination angle $i = 69^{\rm o}.45 \pm 0.20$, and component masses of $M_1 = 0.48 \pm 0.03 M_\odot$ and $M_2 = 0.12 \pm 0.01 M_\odot$ for the hot subdwarf and M dwarf respectively.

With six months of publicly available *Kepler* photometry obtained in short-cadence mode, Barlow et al. (2012) measure centroid times of primary and secondary eclipse by fitting model profiles. On average, secondary eclipses are found to occur 2.06 ± 0.12 s after the midpoint between primary eclipses, which Barlow et al. interpret as a Rømer delay; that is, the delay resulting from the light-travel-time across the binary orbit projected on to an observer's line-of-sight. Assuming circular orbits about the binary centre-of-mass, the time delay corresponds to a mass ratio q = 0.2691 ± 0.0018 and individual masses of $M_1 = 0.372 \pm 0.024 M_\odot$ $M_2 = 0.1002 \pm 0.0065 M_\odot$. A very small orbital eccentricity of $e\cos\omega \simeq 0.00004$ allows Barlow et al. to reconcile their masses with those of Østensen et al. (2010a).

Thirty-seven months of 2M 1938 + 4603 *Kepler* photometry are analysed by Baran et al. (2015b). Eclipse timings from more than 16,000 primary and secondary eclipses exhibit a variation which can be fitted by one or more sinusoids, once orbital motion effects are removed, a periodic variation in the timing signal ascribed to at least one circumbinary body in the system. Upon the assumption that the third body is orbiting in the same plane as the binary, Baran et al. establish that it must be a Jupiter-mass object orbiting with a period of 416 days at a distance of 0.92 AU.

Østensen et al. (2014a) identify two clearly detected pulsation modes with periods of 122 and 132 seconds, as well as a few weaker modes with periods ranging from 118 to 216 seconds, in nearly 3 years of *Kepler* spacecraft photometry of the sdB star KIC 02991276. Unlike other sdB pulsators with similar high-quality *Kepler* light curves, the KIC 02991276 modes do not display long-

term coherency; pulsation frequencies vary substantially in amplitude and phase on timescales of about a month, sometimes disappearing completely. Such stochastic oscillations have been suspected for V361 Hya pulsators, as Reed et al. (2007) infer in the case of PG 0048 + 091, but only with the exceptional coverage of *Kepler* data are Østensen et al. able to unambiguously establish stochastic oscillations in KIC 02991276.

Kepler satellite photometric monitoring of KIC 10553698 continued with a one-minute sampling rate for most of the mission; these results, and radial velocity variations from ground-based spectroscopy are perfectly consistent with a Doppler-beaming effect and lead Østensen et al. (2014b) to conclude that it is a spectroscopic binary with an orbital period of 3.387 days. Østensen et al. introduce the names KIC 10553698A to refer to the V1093 Her component, and KIC 10553698B to refer the $\sim 0.6 M_{\odot}$ white dwarf companion. Like most V1093 Her pulsators, KIC 10553698A displays a rich g-mode pulsation spectrum with several clear $\ell = 1$ and $\ell = 2$ multiplets that maintain a regular frequency splitting; identifying these as being due to rotation, gives a period of ~41 days, which is very much less than the binary orbital period. The detection of $\ell = 1$ modes in KIC 10553698A that interpose in the asymptotic period sequences, and provide a clear indication of mode trapping in a stratified envelope, as predicted by theoretical models, is reported by Østensen et al. for a hot subdwarf for the first time.

Ghasemi et al. (2017) note that the seismic properties of KIC 10553698A provide a test of stellar evolution models, and offer a unique opportunity to determine mixing processes. Mixing due to convective overshooting beyond the boundary of the helium burning core is considered. Chemical stratifications induced by convective shells are found to change the g-mode period spacing pattern of a sdB star appreciably, a model with moderate and small core overshooting being fully consistent with period-spacing and mode trapping Østensen et al. (2014b) observe in KIC 10553698A. Models which include small or very small overshooting with atomic diffusion lead to a decreased extreme horizontal branch lifetime and produce chemical stratification induced by convective shells during the helium burning phase.

Guo and Li (2018) argue that predicted mode trapping in V1093 Her stars is stronger than observed, although the mode trapping efficiency could be reduced by taking diffusion into account. The Helium Flash at the end of Red Giant Branch evolution causes extensive convection that extends very close to the He/H transition zone. Detailed model calculations by Guo and Li show that the mode trapping efficiency could be reduced to approximately the level observed over the whole period range, if the Helium Flash overshoot is taken into account.

Spectroscopic observations of KIC 07664467 by Baran et al. (2016), coupled with Q 5–11 and Q 13–17 *Kepler* satellite photometry to complement earlier observations which Østensen et al. (2011) report, show it to reside in a 1.56-day orbital period binary. A radial velocity amplitude of $K_1 = 57 \pm 3\,\mathrm{kms}^{-1}$ and the Doppler boosting-dominated photometric signal at the orbital period, led Baran et al. to identify the companion as a compact object, almost certainly a white dwarf. An analysis of the amplitude spectrum led to the detection of sixty-one periods, rotationally split multiplets, and an equally spaced sequence in period to facilitate mode identification. Baran et al. derive a rotation period of 35.1 ± 0.6 days for the V1093 Her pulsator, showing this to be another binary system with a subsynchronous sdB star. Spectroscopy of the sdB star gives $T_{\mathrm{eff}} = 27440 \pm 120$ K and $\log g = 5.38 \pm 0.02$ dex with abundances following the general sdB pattern: light metals are subsolar and the iron abundance close to the solar value. Nitrogen enrichment and low carbon and oxygen abundances, resembling the CNO cycle equilibrium, are also found.

Observations over 2.75 years by the *Kepler* spacecraft of the pulsating sdB star KIC 10670103 yield 1.4 million measurements, corresponding to an impressive duty cycle of 93.8%, a frequency resolution of 0.017 μHz, and a 5σ detection limit of 0.1 parts-per-thousand (ppt). KIC 10670103 turns out to be the richest pulsating sdB star hitherto observed as Reed et al. (2014) detect 278 periodicities with frequencies ranging from 23 to 673 μHz (0.4 and 11.8 h) and amplitudes from the detection limit up to 14 ppt. Pulsation modes are identified using asymptotic period spacings and frequency multiplets which indicate a spin period of 88 ± 8 days. Of the 278 periodicities detected in KIC 10670103, Reed et al. associate 163 with low-degree ($\ell \leq 2$) pulsation modes; using these they make detailed examinations of the pulsation structure, including where the pulsation power is concentrated in radial order, over what frequency range mode trapping is inefficient, and how power switches between multiplet members. Amplitudes (and some frequencies) are not stable over the 2.75 years during which *Kepler* satellite photometry was obtained. Reed et al. also obtain follow-up spectroscopic data from which they determine that KIC 10670103 does not show significant radial velocity variations. Updated model stellar atmosphere and line formation calculations give $T_{\mathrm{eff}} = 21485 \pm 540$ K, $\log g = 5.14 \pm 0.05$ and $\log N(\mathrm{He})/N(\mathrm{H}) = -2.60 \pm 0.04$.

KIC 02697388 is a suspected hybrid (DW Lyn) pulsator with a remarkably low $T_{\mathrm{eff}} \simeq 23900$ K (Reed et al., 2010). Kern et al. (2017) analyse 3 years of *Kepler* spacecraft short-cadence data and obtain twenty-one low-resolution spectra of KIC 02697388 giving a radial-velocity scatter of $9.5\,\mathrm{kms}^{-1}$ which, while too large to completely rule out binarity, does rule out short-period, low-inclination orbits for KIC 02697388 and any companion. From short-cadence *Kepler* data, 253 periodicities are detected, most with periods from 1 to 2.5 hours, which Kern *et al.* associate with g-mode pulsations; in addition. twenty-three periods are also detected in the short-period p-mode region. Mode identifications are made for 89% of the periodicities, most being of low degree ($\ell \leq 2$), but forty-two are identified as $\ell \geq 3$. Frequency multiplets correspond to a rotation period for the star of ~42 days. A unique feature is seen in KIC 02697388 data: in all $\ell \geq 2$ multiplets, the splittings decrease over time. If the trend continues, $\ell \geq 2$ multiplets would become singlets within a decade.

Foster et al. (2015) analyze three years of nearly continuous *Kepler* spacecraft short cadence observations of the pulsating sdB star KIC 03527751 (Østensen et al., 2010b; Reed et al., 2010). A

total of 251 periodicities are detected, mostly in the g-mode domain, but also some where p-modes occur, confirming KIC 03527751 is a hybrid (DW Lyn) rather than a V1093 Her pulsator. Asymptotic period spacing relationships, frequency multiplets, and multiplet splitting separations allow 189 of the 251 periods to be associated with pulsation modes; included in these are three sets of $\ell = 4$ multiplets and a possible $\ell = 9$ multiplet. Period spacing sequences indicate respective $\ell = 1$ and 2 overtone spacings of 266.4 ± 0.2 and 153.2 ± 0.2 seconds. Frequency multiplets in the g-mode region, which sample deep into the star, indicate a rotation period of 42.6 ± 3.4 days while p-mode multiplets, which sample the outer envelope, indicate a rotation period of 15.3 ± 0.7 days. Foster et al. therefore report the first example of differential rotation for a sdB star and note that the slower core rotation is contrary to the faster core rotation Kawaler and Hostler (2005) predict.

Mode modulation in amplitude and frequency can be independently inferred by its fine structure in the Fourier spectrum, using a sliding Lomb-Scargle periodogram, or prewhitening methods applied to various parts of the light curve; Zong et al. (2018) apply these techniques to KIC 03527751, a long-period-dominated DW Lyn pulsator already discussed above. All detected modes with amplitudes large enough to be thoroughly studied show amplitude or frequency variations. Three quintuplets around 92, 114, and 253 μHz have components showing signatures that can be linked to non-linear interactions according to the resonant mode coupling theory, an interpretation further supported by many oscillation modes being found to have amplitudes and frequencies showing correlated or anti-correlated variations which may be linked to the amplitude equation formalism, where non-linear frequency corrections are determined by their amplitude variations. The results Zong et al. obtain suggest oscillation modes varying with diverse patterns are a very common phenomenon in pulsating sdB stars and close structures around main frequencies therefore need careful interpretation if a secure identification of real eigenfrequencies (crucial for seismic modeling) is to be obtained.

KIC 07668647 is a V1093 Her pulsator which Østensen et al. (2011) identify in the second half of the *Kepler* survey phase and Reed et al. (2011a) study further, as already reported in the present paper; it has a rich g-mode frequency spectrum, with a few low-amplitude p-modes at short periods, and Telting et al. (2014) therefore make a seismic study aiming to constrain its internal structure, and of sdB stars in general. From the full *Kepler* Q 06–Q 17 light curve, Telting et al. extract 132 significant pulsation frequencies and use period-spacing relations and multiplet splittings to identify the majority of modes. An internal rotation period at the base of the envelope of 46–48 days is derived from g-mode multiplet splittings, while the few p-mode splittings may indicate a slightly longer rotation period further out in the envelope. Mode-visibility considerations lead to an inclination of $\sim 60^{o}$ for the rotation axis of the sdB in KIC 07668647. Another novelty in sdB-star observations made possible by *Kepler* is found by Telting et al.; there is strong evidence for a few multiplets indicative of degree $3 \leq \ell \leq 8$. With ground-based low-resolution spectroscopy, and the near-continuous 2.88 year *Kepler* light curve, Telting et al. find KIC 07668647 to be in a 14.2 day orbital period binary, the companion being a white dwarf. A radial-velocity amplitude of 39 kms^{-1} is consistently determined from spectra, orbital Doppler beaming seen by *Kepler* at 163 parts per million (ppm), and an orbital light-travel delay of 27 s measured using pulsation timing. From their high signal-to-noise average spectra, Telting et al. find nitrogen and iron have abundances close to solar values, while helium, carbon, oxygen and silicon are under-abundant relative to the solar mixture.

KIC 10001893 is one of nineteen sdB pulsators for which the *Kepler* spacecraft obtained time-series photometry in its primary mission; it is one of the five V1093 Her stars Østensen et al. (2011) identify from the second half of the survey and which Reed et al. (2011a) study further. In the full 993.8 days of *Kepler* photometry, Silvotti et al. (2014) find three weak peaks in the KIC 10001893 power spectrum; these are at very low frequencies and cannot be explained in terms of g-modes. Three Earth-size planets (or planetary remnants) in very tight orbits, illuminated by strong stellar radiation, are understood to provide orbital modulation and cause the low frequency peaks. Orbital periods of $P_1 = 5.273$, $P_2 = 7.807$ and $P_3 = 19.48$ h, and ratios $P_2/P_1 = 1.481$ and $P_3/P_2 = 2.495$ very close to the 3:2 and 5:2 resonances, are inferred. One of the main pulsation modes of the star at 210.68 μHz, corresponding to the third harmonic of the orbital frequency of the inner planet, leads Silvotti et al. to suggest this g-mode pulsation in KIC 10001893 is being tidally excited by a planetary companion. The planets Silvotti et al. find orbiting KIC 10001893 are similar to the two Charpinet et al. (2011a) find orbiting KPD 1943 + 4058.

Uzundag et al. (2017) provide a pulsation mode analysis for KIC 10001893, using the same *Kepler* time-series as Silvotti et al. (2014). The amplitude spectrum shows 104 g-mode frequencies between 102 and 496 μHz, as well as six p-modes above 2000 μHz. An absence of multiplets suggests a pole-on orientation; however, modal degrees and relative radial orders are assigned using asymptotic period spacing leading to the assignment of thirty-two dipole $\ell = 1$ and eighteen quadrupole $\ell = 2$ modes. With almost complete sequences of consecutive radial orders for $\ell = 1$ and 2, Uzundag et al. calculate a reduced-period diagram showing almost perfect alignment of the two sequences and in which trapped modes are clearly visible. A similar pattern is a seen in KIC 10553698A (Østensen et al., 2014b) but with all three trapped modes shifted to slightly higher periods. Mode trapping can be caused by transitions between either He/H at the base of the hydrogen envelope or convective and radiative parts of the core and their location, and particularly the spacing, provides a useful tool with which to examine the stellar interior through comparison with suitable models.

KIC 08302197 is another of the nineteen sdB pulsators for which the *Kepler* spacecraft obtained time-series photometry in its primary mission; it is one of the five V1093 Her stars Østensen et al. (2011) identify from the second half of the survey and which Reed et al. (2011a) study further. Baran et al. (2015a) base their extended analysis on *Kepler* satellite photometry from Q 5 to 17, applying a Fourier technique to extract thirty significant pulsation modes. Mode identification relies entirely on period spacing as no multiplets are found; the implication being that KIC 08302197

has a rotation period of more than 1000 days, or it has a unique (pole-on) orientation of its pulsation axis. In addition Baran et al. make spectroscopic observations and obtain twelve radial-velocity measurements, constraining a possible orbital radial-velocity amplitude to be smaller than $\sim 10\,\mathrm{kms}^{-1}$; furthermore, based on colour indices they constrain a possible companion to be a M or later type Main Sequence star, a compact or a substellar object. From their spectra Baran et al. obtain atmospheric parameters $T_{\mathrm{eff}} = 27450 \pm 200$ K, $\log g = 5.438 \pm 0.033$ dex and $\log[N(\mathrm{He})/N(\mathrm{H})] = -2.56 \pm 0.07$ and dex for KIC 08302197, consistent with other V1093 Her stars, and abundances for C, N, O, Si and Fe, setting an upper limit for the S abundance.

Krzesinski (2015) takes another look at the Charpinet et al. (2011a) claim to have found two planets orbiting the V1093 Her star KPD 1943 + 4058. *Kepler* data obtained between Q 5 and Q 17 are analysed, giving particular attention to the low frequency 33 – 49 μHz region where Charpinet et al. find their planetary signatures. As amplitude spectra do not show clear multiplets, Krzesinski uses two stable acoustic modes to determine a theoretical width of gravity mode multiplets and their splittings; this then allows period spacing and histograms of common multiplet component separations to be used to identify pulsation modes and observed gravity mode splittings. Analysis of the low frequency region then shows that the amplitude and frequency change of the signals have similar characteristics to other g-modes. Krzesinski then concludes that the existence of two planets orbiting KPD 1943 + 4058, as Charpinet et al. (2011a) claim, must be in doubt because the two planetary signature frequencies could instead be g-mode pulsations.

Blokesz et al. (2019) demonstrate that the use of a comparison star to provide a local determination of the point-spread function, when extracting *Kepler* satellite photometry, can significantly reduce artifacts. It then appears that amplitudes of Fourier transform signals found in the low-frequency regions for KPD 1943 + 4058 (Charpinet et al., 2011a) and KIC 10001893 (Silvotti et al., 2014) depend on methods used to extract *Kepler* data. Based on their simulations, Blokesz et al. conclude that the two low-frequency Fourier transform signals found in KPD 1943 + 4058 are likely to be combined frequencies of lower amplitude pulsating modes of the star. In the case of KIC 10001893, the strongest signal decreases significantly in amplitude when KIC 10001898 is used to define the local point-spread function and the other two frequencies appear to be spurious.

5 K2 OBSERVATIONS

Following the loss of two reaction wheels, the primary mission of the *Kepler* satellite came to an end, though the same hardware is adopted for the K2 Mission as Howell et al. (2014) describe. K2 makes use of an innovative way of operating the spacecraft to observe target fields along the ecliptic; these were to be observed for approximately seventy-five days providing a unique survey to fill the gaps in duration and sensitivity between the *Kepler* and Transiting Exoplanet Survey Satellite (TESS) missions (Ricker et al., 2015). The K2 mission allows different sdB targets to be continuously monitored photometrically for up to 75 days.

Jeffery and Ramsay (2014) report K2 observations of the pulsating sdB star EQ Psc made during engineering tests in 2014 February. In addition to a rich spectrum of g-mode pulsation frequencies, a light variation with a period of 19.2 hours and full amplitude of 2% is detected. Jeffery and Ramsay propose that the latter is due to reflection from a cool companion, making EQ Psc the hitherto longest-period member of some 30 binaries comprising a hot subdwarf and a cool dwarf companion (sdB + dM).

Baran et al. (2019) present an analysis of PHL 457 and EQ Psc, two pulsating sdB stars observed during the K2 mission. Light curves of both stars show variation consistent with a hot subdwarf irradiating a cooler companion in a binary system. Baran et al. obtain new spectroscopic data with which they determine radial velocity, T_{eff}, log*g*, and $N(\mathrm{He})/N(\mathrm{H})$ for both hot subdwarfs as a function of orbital phase. A previously published spectroscopic orbit of PHL 457 (Schaffenroth et al., 2014) is confirmed, and a spectroscopic orbit of EQ Psc presented; the orbital periods are respectively 0.313 and 0.801 days. By means of multiplets and period spacing, Baran et al. classify several pulsation modes in both stars. The g-mode multiplets indicate sub-synchronous core rotation with periods of 4.6 days (PHL 457) and 9.4 days (EQ Psc). While there is no evidence of a cool companion in the spectral energy distribution (SED) of PHL 457, the SED for EQ Psc shows an infrared excess consistent with a secondary having a temperature of about 6800 K and a radius of 0.23 $R_{\odot}$; this is consistent with the correlation between T_{eff} and orbital phase in the case of EQ Psc, due to a contribution of light from the irradiated companion.

PG 0048 + 091 and PG 1315–123 are in binaries with a F-type Main Sequence companion and have amplitude spectra dominated by p-mode pulsations. Reed et al. (2019) present a spectroscopic and seismic analysis for both objects based in part on seventy-nine days of photometry with K2, giving a frequency resolution 0.22 μHz. The presence of g-modes, as well as p-modes, allows an examination of radial rotation profiles. Frequency multiplets indicate that PG 1315–123 rotates uniformly, as a solid body, while PG 0048 + 091 is rotating faster in the outer envelope. Spectroscopy shows both stars to lie at the hot end of the instability region, these high values for T_{eff} challenging pulsation driving theory, which produces g-mode pulsations only at cooler temperatures. Another challenge is the appearance of pulsations with both driven and stochastic properties.

One of the main results of WET observations by Reed et al. (2007), already mentioned above, is the possible detection of stochastic pulsations in PG 0048 + 091. With a longer-duration, evenly sampled, single-instrument K2 data set, Reed et al. (2019) now conclude that most pulsations in PG 0048 + 091 are not stochastic in nature. Amplitude variations of most peaks are too small for the sensitivity Reed et al. (2007) achieve, and peak shapes are dissimilar to those expected from stochastic oscillations. Yet seven of the Reed et al. (2007) frequencies occur in regions Reed et al. (2019) find to have stochastic properties. Variations Reed et al. (2007) observe in other

frequencies were almost certainly caused by beating between closely-spaced frequencies in the rich pulsation spectrum.

A multi-site campaign on UY Sex has already been mentioned and Koen et al. (1999) identify V1405 Ori (KUV 0442 + 1,416) as a V361 Hya pulsator. Reed et al. (2020b) process and analyse K2 observations of both UY Sex and V1405 Ori, detecting ninety-seven p-mode pulsations in UY Sex and discover V1405 Ori to be a rare rich hybrid pulsator with over 100 p-mode and nineteen g-mode pulsations. From frequency multiplets, Reed et al. derive an envelope rotation period of 24.6 ± 3.5 days for UY Sex. For V1405 Ori, the p-modes give a rotation period of 0.555 ± 0.029 days, while g-modes provide a marginal determination of 4.2 ± 0.4 days. V1405 Ori is therefore found to be rotating differentially, with the core rotating more slowly than the envelope; it is also a short-period (0.398 days) binary with an envelope that is nearly but not quite tidally locked.

Reed et al. (2018a) report K2 observations during Campaign 5 resulting in the discovery of three pulsating sdB stars in binary systems. EPIC 211696659 (SDSS J083603.98 + 155216.4) is a g-mode pulsator having a white dwarf companion and a binary period of 3.16 days. EPIC 211823779 (SDSS J082003.35 + 173914.2) and EPIC 211938328 (LB 378) are both p-mode pulsators in binaries with Main-Sequence F-type companions. The orbital period of EPIC 211938328 is 635 ± 146 days and Reed et al. note that there are insufficient data to constrain the orbital period of EPIC 211823779. Rotationally induced frequency multiplets indicate all three stars to be slow rotators, with EPIC 211696659 sub-synchronous to its orbit.

A time-series analysis of the 83-day Campaign 2 short-cadence data set from K2 reveals EPIC 203948264 as a hitherto newly discovered V1093 Her star. Ketzer et al. (2017) identify twenty-two independent pulsation periods between 0.5 and 2.8 h in the EPIC 203948264 amplitude spectrum. Most pulsations fit the asymptotic period sequences for $\ell = 1$ or 2, with respective average period spacings of 261.3 ± 1.1 and 151.18 ± 0.37 s. Pulsation amplitudes are below 0.77 ppt and vary over time. Ketzer et al. also detect one possible low-amplitude multiplet, which would correspond to a rotation period of 46 days or longer, implying that EPIC 203948264 is another slowly rotating sdB star. Updated spectroscopic parameters, including atmospheric abundances and radial velocities give no indication that EPIC 203948264 is in a binary system.

Bachulski et al. (2016) present an analysis of K2 observations of the pulsating sdB star EPIC 212707862. Thirteen significant frequencies are detected from eighty-one days of photometric monitoring during Campaign 6. As no multiplets could be identified, it was not possible to derive a rotation period although amplitude modulation allows Bachulski et al. to roughly estimate it to be 80 days. Two period-spacing sequences enable Bachulski et al. to assign $\ell = 1$ modes to six frequencies, and $\ell = 2$ to a further five. Radial velocities and the spectral energy distribution hitherto obtained are consistent with EPIC 212707862 being a single hot subdwarf. From their spectra, Bachulski et al. derive $T_{\rm eff} = 28298 \pm 162$ K, $\log g = 5.479 \pm 0.025$ and $\log[N({\rm He})/N({\rm H})] = -2.752 \pm 0.069$.

PG 1142–037 is a new sdB pulsator which Reed et al. (2016) discover from photometry obtained during the first full-length campaign of K2. Fourteen periodicities are detected between 0.9 and 2.5 h with amplitudes below 0.35 ppt, all of which are associated with low-degree, $\ell \leq 2$ modes. Follow-up spectroscopy shows PG 1142–037 to be in a binary with an orbital period of 0.54 days. Phase-folding the K2 photometry reveals a two-component variation, including both Doppler boosting and ellipsoidal deformation. The detection of an ellipsoidal, tidally distorted variable with no indication of rotationally induced pulsation multiplets is a surprise and suggests a sdB rotation period of longer than 45 days, even though the binary period is found to 0.54 day.

From seventy-four days of K2 photometric monitoring during Campaign 5, Baran et al. (2017) discover EPIC 211779126 to be a rare DW Lyn pulsator, having a rich pulsation spectrum in both the p-mode and g-mode regions. Baran et al. find 154 frequencies in the g-mode region as well as twenty-nine frequencies in the p-mode region; they successfully identify modal degrees and relative radial orders for most g-modes using asymptotic period spacing, and modal degrees for some p-modes on the basis of rotational splitting. An important feature for constraining theoretical models are trapped modes, which Baran et al. also detect. Ground-based spectroscopy reveals no companion, suggesting EPIC 211779126 is a single sdB star. An envelope rotation period of approximately 16 days is implied by p-mode multiplet splitting, making EPIC 211779126 the fastest rotating non-binary sdB pulsator observed with *Kepler*. However, Baran et al. do not find resolved multiplets among the high-amplitude g-mode pulsations that correspond to the envelope rotation rate inferred from the p-mode splittings, indicating a much slower core rotation rate.

Menzies and Marang (1986) identify HW Vir (BD −07°3477) to be an eclipsing binary with an extremely short (~ 0.1 day) period. The primary is a hot subdwarf, not hitherto identified as a pulsator from ground-based photometry; the secondary is understood to be a M dwarf. Many such systems have since been discovered, as for example Kupfer et al. (2015) discuss. HW Vir has come to be regarded as "a prototype" and as its position allows K2 observations, it was an obvious target.

From seventy days of observation, Baran et al. (2018) determine the mid-times of eclipses, calculate an $(O - C)$ diagram, find the orbital period to be stable as defined by error limits and deduce a secondary minimum average shift of $\Delta T = 1.62$ s from the mid-point between two consecutive primary eclipses. If the shift is explained solely by light-travel time, the mass of the sdB primary must be $0.26{\rm M}_{\odot}$, which is too low for the star to be core-helium burning. For the sdB star mass to be canonical ($0.47{\rm M}_{\odot}$), this could be achieved for example with an orbital eccentricity of 0.0001, given a favourable longitude of periastron (ω) so that $\cos\omega = 1$. Baran et al. therefore argue that a sdB primary mass of $0.26{\rm M}_{\odot}$ is unlikely to be be correct.

After removing the flux variation caused by the HW Vir binary orbit, Baran et al. calculate an amplitude spectrum which clearly

shows periodic signals from close to the orbital frequency up to 4600 μHz, with a majority of the peaks below 2600 μHz. Peak amplitudes are below 0.1 ppt, too low to be detected with ground-based photometry, but high-precision data from the *Kepler* spacecraft reveals the HW Vir primary to be a pulsating sdB star. Multiplet structure in both p-modes and g-modes does not provide a convincing rotation period for the sdB primary. Baran et al. then argue that the HW Vir sdB pulsation spectrum differs from that in other sdB stars due to the relatively fast rotation Edelmann (2008) infers from spectroscopy which is that it is (nearly) phase-locked with the orbit.

Jeffery et al. (2017) find UVO 0825 + 15 to be a hot bright helium-rich subdwarf lying in K2 Field 5 and for which they obtain spectra using the Subaru High Dispersion Spectrograph and Nordic Optical Telescope, the latter having an intermediate dispersion ($\lambda/\Delta\lambda \simeq 2000$). Analyses of ultraviolet (from the International Ultraviolet Explorer Archive) and intermediate dispersion optical spectra rule out a short-period binary companion and provide fundamental atmospheric parameters of $T_{\rm eff} = 38900 \pm 270$ K, $\log g = 5.97 \pm 0.11$, $\log N({\rm He})/N({\rm H}) = -0.57 \pm 0.01$, $E(B-V) \simeq 0.03$, and an angular radius $\theta = (1.062 \pm 0.006) \times 10^{-11}$ radians. Jeffery et al. find Pb IV absorption lines in the Subaru spectrum, indicative of a very high lead overabundance; they also note carbon is more than 2 dex sub-solar, iron is approximately solar, and all other elements after argon in the Periodic Table are at least 2-4 dex overabundant, including germanium and yttrium. The photosphere is presumed to have a chemical structure determined by radiatively dominated diffusion. Jeffery et al. find the K2 light curve to show a dominant period around 10.8 h, with a variable amplitude, its first harmonic, and another period at 13.3 h. A preferred explanation is multi-periodic non-radial oscillation due to g-modes with very high radial order, although Jeffery *et al.* note this presents difficulties for pulsation theory; alternative explanations fail for lack of radial-velocity evidence.

Silvotti et al. (2019) nicely illustrate the value of using spacecraft to obtain long time-base high precision photometry through their detection of pulsation in the bright (V = 10.2) sdB star HD 4539 (PG 0044 + 097 and EPIC 220641886), a feat which Lynas-Gray (2012) fails to achieve with ground-based photometry using modest facilities. From the K2 light curve (78.7 days) Silvotti et al. extract 169 pulsation frequencies, 124 having a robust detection; most are found in the low-frequency g-mode region but some higher frequency p-modes are also detected, implying that HD 4539 is a hybrid (DW Lyn) pulsator. The lack of any frequency splitting in its amplitude spectrum suggests a HD 4539 rotation period longer than the K2 run, or that the star is seen pole-on. From asymptotic period spacing, many high-degree modes, up to ($\ell = 12$), are seen in the amplitude spectrum of HD 4539, with amplitudes as low as a few ppm. Silvotti et al. obtain $T_{\rm eff} = 22800 \pm 160$ K, $\log g = 5.20 \pm 0.02$, and $\log[N({\rm He})/N({\rm H})] = -2.34 \pm 0.05$ from low-resolution spectroscopy, and by fitting the spectral energy distribution they get $T_{\rm eff} = 23470\,^{+650}_{-210}$ K, $R = 0.26 \pm 0.01 {\rm R}_\odot$, and $M = 0.40 \pm 0.08 {\rm M}_\odot$. Moreover, from eleven high-resolution spectra Silvotti et al. see radial velocity variations caused by stellar pulsations, with amplitudes of $\simeq 150\,{\rm ms}^{-1}$ for the main modes, and exclude the presence of a companion with a minimum mass higher than a few Jupiter masses having orbital periods less than ~300 days.

6 TRANSITING EXOPLANET SURVEY SATELLITE OBSERVATIONS

The NASA Transiting Exoplanet Survey Satellite (TESS, Ricker et al., 2015) was launched on 2018 April 18th. An important feature distinguishing TESS from other facilities referenced above is the intention that most of the celestial sphere will be observed during the initial two-year mission. Hot subdwarfs not accessible to MOST, CoRoT, *Kepler* and K2 may now in principle be photometrically monitored from space for an extended period. Charpinet et al. (2019) discuss the prospects for asteroseismic observations of sdB stars in more detail.

As KIC 10139564 is the only V361 Hya star Østensen et al. (2010b) find in the *Kepler* field, and subsequent searches did not find another, Prins et al. (2019) emphasise the importance of observing as many as possible with TESS, especially at the ecliptic poles where the time-base will be longest. Low-resolution Balmer-line spectroscopy is used to identify thirty-nine new sdB stars around the northern ecliptic pole ($\beta > 73^{\rm o}$); of these, twenty-nine have characteristics ($T_{\rm eff} > 28000$ K or a composite spectrum) that may put them in the p-mode instability strip, and adding to the two (LS Dra and V366 Dra) already known. Prins et al. obtain ground-based time-series photometry for most of their p-mode candidates and discover J19384 + 5824 to be a V361 Hya star in the TESS 189 days viewing zone; it has a period of 172 s and an amplitude of 0.0091 magnitudes.

Charpinet et al. (2019) present the discovery and detailed asteroseismic analysis of a new g-mode hot subdwarf pulsator, EC 21494–7018 (TIC 278659026), monitored in the TESS first sector using a 120-second cadence. The light curve analysis reveals EC 21494–7018 to be a sdB pulsator having up to twenty independent g-mode frequencies. An optimal model solution in full agreement with independent measurements provided by spectroscopy (atmospheric parameters derived from model atmospheres) and astrometry (distance evaluated from the Gaia DR2 trigonometric parallax) is obtained through a seismic analysis. Charpinet et al. derive a mass for EC 21494–7018 ($0.391 \pm 0.009 {\rm M}_\odot$) significantly lower than the canonical mass of sdB stars, suggesting that its progenitor had not undergone the Helium Flash and was therefore a massive ($\geq 2 {\rm M}_\odot$) red giant. Other derived parameters include the H-rich envelope mass ($0.0037 \pm 0.0010\,{\rm M}_\odot$), radius ($0.1694 \pm 0.0081\,{\rm R}_\odot$), and luminosity ($8.2 \pm 1.1\,{\rm L}_\odot$). The optimal model fit has a double-layered He + H composition profile, which Charpinet et al. interpret as an incomplete but ongoing process of gravitational settling of helium at the bottom of a thick H-rich envelope. Properties Charpinet et al. derive for the core indicate EC 21494–7018 has burnt ~ 43% (by mass) of its helium and that it is relatively large core ($M_{\rm core} = 0.198 \pm 0.010\,{\rm M}_\odot$), and mixed in line with trends already uncovered from other g-mode sdB pulsators. In

addition Charpinet et al. make a first estimate of the core oxygen mass fraction $\left(X(\mathrm{O})_{\mathrm{core}} = 0.16^{+0.13}_{-0.05}\right)$, produced at this stage of evolution in a helium-burning core, a result which may help narrow down the still uncertain $^{12}\mathrm{C}(\alpha,\gamma)^{16}\mathrm{O}$ nuclear reaction rate when coupled with estimates for the core-size and stellar age on the ZAHB.

Reed et al. (2020a) report TESS observations showing CD −28°1974 to have an amplitude spectrum in which g-modes dominate, making it a hybrid (DW Lyn) pulsating sdB star; it has thirteen secure periods that form a $\ell = 1$ asymptotic sequence near the expected period spacing. Typical $\ell = 1$ g-mode periods in sdB stars lie between 3300 and 10000 seconds, whereas in CD −28°1974 Reed et al. find them between 1500 and 3300 seconds, indicating a somewhat different internal structure. CD −28°1974 has a F or G-type Main Sequence companion with Gaia proper motions indicating a comoving pair at the same distance (395 ± 7 pc) at which the separation of 1.33 arcsec would correspond to 530 ± 10 au and an orbital period of ~10^4 years.

Sahoo et al. (2020) report the detection of pulsations in three pulsating sdB stars SB 459 (TIC 067584818), SB 815 (TIC 169285097) and PG 0342 + 026 (TIC 457168745) monitored by TESS during single sectors, giving time-series covering twenty-seven days. Six longer period (266.8–387.2 seconds) p-mode frequencies are identified in SB 815 and in all three stars, at least twenty-two frequencies in the g-mode domain are seen. As no multiplets are found, mode identification in these stars is based on an asymptotic period relation; $\ell = 1$ or $\ell = 2$ being assigned to g-modes. Trapped modes are also identified which signify a non-uniform internal chemical profile. Using high precision trigonometric parallaxes from the Gaia mission and spectral energy distributions, Sahoo et al. derive stellar parameters from their atmospheric counterparts. Radii, masses, and luminosities are close to their canonical values for extreme horizontal branch stars. In particular, the stellar masses are close to the canonical 0.47 $M_\odot$ for all three stars but with large uncertainties.

7 SUMMARY AND FUTURE PROSPECTS

A better understanding of the late stages of stellar evolution is one of the main reasons for probing the internal structure of hot subdwarfs with asteroseismology. The point is very well expressed by Van Grootel et al. (2010a) who in the concluding part of their paper write: "As all helium-burning cores have similar characteristics, pulsating sdB stars are found to be excellent probes of Horizontal Branch star internal properties in general, an intermediate stage of stellar evolution experienced by the vast majority of stars." In reviewing papers mentioned above, I was very impressed by the wide diversity among the sdB stars various authors study with the *Kepler* satellite. While similarities exist and are mentioned, every sdB appeared to have its distinguishing characteristics. Diversity was to me at least, a good argument for a binary origin: evolution of binary systems depends on masses, separations and compositions of the two components as well as how that binary formed originally.

Having all too briefly highlighted the enormous contribution to the asteroseismic study of sdB stars achieved through observations made by the *Kepler* satellite, during the main mission and the K2 mission that followed, it was gratifying to find that further time-series data collected by TESS will very probably continue the advance. In this closing section, I have therefore attempted to distill the essential facts about sdB stars that have been learnt from the *Kepler* Missions:

- Precision time-series photometry obtained with the *Kepler* satellite, almost continuously over nearly four years, has allowed some apparently single V1093 Her pulsators to be identified as binaries. KIC 07668647 and KIC 10553698 are found to have white dwarf companions from an orbital signature in the power spectra. M dwarf companions of KIC 02991403, KIC 08302197 and KIC 11179657 are identified from reflection effects seen in raw light curves. 2M 1938 + 4603 turns out to be an eclipsing binary, possibly having a Jupiter-mass object orbiting the binary at a distance of 0.92 AU
- Evidence of trapped modes is found in power spectra of KIC 10001893, KIC 10553698 and KPD 1943 + 4058. Guo and Li (2018) argue that the Helium Flash, at the end of the red giant stage, causes convection extending very close to the He/H transition zone and a convective overshoot during this stage smooths the chemical profile in the He/H transition zone. Detailed model calculations show that the mode trapping efficiency is then reduced to agree with observation.
- For a number of V1093 Her stars observed by *Kepler*, core rotation rates are found to be lower than the corresponding envelope rotation rate. In cases where the V1093 Her star is also known to be in a binary, the orbital time was shorter than its rotation period, indicating that rotation is generally not synchronised with orbital motion. The slow envelope rotation is consistent with a V1093 Her star having a red giant progenitor and the finding by Mosser et al. (2012) that the mean red giant core rotation significantly slows down in the last stages of Red Giant Branch evolution. A slower core rotation rate is consitent with results by Tayar et al. (2019) who find a rapid transfer of angular momentum from the core, to the surrounding envelope, during the core helium burning phase.
- According to Miller Bertolami et al. (2020), stochastic excitation of pulsations in sdB stars are asteroseismic signatures of an earlier helium core flash. Stochastic excitations are identified in WET observations of PG 0048 + 091 and, for some frequencies, confirmed by later K2 observations. In the case of KIC 02991276, *Kepler* observations confirm the presence of stochastically excited pulsations. A new opportunity to study the helium core flash has thus been established.
- Although early *Kepler* observations of KIC 10139564, the only V361 Hya star in the *Kepler* field, suggest pulsations with stable frequencies and amplitudes, the analysis of thirty-eight months of contiguous short-cadence data (Zong et al., 2016) highlights mode multiplets induced by rotation which show intriguing behaviour. For example, Zong et al. find a triplet at 5760 μHz, a quintuplet at 5287 μHz and a $(\ell > 2)$ multiplet at 5412 μHz, all induced by rotation, showing clear frequency and amplitude modulations typical of the intermediate regime of a resonance between components.

Identified frequency and amplitude modulations are signatures of non-linear resonant couplings occurring in pulsating sdB stars. Resonances occurring in pulsating sdB stars appear to follow more complicated patterns than the simple predictions from current non-linear theoretical frameworks; results which should motivate further development of non-linear stellar pulsation theory.

Diversity among the sdB star population means that a point Heber (2009) makes in his review is still valid; every sdB star needs to be studied and its distinguishing characteristics identified. More and better observations will be needed as well as theoretical developments and so the following future developments are proposed:

- In order to study every sdB star, it is first necessary to find them and distinguish pulsators from non-pulsators; several facilities are becoming available to expedite this search. The All-Sky Automated Survey for Supernovae (Kochanek et al., 2017) consists of twenty-four observing stations distributed in latitude and longitude across the globe; each observes with Johnson V, R and I filters and in principle allows the entire celestial sphere to be surveyed to $V \leq 16$ every twenty-four hours. Evryscope (Law et al., 2015, 2016) is deployed in Chile and California and images the entire visible sky every two minutes to $V \leq 16$. The Large Synoptic Survey Telescope (Tyson, 2002; Ivezić et al., 2019) will obtain deep images in six optical bands, with each sky location visited close to 1000 times over 10 years.
- Given the *Kepler* mission success, it is important for TESS to monitor as many sdB pulsators as feasible and for as long as possible, so as to maximise the time-base; this is already in hand. To some extent the asteroseismology community is fortunate because for as long as the current interest in exoplanets persists, and the prospect of finding an Earth-like planet harbouring life continues, satellites will be needed to continue these searches. PLATO (Rauer et al., 2016) is one such mission and so obtaining high quality time-series photometry of hot subdwarfs may be expected to continue.
- Apart from work on the AA Dor secondary (Vučković et al., 2016) there has hitherto, and to the best of my knowledge, been no detailed study of M dwarf companions of pulsating hot subdwarfs in binary systems. Once completed, such studies would help with understanding associated hot subwarf power spectra. The James Webb Space Telescope (Gardner et al., 2006) could in principle be used to obtain transmission spectra immediately before and after primary and secondary eclipses in HW Vir-type systems.
- Atmospheric parameters and element abundances in sdB star atmospheres are an essential guide to the interpretation of asteroseismic time-series. Continued observation of sdB stars in spectroscopic surveys, such as LAMOST (Luo et al., 2016), are therefore needed. Follow-up high dispersion spectroscopy could then be obtained as necessary.
- Derived element abundances in the solar photosphere are compromised, if three-dimensional radiative transfer and hydrodynamic effects are neglected in the atmosphere. Atmospheres of pulsating hot subdwarfs are non-static, almost by definition, and temperature as well as pressure changes which accompany pulsation imply that these quantities are not constant at a given optical depth. I therefore propose that pulsating hot subdwarf atmospheric parameters and element abundances be based on model stellar atmospheres and line formations calculations incorporating hydrodynamics and three-dimensional radiative transfer.
- Stellar evolution calculation results are known to be dependent on the approximation used to model radiation transfer in the stellar atmosphere (VandenBerg et al., 2008). Coupling one-dimensional stellar evolution with three-dimensional hydrodynamical simulations of the stellar surface are now also being extended to asteroseismology (Mosumgaard et al., 2020); the resulting new models are able to predict observed frequencies without additional corrections and are able to do so consistently for all stellar parameters. As far as I am aware, the Mosumgaard et al. technique has not yet been applied to pulsating hot subdwarfs.
- Lynas-Gray et al. (2018) summarise our understanding of astrophysical opacities as it was in 2018. Of particular note is an experimental measurement by Bailey et al. (2015) of iron absorption in plasma conditions existing at the base of the solar convection zone, using the Sandia Z-Facility. When compared with the OP prediction, the Bailey et al. measurement implies an increase in the Rosseland mean opacity of $7 \pm 3\%$. In advance of any new theoretical initiative, it is essential that the Bailey et al. measurement be repeated with a different facility and Perry et al. (2020) report progress towards doing so with the National Ignition Facility.
- In view of various modulation patterns time-series observations of sdB stars uncover, Zong et al. (2018) encourage further developments in the field of non-linear stellar oscillation theory. The idea is hardly new as Cox (1976) proposes the full development of non-linear stellar oscillation theory and, although widely recognised as a difficult problem, its development would allow information in pulsation amplitudes to be more fully exploited. Stars such as KIC 10139564 now offer remarkable test-beds against which new non-linear pulsation theory may be benchmarked.

I end this review with a cautionary note. In the last sentence of their abstract, Zong et al. (2018) write "It also raises a warning to any long-term project aiming at measuring the rate of period change of pulsations caused by stellar evolution, or at discovering stellar (planetary) companions around pulsating stars using timing methods, as both require very stable pulsation modes".

AUTHOR CONTRIBUTIONS

The author confirms being the sole contributor of this work and has approved it for publication.

FUNDING

Work reported in this paper has been funded by the United Kingdom Department of Work and Pensions, as well as the Universities Superannuation Scheme; for these sources of finance, the author is most grateful.

ACKNOWLEDGMENTS

Preparation of this paper made use of facilities provided by the University of Oxford and University College London. I am very grateful to two reviewers for their comments.

REFERENCES

Aerts, C. (2019). Probing the interior physics of stars through asteroseismology. ArXiv e-prints: arXiv:1912.12300.

Bachulski, S., Baran, A. S., Jeffery, C. S., Østensen, R. H., Reed, M. D., Telting, J. H., et al. (2016). Mode identification in a pulsating subdwarf B star EPIC 212707862 observed with K2. *Acta Astron.* 66, 455–467.

Badnell, N. R., Bautista, M. A., Butler, K., Delahaye, F., Mendoza, C., Palmeri, P., et al. (2005). Updated opacities from the opacity project. *Mon. Not. R. Astron. Soc.* 360, 458–464. doi:10.1111/j.1365-2966.2005.08991.x

Baglin, A., Auvergne, M., Barge, P., Deleuil, M., Catala, C., Michel, E., et al. (2006). "Scientific objectives for a minisat: CoRoT," in *The CoRoT mission pre-launch status–stellar seismology and planet finding*. Editors M. Fridlund, A. Baglin, J. Lochard, and L. Conroy (ESA Special Publication), 33.

Bailey, J. E., Nagayama, T., Loisel, G. P., Rochau, G. A., Blancard, C., Colgan, J., et al. (2015). A higher-than-predicted measurement of iron opacity at solar interior temperatures. *Nature* 517, 56–59. doi:10.1038/nature14048

Baran, A. S., and Østensen, R. H. (2013). Detection of multiplets of degree $l = 3$ and $l = 4$ in the subdwarf-B pulsator KIC 10139564. *Acta Astron.* 63, 79–90.

Baran, A., Pigulski, A., Kozieł, D., Ogłoza, W., Silvotti, R., and Zoła, S. (2005). Multicolour photometry of Balloon 090100001: linking the two classes of pulsating hot subdwarfs. *Mon. Not. R. Astron. Soc.* 360, 737–747. doi:10.1111/j.1365-2966.2005.09066.x

Baran, A., Oreiro, R., Pigulski, A., Pérez Hernández, F., Ulla, A., Reed, M. D., et al. (2009). The pulsating hot subdwarf Balloon 090100001: results of the 2005 multisite campaign. *Mon. Not. R. Astron. Soc.* 392, 1092–1105. doi:10.1111/j.1365-2966.2008.14024.x

Baran, A. S., Kawaler, S. D., Reed, M. D., Quint, A. C., O'Toole, S. J., Østensen, R. H., et al. (2011). First Kepler results on compact pulsators–VII. Pulsating subdwarf B stars detected in the second half of the survey phase. *Mon. Not. R. Astron. Soc.* 414, 2871–2884. doi:10.1111/j.1365-2966.2011.18486.x

Baran, A. S., Reed, M. D., Stello, D., Østensen, R. H., Telting, J. H., Pakštienė, E., et al. (2012). A pulsation zoo in the hot subdwarf B star KIC 10139564 observed by Kepler. *Mon. Not. R. Astron. Soc.* 424, 2686–2700. doi:10.1111/j.1365-2966.2012.21355.x

Baran, A. S., Telting, J. H., Németh, P., Bachulski, S., and Krzesiński, J. (2015a). KIC 8302197: a non-rotating or low-inclination pulsating subdwarf B star observed with the Kepler spacecraft. *Astron. Astrophys.* 573, 8. doi:10.1051/0004-6361/201424877

Baran, A. S., Zola, S., Blokesz, A., Østensen, R. H., and Silvotti, R. (2015b). Detection of a planet in the sdB + M dwarf binary system 2M 1938 + 4603. *Astron. Astrophys.* 577, 6. doi:10.1051/0004-6361/201425392

Baran, A. S., Telting, J. H., Németh, P., Østensen, R. H., Reed, M. D., and Kiaeerad, F. (2016). A subsynchronously rotating pulsating subdwarf B star in a short-period binary with a white dwarf companion. *Astron. Astrophys.* 585, 11. doi:10.1051/0004-6361/201527182

Baran, A. S., Reed, M. D., Østensen, R. H., Telting, J. H., and Jeffery, C. S. (2017). EPIC 211779126: a rare hybrid pulsating subdwarf B star richly pulsating in both pressure and gravity modes. *Astron. Astrophys.* 597, 12. doi:10.1051/0004-6361/201629651

Baran, A. S., Østensen, R. H., Telting, J. H., Vos, J., Kilkenny, D., Vučković, M., et al. (2018). Pulsations and eclipse-time analysis of HW Vir. *Mon. Not. R. Astron. Soc.* 481, 2721–2735. doi:10.1093/mnras/sty2473

Baran, A. S., Telting, J. H., Jeffery, C. S., Østensen, R. H., Vos, J., Reed, M. D., et al. (2019). K2 observations of the sdBV + dM/bd binaries PHL 457 and EQ Psc. *Mon. Not. R. Astron. Soc.* 489, 1556–1571. doi:10.1093/mnras/stz2209

Barlow, B. N., Wade, R. A., and Liss, S. E. (2012). The rømer delay and mass ratio of the sdB + dM binary 2M 1938 + 4603 from Kepler eclipse timings. *Astrophys. J.* 753, 7. doi:10.1088/0004-637X/753/2/101

Billères, M., Fontaine, G., Brassard, P., Charpinet, S., Liebert, J., Saffer, R. A., et al. (1997). Discovery of p-mode instabilities in the hot subdwarf B star PG 1047 + 003. *Astrophys. J. Lett.* 487, L81–L84. doi:10.1086/310882

Billéres, M., Fontaine, G., Brassard, P., Charpinet, S., Liebert, J., and Saffer, R. A. (2000). Detection of p-mode pulsations and possible ellipsoidal luminosity variations in the hot subdwarf B star KPD 1930+2752. *Astrophys. J.* 530, 441–453. doi:10.1086/308369

Bíró, I. B., and Nuspl, J. (2011). Photometric mode identification methods of non-radial pulsations in eclipsing binaries–I. Dynamic eclipse mapping. *Mon. Not. R. Astron. Soc.* 416, 1601–1615. doi:10.1111/j.1365-2966.2011.18400.x

Bloemen, S., Hu, H., Aerts, C., Dupret, M. A., Østensen, R. H., Degroote, P., et al. (2014). The blue-edge problem of the V1093 Herculis instability strip revisited using evolutionary models with atomic diffusion. *Astron. Astrophys.* 569, 6. doi:10.1051/0004-6361/201323309

Blokesz, A., Krzesinski, J., and Kedziora-Chudczer, L. (2019). Analysis of putative exoplanetary signatures found in light curves of two sdBV stars observed by Kepler. *Astron. Astrophys.* 627, 8. doi:10.1051/0004-6361/201835003

Borucki, W. J., Koch, D., Basri, G., Batalha, N., Brown, T., Caldwell, D., et al. (2010). Kepler planet-detection mission: introduction and first results. *Science* 327, 977. doi:10.1126/science.1185402

Charpinet, S., Fontaine, G., Brassard, P., and Dorman, B. (1996). The potential of asteroseismology for hot, subdwarf B stars: a new class of pulsating stars? *Astrophys J.* 471, L103. doi:10.1086/310335

Charpinet, S., Fontaine, G., Brassard, P., Chayer, P., Rogers, F. J., Iglesias, C. A., et al. (1997). A driving mechanism for the newly discovered class of pulsating subdwarf B stars. *Astrophys. J. Lett.* 483, L123–L126. doi:10.1086/310741

Charpinet, S., Fontaine, G., Brassard, P., and Dorman, B. (2000). Adiabatic survey of subdwarf B star oscillations. I. Pulsation properties of a representative evolutionary model. *Astrophys J. Suppl. Ser.* 131, 223–247. doi:10.1086/317359

Charpinet, S., Fontaine, G., Brassard, P., and Dorman, B. (2002a). Adiabatic survey of subdwarf B star oscillations. II. Effects of model parameters on pulsation modes. *Astrophys J. Suppl. Ser.* 139, 487–537. doi:10.1086/338822

Charpinet, S., Fontaine, G., Brassard, P., and Dorman, B. (2002b). Adiabatic survey of subdwarf B star oscillations. III. Effects of extreme horizontal branch stellar evolution on pulsation modes. *Astrophys J. Suppl. Ser.* 140, 469–561. doi:10.1086/339707

Charpinet, S., Silvotti, R., Bonanno, A., Fontaine, G., Brassard, P., Chayer, P., et al. (2006). The rapidly pulsating subdwarf B star PG 1325 + 101. II. Structural parameters from asteroseismology. *Astron. Astrophys.* 459, 565–576. doi:10.1051/0004-6361:20065316

Charpinet, S., Green, E. M., Baglin, A., Van Grootel, V., Fontaine, G., Vauclair, G., et al. (2010). CoRoT opens a new era in hot B subdwarf asteroseismology. Detection of multiple g-mode oscillations in KPD 0629-0016. *Astron. Astrophys.* 516, 5. doi:10.1051/0004-6361/201014789

Charpinet, S., Fontaine, G., Brassard, P., Green, E. M., Van Grootel, V., Randall, S. K., et al. (2011a). A compact system of small planets around a former red-giant star. *Nature* 480, 496–499. doi:10.1038/nature10631

Charpinet, S., Van Grootel, V., Fontaine, G., Green, E. M., Brassard, P., Randall, S. K., et al. (2011b). Deep asteroseismic sounding of the compact hot B subdwarf

pulsator KIC02697388 from Kepler time series photometry. *Astron. Astrophys.* 530, 20. doi:10.1051/0004-6361/201016412

Charpinet, S., Brassard, P., Fontaine, G., Van Grootel, V., Zong, W., Giammichele, N., et al. (2019). TESS first look at evolved compact pulsators discovery and asteroseismic probing of the g-mode hot B subdwarf pulsator EC 21494-7018. *Astron. Astrophys.* 632, 23. doi:10.1051/0004-6361/201935395

Clausen, D., and Wade, R. A. (2011). How to make a singleton sdB star via accelerated stellar evolution. *Astrophys. J. Lett.* 733. doi:10.1088/2041-8205/733/2/L42

Clausen, D., Wade, R. A., Kopparapu, R. K., and O'Shaughnessy, R. (2012). Population synthesis of hot subdwarfs: a parameter study. *Astrophys. J.* 746, 18. doi:10.1088/0004-637X/746/2/186

Cox, J. P. (1976). Nonradial oscillations of stars - theories and observations. *Annu. Rev. Astron. Astrophys.* 14, 247–273. doi:10.1146/annurev.aa.14.090176.001335

Edelmann, H. (2008). "HW vir's companion: an M-type dwarf, or maybe a giant rotating spherical mirror?," in *Hot subdwarf stars and related objects*. Editors U. Heber, C. S. Jeffery, and R. Napiwotzki (Astronomical Society of the Pacific Conference Series), 392, 187.

Fontaine, G., Brassard, P., Charpinet, S., Green, E. M., Chayer, P., Billères, M., et al. (2003). A driving mechanism for the newly discovered long-period pulsating subdwarf B stars. *Astrophys. J.* 597, 518–534. doi:10.1086/378270

Fontaine, G., Brassard, P., Charpinet, S., Green, E. M., Chayer, P., Randall, S. K., et al. (2008). "Achievements and challenges in the field of sdB asteroseismology," in *Hot subdwarf stars and related objects*. Editors U. Heber, C. S. Jeffery, and R. Napiwotzki (Astronomical Society of the Pacific Conference Series), 231.

Foster, H. M., Reed, M. D., Telting, J. H., Østensen, R. H., and Baran, A. S. (2015). The discovery of differential radial rotation in the pulsating subdwarf B star KIC 3527751. *Astrophys. J.* 805, 12. doi:10.1088/0004-637X/805/2/94

Gardner, J. P., Mather, J. C., Clampin, M., Doyon, R., Greenhouse, M. A., Hammel, H. B., et al. (2006). The James Webb space telescope. *Space Sci. Rev.* 123, 485–606. doi:10.1007/s11214-006-8315-7

Ghasemi, H., Moravveji, E., Aerts, C., Safari, H., and Vučković, M. (2017). The effects of near-core convective shells on the gravity modes of the subdwarf B pulsator KIC 10553698A. *Mon. Not. R. Astron. Soc.* 465, 1518–1531. doi:10.1093/mnras/stw2839

Green, E. M., Fontaine, G., Reed, M. D., Callerame, K., Seitenzahl, I. R., White, B. A., et al. (2003). Discovery of A New class of pulsating stars: gravity-mode pulsators among subdwarf B stars. *Astrophys. J.* 583, L31–L34. doi:10.1086/367929

Greenstein, J. L. (1957). "Evidence for instability among subluminous stars," in *Non-stable stars*. Editor G. H. Herbig (IAU Symposium), 41

Guo, J. J., and Li, Y. (2018). Influence of the He-flash convective overshoot on mode trapping efficiency in g-mode pulsating subdwarf B stars. *Mon. Not. R. Astron. Soc.* 478, 3290–3297. doi:10.1093/mnras/sty1010

Han, Z., Podsiadlowski, P., Maxted, P. F. L., Marsh, T. R., and Ivanova, N. (2002). The origin of subdwarf B stars–I. The formation channels. *Mon. Not. R. Astron. Soc.* 336, 449–466. doi:10.1046/j.1365-8711.2002.05752.x

Han, Z., Podsiadlowski, P., Maxted, P. F. L., and Marsh, T. R. (2003). The origin of subdwarf B stars–II. *Mon. Not. R. Astron. Soc.* 341, 669–691. doi:10.1046/j.1365-8711.2003.06451.x

Heber, U. (2009). Hot subdwarf stars. *Annu. Rev. Astron. Astrophys.* 47, 211–251. doi:10.1146/annurev-astro-082708-101836

Heber, U. (2016). Hot subluminous stars. *Publ. Astron. Soc. Pac.* 128, 082001. doi:10.1088/1538-3873/128/966/082001

Howell, S. B., Sobeck, C., Haas, M., Still, M., Barclay, T., Mullally, F., et al. (2014). The K2 mission: characterization and early results. *Publ. Astron. Soc. Pac.* 126, 25. doi:10.1086/676406

Ivezić, Ž., Kahn, S. M., Tyson, J. A., Abel, B., Acosta, E., Allsman, R., et al. (2019). LSST: from science drivers to reference design and anticipated data products. *Astrophys. J.* 873, 111. doi:10.3847/1538-4357/ab042c

Jeffery, C. S., and Ramsay, G. (2014). K2 observations of the pulsating subdwarf B star EQ Piscium: an sdB + dM binary. *Mon. Not. R. Astron. Soc.* 442, L61–L65. doi:10.1093/mnrasl/slu059

Jeffery, C. S., and Saio, H. (2006). Gravity-mode pulsations in subdwarf B stars: a critical test of stellar opacity. *Mon. Not. R. Astron. Soc. Lett.* 372, L48–L52. doi:10.1111/j.1745-3933.2006.00223.x

Jeffery, C. S., and Saio, H. (2007). Improved opacities and pulsation stability in subluminous B and O stars. *Mon. Not. R. Astron. Soc.* 378, 379–383. doi:10.1111/j.1365-2966.2007.11794.x

Jeffery, C. S., Baran, A. S., Behara, N. T., Kvammen, A., Martin, P., Naslim, N., et al. (2017). Discovery of a variable lead-rich hot subdwarf: UVO 0825 + 15. *Mon. Not. R. Astron. Soc.* 465, 3101–3124. doi:10.1093/mnras/stw2852

Kawaler, S. D., and Hostler, S. R. (2005). Internal rotation of subdwarf B stars: limiting cases and asteroseismological consequences. *Astrophys. J.* 621, 432–444. doi:10.1086/427403

Kawaler, S. D., Reed, M. D., Østensen, R. H., Bloemen, S., Kurtz, D. W., Quint, A. C., et al. (2010a). First Kepler results on compact pulsators–V. Slowly pulsating subdwarf B stars in short-period binaries. *Mon. Not. R. Astron. Soc.* 409, 1509–1517. doi:10.1111/j.1365-2966.2010.17475.x

Kawaler, S. D., Reed, M. D., Quint, A. C., Østensen, R. H., Silvotti, R., Baran, A. S., et al. (2010b). First Kepler results on compact pulsators–II. KIC 010139564, a new pulsating subdwarf B (V361 Hya) star with an additional low-frequency mode. *Mon. Not. R. Astron. Soc.* 409, 1487–1495. doi:10.1111/j.1365-2966.2010.17528.x

Kern, J. W., Reed, M. D., Baran, A. S., Østensen, R. H., and Telting, J. H. (2017). Kepler observations of the pulsating subdwarf B star KIC 2697388: the detection of converging frequency multiplets in the full data set. *Mon. Not. R. Astron. Soc.* 465, 1057–1065. doi:10.1093/mnras/stw2794

Ketzer, L., Reed, M. D., Baran, A. S., Németh, P., Telting, J. H., Østensen, R. H., et al. (2017). K2 observations of pulsating subdwarf B stars: analysis of EPIC 203948264 observed during Campaign 2. *Mon. Not. R. Astron. Soc.* 467, 461–468. doi:10.1093/mnras/stx104

Kilkenny, D., Koen, C., O'Donoghue, D., and Stobie, R. S. (1997). A new class of rapidly pulsating star–I. EC 14026-2647, the class prototype. *Mon. Not. R. Astron. Soc.* 285, 640–644. doi:10.1093/mnras/285.3.640

Kilkenny, D., O'Donoghue, D., Koen, C., Lynas-Gray, A. E., and van Wyk, F. (1998). The EC 14026 stars–VIII. PG 1336-018: a pulsating sdB star in an HWVir-type eclipsing binary. *Mon. Not. R. Astron. Soc.* 296, 329–338. doi:10.1046/j.1365-8711.1998.01432.x

Kilkenny, D., Koen, C., O'Donoghue, D., van Wyk, F., Larson, K. A., Shobbrook, R., et al. (1999). The EC 14026 stars–X. A multi-site campaign on the sdBV star PG 1605 + 072. *Mon. Not. R. Astron. Soc.* 303, 525–534. doi:10.1046/j.1365-8711.1999.02256.x

Kilkenny, D., Billères, M., Stobie, R. S., Fontaine, G., Shobbrook, R. R., O'Donoghue, D., et al. (2002). A multisite campaign on the pulsating subdwarf B star PG 1047 + 003. *Mon. Not. R. Astron. Soc.* 331, 399–406. doi:10.1046/j.1365-8711.2002.05198.x

Kilkenny, D., Reed, M. D., O'Donoghue, D., Kawaler, S. D., Mukadam, A., Kleinman, S. J., et al. (2003). A Whole Earth Telescope campaign on the pulsating subdwarf B binary system PG 1336-018 (NY Vir). *Mon. Not. R. Astron. Soc.* 345, 834–846. doi:10.1046/j.1365-8711.2003.07007.x

Kilkenny, D. (2010). Amplitude variations in pulsating sdB stars. *Astrophys. Space Sci.* 329, 175–181. doi:10.1007/s10509-010-0324-z

Kochanek, C. S., Shappee, B. J., Stanek, K. Z., Holoien, T. W.-S., Thompson, T. A., Prieto, J. L., et al. (2017). The all-sky automated survey for Supernovae (ASAS-SN) light curve server v1.0. *Publ. Astron. Soc. Pac.* 129, 104502. doi:10.1088/1538-3873/aa80d9

Koen, C., Kilkenny, D., O'Donoghue, D., van Wyk, F., and Stobie, R. S. (1997). A new class of rapidly pulsating star–II. PB 8783. *Mon. Not. R. Astron. Soc.* 285, 645–650. doi:10.1093/mnras/285.3.645

Koen, C., O'Donoghue, D., Kilkenny, D., Lynas-Gray, A. E., Marang, F., and van Wyk, F. (1998). The EC 14026 stars–VII. PG 1605 + 072, a star with many pulsation modes. *Mon. Not. R. Astron. Soc.* 296, 317–328. doi:10.1046/j.1365-8711.1998.01435.x

Koen, C., O'Donoghue, D., Kilkenny, D., Stobie, R. S., and Saffer, R. A. (1999). The EC 14026 stars–XIII. EC 05217-3914 and KUV 0442 + 1416. *Mon. Not. R. Astron. Soc.* 306, 213–222. doi:10.1046/j.1365-8711.1999.02506.x

Koen, C., O'Donoghue, D., Kilkenny, D., and Pollacco, D. L. (2004). Two new EC14026 stars: PG 0048 + 091 and PG 0154 + 182. *New Astron.* 9, 565–572. doi:10.1016/j.newast.2004.03.001

Krzesinski, J. (2015). Planetary candidates around the pulsating sdB star KIC 5807616 considered doubtful. *Astron. Astrophys.* 581, 7. doi:10.1051/0004-6361/201526346

Kupfer, T., Geier, S., Heber, U., Østensen, R. H., Barlow, B. N., Maxted, P. F. L., et al. (2015). Hot subdwarf binaries from the MUCHFUSS project. Analysis of 12 new systems and a study of the short-period binary population. *Astron. Astrophys.* 576, 24. doi:10.1051/0004-6361/201425213

Law, N. M., Fors, O., Ratzloff, J., Wulfken, P., Kavanaugh, D., Sitar, D. J., et al. (2015). Evryscope science: exploring the potential of all-sky gigapixel-scale telescopes. *Publ. Astron. Soc. Pac.* 127, 234. doi:10.1086/680521

Law, N. M., Fors, O., Ratzloff, J., Corbett, H., del Ser, D., and Wulfken, P. (2016). "The Evryscope: design and performance of the first full-sky gigapixel-scale telescope," in *Ground-based and airborne telescopes VI* (Bellingham, WA: SPIE). doi:10.1117/12.2233349

Luo, Y.-P., Németh, P., Liu, C., Deng, L.-C., and Han, Z.-W. (2016). Hot subdwarf stars observed in LAMOST DR1—atmospheric parameters from single-lined spectra. *Astrophys. J.* 818, 13. doi:10.3847/0004-637X/818/2/202

Lynas-Gray, A. E., Basu, S., Bautista, M. A., Colgan, J., Mendoza, C., Tennyson, J., et al. (2018). "Current state of astrophysical opacities: a white paper," in *Workshop on astrophysical opacities* (Astronomical Society of the Pacific Conference Series), 301–318.

Lynas-Gray, A. E. (2012). "Photometric variability of HD 4539?," in *Fifth Meeting on Hot Subdwarf Stars and Related Objects*. Editors D. Kilkenny, C. S. Jeffery, and C. Koen (Astronomical Society of the Pacific Conference Series), 213.

Maxted, P. F. L., Marsh, T. R., and North, R. C. (2000). KPD 1930+2752: a candidate Type Ia supernova progenitor. *Mon. Not. R. Astron. Soc.* 317, L41–L44. doi:10.1046/j.1365-8711.2000.03856.x

Menzies, J. W., and Marang, F. (1986). "A new B-subdwarf eclipsing binary with an extremely short period," in *Instrumentation and research programmes for small telescopes*. Editors J. B. Hearnshaw and P. L. Cottrell (IAU Symposium), 305

Miller Bertolami, M. M., Battich, T., Córsico, A. H., Christensen-Dalsgaard, J., and Althaus, L. G. (2020). Asteroseismic signatures of the helium core flash. *Nat. Astron.* 4, 67–71. doi:10.1038/s41550-019-0890-0

Mosser, B., Goupil, M. J., Belkacem, K., Marques, J. P., Beck, P. G., Bloemen, S., et al. (2012). Spin down of the core rotation in red giants. *Astron. Astrophys.* 548. doi:10.1051/0004-6361/201220106

Mosumgaard, J. R., Jørgensen, A. C. S., Weiss, A., Silva Aguirre, V., and Christensen-Dalsgaard, J. (2020). Coupling 1D stellar evolution with 3D-hydrodynamical simulations on-the-fly II: stellar evolution and asteroseismic applications. *Mon. Not. R. Astron. Soc.* 491, 1160–1173. doi:10.1093/mnras/stz2979

Nather, R. E., Winget, D. E., Clemens, J. C., Hansen, C. J., and Hine, B. P. (1990). The whole Earth telescope: a new astronomical instrument. *Astrophys. J.* 361, 309–317. doi:10.1086/169196

O'Donoghue, D., Lynas-Gray, A. E., Kilkenny, D., Stobie, R. S., and Koen, C. (1997). A new class of rapidly pulsating star–IV. Oscillations in EC 20117-4014 and atmospheric analyses. *Mon. Not. R. Astron. Soc.* 285, 657–672. doi:10.1093/mnras/285.3.657

O'Donoghue, D., Koen, C., Lynas-Gray, A. E., Kilkenny, D., and van Wyk, F. (1998). The EC14026 stars–VI. PG1047 + 003. *Mon. Not. R. Astron. Soc.* 296, 306–316. doi:10.1046/j.1365-8711.1998.01311.x

O'Toole, S. J., Heber, U., Jeffery, C. S., Dreizler, S., Schuh, S. L., Woolf, V. M., et al. (2005). The MultiSite spectroscopic telescope campaign: 2 m spectroscopy of the V361 Hya variable PG 1605 + 072. *Astron. Astrophys.* 440, 667–674. doi:10.1051/0004-6361:20053352

Oreiro, R., Ulla, A., Pérez Hernández, F., Østensen, R., Rodríguez López, C., and MacDonald, J. (2004). Balloon 090100001: a bright, high amplitude sdB pulsator. *Astron. Astrophys.* 418, 243–247. doi:10.1051/0004-6361:20035844

Oreiro, R., Pérez Hernández, F., Ulla, A., Garrido, R., Østensen, R., and MacDonald, J. (2005). Balloon 090100001: a short and long period pulsating sdB star. *Astron. Astrophys.* 438, 257–263. doi:10.1051/0004-6361:20052681

Østensen, R. H., Green, E. M., Bloemen, S., Marsh, T. R., Laird, J. B., Morris, M., et al. (2010a). 2M1938 + 4603: a rich, multimode pulsating sdB star with an eclipsing dM companion observed with Kepler. *Mon. Not. R. Astron. Soc.* 408, L51–L55. doi:10.1111/j.1745-3933.2010.00926.x

Østensen, R. H., Silvotti, R., Charpinet, S., Oreiro, R., Handler, G., Green, E. M., et al. (2010b). First Kepler results on compact pulsators - I. Survey target selection and the first pulsators. *Mon. Not. R. Astron. Soc.* 409, 1470–1486. doi:10.1111/j.1365-2966.2010.17366.x

Østensen, R. H., Silvotti, R., Charpinet, S., Oreiro, R., Bloemen, S., Baran, A. S., et al. (2011). First Kepler results on compact pulsators–VI. Targets in the final half of the survey phase. *Mon. Not. R. Astron. Soc.* 414, 2860–2870. doi:10.1111/j.1365-2966.2011.18405.x

Østensen, R. H., Reed, M. D., Baran, A. S., and Telting, J. H. (2014a). Stochastic pulsations in the subdwarf-B star KIC 2991276. *Astron. Astrophys.* 564, 4. doi:10.1051/0004-6361/201423734

Østensen, R. H., Telting, J. H., Reed, M. D., Baran, A. S., Nemeth, P., and Kiaeerad, F. (2014b). Asteroseismology revealing trapped modes in KIC 10553698A. *Astron. Astrophys.* 569, 14. doi:10.1051/0004-6361/201423611

Østensen, R. H. (2010). Observational asteroseismology of hot subdwarf stars. *Astron. Nachr.* 331, 1026–1033. doi:10.1002/asna.201011450

Pablo, H., Kawaler, S. D., Reed, M. D., Bloemen, S., Charpinet, S., Hu, H., et al. (2012). Seismic evidence for non-synchronization in two close sdb+dM binaries from Kepler photometry. *Mon. Not. R. Astron. Soc.* 422, 1343–1351. doi:10.1111/j.1365-2966.2012.20707.x

Perry, T. S., Heeter, R. F., Opachich, Y. P., Johns, H. M., King, J. A., Dodd, E. S., et al. (2020). Progress toward NIF opacity measurements. *High Energy Density Phys.* 35, 100728. doi:10.1016/j.hedp.2019.100728

Preece, H. P., Tout, C. A., and Jeffery, C. S. (2018). Tidal interactions of close hot subdwarf binaries. *Mon. Not. R. Astron. Soc.* 481, 715–726. doi:10.1093/mnras/sty2091

Prins, S., Telting, J., and Østensen, R. (2019). A small survey of UV-bright stars around the northern ecliptic pole: seeking new p-mode sdB variables for the TESS mission. *Open Astron.* 28, 61–67. doi:10.1515/astro-2019-0005

Randall, S. K., Fontaine, G., Brassard, P., and Bergeron, P. (2005a). The potential of multicolor photometry for pulsating subdwarf B stars. *Astrophys J.* 161, 456–479. doi:10.1086/468186

Randall, S. K., Matthews, J. M., Fontaine, G., Rowe, J., Kuschnig, R., Green, E. M., et al. (2005b). Detection of long-period variations in the subdwarf B star PG 0101 + 039 on the basis of photometry from the MOST satellite. *Astrophys J.* 633, 460–464. doi:10.1086/452628

Randall, S. K., Fontaine, G., Green, E. M., Brassard, P., Kilkenny, D., Crause, L., et al. (2006a). Asteroseismological studies of long-period variable subdwarf B stars. I. A multisite campaign on PG 1627 + 017. *Astrophys J.* 643, 1198–1218. doi:10.1086/502964

Randall, S. K., Green, E. M., Fontaine, G., Brassard, P., Terndrup, D. M., Brown, N., et al. (2006b). Asteroseismological studies of long-period variable subdwarf B stars. II. Two-color photometry of PG 1338 + 481. *Astrophys J.* 645, 1464–1484. doi:10.1086/504459

Rauer, H., Aerts, C., and Cabrera, J. (2016). The PLATO mission. *Astron. Nachrichten* 337, 961. doi:10.1002/asna.201612408

Reed, M. D., Brondel, B. J., and Kawaler, S. D. (2005). Pulsating stars in close binaries. I. Investigations of eclipse mapping and oblique pulsations. *Astrophys J.* 634, 602–615. doi:10.1086/491666

Reed, M. D., O'Toole, S. J., Terndrup, D. M., Eggen, J. R., Zhou, A.-Y., An, D., et al. (2007). Follow-up observations of pulsating subdwarf B stars: multisite campaigns on PG 1618 + 563B and PG 0048 + 091. *Astrophys. J.* 664, 518–535. doi:10.1086/518878

Reed, M. D., Kawaler, S. D., Østensen, R. H., Bloemen, S., Baran, A., Telting, J. H., et al. (2010). First Kepler results on compact pulsators–III. Subdwarf B stars with V1093 Her and hybrid (DW Lyn) type pulsations. *Mon. Not. R. Astron. Soc.* 409, 1496–1508. doi:10.1111/j.1365-2966.2010.17423.x

Reed, M. D., Baran, A., Quint, A. C., Kawaler, S. D., O'Toole, S. J., Telting, J., et al. (2011a). First Kepler results on compact pulsators–VIII. Mode identifications via period spacings in g-mode pulsating subdwarf B stars. *Mon. Not. R. Astron. Soc.* 414, 2885–2892. doi:10.1111/j.1365-2966.2011.18532.x

Reed, M. D., Harms, S. L., Poindexter, S., Zhou, A. Y., Eggen, J. R., Morris, M. A., et al. (2011b). Whole Earth Telescope observations of the subdwarf B star KPD 1930 + 2752: a rich, short-period pulsator in a close binary. *Mon. Not. R. Astron. Soc.* 412, 371–390. doi:10.1111/j.1365-2966.2010.17912.x

Reed, M. D., Kilkenny, D., O'Toole, S., Østensen, R. H., Honer, C., Gilker, J. T., et al. (2012). Multiyear and multisite photometric campaigns on the bright high-amplitude pulsating subdwarf B star EC 01541-1409. *Mon. Not. R. Astron. Soc.* 421, 181–189. doi:10.1111/j.1365-2966.2011.20289.x

Reed, M. D., Foster, H., Telting, J. H., Østensen, R. H., Farris, L. H., Oreiro, R., et al. (2014). Analysis of the rich frequency spectrum of KIC 10670103 revealing the most slowly rotating subdwarf B star in the Kepler field. *Mon. Not. R. Astron. Soc.* 440, 3809–3824. doi:10.1093/mnras/stu412

Reed, M. D., Baran, A. S., Østensen, R. H., Telting, J. H., Kern, J. W., Bloemen, S., et al. (2016). A pulsation analysis of K2 observations of the subdwarf B star PG 1142-037 during Campaign 1: a subsynchronously rotating ellipsoidal variable. *Mon. Not. R. Astron. Soc.* 458, 1417–1426. doi:10.1093/mnras/stw348

Reed, M. D., Armbrecht, E. L., Telting, J. H., Baran, A. S., Østensen, R. H., Blay, P., et al. (2018a). K2 Campaign 5 observations of pulsating subdwarf B stars: binaries and super-Nyquist frequencies. *Mon. Not. R. Astron. Soc.* 474, 5186–5198. doi:10.1093/mnras/stx3133

Reed, M. D., Baran, A. S., Telting, J. H., Østensen, R. H., Jeffery, C. S., Kern, J. W., et al. (2018b). A review of seismic observations of Kepler and K2-Observed sdBV stars. *Open Astron.* 27, 157–166. doi:10.1515/astro-2018-0015

Reed, M. D., Telting, J. H., Ketzer, L., Crooke, J. A., Baran, A. S., Vos, J., et al. (2019). Two p-mode-dominated subdwarf B pulsators in binaries with F-star companions observed with K2. *Mon. Not. R. Astron. Soc.* 483, 2282–2299. doi:10.1093/mnras/sty3025

Reed, M. D., Shoaf, K. A., Németh, P., Vos, J., Uzundag, M., Baran, A. S., et al. (2020a). TESS observations of pulsating subdwarf B stars: extraordinarily short-period gravity modes in CD–28° 1974. *Mon. Not. R. Astron. Soc.* 493, 5162–5169. doi:10.1093/mnras/staa661

Reed, M. D., Yeager, M., Vos, J., Telting, J. H., Østensen, R. H., Slayton, A., et al. (2020b). K2 observations of the pulsating subdwarf B stars UY Sex and V1405 Ori. *Mon. Not. R. Astron. Soc.* 492, 5202–5217. doi:10.1093/mnras/staa144

Reed, M. D. (2006). Whole Earth Telescope Xcov 21 and 23 CollaborationsThe observational search for tidally tipped pulsation axes in subdwarf B stars. *Memorie della Societa Astron. Italiana* 77, 417.

Reed, M. D. (2016). Progress in the study of pulsating subdwarf B stars. *Proc. Int. Astron. Union* 11, 589–595. doi:10.1017/S1743921316006165

Ricker, G. R., Winn, J. N., Vanderspek, R., Latham, D. W., Bakos, G. Á., Bean, J. L., et al. (2015). Transiting exoplanet survey satellite (TESS). *J. Astron. Telesc. Instrum. Syst.* 1, 014003. doi:10.1117/1.JATIS.1.1.014003

Rogers, F. J., and Iglesias, C. A. (1992a). Radiative atomic Rosseland mean opacity tables. *Astrophys. J.* 79, 507–568. doi:10.1086/191659

Rogers, F. J., and Iglesias, C. A. (1992b). Rosseland mean opacities for variable compositions. *Astrophys. J.* 401, 361–366. doi:10.1086/172066

Sahoo, S. K., Baran, A. S., Heber, U., Ostrowski, J., Sanjayan, S., Silvotti, R., et al. (2020). Mode identification in three pulsating hot subdwarfs observed with TESS satellite. *Mon. Not. R. Astron. Soc.* 495, 2844–2857. doi:10.1093/mnras/staa1337

Schaffenroth, V., Classen, L., Nagel, K., Geier, S., Koen, C., Heber, U., et al. (2014). Two candidate brown dwarf companions around core helium-burning stars. *Astron. Astrophys.* 570, 2844–2857. doi:10.1051/0004-6361/201424616

Schoenaers, C., and Lynas-Gray, A. E. (2006). Line-profile variations in pulsating sdb stars as a pulsation mode diagnostic. *Balt. Astron.* 15, 219–226.

Schoenaers, C., and Lynas-Gray, A. E. (2008). "Spectroscopic mode identification in slowly-pulsating subdwarf B stars," in *Hot subdwarf stars and related objects*. Editors U. Heber, C. S. Jeffery, and R. Napiwotzki (Astronomical Society of the Pacific Conference Series), 253.

Schuh, S., Huber, J., Green, E. M., O'Toole, S. J., Dreizler, S., Heber, U., et al. (2005). "Discovery of a long-period photometric variation in the V361 Hya star HS 0702+6043," in *14th European workshop on white dwarfs*. Editors D. Koester and S. Moehler (Astronomical Society of the Pacific Conference Series), 530. of

Seaton, M. J., Yan, Y., Mihalas, D., and Pradhan, A. K. (1994). Opacities for stellar envelopes. *Mon. Not. R. Astron. Soc.* 266, 805–828. doi:10.1093/mnras/266.4.805

Silvotti, R., Østensen, R., Heber, U., Solheim, J.-E., Dreizler, S., and Altmann, M. (2002). PG 1325 + 101 and PG 2303 + 019: two new large amplitude subdwarf B pulsators. *Astron. Astrophys.* 383, 239–243. doi:10.1051/0004-6361:20011712

Silvotti, R., Bonanno, A., Bernabei, S., Fontaine, G., Charpinet, S., Leccia, S., et al. (2006). The rapidly pulsating subdwarf B star PG 1325+101. I. Oscillation modes from multisite observations. *Astron. Astrophys.* 459, 557–564. doi:10.1051/0004-6361:20065314

Silvotti, R., Charpinet, S., Green, E., Fontaine, G., Telting, J. H., Østensen, R. H., et al. (2014). Kepler detection of a new extreme planetary system orbiting the subdwarf-B pulsator KIC 10001893. *Astron. Astrophys.* 570, 6. doi:10.1051/0004-6361/201424509

Silvotti, R., Uzundag, M., Baran, A. S., Østensen, R. H., Telting, J. H., Heber, U., et al. (2019). High-degree gravity modes in the single sdB star HD 4539. *Mon. Not. R. Astron. Soc.* 489, 4791–4801. doi:10.1093/mnras/stz2244

Stobie, R. S., Kawaler, S. D., Kilkenny, D., O'Donoghue, D., and Koen, C. (1997a). A new class of rapidly pulsating star - III. Oscillations in EC 10228-0905 and pulsation analysis. *Mon. Not. R. Astron. Soc.* 285, 651–656. doi:10.1093/mnras/285.3.651

Stobie, R. S., Kilkenny, D., O'Donoghue, D., Chen, A., Koen, C., Morgan, D. H., et al. (1997b). The edinburgh-cape blue object survey - I. Description of the survey. *Mon. Not. R. Astron. Soc.* 287, 848–866. doi:10.1093/mnras/287.4.848

Tayar, J., Beck, P. G., Pinsonneault, M. H., García, R. A., and Mathur, S. (2019). Core-envelope coupling in intermediate-mass core-helium burning stars. *Astrophys. J.* 887, 16. doi:10.3847/1538-4357/ab558a

Telting, J. H., Baran, A. S., Nemeth, P., Østensen, R. H., Kupfer, T., Macfarlane, S., et al. (2014). KIC 7668647: a 14 day beaming sdB + WD binary with a pulsating subdwarf. *Astron. Astrophys.* 570, 18. doi:10.1051/0004-6361/201424169

Telting, J. H. (2008). Constraints on angular numbers of pulsation modes from spectroscopy. *Commun. Asteroseismol.* 157, 112–117.

Tillich, A., Heber, U., O'Toole, S. J., Østensen, R., and Schuh, S. (2007). The Multi-Site Spectroscopic Telescope Campaign. II. Effective temperature and gravity variations in the multi-periodic pulsating subdwarf B star PG 1605 + 072. *Astrron. Astrophy.* 473, 219–228. doi:10.1051/0004-6361:20077949

Tyson, J. A. (2002). "Large synoptic survey telescope: overview," in *Survey and other telescope technologies and discoveries*. Editors J. A. Tyson and S. Wolff (Bellingham, WA: SPIE), 10–20. doi:10.1117/12.456772

Uzundag, M., Baran, A. S., Østensen, R. H., Reed, M. D., Telting, J. H., and Quick, B. K. (2017). KIC 10001893: a pulsating sdB star with multiple trapped modes. *Mon. Not. R. Astron. Soc.* 472, 700–707. doi:10.1093/mnras/stx2011

Van Grootel, V., Charpinet, S., Fontaine, G., Brassard, P., Green, E. M., Randall, S. K., et al. (2010a). Early asteroseismic results from Kepler: structural and core parameters of the hot B subdwarf KPD 1943 + 4058 as inferred from g-mode oscillations. *Astrophys. J.* 718, L97–L101. doi:10.1088/2041-8205/718/2/L97

Van Grootel, V., Charpinet, S., Fontaine, G., Green, E. M., and Brassard, P. (2010b). Structural and core parameters of the hot B subdwarf KPD 0629-0016 from CoRoT g-mode asteroseismology. *Astron. Astrophys.* 524, 6. doi:10.1051/0004-6361/201015437

VandenBerg, D. A., Edvardsson, B., Eriksson, K., and Gustafsson, B. (2008). On the use of blanketed atmospheres as boundary conditions for stellar evolutionary models. *Astrophys. J.* 675, 746–763. doi:10.1086/521600

Vos, J., Vučković, M., Chen, X., Han, Z., Boudreaux, T., Barlow, B. N., et al. (2019). The orbital period-mass ratio relation of wide sdB+MS binaries and its application to the stability of RLOF. *Mon. Not. R. Astron. Soc.* 482, 4592–4605. doi:10.1093/mnras/sty3017

Vučković, M., Kawaler, S. D., O'Toole, S., Csubry, Z., Baran, A., Zola, S., et al. (2006). Whole Earth telescope observations of the pulsating subdwarf B star PG 0014+067. *Astrophys. J.* 646, 1230–1240. doi:10.1086/505137

Vučković, M., Østensen, R. H., Németh, P., Bloemen, S., and Pápics, P. I. (2016). Looking on the bright side: the story of AA Doradus as revealed by its cool companion. *Astron. Astrophys.* 586, 12. doi:10.1051/0004-6361/201526552

Walker, G., Matthews, J., Kuschnig, R., Johnson, R., Rucinski, S., Pazder, J., et al. (2003). The MOST asteroseismology mission: ultraprecise photometry from space. *Publ. Astron. Soc. Pac.* 115, 1023–1035. doi:10.1086/377358

Zong, W., Charpinet, S., and Vauclair, G. (2016). Signatures of nonlinear mode interactions in the pulsating hot B subdwarf star KIC 10139564. *Astron. Astrophys.* 594, 19. doi:10.1051/0004-6361/201629132

Zong, W., Charpinet, S., Fu, J.-N., Vauclair, G., Niu, J.-S., and Su, J. (2018). Oscillation mode variability in evolved compact pulsators from Kepler photometry. I. The hot B subdwarf star KIC 3527751. *Astrophys. J.* 853, 98. doi:10.3847/1538-4357/aaa548

Conflict of Interest: The author declares that the research was conducted in the absence of any commercial or financial relationships that could be construed as a potential conflict of interest.

frontiers in Astronomy and Space Sciences

REVIEW
published: 14 May 2021
doi: 10.3389/fspas.2021.663026

Asteroseismology of Close Binary Stars: Tides and Mass Transfer

*Zhao Guo**

Department of Applied Mathematics and Theoretical Physics, University of Cambridge, Cambridge, United Kingdom

The study of stellar oscillations allows us to infer the properties of stellar interiors. Meanwhile, fundamental parameters such as mass and radius can be obtained by studying stars in binary systems. The synergy between binarity and asteroseismology can constrain the parameter space of stellar properties and facilitate the asteroseismic inference. On the other hand, binarity also introduces additional complexities such tides and mass transfer. From an observational perspective, we briefly review the recent advances in the study of tidal effects on stellar oscillations, focusing on upper main sequence stars (F-, A-, or OB- type). The effect can be roughly divided into two categories. The first one concerns the tidally excited oscillations (TEOs) in eccentric binaries where TEOs are mostly due to resonances between dynamical tides and gravity modes of the star. TEOs appear as orbital-harmonic oscillations on top of the eccentric ellipsoidal light curve variations (the "heartbeat" feature). The second category is regarding the self-excited oscillations perturbed by static tides in circularized and synchronized close binaries. It includes the tidal deformation of the propagation cavity and its effect on eigenfrequencies, eigenfunctions, and the pulsation alignment. We list binary systems that show these two types of tidal effect and summarize the orbital and pulsation observables. We also discuss the theoretical approaches used to model these tidal oscillations and relevant complications such as non-linear mode coupling and resonance locking. Further information can be extracted from the observations of these oscillations which will improve our understanding of tides. We also discuss the effect of mass transfer, the extreme result of tides, on stellar oscillations. We bring to the readers' attention: (1) oscillating stars undergoing mass accretion (A-, F-, and OB type pulsators and white dwarfs), for which the pulsation properties may be changed significantly by accretion; (2) post-mass transfer pulsators, which have undergone a stable or unstable Roche-Lobe overflow. These pulsators have great potential in probing detailed physical processes in stellar interiors and mass transfer, as well as in studying the binary star populations.

Keywords: stars early-type, evolution, oscillations, stars: binaries, asteroseismology

OPEN ACCESS

Edited by:
Andrzej S. Baran, Pedagogical University of Kraków, Poland

Reviewed by:
Jim Fuller, California Institute of Technology, United States
Dominic Bowman, KU Leuven, Belgium

***Correspondence:**
Zhao Guo
zg281@cam.ac.uk

Specialty section:
This article was submitted to Stellar and Solar Physics, a section of the journal Frontiers in Astronomy and Space Sciences

Received: *02 February 2021*
Accepted: *06 April 2021*
Published: *14 May 2021*

Citation:
Guo Z (2021) Asteroseismology of Close Binary Stars: Tides and Mass Transfer. Front. Astron. Space Sci. 8:663026. doi: 10.3389/fspas.2021.663026

1. INTRODUCTION

Stars tend to reside in binary or multiple systems, especially for those of early-type (Raghavan et al., 2010; Moe and Di Stefano, 2017). The intermediate and massive stars also possess a stably stratified radiative envelope which facilitates the propagation of gravity waves. When forming global normal modes, these gravity (g) modes can be observed in photometry or spectroscopy and be used to

study the stellar interiors. Thanks to the recent space telescopes, significant advances have been made in asteroseismology (Aerts et al., 2010; Bowman, 2020) including, e.g., the self-excited g-mode pulsators such as the F or A type γ Dor stars (Van Reeth et al., 2016; Li et al., 2020b) and the Slowly Pulsating B-stars (SPB) (Pápics et al., 2017). In binary stars, tidal forcing from the companion star naturally falls into the low-frequency (inertial and gravity mode) regime[1], with characteristic periods on the order of days. The tidally excited oscillations are crucial for the orbital evolution of binaries (Zahn, 1975, 1977; Ogilvie, 2014). It requires precise (generally $<10^{-4}$ magnitude), long, and continuous observations to detect the direct effect of tides on stellar oscillations. We are witnessing a huge amount of evidence of tidal effects on stellar oscillations, including both the tidally excited modes and perturbed modes.

The effect of tides can be classified into two categories. First, the non-wavelike, equilibrium tide regime, where the tidal effect is a global static deformation (Remus et al., 2012). The shape can be approximated as a spheroid or, more generally, as the Roche model, which is frequently used in the modeling of binary star light curves (Wilson and Devinney, 1971; Prša and Zwitter, 2005; Sepinsky et al., 2007). Second, in the wave-like, dynamical tide regime, the harmonic tidal forcing induces gravity waves in the radiative envelope and inertial waves in the convective core. If the waves suffer from less damping and manifest themselves as temperature variations on the stellar surface, they can be observed and studied.

Observationally, we discuss two classes of pulsating binaries. The first is pulsating eccentric binaries, i.e., the heartbeat stars (HBs). HBs are eccentric binary systems showing the eccentric ellipsoidal variations (the "heartbeat," sometimes similar to the electrocardiogram) near the periastron passage. **Figure 1** shows the typical light curves of three HBs observed by *Kepler* from low to high inclinations. The heartbeat feature stems from the ellipsoidal variation (mainly from the temperature and geometric perturbations due to tidal deformation) and the reflection effect (mutual heating). Doppler boosting also contributes to the feature but to a much lesser degree (Loeb and Gaudi, 2003; van Kerkwijk et al., 2010; Hambleton et al., 2016). The prototype of HB is KOI-54, which consists of two A-type main-sequence stars in a face-on, very eccentric orbit (Welsh et al., 2011). Later compilations of HBs include Thompson et al. (2012) and Kirk et al. (2016). The spectroscopic follow-up studies include Smullen and Kobulnicky (2015), Shporer et al. (2016), Kjurkchieva et al. (2016), and Dimitrov et al. (2017). Detailed studies of individual systems have been performed (see below). Some HBs show tidally excited oscillations (TEOs) on top of the heartbeat feature, i.e., additional g-mode oscillations induced by the dynamical tide.

The other class is circularized and synchronized close binaries with self-excited oscillations. For example, the A or F-type, pressure(p)-mode pulsating stars of δ Scuti type (Breger, 1979; Rodríguez et al., 2000) have been frequently found in close binaries. Some systems show p-modes perturbed by static tides. The manifestation can be seen in the perturbed eigenfrequencies and pulsational alignment (tidal splittings) and the modified eigenfunctions (e.g., flux may be non-uniformly distributed on the stellar surface).

Lastly, in section 4, we also discuss the extreme case of tides: mass transfer, and its effect on stellar oscillations. Particular attention is paid to the mode excitation and the binary-channel formation of pulsating stars via mass transfer.

2. ECCENTRIC BINARIES WITH TIDALLY EXCITED OSCILLATIONS (TEOs)

The HBs depict the upper envelope of the classical orbital period-eccentricity diagram (Shporer et al., 2016). The relatively short period (mostly $P \lesssim 50$ d) and high eccentricity ($e \gtrsim 0.2$) indicate an on-going strong tidal evolution (Dong et al., 2013). Zimmerman et al. (2017) showed that about 20 HBs have a surface rotation period $\approx$ 1.5 times longer than the pseudo-synchronous rotation period (Hut, 1981). Some heartbeat stars are actually in a hierarchical system. For example, high-resolution spectroscopy reveals a third spectral component in KIC 3230227 (Guo et al., 2017a; Lampens, 2017[2]). The high eccentricity ($e = 0.89$) and spin-orbit misalignment of the heartbeat binary KIC 8164262 (Hambleton et al., 2018) suggest that it is probably formed via the Kozai-Lidov mechanism (Kozai, 1962; Lidov, 1962; Naoz, 2016), a possible formation channel for some HBs. It is quite possible that many HBs have a hidden tertiary companion (Anderson et al., 2017).

The heartbeat signature can be present in the light curve irrespective of the spectral type. We will not discuss HBs with red giant components (Nicholls and Wood, 2012; Gaulme et al., 2013, 2014; Beck et al., 2014; Kuszlewicz et al., 2019) but focus on HBs with A- F- and OB-type stars. These stars possess radiative envelopes which facilitate the observability of tidally excited oscillations.

Observationally, we subtract the contribution from the equilibrium tide (the heartbeat feature, red lines in **Figure 1**) before studying the oscillations in the Fourier domain (**Figure 1**, right panel). TEOs represent the dynamical tidal response of the star to the companion, mostly manifest as exact orbital-harmonic frequencies (except for non-linear TEOs, see section 2.2 below). In the right panels of **Figure 1**, the peaks labeled with red numbers or gray squares are orbital-harmonic TEOs. Very-low-inclination HBs usually show $l = 2, m = 0$ TEOs while near-edge-on HBs tend to show $l = 2, m = 2$ TEOs. Tentative mode identification (l and m) of TEOs are labeled in **Figure 1**. The amplitude and frequency range (orbital harmonic number N) of TEOs can be predicted from theory and these expectations can be used to distinguish from the aliases resulting from imperfect equilibrium-tide light curve removal and other artifacts generated in the data reduction (e.g., frequency peaks without labels in the Fourier spectra of the upper and middle panels of **Figure 1**). An estimate can be made to the largest possible amplitude of these aliases and thus they can usually be distinguished from real TEOs. Note that the Fourier spectrum

[1]In some rare cases, pressure modes can also be tidally excited, e.g., in the central red giant star of the triple system HD181068 (Fuller et al., 2013).

[2]Presented as a poster at the KASOC conference.

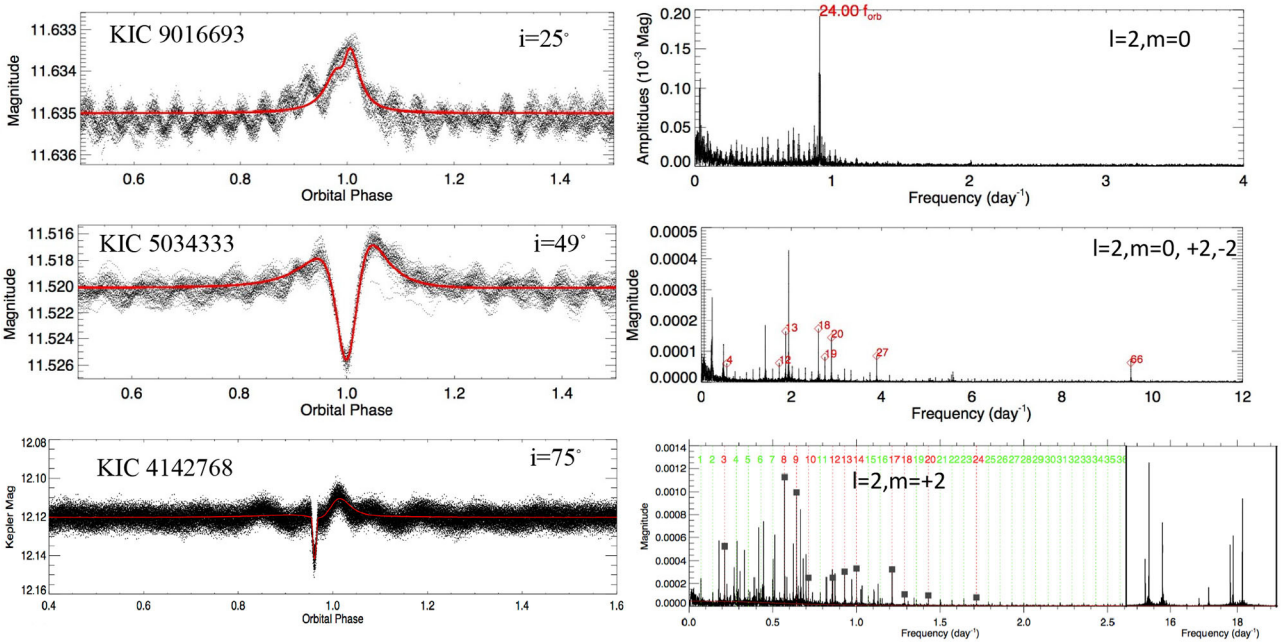

FIGURE 1 | (Left) *Kepler* Light curves of three heartbeat binaries with TEOs, from low to high orbital inclinations (*i*). In particular, KIC 4142768 has an eclipse near the periastron (phase = 1.0). **(Right)** Fourier spectrum of the light curves after removing the equilibrium tide contribution (red lines in left panels). The TEOs (red symbols or gray squares) are labeled by their orbital harmonic number (*N*) in red, and their tentative mode identification (*l* and *m*) are also shown. In the lower panel, intrinsic self-excited oscillations (γ Dor g-modes in the frequency range $f < 2$ d^{-1} and δ Scuti p-modes in $f > 15$ d^{-1}) are also present. Imperfect equilibrium-tide removal also generates a series of consecutive low-amplitude peaks, most notably in the upper and middle panels (see text). Adopted from Guo et al. (2019, 2020).

can also contain self-excited oscillations (e.g., γ Dor type g-modes and δ Scuti p-modes in KIC 4142768, lower panel of **Figure 1**). Furthermore, modulations from the stellar spin also introduce frequency peaks at the rotation frequency and its harmonics.

We compile a list of 22 heartbeat binaries with TEOs:

OB- type: HD 177863 (Willems and Aerts, 2002); ι Ori (Pablo et al., 2017); MACHO80.7443.1718 (Jayasinghe et al., 2019); QX Car and V1294 Sco (Kołaczek-Szymański et al., 2020); two possible candidates: η Car (Richardson et al., 2018); R81 (Tubbesing et al., 2002).

A-F- type: HD209295 (Handler et al., 2002); KOI-54 (Welsh et al., 2011); KIC 3230227 (Guo et al., 2017a); KIC 4142768 (Guo et al., 2019); KIC 9016693, KIC 8719324 and KIC 4248941, KIC 5034333 (Guo et al., 2020); KIC 11494130 and KIC 5790807 (Cheng et al., 2020), KIC 4544587 (Hambleton et al., 2013); KIC 3749404 (Hambleton et al., 2016), KIC 8164262 (Fuller et al., 2017; Hambleton et al., 2018); p Vel, θ^1 Cru, η^1 UMa, HD158013 and 14 Peg (Kołaczek-Szymański et al., 2020).

This list is of course incomplete. Kirk et al. (2016) included 24 HBs with TEOs, which is about 15% of all heartbeat binaries in the *Kepler* eclipsing catalog. Only ten systems are included here since TEOs in the rest have not been studied in detail. **Table 1** contains the stellar, orbital and oscillation parameters of 22 heartbeat binaries (A detailed online version can be found at: http://www.astro.gsu.edu/~guo/tides_review_table.pdf).

2.1. Tidally Excited Oscillations (TEOs) in Heartbeat Stars

We briefly describe the general physical picture of tidally excited waves in early-type stars. Early seminal studies used asymptotic approximations of gravity waves (Zahn, 1975, 1977; Goldreich and Nicholson, 1989), and it was extended to include the effect of rotation (Mathis, 2009). Later numerical calculations include the effect of non-adiabaticity and rotation (Savonije et al., 1995; Papaloizou and Savonije, 1997; Savonije and Papaloizou, 1997). Dedicated calculations (Witte and Savonije, 1999a,b) on massive stars studied the binary evolution and the intricate effects such as resonance locking. Other studies implemented the mode decomposition approach (Alexander, 1987; Lai et al., 1993; Lai, 1997; Schenk et al., 2002; Fuller, 2017).

Intermediate and massive stars possess a convective core and radiative envelope. In binaries containing these stars, internal gravity waves (IGW) are generated by the tidal potential (also by the convective motion in the core) at the radiative-convective boundary and propagate outward (Goldreich and Nicholson, 1989; Lecoanet and Quataert, 2013; Rogers et al., 2013; Edelmann et al., 2019; Lecoanet et al., 2019; Horst et al., 2020). They suffer from linear damping due to radiative diffusion (Press, 1981; Garcia Lopez and Spruit, 1991; Zahn et al., 1997). The low-frequency, short-wavelength waves are damped strongly and behave like traveling waves (Ratnasingam et al., 2019). Higher-frequency waves can be reflected at the outer turning points and

interfere constructively to form global normal modes (Prat et al., 2016).

Most of the observed prominent TEOs in HBs are standing waves, suffering from less damping. When the TEO amplitudes surpass the parametric instability threshold, the TEOs begin to suffer from non-linear mode coupling and transfer energy to daughter modes or multiple pairs of daughter modes (Weinberg et al., 2012; Yu et al., 2020). The daughter modes may again become unstable and couple with grand-daughter modes. In general, a mode coupling network can be formed. Observationally, this can be seen as mode triplets or multiplets satisfying the resonance conditions. This weakly-nonlinear regime will be discussed in the next section.

The amplitudes of the tidally excited gravity waves, when propagating to the near-surface layers with smaller densities, increase significantly. If the waves become significantly non-linear (the multiplication of the radial wavenumber and radial displacement $k_r\xi_r \gtrsim 1$), they overturn the stratification and break (Su et al., 2020). Thus, they deposit their energy (tidal heating) and angular momentum (tidal synchronization), and turn into small-scale turbulence. Thus, the surface layers are synchronized first and a differential rotation profile may be produced (Goldreich and Nicholson, 1989), although the hydromagnetic effects tend to smooth out differential rotation (Rüdiger et al., 2015; Townsend et al., 2018). Critical layers where the Doppler-shifted wave frequency approaches zero, may form and move inward (Alvan et al., 2013). The subsequent gravity waves cannot pass the critical layer and waves dissipate strongly. Observationally, single upper main-sequence stars tend to have a nearly uniform rotation profile in the radiative envelope, inferred from asteroseismology (Bowman, 2020; Aerts, 2021)[3]. The g-mode pulsating γ Dor stars (spectral type A-F-) in close binaries with $P_{orb} \leq 10$ d show a convective-core-boundary rotation period that is similar to the orbital period, suggesting that the tidal synchronization has already reached the deep interior (Guo et al., 2019; Li et al., 2020a; Saio, 2020). Nevertheless, Kallinger et al. (2017) found a Slowly Pulsating B-star in a triple system that appears to show a faster-rotating surface layer, which may fall into the Goldreich and Nicholson's outside-in synchronization scenario.

Since the TEOs are direct manifestation of dynamical tides, they are crucial for our understanding of the above physical processes. First, we show some general properties of the TEOs in heartbeat stars.

The overall strength of the tidal response of star 1 due to star 2 is determined by the tidal parameter ϵ_l:

$$\epsilon_l = \left(\frac{M_2}{M_1}\right)\left(\frac{R_1}{D_{peri}}\right)^{l+1} \quad (1)$$

where $D_{peri} = a(1-e)$. Since $\frac{R_1}{D_{peri}} \ll 1$, it is usually sufficient to consider the dominant $l = 2$ component.

Thus, to have a larger tidal amplitude, one could (1) make the mass ratio M_2/M_1[4] larger (i.e., close to 1.0); (2) make the stellar radius R_1 bigger; (3) have a smaller periastron distance D_{peri}. And indeed, observationally: (1) many heartbeat stars have a mass ratio close to unity[5]; (2) lots of heartbeat stars with tidally excited oscillations are slightly evolved main-sequence stars (e.g., KIC 4142768 has a primary star with $M = 2.05M_\odot, R = 2.96R_\odot$, Guo et al., 2019); (3) heartbeat binaries have a high eccentricity ($\approx 0.2 - 0.9$) and short periastron distance. The $D_{\rm peri}$ of 19 HBs in Shporer et al. (2016) ranges from 0.05 to 0.1AU, and the corresponding tidal parameter ϵ_2 values are $\approx 10^{-3}$.

The observed TEOs correspond to the frequencies of stellar g-modes with radial orders from $\approx$ 10 to a few tens. For example, the primary star in KIC 3230227 ($M = 1.84M_\odot, R = 2.01R_\odot$, Guo et al., 2017a) shows orbital-harmonic oscillations corresponding to $l = 2, m = 2$ g modes, with radial order $n_g \sim 10 - 30$; KOI 54 ($M = 2.05M_\odot, R = 2.33R_\odot$, O'Leary and Burkart, 2014) shows TEOs that mostly have $l = 2, m = 0$, corresponding to radial order $n_g \sim 10 - 50$. The slightly evolved primary in KIC4142768 (Guo et al., 2017a) shows TEOs that are in agreement with $n_g \approx 30 - 70$ g modes.

In **Figure 2**, we stack the observed TEOs in 22 heartbeat binaries together, with decreasing orbital eccentricities from the top to the bottom. These Fourier spectra show that the TEOs generally have oscillation frequencies $<\sim 5$ d^{-1}. They mostly correspond to orbital harmonics N from 4 to 40, although in some special cases the N can reach much larger values ($N \sim 300$ in KIC 8164262). The TEO amplitudes can be as large as > 10 milli-mag although the majority are lower than 0.5 milli-mag (right panel in **Figure 2**).

In general, most of the observed TEOs are likely (linearly) excited by the dynamical tide (exact orbital-harmonic frequencies ($Nf_{\rm orb}$, see next section for nonlinear non-harmonic TEOs), with the stellar response dominated by the closest frequency g-mode. But which orbital harmonics N are favorably excited? Following Burkart et al. (2012), the favorable range of orbital harmonics depends essentially on the multiplication of Q_{nl} and X_{lm} (see immediately later in this paragraph for the definitions). First, not all g-modes couple with the tidal potential equally. The weights are described by the tidal overlap integral Q_{nl}, which peaks around the dynamical frequency of the star. Q_{nl} decreases toward lower frequencies since higher order g-modes have shorter wavelength and cannot couple well spatially with the tidal potential. Secondly, stars in eccentric orbits experience a series of forcing frequencies ($Nf_{\rm orb}$, with $|N| < \infty$) which are weighted by the eccentricity-dependent Hansen coefficient X_{lm}. $X_{l=2,m=2}$ peaks at the periastron-passage frequency and decreases toward larger N; $X_{l=2,m=0}$ monotonically decreases as N increases (Willems, 2003, Figures 1, 2; Fuller, 2017, Figure 3). Thus, the favored range of orbital harmonics N is between the peaks of Q_{nl} and X_{lm} (Burkart et al., 2012, Figures 2, 3).

In **Figure 3**, we show the observed TEO amplitudes (in magnitude variation Δmag or luminosity variation $\Delta L/L$, related by $\Delta L/L \approx 1.086\Delta mag$) as a function of the orbital harmonic

[3]Asteroseismology of pre-Kepler β Cephei stars (since none were observed by Kepler) have a large range in their inferred interior rotation profiles.

[4]Usually defined so that $M_2 \leq M_1$.

[5](if the two components can be resolved in the spectra).

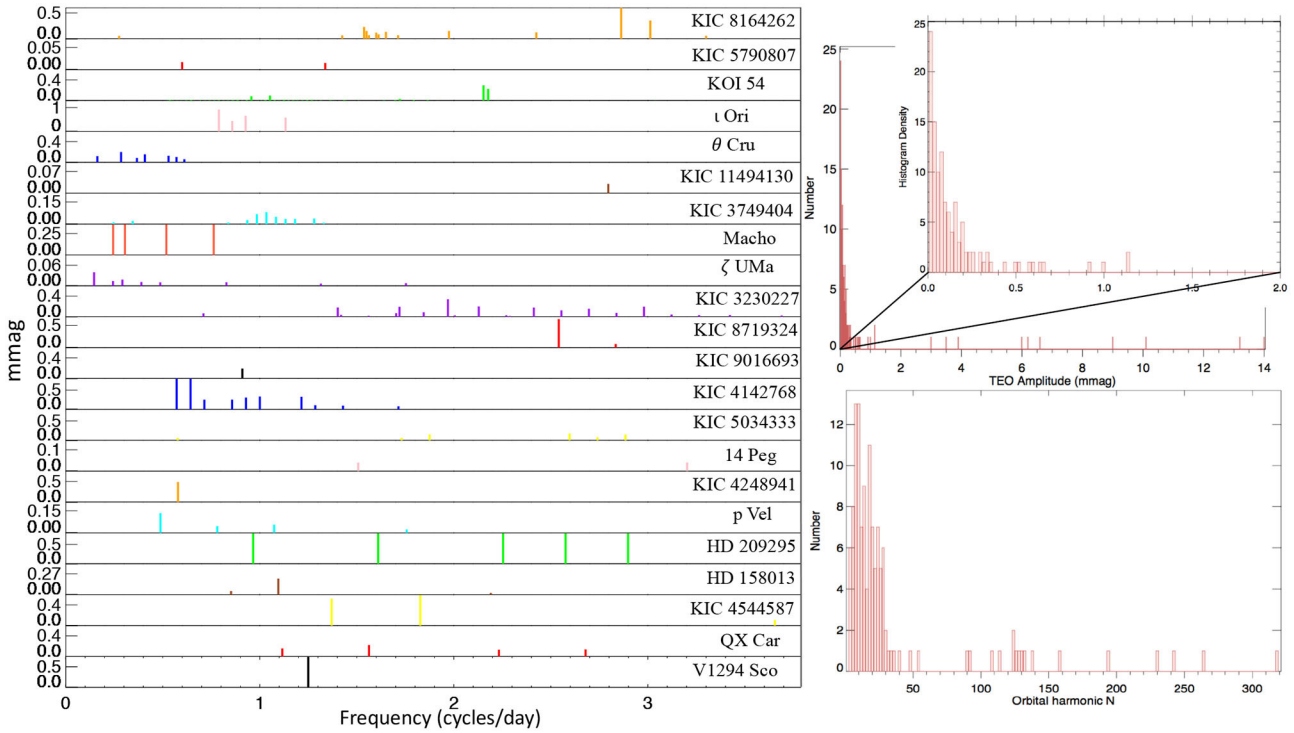

FIGURE 2 | Fourier amplitude spectrum of all 22 heartbeat binaries with TEOs. The TEO amplitudes are shown in mmag. The inset plots show the TEO amplitude histogram (upper) and the orbital harmonic N histogram (lower).

number (N) in four HBs KIC4142768, KIC3230227, ι Ori and KOI-54 (gray squares, circles, red squares, and red crosses, respectively). These observed TEOs should be compared with the theoretical amplitudes for $m = 2$, $m = 2$, $m = 2$, $m = 0$ modes (blue diamonds, open diamonds, blue circles, and open triangles, respectively, same ordering as above). It can be seen that the observed TEO range (between the two vertical lines) matches well with the theoretical expectations (the "bump" formed by background symbols. For ι Ori, the theoretical TEO amplitudes of $m = 0$ modes (cyan open circles) are below the detection limit and much lower than observed TEOs ($m = 2$). For KOI-54, the Δmag from the temperature effect (Δmag_T; upper) and geometrical effect (Δmag_G; lower) are distinguished. Note that the observed magnitude variations are primarily due to the temperature perturbations (slightly overestimated in Fuller and Lai, 2012).

However, to model the TEO amplitudes individually, one needs to consider the Lorentzian term Δ_{nlmN} (a term describing the resonances, see Equation 13, Burkart et al., 2012), which depends sensitively on the frequency detuning, i.e., the closeness of a certain forcing frequency ($Nf_{\rm orb}$) to the nearest eigenmode frequency. Unfortunately, even a change of $0.001M_\odot$ in stellar models can significantly change the detuning parameter, thus the Lorentzian term. A better way is to treat the detuning parameter as a random variable, which is uniformly distributed between its minimum value (= 0, perfect resonance) and maximum values (half of the adjacent g-mode spacing). In this way, a credible interval can be calculated for the Lorentzian term and thus the observed TEO amplitude (Fuller, 2017). For example, the 95% credible interval ($\pm 2\sigma$) of theoretical TEO amplitude for KIC 4142768 is shown as the shaded region in the upper left panel of **Figure 3**.

TEO phases, measured with respect to the periastron, deserve a particular discussion. We expect most observed TEOs are standing waves and nearly adiabatic, and their phases are close to the adiabatic expectations which are essentially only a function of ω (argument of periastron) and m (Burkart et al., 2012; Guo et al., 2020). In **Figure 4**, we show the observed TEO phases (symbols) and the theoretical adiabatic phases (vertical lines) for five HBs. As expected, low inclination HBs tend to show $m = 0$ modes (top two systems), and intermediate/high inclination HBs usually present both $m = 0$ and $m = 2$ modes. The low-frequency TEOs experience more radiative damping, and they can be distinguished by their relatively large phase offset from adiabatic phases (O'Leary and Burkart, 2014, Figure 4; Guo et al., 2019, Figure 7). Weakly non-linear TEOs that experience non-linear mode coupling also show deviations from the adiabatic phases. It is possible that TEOs locked in resonance with the orbit still have relatively large frequency detuning compared with the mode damping rate, and thus they do not show arbitrary phases as in the perfect-resonance case.

To summarize, the tidal response to a forcing frequency ($Nf_{\rm orb}$) is a summation of the mode eigenfunctions weighted by the mode amplitude $A_{nlmN} \propto \epsilon_l Q_{nl} X_{lm} \Delta_{nlmN}$ (Burkart et al.,

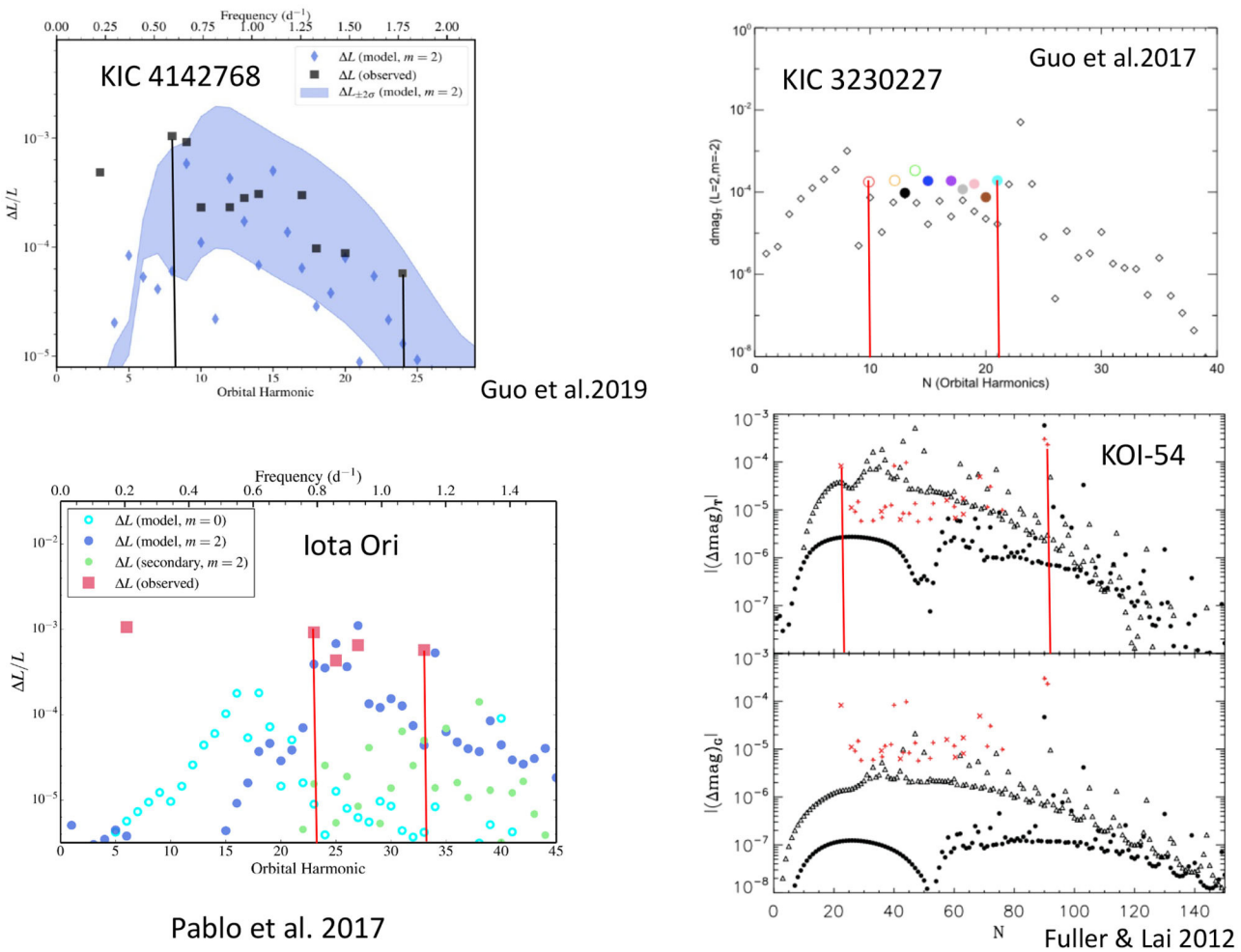

FIGURE 3 | The amplitude of TEOs in magnitude variation (Δmag) or relative luminosity variation ($\Delta L/L$) as a function of orbital harmonic (N) for four heartbeat binaries. The observed TEOs are indicated by the gray squares (**upper left**, KIC 4142768), open circles (**upper right**, KIC 3230227), red squares (**lower left**, ι Ori), and red crosses (**lower right**, KOI-54). The theoretical TEO amplitudes are shown as blue diamonds (**upper left**, $m = 2$ modes), open diamonds (**upper right**, $m = 2$ modes), blue/cyan circles (**lower left**, $m = 2/m = 0$ modes), and open triangles/filled circles (**lower right**, $m = 0/m = 2$ modes, respectively). The two vertical lines in each panel show the lower and upper frequency limits of the observed TEOs.

2012; Fuller, 2017). Roughly speaking, ϵ_l determines the overall strength, $Q_{nl}X_{lm}$ controls the range of excited orbital harmonics N, and Δ_{nlmN} sets the detailed amplitude of each TEO. TEO phases are primarily determined by the orbital orientation. Most observed TEOs in HBs are chance resonances (i.e., random frequency detuning) with g-modes and can be modeled by the above theoretical framework. In fact, the aforementioned statistical approach is good for finding TEOs larger than expectation. These TEOs may be locked in resonance with the orbit and require a different modeling approach (see section 2.3).

2.2. Weakly Non-linear TEOs: Mode Coupling

Modes near resonances can non-linearly interact and observationally, this can generate combination frequencies in the form of $mf_a \pm nf_b$, with m and n being integers. Resonance mode couplings have been observed and studied in free oscillations for B-type pulsators (Degroote et al., 2009), δ Scuti pulsators (Breger and Montgomery, 2014; Bowman et al., 2016) as well as compact pulsators (Zong et al., 2016a,b) and other types of variables. Theoretical studies include, e.g., Dziembowski and Krolikowska (1985), Van Hoolst (1994), and Buchler et al. (1997).

In the context of tidal oscillations, a striking feature in the observed TEOs is that some of them are not orbital harmonics. And the anharmonic frequencies can pair up and sum to an orbital harmonic ($f_a + f_b \approx Nf_{\rm orb}$). This can be explained by the non-linear resonance mode coupling.

When the tidally excited oscillations surpass the linear regime and become weakly non-linear, the oscillation mode can suffer from parametric instability (Schenk et al., 2002; Arras et al.,

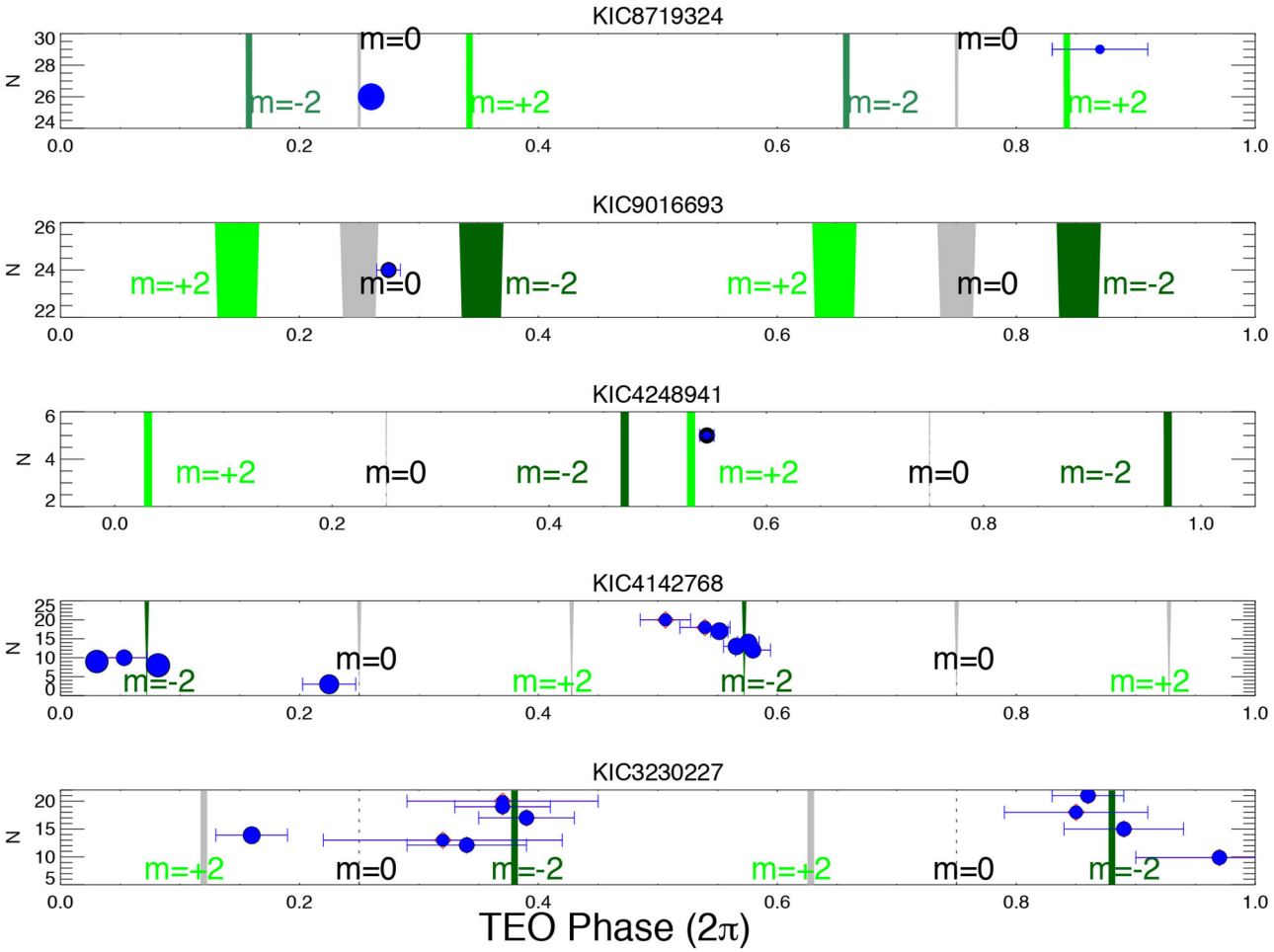

FIGURE 4 | Observed TEO phases (symbols) as a function of orbital harmonics (N) for five heartbeat binary systems. The theoretical phases in the adiabatic approximation are indicated by vertical lines, with the azimuthal number $m = 0$, or ± 2 labeled. Adopted from Guo et al. (2017a, 2020).

2003), which is the leading-order non-linear effect (Weinberg et al., 2012). In the dominant three-mode resonance coupling scenario ($f_A = f_a + f_b$), the parent mode A is resonantly excited by a linear dynamical tide (an orbital harmonic Nf_{orb}); and when its amplitude exceeds the three-mode instability threshold, it can transfer energy to two daughter modes (a, b). In **Figure 5**, we show different mode coupling patterns. The upper left is the aforementioned basic three-mode coupling. The mode-coupling triplet (A, a, b) can also couple to other mode triplets, either by sharing the parent (lower left) or sharing a daughter mode (upper middle panel). Multiple mode-triplets can also couple together (lower middle panel). In KIC 3230227, we find that two mode-coupling triplets share one daughter mode. And the resonance conditions for the two mode triplets are labeled in **Figure 5**: $f_A(22) = f_a(9.88) + f_b(12.12)$ and $f_B(26) = f_d(13.88) + f_b(12.12)$, where all frequencies are in units of the orbital frequency. In KOI-54, it is found that the 91st orbital harmonic resonantly excites an eigenmode very close to it, and this parent mode has at least four pairs of daughter modes. Some of the pairs even share daughters (O'Leary and Burkart, 2014). Furthermore, third-order mode coupling is also evidenced (the rightmost panel in **Figure 5**).

Observationally, these non-linear coupled TEOs can offer us lots of information beyond the linear theory. Firstly, the selection rules (relating the modes' l and m, Dziembowski, 1982) in mode coupling can help to identify the daughter modes (O'Leary and Burkart, 2014; Guo, 2020). If we have a large number of these mode triplets, since the linearly driven parent modes can be identified from phases, we may be able to discern the g-mode period spacings among the daughter modes and possibly among the close-to-resonance parent modes. The asymptotic period spacing pattern has been routinely found in self-excited g-modes in γ Dor stars and SPB stars, but not in tidally excited modes. Secondly, parent modes that suffer from mode-coupling instability should be close to the eigenmode frequency (although they do not necessarily have a larger amplitude than the daughter modes). Together with the anharmonic daughter modes, these mode frequencies provide a list of eigenmodes that can be compared with stellar models. This kind of tidal asteroseismology can thus be performed. After the preliminary effort by Burkart

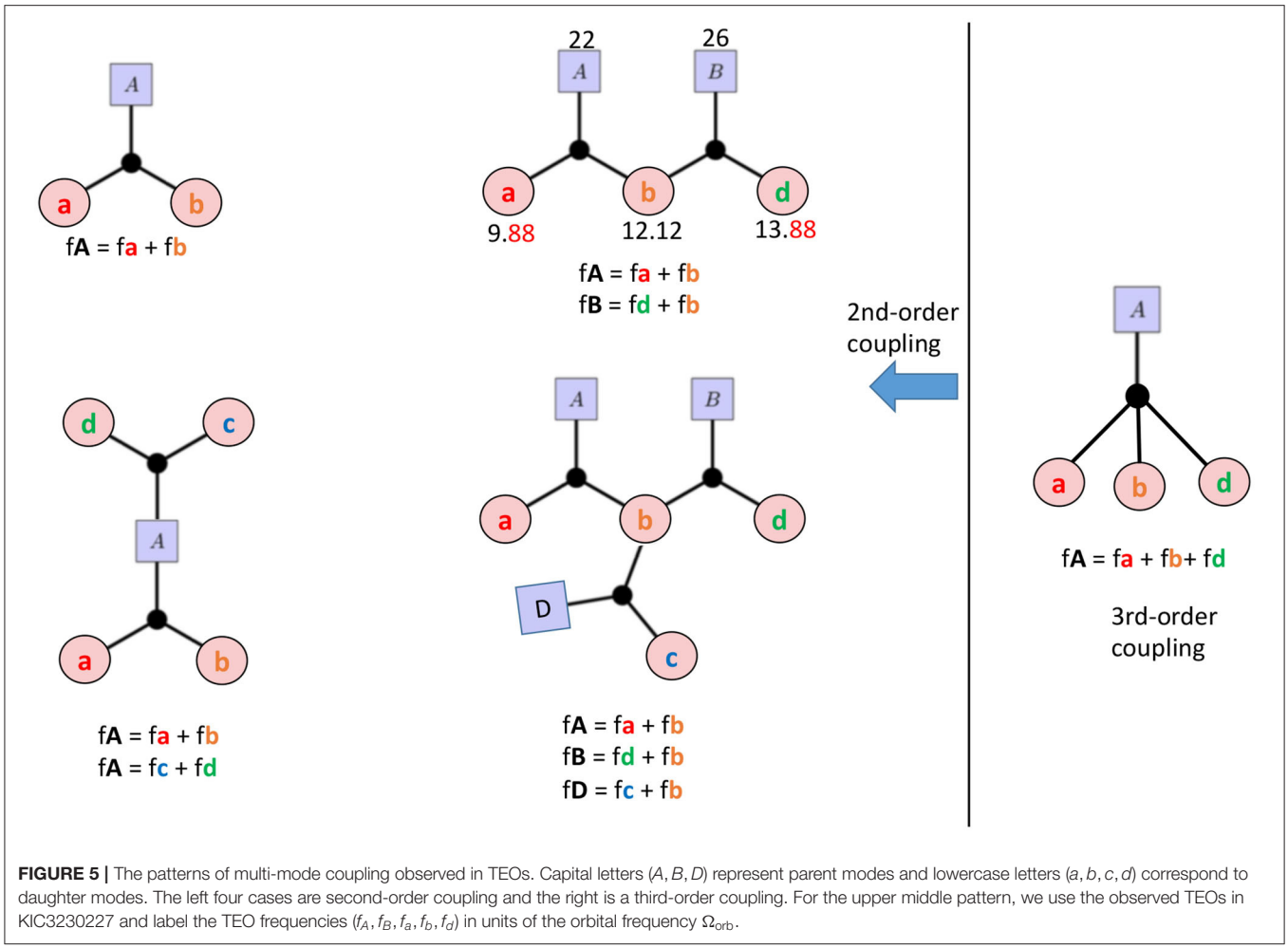

FIGURE 5 | The patterns of multi-mode coupling observed in TEOs. Capital letters (A, B, D) represent parent modes and lowercase letters (a, b, c, d) correspond to daughter modes. The left four cases are second-order coupling and the right is a third-order coupling. For the upper middle pattern, we use the observed TEOs in KIC3230227 and label the TEO frequencies (f_A, f_B, f_a, f_b, f_d) in units of the orbital frequency $\Omega_{\rm orb}$.

et al. (2012), we are still waiting for its first concrete application in a real star. Thirdly, the observed parent mode amplitude can be compared to the mode-coupling threshold. This helps to determine the nature of coupling. For KOI-54, O'Leary and Burkart (2014) showed that five-mode coupling can decrease the threshold amplitude of parametric instability (i.e., smaller than three-mode coupling threshold). This explains the observed parent-mode amplitude being much smaller than the three-mode instability threshold. In fact, Weinberg et al. (2012) showed that, if the parent mode couples to N daughter-mode pairs, the threshold amplitude can decrease by a factor of N. Fourthly, the mode coupling systems can have different behavior (Wersinger et al., 1980; Wu and Goldreich, 2001), depending on the frequency detuning (the difference between the parent-mode frequency f_A and the resonant linear tide at $Nf_{orb} \approx f_A$, and also between the parent-mode frequency and the daughter-mode frequency sum $f_a + f_b$) and the daughter-mode damping rates. Guo (2020) showed that the observed stable amplitudes/phases of the parent and daughter modes in KIC3230227 indicate the five-mode-coupling system has settled into an equilibrium state, and this agrees with the theoretical mode damping rates. The mode-coupling systems can show limit cycles (Moskalik, 1985) and observables such as cycle period can help to constrain mode parameters (e.g., damping rates). In ZZ Ceti (DAV) type pulsating white dwarfs, it is in fact limit cycles that explain the observed outbursts in the light curves (Luan and Goldreich, 2018). Non-linear mode coupling is believed to be the dominant amplitude limitation mechanism in many types of pulsators such as δ Scuti (Dziembowski and Krolikowska, 1985; Dziembowski et al., 1988) and SPB stars (Lee, 2012). The same limitation mechanism applies to the tidally excited g modes. Unfortunately, relevant studies in this direction are rare.

2.3. Resonance Locking

When the evolution of a mode frequency is in pace with that of the forcing frequency (i.e., their time derivatives are the same), the oscillation mode can be locked into resonance with the orbit. This resonance locking phenomenon can have significant consequences on the orbital evolution of not only stellar binaries, but also satellites of gaseous giant planets (Fuller et al., 2016; Lainey et al., 2020). In the context of heartbeat stars, it can have several observational implications. Firstly, the mode in resonance locking has a larger-than-expected amplitude (i.e., compared to

the amplitude from the aforementioned statistical approach). This has been demonstrated for the dominant oscillation mode in the primary star of KIC 8164262 (Fuller et al., 2017; Hambleton et al., 2018). The mode in resonance locking has an orbital harmonic of $N = 229$ and is likely an $m = 1$ mode in this misaligned binary. Cheng et al. (2020) found that the oscillation at 53rd orbital harmonic is a possible candidate for resonance locking in KIC 11494130. Resonance locking can significantly enhance the tidal dissipation and orbital evolution (e.g., see Figure 3 in Witte and Savonije, 1999b for a $10M_\odot + 1.4M_\odot$ binary). For KIC 8164262, Fuller et al. (2017) estimated that the tidal quality factor Q' is reduced from $\approx 2 \times 10^7$ to $\approx 5 \times 10^4$ due to the mode in resonance locking. Secondly, it remains to be seen observationally whether the TEOs in resonance locking suffer more from the (weakly) non-linear mode coupling and strong non-linear damping. In fact, the dominant TEO in KOI-54 at 91 times of orbital frequency has multiple daughter pairs, although the resonance-locking nature of this $l = 2, m = 0$ mode is still under debate. An examination of the resonantly-locked TEO amplitude and phase is desirable. Resonance locking depends on the evolutionary speed of the oscillation mode due to stellar evolution, and thus it is sensitive to the stellar age. A study of the resonance-locking condition spanning from ZAMS to TAMS, and for different orbital parameters would be very useful. The orbital harmonic N of a resonantly locked mode as a limited range and a predictable amplitude, allow for inference about whether resonance locking is occurring (Fuller and Lai, 2012; Burkart et al., 2014; Fuller, 2017).

3. CIRCULAR BINARIES WITH TIDALLY PERTURBED MODES

In the circularized and synchronized close binaries, tides do not dynamically excite oscillation modes but rather perturb the propagation cavity and pulsation alignment. The effects of equilibrium tides on stellar oscillations include:

(a) perturbed eigenfrequencies (tidal splitting):

The study of oscillations of tidally distorted polytropes can date back to early work by Chandrasekhar (1969). Other works using polytrope models include Saio (1981), Horedt (2004), Reyniers and Smeyers (2003), and also Roxburgh (unpublished). These works use the perturbative method and concentrate on the perturbing effect on eigenfrequencies. Preece et al. (2019) implemented a different method to calculate the oscillation frequencies of a tidally distorted sub-dwarf B star. It involves performing the surface-averaging of local oscillation frequencies calculated from the local density profile.

Observational work includes Balona (2018), in which he applied the above perturbative theory to KIC 4142768[6]. Tidally perturbed oscillations have been found in U Gru (Bowman et al., 2019b), V453 Cyg (Southworth et al., 2020), VV Ori (Southworth et al., 2021), and RS Cha (Steindl et al., 2021). These are mostly close, nearly circular and synchronous, Algol-like binary systems with self-excited oscillations. In addition, tidally perturbed gravity modes (tidal splittings) have been found in the SPB star π^5 Orionis (Jerzykiewicz et al., 2020), and this 3.7-day-binary also shows ellipsoidal variations[7].

(b) perturbed eigenfunctions and pulsation alignment.

Recently, tidally tilted binaries have been found which show modulated oscillation amplitude and phase (similar to the oblique roAp pulsators, Kurtz, 1982). The pulsation axis is almost aligned with the tidal axis, and thus pulsation frequencies have side-lobes separated by the orbital frequencies. The first system HD74423, was found by Handler et al. (2020) and was termed a "single-sided pulsator." Subsequent discoveries include CO Cam by Kurtz et al. (2020) and TIC 63328020 by Rappaport et al. (2021). Fuller et al. (2020) used the more general operator-perturbation method in Dahlen and Tromp (1998) and modeled the stellar response to the static tides by decomposing it into free-oscillation eigenfunctions. Thus, they obtained not only tidally perturbed eigenfrequencies, but also eigenfunctions. It is found that modes can be trapped at the pole, equator, or some intermediate latitude. The amplitude/phase modulation can be modeled and thus be used to as a mode identification method. Springer and Shaviv (2013) studied the propagation and damping of high-frequency acoustic waves in a Roche-lobe filling star.

The above tidal perturbation effect due to equilibrium tide should also work in the case of eccentric orbits, maybe in a different fashion since the tidal deformation is quite different at different orbital phases. In fact, in the eccentric binary KIC 4544587 (Hambleton et al., 2013), in addition to the orbital harmonic g-modes excited by the dynamical tide, p-modes separated by orbital frequency are also present. These modes are interpreted as tidally perturbed p modes. It would be interesting to re-examine this system and study the equilibrium tidal effect on the self-excited oscillations.

4. OSCILLATING CLOSE BINARIES WITH MASS TRANSFER

4.1. Mass-Accreting Pulsators

In the strong-tide regime when a star fills its Roche lobe, tides induce mass transfer. Depending on the adjustment of the stellar radius and the Roche-lobe radius, the mass transfer can be in the form of stable or unstable Roche-lobe overflow (RLOF) (Vanbeveren and De Loore, 1994; Soberman et al., 1997). Mass transfer affects the evolution of the binary orbit (Dosopoulou and Kalogera, 2016a,b). But the asteroseismic consequences of accretion have not been studied. How does the mixing process modify the excitation of heat-driven pulsations? The κ-mechanism excitation occurs at the near-surface layer where the opacity due to the hydrogen/helium or iron-group elements ionization zones have a local maximum (Unno et al., 1989, chapter 5). In addition, another necessary condition for the driving is that the local thermal timescale has to be comparable to the oscillation period (Pamyatnykh, 1999). Even

[6] Although the method is valid, this system is found to be an eccentric binary with TEOs and the application is thus questionable.

[7] Some of these systems may be slightly out of synchronization, and dynamical tides can also be viable in asynchronous rotating stars in circular orbits.

without material mixing, the accretion may drive the star out of thermal equilibrium, and this may also change the geometric depth of the ionization zone and thus the pulsation excitation and frequencies. If mixing (e.g., thermohaline mixing when a negative chemical composition gradient is present) does happen (Stancliffe and Glebbeek, 2008), the change of composition also needs to be taken into account.

Observationally, many mass-accreting stars do show pulsations. The Oscillating Algol (oEA) systems are a class of δ Scuti/γ Dor pulsators in Algol-type binaries with mass accretion (Mkrtichian et al., 2004, 2020). The companion is usually a low-mass star filling or nearly-filling its Roche lobe, depending on whether the mass transfer process is finished or not. To name a few, AS Eri (Mkrtichian et al., 2004), KIC 4739791 (Lee et al., 2016), KIC 8553788 (Liakos, 2018), V392 Orionis (Hong et al., 2019), KIC 10736223 (Cheng et al., 2020). Guo and Li (2019) found the period spacing pattern of dipole g modes in mass-accreting γ Dor star in KIC 9592855. A comparison with theoretical g-mode period spacings suggests that the mass of this primary star is lower than previously reported. Streamer et al. (2018) did detailed binary star evolution modeling and calculate the pulsation properties of the mass-accreting δ Scuti primary ($\approx 2.2M_{\odot}$) in TT Hor. They managed to match the observed oscillation frequencies and found a likely evolutionary history for the δ Scuti pulsator. It was initially a $1.3M_{\odot}$ star and accreted about $0.9M_{\odot}$ from the companion. Accretion-driven variability in oEA binaries has been studied (Mkrtichian et al., 2018) and the Fourier spectrum of accreting δ Scuti pulsators can change during the outburst. Although some of these variabilities may be attributed to the variation of mass transfer rate, the pulsation changes also contribute to the variability. A significant number of Agol-type eclipsing binaries have δ Scuti pulsating components and it seems that many of them show very high-frequency p-modes (~ 60 d^{-1}), which is a signature of youth and probably the result of rejuvenation from RLOF (Dray and Tout, 2007).

Previous works on how mass-transfer modifies stellar oscillations are scarce. Note that numerous oscillations of mass-accreting white dwarfs (WD) in Cataclysmic Variables (CVs) have been discovered (Mukadam et al., 2007, 2011). Arras et al. (2006) studied the g-mode pulsational instabilities of accreting WDs in CVs. He found that an envelope of solar-like composition (accreted material) on top of the pure-hydrogen layer of the WD can change the edge of the instability strip significantly. During the accretion, outbursts can heat the WD, bringing it out of the instability strip. Similar work to the pulsational instability of other types of opacity-driven pulsators would be interesting.

4.2. Post-mass Transfer Pulsating Binaries

Post-mass transfer binaries with a δ Scuti pulsating component have been discovered, including KIC 10661783 (Southworth et al., 2011; Lehmann et al., 2013), KIC 8262223 (Guo et al., 2017c), and the aforementioned TIC 63328020 (Rappaport et al., 2021). The previous-mass-gainer δ Scuti star in KIC 8262223 pulsates at about 60 d^{-1}, suggesting that the system only just finished the mass transfer, i.e., the effect of rejuvenation is still present. In contrast, KIC 10661783 pulsates at much lower frequencies (15 d^{-1}). This is likely due to the fact that it has finished the mass transfer long ago and the δ Scuti pulsator is already evolved. Similarly, post-mass transfer γ Dor and SPB-type pulsating binaries have also been identified (Matson et al., 2015; Guo et al., 2017b). It is quite clear that δ Scuti and γ Dor type pulsations are not suppressed in close binaries. This is in contrast with red giants in binaries, in which solar-like oscillations seem to be suppressed by binarity, probably due to the enhanced magnetic activity. The majority of the aforementioned binary can be formed in the formation channel of EL CVn binaries[8] (Maxted et al., 2013, 2014). The formation involves the evolution of two low-mass stars with stable RLOF and mass reversal (Chen et al., 2017). In **Figure 6**, we show typical evolutionary tracks of an EL CVn type binary. Staring with two low-mass stars ($M_1 = 1.35, M_2 = 1.15M_{\odot}$), the mass gainer can evolve to a δ Scuti/γ Dor pulsator ($M = 1.72M_{\odot}$) or even an SPB star with slightly changed initial conditions. The mass donor can become a pre-ELM WD (extremely low-mass white dwarf precursor) pulsator ($M \lesssim 0.2M_{\odot}$) with p, or g-mode pulsations (Maxted et al., 2013; Gianninas et al., 2016; Istrate et al., 2016), and possibly later on the WD cooling track, become a g-mode pulsating helium WD. These five types of post-mass transfer pulsators have been marked in **Figure 6** as ellipses.

Post-mass transfer RR Lyrae and Cepheid pulsators have been found by Pietrzyński et al. (2012) and Pilecki et al. (2017), respectively. Gautschy and Saio (2017) studied the binary evolution channel to form anomalous Cepheids via RLOF and merger-like evolution. Similar work by Karczmarek et al. (2017) found stars crossing the classical instability strip of RR Lyrae and Cepheids via the binary channel. The formation of recently-discovered Blue Large-Amplitude Pulsators (BLAP) also involves binary evolution with mass transfer (Pietrukowicz et al., 2017). Recently, Byrne and Jeffery (2020) studied the non-adiabatic pulsational properties by using the post-mass-transfer stellar models. We also know sub-dwarf B-stars (sdB) and blue stragglers can be formed by mass-transfer or merger (Han et al., 2002, 2003). The list of post-mass transfer pulsators can go on and on. Binary channels can generate all kinds of exotic binary systems (de Loore and Doom, 1992; Hurley et al., 2002; Eggleton, 2006). It can also generate new types of pulsating stars and also contaminate the existing pulsators (Jeffery and Saio, 2016). Pulsational analysis of post-mass transfer systems is still the frontier of asteroseismology, and it holds great promise to improve our understanding on stellar structure and evolution.

5. DISCUSSION AND FUTURE PROSPECTS

Detailed analysis of existing *Kepler* HBs needs to be done on a one-by-one basis. There are also tidal oscillations in binaries that are not identified yet in *Kepler* data. Gaulme and Guzik (2019) identified KIC 11572363 as an HB with TEOs. They also find some other "tidal pulsators," and most of them have circular orbits with self-excited modes, probably perturbed by tides. Sekaran et al. (2020) compiled 95 g-mode pulsators in eclipsing binaries. The sample may contain tidally perturbed

[8] EL CVn binary is a type of binary consisting of an F-,A-type dwarf and a low-mass helium white dwarf precursor.

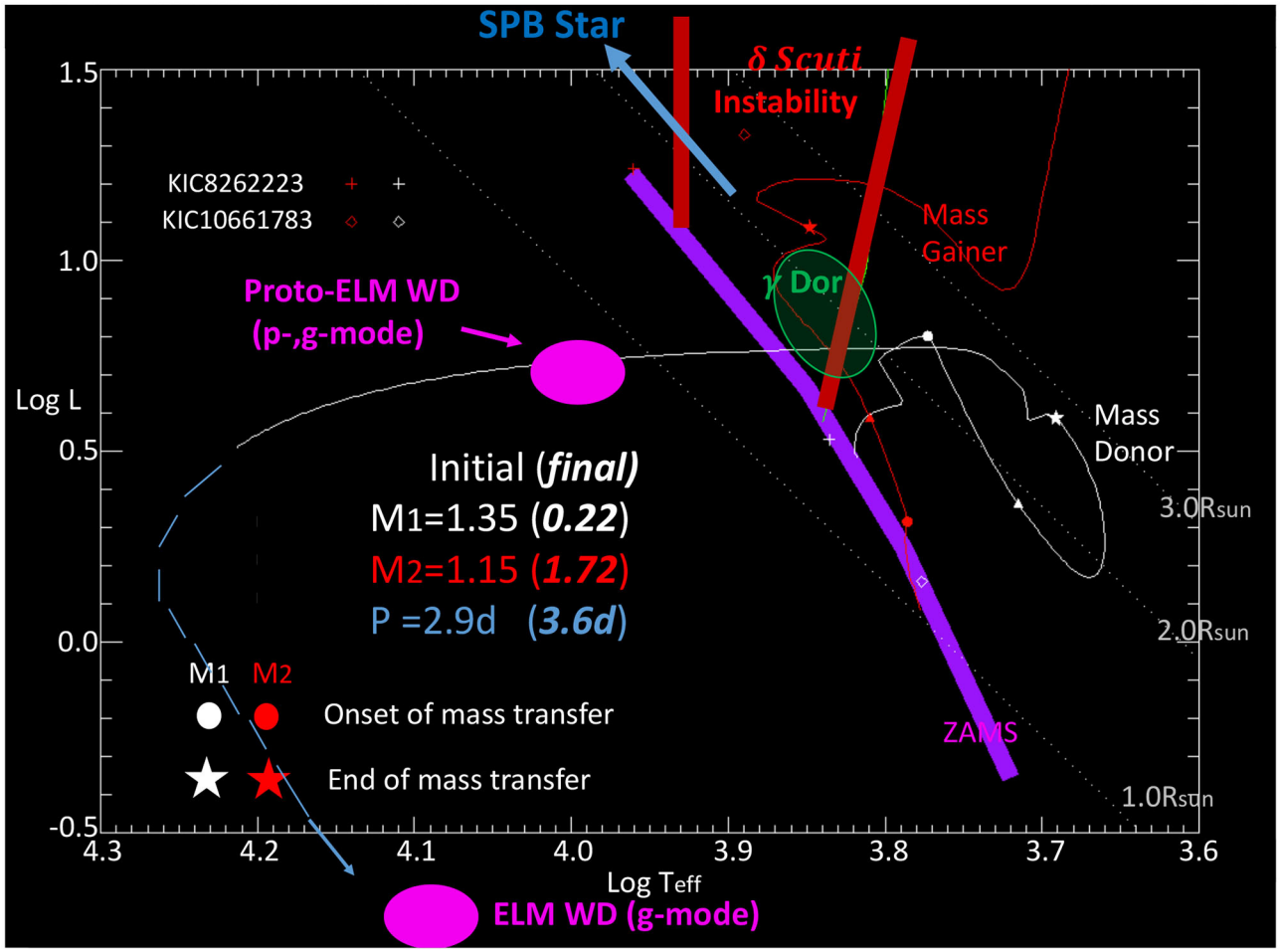

FIGURE 6 | Typical evolutionary tracks for the formation an EL CVn type binary via stable RLOF mass transfer. This binary channel can generate 5 type of pulsating stars: Slowly Pulsating B-stars (SPB), δ Scuti stars (indicated by the red instability strip edges), γ Dor pulsators (green ellipses), Pre-ELM white dwarf, and He white dwarf pulsator (purple ellipses).

modes or tidally excited modes. More tidally excited or perturbed oscillations can be obtained from the on-going surveys such as TESS (Ricker et al., 2015), KELT (Pepper et al., 2007), etc.

Willems and Aerts (2002) modeled the radial velocity (RV) variation from tides in an eccentric binary HD177863 with a B-type star component. Arras et al. (2012) predicted the tidally induced RV amplitude in exoplanet hosts. For heartbeat binaries, it was already noted by Welsh et al. (2011) that the radial velocity variations Δv_r in KOI-54 show significant non-Gaussian RV residuals after removing the Keplerian orbit. The RV variations due to the equilibrium tide and dynamical tide can be calculated and compared with observations (Bunting and Terquem, 2021). Massive stars can show periastron activities, including non-Keplerian RV variations and line-profile variations (Koenigsberger et al., 2012; Richardson et al., 2017; Koenigsberger and Schmutz, 2020). It is worth a modeling effort although other effects (e.g., stellar wind and magnetic field) are also important in these hot stars. Other types of observation can also reveal the signature of tides, e.g., line profile variations from high-resolution spectroscopy, and spectro-polarimetric observations. In particular, multi-color observations of stellar oscillations are going to gain importance as more space surveys are underway.

The potential of tidal asteroseismology in constraining stellar parameters has not been exploited yet. Fuller et al. (2017) experimented with KIC 8164262 and found small amounts of convective core overshoot and diffusive mixing can yield better agreement with observed TEO amplitude. The convective boundary criterion adopted can also be important (Chernov, 2017). A detailed analysis would involve scanning the large multi-dimensional parameter space. Actually, Burkart et al. (2012) did preliminary asteroseismic modeling of the TEOs in KOI-54 by varying the stellar masses and radii, assuming fixed metallicity and the rotation period. They found that the TEO amplitude sensitively depends on the stellar models, and to match with observations requires a fined-tuned degree of resonance which is very difficult to capture in a grid of stellar models. Even a small difference in stellar models can significantly change the degree

TABLE 1 | Heartbeat binaries with Tidally Excited Oscillations.

Name	P_{orb}(d) f_{orb}(d^{-1})	i e ω	$T_{\rm eff}$ log g $M(M_\odot)$ $R(R_\odot)$	TEO harmonic ($N = f/f_{orb}$)	TEO amplitude (mmag)	Remark
KIC 8164262	87.45717	65°	6890/3500 K	229	10.1	
	0.01143417	0.886	3.9/–	241	0.353	
		84.79°	1.70, 0.36$M_\odot$	123	0.229	
			2.4, $-R_\odot$	158	0.152	
				124	0.151	
				132	0.133	
				194	0.123	
				128	0.118	
				317	0.095	
				129	0.083	
				125	0.069	
				137	0.068	
				114	0.064	
				264	0.056	
				22	0.056	
KIC 5790807	79.996246	85.82°	6466 K	48	0.017	m = 2
	0.01250	0.855	3.42	107	0.015	m = 2
		155.6°	1.74, 0.44$M_\odot$			
KOI54	41.8050	5.5°	8500/8800 K			
=KIC8112039	0.023921	0.8335	4.12/4.08	90	0.294	m = 0
		36.7°	2.33, 2.39$M_\odot$	91	0.227	m = 0
Only A$\geq 2\mu mag$			2.20, 2.33$R_\odot$	44	0.0958	
				40	0.0826	
				72	0.0297	
				27	0.0013	
				53	0.0144	
				47	0.0134	
				39	0.0112	
				60	0.0068	
				37	0.0103	
				71	0.0110	
				75	0.0104	
				27	0.0084	
				43	0.0085	
				45	0.0088	
				36	0.0063	
				52	0.0071	
				33	0.0057	
				29	0.0044	
				48	0.0059	
				78	0.0051	
				49	0.0051	
				32	0.0047	
				57	0.0045	
				46	0.0043	
				31	0.0042	
				26	0.0041	

(Continued)

TABLE 1 | Continued

Name	P_{orb}(d) f_{orb}(d^{-1})	i e ω	$T_{\rm eff}$ log g $M(M_\odot)$ $R(R_\odot)$	TEO harmonic ($N = f/f_{orb}$)	TEO amplitude (mmag)	Remark
				42	0.0040	
				51	0.0040	
				55	0.0036	
				35	0.0034	
				50	0.0034	
				25	0.0030	
				38	0.0029	
				22	0.0028	
				34	0.0026	
				30	0.0025	
				24	0.0025	
				23	0.0021	
				127	0.0021	
				54	0.0020	
				Aharmonic:		
				22.419	0.00787	
				68.582	0.00490	
				63.076	0.00246	
				57.577	0.00157	
				25.846	0.00112	
				35.844	0.00090	
				60.419	0.00059	
				42.106	0.00066	
				59.969	0.00057	
				41.417	0.00041	
				49.589	0.00036	
				25.076	0.00030	
				24.844	0.00029	
				44.078	0.00029	
				93.197	0.00029	
				80.087	0.00021	
				72.088	0.00020	
				27.581	0.00020	
ι Ori	29.13376	62.86°			Red/Blue	
	0.034324	0.7452	31,18.3(10^3K)	23	0.92/0.97	m = 2
		122.15°	3.89, 4.18	25	0.44/–	m = 2
			23.18,13.94$M_\odot$	27	0.66/0.78	m = 2
			9.10, 4.94$R_\odot$	33	0.58/0.7	m = 2
θ^1 Cru	24.5314	26.12°				
A3-A8	0.04076	0.707		4	0.1184	
		119.96°		7	0.1999	
KIC 11494130	18.9554	79.2°	6600 K,	53	0.03	m = 0
	0.052755	0.66	4.2			
		263°	∼1.4, ∼0.5$M_\odot$			
KIC 3749404	20.3063852	62°	8000/6900 K	21	0.0807	
	0.04924567	0.659	4.4/4.1	20	0.0670	
		123.2°	1.78, 1.32$M_\odot$	26	0.0374	
			1.98,1.20$R_\odot$	22	0.0491	

(Continued)

TABLE 1 | Continued

Name	P_{orb}(d) f_{orb}(d^{-1})	i e ω	$T_{\rm eff}$ log g $M(M_\odot)$ $R(R_\odot)$	TEO harmonic ($N = f/f_{orb}$)	TEO amplitude (mmag)	Remark
				19	0.0266	
				7	0.021	
				24	0.0347	
				23	0.0344	
				5	0.0121	
				17	0.0096	
				27	0.0091	
MACHO	32.83	44.9°		8	3	
80.7443.1718	0.0305	0.565		10	6	
		61.1°	$\sim 30M_\odot$	17	9	
				25	14	
ζ^1 UMa	20.5351	44.66°		3	0.0394	
A2,A2	0.048697	0.621		5	0.0140	
		114.5°	$\sim$2.2, 2.2$M_\odot$	6	0.0181	
				8	0.0111	
				10	0.0101	
KIC 3230227	7.0471062	73.42°	8000/8180 K	13.88	0.338	
	0.141902	0.60	4.10/4.23	21	0.194	m = 2
		293.0°	1.84, 1.73$M_\odot$	15	0.198	m = 2
			2.01,1.68$R_\odot$	17	0.177	m = 2
				19	0.154	m = 2
				12.12	0.192	
				18	0.124	m = 2
				9.88	0.179	
				20	0.073	m = 2
				13	0.085	m = 2
				22	0.043	m = 2
				12	0.069	m = 2
				24.12	0.033	
				23	0.031	m = 2
				26	0.024	m = 2
				13	0.042	m = 2
				31	0.016	m = 2
				28	0.017	m = 2
				16	0.027	m = 2
				27	0.017	m = 2
				10	0.036	m = 2
				5	0.065	m = 2
				14.13	0.025	
				40	0.010	m = 2
				30	0.009	m = 2
				16.13	0.014	
				11	0.018	m = 2
KIC8719324	10.2326979	73.54°	7,750 K	26	0.64472	m = 0
	0.0977259	0.6	4.5	29	0.0789	m = 2
		-17.1°	–			
			–			

(Continued)

TABLE 1 | Continued

Name	P_{orb}(d) f_{orb}(d^{-1})	i e ω	$T_{\rm eff}$ log g $M(M_\odot)$ $R(R_\odot)$	TEO harmonic ($N = f/f_{orb}$)	TEO amplitude (mmag)	Remark
KIC9016693	26.3680271	25.6°	7,262 K	24	0.19238	m = 0
	0.0379247	0.596	–			
		108.4°	≈ 1.6			
			-			
KIC 4142768	13.9958015	75.81°	7327/7383 K	9	0.995	m = 2
	0.071449999	0.582	3.81/3.95	8	1.129	m = 2
		328.2°	2.05, 2.05$M_\odot$	17	0.325	m = 2
			2.96,2.51$R_\odot$	14	0.332	m = 2
				13	0.304	m = 2
				12	0.252	m = 2
				10	0.251	m = 2
				18	0.105	m = 2
				20	0.096	m = 2
				24	0.078	m = 2
KIC 5034333	6.9322800	49.88°	9,250 K	18	0.1760	
	0.1442527	0.58	4.5	13	0.1500	
		−17.1°	–	20	0.1465	
			–	27	0.0878	
				19	0.0802	
				66	0.0723	
				4	0.0613	
				12	0.0602	
14 Peg	5.30824	17.32°		8	0.040	
A1V,A1V	0.18839	0.5333		17	0.041	
		310.9°				
KIC4248941	8.6445976	68.3°	6,750 K	5	0.48790	m = 2
	0.1156792	0.423	4.5			
		-50.5°				
p Vel A	10.2437	32.72°		5	0.1346	
F5 IV, F1 V	0.09762	0.3528		8	0.0458	
		169.4°		11	0.0562	
				18	0.0235	
HD209295	3.10575	40-45°	7,750 K		B, V (filter)	
	0.32198	0.352	4.3	8	18.3, 13.2	
		31.1°	1.84,0.6-1$M_\odot$	7	8.4, 6.6	
			–	3	7.0, 6.2	
				5	4.6, 3.9	
				9	4.5, 3.5	
HD158013	8.21675	50.97°		7	0.0468	
Am	0.12170	0.3327		9	0.2078	
		129.57°		18	0.0229	
KIC 4544587	2.189 094	87.9°	8,600/7,750 K			
	0.456810	0.275	4.24/4.33	4	0.593	
		328.9°	1.98, 1.61$M_\odot$	3	0.520	
			1.76, 1.42$R_\odot$	97	0.134	
				10	0.116	
				8	0.106	

(Continued)

TABLE 1 | Continued

Name	P_{orb}(d) f_{orb}(d^{-1})	i e ω	$T_{\rm eff}$ log g $M(M_\odot)$ $R(R_\odot)$	TEO harmonic ($N = f/f_{orb}$)	TEO amplitude (mmag)	Remark
				9	0.093	
QX Car	4.47948	34.77°		5	0.156	
B2V, B2V	0.22324	0.2677		7	0.221	
		174.7°		10	0.131	
				12	0.137	
V1294 Sco	5.6010	46.2°		7	1.14	
O9IV,O9.7V	0.17854	0.2578				
		130.8°				
HD174884	3.65705	73.35°	13140,12044 K	8	0.120	
	0.27344	0.2939	3.89,4.26	13	0.111	
		51.31°	4.04,2.72$M_\odot$	3	0.091	
			3.77,2.04$R_\odot$	4	0.097	

of resonance and thus the TEO amplitude. Their final adopted models have Fourier spectra semi-quantitatively consistent with the observations, although they also find that there are many local minima which can produce comparably good fits. Other factors also make tidal seismic modeling challenging, e.g., weak non-linearity of TEOs can set in and detailed mode-coupling calculations may involve many mode-coupling networks (Essick and Weinberg, 2016; Yu et al., 2020).

Convective motion in the core can excite internal gravity waves (Lecoanet and Quataert, 2013; Rogers et al., 2013; Edelmann et al., 2019; Lecoanet et al., 2019). This has have been observed as the low-frequency power excess of OB stars by Bowman et al. (2019a, 2020) (Other interpretation also exists, e.g., arising from the subsurface convection zone, Cantiello et al., 2021). Similarly, tidally excited internal gravity/gravito-inertial waves are also expected to be present in the observed Fourier spectra. It would be interesting to do a similar study of the low-frequency background of the Fourier spectrum and check if there is evidence of tidal origin.

The Rossby (r) modes and inertial modes constitute the very low-frequency part of the tidal response. Global r-modes have been discovered (Van Reeth et al., 2016; Saio et al., 2018; Saio, 2019) in many single γ Dor stars, B-type stars, eclipsing binaries including HBs, and white dwarfs in Cataclysmic Variables. Although r-modes can be heat-driven, the observations seem to favor a mechanical origin since most discoveries are related to fast-rotating systems. Theoretically, tidally excited r-modes can also be present in rotating early-type stars (e.g., see Witte and Savonije, 1999b, Figure 2 for a $10M_\odot$ example), although an observational confirmation is still awaiting. Recently, indirect evidence of pure inertial modes in the convective core has been discovered from their coupling effect with the dipole g-modes in the radiative envelope of γ Dor stars (Ouazzani et al., 2020; Saio et al., 2021). Observationally, this is inferred from the unexpected dips in the g-mode period spacing pattern which requires computations beyond the traditional approximation for rotation. Pure inertial waves can be induced by tides, similar to the inertial waves in the convective envelope of solar-type stars (Ogilvie and Lin, 2007). Again, the confirmation of theory awaits future observations.

In addition to the tidally excited oscillation, self-excited oscillations may also affect the orbital evolution. In the "inverse-tide" scenario (Fuller, 2021), angular momentum can be transferred from the self-excited modes to the orbit, and this may explain some of the very-slowly rotating convective cores discovered in γ Dor binaries (Guo and Li, 2019; Li et al., 2020a).

Studies on the tidal perturbative effect on the mode properties are still at an early stage, e.g., oscillations of tidally distorted stars are generally limited to simplified stellar models. Also some important factors have not been included. For example, detailed calculations in Fuller et al. (2020) only considered the effect of static tidal distortion on the mode eigenfrequencies and eigenfunctions and ignored the effect of Coriolis force. Close binaries with circular/synchronized orbits are easier to follow up observationally. Their oscillation properties are only studied on a one-by-one basis. Observationally, photometric and spectroscopic surveys are starting to offer a large sample of binary stars. The potential of these stars in constraining the tidal theory is still yet to be fully exploited (Justesen and Albrecht, 2021). With a large sample of various of binaries with pulsations and better theoretical understanding on mode properties, we may begin to perform the binary population synthesis with stellar oscillations included. The studies of stellar oscillations in binaries are, and will continue, revolutionizing the field of stellar astrophysics.

AUTHOR CONTRIBUTIONS

The author confirms being the sole contributor of this work and has approved it for publication.

FUNDING

This work was supported by STFC (grant ST/T00049X/1).

ACKNOWLEDGMENTS

We thank the referees for the pertinent comments and suggestions. ZG is in debt to Gordon Ogilvie for the thorough reading of this article and his enlightening comments, to Phil Arras, Nevin Weinberg, Rich Townsend, and Meng Sun for illuminating discussions on tides. Jim Fuller kindly grants us permission to use his plots in **Figure 2**. We acknowledge the usage of *Kepler* data by NASA.

REFERENCES

Aerts, C. (2021). Probing the interior physics of stars through asteroseismology. *Rev. Modern Phys*. 93:015001. doi: 10.1103/RevModPhys.93.015001

Aerts, C., Christensen-Dalsgaard, J., and Kurtz, D. W. (2010). *Asteroseismology*. Heidelberg: Springer. Available online at: https://ui.adsabs.harvard.edu/abs/2010aste.book.....A/abstract

Alexander, M. E. (1987). Tidal resonances in binary star systems. *Mon. Not. R. Astron. Soc*. 227, 843–861. doi: 10.1093/mnras/227.4.843

Alvan, L., Mathis, S., and Decressin, T. (2013). Coupling between internal waves and shear-induced turbulence in stellar radiation zones: the critical layers. *Astron. Astrophys*. 553:A86. doi: 10.1051/0004-6361/201321210

Anderson, K. R., Lai, D., and Storch, N. I. (2017). Eccentricity and spin-orbit misalignment in short-period stellar binaries as a signpost of hidden tertiary companions. *Mon. Not. R. Astron. Soc*. 467, 3066–3082. doi: 10.1093/mnras/stx293

Arras, P., Burkart, J., Quataert, E., and Weinberg, N. N. (2012). The radial velocity signature of tides raised in stars hosting exoplanets. *Mon. Not. R. Astron. Soc*. 422, 1761–1766. doi: 10.1111/j.1365-2966.2012.20756.x

Arras, P., Flanagan, E. E., Morsink, S. M., Schenk, A. K., Teukolsky, S. A., and Wasserman, I. (2003). Saturation of the R-mode instability. *Astrophys. J*. 591, 1129–1151. doi: 10.1086/374657

Arras, P., Townsley, D. M., and Bildsten, L. (2006). Pulsational instabilities in accreting white dwarfs. *Astrophys. J. Lett*. 643, L119–L122. doi: 10.1086/505178

Balona, L. A. (2018). The effect of tides on self-driven stellar pulsations. *Mon. Not. R. Astron. Soc*. 476, 4840–4847. doi: 10.1093/mnras/sty544

Beck, P. G., Hambleton, K., Vos, J., Kallinger, T., Bloemen, S., Tkachenko, A., et al. (2014). Pulsating red giant stars in eccentric binary systems discovered from Kepler space-based photometry. A sample study and the analysis of KIC 5006817. *Astron. Astrophys*. 564:A36. doi: 10.1051/0004-6361/201322477

Bowman, D. M. (2020). Asteroseismology of high-mass stars: new insights of stellar interiors with space telescopes. *Front. Astron. Space Sci*. 7:70. doi: 10.3389/fspas.2020.578584

Bowman, D. M., Aerts, C., Johnston, C., Pedersen, M. G., Rogers, T. M., Edelmann, P. V. F., et al. (2019a). Photometric detection of internal gravity waves in upper main-sequence stars. I. Methodology and application to CoRoT targets. *Astron. Astrophys*. 621:A135. doi: 10.1051/0004-6361/201833662

Bowman, D. M., Burssens, S., Simón-Díaz, S., Edelmann, P. V. F., Rogers, T. M., Horst, L., et al. (2020). Photometric detection of internal gravity waves in upper main-sequence stars. II. Combined TESS photometry and high-resolution spectroscopy. *Astron. Astrophys*. 640:A36. doi: 10.1051/0004-6361/202038224

Bowman, D. M., Johnston, C., Tkachenko, A., Mkrtichian, D. E., Gunsriwiwat, K., and Aerts, C. (2019b). Discovery of tidally perturbed pulsations in the eclipsing binary U Gru: a crucial system for tidal asteroseismology. *Astrophys. J. Lett*. 883:L26. doi: 10.3847/2041-8213/ab3fb2

Bowman, D. M., Kurtz, D. W., Breger, M., Murphy, S. J., and Holdsworth, D. L. (2016). Amplitude modulation in δSCT stars: statistics from an ensemble study of Kepler targets. *Mon. Not. R. Astron. Soc*. 460, 1970–1989. doi: 10.1093/mnras/stw1153

Breger, M. (1979). Delta Scuti and related stars. *Publ. Astron. Soc. Pac*. 91, 5–26. doi: 10.1086/130433

Breger, M., and Montgomery, M. H. (2014). Evidence of resonant mode coupling and the relationship between low and high frequencies in a rapidly rotating a star. *Astrophys. J*. 783:89. doi: 10.1088/0004-637X/783/2/89

Buchler, J. R., Goupil, M. J., and Hansen, C. J. (1997). On the role of resonances in nonradial pulsators. *Astron. Astrophys*. 321, 159–176.

Bunting, A., and Terquem, C. (2021). Tidally induced stellar oscillations: converting modelled oscillations excited by hot Jupiters into observables. *Mon. Not. R. Astron. Soc*. 500, 2711–2731. doi: 10.1093/mnras/staa3394

Burkart, J., Quataert, E., and Arras, P. (2014). Dynamical resonance locking in tidally interacting binary systems. *Mon. Not. R. Astron. Soc*. 443, 2957–2973. doi: 10.1093/mnras/stu1366

Burkart, J., Quataert, E., Arras, P., and Weinberg, N. N. (2012). Tidal asteroseismology: Kepler's KOI-54. *Mon. Not. R. Astron. Soc*. 421, 983–1006. doi: 10.1111/j.1365-2966.2011.20344.x

Byrne, C. M., and Jeffery, C. S. (2020). Pulsation in faint blue stars. *Mon. Not. R. Astron. Soc*. 492, 232–244. doi: 10.1093/mnras/stz3486

Cantiello, M., Lecoanet, D., Jermyn, A. S., and Grassitelli, L. (2021). On the origin of stochastic, low-frequency photometric variability in massive stars. *arXiv* [e-prints] arXiv:2102.05670

Chandrasekhar, S. (1969). *The Silliman Foundation Lectures*. New Haven, CT: Yale University Press. Available online at: https://ui.adsabs.harvard.edu/abs/1969efe..book.....C/abstract

Chen, X., Maxted, P. F. L., Li, J., and Han, Z. (2017). The formation of EL CVn-type binaries. *Mon. Not. R. Astron. Soc*. 467, 1874–1889. doi: 10.1093/mnras/stx115

Cheng, S. J., Fuller, J., Guo, Z., Lehman, H., and Hambleton, K. (2020). Detailed characterization of heartbeat stars and their tidally excited oscillations. *Astrophys. J*. 903:122. doi: 10.3847/1538-4357/abb46d

Chernov, S. V. (2017). Zahn's theory of dynamical tides and its application to stars. *Astron. Lett*. 43, 429–437. doi: 10.1134/S1063773717060020

Dahlen, F., and Tromp, J. (1998). *Theoretical Global Seismology*. Princeton, New Jersey: Princeton University Press. doi: 10.1515/9780691216157

de Loore, C. W. H., and Doom, C. D. (1992). *Structure and Evolution of Single and Binary Stars*, Vol. 179. Boston, MA: Kluwer Academic Publisher. Available online at: https://ui.adsabs.harvard.edu/abs/1992ASSL..179.....D/abstract

Degroote, P., Briquet, M., Catala, C., Uytterhoeven, K., Lefever, K., Morel, T., et al. (2009). Evidence for nonlinear resonant mode coupling in the βCephei star HD 180642 (V1449 Aquilae) from CoRoT photometry. *Astron. Astrophys*. 506, 111–123. doi: 10.1051/0004-6361/200911782

Dimitrov, D. P., Kjurkchieva, D. P., and Iliev, I. K. (2017). Simultaneous solutions of Kepler light curves and radial velocity curves of seven heartbeat variables. *Mon. Not. R. Astron. Soc*. 469, 2089–2101. doi: 10.1093/mnras/stx745

Dong, S., Katz, B., and Socrates, A. (2013). Exploring a "flow" of highly eccentric binaries with Kepler. *Astrophys. J. Lett*. 763:L2. doi: 10.1088/2041-8205/763/1/L2

Dosopoulou, F., and Kalogera, V. (2016a). Orbital evolution of mass-transferring eccentric binary systems. I. Phase-dependent evolution. *Astrophys. J*. 825:70. doi: 10.3847/0004-637X/825/1/70

Dosopoulou, F., and Kalogera, V. (2016b). Orbital evolution of mass-transferring eccentric binary systems. II. Secular evolution. *Astrophys. J*. 825:71. doi: 10.3847/0004-637X/825/1/71

Dray, L. M., and Tout, C. A. (2007). On rejuvenation in massive binary systems. *Mon. Not. R. Astron. Soc*. 376, 61–70. doi: 10.1111/j.1365-2966.2007.11431.x

Dziembowski, W. (1982). Nonlinear mode coupling in oscillating stars. I - Second order theory of the coherent mode coupling. *Acta Astron*. 32, 147–171.

Dziembowski, W., and Krolikowska, M. (1985). Nonlinear mode coupling in oscillating stars. II - Limiting amplitude effect of the parametric resonance in main sequence stars. *Acta Astron*. 35, 5–28.

Dziembowski, W., Krolikowska, M., and Kosovichev, A. (1988). Nonlinear mode coupling in oscillating stars. III. Amplitude limitingeffect of the rotation in the Delta Scuti stars. *Acta Astron*. 38, 61–75.

Edelmann, P. V. F., Ratnasingam, R. P., Pedersen, M. G., Bowman, D. M., Prat, V., and Rogers, T. M. (2019). Three-dimensional simulations of massive stars. I. Wave generation and propagation. *Astrophys. J*. 876:4. doi: 10.3847/1538-4357/ab12df

Eggleton, P. (2006). *Evolutionary Processes in Binary and Multiple Stars*. Cambridge: Cambridge University Press. Available online at: https://ui.adsabs.harvard.edu/abs/2006epbm.book.....E/abstract

Essick, R., and Weinberg, N. N. (2016). Orbital decay of hot jupiters due to nonlinear tidal dissipation within solar-type hosts. *Astrophys. J.* 816:18. doi: 10.3847/0004-637X/816/1/18

Fuller, J. (2017). Heartbeat stars, tidally excited oscillations and resonance locking. *Mon. Not. R. Astron. Soc.* 472, 1538–1564. doi: 10.1093/mnras/stx2135

Fuller, J. (2021). Inverse tides in pulsating binary stars. *Mon. Not. R. Astron. Soc.* 501, 483–490. doi: 10.1093/mnras/staa3636

Fuller, J., Derekas, A., Borkovits, T., Huber, D., Bedding, T. R., and Kiss, L. L. (2013). Tidally induced oscillations and orbital decay in compact triple-star systems. *Mon. Not. R. Astron. Soc.* 429, 2425–2441. doi: 10.1093/mnras/sts511

Fuller, J., Hambleton, K., Shporer, A., Isaacson, H., and Thompson, S. (2017). Accelerated tidal circularization via resonance locking in KIC 8164262. *Mon. Not. R. Astron. Soc.* 472, L25–L29. doi: 10.1093/mnrasl/slx130

Fuller, J., Kurtz, D. W., Handler, G., and Rappaport, S. (2020). Tidally trapped pulsations in binary stars. *Mon. Not. R. Astron. Soc.* 498, 5730–5744. doi: 10.1093/mnras/staa2376

Fuller, J., and Lai, D. (2012). Dynamical tides in eccentric binaries and tidally excited stellar pulsations in Kepler KOI-54. *Mon. Not. R. Astron. Soc.* 420, 3126–3138. doi: 10.1111/j.1365-2966.2011.20237.x

Fuller, J., Luan, J., and Quataert, E. (2016). Resonance locking as the source of rapid tidal migration in the Jupiter and Saturn moon systems. *Mon. Not. R. Astron. Soc.* 458, 3867–3879. doi: 10.1093/mnras/stw609

Garcia Lopez, R. J., and Spruit, H. C. (1991). Li depletion in F stars by internal gravity waves. *Astrophys. J.* 377:268. doi: 10.1086/170356

Gaulme, P., and Guzik, J. A. (2019). Systematic search for stellar pulsators in the eclipsing binaries observed by Kepler. *Astron. Astrophys.* 630:A106. doi: 10.1051/0004-6361/201935821

Gaulme, P., Jackiewicz, J., Appourchaux, T., and Mosser, B. (2014). Surface activity and oscillation amplitudes of red giants in eclipsing binaries. *Astrophys. J.* 785:5. doi: 10.1088/0004-637X/785/1/5

Gaulme, P., McKeever, J., Rawls, M. L., Jackiewicz, J., Mosser, B., and Guzik, J. A. (2013). Red giants in eclipsing binary and multiple-star systems: modeling and asteroseismic analysis of 70 candidates from Kepler data. *Astrophys. J.* 767:82. doi: 10.1088/0004-637X/767/1/82

Gautschy, A., and Saio, H. (2017). On binary channels to anomalous Cepheids. *Mon. Not. R. Astron. Soc.* 468, 4419–4428. doi: 10.1093/mnras/stx811

Gianninas, A., Curd, B., Fontaine, G., Brown, W. R., and Kilic, M. (2016). Discovery of three pulsating, mixed-atmosphere, extremely low-mass white dwarf precursors. *Astrophys. J. Lett.* 822:L27. doi: 10.3847/2041-8205/822/2/L27

Goldreich, P., and Nicholson, P. D. (1989). Tidal friction in early-type stars. *Astrophys. J.* 342:1079. doi: 10.1086/167665

Guo, Z. (2020). Tidal asteroseismology: possible evidence of nonlinear mode coupling in an equilibrium state in Kepler eclipsing binary KIC 3230227. *Astrophys. J.* 896:161. doi: 10.3847/1538-4357/ab911f

Guo, Z., Fuller, J., Shporer, A., Li, G., Hambleton, K., Manuel, J., et al. (2019). KIC 4142768: an evolved gamma doradus/delta scuti hybrid pulsating eclipsing binary with tidally excited oscillations. *Astrophys. J.* 885:46. doi: 10.3847/1538-4357/ab41f6

Guo, Z., Gies, D. R., and Fuller, J. (2017a). Tidally induced pulsations in Kepler eclipsing binary KIC 3230227. *Astrophys. J.* 834:59. doi: 10.3847/1538-4357/834/1/59

Guo, Z., Gies, D. R., and Matson, R. A. (2017b). Gravity modes reveal the internal rotation of a post-mass-transfer gamma Doradus/Delta Scuti hybrid pulsator in Kepler eclipsing binary KIC 9592855. *Astrophys. J.* 851:39. doi: 10.3847/1538-4357/aa978c

Guo, Z., Gies, D. R., Matson, R. A., García Hernández, A., Han, Z., and Chen, X. (2017c). KIC 8262223: a post-mass transfer eclipsing binary consisting of a delta scuti pulsator and a helium white dwarf precursor. *Astrophys. J.* 837:114. doi: 10.3847/1538-4357/aa61a4

Guo, Z., and Li, G. (2019). A mass-accreting gamma doradus pulsator with a synchronized core in Kepler eclipsing binary KIC 7385478. *Astrophys. J. Lett.* 882:L5. doi: 10.3847/2041-8213/ab3a53

Guo, Z., Shporer, A., Hambleton, K., and Isaacson, H. (2020). Tidally excited oscillations in heartbeat binary stars: pulsation phases and mode identification. *Astrophys. J.* 888:95. doi: 10.3847/1538-4357/ab58c2

Hambleton, K., Fuller, J., Thompson, S., Prša, A., Kurtz, D. W., Shporer, A., et al. (2018). KIC 8164262: a heartbeat star showing tidally induced pulsations with resonant locking. *Mon. Not. R. Astron. Soc.* 473, 5165–5176. doi: 10.1093/mnras/stx2673

Hambleton, K., Kurtz, D. W., Prša, A., Quinn, S. N., Fuller, J., Murphy, S. J., et al. (2016). KIC 3749404: a heartbeat star with rapid apsidal advance indicative of a tertiary component. *Mon. Not. R. Astron. Soc.* 463, 1199–1212. doi: 10.1093/mnras/stw1970

Hambleton, K. M., Kurtz, D. W., Prša, A., Guzik, J. A., Pavlovski, K., Bloemen, S., et al. (2013). KIC 4544587: an eccentric, short-period binary system with δSct pulsations and tidally excited modes. *Mon. Not. R. Astron. Soc.* 434, 925–940. doi: 10.1093/mnras/stt886

Han, Z., Podsiadlowski, P., Maxted, P. F. L., and Marsh, T. R. (2003). The origin of subdwarf B stars - II. *Mon. Not. R. Astron. Soc.* 341, 669–691. doi: 10.1046/j.1365-8711.2003.06451.x

Han, Z., Podsiadlowski, P., Maxted, P. F. L., Marsh, T. R., and Ivanova, N. (2002). The origin of subdwarf B stars - I. The formation channels. *Mon. Not. R. Astron. Soc.* 336, 449–466. doi: 10.1046/j.1365-8711.2002.05752.x

Handler, G., Balona, L. A., Shobbrook, R. R., Koen, C., Bruch, A., Romero-Colmenero, E., et al. (2002). Discovery and analysis of p-mode and g-mode oscillations in the A-type primary of the eccentric binary HD 209295*. *Mon. Not. R. Astron. Soc.* 333, 262–279. doi: 10.1046/j.1365-8711.2002.05295.x

Handler, G., Kurtz, D. W., Rappaport, S. A., Saio, H., Fuller, J., Jones, D., et al. (2020). Tidally trapped pulsations in a close binary star system discovered by TESS. *Nat. Astron.* 4, 684–689. doi: 10.1038/s41550-020-1035-1

Hong, K., Lee, J. W., Koo, J.-R., Park, J.-H., Kim, S.-L., Rittipruk, P., et al. (2019). Time-series spectroscopy of the oscillating eclipsing algol system V392 orionis. *Astron. J.* 157:28. doi: 10.3847/1538-3881/aaf39f

Horedt, G. P. (2004). *Polytropes - Applications in Astrophysics and Related Fields*, Vol. 306. Dordrecht; Wessling: Deutsches Zentrum für Luft- und Raumfahrt DLR; Kluwer Academic Publishers. Available online at: https://ui.adsabs.harvard.edu/abs/2004ASSL..306.....H/abstract

Horst, L., Edelmann, P. V. F., Andrássy, R., Röpke, F. K., Bowman, D. M., Aerts, C., et al. (2020). Fully compressible simulations of waves and core convection in main-sequence stars. *Astron. Astrophys.* 641:A18. doi: 10.1051/0004-6361/202037531

Hurley, J. R., Tout, C. A., and Pols, O. R. (2002). Evolution of binary stars and the effect of tides on binary populations. *Mon. Not. R. Astron. Soc.* 329, 897–928. doi: 10.1046/j.1365-8711.2002.05038.x

Hut, P. (1981). Tidal evolution in close binary systems. *Astron. Astrophys.* 99, 126–140.

Istrate, A. G., Fontaine, G., Gianninas, A., Grassitelli, L., Marchant, P., Tauris, T. M., et al. (2016). Asteroseismic test of rotational mixing in low-mass white dwarfs. *Astron. Astrophys.* 595:L12. doi: 10.1051/0004-6361/201629876

Jayasinghe, T., Stanek, K. Z., Kochanek, C. S., Thompson, T. A., Shappee, B. J., and Fausnaugh, M. (2019). An extreme amplitude, massive heartbeat system in the LMC characterized using ASAS-SN and TESS. *Mon. Not. R. Astron. Soc.* 489, 4705–4711. doi: 10.1093/mnras/stz2460

Jeffery, C. S., and Saio, H. (2016). Radial pulsation as a function of hydrogen abundance. *Mon. Not. R. Astron. Soc.* 458, 1352–1373. doi: 10.1093/mnras/stw388

Jerzykiewicz, M., Pigulski, A., Handler, G., Moffat, A. F. J., Popowicz, A., Wade, G. A., et al. (2020). BRITE-Constellation photometry of π^5 Orionis, an ellipsoidal SPB variable. *Mon. Not. R. Astron. Soc.* 496, 2391–2401. doi: 10.1093/mnras/staa1665

Justesen, A. B., and Albrecht, S. (2021). Temperature and distance dependence of tidal circularization in close binaries: a catalog of eclipsing binaries in the southern hemisphere observed by the TESS satellite. *arXiv* [e-prints] arXiv:2103.09216.

Kallinger, T., Weiss, W. W., Beck, P. G., Pigulski, A., Kuschnig, R., Tkachenko, A., et al. (2017). Triple system HD 201433 with a SPB star component seen by BRITE - Constellation: pulsation, differential rotation, and angular momentum transfer. *Astron. Astrophys.* 603:A13. doi: 10.1051/0004-6361/201730625

Karczmarek, P., Wiktorowicz, G., Iłkiewicz, K., Smolec, R., Stepień, K., Pietrzyński, G., et al. (2017). The occurrence of binary evolution pulsators in classical instability strip of RR Lyrae and Cepheid variables. *Mon. Not. R. Astron. Soc.* 466, 2842–2854. doi: 10.1093/mnras/stw3286

Kirk, B., Conroy, K., Prša, A., Abdul-Masih, M., Kochoska, A., Matijevič, G., et al. (2016). Kepler eclipsing binary stars. VII. The catalog of eclipsing binaries found in the entire Kepler data set. *Astron. J.* 151:68. doi: 10.3847/0004-6256/151/3/68

Kjurkchieva, D., Vasileva, D., and Dimitrov, D. (2016). Light curve solutions of 12 eccentric Kepler binaries and analysis of their out-of-eclipse variability. *Astron. J.* 152:189. doi: 10.3847/0004-6256/152/6/189

Koenigsberger, G., Moreno, E., and Harrington, D. M. (2012). Tidal effects on the radial velocity curve of HD 77581 (Vela X-1). *Astron. Astrophys.* 539:A84. doi: 10.1051/0004-6361/201118397

Koenigsberger, G., and Schmutz, W. (2020). The nature of the companion in the Wolf-Rayet system EZ Canis Majoris. *Astron. Astrophys.* 639:A18. doi: 10.1051/0004-6361/201937305

Kołaczek-Szymański, P. A., Pigulski, A., Michalska, G., Moździerski, D., and Różański, T. (2020). Massive heartbeat stars from TESS. I. TESS sectors 1-16. *arXiv e-prints. arXiv:2012.11559*. doi: 10.1051/0004-6361/202039553

Kozai, Y. (1962). Secular perturbations of asteroids with high inclination and eccentricity. *Astron. J.* 67, 591–598. doi: 10.1086/108790

Kurtz, D. W. (1982). Rapidly oscillating AP stars. *Mon. Not. R. Astron. Soc.* 200, 807–859. doi: 10.1093/mnras/200.3.807

Kurtz, D. W., Handler, G., Rappaport, S. A., Saio, H., Fuller, J., Jacobs, T., et al. (2020). The single-sided pulsator CO Camelopardalis. *Mon. Not. R. Astron. Soc.* 494, 5118–5133. doi: 10.1093/mnras/staa989

Kuszlewicz, J. S., North, T. S. H., Chaplin, W. J., Bieryla, A., Latham, D. W., Miglio, A., et al. (2019). KOI-3890: a high-mass-ratio asteroseismic red giant+M-dwarf eclipsing binary undergoing heartbeat tidal interactions. *Mon. Not. R. Astron. Soc.* 487, 14–23. doi: 10.1093/mnras/stz1185

Lai, D. (1997). Dynamical tides in rotating binary stars. *Astrophys. J.* 490, 847–862. doi: 10.1086/304899

Lai, D., Rasio, F. A., and Shapiro, S. L. (1993). Collisions and close encounters between massive main-sequence stars. *Astrophys. J.* 412:593. doi: 10.1086/172946

Lainey, V., Casajus, L. G., Fuller, J., Zannoni, M., Tortora, P., Cooper, N., et al. (2020). Resonance locking in giant planets indicated by the rapid orbital expansion of Titan. *Nat. Astron.* 4, 1053–1058. doi: 10.1038/s41550-020-1120-5

Lecoanet, D., Cantiello, M., Quataert, E., Couston, L.-A., Burns, K. J., Pope, B. J. S., et al. (2019). Low-frequency variability in massive stars: core generation or surface phenomenon? *Astrophys. J. Lett.* 886:L15. doi: 10.3847/2041-8213/ab5446

Lecoanet, D., and Quataert, E. (2013). Internal gravity wave excitation by turbulent convection. *Mon. Not. R. Astron. Soc.* 430, 2363–2376. doi: 10.1093/mnras/stt055

Lee, J. W., Kim, S.-L., Hong, K., Koo, J.-R., Lee, C.-U., and Youn, J.-H. (2016). KIC 4739791: a new R CMa-type eclipsing binary with a pulsating component. *Astron. J.* 151:25. doi: 10.3847/0004-6256/151/2/25

Lee, U. (2012). Amplitudes of low-frequency modes in rotating B-type stars. *Mon. Not. R. Astron. Soc.* 420, 2387–2398. doi: 10.1111/j.1365-2966.2011.20204.x

Lehmann, H., Southworth, J., Tkachenko, A., and Pavlovski, K. (2013). Physical properties of the eclipsing δScuti star KIC 10661783. *Astron. Astrophys.* 557:A79. doi: 10.1051/0004-6361/201321400

Li, G., Guo, Z., Fuller, J., Bedding, T. R., Murphy, S. J., Colman, I. L., et al. (2020a). The effect of tides on near-core rotation: analysis of 35 Kepler γDoradus stars in eclipsing and spectroscopic binaries. *Mon. Not. R. Astron. Soc.* 497, 4363–4375. doi: 10.1093/mnras/staa2266

Li, G., Van Reeth, T., Bedding, T. R., Murphy, S. J., Antoci, V., Ouazzani, R.-M., et al. (2020b). Gravity-mode period spacings and near-core rotation rates of 611 γDoradus stars with Kepler. *Mon. Not. R. Astron. Soc.* 491, 3586–3605. doi: 10.1093/mnras/stz2906

Liakos, A. (2018). KIC 8553788: A pulsating Algol with an extreme mass ratio. *Astron. Astrophys.* 616:A130. doi: 10.1051/0004-6361/201832639

Lidov, M. L. (1962). The evolution of orbits of artificial satellites of planets under the action of gravitational perturbations of external bodies. *Planet. Space Sci.* 9, 719–759. doi: 10.1016/0032-0633(62)90129-0

Loeb, A., and Gaudi, B. S. (2003). Periodic flux variability of stars due to the reflex doppler effect induced by planetary companions. *Astrophys. J. Lett.* 588, L117–L120. doi: 10.1086/375551

Luan, J., and Goldreich, P. (2018). DAVs: red edge and outbursts. *Astrophys. J.* 863:82. doi: 10.3847/1538-4357/aad0f4

Mathis, S. (2009). Transport by gravito-inertial waves in differentially rotating stellar radiation zones. I - Theoretical formulation. *Astron. Astrophys.* 506, 811–828. doi: 10.1051/0004-6361/200810544

Matson, R. A., Gies, D. R., Guo, Z., Quinn, S. N., Buchhave, L. A., Latham, D. W., et al. (2015). HST/COS detection of the spectrum of the subdwarf companion of KOI-81. *Astrophys. J.* 806:155. doi: 10.1088/0004-637X/806/2/155

Maxted, P. F. L., Bloemen, S., Heber, U., Geier, S., Wheatley, P. J., Marsh, T. R., et al. (2014). EL CVn-type binaries - discovery of 17 helium white dwarf precursors in bright eclipsing binary star systems. *Mon. Not. R. Astron. Soc.* 437, 1681–1697. doi: 10.1093/mnras/stt2007

Maxted, P. F. L., Serenelli, A. M., Miglio, A., Marsh, T. R., Heber, U., Dhillon, V. S., et al. (2013). Multi-periodic pulsations of a stripped red-giant star in an eclipsing binary system. *Nature* 498, 463–465. doi: 10.1038/nature 12192

Mkrtichian, D., Gunsriwiwat, K., Engelbrecht, C., A-thano, N., Lehmann, H., Lampens, P., et al. (2020). "The pulsation spectrum of a mass-accreting component of AS Eri," in *Stars and their Variability Observed from Space*, eds C. Neiner, W. W. Weiss, D. Baade, R. E. Griffin, and C. C. Lovekin, and A. F. J. Moffat, 113–114. Available online at: https://ui.adsabs.harvard.edu/abs/2020svos.conf..113M/abstract

Mkrtichian, D. E., Kusakin, A. V., Rodriguez, E., Gamarova, A. Y., Kim, C., Kim, S. L., et al. (2004). Frequency spectrum of the rapidly-oscillating mass-accreting component of the Algol-type system AS Eri. *Astron. Astrophys.* 419, 1015–1024. doi: 10.1051/0004-6361:20040095

Mkrtichian, D. E., Lehmann, H., Rodríguez, E., Olson, E., Kim, S. L., Kusakin, A. V., et al. (2018). The eclipsing binary star RZ Cas: accretion-driven variability of the multimode oscillation spectrum. *Mon. Not. R. Astron. Soc.* 475, 4745–4767. doi: 10.1093/mnras/stx2841

Moe, M., and Di Stefano, R. (2017). Mind your Ps and Qs: the interrelation between period (P) and mass-ratio (Q) distributions of binary stars. *Astrophys. J. Suppl. Ser.* 230:15. doi: 10.3847/1538-4365/aa6fb6

Moskalik, P. (1985). Modulation of amplitudes in oscillating stars due to resonant mode coupling. *Acta Astron.* 35, 229–254.

Mukadam, A. S., Gänsicke, B. T., Szkody, P., Aungwerojwit, A., Howell, S. B., Fraser, O. J., et al. (2007). Discovery of two new accreting pulsating white dwarf stars. *Astrophys. J.* 667, 433–441. doi: 10.1086/520700

Mukadam, A. S., Townsley, D. M., Szkody, P., Gänsicke, B. T., Winget, D. E., Hermes, J. J., et al. (2011). First unambiguous detection of the return of pulsations in the accreting white dwarf SDSS J074531.92+453829.6 after an outburst. *Astrophys. J. Lett.* 728:L33. doi: 10.1088/2041-8205/728/2/L33

Naoz, S. (2016). The eccentric Kozai-Lidov effect and its applications. *Annu. Rev. Astron. Astrophys.* 54, 441–489. doi: 10.1146/annurev-astro-081915-023315

Nicholls, C. P., and Wood, P. R. (2012). Eccentric ellipsoidal red giant binaries in the LMC: complete orbital solutions and comments on interaction at periastron. *Mon. Not. R. Astron. Soc.* 421, 2616–2628. doi: 10.1111/j.1365-2966.2012.20492.x

Ogilvie, G. I. (2014). Tidal dissipation in stars and giant planets. *Annu. Rev. Astron. Astrophys.* 52, 171–210. doi: 10.1146/annurev-astro-081913-035941

Ogilvie, G. I., and Lin, D. N. C. (2007). Tidal dissipation in rotating solar-type stars. *Astrophys. J.* 661, 1180–1191. doi: 10.1086/515435

O'Leary, R. M., and Burkart, J. (2014). It takes a village to raise a tide: non-linear multiple-mode coupling and mode identification in KOI-54. *Mon. Not. R. Astron. Soc.* 440, 3036–3050. doi: 10.1093/mnras/stu335

Ouazzani, R. M., Ligniéres, F., Dupret, M. A., Salmon, S. J. A. J., Ballot, J., Christophe, S., et al. (2020). First evidence of inertial modes in γDoradus stars: the core rotation revealed. *Astron. Astrophys.* 640:A49. doi: 10.1051/0004-6361/201936653

Pablo, H., Richardson, N. D., Fuller, J., Rowe, J., Moffat, A. F. J., Kuschnig, R., et al. (2017). The most massive heartbeat: an in-depth analysis of ιOrionis. *Mon. Not. R. Astron. Soc.* 467, 2494–2503. doi: 10.1093/mnras/stx207

Pamyatnykh, A. A. (1999). Pulsational instability domains in the upper main sequence. *Acta Astron.* 49, 119–148.

Papaloizou, J. C. B. and Savonije, G. J. (1997). Non-adiabatic tidal forcing of a massive, uniformly rotating star - III. Asymptotic treatment for low frequencies in the inertial regime. *Mon. Not. R. Astron. Soc.* 291, 651–657. doi: 10.1093/mnras/291.4.651

Pápics, P. I., Tkachenko, A., Van Reeth, T., Aerts, C., Moravveji, E., Van de Sande, M., et al. (2017). Signatures of internal rotation discovered in the

Kepler data of five slowly pulsating B stars. *Astron. Astrophys.* 598:A74. doi: 10.1051/0004-6361/201629814

Pepper, J., Pogge, R. W., DePoy, D. L., Marshall, J. L., Stanek, K. Z., Stutz, A. M., et al. (2007). The Kilodegree Extremely Little Telescope (KELT): a small robotic telescope for large-area synoptic surveys. *Publ. Astron. Soc. Pac.* 119, 923–935. doi: 10.1086/521836

Pietrukowicz, P., Dziembowski, W. A., Latour, M., Angeloni, R., Poleski, R., di Mille, F., et al. (2017). Blue large-amplitude pulsators as a new class of variable stars. *Nat. Astron.* 1:0166. doi: 10.1038/s41550-017-0166

Pietrzyński, G., Thompson, I. B., Gieren, W., Graczyk, D., Stepień, K., Bono, G., et al. (2012). RR-Lyrae-type pulsations from a 0.26-solar-mass star in a binary system. *Nature* 484, 75–77. doi: 10.1038/nature10966

Pilecki, B., Gieren, W., Smolec, R., Pietrzyński, G., Thompson, I. B., Anderson, R. I., et al. (2017). Mass and p-factor of the Type II Cepheid OGLE-LMC-T2CEP-098 in a binary system. *Astrophys. J.* 842:110. doi: 10.3847/1538-4357/aa6ff7

Prat, V., Ligniéres, F., and Ballot, J. (2016). Asymptotic theory of gravity modes in rotating stars. I. Ray dynamics. *Astron. Astrophys.* 587:A110. doi: 10.1051/0004-6361/201527737

Preece, H. P., Jeffery, C. S., and Tout, C. A. (2019). Asteroseismology of tidally distorted sdB stars. *Mon. Not. R. Astron. Soc.* 489, 3066–3072. doi: 10.1093/mnras/stz2292

Press, W. H. (1981). Radiative and other effects from internal waves in solar and stellar interiors. *Astrophys. J.* 245, 286–303. doi: 10.1086/158809

Prša, A., and Zwitter, T. (2005). A computational guide to physics of eclipsing binaries. I. Demonstrations and perspectives. *Astrophys. J.* 628, 426–438. doi: 10.1086/430591

Raghavan, D., McAlister, H. A., Henry, T. J., Latham, D. W., Marcy, G. W., Mason, B. D., et al. (2010). A survey of stellar families: multiplicity of solar-type stars. *Astrophys. J. Suppl. Ser.* 190, 1–42. doi: 10.1088/0067-0049/190/1/1

Rappaport, S. A., Kurtz, D. W., Handler, G., Jones, D., Nelson, L. A., Saio, H., et al. (2021). A tidally tilted sectoral dipole pulsation mode in the eclipsing binary TIC 63328020. *Mon. Not. R. Astron. Soc.* 503, 254–269. doi: 10.1093/mnras/stab336

Ratnasingam, R. P., Edelmann, P. V. F., and Rogers, T. M. (2019). Onset of non-linear internal gravity waves in intermediate-mass stars. *Mon. Not. R. Astron. Soc.* 482, 5500–5512. doi: 10.1093/mnras/sty3086

Remus, F., Mathis, S., and Zahn, J. P. (2012). The equilibrium tide in stars and giant planets. I. The coplanar case. *Astron. Astrophys.* 544:A132. doi: 10.1051/0004-6361/201118160

Reyniers, K., and Smeyers, P. (2003). Tidal perturbations of linear, isentropic oscillations in components of circular-orbit close binaries. I. Synchronously rotating components. *Astron. Astrophys.* 404, 1051–1065. doi: 10.1051/0004-6361:20030501

Richardson, N. D., Pablo, H., Sterken, C., Pigulski, A., Koenigsberger, G., Moffat, A. F. J., et al. (2018). BRITE-Constellation reveals evidence for pulsations in the enigmatic binary ηCarinae. *Mon. Not. R. Astron. Soc.* 475, 5417–5423. doi: 10.1093/mnras/sty157

Richardson, N. D., Russell, C. M. P., St-Jean, L., Moffat, A. F. J., St-Louis, N., Shenar, T., et al. (2017). The variability of the BRITE-est Wolf-Rayet binary, γ^2 Velorum-I. Photometric and spectroscopic evidence for colliding winds. *Mon. Not. R. Astron. Soc.* 471, 2715–2729. doi: 10.1093/mnras/stx1731

Ricker, G. R., Winn, J. N., Vanderspek, R., Latham, D. W., Bakos, G. Á., Bean, J. L., et al. (2015). Transiting Exoplanet Survey Satellite (TESS). *J. Astron. Telesc. Instrum. Syst.* 1:014003. doi: 10.1117/1.JATIS.1.1.014003

Rodríguez, E., López-González, M. J., and López de Coca, P. (2000). A revised catalogue of delta Sct stars. *Astron. Astrophys. Suppl. Ser.* 144, 469–474. doi: 10.1051/aas:2000221

Rogers, T. M., Lin, D. N. C., McElwaine, J. N., and Lau, H. H. B. (2013). Internal gravity waves in massive stars: angular momentum transport. *Astrophys. J.* 772:21. doi: 10.1088/0004-637X/772/1/21

Rüdiger, G., Gellert, M., Spada, F., and Tereshin, I. (2015). The angular momentum transport by unstable toroidal magnetic fields. *Astron. Astrophys.* 573:A80. doi: 10.1051/0004-6361/201424060

Saio, H. (1981). Rotational and tidal perturbations of nonradial oscillations in polytropic star. *Astrophys. J.* 244, 299–315. doi: 10.1086/158708

Saio, H. (2019). R-mode oscillations in accreting white dwarfs in cataclysmic variables. *Mon. Not. R. Astron. Soc.* 487, 2177–2190. doi: 10.1093/mnras/stz1407

Saio, H. (2020). "R-mode oscillations in eclipsing binaries," in *Proceedings of the Conference Stars and their Variability Observed from Space*, eds C. Neiner, W. W. Weiss, D. Baade, R. E. Griffin, C. C. Lovekin, A. F. J. Moffat (Vienna: University of Vienna), 321–324. Available online at: https://ui.adsabs.harvard.edu/abs/2020svos.conf..321S/abstract

Saio, H., Kurtz, D. W., Murphy, S. J., Antoci, V. L., and Lee, U. (2018). Theory and evidence of global Rossby waves in upper main-sequence stars: r-mode oscillations in many Kepler stars. *Mon. Not. R. Astron. Soc.* 474, 2774–2786. doi: 10.1093/mnras/stx2962

Saio, H., Takata, M., Lee, U., Li, G., and Van Reeth, T. (2021). Rotation of the convective core in γDor stars measured by dips in period spacings of g modes coupled with inertial modes. *Mon. Not. R. Astron. Soc.* 502, 5856–5874. doi: 10.1093/mnras/stab482

Savonije, G. J., and Papaloizou, J. C. B. (1997). Non-adiabatic tidal forcing of a massive, uniformly rotating star - II. The low-frequency, inertial regime. *Mon. Not. R. Astron. Soc.* 291, 633–650. doi: 10.1093/mnras/291.4.633

Savonije, G. J., Papaloizou, J. C. B., and Alberts, F. (1995). Nonadiabatic tidal forcing of a massive uniformly rotating star. *Mon. Not. R. Astron. Soc.* 277:471. doi: 10.1093/mnras/277.2.471

Schenk, A. K., Arras, P., Flanagan, É. É., Teukolsky, S. A., and Wasserman, I. (2002). Nonlinear mode coupling in rotating stars and the r-mode instability in neutron stars. *Phys. Rev. D* 65:024001. doi: 10.1103/PhysRevD.65.024001

Sekaran, S., Tkachenko, A., Abdul-Masih, M., Prša, A., Johnston, C., Huber, D., et al. (2020). Tango of celestial dancers: A sample of detached eclipsing binary systems containing g-mode pulsating components. A case study of KIC9850387. *Astron. Astrophys.* 643:A162. doi: 10.1051/0004-6361/202038989

Sepinsky, J. F., Willems, B., and Kalogera, V. (2007). Equipotential surfaces and lagrangian points in nonsynchronous, eccentric binary and planetary systems. *Astrophys. J.* 660, 1624–1635. doi: 10.1086/513736

Shporer, A., Fuller, J., Isaacson, H., Hambleton, K., Thompson, S. E., Prša, A., et al. (2016). Radial velocity monitoring of Kepler heartbeat stars. *Astrophys. J.* 829:34. doi: 10.3847/0004-637X/829/1/34

Smullen, R. A., and Kobulnicky, H. A. (2015). Heartbeat stars: spectroscopic orbital solutions for six eccentric binary systems. *Astrophys. J.* 808:166. doi: 10.1088/0004-637X/808/2/166

Soberman, G. E., Phinney, E. S., and van den Heuvel, E. P. J. (1997). Stability criteria for mass transfer in binary stellar evolution. *Astron. Astrophys.* 327, 620–635.

Southworth, J., Bowman, D. M., and Pavlovski, K. (2021). A βCephei pulsator and a changing orbital inclination in the high-mass eclipsing binary system VV Orionis. *Mon. Not. R. Astron. Soc.* 501, L65–L70. doi: 10.1093/mnrasl/slaa197

Southworth, J., Bowman, D. M., Tkachenko, A., and Pavlovski, K. (2020). Discovery of βCep pulsations in the eclipsing binary V453 Cygni. *Mon. Not. R. Astron. Soc.* 497, L19–L23. doi: 10.1093/mnrasl/slaa091

Southworth, J., Zima, W., Aerts, C., Bruntt, H., Lehmann, H., Kim, S. L., et al. (2011). Kepler photometry of KIC 10661783: a binary star with total eclipses and δScuti pulsations. *Mon. Not. R. Astron. Soc.* 414, 2413–2423. doi: 10.1111/j.1365-2966.2011.18559.x

Springer, O. M., and Shaviv, N. J. (2013). Asteroseismic effects in close binary stars. *Mon. Not. R. Astron. Soc.* 434, 1869–1882. doi: 10.1093/mnras/stt1041

Stancliffe, R. J., and Glebbeek, E. (2008). Thermohaline mixing and gravitational settling in carbon-enhanced metal-poor stars. *Mon. Not. R. Astron. Soc.* 389, 1828–1838. doi: 10.1111/j.1365-2966.2008.13700.x

Steindl, T., Zwintz, K., and Bowman, D. M. (2021). Tidally perturbed pulsations in the pre-main sequence δScuti binary RS Cha. *Astron. Astrophys.* 645:A119. doi: 10.1051/0004-6361/202039093

Streamer, M., Ireland, M. J., Murphy, S. J., and Bento, J. (2018). A window into δSct stellar interiors: understanding the eclipsing binary system TT Hor. *Mon. Not. R. Astron. Soc.* 480, 1372–1383. doi: 10.1093/mnras/sty1881

Su, Y., Lecoanet, D., and Lai, D. (2020). Physics of tidal dissipation in early-type stars and white dwarfs: hydrodynamical simulations of internal gravity wave breaking in stellar envelopes. *Mon. Not. R. Astron. Soc.* 495, 1239–1251. doi: 10.1093/mnras/staa1306

Thompson, S. E., Everett, M., Mullally, F., Barclay, T., Howell, S. B., Still, M., et al. (2012). A class of eccentric binaries with dynamic tidal distortions discovered with Kepler. *Astrophys. J.* 753:86. doi: 10.1088/0004-637X/753/1/86

Townsend, R. H. D., Goldstein, J., and Zweibel, E. G. (2018). Angular momentum transport by heat-driven g-modes in slowly pulsating B stars. *Mon. Not. R. Astron. Soc.* 475, 879–893. doi: 10.1093/mnras/stx3142

Tubbesing, S., Kaufer, A., Stahl, O., Wolf, B., Schmid, H. M., Korn, A. J., et al. (2002). The eclipsing hypergiant R 81 (B2.5Ia-O) in the Large Magellanic Cloud. System properties from spectroscopic and photometric monitoring. *Astron. Astrophys.* 389, 931–944. doi: 10.1051/0004-6361:20020682

Unno, W., Osaki, Y., Ando, H., Saio, H., and Shibahashi, H. (1989). *Nonradial Oscillations of Stars, 2nd Edn*. Tokyo: Tokyo Univ. Press). Available online at: https://ui.adsabs.harvard.edu/abs/1989nos..book.....U/abstract

Van Hoolst, T. (1994). Coupled-mode equations and amplitude equations for nonadiabatic, nonradial oscillations of stars. *Astron. Astrophys.* 292, 471–480.

van Kerkwijk, M. H., Rappaport, S. A., Breton, R. P., Justham, S., Podsiadlowski, P., and Han, Z. (2010). Observations of doppler boosting in Kepler light curves. *Astrophys. J.* 715, 51–58. doi: 10.1088/0004-637X/715/1/51

Van Reeth, T., Tkachenko, A., and Aerts, C. (2016). Interior rotation of a sample of γDoradus stars from ensemble modelling of their gravity-mode period spacings. *Astron. Astrophys.* 593:A120. doi: 10.1051/0004-6361/201628616

Vanbeveren, D., and De Loore, C. (1994). The evolution of the mass gainer in massive close binaries. *Astron. Astrophys.* 290, 129–132. doi: 10.1007/978-94-011-1080-8

Weinberg, N. N., Arras, P., Quataert, E., and Burkart, J. (2012). Nonlinear tides in close binary systems. *Astrophys. J.* 751:136. doi: 10.1088/0004-637X/751/2/136

Welsh, W. F., Orosz, J. A., Aerts, C., Brown, T. M., Brugamyer, E., Cochran, W. D., et al. (2011). KOI-54: the Kepler discovery of tidally excited pulsations and brightenings in a highly eccentric binary. Astrophys. *J. Suppl. Ser.* 197:4. doi: 10.1088/0067-0049/197/1/4

Wersinger, J.-M., Finn, J., and Ott, E. (1980). Bifurcation and "strange" behavior in instability saturation by nonlinear three-wave mode coupling. *Phys. Fluids* 23, 1142–1154. doi: 10.1063/1.863116

Willems, B. (2003). Excitation of oscillation modes by tides in close binaries: constraints on stellar and orbital parameters. *Mon. Not. R. Astron. Soc.* 346, 968–976. doi: 10.1111/j.1365-2966.2003.07151.x

Willems, B., and Aerts, C. (2002). Tidally induced radial-velocity variations in close binaries. *Astron. Astrophys.* 384, 441–451. doi: 10.1051/0004-6361:20020021

Wilson, R. E., and Devinney, E. J. (1971). Realization of accurate close-binary light curves: application to MR Cygni. *Astrophys. J.* 166:605. doi: 10.1086/150986

Witte, M. G., and Savonije, G. J. (1999a). The dynamical tide in a rotating 10 Msun main sequence star. A study of G- and R-mode resonances. *Astron. Astrophys.* 341, 842–852.

Witte, M. G., and Savonije, G. J. (1999b). Tidal evolution of eccentric orbits in massive binary systems. A study of resonance locking. *Astron. Astrophys.* 350, 129–147.

Wu, Y., and Goldreich, P. (2001). Gravity modes in ZZ Ceti stars. IV. Amplitude saturation by parametric instability. *Astrophys. J.* 546, 469–483. doi: 10.1086/318234

Yu, H., Weinberg, N. N., and Fuller, J. (2020). Non-linear dynamical tides in white dwarf binaries. *Mon. Not. R. Astron. Soc.* 496, 5482–5502. doi: 10.1093/mnras/staa1858

Zahn, J. P. (1975). The dynamical tide in close binaries. *Astron. Astrophys.* 41, 329–344.

Zahn, J. P. (1977). Reprint of 1977A&A....57..383Z. Tidal friction in close binary stars. *Astron. Astrophys.* 500, 121–132.

Zahn, J. P., Talon, S., and Matias, J. (1997). Angular momentum transport by internal waves in the solar interior. *Astron. Astrophys.* 322, 320–328.

Zimmerman, M. K., Thompson, S. E., Mullally, F., Fuller, J., Shporer, A., and Hambleton, K. (2017). The pseudosynchronization of binary stars undergoing strong tidal interactions. *Astrophys. J.* 846:147. doi: 10.3847/1538-4357/aa85e3

Zong, W., Charpinet, S., and Vauclair, G. (2016a). Signatures of nonlinear mode interactions in the pulsating hot B subdwarf star KIC 10139564. *Astron. Astrophys.* 594:A46. doi: 10.1051/0004-6361/201629132

Zong, W., Charpinet, S., Vauclair, G., Giammichele, N., and Van Grootel, V. (2016b). Amplitude and frequency variations of oscillation modes in the pulsating DB white dwarf star KIC 08626021. The likely signature of nonlinear resonant mode coupling. *Astron. Astrophys.* 585:A22. doi: 10.1051/0004-6361/201526300

Conflict of Interest: The author declares that the research was conducted in the absence of any commercial or financial relationships that could be construed as a potential conflict of interest.

ASTEROSEISMOLOGY IN THE KEPLER ERA

EDITED BY: Andrzej S Baran, Anthony Eugene Lynas-Gray and Karen Kinemuchi
PUBLISHED IN: Frontiers in Astronomy and Space Sciences

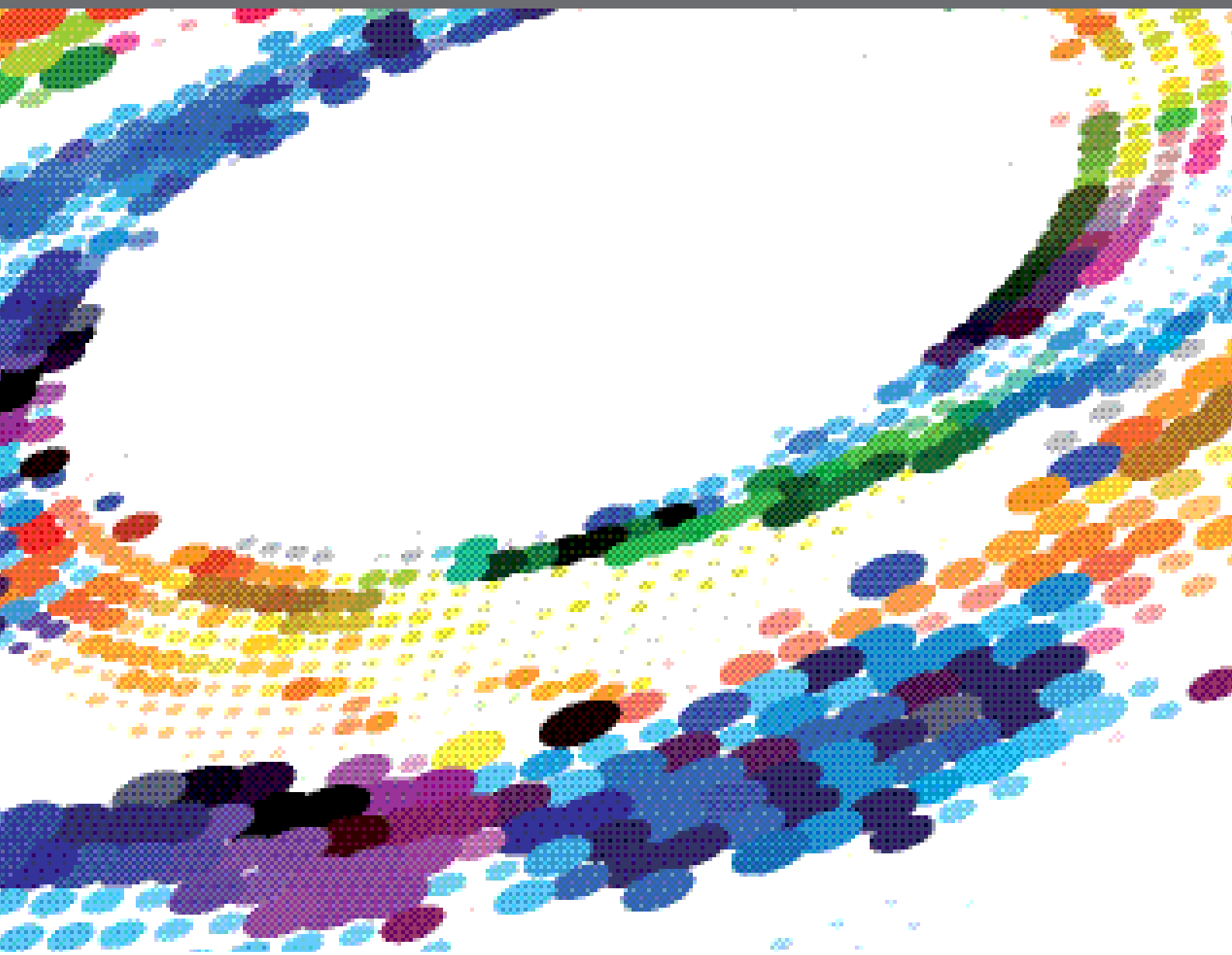

frontiers Research Topics

ISSN 1664-8714
ISBN 978-2-88971-477-3
DOI 10.3389/978-2-88971-477-3

About Frontiers

Frontiers is more than just an open-access publisher of scholarly articles: it is a pioneering approach to the world of academia, radically improving the way scholarly research is managed. The grand vision of Frontiers is a world where all people have an equal opportunity to seek, share and generate knowledge. Frontiers provides immediate and permanent online open access to all its publications, but this alone is not enough to realize our grand goals.

Frontiers Journal Series

The Frontiers Journal Series is a multi-tier and interdisciplinary set of open-access, online journals, promising a paradigm shift from the current review, selection and dissemination processes in academic publishing. All Frontiers journals are driven by researchers for researchers; therefore, they constitute a service to the scholarly community. At the same time, the Frontiers Journal Series operates on a revolutionary invention, the tiered publishing system, initially addressing specific communities of scholars, and gradually climbing up to broader public understanding, thus serving the interests of the lay society, too.

Dedication to Quality

Each Frontiers article is a landmark of the highest quality, thanks to genuinely collaborative interactions between authors and review editors, who include some of the world's best academicians. Research must be certified by peers before entering a stream of knowledge that may eventually reach the public - and shape society; therefore, Frontiers only applies the most rigorous and unbiased reviews.
Frontiers revolutionizes research publishing by freely delivering the most outstanding research, evaluated with no bias from both the academic and social point of view. By applying the most advanced information technologies, Frontiers is catapulting scholarly publishing into a new generation.

What are Frontiers Research Topics?

Frontiers Research Topics are very popular trademarks of the Frontiers Journals Series: they are collections of at least ten articles, all centered on a particular subject. With their unique mix of varied contributions from Original Research to Review Articles, Frontiers Research Topics unify the most influential researchers, the latest key findings and historical advances in a hot research area! Find out more on how to host your own Frontiers Research Topic or contribute to one as an author by contacting the Frontiers Editorial Office: frontiersin.org/about/contact

ASTEROSEISMOLOGY IN THE KEPLER ERA

Topic Editors:
Andrzej S Baran, Pedagogical University of Kraków, Poland
Anthony Eugene Lynas-Gray, University College London, United Kingdom
Karen Kinemuchi, New Mexico State University, United States

Citation: Baran, A. S., Lynas-Gray, A. E., Kinemuchi, K., eds. (2021). Asteroseismology in the Kepler Era. Lausanne: Frontiers Media SA.
doi: 10.3389/978-2-88971-477-3

Table of Contents

Advantages of publishing in Frontiers

OPEN ACCESS
Articles are free to read for greatest visibility and readership

FAST PUBLICATION
Around 90 days from submission to decision

HIGH QUALITY PEER-REVIEW
Rigorous, collaborative, and constructive peer-review

TRANSPARENT PEER-REVIEW
Editors and reviewers acknowledged by name on published articles

Frontiers
Avenue du Tribunal-Fédéral 34
1005 Lausanne | Switzerland

Visit us: www.frontiersin.org
Contact us: frontiersin.org/about/contact

REPRODUCIBILITY OF RESEARCH
Support open data and methods to enhance research reproducibility

DIGITAL PUBLISHING
Articles designed for optimal readership across devices

FOLLOW US
@frontiersin

IMPACT METRICS
Advanced article metrics track visibility across digital media

EXTENSIVE PROMOTION
Marketing and promotion of impactful research

LOOP RESEARCH NETWORK
Our network increases your article's readership